

GA-A15738  
UC-77

## HTGR GAS TURBINE PROGRAM

SEMIANNUAL PROGRESS REPORT  
FOR THE PERIOD ENDING SEPTEMBER 30, 1979

by  
PROJECT STAFF

Prepared under  
Contract DE-AT03-76SF70046  
for the San Francisco Operations Office  
Department of Energy

DATE PUBLISHED: MAY 1980

---

**GENERAL ATOMIC COMPANY**

---

8008130540

## NOTICE

This report was prepared as an account of work sponsored by an agency of the United States Government. Neither the United States nor any agency thereof, nor any of their employees, makes any warranty, expressed or implied, or assumes any legal liability or responsibility for any third party's use or the results of such use of any information, apparatus, product or process disclosed in this report, or represents that its use by such third party would not infringe privately owned rights.

Printed in the United States of America  
Available from  
National Technical Information Service  
U.S. Department of Commerce  
5285 Port Royal Road  
Springfield, VA 22161

Price codes: printed copy A18; microfiche A01

**GA-A15738  
UC-77**

## **HTGR GAS TURBINE PROGRAM**

**SEMIANNUAL PROGRESS REPORT  
FOR THE PERIOD ENDING SEPTEMBER 30, 1979**

**by  
PROJECT STAFF**

**Prepared under  
Contract DE-AT03-76SF70046  
for the San Francisco Operations Office  
Department of Energy**

**GENERAL ATOMIC PROJECT 68  
DATE PUBLISHED: MAY 1980**

---

**GENERAL ATOMIC COMPANY**

---

## ABSTRACT

This report describes conceptual design and analysis performed by General Atomic Company for the U.S. Department of Energy on the direct cycle gas turbine high-temperature gas-cooled reactor (HTGR-GT).

General Atomic cooperated with the German/Swiss HHT project on the development of the HTGR-GT concept in the areas of systems analysis, safety and accident analysis, and PCRV-liner-internals design.

## CONTENTS

ABSTRACT . . . . .	111
1. INTRODUCTION . . . . .	1-1
2. SYSTEMS DESIGN METHODS DEVELOPMENT . . . . .	2-1
2.1. Scope . . . . .	2-1
2.2. Summary . . . . .	2-1
2.2.1. Computer Program CODER . . . . .	2-1
2.2.2. Computer Program RECA3/GT . . . . .	2-2
2.2.3. Computer Program ECSEL8 . . . . .	2-2
2.3. Discussion . . . . .	2-2
3. SYSTEM DYNAMICS METHODS DEVELOPMENT . . . . .	3-1
3.1. Scope . . . . .	3-1
3.2. Summary . . . . .	3-1
3.3. Discussion . . . . .	3-1
3.3.1. CWS/Precooler . . . . .	3-1
3.3.2. Preliminary Two-Loop, 800-MW(e) Plant Model . . . . .	3-4
4. ALTERNATE DESIGN . . . . .	4-1
4.1. Scope . . . . .	4-1
4.2. Summary . . . . .	4-1
4.3. Discussion . . . . .	4-2
4.3.1. Intercooled Versus Non-intercooled Plant Study . . . . .	4-2
4.3.2. Advanced Features Study . . . . .	4-25
5. MISCELLANEOUS CONTROLS AND AUXILIARY SYSTEMS . . . . .	5-1
5.1. Scope . . . . .	5-1
5.2. Summary . . . . .	5-1
5.3. Discussion . . . . .	5-1
6. STRUCTURAL MECHANICS . . . . .	6-1
6.1. Scope . . . . .	6-1
6.2. Summary . . . . .	6-1

6.3.	Discussion . . . . .	6-2
6.3.1.	RCB/PCRV Plant . . . . .	6-2
6.3.2.	Prismatic Block Gas Turbine Reactor Core . . . . .	6-4
6.3.3.	Gas Turbine Pebble Bed Core . . . . .	6-9
7.	SHIELDING ANALYSIS AND DESIGN . . . . .	7-1
7.1.	Scope . . . . .	7-1
7.2.	Summary . . . . .	7-1
7.3.	Discussion . . . . .	7-1
7.3.1.	Thermal Barrier Evaluation . . . . .	7-1
7.3.2.	Turbomachine Disassembly and Decontamination . . . . .	7-2
7.3.3.	Hot Duct Removal . . . . .	7-4
7.3.4.	Helium Control Valve Maintenance . . . . .	7-6
8.	LICENSING . . . . .	8-1
8.1.	Scope . . . . .	8-1
8.2.	Summary . . . . .	8-1
8.3.	Discussion . . . . .	8-2
8.3.1.	Design Reviews . . . . .	8-2
8.3.2.	Nuclear Safety Plant Specification . . . . .	8-6
8.3.3.	Proposed HTGR-GT Specific LTRs . . . . .	8-6
9.	SAFETY . . . . .	9-1
9.1.	Scope . . . . .	9-1
9.2.	Summary . . . . .	9-1
9.3.	Discussion . . . . .	9-3
9.3.1.	Pressure Equilibration Rates . . . . .	9-3
9.3.2.	TUBE Program Development and Verification . . . . .	9-4
9.3.3.	Review of Primary Coolant System Boundary . . . . .	9-5
9.3.4.	HuT Support . . . . .	9-12
9.4.	Reference . . . . .	9-16
10.	AVAILABILITY . . . . .	10-1
10.1.	Scope . . . . .	10-1
10.2.	Summary . . . . .	10-1
10.3.	Discussion . . . . .	10-1
10.3.1.	HTGR-GT Preliminary Availability Evaluation . . . . .	10-1
10.3.2.	Intercooled/Non-Intercooled Plant Availability Comparison . . . . .	10-2
10.3.3.	Conclusions . . . . .	10-7

11. REACTOR TURBINE SYSTEM/BALANCE OF PLANT INTEGRATION . . . . .	11-1
11.1. Scope . . . . .	11-1
11.2. Summary . . . . .	11-1
11.3. Discussion . . . . .	11-2
11.3.1. BOP Plant Layouts . . . . .	11-2
11.3.2. BOP Systems . . . . .	11-4
11.3.3. Intercooled Versus Non-intercooled Plant Impact on BOP . . . . .	11-8
11.3.4. Maintenance/Contamination Study . . . . .	11-9
12. SYSTEMS DESIGN . . . . .	12-1
12.1. Scope . . . . .	12-1
12.2. Summary . . . . .	12-1
12.3. Discussion . . . . .	12-17
12.3.1. Primary System Parameter-Related Design Issues . .	12-17
12.3.2. Primary System Parameter Review . . . . .	12-22
12.3.3. Non-Intercooled Versus Intercooled Plant Optimization Study . . . . .	12-24
12.3.4. Helium Inventory Control System for 3000-MW(t) HTGR-GT Plant . . . . .	12-25
12.3.5. $\Delta P/P$ and Bypass Flows for 3000-MW(t) HTGR-GT Plant . . . . .	12-33
12.3.6. Evaluation of Cooling Towers and Ambient Design Temperatures . . . . .	12-35
12.3.7. CACS Design Criteria . . . . .	12-37
12.3.8. CACS Component Sizing . . . . .	12-38
13. SYSTEM DYNAMICS . . . . .	13-1
13.1. Scope . . . . .	13-1
13.2. Summary . . . . .	13-1
13.3. Discussion . . . . .	13-3
13.3.1. Three-Loop, 1200-MW(e) and Two-Loop, 800-MW(e) Plant Analyses and Comparison . . . . .	13-3
13.3.2. Plant Control and Protection Systems Functional Design . . . . .	13-10
13.3.3. Intercooled Versus Non-Intercooled and Warm Liner Versus Cold Liner Studies . . . . .	13-15

13.3.4.	Sound Pressure Level, Natural Convection, and Flow Mixing Studies . . . . .	13-16
13.3.5.	HTGR-GT Loop Natural Convection With No Forced Flow . . . . .	13-17
13.3.6.	Mixing of Turbine and Bypass Valve Gas Streams in HTGR-GT . . . . .	13-19
13.4.	Reference . . . . .	13-21
14.	PCRV LINERS, PENETRATIONS, AND CLOSURES . . . . .	14-1
14.1.	Scope . . . . .	14-1
14.2.	Summary . . . . .	14-1
14.3.	Discussion . . . . .	14-5
14.4.	Reference . . . . .	14-14
15.	PCRV STRUCTURES . . . . .	15-1
15.1.	Scope . . . . .	15-1
15.2.	Summary . . . . .	15-1
15.3.	Discussion . . . . .	15-2
15.3.1.	Effectiveness of PCRV Pressurizing at Turbo- machine Cavity Region . . . . .	15-2
15.3.2.	Two-Loop Intercooled and Non-Intercooled Plant Study . . . . .	15-10
16.	THERMAL BARRIER . . . . .	16-1
16.1.	Scope . . . . .	16-1
16.2.	Summary . . . . .	16-1
16.3.	Discussion . . . . .	16-1
16.3.1.	Evaluation of HHT Thermal Barrier Designs . . . . .	16-1
16.3.2.	High-Temperature Thermal Barrier Design Development . . . . .	16-4
17.	REACTOR INTERNALS . . . . .	17-1
17.1.	Reactor Internals Design . . . . .	17-1
17.1.1.	Scope . . . . .	17-1
17.1.2.	Summary . . . . .	17-1
17.1.3.	Discussion . . . . .	17-2
17.2.	Hot Duct Design - Free-Standing Section . . . . .	17-5
17.2.1.	Scope . . . . .	17-5
17.2.2.	Summary . . . . .	17-5
17.2.3.	Discussion . . . . .	17-5



17.3. Hot Duct Design - Thermal Barrier . . . . .	17-19
17.3.1. Scope . . . . .	17-19
17.3.2. Summary . . . . .	17-19
17.3.3. Discussion . . . . .	17-19
17.4. Reference . . . . .	17-32
18. TURBOMACHINERY . . . . .	18-1
18.1. Scope . . . . .	18-1
18.2. Summary . . . . .	18-1
18.3. Discussion . . . . .	18-2
18.3.1. 400-MW(e) Turbomachine Conceptual Design . . . . .	18-2
18.3.2. Sound Power Level Study . . . . .	18-5
18.3.3. Turbomachine Weight Summary . . . . .	18-6
18.3.4. Turbine Cooling Flow Distribution . . . . .	18-6
18.3.5. 400-MW(e) Intercooled Turbomachine Conceptual Design . . . . .	18-6
18.3.6. Compressor Map . . . . .	18-11
18.3.7. In Situ Bearing Maintenance . . . . .	18-11
18.3.8. Turbomachine Noise Reduction . . . . .	18-22
18.3.9. Depressurization During Deblading . . . . .	18-22
18.3.10. Welded Rotor Failure Mechanism . . . . .	18-31
18.3.11. Turbine Disk Rim Stress Studies . . . . .	18-37
18.3.12. Creep/Fatigue Interaction . . . . .	18-50
18.3.13. Turbomachine Materials Selection Review . . . . .	18-51
18.3.14. Turbomachine Development Program . . . . .	18-61
18.3.15. Turbomachine/Generator Development Schedule . . . . .	18-65
18.3.16. Turbomachine/Generator Development Cost . . . . .	18-65
18.3.17. Preliminary Evaluation of Impact of Codes and Licensing Criteria on Turbomachinery Design . . . . .	18-65
18.4. References . . . . .	18-77
19. TURBOMACHINE REMOTE MAINTENANCE . . . . .	19-1
19.1. Scope . . . . .	19-1
19.2. Summary . . . . .	19-1
19.3. Discussion . . . . .	19-2
19.3.1. Introduction . . . . .	19-2
19.3.2. Maintenance Criteria . . . . .	19-3

19.3.3. Maintenance Procedure . . . . .	19-8
19.3.4. Remote Maintenance Facility . . . . .	19-20
19.3.5. Conclusions and Recommendations . . . . .	19-31
19.4. References . . . . .	19-31
20. REMOTE MAINTENANCE FACILITY . . . . .	20-1
20.1. Scope . . . . .	20-1
20.2. Summary . . . . .	20-1
20.3. Discussion . . . . .	20-2
20.4. Reference . . . . .	20-7
21. CONTROL VALVE . . . . .	21-1
21.1. Scope . . . . .	21-1
21.2. Summary . . . . .	21-1
21.3. Discussion . . . . .	21-1
22. HEAT EXCHANGERS . . . . .	22-1
22.1. Scope . . . . .	22-1
22.2. Summary . . . . .	22-2
22.3. Discussion . . . . .	22-4
22.3.1. Heat Exchanger Design Issues Study . . . . .	22-4
22.3.2. Evaluation of Sulzer/GA Heat Exchanger Design Criteria . . . . .	22-9
22.3.3. 500-MW(e) HTGR-GT Heat Exchanger Study . . . . .	22-10
22.3.4. Alternate Heat Exchanger Design . . . . .	22-10
23. PLANT PROTECTION SYSTEM . . . . .	23-1
23.1. Scope . . . . .	23-1
23.2. Summary . . . . .	23-1
23.3. Discussion . . . . .	23-1
23.3.1. Review and Problem Areas . . . . .	23-1
23.3.2. Design . . . . .	23-2
24. PLANT CONTROL SYSTEM . . . . .	24-1
24.1. Scope . . . . .	24-1
24.2. Summary . . . . .	24-1
24.3. Discussion . . . . .	24-1
APPENDIX A: TURBOMACHINE NOISE REDUCTION . . . . .	A-

## FIGURES

3-1.	Diagram of circulating water system . . . . .	3-3
3-2.	Isothermal temperature coefficients for HEU and MEU cores .	3-5
4-1.	Plan view of PCRV top head for two-loop, 800-MW(e) HTGR-GT non-intercooled plant . . . . .	4-5
4-2.	Elevation view through PLC for two-loop, 800-MW(e) HTGR-GT non-intercooled plant . . . . .	4-7
4-3.	Elevation view through core cavity for two-loop, 800-MW(e) non-intercooled plant . . . . .	4-9
4-4.	Plan view of PCRV top head for two-loop, 800-MW(e) intercooled plant . . . . .	4-11
4-5.	Elevation view through PCI for two-loop, 800-MW(e) intercooled plant . . . . .	4-13
4-6.	Elevation view through core cavity for two-loop, 800-MW(e) intercooled plant . . . . .	4-15
4-7.	Three-loop HTGR-GT integrated design with separate turbo- machine PCRVs . . . . .	4-28
4-8.	Turbomachine PCRV prestressing . . . . .	4-29
4-9.	Isometric view of monolithic turbomachine module . . . . .	4-30
4-10.	Three-loop plant concept embodying "power block" layout approach with vertical heat exchanger . . . . .	4-32
4-11.	Two-loop plant concept embodying "power block" layout approach with vertical heat exchanger . . . . .	4-33
4-12.	Elevation view through PCRV showing "power block" concept with horizontal heat exchangers . . . . .	4-34
4-13.	Plan view of PCRV with three "power blocks" embodying horizontal heat exchangers . . . . .	4-35
4-14.	View showing details of "power block" for case with horizontal heat exchangers . . . . .	4-36
4-15.	Example of PCL liner "pattern" for precast PCRV block approach . . . . .	4-37
4-15.	Precast modular concept for circular PCRV . . . . .	4-39
4-17.	Precast modular concept for rectangular PCRV . . . . .	4-40
5-1.	Primary bypass valve actuation system . . . . .	5-3
5-2.	Control module for primary bypass valve . . . . .	5-4
6-1.	Dynamic model of HHT demonstration plant RCB/PCRV with mass point locations . . . . .	6-3
6-2.	Horizontal response spectra for 1-g OBE with PCRV support pads . . . . .	6-5

6-3.	Horizontal response spectra for 1-g OBE without PCRV support pads . . . . .	6-6
6-4.	MCOCO model of full-scale gas turbine reactor core . . . . .	6-7
6-5.	OBE horizontal response at mid-core . . . . .	6-8
6-6.	Dynamic model simulated by modified CRUNCH-2D program . . . . .	6-10
7-1.	Dose rates for separated turbine and compressor . . . . .	7-3
7-2.	Hot duct removal cask steel thicknesses . . . . .	7-5
9-1.	Fault tree showing events that could lead to PCRV overpressurization . . . . .	9-8
11-1.	Plot plan showing overall HTGR-GT plant arrangement . . . . .	11-5
12-1.	Conceptual piping and storage system for a helium inventory control system . . . . .	12-7
12-2.	Pressure loss/leakage diagram for three-loop 3000-MW(t) HTGR-GT . . . . .	12-9
12-3.	Turbine inlet temperature and system pressure variations versus change in power cost at 80% capacity factor . . . . .	12-23
12-4.	Process flow diagram for two-loop, 800-MW(e) HTGR-GT non-intercooled plant using CODER8 (Run No. H03B/H05 optimized) . . . . .	12-26
12-5.	Process flow diagram for two-loop, 800-MW(e) HTGR-GT intercooled plant using CODER7 (Run No. G03B/G04 optimized) . . . . .	12-27
12-6.	Representation of load-following cycle . . . . .	12-29
12-7.	Part-load efficiency for various control modes . . . . .	12-30
13-1.	Part-load efficiency for various plant control modes . . . . .	13-14
13-2.	Bypass valve/turbine exhaust flow mixing . . . . .	13-20
14-1.	Liner leak chase collection system . . . . .	14-7
14-2.	Core cavity liner venting system . . . . .	14-15
14-3.	Steel ring and concrete plug closure concept . . . . .	14-17
15-1.	PCRV for reference three-loop HTGR-GT plant . . . . .	15-3
15-2.	Horizontal tendon layout for PCRV bottom head . . . . .	15-7
15-3.	Three-dimensional finite element model of PCRV . . . . .	15-9
15-4.	Plan view of PCRV for two-loop, 800-MW(e) non-intercooled HTGR-GT plant . . . . .	15-11
15-5.	Plan view of PCRV top head for two-loop, 800-MW(e) intercooled HTGR-GT plant . . . . .	15-12
15-6.	PCRV for non-intercooled HTGR-GT . . . . .	15-14
15-17.	PCRV for intercooled HTGR-GT . . . . .	15-16

16-1.	Thermal barrier coverplate with integrated attachment fixture . . . . .	16-8
17-1.	Conceptual core inlet and core outlet ducts . . . . .	17-7
17-2.	Carbon-carbon/insulation washer hot duct thermal barrier concept . . . . .	17-21
17-3.	Cast coverplate hot duct thermal barrier concept . . . . .	17-23
17-4.	Castable thermal barrier coverplate . . . . .	17-25
17-5.	Castable hot duct thermal shield concept . . . . .	17-27
18-1.	400-MW(e) turbomachine assembly and installation layout . .	18-3
18-2.	Estimated secondary cooling flow distribution . . . . .	18-8
18-3.	400-MW(e) intercooled turbomachine design . . . . .	18-9
18-4.	Turbomachine compressor map high efficiencies . . . . .	18-12
18-5.	Turbomachine compressor map low efficiencies . . . . .	18-13
18-6.	Self-propelled maintenance truck . . . . .	18-14
18-7.	Removal of engine services . . . . .	18-15
18-8.	Removal of compartment cover/bearing sideplate . . . . .	18-17
18-9.	Jacking system . . . . .	18-18
18-10.	Bearing pad removal . . . . .	18-19
18-11.	Removal of shaft and thrust bearings . . . . .	18-20
18-12.	Removal of shaft coupling . . . . .	18-21
18-13.	Turbine deblading computer simulation - gross power versus time . . . . .	18-24
18-14.	Turbine deblading computer simulation - pressure versus time . . . . .	18-25
18-15.	Turbine deblading computer simulation - pressure versus time . . . . .	18-26
18-16.	Turbine deblading computer simulation - temperature versus time . . . . .	18-27
18-17.	Turbine deblading computer simulation - mass flow rate versus time . . . . .	18-28
18-18.	HTGR-GT Volume Dynamics Simulation system schematic . . . .	18-29
18-19.	Depressurization during turbine failure with 0 to 1.0 s period expanded . . . . .	18-32
18-20.	Depressurization during turbine failure . . . . .	18-33
18-21.	Rotor disk crack growth diagram . . . . .	18-35
18-22.	Ladish D6AC minimum yield strength versus temperature . . .	18-39

18-23.	Disk stress versus maximum allowable short-time rim temperature . . . . .	18-41
18-24.	Ladish D6AC stress rupture strength . . . . .	18-42
18-25.	400-MW(e) turbine section . . . . .	18-44
18-26.	Estimated secondary cooling flow distribution . . . . .	18-47
18-27.	400-MW(e) HTGR-GT turbomachine/generator development schedule . . . . .	18-66
19-1.	Turbomachine radiation level after 100-day decay . . . . .	19-6
19-2.	Turbine and compressor dose rates . . . . .	19-7
19-3.	Turbomachine - exploded view . . . . .	19-10
19-4.	First level functional flow diagram . . . . .	19-11
19-5.	Second level - repair gas turbine . . . . .	19-13
19-6.	Schematic for removing 180-deg split cases . . . . .	19-15
19-7.	Turbomachine envelope dimensions and weight . . . . .	19-19
19-8.	400-MW(e) gas turbine . . . . .	19-21
19-9.	Functional arrangement of a remote repair facility . . . . .	19-23
19-10.	Functional layout of a remote repair facility . . . . .	19-25
20-1.	Remote maintenance facility floor plan . . . . .	20-5
22-1.	Heat exchanger module arrangement with expansion joint . . . . .	22-5
22-2.	Design modification of hexagonal heat exchanger module support structure . . . . .	22-7
22-3.	GE alternate recuperator design . . . . .	22-11
22-4.	"Eggcrate" tube supports for heat exchanger module . . . . .	22-15
22-5.	GA seven-module alternate recuperator design . . . . .	22-19
22-6.	GA stayed tubesheet alternate recuperator design . . . . .	22-21
23-1.	Plant protection system instrument block diagram . . . . .	23-3
24-1.	Instrument diagram for primary bypass valve . . . . .	24-3
24-2.	Frequency response of electrohydraulic servo valve for primary bypass valve actuation system . . . . .	24-5
24-3.	Instrument diagram for plant control system . . . . .	24-7
A-1.	Estimated compressor discharge spectra for 400-MW(e) HTGR-GT . . . . .	A-9
A-2.	Estimated turbine discharge spectra for 400-MW(e) HTGR-GT . . . . .	A-10
A-3.	Estimated noise reduction potential at compressor inlet of 400-MW(e) HTGR-GT . . . . .	A-12
A-4.	Estimated noise reduction potential at turbine inlet of 400-MW(e) HTGR-GT . . . . .	A-13

TABLES

2-1.	Performance parameters for two-loop, 2000-MW(t) HTGR-GT non-intercooled reference plant . . . . .	2-3
2-2.	Performance parameters for two-loop, 2000-MW(t) HTGR-GT intercooled plant . . . . .	2-4
4-1.	Major factors related to intercooling . . . . .	4-4
4-2.	Two-loop, 400-MW(e) intercooled vs non-intercooled plant comparison . . . . .	4-18
4-3.	Additional plant complexities associated with intercooled cycle . . . . .	4-20
4-4.	Cost comparison summary for intercooled (INT) versus non-intercooled (NINT) study . . . . .	4-22
4-5.	Comparison of intercooled and non-intercooled cycle salient features . . . . .	4-23
10-1.	Unscheduled outage hours allocated to the 900-MW(e) HTGR-SC reference plant common to the HTGR-GT . . . . .	10-3
10-2.	Preliminary availability summary for three-loop non-intercooled HTGR-GT . . . . .	10-4
10-3.	Two-loop HTGR-GT availability summary . . . . .	10-5
12-1.	Parameters evaluated in primary system parameter study . . . . .	12-3
12-2.	Performance parameters for two-loop, 2000-MW(t) HTGR-GT non-intercooled reference plant . . . . .	12-4
12-3.	Performance parameters for two-loop, 2000-MW(t) HTGR-GT Intercooled plant . . . . .	12-5
12-4.	Primary coolant system pressure losses . . . . .	12-10
12-5.	Primary coolant system performance . . . . .	12-13
12-6.	Core auxiliary circulator (System 28-1) conceptual study results . . . . .	12-14
12-7.	Core auxiliary heat exchanger (System 28-2) conceptual study results . . . . .	12-14
12-8.	Core auxiliary cooling water system (System 47) conceptual study results . . . . .	12-15
12-9.	Engineering cost estimate for CACS and CACWS components . . . . .	12-16
12-10.	Anticipated transients for 3000-MW(t) HTGR-GT commercial plant . . . . .	12-28
12-11.	Plant efficiency/cost savings associated with HICS . . . . .	12-32
12-12.	Primary system pressure loss summary . . . . .	12-34
12-13.	Primary coolant system bypass/leakage flows . . . . .	12-36

13-1.	1200-MW(e) HTGR-GT reference commercial plant transient performance comparison . . . . .	13-4
13-2.	Two-loop 800-MW(e) HTGR-GT plant transient performance comparison . . . . .	13-6
13-3.	Plant conditions two days after scram . . . . .	13-12
13-4.	Primary circuit mean square pressures in one-octave bands . . . . .	13-18
14-1.	Summary comparison of warm and cold liner concepts . . . . .	14-2
16-1.	Major candidate thermal barrier metallics and design temperature limits . . . . .	16-6
18-1.	400-MW(e) turbomachine weight summary . . . . .	18-7
18-2.	HTGR-GT Volume Dynamics Simulation . . . . .	18-30
18-3.	Major parameters for reactor scram coastdown and plant loss of load transients . . . . .	18-45
18-4.	Estimated gas temperatures for coastdown initiated by	
(a)	reactor scram . . . . .	18-48
18-4.	Estimated gas temperatures for plant loss of load . . . . .	18-48
(b)		
18-5.	Updated HTGR-GT turbomachinery materials selection . . . . .	18-53
18-6.	Initial HTGR-GT turbomachinery materials selection . . . . .	18-59
18-7.	Chemical compositions of candidate materials for HTGR-GT turbomachinery . . . . .	18-60
18-8.	400-MW(e) HTGR-GT turbomachine/generator development cost . . . . .	18-73
19-1.	First level time summary for gas turbine repair outage . . . . .	19-14
19-2.	8.0 repair gas turbine - time summary . . . . .	19-17
19-3.	Tooling requirements summary . . . . .	19-27
21-1.	Valve criteria for three-loop, 400-MW(e) HTGR-GT non-intercooled reference plant . . . . .	21-2
22-1.	Recuperator concept comparison . . . . .	22-14



## 1. INTRODUCTION

This report describes the gas turbine high-temperature gas-cooled reactor (HTGR-GT) program effort funded under DOE Contract DE-AT03-76SF-70046 for the period April 1, 1979 through September 30, 1979. It reflects the shift of the major General Atomic design effort from the steam cycle HTGR (HTGR-SC) to the direct cycle HTGR-GT.

In Section 2, the systems design methods development is reviewed. This effort encompassed the development of the performance and cost optimization codes CODER7 and CODER8 as well as the modification of the RECA and ECSEL core auxiliary cooling codes to cover the HTGR-GT conditions.

Section 3 describes the system dynamics methods development related to the dynamic modeling of the HTGR-GT plant, including the functional design of the plant protection system (PPS). This effort will provide the basis for controlling design transients as well as the basis for the design of the PPS.

The alternative design studies are reviewed in Section 4. These studies addressed intercooled versus non-intercooled plants as well as advanced features which offer the potential for plant cost reduction and design simplification. As a result of the intercooled versus non-intercooled plant studies, the non-intercooled plant was selected as the reference configuration for all further design studies. This selection was made on the basis of cost, reliability, availability, and design complexity considerations.

In Section 5, the design of the bypass valve auxiliary systems is discussed. The purpose of this design effort is to establish requirements and interfaces for the auxiliary systems. Of major concern in the design of these auxiliary systems is their speed of response and reliability to ensure

that the turbomachinery does not overspeed, which could result in distraction of the turbomachinery as well as a severe primary system transient.

Section 6 describes the seismic studies conducted on the prestressed concrete reactor vessel (PCRVR), the core, and the secondary containment. All studies were based on the maximum ground acceleration for the operating basis earthquake (OBE) and the safe shutdown earthquake (SSE).

Shielding analysis and design effort is discussed in Section 7. The impact of high neutron fluxes on the materials in and adjacent to the core area is addressed. In all these areas, except the top head region, the neutron activation of materials proved to be of concern. In the top head area, material selection is based upon physical properties rather than the consideration of radiation effects.

The licensing effort is discussed in Section 8. Licensing reviews were conducted in the following areas:

1. Design requirements for components which may be relied upon for core cooling during turbomachinery coastdown.
2. Core auxiliary cooling system (CACS) design basis.
3. Precooler safety classification.
4. Safety classification of the turbomachinery shaft and shaft seal.

In addition, the initial issue of the HTGR-GT Nuclear Safety Specification was prepared, as well as suggestions for preapplication Licensing Topical Reports (LTRs).

Plant safety studies are reviewed in Section 9. The major tasks in this area are related to the development of the German Safety Criteria and the study of the pressure equilibration accident as caused by a turbomachinery

failure. In addition, the basis for the design basis depressurization accident (DBDA) and the internal pressure relief system using the bypass valves and the internal high- and low-pressure areas are reviewed.

Section 10 reviews the HTGR-GT availability studies. The conclusion from this effort is that the 90% availability goal is realizable.

Reactor turbine system/balance of plant (BOP) integration is discussed in Section 11. This effort provides the basis for all further reference plant BOP design by the architect-engineer.

Section 12 covers the systems design effort. This effort is related to overall system studies including technical issues review, cycle selection, helium inventory control economic impact, pressure drop and bypass studies, ambient air efficiency impact, and CACS studies. The results from this effort form the basis for work by the component designers.

The system dynamic effort is described in Section 13. The purpose of this task is to analyze the plant transient performance, provide component designers with the controlling plant transients, and develop the basis for the PPS and the plant control system (PCS). In addition, plant acoustic aspects, natural convection, and flow mixing are studied.

Sections 14, 15, 16, and 17 cover the structural engineering effort on the liners, penetrations, and closures, the PCRV, the thermal barrier, and the reactor internals, respectively. This work encompasses studies of the warm liner concept, liner leak detection systems, closure, PCRV for inter-cooled and non-intercooled plants, thermal barrier and hot duct, and reactor internals related to the U.S. and HHT plants.

The United Technologies Corporation (UTC) effort in the development of the turbomachinery for the HTGR-GT plant is described in Section 18. Sections 19 and 20 describe GA studies related to remote maintenance tooling and facilities for the disassembly and reassembly of a contaminated turbo-machine.

The bypass control valve development effort is reviewed in Section 21. This task addresses the trim, attemperation, primary bypass, and safety valve functional requirements. The task is conducted in conjunction with the valve auxiliary system development discussed in Section 5.

Section 22 covers the heat exchanger development effort by Combustion Engineering (CE) under subcontract to GA. This task is primarily aimed at the resolution of design issues which had been identified as a result of a detailed review of the heat exchanger designs developed in FY-78.

Sections 23 and 24 describe the effort on the PPS and the PCS. This effort was small because of funding limitations and as a result addressed only the bypass control valve controls and the development of design issues to be resolved in the future.

## 2. SYSTEMS DESIGN METHODS DEVELOPMENT (261002)

### 2.1. SCOPE

The purpose of this task in FY-79 was to develop optimization and design evaluation computer programs and to modify CACS analysis codes for HTGR-GT conditions.

### 2.2. SUMMARY

Two cost optimization and design evaluation computer programs, CODER7 and CODER8, were developed. In addition, two core auxiliary cooling system (CACS) analysis codes, RECA3/GT and ECSEL8, were modified for HTGR-GT use.

#### 2.2.1. Computer Program CODER

Development of CODER program versions for the two-loop, 2000-MW(t) intercooled plant (CODER7) and the two-loop, 2000-MW(t) non-intercooled plant (CODER8) was completed in FY-79. The present versions of these programs are based on previous versions of the same code for non-intercooled and intercooled designs with major modifications in the prestressed concrete reactor vessel (PCRVR), thermal barrier area, precooler cost, and duct sizing/pressure drop algorithms. Additional algorithms were developed and added for wet/dry as well as all-dry cooling towers. The base case cost subroutine was generally updated, and a new design data base was generated for the remainder of the program subroutines, such as turbomachine performance and the containment/balance of plant (BOP). Many input/output formats were expanded and updated, including the addition of a plot package facilitating rapid visualization of cost versus parameter sensitivities.

Tables 2-1 and 2-2 give the performance parameters for the reference non-intercooled and intercooled plants, respectively. These data, which were generated by component specialists and cost estimators, serve as the reference point for further evaluations. As shown in the tables, plant efficiency is 38.0% for the two-loop non-intercooled design compared with 41.6% for the intercooled design.

#### 2.2.2. Computer Program RECA3/GT

An HTGR-GT version of RECA, the primary core cooling evaluation code, was prepared and is identified as RECA3/GT. It is generally a merger of RECA3 and REALLY (the code used to evaluate transients in the gas turbine). This code has not been checked out to any significant degree and is not considered fully operational. Work is in progress to complete the operational checkout and to apply RECA3/GT to the initial 800-MW(e) HTGR-GT two-loop plant design to evaluate its readiness.

#### 2.2.3. Computer Program ECSEL8

The computer program ECSEL8 is used to select cost-optimized CACS configuration and sizing in the preliminary design phase. Because it is expected that such analyses will frequently be required in the HTGR-GT program in the near future, this code was the subject of significant updating and improvement under the Generic Program. Changes were also made to the code under the HTGR-GT Project.

### 2.3. DISCUSSION

A shift in emphasis occurred during code development from the three-loop 3000-MW(t) plant toward a two-loop 2000-MW(t) plant. This shift in emphasis and the associated configuration differences resulted in the requirement to perform a major configuration update in CODER. The configuration was updated to provide a reference case closer to the points of interest in system evaluations and to provide greater confidence in the

TABLE 2-1  
 PERFORMANCE PARAMETERS FOR TWO-LOOP, 2000-MW(t) HTGR-GT  
 NON-INTERCOOLED REFERENCE PLANT

Conditions: No intercooling; no blade cooling for turbomachine; standard  
 day ambient air temperature; CODER8 run H01.

Reactor rating	2000 MW(t)
Number of loops	2
Liner option	Conventional
Compressor pressure ratio	2.5
Compressor flow, M	586.27 kg/s (4,653,000 lb/h)
HP compressor outlet pressure	7.929 MPa (1150 psia)
Reactor inlet temperature	507°C (945°F)
Reactor outlet temperature	850°C (1562°F)
Turbine inlet temperature	849°C (1560°F)
Compressor inlet temperature	26.7°C (80.1°F)
Minimum cycle helium temperature	26.1°C (79.0°F)
Primary system pressure loss	529 kPa (76.7 psi)
Recuperator high-pressure $\Delta P$	75.83 kPa (11.0 psi)
Core $\Delta P$	114.4 kPa (16.6 psi)
Turbine $\Delta P$	4226 kPa (613 psi)
Recuperator low-pressure $\Delta P$	103.4 kPa (15.5 psi)
Precooler $\Delta P$	38.6 kPa (5.6 psi)
Compressor pressure rise	4757 kPa (690 psi)
Recuperator effectiveness	0.898
Turbine isentropic efficiency	91.8%
Compressor isentropic efficiency	89.8%
Generator efficiency	98.8%
Turbine blade cooling flow, M	0%
Turbine disk cooling flow, M	2.96%
Ambient air temperature	15°C (59°F)
Cooling water temperature	20.6°C (69°F)
Precooler outlet water temperature	132°C (270°F)
Heat losses	11.87 MW(t)
Auxiliary power	8.0 MW(e)
Plant efficiency	38.0%
Net electrical output	759 MW(e)

TABLE 2-2  
 PERFORMANCE PARAMETERS FOR TWO-LOOP, 2000-MW(t)  
 HTGR-GT INTERCOOLED PLANT

Conditions: Intercooling; no blade cooling for turbomachine; standard day ambient air temperature; CODER7 run G01.

Reactor rating	2000 MW(t)
Number of loops	2
Liner option	Conventional
Compressor pressure ratio, each	1.75
Compressor pressure ratio, overall	3.06
Compressor flow, M	501.72 kg/s (3,982,000 lb/h)
HP compressor outlet pressure	7.874 MPa (1142 psia)
Reactor inlet temperature	449.4°C (841°F)
Reactor outlet temperature	850.0°C (1562°F)
Turbine inlet temperature	848.9°C (1560°F)
LP compressor inlet temperature	26.4°C (79.6°F)
HP compressor inlet temperature	26.6°C (80.0°F)
Minimum cycle helium temperature	26.1°C (79.0°F)
Primary system pressure loss	499.8 kPa (72.5 psi)
Recuperator high-pressure $\Delta P$	40.67 kPa (5.9 psi)
Core $\Delta P$	86.2 kPa (12.5 psi)
Turbine $\Delta P$	4833 kPa (701 psi)
Recuperator low-pressure $\Delta P$	88.93 kPa (12.9 psi)
Precooler $\Delta P$	47.6 kPa (6.9 psi)
LP compressor pressure rise	1958 kPa (284 psi)
HP compressor pressure rise	3371 kPa (489 psi)
Recuperator effectiveness	0.898
Turbine isentropic efficiency	92.2%
HP compressor isentropic efficiency	90.2%
LP compressor isentropic efficiency	90.8%
Generator efficiency	98.8%
Turbine blade cooling flow, M	0%
Turbine disk cooling flow, M	2.96%
Ambient air temperature	15.0°C (59°F)
Cooling water temperature	20.6°C (69°F)
Precooler outlet water temperature	86.9°C (188.5°F)
Intercooler outlet water temperature	65.6°C (150.0°F)
Heat losses	9.93 MW(t)
Auxiliary power	8.0 MW(e)
Plant efficiency	41.6%
Net electrical output	832 MW(e)



sensitivity results developed through the application of CODER. The reference case itself is consistent with major component descriptions as defined by engineering evaluations conducted by the component specialists.

CODER7 is based on an amalgamation of CODER6 [three-loop, 3000-MW(t) non-intercooled configuration version] and CODER2 [two-loop, 3000-MW(t) intercooled configuration version]. A new PCRV model based on Figs. 4-4 through 4-6 has been incorporated in CODER7. CODER8 is based on CODER6 and also includes a new PCRV model, based on Figs. 4-1 through 4-3.

Thermal barrier algorithms and base case areas were developed from the reference intercooled design drawings and included new thermal barrier zones to cover intercooler-related equipment and ducts. Thermal barrier areas for the non-intercooled design (CODER8) were derived from the three-loop design data included in CODER6.

Duct pressure drop algorithms were upgraded for the intercooled design, and the number of pressure drop nodes was increased to account for the intercooler ducts and heat exchangers. For both CODER7 and CODER8, all heat exchanger algorithms were modified to enable more accurate pressure loss calculations and ensure consistency with recent heat exchanger pressure loss estimates.

Printout formats were upgraded to enhance usability and tractability of calculational results. Also, cost and design data were upgraded to be consistent with the latest information available. A revision to the pre-cooler cost algorithm was made to reflect results which showed that pre-cooler/intercooler costs are labor intensive and therefore primarily dependent on tube quantity rather than surface area.

A plot routine was integrated into CODER to allow automatic plotting of cost sensitivity results.

In CODER7 a new subroutine named HELVOL was added to handle PCRV calculations related to concrete, rebar, prestressing, liner, and helium quantities required by cost routines. Also, the automated multiparameter optimization feature in CODER7 and CODER8 was made operational.

General Atomic is collaborating with United Engineers and Constructors (UE&C) for the purpose of providing GA with the capability to size, cost, and predict the performance of HTGR-GT power plants with different cooling tower arrangements. UE&C has provided GA with sizing, cost, and performance data for all-dry natural draft cooling tower arrangements and for wet/dry cooling tower arrangements for both the non-intercooled and the intercooled HTGR-GT plant configurations. General Atomic has developed cooling tower sizing and cost models for the above-mentioned tower arrangements for use with the cost evaluation computer code CODER. General Atomic has also developed a performance model for the all-dry natural draft cooling tower arrangements for the non-intercooled plant configuration to be used with the performance evaluation code POPOFF. The performance models for the wet/dry tower arrangements have not been developed for either the non-intercooled or the intercooled plant configuration.

The sizing and cost cooling tower models are based on standard linear regression techniques and the UE&C sizing and cost data. An exception is the intermediate heat exchanger of the wet/dry tower system. The sizing of this equipment is based on first-principle heat exchanger sizing techniques, and the cost is based on the weights of the shell and tube materials. These models have been added to the cost evaluation code CODER and have been tested. The inputs to the models are tower approach temperature, tower range, heat rejected, and design ambient temperature (dry bulb). Additional inputs for the wet/dry tower arrangement are wet bulb temperature and dryness fraction. The outputs are cost and tower sizing information such as height, heat transfer surface area, etc. The sizing information is the input to the performance models.

The performance model for the all-dry natural draft cooling tower arrangement is based on applicable basic engineering principles and the sizing information from the sizing and cost models. The output of this model is the pre-cooler inlet water temperature, which ultimately affects total plant output. This model has been added to the performance code POPOFF, and it has been tested.

The RECA3 computer code has been updated to permit the user to simulate, during core cooling transients, the flow leak paths around the gas turbine main loops as well as the CACS. Each transient simulated using the RECA3 computer code may, by proper card input, be divided into three time periods. The first period corresponds to the time following a trip when the core is cooled by the spindown of the turbomachinery. The second period of the transient simulation assumes no forced circulation cooling to the core, while the third and last period covers the time when the core is cooled by CACS operation. The conditions of the primary and/or plant systems during each of these time periods may be input into this updated RECA3 program from the HTGR-GT transient performance code. During the first period of cooling, the thermal conditions of the primary system, in the form of core inlet flow and temperature, core power, and PCRV pressure histories, may be read from a file previously created from the REALY2 system program. In the second no forced cooling period, the primary system parameters defined at the end of the first period are assumed to remain constant throughout this time. Finally, at the beginning of the third period of simulation (the time of forced CACS cooling), a complete model of the gas turbine loops along with their corresponding flow and temperature conditions can be read into the RECA program from another file created from the REALY2 systems program.

ECSEL sizes the major components of both the reactor turbine system (RTS) and BOP portions of the CACS for given sets of input data. Components sized are the core auxiliary heat exchanger (CAHE), air blast heat

exchanger (ABHX) (i.e., auxiliary loop cooler) and its fans, auxiliary primary coolant circulator, core auxiliary cooling water system (CACWS) pump, CACWS pipe, etc. The sizing of the CACS is based upon the iterative solution to several simultaneous equations which model the heat exchange and fluid flow process in the three coolant loops (i.e., primary coolant, CACWS, and air - the ultimate heat sink) at three separate design points. These three design points are the heat balances at the points of time in peak core temperature in the following three CACS design basis transients:

1. Pressurized core cooldown with either helium or helium with moisture as the primary coolant.
2. Depressurized core cooldown with pure helium as the primary coolant.
3. The design basis depressurization accident (DBDA), depressurized cooldown with air added to the helium.

ECSELS, the present program version, has the following improvements:

1. The water circuit is modeled as having constant volumetric flow in all three design point cases, unlike the former model, which had constant mass flow. (Output can now be directly transcribed to the piping and instrumentation diagram.)
2. The moisture factor formerly built into pressurized cooldown calculations as an input option and the molar fraction of  $H_2O$  can be specified as input. Calculations of primary coolant properties with (or without) moisture addition were entirely revised.

3. The molecular weight at the DBDA design point is likewise now an input variable. This feature also makes use of the revised primary coolant property calculation method.
4. Core flow bypasses are now input variables, differing for pressurized or depressurized cooldown.
5. The number of CACS loops was added as an input, rather than a built-in, variable, with different values for pressurized and depressurized cooldown.

### 3. SYSTEM DYNAMICS METHODS DEVELOPMENT (261003)

#### 3.1. SCOPE

The purpose of this task in FY-79 was to develop system dynamics models for HTGR-GT transient analyses and control/plant protection system (PPS) functional design.

#### 3.2. SUMMARY

The plant dynamics code REALY2 was subjected to general maintenance via improvement of input, output, and storage management. Specific developments included development of a secondary system [circulating water system (CWS)] model and development of the new reference two-loop, 800-MW(e) HTGR-GT, medium-enriched uranium (MEU) fueled plant.

#### 3.3. DISCUSSION

##### 3.3.1. CWS/Precooler

A newly developed model of the CWS will allow better utilization of REALY2 in support of HTGR-GT PPS and plant control system (PCS) design efforts. Combined with changes in REALY2 subroutines, the new model provides a reasonable simulation of precooler and CWS transients such as pump or tower shutdown, thereby improving the realism of the gas turbine transient model by simulating the CWS interaction and increasing the number of secondary system transients which may be studied in PPS and PCS analysis work.

The new model is called CWS DYN. CWS DYN can be used with combinations of heat exchanger systems and dry cooling towers. Single or multiple dry cooling tower arrangements can be represented. The geometry of the towers, piping, and pumping is easily described by design input variables. The subroutine is currently limited to non-boiling secondary systems.

The test model and current input were based on the twin-tower CWS arrangement shown in Fig. 3-1. Since the available data for the CWS predate the reference commercial plant precooler design, it was necessary to revise the CWS design and make it compatible with the currently planned 132°C (270°F) precooler outlet temperature. After reviewing the problem, it was decided to use the water flow velocities developed in 1976 for a CWS optimization study. Similarly, the cooling tower has been updated to the current conditions of precooler discharge.

The tower "draft effect" provides the air velocity ( $V_1$ ) at the tower heat exchanger. The tower heat transfer is therefore a function of  $V_1$ . Since there is an implicative use of  $V_1$  in the solution for tower exit air temperature, water temperatures, and tower heat-exchanger heat flux, an iterative solution for  $V_1$  has been formulated.

A rough assessment of CWS time constants was made prior to creating the model. The predominant dynamic effect came from the cooling water circuit time, which tends to delay the propagation of precooler temperature change to the tower and vice versa. The long transient delay through the approximately 975 m (3200 ft) of CWS piping and tower necessitated adoption of a slug-flow subroutine.

Several slug-flow codes were investigated. However, none of the slug-flow routines present a convenient way of allowing for boiling in the precooler to interact with the CWS simulation. Therefore, it was decided to postpone the modeling required to cover boiling events. The studies may be tentatively limited for this reason. The limitations would affect improbable events involving massive failure of precooler or CWS piping.

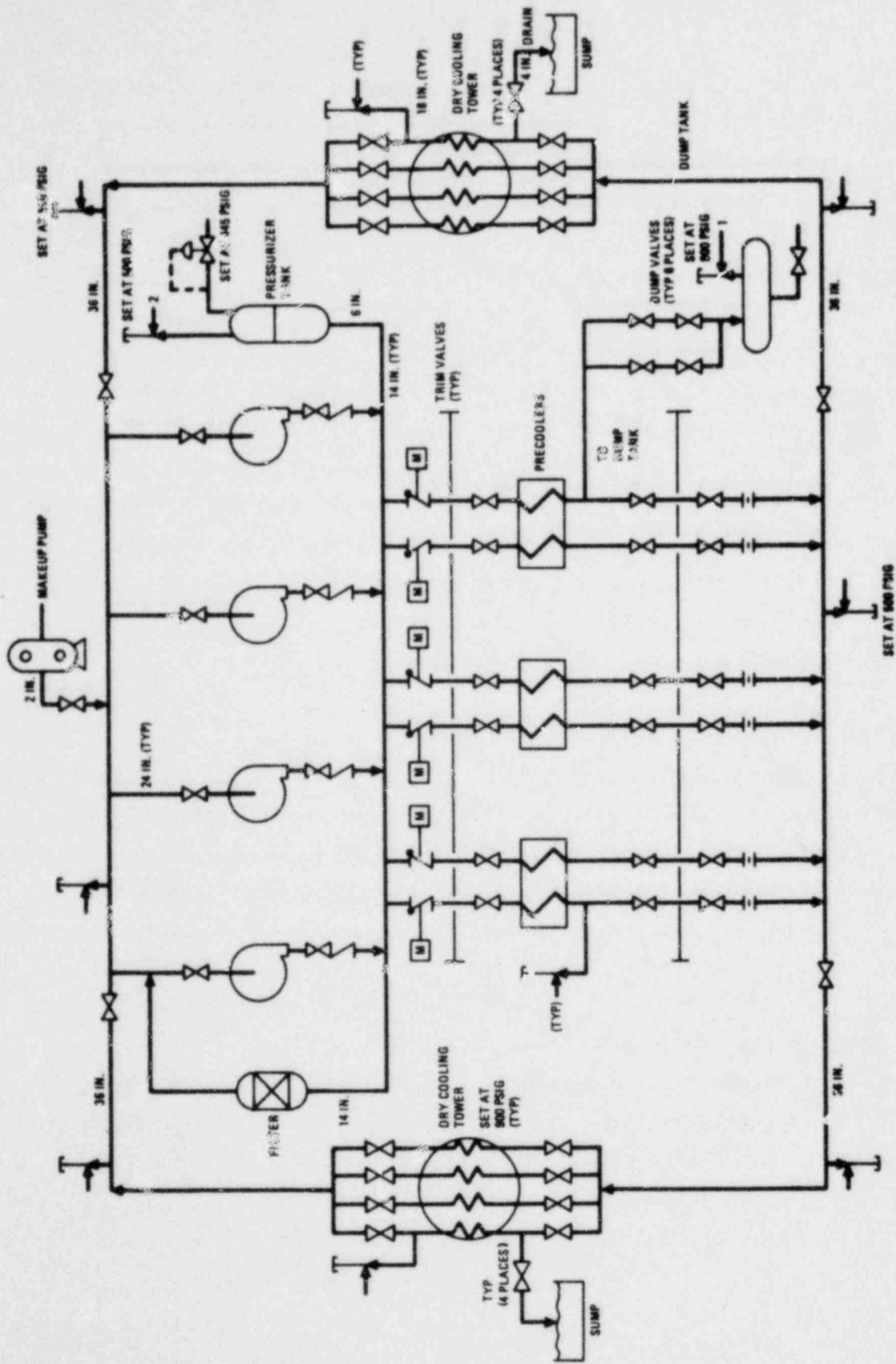


Fig. 3-1. Diagram of circulating water system



There are additional capabilities to initiate transients which could originate within the CWS. For example, the pumping capacity can be increased or decreased by changing bypass flow rates, by dropping pumps, or by activating a standby pump. In addition, cooling tower flow path geometry can be varied to simulate closing off tower heat exchanger modules. These capabilities have been tested and function as expected.

### 3.3.2. Preliminary Two-Loop, 800-MW(e) Plant Model

The simulation capability of the REALY2 code was updated by the addition of a preliminary model of the two-loop, 800-MW(e) HTGR-GT plant. This model contains a new core layout with a core power density of  $6.6 \text{ W/cm}^3$  and a 4-yr MEU/Th fuel cycle. Owing to the conceptual nature of the core design, axial power distribution, radial power distribution, and core flow distribution were assumed to be the same for this core as for the core of the 1200-MW(e) plant.

The use of an MEU/Th fuel cycle required remodeling of the reactor kinetics and the temperature coefficients. As shown in Fig. 3-2, which compares isothermal temperature coefficients for highly enriched uranium (HEU) and MEU cores, the contribution of Doppler broadening of absorbing resonances and spectral hardening to the temperature coefficients greatly affects the core power level as a function of coolant temperature in the normal operation range of the HTGR-GT.

Owing to the preliminary state of the 800-MW(e) HTGR-GT plant layout, loop flow requirements, loop geometries, and loop volumes were assumed to be the same for this model as for the 1200-MW(e) HTGR-GT, since the loop power rating will likely remain close if not the same for the two plant designs.

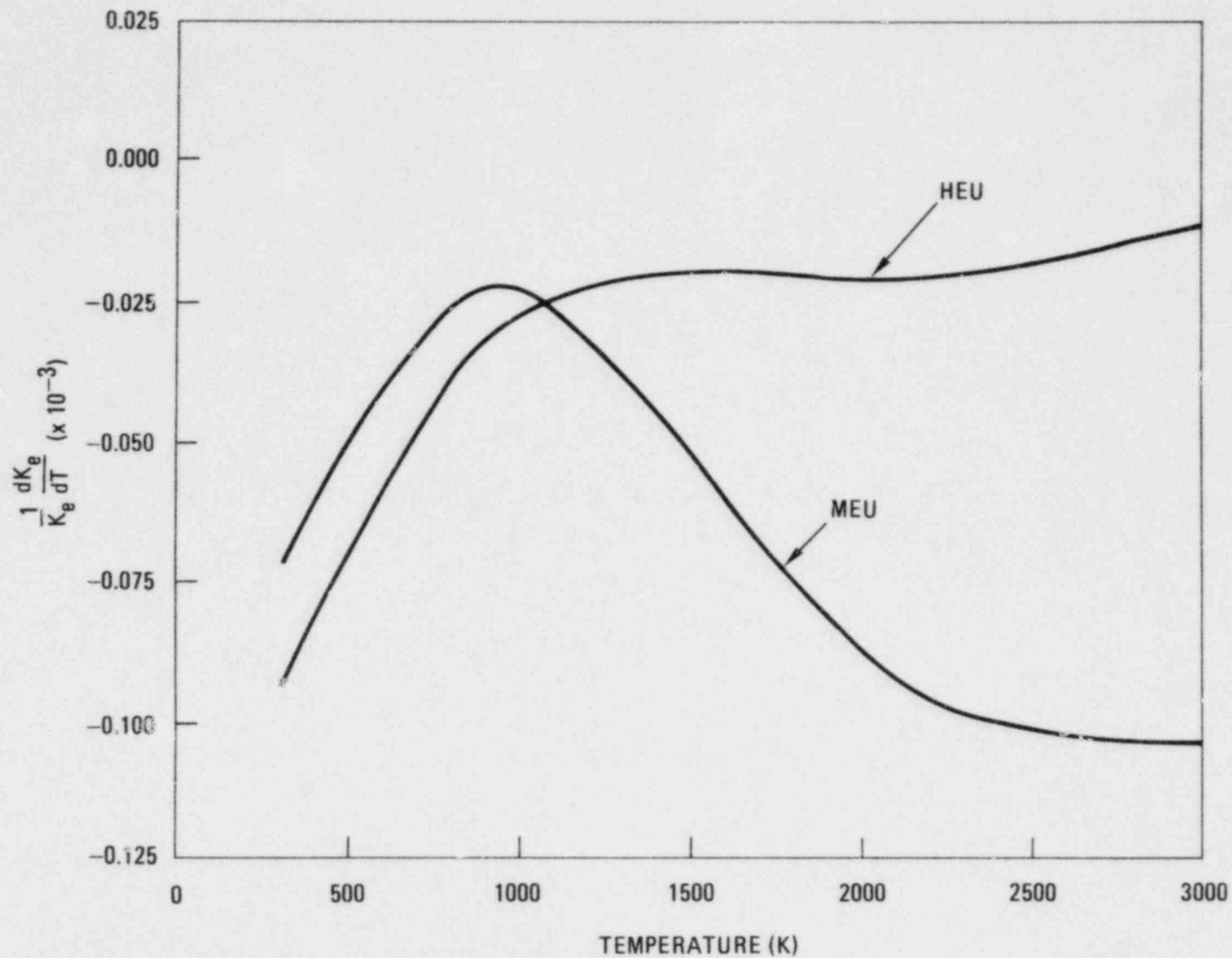


Fig. 3-2. Isothermal temperature coefficients for HEU and MEU cores

#### 4. ALTERNATE DESIGN (630101)

##### 4.1. SCOPE

The purpose of this task in FY-79 was to perform an intercooled versus non-intercooled plant study and advanced features studies.

##### 4.2. SUMMARY

Two major studies were conducted in which the efforts of the GA Resource and subcontractor organizations were integrated. The first was the intercooled versus the non-intercooled HTGR-GT plant study; and the second consisted of advanced features studies, which were conducted to identify advanced plant features having a significant impact on cost, construction time, plant simplicity, plant maintainability, and/or plant efficiency.

In the intercooled versus non-intercooled study, the following key areas were addressed:

1. Systems analysis.
2. Plant layout.
3. Power conversion loop (PCL) components.
4. Assessment of relative plant reliability/operability, maintenance, and ISI.
5. Plant cost.

Plant efficiencies were calculated at 38.0% for the non-intercooled plant and 41.6% for the intercooled plant. This efficiency difference did not manifest itself in a significant power generation cost savings. Based on this result and the greater degree of complexity of the intercooled plant, the non-intercooled plant was recommended as the reference configuration for further design efforts.

In the advanced design studies, several concepts were identified which have the potential for reduced plant cost. Essentially, the approaches involved modularization of the PCRV to permit construction of critical path items in parallel. These concepts will continue to be pursued and incorporated into the reference design when they have progressed to a more advanced level of maturity.

#### 4.3. DISCUSSION

##### 4.3.1. Intercooled Versus Non-intercooled Plant Study

4.3.1.1. Introduction. In the HTGR-GT plant studies performed by GA over the last few years, there has been a strong motivation to use the non-intercooled cycle for the following reasons: (1) plant simplicity in both turbomachine and primary system and (2) high reject temperature for economic dry cooling and optional bottoming cycle. In Europe, on the other hand, the intercooled cycle has always been favored because of (1) its higher efficiency, (2) the fact that reject water temperature is well suited to district heating, and (3) a carry-over from the European fossil-fired closed cycle gas turbine (CCGT) plants, which have all been intercooled.

In any compression process involving a multi-stage system, cooling the gas between the stages reduces the compression work, and in the case of the CCGT the plant efficiency is increased by virtue of the higher net turbine

output. Periodically since initiation of HTGR-GT studies in 1971, performance estimates have been carried out revealing an efficiency gain of 2 to 3 percentage points for the intercooled cycle. However, with emphasis early in the program on simplicity, it was felt that for an integrated HTGR-GT plant concept, the addition of yet another heat exchanger in the reactor pressure vessel, together with a more complicated turbomachine and more difficult gas flow paths, resulted in an overall plant of unwarranted complexity. Accordingly, while an efficiency gain was projected, plant designs based on the intercooled cycle were not pursued because of the complexity element, although the major factors relating to intercooling were known (Table 4-1).

In 1979, a study was initiated to evaluate the intercooled cycle from the design, performance, and economics standpoints. Details of the intercooled and non-intercooled plants, both based on two 1000-MW(t) loops, are outlined below. Both plants are based on cycle parameter selection for minimum power generation costs. The various plant technical, economic, and operability endeavors were directed toward establishing a technology data bank from which a rational decision could be made regarding the selection of the thermodynamic cycle. The work done in various disciplines leading to the recommendation of the thermodynamic cycle is documented in this section of the present report.

4.3.1.2. Plant Layout Configuration Studies. The bases for the comparison of an intercooled and a non-intercooled cycle were two plant concepts, both embodying two 1000-MW(t) power conversion loops (PCLs). For the non-intercooled variant, a plan view of the PCRV is shown in Fig. 4-1 and elevation views through the PCL and the core cavity are shown in Figs. 4-2 and 4-3, respectively. Corresponding conceptual layout views for the intercooled plant are shown in Figs. 4-4, 4-5, and 4-6.

TABLE 4-1  
MAJOR FACTORS RELATED TO INTERCOOLING

---

Non-Intercooled Plant

1. Simpler turbomachine (shorter rotor, fewer duct connections).
2. Simpler gas flow paths and primary system layout.
3. Improved availability and reliability resulting from less complex system.
4. High reject temperature well suited for cogeneration (i.e., binary cycle, process steam, district heating, etc.).
5. Reduced plant construction time (simpler PCRV).
6. Reduced complexity and risk.

Intercooled Plant

1. Increased cycle thermodynamic efficiency.
  2. Reduced helium mass flow rate (i.e., smaller components).
  3. Source of cooler high-pressure gas available for cavity liner cooling.
  4. Reduced core inlet gas temperature.
  5. Possible use of additional water-to-helium heat exchanger (intercooler) for decay heat removal.
  6. Heat rejection split between two water-to-helium exchangers (pre-cooler and intercooler), resulting in smaller unit assemblies.
  7. Utilization of European experience with small fossil-fired CCGTs.
  8. Water outlet temperature well suited for district heating.
  9. Additional maintenance requirements.
  10. Increased plant capital cost.
  11. Additional source of water ingress to primary system.
-



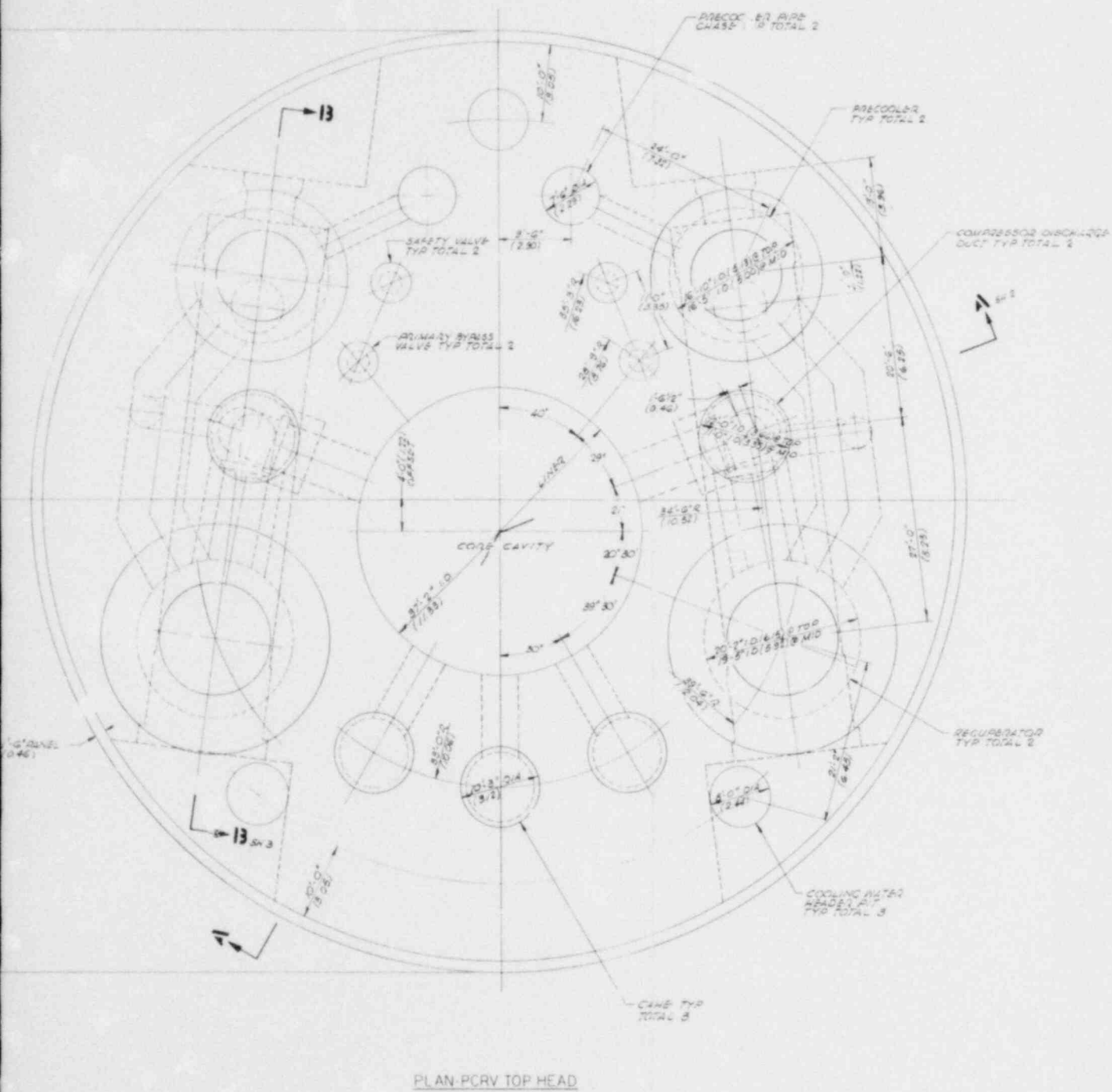


Fig. 4-1. Plan view of PCRV top head for two-loop, 800-MW(e) HTGR-GT non-intercooled plant



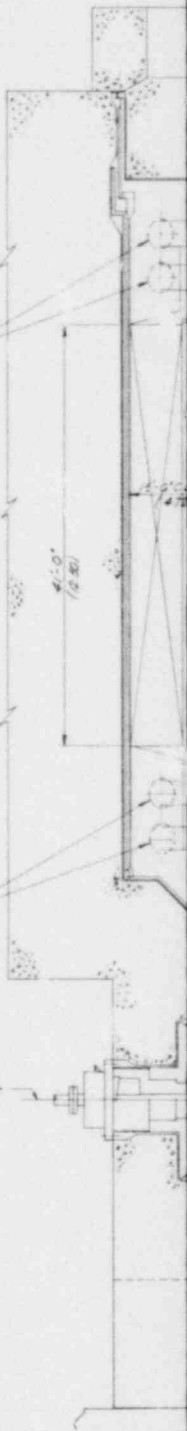
AIR COOLER

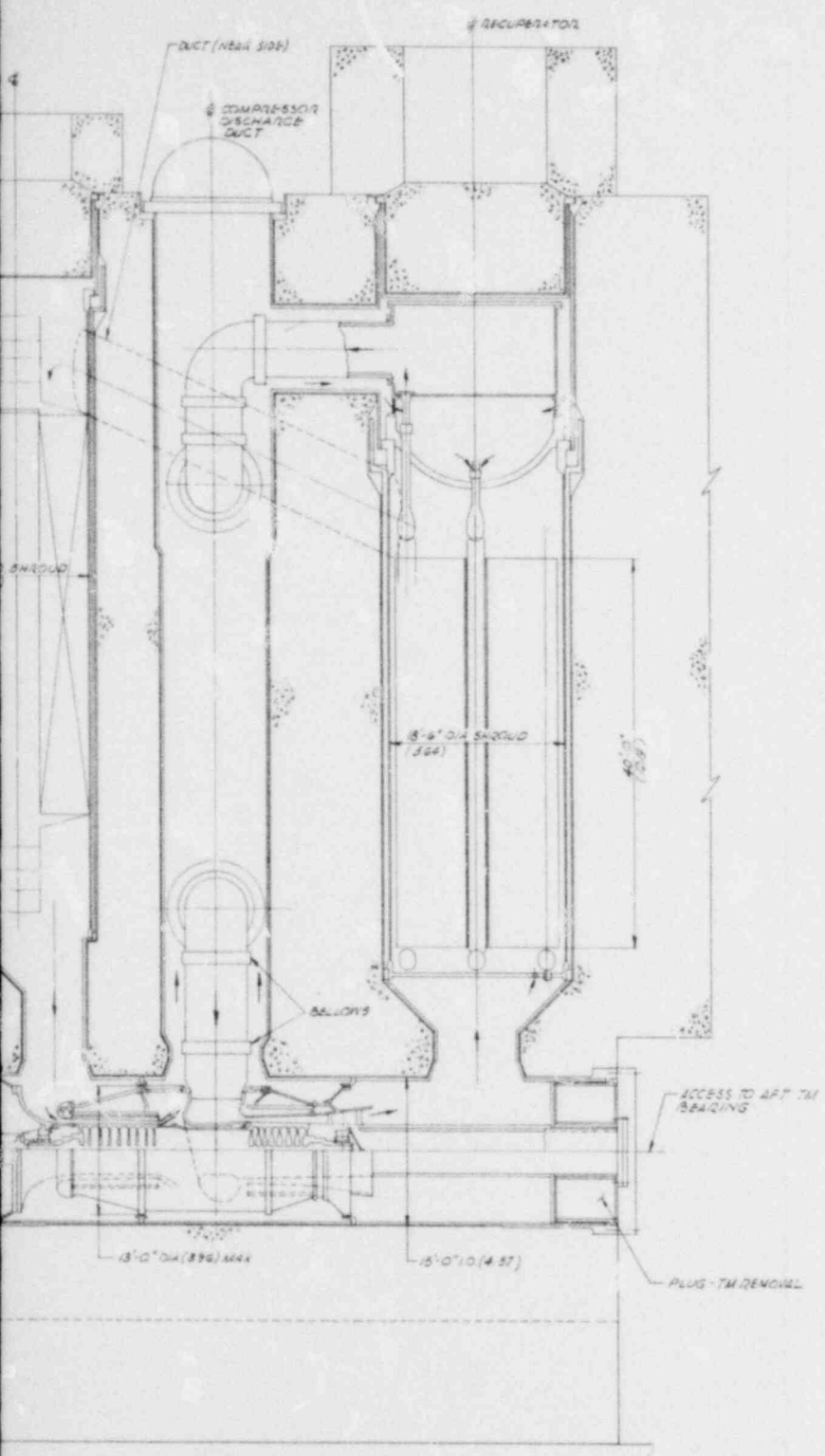
WATER LINES TO PIPE  
CHASE (FAR SIDE)

4'-0"  
(F. 80)

WATER LINES TO PIPE  
CHASE (FAR SIDE)

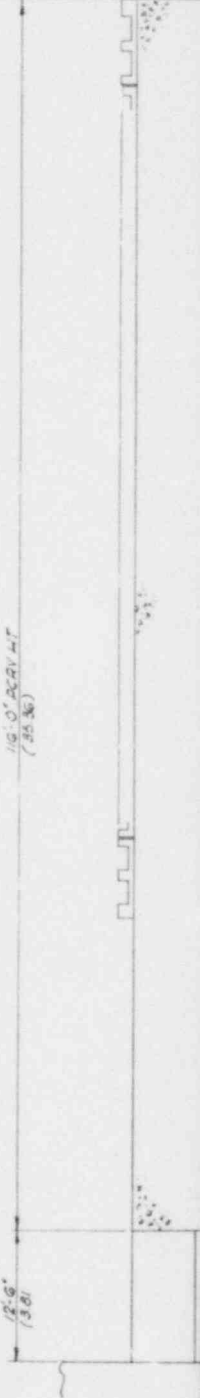
6 TURBOMACHINE





SECTION 13 - 13 SH1

Fig. 4-2. Elevation view through PLC for two-loop, 800-MW(e) HTGR-GT non-intercooled plant



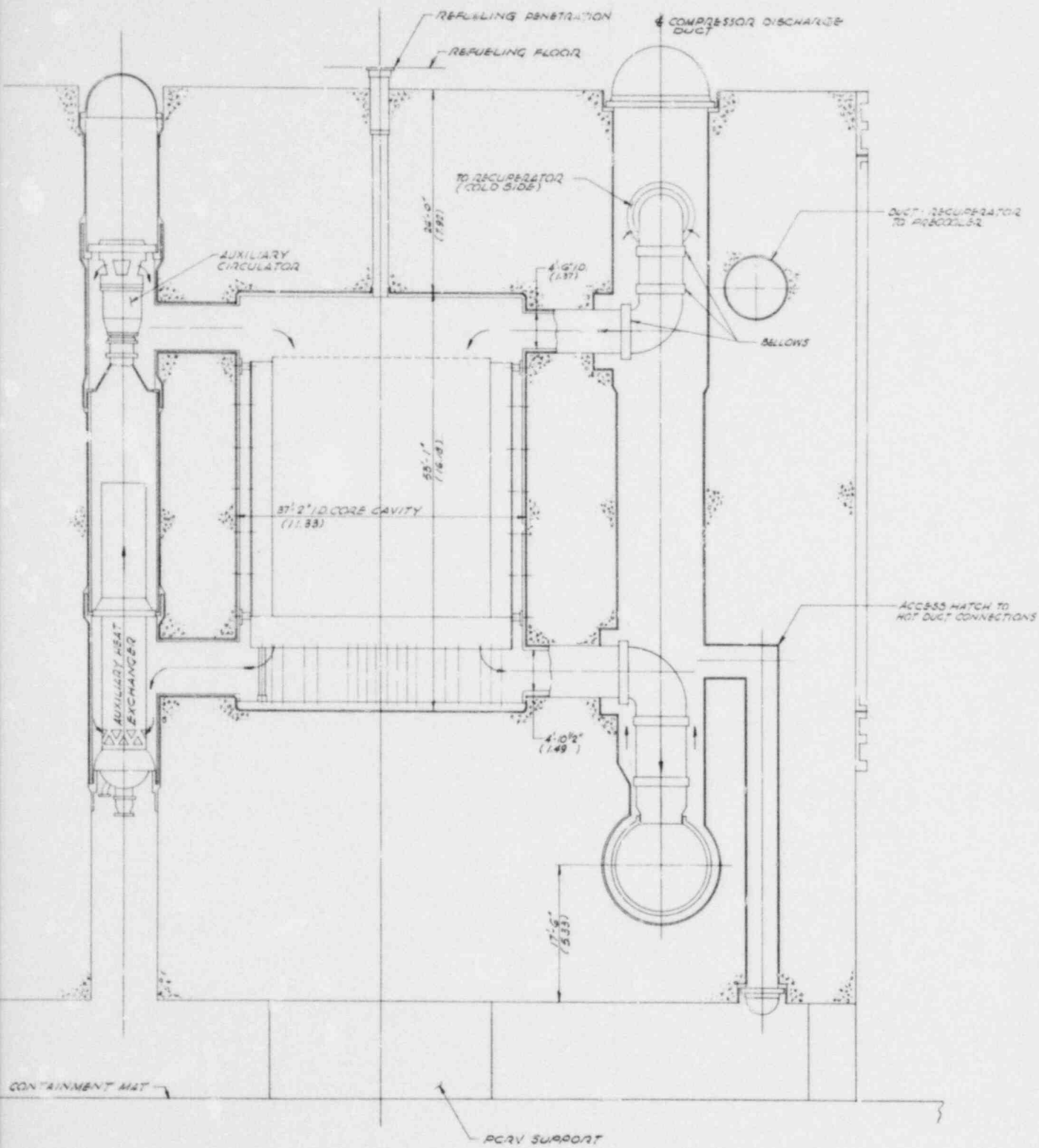
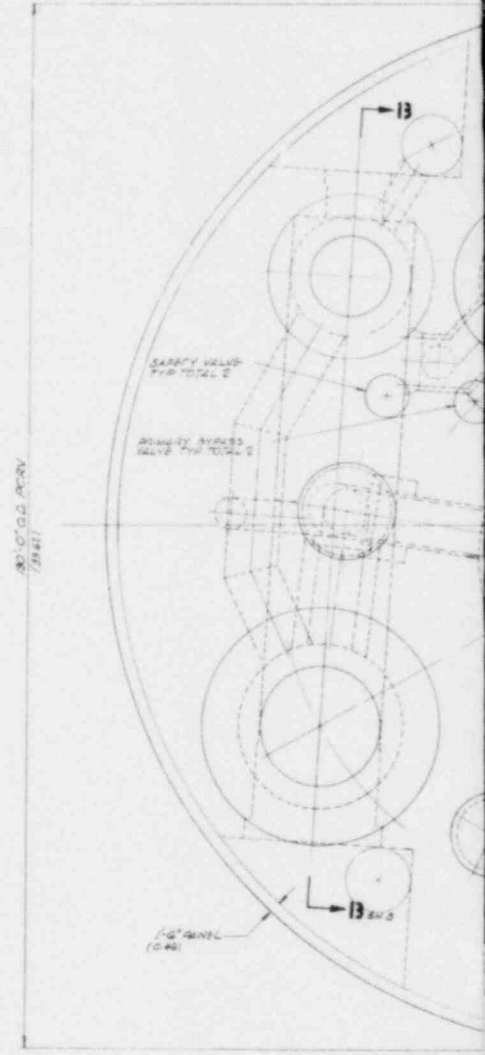


Fig. 4-3. Elevation view through core cavity for two-loop, 800-MW(e) non-intercooled plant



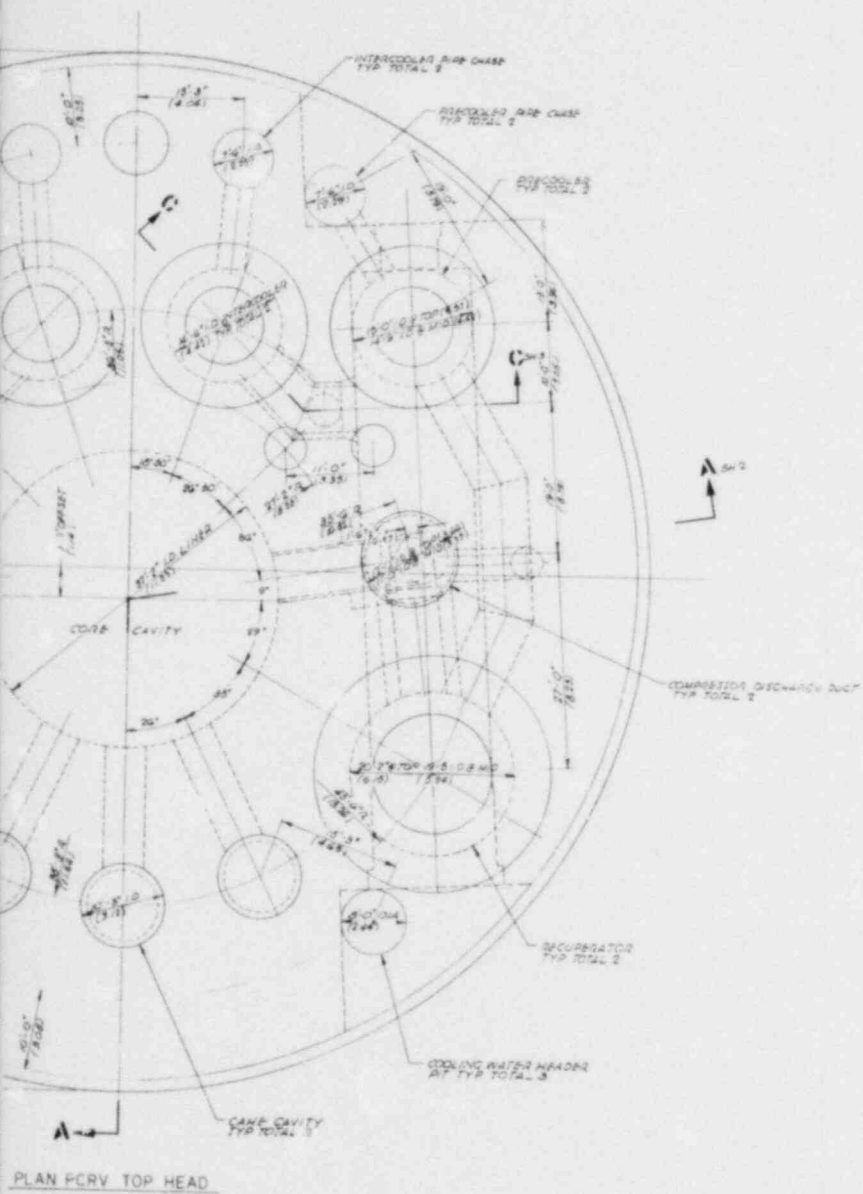
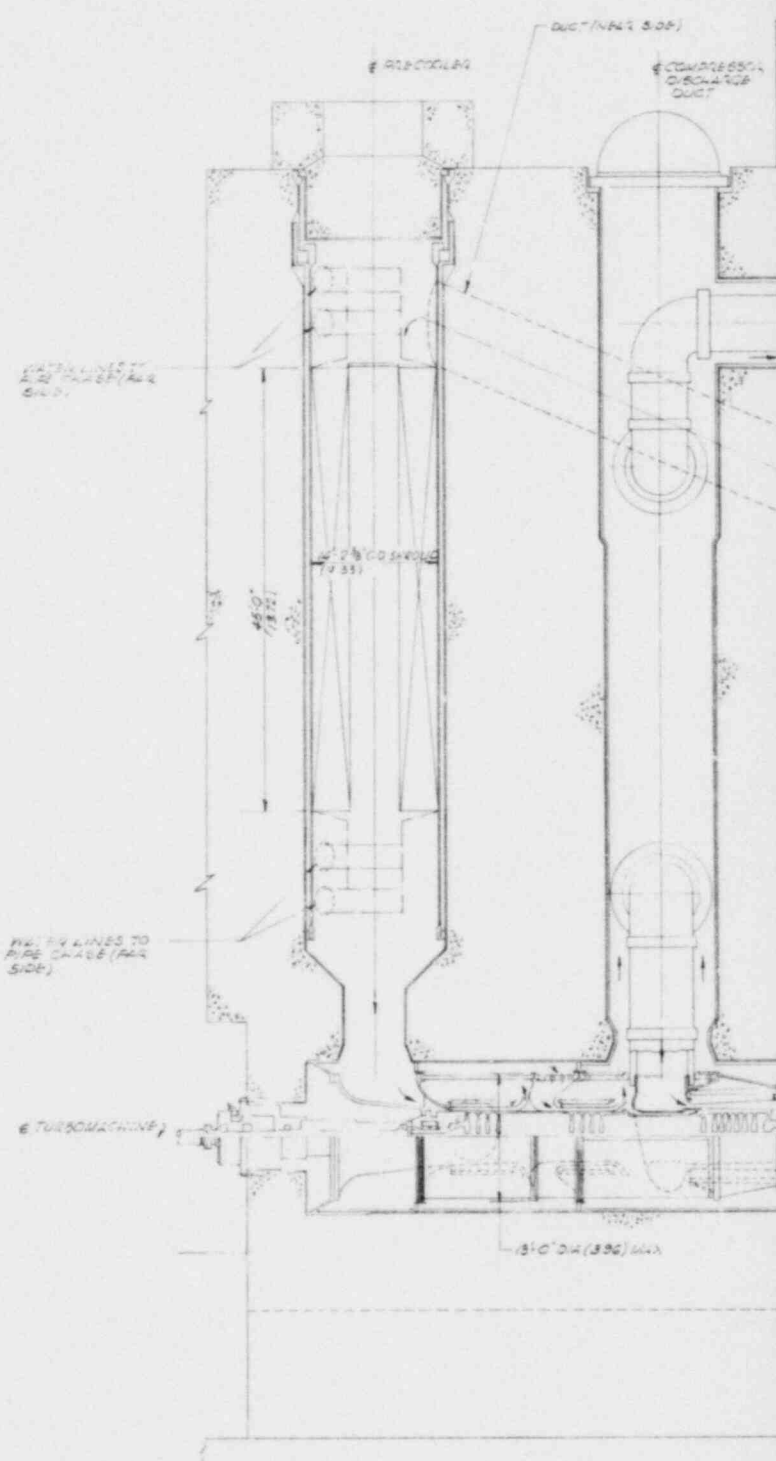


Fig. 4-4. Plan view of PCRV top head  
for two-loop, 800-MW(e)  
intercooled plant



SECTION 13 - 13 SH 1

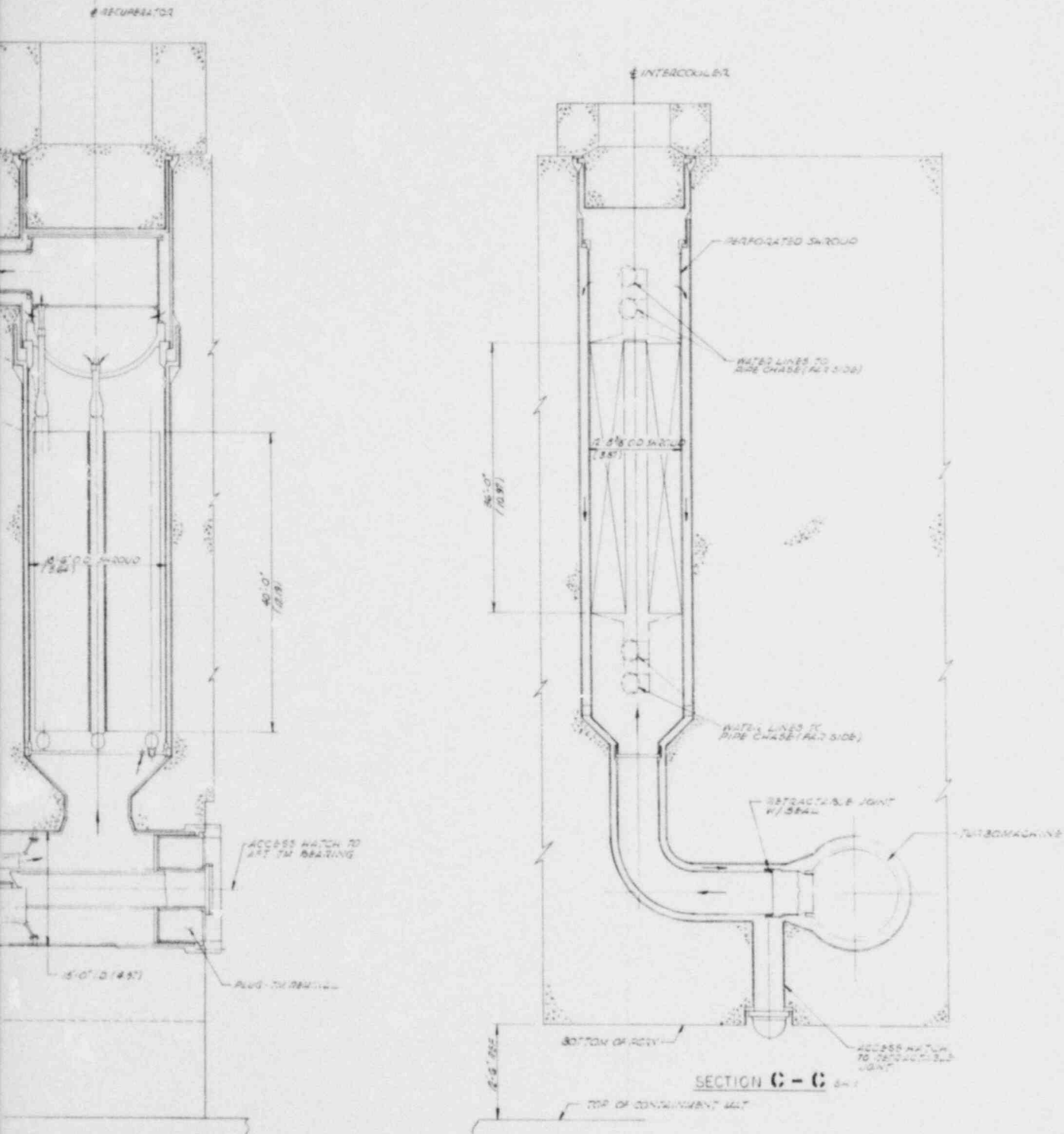
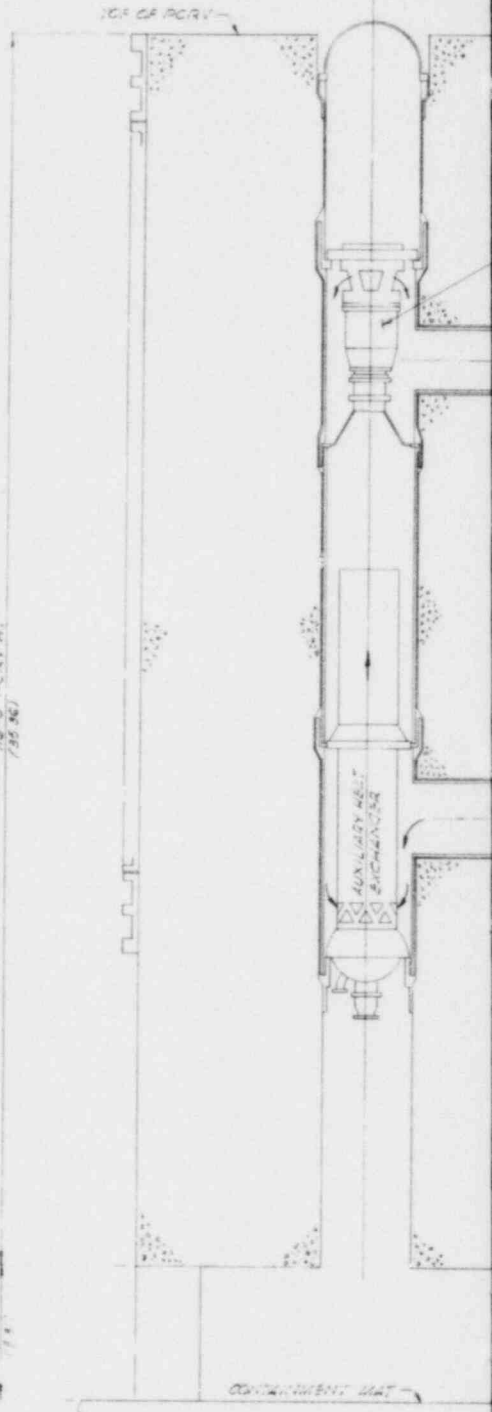
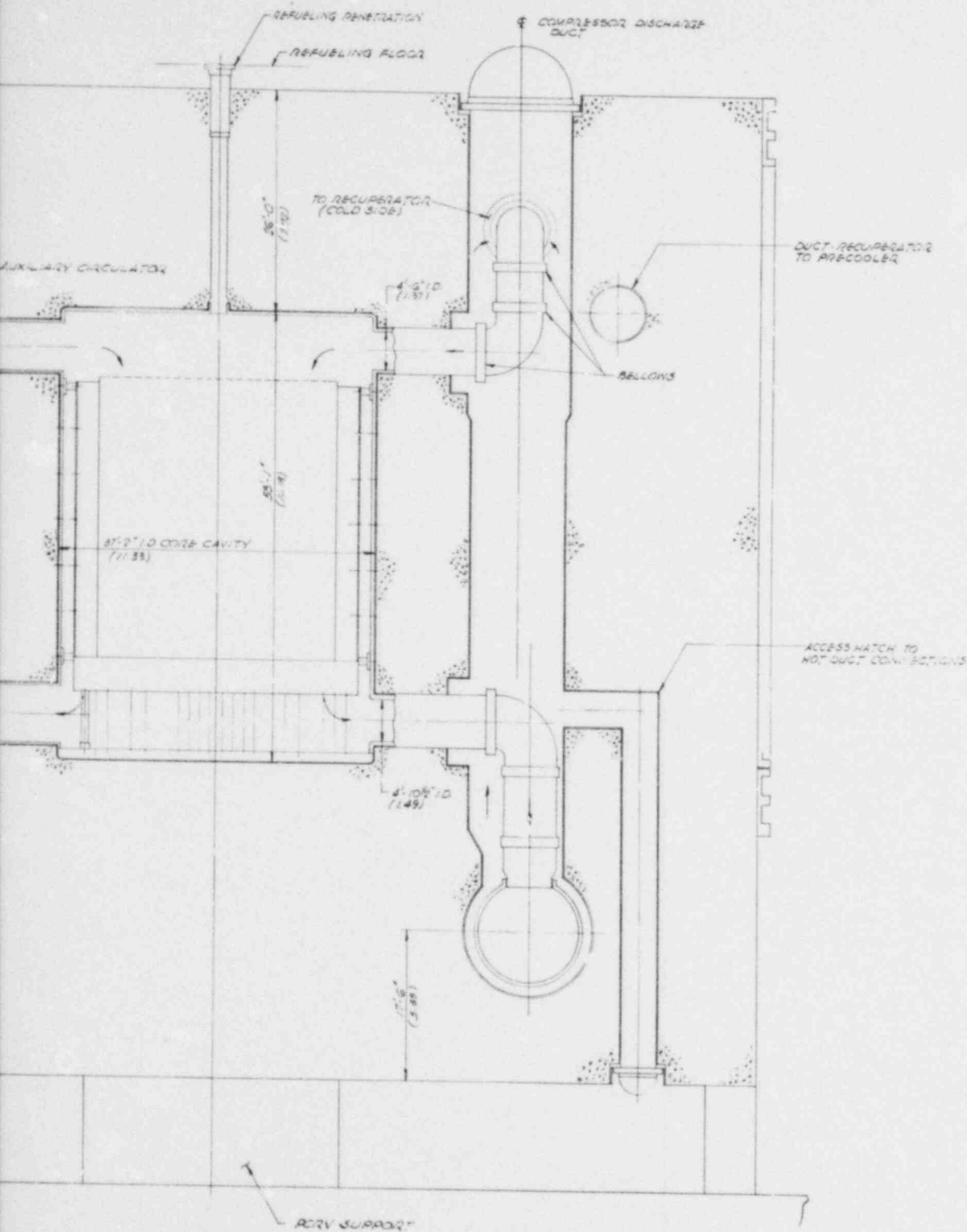


Fig. 4-5. Elevation view through PCL  
 for two-loop, 800-MW(e)  
 intercooled plant







SECTION **A - A** 341

Fig. 4-6. Elevation view through core cavity for two-loop, 800-Mw(e) intercooled plant

4.3.1.3. Evaluation of Plant Concepts. The power plant efficiency data given in Table 4-2 (38.0% and 41.6% for the base case non-intercooled and intercooled variants, respectively) must be regarded as preliminary. These values must be regarded as tentative since the object of the study was to compare the two cycle types on the same basis, rather than to perform design refinements. It is recognized that the design of a new power plant is an iterative process, and the status of the two base cases is that efforts to improve performance were not pursued beyond the first design iteration. For the non-intercooled plant, for example, the cycle efficiency of 38% includes unrealistically high pressure loss projections for the heat exchangers, which were not upgraded to reflect design improvements made downstream of the CODER heat exchanger algorithm development. Analytical studies for the two cycles were pursued to the point of identifying optimized solutions, and efficiency values of 40.0% and 43.3% were computed for the non-intercooled and intercooled plant variants. However, these values should be viewed as goals owing to the optimism used in selecting performance parameters.

Based on the first design iteration and the associated systems-related assumptions, the base case non-intercooled plant has an estimated efficiency of 38.0%. The results of the tentative optimization effort indicated an efficiency value of 40.0%. With design evolution factored into these projections for the non-intercooled plant, an efficiency value between these two numbers can be expected. Experience suggests that 39% is realizable.

The large difference in plant efficiencies of 3.6 percentage points for the two base case designs did not manifest itself in an equivalent power-generating cost differential. The higher efficiency of the intercooled plant is achieved by the inclusion of extra equipment and additional plant complexity, both resulting in higher capital cost. The various elements of the additional complexity associated with the intercooled plant are given in Table 4-3.

TABLE 4-3  
 ADDITIONAL PLANT COMPLEXITIES ASSOCIATED WITH INTERCOOLED CYCLE

Area	Major Impact(s)
<u>PCRV</u>	
Propagating effect of larger diameter	<ul style="list-style-type: none"> <li>● Increased construction time</li>   <li>● Increased capital cost</li> </ul>
Two additional cavities	
More complex tendon arrangement	
Increased liner area	
Increased thermal barrier	
More complex top head	
More complex gas flow paths	
<u>Turbomachine</u>	
Longer turbomachine length	<ul style="list-style-type: none"> <li>● Maintenance</li> <li>● Reliability/availability</li> <li>● Increased development</li> <li>● Higher capital cost</li>   <li>● Higher development risk</li> </ul>
Critical speed(s) uncertainty	
More complex casing and structure	
Additional cavity seal	
Additional duct retraction	
Impact of higher fission product release	
More complex burst shield	
<u>Heat Exchangers</u>	
Two additional exchanger assemblies	<ul style="list-style-type: none"> <li>● Maintenance</li> <li>● Reliability/availability</li> </ul>
Increased number of tube ends	
Added water pipes, valves, controls	
Larger water inventory	

There was substantial commonality in the PCRV plan views for the two plant variants. Both PCRV configurations have a chordal arrangement of the turbomachines, and both the recuperators and precoolers are positioned directly above the turbomachine cavities with straight vertical connections to the turbomachines. This arrangement offers the smallest projected area and, therefore, a minimum number of vertical tendons; it also provides the best distribution of the vertical tendons around the core. The ducts are arranged so that the core inlet and outlet ducts for each PCL lead horizontally into the compressor discharge duct cavity, which permits both ducts to operate at nearly pressure-balanced conditions. The ducts connecting the recuperators with the precoolers are curved around the compressor discharge ducts.

The intercoolers for the intercooled plant are arranged between the precooler cavities on the opposite side from the CACS cavities (as shown in Fig. 4-4) and are connected to the turbomachines by concentric ducts that enter the cavity on the side (as illustrated in Fig. 4-5). For this orientation of the major components, it was found that the two intercoolers could be embodied in the primary system without a major increase in PCRV diameter.

The PCRV is longitudinally prestressed by linear tendons. The circumferential prestressing is conventional for the top head and barrel section of the PCRV with wire winding in steel-lined channels of precast panels. In the bottom head section of the PCRV, the wire winding is replaced by diagonal tendons.

Analytical modeling of both plant concepts was performed, and versions of the optimization computer program CODER were refined. Algorithms for the various elements of the primary system were developed and incorporated in CODER. The salient features and performance estimates for the two base-case plant design concepts are given in Table 4-2.

TABLE 4-2  
TWO-LOOP, 400-MW(e) INTERCOOLED VERSUS NON-INTERCOOLED PLANT  
COMPARISON (BASE CASE)

	Non-Intercooled	Intercooled
Core thermal rating, MW(t)	2000	
Reactor outlet temp., °C(°F)	850(1562)	
Heat rejection	Dry-cooled	
Nominal loop rating, MW(t)	1000	
No. of loops	2	
Liner type	Insulated and water cooled	
Plant layout drawing	025113	025100
Core position	Offset	Offset
Turbomachine orientation	Chordal	Chordal
PCRV diameter, m(ft)	37.2(122)	39.6(130)
PCRV height, m(ft)	35.4(116)	35.4(116)
No. of major cavities	12	14
No. of CACS units	3	3
Hot duct replaceability	Yes	Yes
Thermal barrier replaceability	No	No
Maximum system pressure, MPa (psia)	7.93(1150)	7.93(1150)
Turbomachine type	Single-shaft	Single-shaft
Compressor/turbine stages	18/8	8 + 8/9
Compressor pressure ratio	2.5	3.0
No. of journal bearings	2	2
Overall diameter, m(ft)	3.96(13.0)	3.96(13.0)
Overall length, m(ft)	11.3(37)	15.2(50)
Overall weight, tonnes (tons)	277(305)	-
Recuperator type	Straight tube, modular	
Effectiveness	0.90	
Exchanger diameter, m(ft)	5.6(18.5)	
Overall length, m(ft)	20.4(67)	
Overall weight, tonnes (tons)	726(800)	
Precooler/intercooler type	Helical bundle	
Water outlet temp., °C(°F)	132(270)	87/65(189/150)
Exchanger dia., m(ft)	4.7(15.5)	4.1/3.8(13.5/12.5)
Overall length, m(ft)	19.8(65)	21.3/18.3(70/60)
Overall weight, tonnes (tons)	435(480)	-
Ambient temp., °C(°F)	15(59)	15(59)
Plant output, MW(e)	760	832
Approx. plant efficiency, %	38.0	41.6

There was close agreement between the CODER cost projections and the actual cost estimates based on the design layouts. In addition to comparing the two base case designs, power generation costs were compared for two optimized cases: (1) plants with the same reactor thermal power and (2) plants with the same electrical output. Table 4-4 summarizes the pertinent results of this comparison. As expected, the intercooled plant shows a slight power generation cost advantage for all comparisons, but these differences were not felt to be significant at this stage when weighed against other cycle selection factors that influence the program.

In Table 4-5, an attempt has been made to compare the salient features of the two base case designs. It is recognized that not all of the elements portrayed have the same weight ranking, but the data are presented to indicate major areas of merit. With the aforementioned cost differential not being a major deciding element, the choice of plant concept was based on an evaluation of the technical issues and other factors outlined in Table 4-5.

4.3.1.4. Conclusions. The comparison of two power plants based on intercooled and non-intercooled cycles (at the same core thermal power rating), while lacking in technical depth, was of sufficient scope to enable salient differences to be identified and assessed. Key elements in the study included (1) systems analysis and parameter definition, (2) plant layout evaluation, (3) PCI component design, (4) cost comparison, and (5) assessment of relative plant operability issues (reliability/availability, maintenance and ISI, etc.).

For the two base case designs, the plant efficiency estimates were 38.0% and 41.6% for the non-intercooled and intercooled variants, respectively. This large difference in efficiency (3.6 percentage points) did not manifest itself in equivalent power generation cost savings. The accuracy to which it was possible to pursue cost differences is defined as a

TABLE 4-4  
 COST COMPARISON SUMMARY FOR INTERCOOLED (INT) VERSUS  
 NON-INTERCOOLED (NINT) STUDY

	Base Case		Optimized Case		
	NINT	INT	NINT	INT	INT
Net output, MW(e)	759.3	832.1	800	800	869.5
Core thermal power, MW(t)	2000	2000	2000	1818	2000
Efficiency, %	38.0	41.6	40.0	44.0	43.5
Normalized capital cost <sup>(a)</sup>	Base	1.05	Opt. base	1.01	1.03
Normalized \$/kW(e) <sup>(a)</sup>	Base	0.96	Opt. base	1.01	0.95
Normalized power generation cost	Base	0.94	Opt. base	0.99	0.95

(a) Fuel costs not included. Comparison is based on 1979 dollars.



TABLE 4-5  
COMPARISON OF INTERCOOLED AND NON-INTERCOOLED CYCLE SALIENT FEATURES

	Non- Intercooled	Intercooled	Comment
<u>Technical Issues</u>			
PCRIV tendon layout	X <sup>(a)</sup>		
Gas flow path complexity	X		
Liner cooling flexibility		X	Possible advantage for partial warm liner concepts
PCRIV construction time	X		
PCRIV top head complexity	X		
Core gas inlet temperature		X	Two less cavities 449°C(840°F) instead of 507°C (945°F)
Fission product release	X		
Fuel element thermal stress	X		Reduced $\Delta T$
Heat exchanger diameters		X	Small difference
Heat exchanger metal temperatures		X	Slight advantage for recuperator
Turbomachine bearing span	X		Greater critical speed margin
Seals in turbomachine cavity	X		Less cavity seals
Control valves		X	Lower operating temperature
Scalability	X		Viable three-loop option
<u>Other Factors</u>			
Operability	X		Fewer systems
Availability and reliability	X		Less equipment
Maintenance and ISI	X		
Power generation cost		X	Marginal advantage
Capital cost	X		Small advantage
Complexity and risk	X		
Process steam production	X		Higher reject temperature
Binary cycle option	X		Higher reject temperature
International cooperation		X	Cooperation with HHT
High efficiency		X	Resource conservation
Cogeneration	X		Binary cycle or steam supply
Program cost		X?	Cost sharing with FRG
Technology transfer		X	Indirect cycle, fission, coal CCGT

(a) X indicates an advantage.

conceptual estimate. It was not possible to provide a more precise cost estimate because (1) the plant designs lacked detailed definition, and (2) funds and time were not available for detailed cost analyses.

A comparison of analytically optimized intercooled and non-intercooled plant designs, via the system optimization code CODER, revealed that the economic incentive for intercooling is even smaller, regardless of whether the plants are compared on an equal electrical output or an equal core thermal power rating basis. In addition to reinforcing the general conclusions of the base case comparison, the optimized case results provide an indication of the efficiency potentials for these two options. In the selection of the HTGR-GT plant thermodynamic cycle, it was not felt prudent to let this small economic increment be the deciding factor. The non-intercooled cycle was favored because of a combination of the following advantages:

1. Simpler overall plant arrangement, particularly the PCRV and primary system.
2. Reduced complexity and risk.
3. Better projections of plant operability, reliability/availability, and maintenance and ISI.
4. Scaling flexibility should plants of higher rating be required in the future (i.e., two and three-loop options open).
5. Superior cogeneration capability (i.e., binary cycle and process steam production).

It should be pointed out that the above factors are consistent with a decision made at the onset of HTGR-GT plant activities in 1971, namely that the plant should be kept as simple as possible.

The conclusion of the study to pursue the design of a two-loop plant based on a non-intercooled cycle has inherent in it the motivation that successful operation of the first plant will be more realizable with the simpler system. Operation of the first plant with a minimum of development and commissioning problems is of the essence, and this is regarded as a much stronger factor in the decision-making process than the very small power-generating cost advantage identified in this study for the more complex intercooled variant.

#### 4.3.2. Advanced Features Study

4.3.2.1. Introduction. The current HTGR-GT reference plant embodies many features in both the primary system and BOP that were established for the HTGR-SC. The major purpose of the advanced features study is to examine the validity of these assumptions, particularly with regard to reducing the cost of the HTGR-GT plant. A study was made of advanced and novel features to ensure that the plant concept selection will yield a competitive plant for commercial service in the early decades of the 21st century.

With the PCF/ size literally dominating the plant design, initial efforts were directed toward screening possible alternatives to both the design and construction of the vessel, while retaining the safety features of the prestressed concrete approach but with potential reduction in capital cost. The various approaches outlined in the following section are regarded as being very conceptual in nature and have been developed only to the extent necessary to permit a qualitative indication of their merits and drawbacks.

At the start of the study, a review of possible concepts and the basic criteria of primary system integration again (as in previous investigations) led to the adoption of a fully integrated approach, the motivation being

safety related. The integrated design is defined as a configuration where all components are either in a common prestressed concrete vessel or in several concrete vessels connected to each other so that all connecting ducts are embedded in these vessels.

#### 4.3.2.2. Plant Configurations Embodying Advanced Primary System Features.

As discussed in other sections of this report, the HTGR-GT program underwent modification during FY-79 whereby the reference plant was changed from a three-loop to a two-loop configuration. The advanced features study addressed both three- and two-loop variants. An obvious goal in power plant design studies is to establish a configuration for which the construction schedule is minimized, since a large percentage of plant cost is represented by escalation and interest costs during construction. Clearly, at the conceptual design stage it is not possible to be definitive with regard to comparing the construction times required for different plant configurations. Indeed, several plants would have to be built before a thorough knowledge of construction sequences and actual cost data were realized.

The advanced features study was essentially concentrated on the PCRV layout itself to explore possible design changes that might permit paralleling of construction operations, such as adopting a modular or precast approach for the vessel or vessels. The initial effort of exploring alternate PCRV design approaches was justified since previous HTGR work has indicated that the construction schedule critical path for a large HTGR is dominated by the PCRV erection. The following sections outline conceptual design approaches which were generated consistent with the goal of identifying features conducive to reduction of construction time.

#### "Gondola" Turbomachine Vessel Concept

In an effort to "uncouple" the turbomachine cavity from the main body of the PCRV, a "gondola" concept was generated with the turbomachine module

positioned below the PCRV. As shown in Fig. 4-7, the turbomachine is installed in its own prestressed concrete vessel, and the overall arrangement is in compliance with the fully integrated plant approach. An advantage postulated for this scheme is that the turbomachine module (Figs. 4-8 and 4-9) can be fabricated separately and installed at a convenient time in the schedule so that the plant construction schedule will be reduced.

The construction of the turbomachine vessel can be planned so that, after construction and prestressing, the installation of the turbomachine can be performed with a machine mock-up and the turbomachine cavity can be prepared for the final installation of the gas turbine. At the appropriate time in the construction schedule, the turbomachine cavity will be moved into place. Moving the cavity can be accomplished using specially designed air pallets, and for this operation a smooth and level concrete platform has to be provided. After the turbomachine vessel element is in place, it will be jacked up to the bottom surface of the main PCRV and, after matching up the seismic lugs, will be secured in this position. The duct flanges will then be connected through access ducts provided in the bottom part of the main PCRV as shown in Fig. 4-7.

It was felt that this novel approach would have the following advantages: (1) potential for reduced construction time and (2) reduction in PCRV diameter. A disadvantage is an increase in height from the top of the PCRV to the base mat. The "gondola" approach was not pursued beyond the conceptual form, and in-depth structural evaluation was felt to be necessary prior to establishing a construction and prestressing sequence for the combined structure. While shown in Fig. 4-7 for a three-loop plant, the concept of separate turbomachine concrete structures is equally applicable to a two-loop plant variant.

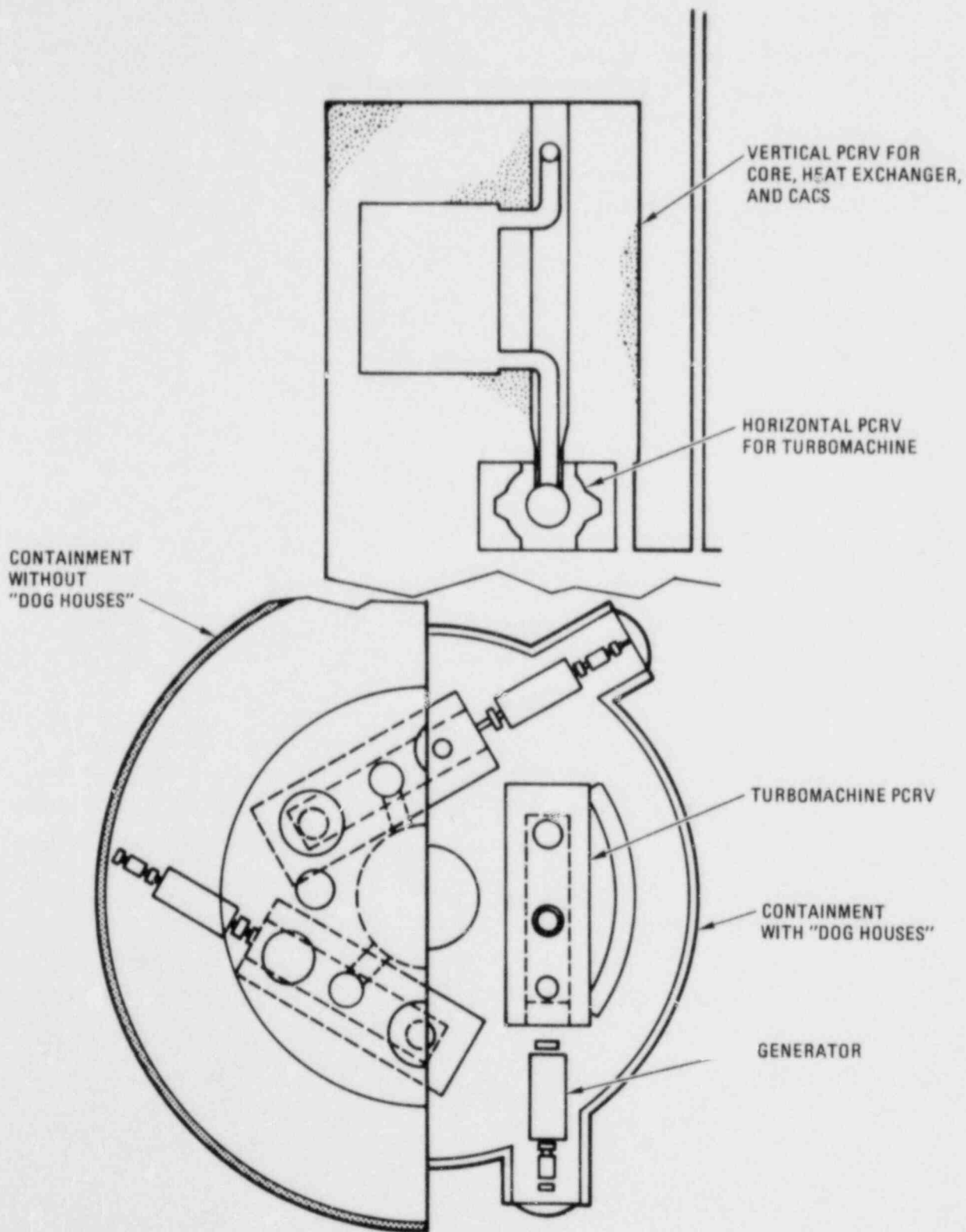


Fig. 4-7. Three-loop HTGR-GT integrated design with separate turbomachine PCRVs

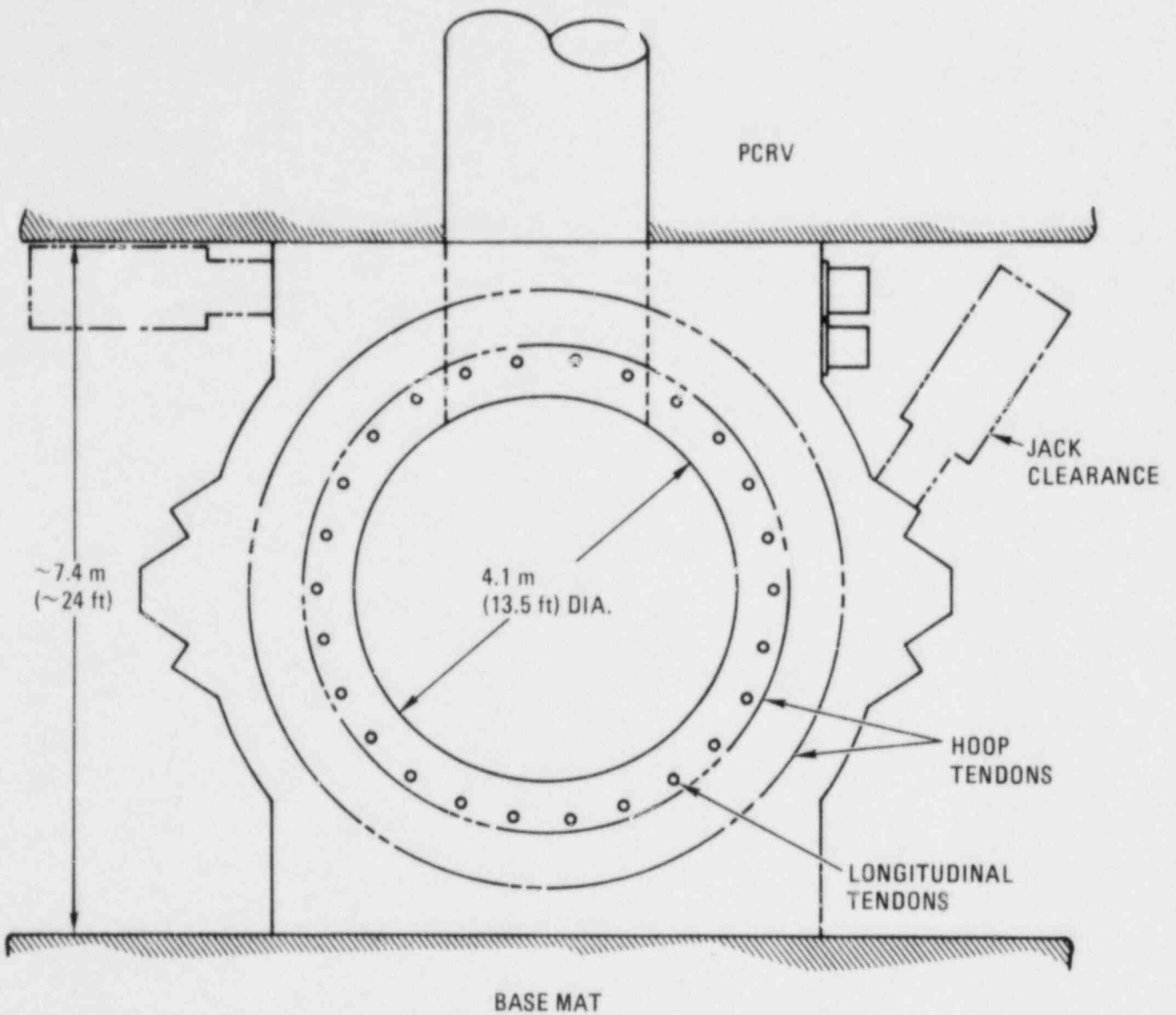


Fig. 4-8. Turbomachine PCRV prestressing

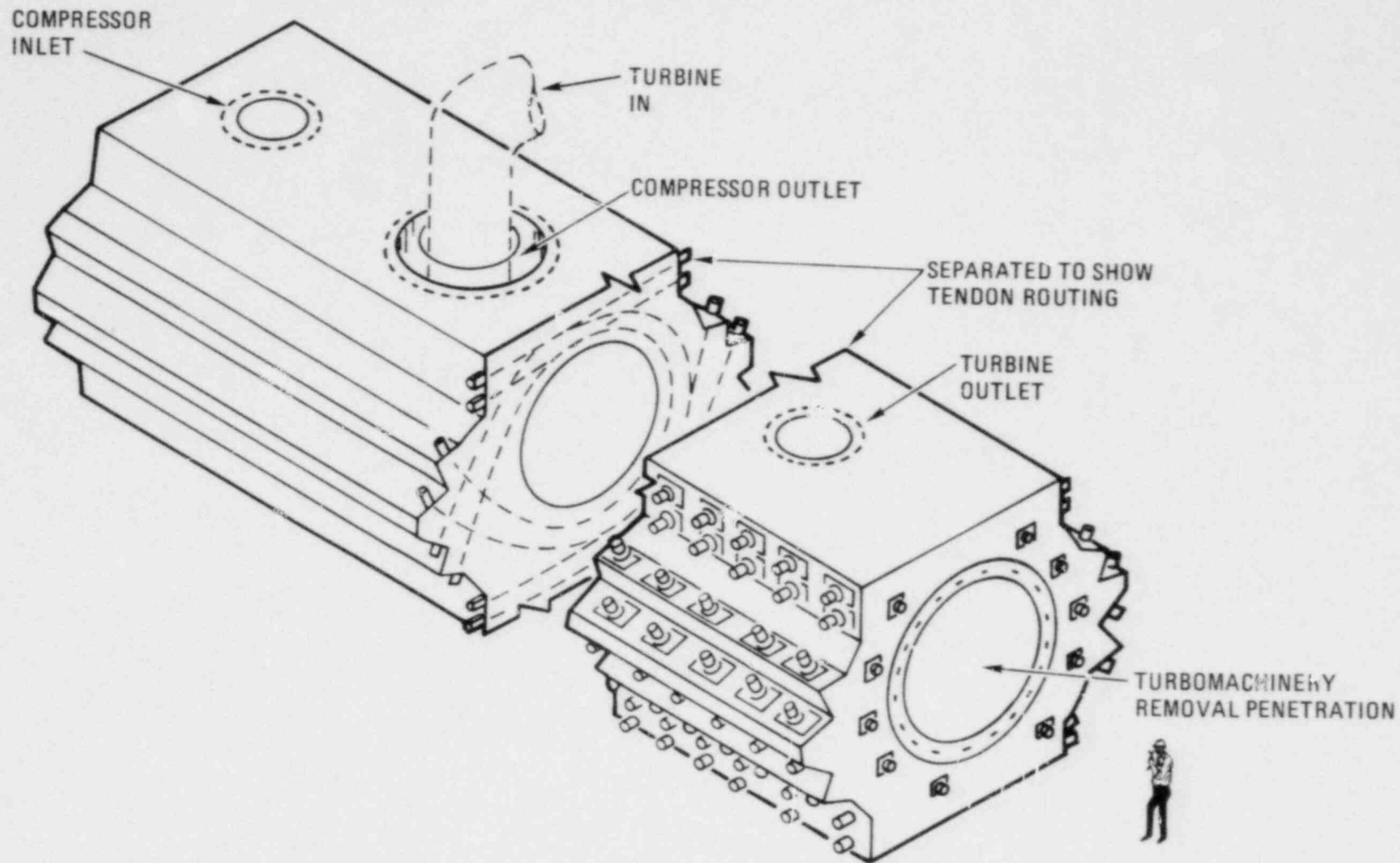


Fig. 4-9. Isometric view of monolithic turbomachine module



### "Power Block" PCRV Layout Concept

An obvious extension of the "gondola" concept involved the study of a "power block" concept in which all the power conversion equipment was installed in a separate concrete structure, with the main body of the vessel containing only the core cavity and CACS cavities. The overall approach of this concept for variants embodying vertical heat exchangers is illustrated in Figs. 4-10 and 4-11 for three- and two-loop plants, respectively. Versions of this approach with horizontal heat exchangers were also explored. These versions are illustrated in Figs. 4-12 and 4-13 for the three-loop plant, and details of the power block are shown in Fig. 4-14.

The advantages postulated for the "power block" concept were as follows: (1) material quantities are reduced; (2) no wire-winding machine is required; and (3) the construction schedule is reduced by constructing the PCRVs in parallel. A disadvantage would be the larger containment building owing to the larger plan area. Work beyond the conceptual phase was not pursued because of budgeting and priority considerations.

### Precast PCRV Block Layout Concept

The ultimate in modularization of the PCRV involves a structure assembled from a multiplicity of precast elements. A very cursory investigation was carried out for a PCRV layout concept assembled from precast concrete modules. It was postulated that such an approach would permit many operations to be done in parallel, which would have a positive impact on construction time. The basic metallic liners and interconnecting ducts could perhaps be assembled as a structure, as shown in Fig. 4-15. The precast concrete elements, with as many "standardized blocks" as possible, could be fabricated on a batch production basis. The construction of the PCRV would then take the form of assembling the precast concrete elements around the "steel pattern." This approach is shown conceptually for

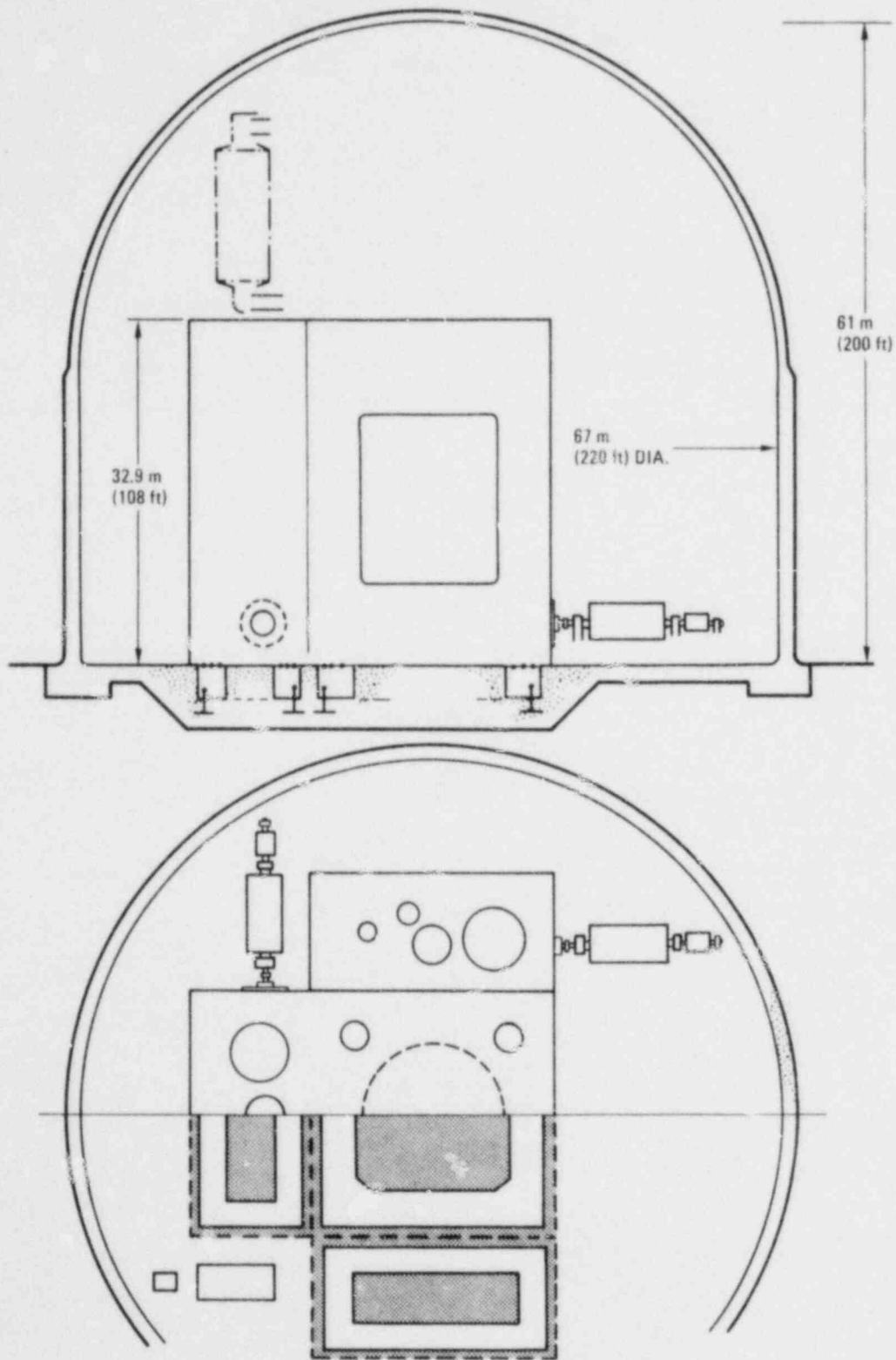


Fig. 4-10. Three-loop plant concept embodying "power block" layout approach with vertical heat exchanger

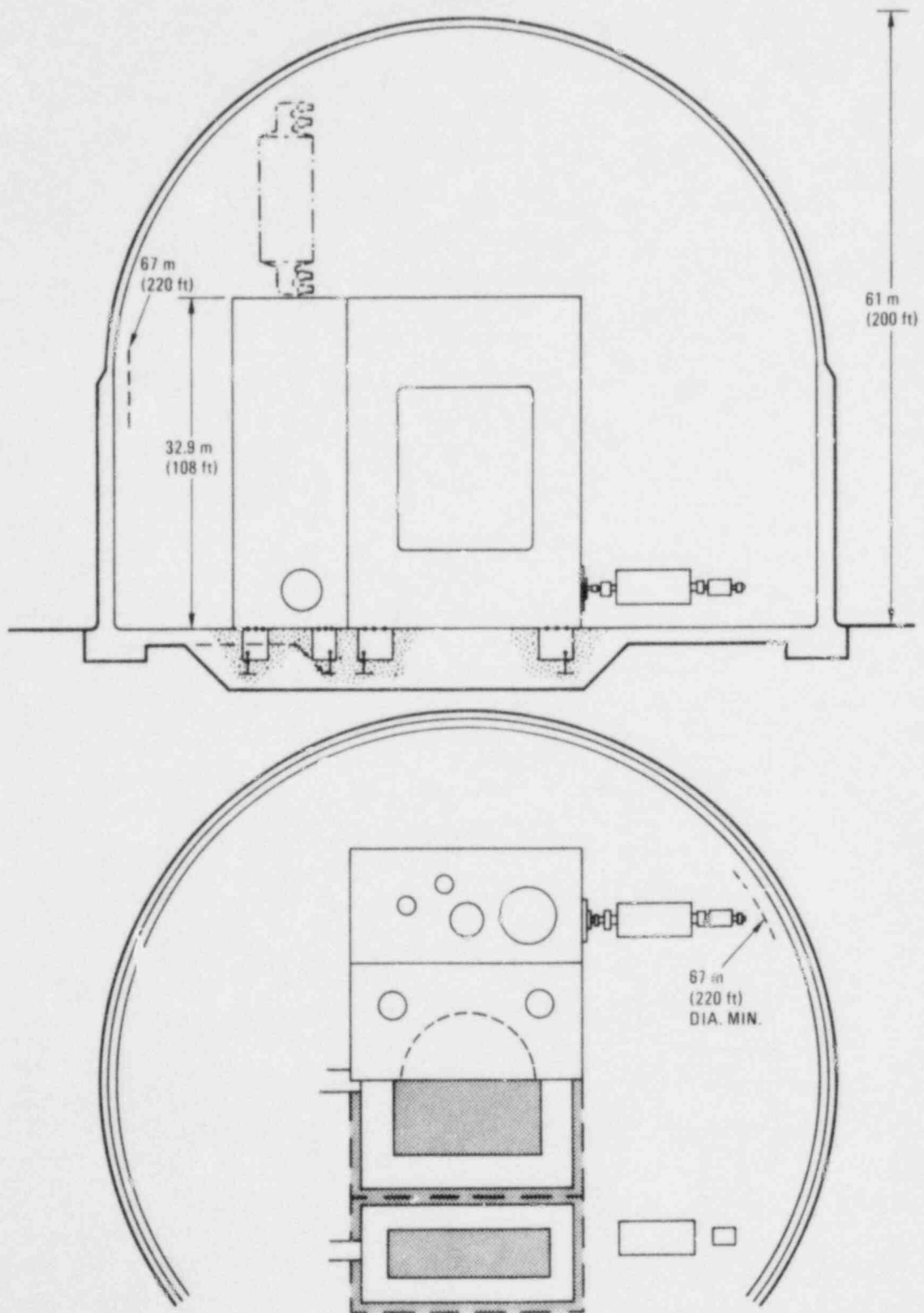
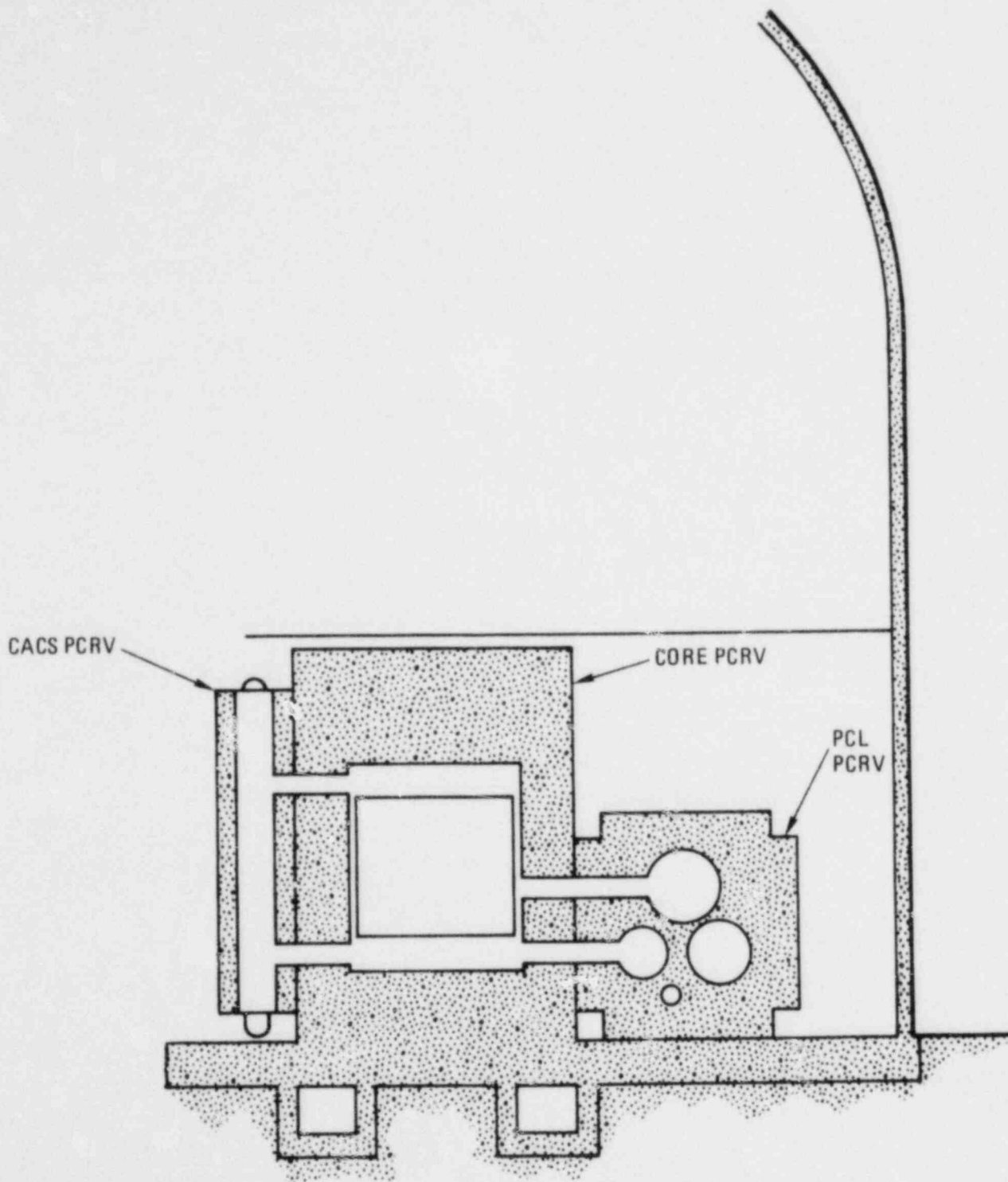


Fig. 4-11. Two-loop plant concept embodying "power block" layout approach with vertical heat exchanger



SECTION A-A

Fig. 4-12. Elevation view through PCRV showing "power block" concept with horizontal heat exchangers

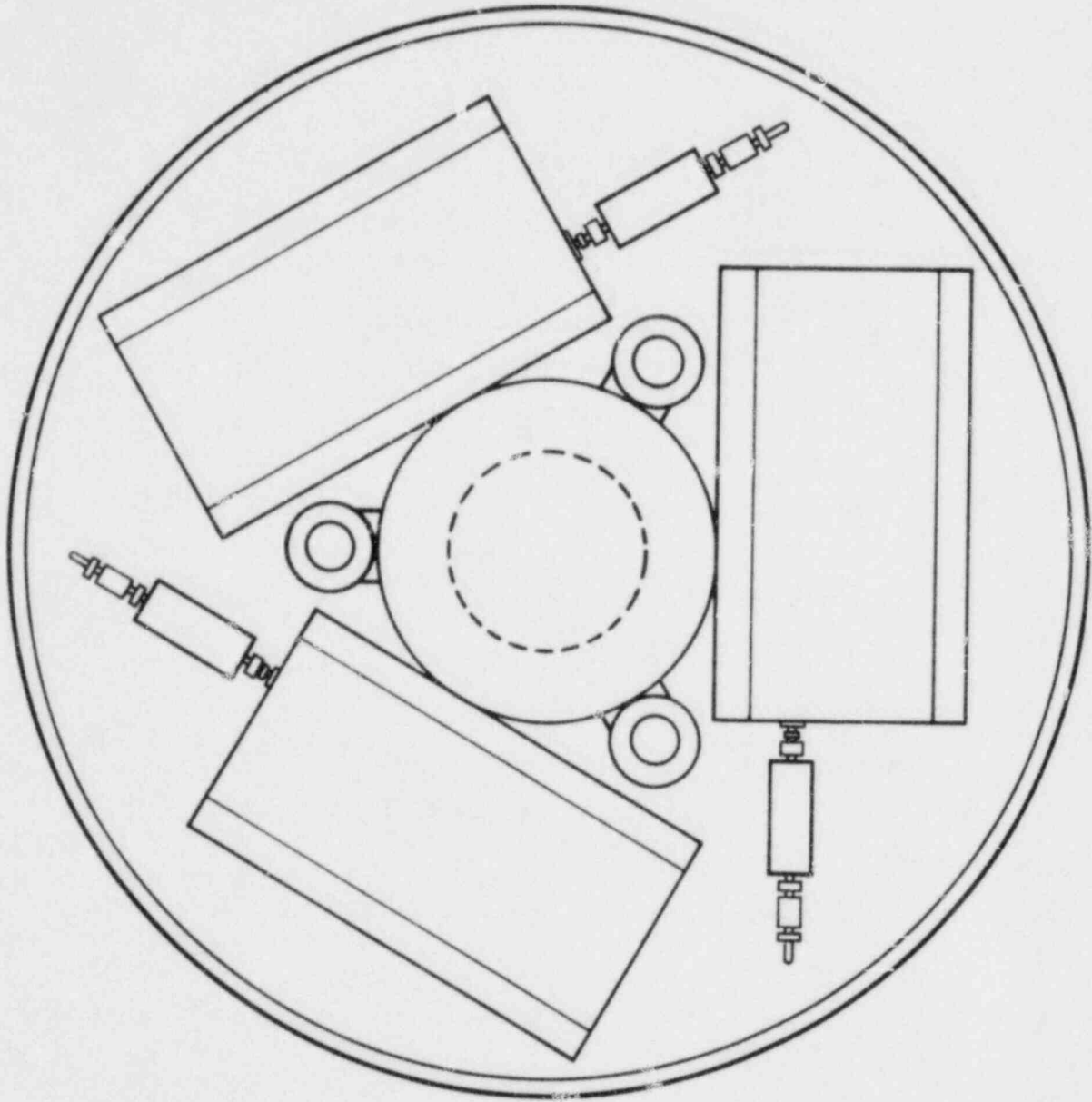


Fig. 4-13. Plan view of PCRV with three "power blocks" embodying horizontal heat exchangers

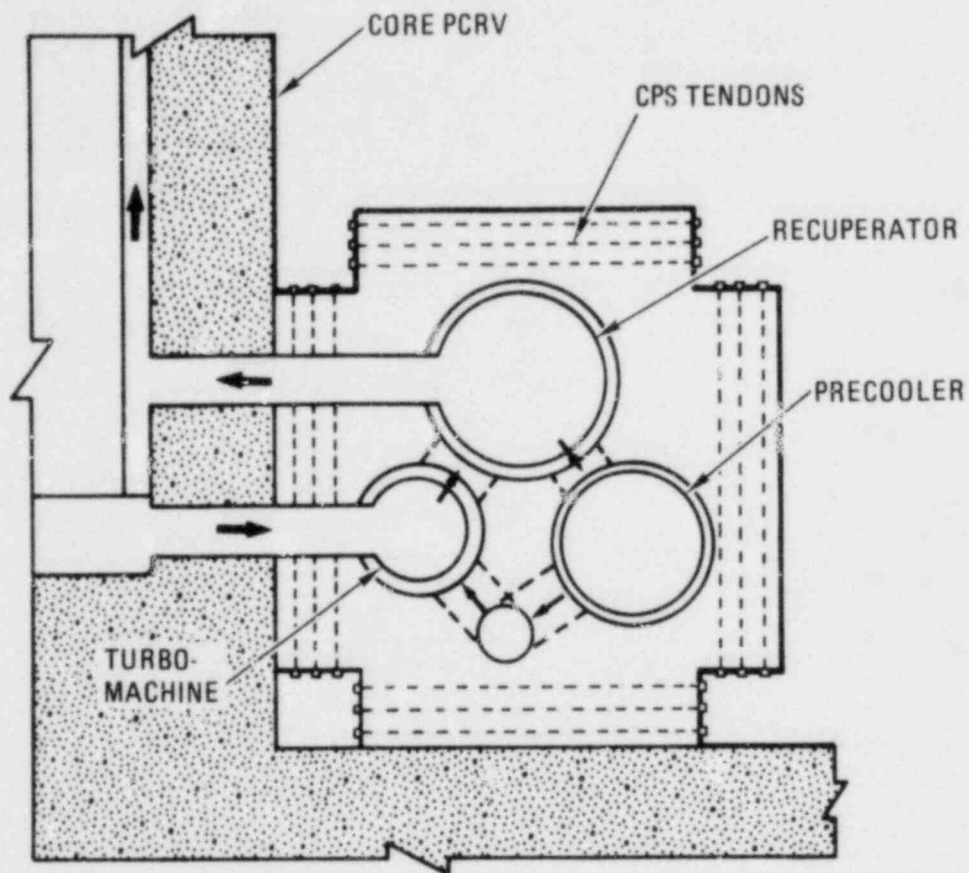


Fig. 4-14. View showing details of "power block" for case with horizontal heat exchangers

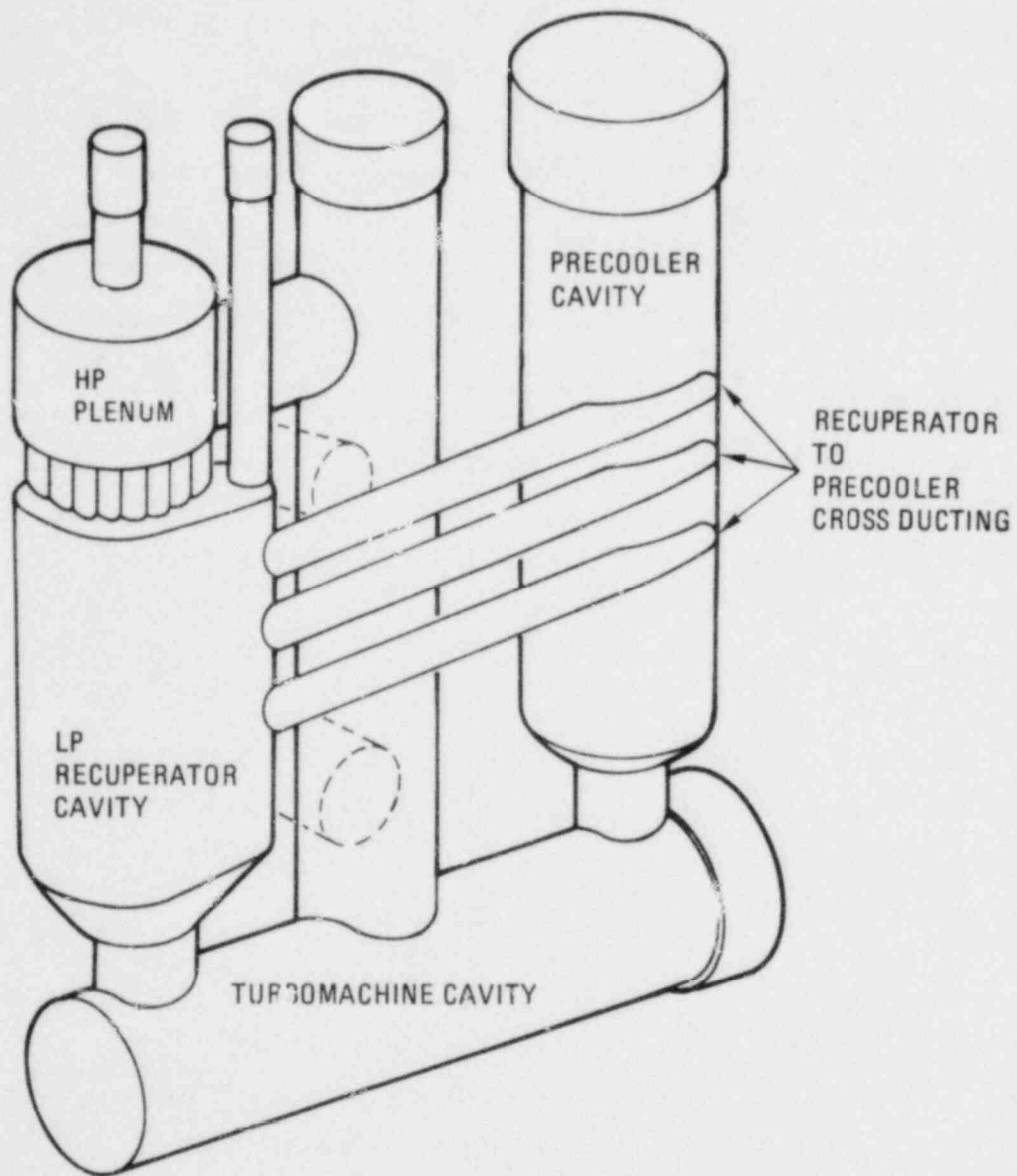


Fig. 4-15. Example of PCL liner "pattern" for precast PCRV block approach (temporary bracing not shown)

circular and rectangular PCRV approaches in Figs. 4-16 and 4-17, respectively. Steel rebar splicing and continuity between the precast blocks and the task of pumping in grout between the precast modular elements to form a homogeneous vessel structure were recognized as problems. The precast modular approach for PCRV construction represents perhaps the most radical approach investigated during the advanced features study. Advantages postulated for this scheme essentially related to reduced construction schedule resulting from parallel operations and elimination of soffit framework ordinarily required in conventional PCRV construction. Disadvantages included (1) too many different PCRV precast block shapes, (2) complexity of precast block shapes, (3) complex interaction of precast blocks with crossducts and liners during PCRV assembly, and (4) tendon/rebar congestion in the turbomachine PCRV (due to exclusive use of linear tendons). Because of budgetary constraints and the large effort envisioned to prove this type of construction feasible, the precast PCRV approach was not pursued beyond the embryonic stage.

4.3.2.3. Summary. Although the limited budget prevented in-depth studies of advanced features, several concepts were identified which have potential for reducing plant cost. The novel design approaches described above were not directed toward improvement of a particular plant concept, but rather were based on quite different design thinking hitherto not explored for the HTGR-GT plant. Essentially the approaches involved modularization of the PCRV (to varying degrees) to permit construction of critical path items to be done in parallel. Clearly, some of the approaches are quite radical. Nevertheless, continued study is encouraged to pursue them to the point of establishing feasibility and determining potential capital cost savings.



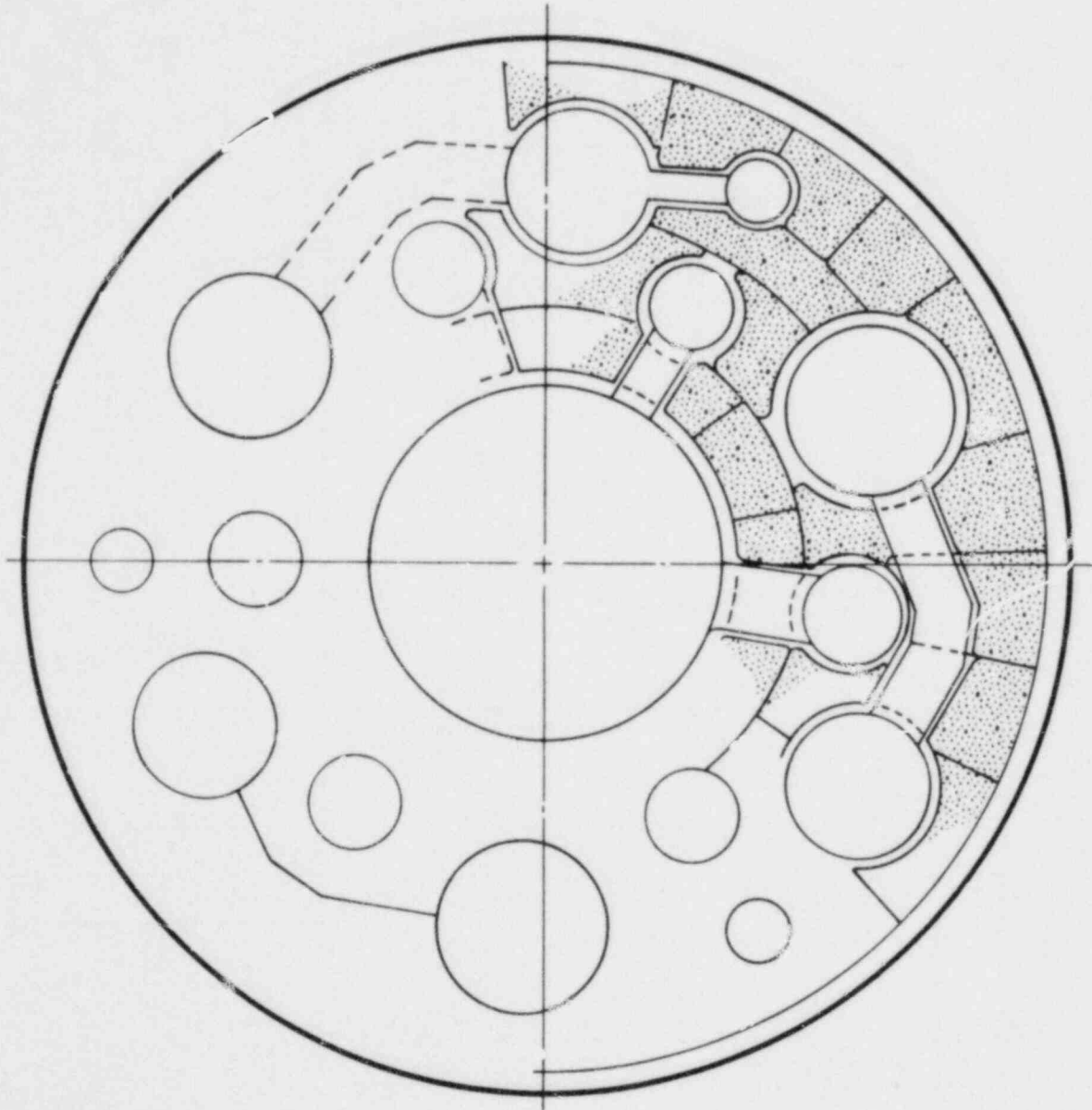


Fig. 4-16. Precast modular concept for circular PCRV

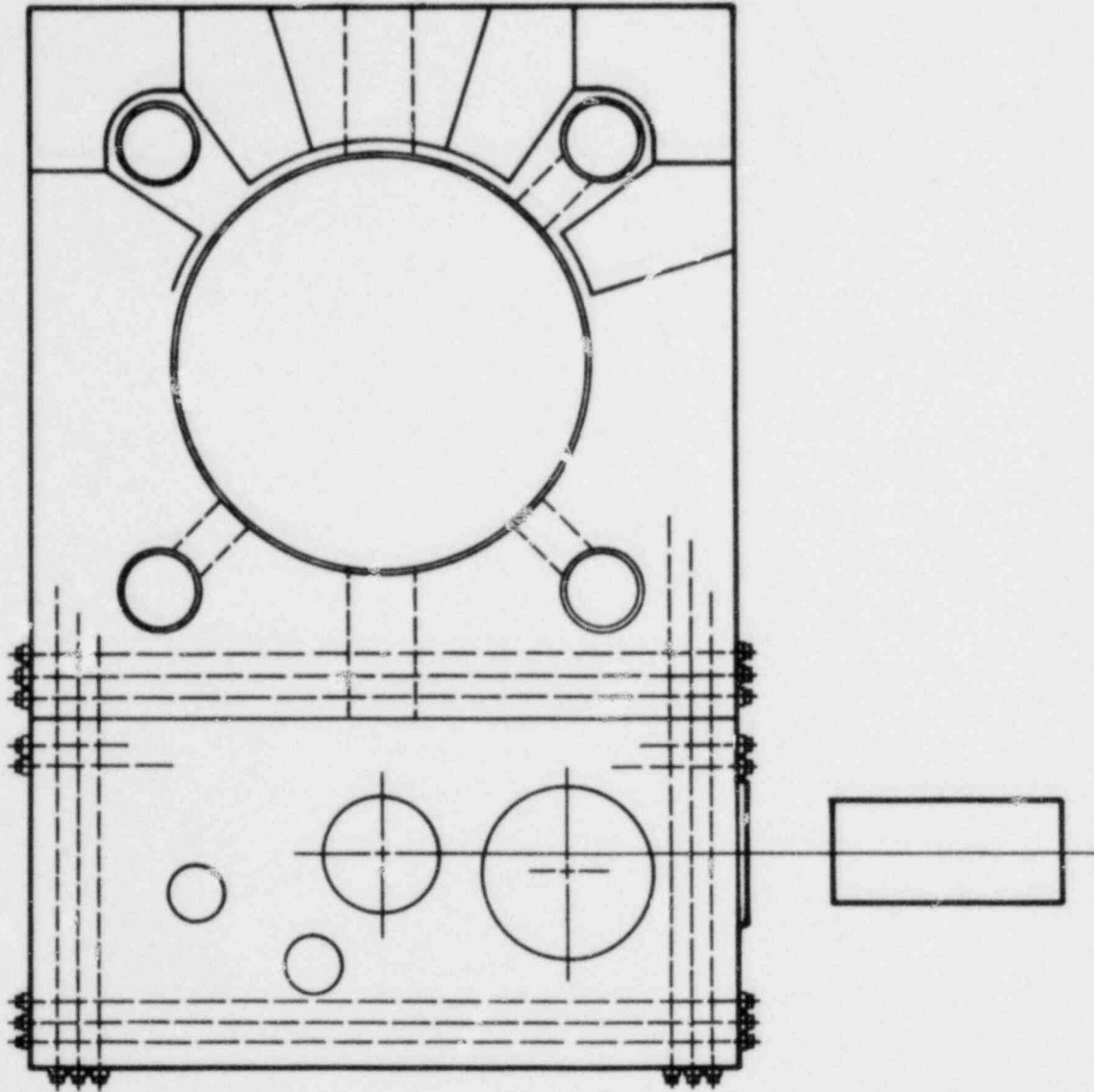


Fig. 4-17. Precast modular concept for rectangular PCRV

## 5. MISCELLANEOUS CONTROLS AND AUXILIARY SYSTEMS (630102)

### 5.1. SCOPE

The purpose of this task in FY-79 was to establish the helium bypass valve service system requirements and interfaces.

### 5.2. SUMMARY

A preliminary design for the valve actuating system has been completed. A portion of this design is shown in Fig. 5-1.

### 5.3. DISCUSSION

The valve actuating system preliminary design has the following features:

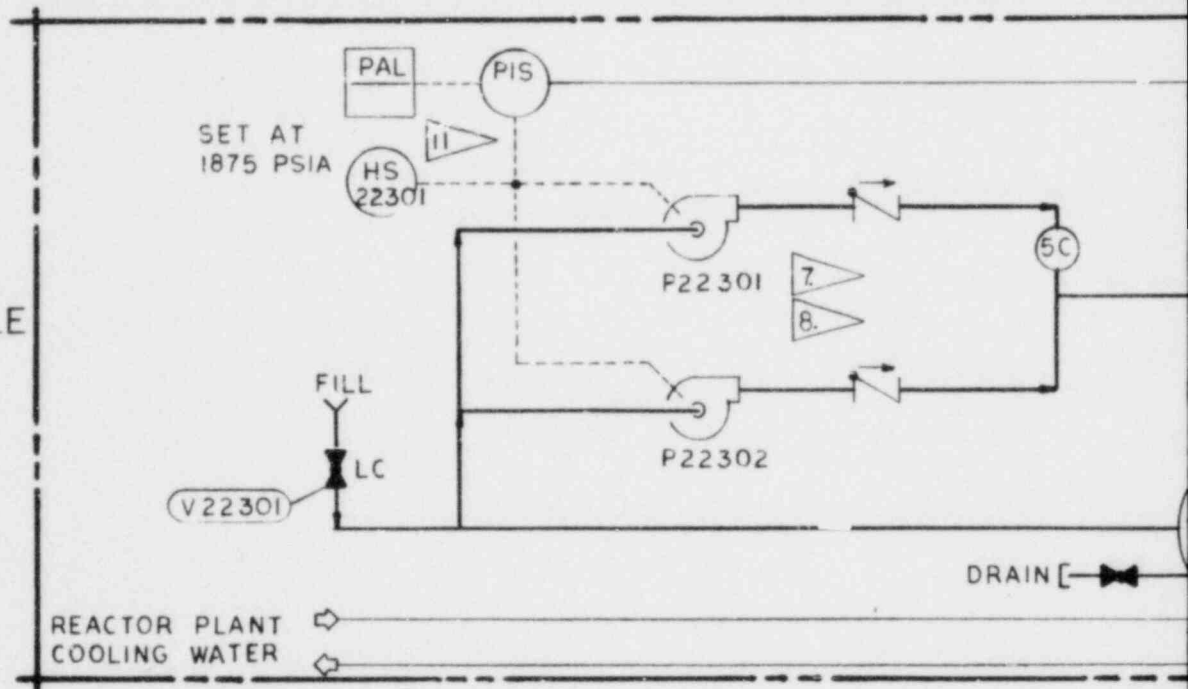
1. Hydraulic actuators are used to serve all valves. This design approach allows all moving parts (except the actuator piston assembly and position instrumentation) to be located out of the PCRV cavities for ease of maintenance and testing.
2. Actuators are served from high-speed servo valves to achieve design simplicity and speed of operation.
3. Each valve is served from its own independent actuation system or module. In addition to achieving design simplicity, this approach prohibits the failure of one valve or actuation system from affecting the operation of other valves in the same primary coolant loop or valves in other loops. Valve function is also made independent

in the primary bypass valve. Since this valve has two basic operating functions (a safety function, to serve as a redundant safety valve, and a non-safety function, to serve as a turbo-machine bypass flow control valve), two independent actuation systems have been designed to serve this valve. Figure 5-2 depicts one of five actuation systems or modules serving the valves in a typical loop.

This preliminary design is intended for use by GA in evaluating valve control dynamics with the aid of a "hybrid" computer. Work is in progress to develop a computer model of the valves, their actuation systems, and the primary coolant loop to evaluate system performance. This design is also intended for use by a large-valve design consultant in his nationwide survey of large-valve designers and fabricators. A large-valve design contract will be let by GA in FY-80.

In parallel with the tasks outlined above, GA will revise the current actuation system design to accommodate larger valves. The current design is based on 670 mm (26.4-in.) primary bypass and safety valves. Recent primary loop flow and pressure drop analysis indicates the valves could be as large as 792 mm (31.2 in.). See Section 21 for further discussion of control valves.

S 2203  
CONTROL MODULE



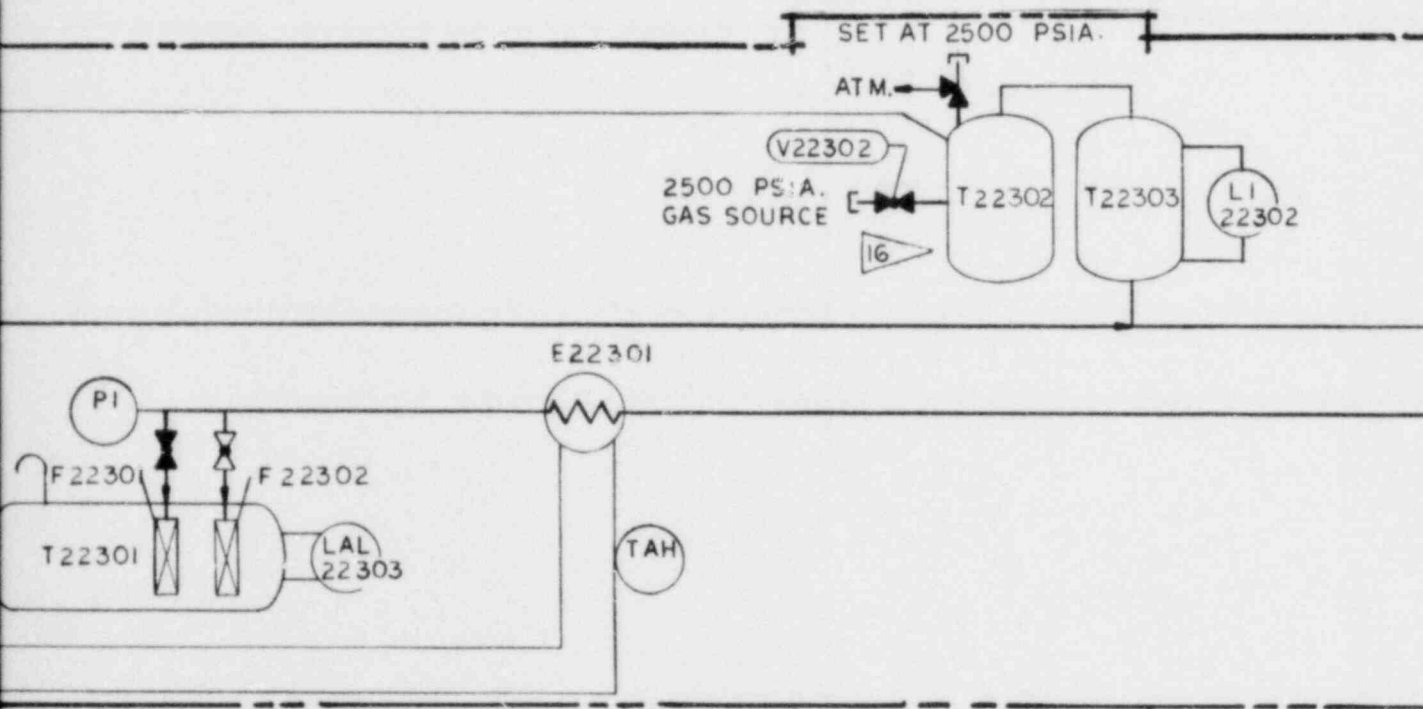


Fig. 5-1. Primary bypass valve actuation system

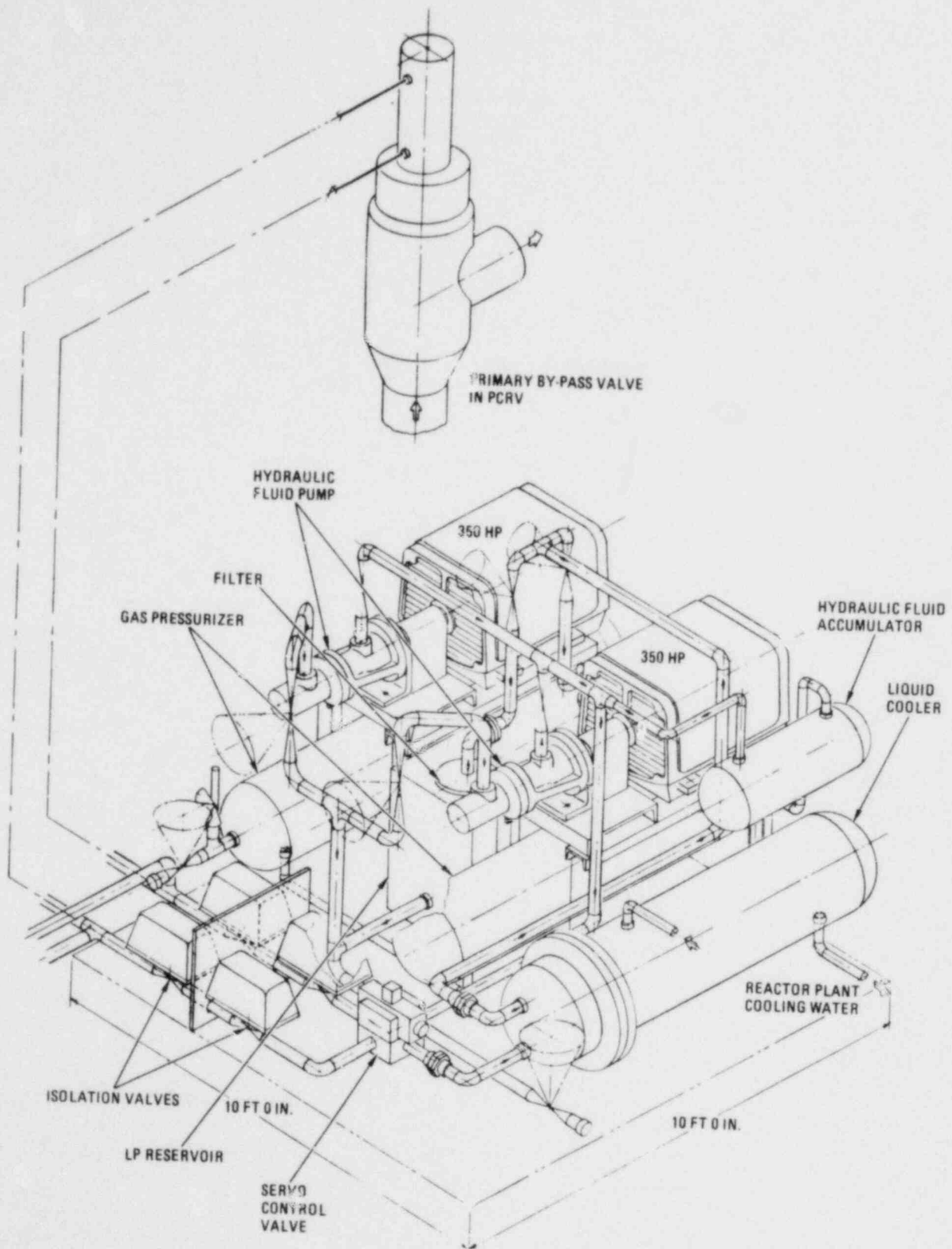


Fig. 5-2. Control module for primary bypass valve

## 6. STRUCTURAL MECHANICS (630103)

### 6.1. SCOPE

The purpose of this task in FY-79 was to evaluate the seismic response of a representative plant PCRV and containment building and examine the seismic problems associated with a graphite core.

### 6.2. SUMMARY

Three task items were completed: (1) a seismic analysis of a gas turbine PCRV and reactor containment building (RCB), (2) a seismic evaluation of a prismatic block gas turbine core, and (3) a seismic evaluation of a gas turbine pebble bed core.

A seismic analysis of the RCB and PCRV based on the German HHT Demonstration Plant has been completed. This configuration was used because it was considered representative of both the U.S. and German configurations. The analysis included the basic dynamic model formulation, calculation of structural properties, seismic excitation and site parameter selection, structural damping, eigenvalue solution, response spectrum, and time-history analyses. Analytical results were generated and presented in terms of forces, moments, deformations, and in-structure response spectra at various critical locations of the RCB/PCRV for two PCRV support conditions (one with PCRV neoprene support pads and one without) at a German site specified by Hochttemperatur-Reaktorbau (HRB). All numerical results were based on a 1.0-g maximum horizontal ground acceleration for the operating basis earthquake (OBE) as well as the safe shutdown earthquake (SSE). The resultant loads and response are close to those for a soft soil, 900-MW HTGR-SC analysis.



Preliminary seismic design loads for a prismatic block gas turbine reactor core have been generated with the MCOCO computer program. In order to envelope all expected response spectra, one artificial horizontal and one vertical time history were developed covering the response spectra at the core level of five sites ranging from soft soil to competent rock. The analytical model represented the core at 100% power for a 0.15-g OBE. Unfortunately, the time history developed from this envelope produces a much higher rigid-range  $g$  level than is necessary. The "envelope" analysis was used because of the high cost of obtaining a large number of MCOCO runs for various soil conditions. The loads produced, however, are too conservative and illustrate the need for more work to produce a more accurate time history from a response spectrum.

Seismic analysis of a pebble bed core with core barrel has been initiated by using a modified version of the CRUNCH-2D computer program. The major code modifications involve the addition of a flexible cylinder type structure for the simulation of the core barrel. The "pebbles" are represented by hexagonal block elements with nonlinear block stiffness based upon the force-deformation characteristics of identical spheres in compression.

### 6.3. DISCUSSION

#### 6.3.1. RCB/PCRIV Plant

The RCB is a cylindrical, reinforced concrete structure with a dome roof of spherical shape. The RCB houses the PCRIV and an inner crane support frame structure, all of which are situated on a common foundation base slab. The PCRIV is a multicavity reactor pressure vessel which houses all components carrying a primary gas coolant.

The dynamic model of the surface-founded RCB/PCRIV configuration is shown in Fig. 6-1. The structure is simulated as a multiple-degree-of-freedom lumped-parameter model supported by a rigid base slab which is

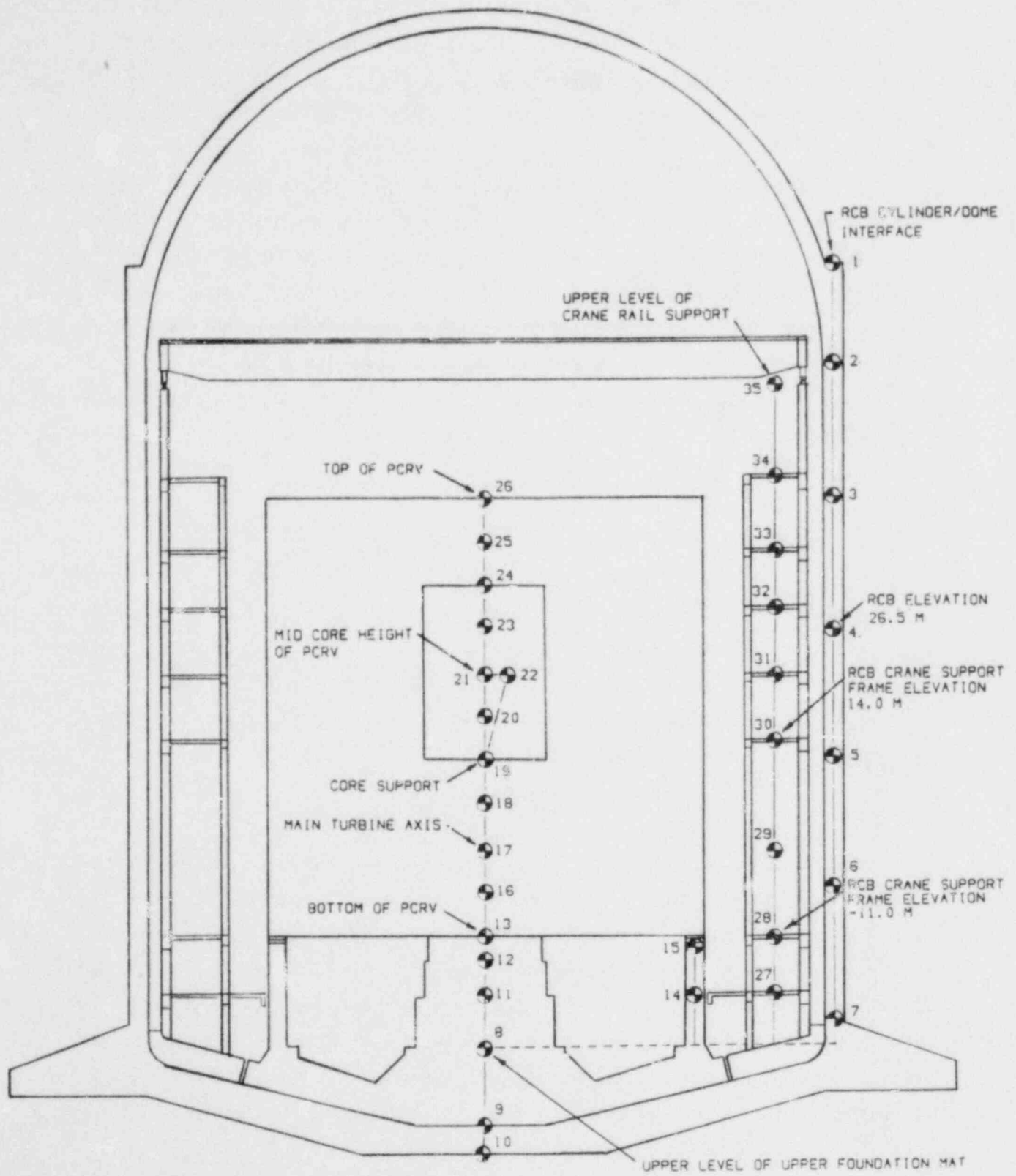


Fig. 6-1. Dynamic model of HHT demonstration plant RCB/PCRV with mass point locations

founded on an elastic half-space. Two separate analyses, one with PCRV neoprene support pads and one without, were performed. Typical response spectra with and without PCRV support pads are shown in Figs. 6-2 and 6-3.

A comparison of the response quantities shows that there is essentially no difference between the vibrational characteristics and the structural responses of the plant when the PCRV is situated on neoprene pads and when it is not. The neoprene pads behave in a rigid manner in comparison with the soft soil. The displacement response values represent the maximum values computed for a soft soil site characterized by a dynamic shear modulus of  $60 \text{ MN/m}^2$  (10,000 psi), are relative to the ground, and include the deformation resulting from the soil compliance functions of the elastic half-space analysis.

#### 6.3.2. Prismatic Block Gas Turbine Reactor Core

A modified MCOCO computer program was used for the seismic analysis of the prismatic block gas turbine reactor core. In order to better represent the gas turbine reactor core design, a new side shield arrangement was incorporated. One case was run: horizontal and vertical "envelopes" at a 0.15-g OBE with a total cross core gap of approximately 30 mm (1.1 in.), which is a new core at 100% operating condition.

The MCOCO model of the gas turbine reactor core is shown in Fig. 6-4. It consists of 34 columns, each containing six to 14 elements. These columns are supported on core support floor blocks which are in turn held up by support posts. The conservatism of the "enveloping" technique used is illustrated in Fig. 6-5, where the response envelope to be matched is compared with the actual spectra developed. The match is good above a period of 0.09 s, but the magnitudes separate to a ratio of more than 2 to 1 in the rigid range. This is typical for present techniques for producing time histories from response spectra.

# UPPER LEVEL OF UPPER FOUNDATION MAT

HORIZONTAL RESPONSE SPECTRA FOR 1.0G OPERATING BASIS EARTHQUAKE

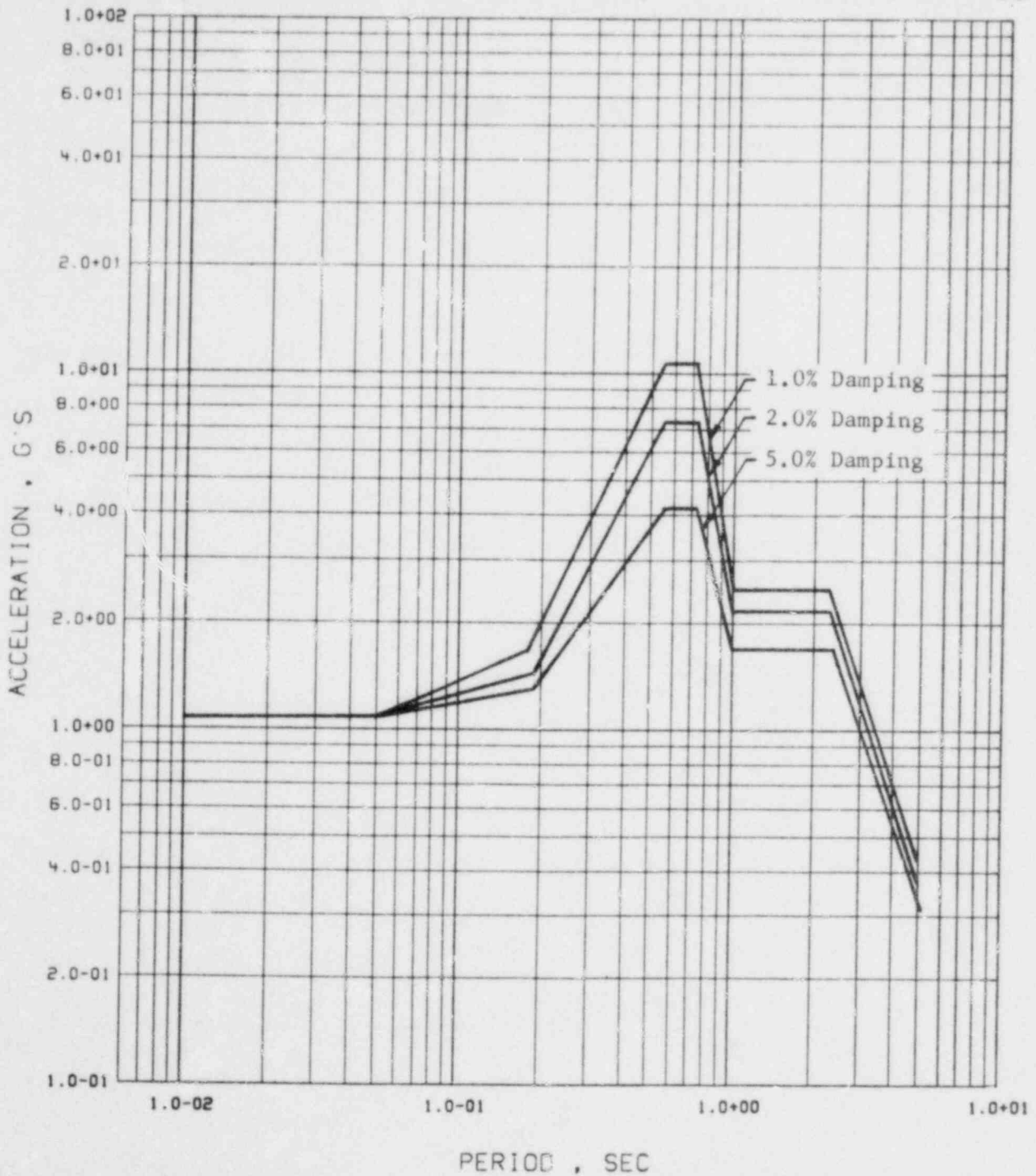


Fig. 6-2. Horizontal response spectra for 1-g OBE with PCR support pads

# UPPER LEVEL OF UPPER FOUNDATION MAT

## HORIZONTAL RESPONSE SPECTRA FOR 1.0G OPERATING BASIS EARTHQUAKE

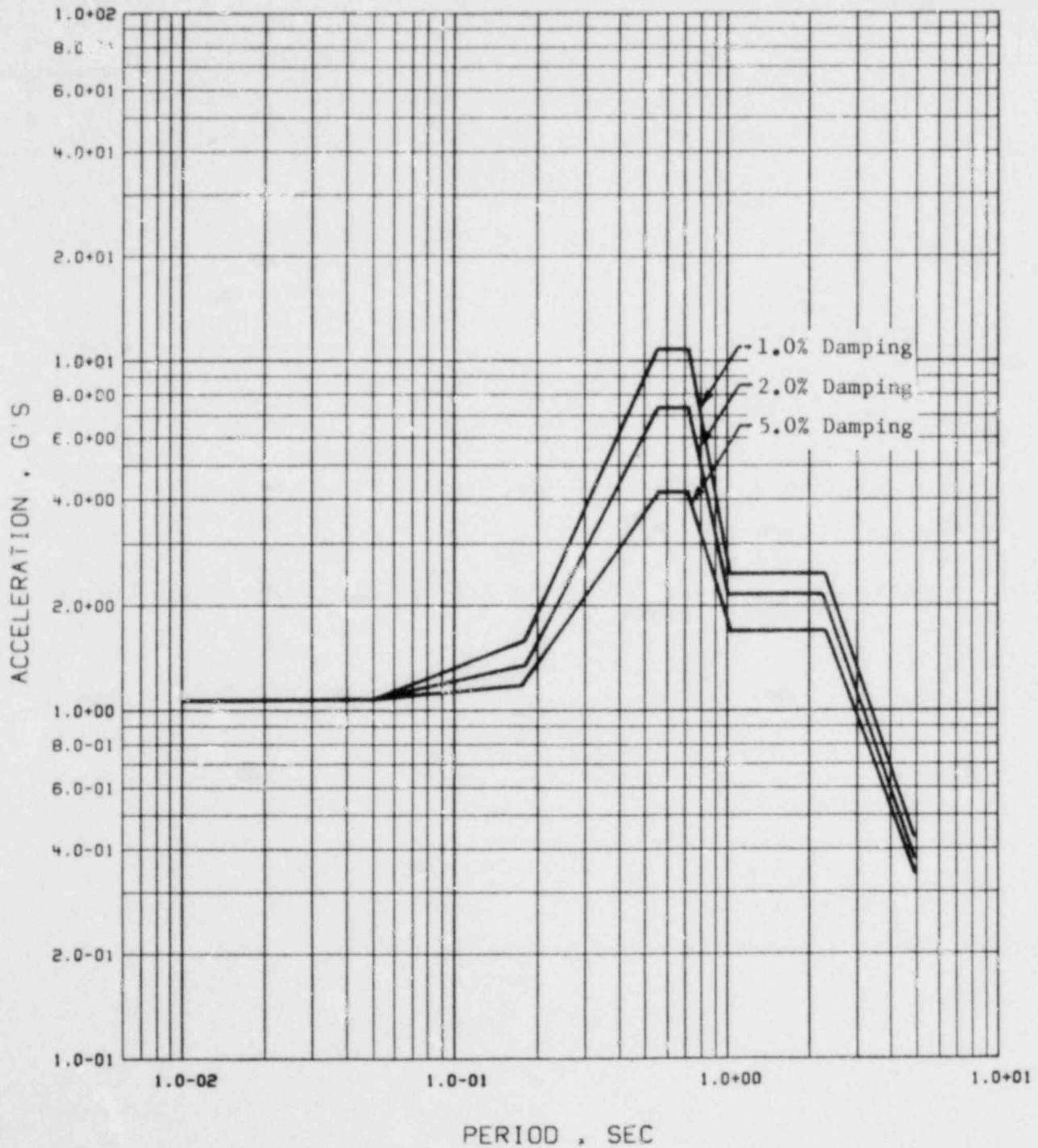
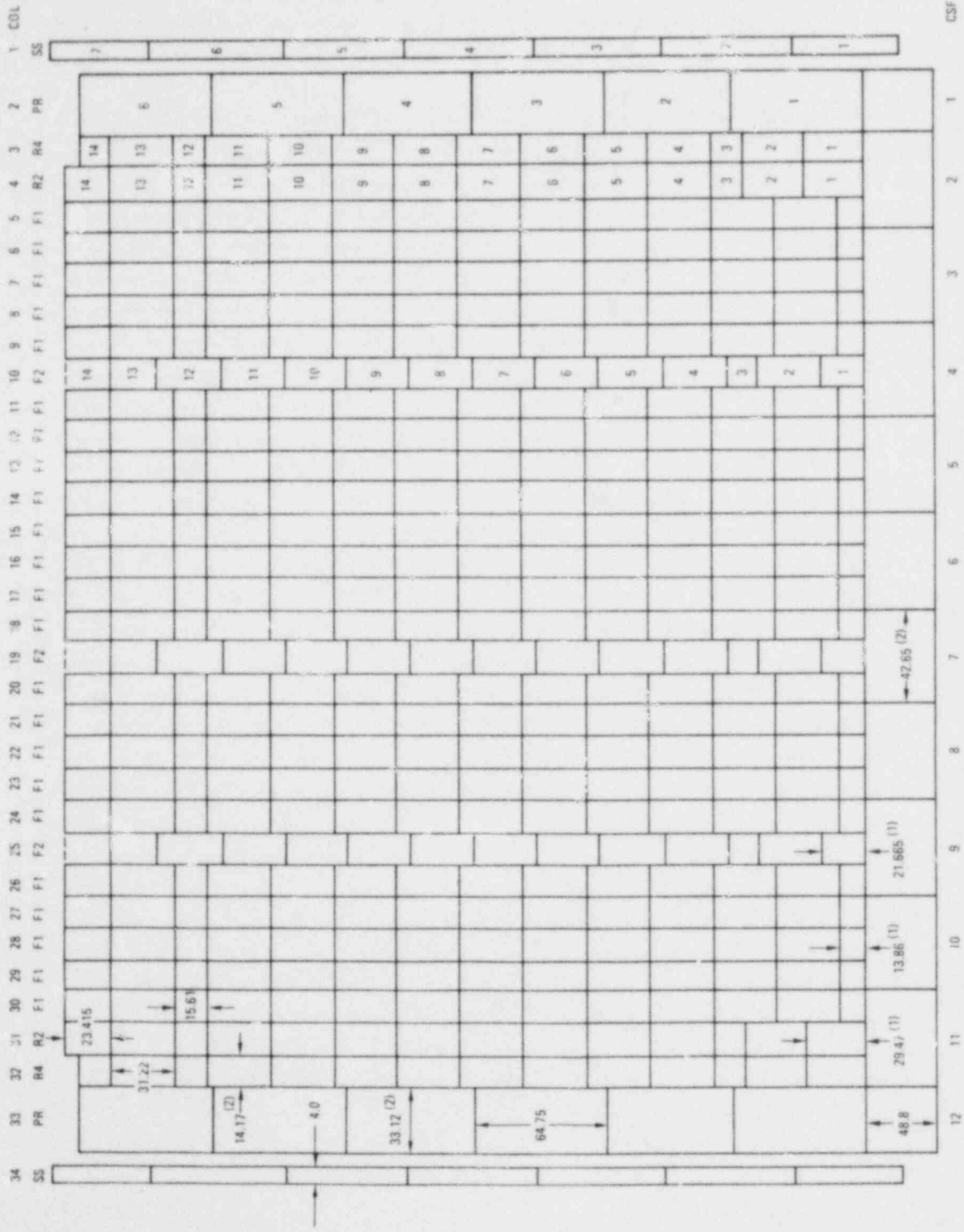


Fig. 6-3. Horizontal response spectra for 1-g OBE without PCR support pads



(1) ELEMENTS AT LEVEL 1 HAVE 1/5 IN. SUBTRACTED FROM HEIGHT FOR FLOOR INSERT.  
 (2) AT 100% POWER, REFLECTOR, FUEL AND FLOOR ELEMENT WIDTHS ARE 33.375, 14.2116 AND 42.745 IN., RESPECTIVELY.

Fig. 6-4. MCOCO model of full-scale gas turbine reactor core

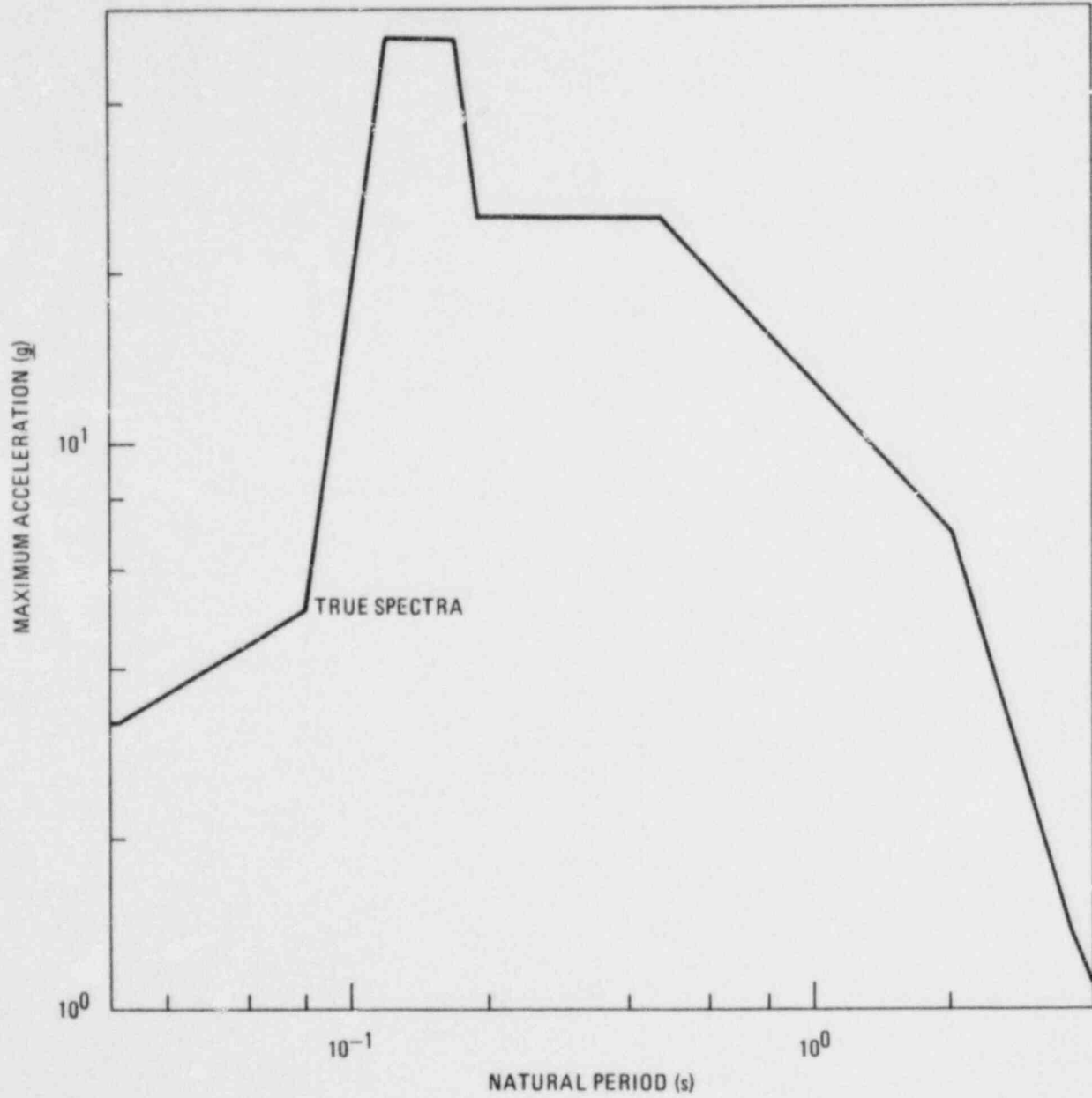


Fig. 6-5. OBE horizontal response at mid-core

### 6.3.3. Gas Turbine Pebble Bed Core

The dynamic response of a pebble bed core under seismic disturbances has been analyzed by studying the behavior of a horizontal slice of the core. The core model was chosen to be similar to that in the German HHT 1637-MW(t) Pebble Bed Demonstration Plant in which the graphite core is contained within a cylinder type core barrel.

The development of a three-dimensional computer model is time consuming, and alternative approaches seeking an approximate first solution to the problem were explored. The CRUNCH-2D computer program was utilized to conduct a first study of the problem.

The CRUNCH-2D computer program was modified to simulate a pebble bed core with core barrel by incorporating a flexible core barrel around the side reflectors as shown in Fig. 6-6. The code was originally developed for a prismatic block core, and an approximation has been made by grouping the pebbles together as solid lumps. In the modified version, the input motions are applied at the bottom of the core and transmitted upward through the barrel, which is supported on a series of shear springs simulating the effects of an elastic shell. Major modifications include the replacement of original core block stiffness by a nonlinear force-displacement relation derived from the consideration of Hertzian theory of spherical bodies in contact.

At this time, the results are only qualitative since the pebbles were represented by hexagonal block elements and a three-dimensional system was modeled by a horizontal planar array. However, these inherent limitations of the current computer program may be remedied in the future by code development and modifications.



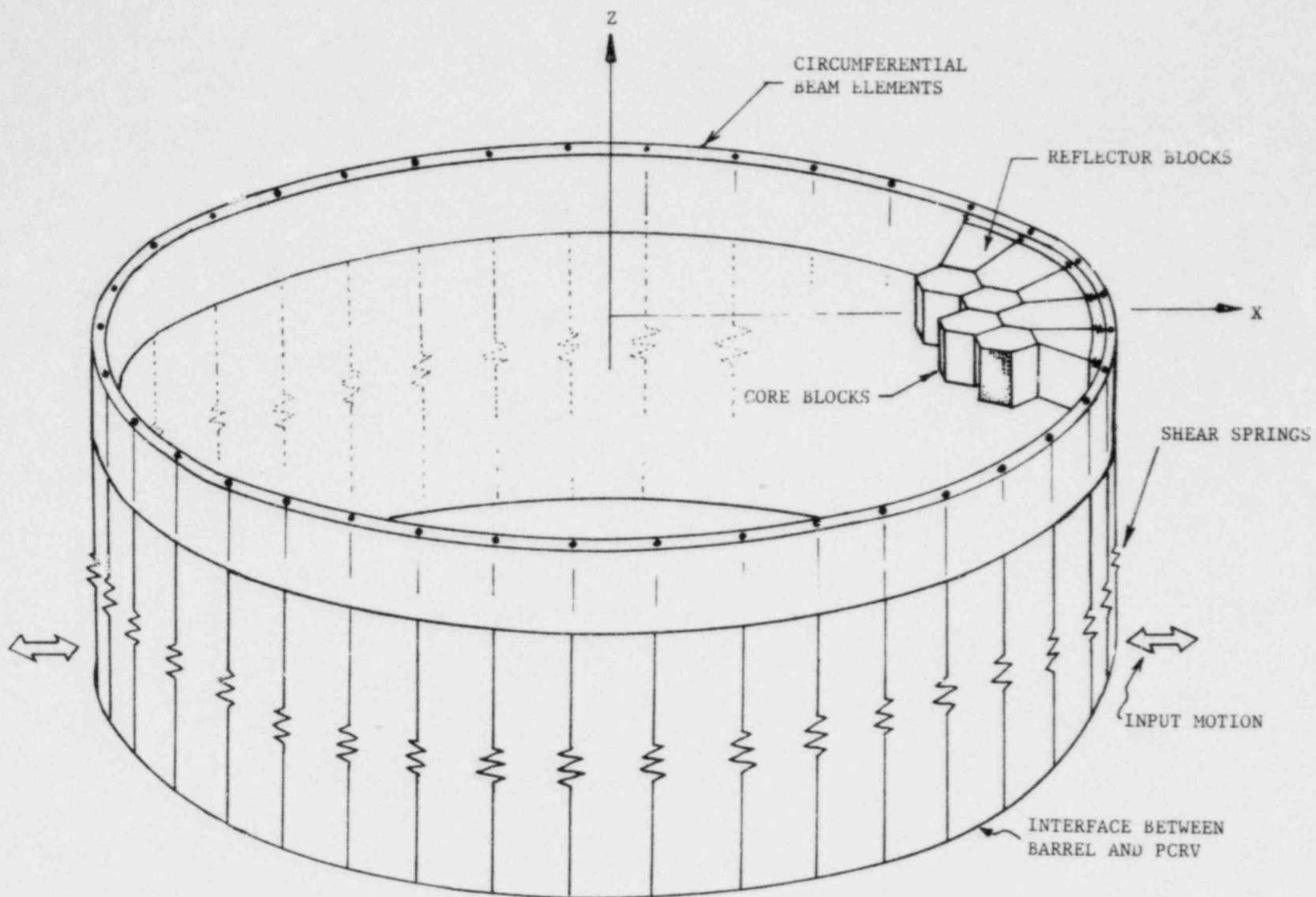


Fig. 6-6. Dynamic model simulated by modified CRUNCH-2D program

## 7. SHIELDING ANALYSIS AND DESIGN (630104)

### 7.1. SCOPE

The purpose of this task in FY-79 was to provide radiation protection and shielding analysis and design support to the HTGR-GT project.

### 7.2. SUMMARY

Thermal barrier evaluation included assessment of candidate materials for the thermal barrier coverplate, top head region, and center and lower sidewalls. Dose rates were calculated for the disassembled parts of the turbomachine, and decontamination procedures were investigated. Calculations were performed to determine the shielding requirements for the hot duct removal cask. In the area of helium control valve maintenance, calculations of dose rate on top of the control valve bonnet versus bonnet thickness were performed.

### 7.3. DISCUSSION

#### 7.3.1. Thermal Barrier Evaluation

The candidate materials proposed for the thermal barrier coverplates were qualitatively assessed from a shielding standpoint. The major areas of concern are radiation damage in the form of high-temperature embrittlement and neutron activation of the coverplate materials. The amounts of boron and cobalt in the materials dictate the degree of radiation damage and neutron activation, respectively. In general, use of materials with significant amounts of boron and/or cobalt is discouraged, especially in an environment of high operating temperature and/or high thermal neutron flux.

In the top head region where the thermal neutron flux is fairly low, material selection may be based upon the merits of physical properties rather than the consideration of radiation effects. Similarly, there is no radiation problem with the materials proposed for the upper sidewall region, since the thermal flux and operating temperature are still sufficiently low.

Because of the high thermal neutron flux at the center sidewall, the use of such materials as IN 100, Hastelloy X, Rene 100, and IN 738 would result in significant Co-60 activity. It is advisable to avoid these materials if possible.

Carbon-carbon, a preferred material for the lower sidewall, is able to withstand a neutron fluence much higher than the current limit of  $10^{17}$  nvt thermal. Fast neutrons rather than thermal neutrons are of concern for carbon-carbon. If carbon-carbon is selected, it may be possible to reduce the height of the bottom reflector and core support by removing or relaxing the current constraint on the thermal neutron fluence at the lower sidewall.

#### 7.3.2. Turbomachine Disassembly and Decontamination

Dose rates were calculated for the disassembled parts of the turbomachine. Figure 7-1 shows the results for the case in which the split casing between the turbine and compressor has been removed and the turbine and compressor units are separated. The results are based upon the plate-out data for Level A activity, 6-yr operating time, and 100-day decay in the various regions of the turbomachine. All dose points are 61 cm (2 ft) from surfaces.

After the stator casing and containment ring are removed, the dose rate at 61 cm (2 ft) from the tip of the exposed turbine blades was found to be 12.6 rads/h. The corresponding configuration for the compressor gave 0.26 rad/h.

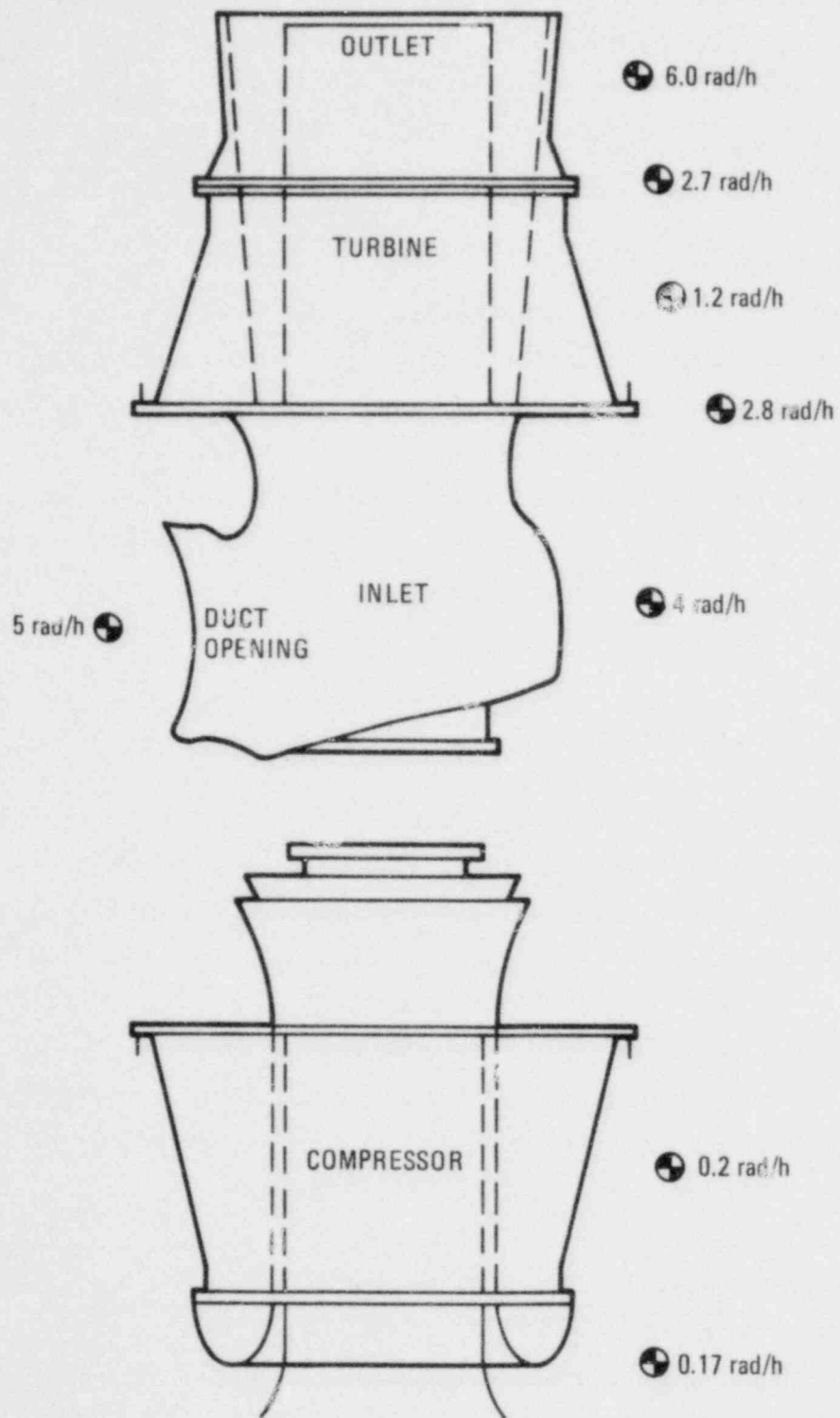


Fig. 7-1. Dose rates for separated turbine and compressor

The predominant contributor to the dose rate for the turbine unit is Ag-110m, whereas cesium nuclides are most important for the compressor unit dose rate. If the expected rather than design plateout distributions were used, the effect on the dose rate for the turbine would be small, but the dose rate for the compressor could drop a factor of 35.

Decontamination is required in order to perform contact maintenance on the turbomachine. For most external surfaces of the turbine and compressor, where the decontamination factor is 200 or less, standard procedures using such solutions as water, steam, and acid may reduce dose rates in the absence of shielding to the 10 mrad/h level. However, the situation for the rotor and stator blades is complicated by the high dose rate (12.6 rad/h) without shielding and the inaccessibility with the stator casing in place. Pending further investigation, remote handling should be considered in this situation.

### 7.3.3. Hot Duct Removal

Detailed calculations were performed to determine the shielding requirements for the hot duct removal cask. The dose rate criteria are prescribed as 20 mrem/h at the personnel level, or below the 244-cm (8-ft) height, and 100 mrem/h above the 244-cm height.

The source terms used for shielding design were the plateout activities for Level B, 40-yr operation, and 10-day decay. Preferential plateout was used on the hot (or inner) surface of the duct, whereas uniform plateout was assumed on the cold surface.

The preliminary steel thicknesses required for the various portions of the removal cask are shown in Fig. 7-2. Ag-110m is a principal contributor to the dose rate outside the cask.

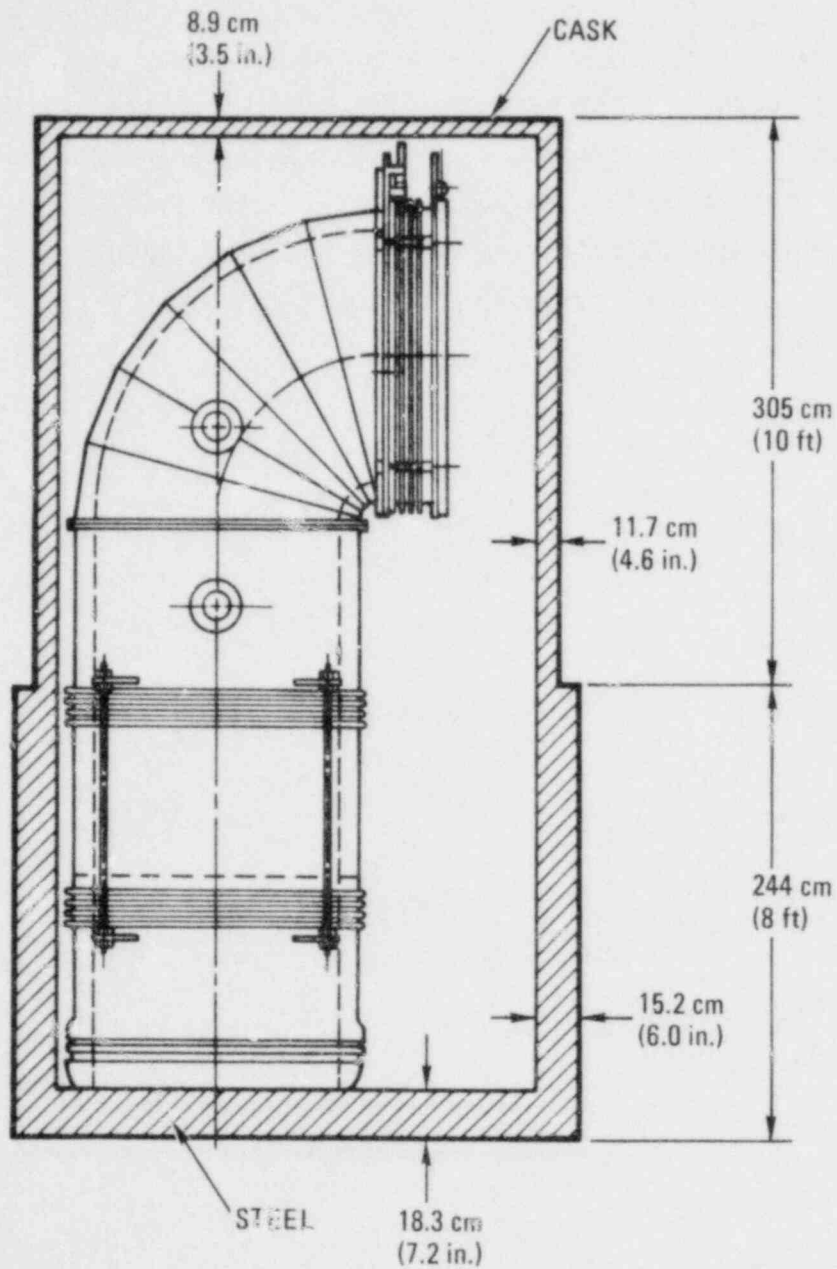


Fig. 7-2. Hot duct removal cask steel thicknesses

#### 7.3.4. Helium Control Valve Maintenance

For access to the helium control valves in the PCRV top head, calculations were performed of the dose rate on top of the control valve bonnet as a function of bonnet thickness. It was found that designing the bonnet with a 10-cm (3.9-in.) steel thickness will keep the dose rate below 10 mrem/h at 10 days after shutdown. With this thickness, the dose rate above the bonnet during operation will be less than 20 mrem/h. These dose rates correspond to a 40-yr Level B plateout accumulation.

## 8. LICENSING (6302)

### 8.1. SCOPE

The purpose of this task in FY-79 was to provide design reviews and licensing positions, develop and maintain an HTGT-GT Nuclear Safety Plant Specification, and provide recommendations on preapplication review topics.

### 8.2. SUMMARY

Principal design reviews were as follows:

1. Nuclear industry precedents and Nuclear Regulatory Commission (NRC) guidance were reviewed to determine the design requirements for HTGR-GT components which might be relied upon to ensure core cooling during turbomachine coastdown. The conclusion reached is that such components must be Safety Class 2 and Seismic Category I.
2. Proposed CACS criteria, design basis events, and component safety classes were reviewed for compatibility with prior requirements and to ensure the consideration of required safety functions at accident scenarios.
3. The licensing implications of precooler safety class and seismic requirements were examined to delineate the advantages and disadvantages of designing the precoolers as non-safety related or safety related. A final decision has not been reached.



4. Proposed safety classifications for the turbomachine shaft and shaft seals were reviewed to identify minimum requirements for safety class components. Preliminary conclusions are that the shaft, shaft seal, and shaft seal housing constitute portions of the primary coolant system boundary and are therefore Safety Class 1.

The initial issue of the Nuclear Safety Plant Specification for the HTGR-GT was prepared. The specification developed over the past several years for the HTGR-SC plant has been modified by incorporating information specific to systems, design criteria, and transients and accidents for the HTGR-GT.

Recommendations for preapplication review licensing topical reports (LTRs) specific to the HTGR-GT were made and distributed for comment. The recommended topics are intended to address major safety issues that are expected to arise in licensing an HTGR-GT plant.

### 8.3. DISCUSSION

#### 8.3.1. Design Reviews

8.3.1.1. Component Design Requirements. In considering the possibility of taking credit for turbomachine coastdown prior to initiating CACS cooling in order to lessen the heat load on the CACS, the question of whether the turbomachine, recuperator, and precoolers must be safety class and/or Seismic Category I has arisen. The answer to this question can have a significant impact on design and cost; a licensing position was therefore developed based on nuclear industry precedents and NRC guidance.

There are two clear precedents from the light water reactor (LWR) licensing activities which are applicable to the above question. The first of these is the requirement for seismic capability of pressurized water reactor (PWR) main coolant pumps. PWR plants must take credit for main

coolant pump coastdown during certain reactor transients. To ensure that the pumps can reliably supply this coastdown, the pump/motor system is designed for the SSE. In addition, it is reasonable to conclude that any other component or system which is essential to assuring coastdown would have to be Seismic Category I. Application of this precedent and reasoning to the HTGR-GT indicates that the turbomachine, the precooler, and any other main loop components which could reduce helium flow or heat removal would have to be Seismic Category I. Furthermore, Regulatory Guide 1.29 is explicit in requiring that "systems or portions of systems that are required for emergency core cooling" and/or "residual heat removal" be designed to Seismic Category I requirements.

The second LWR precedent concerns the safety class of components which are relied upon to ensure core cooling during coastdown. For the LWR, main coolant pump parts which ensure coastdown are designed to Safety Class 2 requirements. This choice of safety class is obvious based on the requirements of Regulatory Guide 1.26 and the American Nuclear Society classification system, since both require Safety Class 2 for systems or portions of systems necessary to ensure adequate reactor core cooling. This same safety function, reactor core cooling, is the purpose of ensuring turbomachine coastdown in the HTGR-GT. Therefore, the HTGR-GT main loop components necessary to perform this function would have to be Safety Class 2.

8.3.1.2. CACS Criteria. Criteria for the HTGR-GT plant CACS, which are under development, may be somewhat different from those for an HTGR-SC plant. Criteria proposed by the system designers have been reviewed to ensure that the necessary safety functions and accident scenarios are considered in the design. Precedents as expressed in the Nuclear Safety Plant Specification for the HTGR-SC are largely appropriate, but the HTGR-GT introduces some different considerations, such as potential core bypasses for coolant flow resulting from failures in ducts, heat exchangers, and the turbomachine. This leads to consideration of safety classifications for

components of the power conversion loop, as well as accidents initiated by failures within the loop. Comments on the safety classification and accident scenarios were provided.

8.3.1.3. Precooler Safety Class. The safety class and seismic requirements for the precoolers have not been entirely resolved. It is desirable to minimize the cost of these large heat exchangers by making them non-safety related and non-Seismic Category I. However, such minimum requirements have significant ramifications with regard to licensability, which have been examined.

There are several combinations of safety class and seismic requirements which may be considered for the precoolers. Those listed below are judged to be representative of the spectrum of choices. The cases are listed in the order of increasingly stringent designs.

Case 1: Safety Class Non-Nuclear, Non-Seismic Category I

Advantage: 1. Minimum cost

Disadvantages: 1. Must assume simultaneous failure of all precoolers during a seismic event.  
2. Can take no credit for heat removal during turbomachine coastdown.  
3. Primary coolant system boundary (PCSB) is extended out of the PCRV to the pipes and valves of the CWS.

Case 2: Safety Class Non-Nuclear, Seismic Category I

Advantage: 1. Can take credit for integrity during a seismic event.

Disadvantages: 1. More costly than Case 1.  
2. Same as Case 1, disadvantages 2 and 3.

Case 3: Safety Class 2, Seismic Category I

- Advantages:
1. Same as Case 2, advantage 1.
  2. Can take credit for heat removal during turbomachine coastdown.
  3. Can take credit for the precooler tubes following CWS pipe rupture.

- Disadvantages:
1. More costly than Case 2.
  2. Same as Case 1, disadvantage 3.

Case 4: Safety Class 1, Seismic Category I

- Advantages:
1. Same as Case 3, advantages 1, 2, and 3.
  2. PCSB does not extend into the CWS.
  3. Minimum licensing risk.

- Disadvantages:
1. Highest cost for analysis; cost impact on hardware not determined.

Before a final conclusion can be reached, it will be necessary to analyze the consequences of two events. These are the simultaneous massive failure of the precoolers during a seismic event and the blowdown of the PCRV via the largest cooling water pipe. The latter event must be considered for a non-nuclear precooler because the PCSB extends outside the PCRV and the assumption of a pipe rupture is required without benefit of credit for precooler integrity.

8.3.1.4. Turbomachine Shaft and Shaft Seal Safety Class. The turbomachine for the most part is considered to be non-safety related. However, because the shaft penetrates the PCRV, a portion is PCSB, and therefore Safety Class 1. The proposed safety classes of various components were reviewed, and it was concluded that the PCSB includes, as a minimum, the primary shaft seal, the shutdown seal, the seal housing, and the section of shaft penetrating the PCRV. Other components, including the thrust bearing, were tentatively judged to be non-safety related based on a preliminary analysis of failure consequences.

### 8.3.2. Nuclear Safety Plant Specification

The initial issue of the Nuclear Safety Plant Specification for the two-loop HTGR-GT has been prepared. The basic design philosophy as expressed in such topics as Plant Conditions and Plant Safety Criteria, Single Failure, Seismic Category, Loading Combinations and Service Limits, and Safety Class is essentially the same as in the predecessor documents for the HTGR-SC plant. The principal revisions affect the sections on Systems Criteria and Transients and Accidents for Design Considerations. Since the information in both of these areas is still quite preliminary, the specification will require revision as the design develops and analyses of transients and accidents proceed.

### 8.3.3. Proposed HTGR-GT Specific LTRs

An HTGR-GT plant is a significant departure from previous safety and licensing experience as exemplified by the HTGR-SC plant. Therefore, a number of different safety issues or potential safety issues have been identified which must be addressed in the licensing process. One method of obtaining NRC review of issues is through Licensing Topical Reports (LTRs) submitted on specific topics, as is presently in progress for the Generic Technology Program preapplication review program.

A review of the various issues was made, and the following were selected as the most appropriate LTR topics:

- Analyses of Rotating Machinery Failures.
- Internal Pressure Equilibration Accidents.
- Design Bases for the Turbomachine Shaft and Seal.
- Design Bases for the Bypass/Safety Valves and Actuators.
- Systems Dynamics Code, REALY2.
- Performance Criteria for the CACS.

## 9. SAFETY (6307)

### 9.1. SCOPE

The purpose of this task in FY-79 was to provide a safety assessment of design issues and to support the HHT program by reviewing Federal Republic of Germany (FRG) general safety design criteria and HHT safety criteria.

### 9.2. SUMMARY

Because of the significant impact on the core, thermal barrier, and reactor internals and components, considerable emphasis has been placed on the evaluation of the transient behavior of the primary coolant system during postulated turbine deblading accidents. For conservatism, complete deblading events have been considered. Such events can result in extremely high-pressure transients throughout the primary coolant system. The rate of pressure decay in the core outlet plenum and hot duct and the maximum differential pressure across the core during these transients are of particular importance. Simulation of the turbine deblading accident has been performed using the RATSAM program. A preliminary HTGR-GT version of this program was completed, and both two- and three-loop HTGR-GT designs were modeled. However, these designs were not consistent, so only the two-loop results are reported here. Core outlet plenum depressurization rates as high as 15.0 MPa/s\* (2180 psi/s\*) have been calculated. Corresponding maximum core differential pressures for the two-loop plant are greater than approximately 0.48 MPa (70 psi). Both the core outlet plenum depressurization rate and maximum core differential pressure are relatively strong

---

\*These rates are the maximum calculated over any 0.010-s period.

functions of the core flow resistance. If the first stage inlet nozzle vanes are assumed to remain intact, the maximum core outlet plenum depressurization rate is limited to approximately 7.31 MPa/s\* (1060 psi/s\*), and the maximum differential pressure across the core is approximately 0.28 MPa (40 psi).

The TUBE program was used in earlier HTGR-GT studies of turbomachine deblading events to study local effects in ducts. However, it requires a priori knowledge of the time dependent boundary conditions. Development of the program has continued. An initialization routine to determine steady-state flow conditions in an arbitrary flow path, given a mass flow rate and upstream reservoir condition, has been developed and included in the program. In addition, modifications have been made to limit numerically induced secondary transients which had been observed to result from the program's model for gradual area changes.

Considerable effort was also devoted to support of the HHT program. Most of this effort was in the development of German HTR specific safety criteria and was provided by a GA staff member assigned to HRB in Mannheim for 3 months. In addition, a RATSAM simulation of an HHT turbine deblading accident was performed as a "benchmark calculation." This simulation was reasonably successful and serves, in part, as verification of the analytical tools used by GA and the HHT program.

A review of the selection of a DBDA for the HTGR-GT was also performed. This review has resulted in the recommendation that the HTGR-GT adopt the HTGR-SC plant philosophy which contends that failures of ASME Section III, Division I, Class 1 penetrations and closures need not be postulated. Accordingly, the DBDA flow area should be related to some other feature of the primary coolant system boundary (PCSB) design which may credibly be assumed to fail (e.g., connecting pipe or rotating shaft seal).

The potential for pressure buildup in the PCRV resulting from various sources was estimated to evaluate the adequacy of internal pressure relief. It was concluded that sources of water and helium ingress did not have the potential for overpressurizing the PCRV. The accidental pumping of the complete oil inventory into the PCRV, through defective journal bearing seals, might increase the PCRV pressure to undesirable levels if the injected oil decomposed at the temperatures prevailing in the reactor core. However, the overall size of the PCRV relief line penetration required to mitigate this conservative accident is such that no redesign of the PCRV would be necessary. Thus, the event can be studied at a later date when design details are available.

### 9.3. DISCUSSION

#### 9.3.1. Pressure Equilibration Rates

Pressure equilibration rates for turbine deblading events have been estimated using the RATSAM program for both two-loop [800-MW(e)] and three-loop [1200-MW(e)] plants. These studies were performed with and without turbomachine dynamics and control valve actions; however, these variations did not impact the results dramatically. The rates of depressurization in the core outlet plenum have been shown to be significantly affected by the plenum volume and the flow resistance of the core.

The RATSAM model for the three-loop, 1200-MW(e) plant was based on very preliminary design data, whereas the model for the two-loop, 800-MW(e) plant reflected more recent design information. Accordingly, only the two-loop results are reported here. Owing to the larger volume of the core outlet plenum for the 1200-MW(e) plant, it is expected that depressurization rates will be smaller for that plant than for the 800-MW(e) plant with identical main loops.



Maximum depressurization rates (over any 0.010-s period) in the core outlet plenum and turbine inlet plenum have been calculated to be 15 MPa/s (2180 psi/s) and 56.9 MPa/s (8255 psi/s), respectively. The maximum core differential pressure for this case is estimated to be greater than approximately 0.48 MPa (70 psi). However, if the first stage inlet nozzle vanes can be assumed to remain intact during the deblading, the above rates can be reduced to 7.3 MPa/s (1054 psi/s) and 17.6 MPa/s (2555 psi/s). The corresponding maximum core differential pressure for this case is calculated to be only 0.28 MPa (40 psi). This dramatic reduction in depressurization rates is caused by the increased resistance to flow offered by the intact nozzle vanes. At normal conditions, the pressure drop across these vanes has been estimated by the turbine designer to be 1/12 of the total turbine pressure loss.

The turbomachinery designer is designing with greater than normal separation between the first stage inlet nozzle vanes and the first stage turbine blades in an attempt to ensure nozzle integrity and to attenuate inlet sound power levels. If the flow resistance of the former can be assumed to remain intact during the turbine deblading event with a high degree of assurance, it is clear that the design basis depressurization rates for this event will be reduced considerably.

### 9.3.2. TUBE Program Development and Verification

The TUBE program was developed primarily for the pressure equilibration transients associated with HTCR-GT turbomachine deblading accidents. However, it is written in a very general manner and can be applied to a variety of fluid flow transients for which time dependent boundary conditions are prescribed. The program solves the general one-dimensional transient equations (i.e., conservation laws) for the flow of an ideal gas through a variable area tube assuming no heat transfer between the gas and the tube walls and no source of momentum within the control volume.

In applying the program to variable area ducts, it was observed that transients could be induced in the absence of a forcing function. Further investigation indicated that these self-induced transients originated at the "ends" of variable area ducts and were due to the manner in which the conservation equations were expressed prior to finite differencing. The original formulation of the equations, once expressed in divided difference form, required interpolation in flow area and gradient of flow area, which introduces errors when the area varies with distance. By rewriting the conservation equations in a slightly different form before differencing, most of this interpolation error has been eliminated.

A steady-state routine has also been incorporated into the TUBE program to allow the calculation of a non-zero initial velocity and corresponding pressure distribution throughout the system of ducts. Because some difficulties have been experienced with this routine, its development will continue in FY-80.

Some effort was also devoted to developing a TUBE model for turbine deblading. Attempts to simulate a very large pressure drop through a turbine cavity by large, local friction factors have met with some success. However, this method has problems which must be resolved before it can be accepted. Resolution of these problems will be addressed in FY-80.

### 9.3.3. Review of Primary Coolant System Boundary

The purpose of this task was to review safety problems associated with loss of integrity of the PCSB. This effort consisted primarily of an attempt (1) to define the DBDA for the HTGR-GT and (2) to determine the potential for overpressurization of the PCRV resulting from the ingress of secondary fluids.

9.3.3.1. DBDA Definition. For the HTGR-GT, maximum depressurization rates and corresponding dynamic component loads will most likely occur during postulated turbomachine deblading events or catastrophic failure of the recuperator, i.e., pressure equilibration accidents. However, these events will not release any primary coolant from the PCRV. Thus, for the HTGR-GT, the DBDA will be associated with the loss of integrity of the primary coolant system, which results in the highest peak containment pressure. For the large HTGRs designed for the Summit Power Station and Fulton Generating Station, the DBDA was associated with a penetration closure failure. However, it is currently recommended for both the HTGR-SC and the direct cycle HTGR that failures of ASME Section III, Division I, Class 1 penetrations and closures not be considered as design basis events. The proposed DBDA flow area would be related to some other feature of the PCSB design which may credibly be assumed to fail (e.g., connecting pipe or rotating shaft seal).

The selection of a DBDA for the HTGR-GT is also clouded by the safety classification of the precoolers. If the precooler is designated non-nuclear and the circulating water system (CWS) piping within the containment is defined as part of the PCSB, it may be necessary to postulate failure of this piping. What credit can be taken for the non-nuclear pre-cooler tubing during this event is not clear at this time.

9.3.3.2. PCRV Overpressurization. Although the HTGR-GT primary coolant system contains a large helium inventory, and hence the containment free volume must be sufficiently large to accommodate this inventory without excessive design pressures, the arrangement of the PCSB is such that there appears to be no potential for a "hot leg" blowdown. The so-called hot leg of the HTGR-GT consists only of the core outlet plenum, turbine inlet ducts, and lower CACS ducts. These regions have virtually no potential for gross leakage to the containment.

To assess the adequacy of the internal pressure relief system currently considered for the HTGR-GT (i.e., the ability of turbine bypass valves to relieve high pressure to the low-pressure regions of the PCSB), accident events with a potential for long-term pressure buildup on the primary coolant system were identified and evaluated. The basic approach was to determine if all events would fall into one of two categories:

1. The event is so unlikely that it would never become a design basis event, even in the licensing process.
2. The event would not require redesign of the PCRV even if a relief line were required later and irrespective of whether the probability is very low.

The basic approach was therefore to show the degree of assurance that the PCRV design may proceed without risking redesign, rather than to assess the likelihood that NRC or code committees would require relief trains in the future. Also, the task did not include new methods or designs to avoid pressure rise in the PCRV.

The fault tree in Fig. 9-1 shows those events which could possibly lead to PCRV overpressurization. Of the four branches shown in the figure, a decrease of the PCRV volume is not considered credible, while flow transients in the PCRV have only a negligible effect on pressure. The behavior of the compressors is responsible for the latter. Unrestricted core heatup and failure to trip with resulting large temperature increases in the PCRV and associated pressure increase are not design basis accidents because they are very unlikely to occur. Therefore, only material added to the PCRV atmosphere need be considered to determine if it poses a potential overpressurization hazard. PCRV redesign could be required for such events, which are identified as cases 1 through 5 in Fig. 9-1.

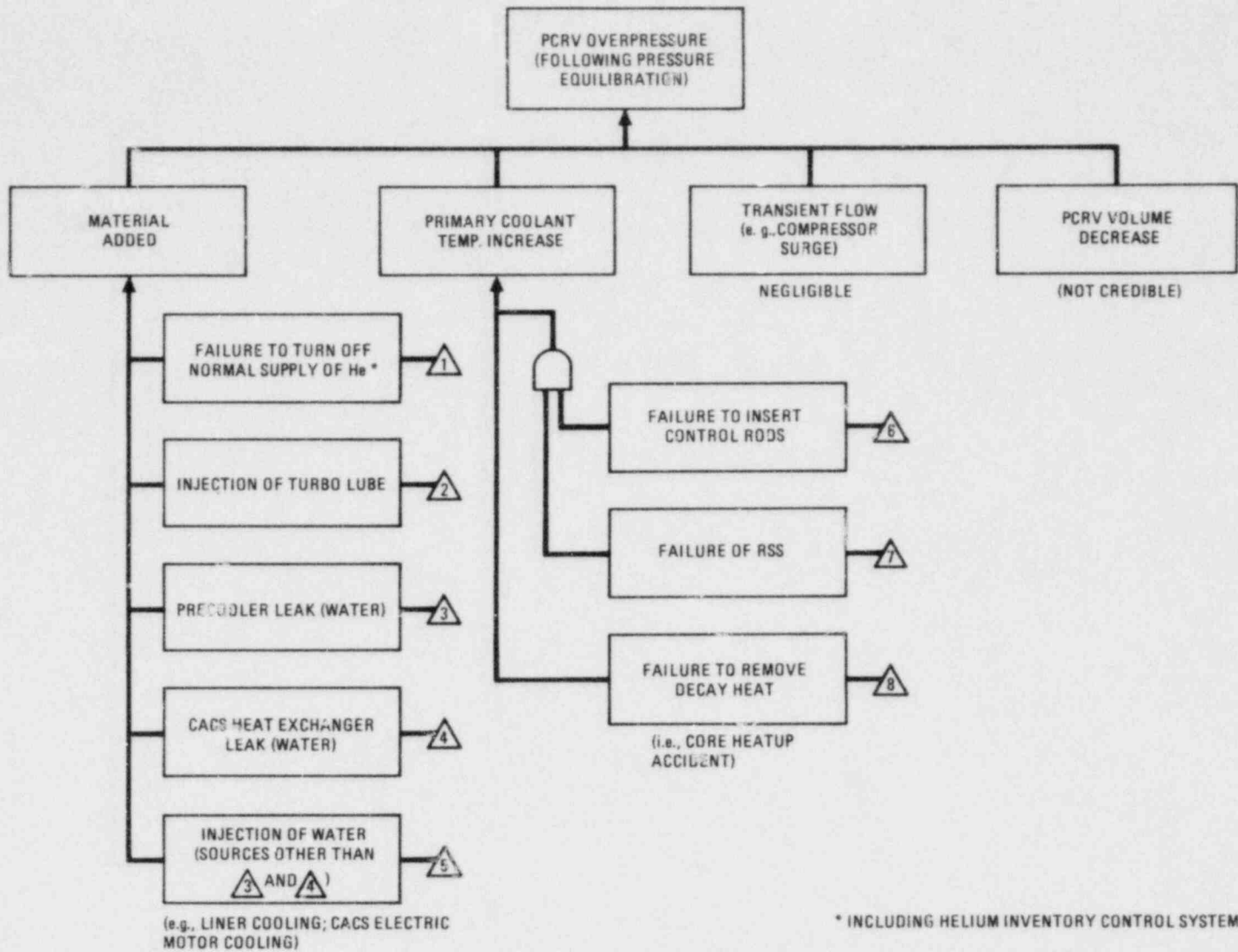


Fig. 9-1. Fault tree showing events that could lead to PCR V overpressurization

Case 1 corresponds not only to the helium purification system but also to the helium inventory control system. Since Case 5 is less severe than case 2, the latter, referred to as "oil ingress," has been selected for investigation.

#### Helium Injection into the PCRV (Case 1)

If the temperatures inside the PCRV remain essentially invariable during some accidental or inadvertent helium injection, then the total injection must not exceed 5811 kg (12,800 lb). To avoid PCRV pressures over 8.3 MPa (1200 psia) under equilibrium conditions. Thus, the tolerable amount of injected helium represents 30.4% of the nominal PCRV inventory.

Helium may be injected into the PCRV from two different sources:

1. Helium purification system. The total inventory of the helium purification system is 2722 kg (6000 lb), well below the 5811 kg (12,800 lb) allowable. Consequently, no overpressurization of the PCRV is posed by this helium inventory.
2. Helium inventory control system (includes a helium purification system). For the bladder configuration, the total inventory is 3405 kg (7500 lb), which can be driven by either water or oil. For the compressor system, the total inventory is about 7264 kg (16,000 lb). Thus, while the former configuration does not pose any overpressurization hazards for the PCRV in case of helium injection, the latter configuration contains sufficient helium to overpressurize the system. Knowledge of all the compressor-motor characteristics is required to compute the surge or stall point of the compressors, which limits the maximum amount of helium that may likely be below the amount required to overpressurize the PCRV [i.e., 5811 kg (12,800 lb)].

### Oil Ingress (Case 2)

An unintentional diversion of the complete oil inventory into the PCRV, through defective journal bearing seals, may increase the PCRV pressure if the injected oil decomposes at the temperatures prevailing in the reactor core. To conservatively assess the PCRV pressurization due to oil ingress, the oil is assumed to decompose into methane and carbon immediately after ingress. Since the oil pumping rate is maintained constant, the pressure increase rate is also constant, reaching the safety valve setpoint approximately 20 min after initiation of oil ingress.

At the opening of the safety relief valve, the rate of the PCRV efflux must be equal to the generation rate of methane to avoid further pressurization of the PCRV. This condition is satisfied by a valve with a net flow area of approximately  $14.8 \text{ cm}^2$  ( $2.3 \text{ in.}^2$ ) [i.e.,  $4.3 \text{ cm}$  ( $1.70 \text{ in.}$ ) diameter], which is well below the size which could be added to the PCRV later without requiring redesign of the vessel.

### Precooler Water Ingress (Case 3)

Assuming that the precoolers are non-safety, non-seismic components, then in the event of an earthquake, the simultaneous rupture of the pre-cooler tubes may allow the ingress of the total water inventory of the two precoolers into the PCRV. The water would cascade down to the turbomachinery cavities. Since there are flow passages between the compressor and turbine, the water would fill the cavities evenly, reaching thermal equilibrium with the metal masses. A thermal balance calculation indicates that the equilibrium temperature of the water would not exceed  $204^\circ\text{C}$  ( $400^\circ\text{F}$ ), and consequently it would not boil [saturation pressure  $1.6 \text{ MPa}$  ( $230 \text{ psia}$ ), i.e., below the initial equilibrium pressure of  $63 \text{ MPa}$  ( $920 \text{ psia}$ )]. Under these conditions, the PCRV atmosphere can be saturated (100% moisture) and still remain well below the  $8.2\text{-MPa}$  ( $1200\text{-psia}$ ) setpoint of a relief valve into the containment building (should such a valve be part of the design). This will be true as long as the pool of water is maintained below  $204^\circ\text{C}$  ( $400^\circ\text{F}$ ).

For the worst case conditions during a pressurized cooldown at approximately 1/2 to 1 h after start of CACS operation, inlet and outlet water temperatures of 153°C (308°F) and 284°C (544°F), respectively, are estimated.

An estimate of the mass transfer by natural circulation indicates that in about 1 week, the PCRV atmosphere can be saturated with water vapor. However, its reaction rate with the graphite is so low at the temperatures established by the CACS [260°C (500°F)] that the pressure rise due to water gas formation is negligible.

#### CACS Water Ingress (Case 4)

The total amount of water in the CACS which can be transferred to the PCRV is about 16,300 l (4300 gal). The instantaneous vaporization of the accidentally transferred water does not pose any overpressurization hazard for the PCRV, since the maximum allowable amount of vaporized water to reach 8.27 MPa (1200 psia) is almost 26,500 l (7000 gal).

#### Core Heatup

Although core heatup is not a case chosen for investigation since it is not a design basis event, it was examined briefly to provide more understanding of the problem of overpressurization.

For comparative purposes, calculations were performed to determine the net flow area of a HTGR-GT PCRV relief valve required to vent the helium flow rate to compensate for the pressure buildup at the initiation of the blowdown during the unrestricted core heatup accident. The minimum area to prevent pressure buildup in the PCRV [0.38-cm (0.15-in.) dia.] is so small in comparison with the net flow area of 14.8 cm<sup>2</sup> (2.3 in.<sup>2</sup>) determined for the oil ingress accident (case 5) for the HTGR-GT that no redesign of the PCRV with regard to the relief line penetration would be required.



When an equilibration pressure of 8.2 MPa (1200 psia) is reached in the HTGR-GT PCRV, the temperature of its boundaries has probably already affected their integrity. Therefore, a manually or temperature actuated valve would be required if it were desired to initiate the controlled PCRV blowdown into the containment building. This would be done only if the pressure could not be relieved through the helium purification system to the storage system.

#### 9.3.4. HHT Support

9.3.4.1. Safety Criteria. The effort in support of the HHT Program consisted primarily of the 3-month assignment of a GA employee at Hochtemperatur-Reaktorbau GmbH (HRB), Mannheim, FRG. During this time he participated in meetings between HRB and German licensing authorities to develop a draft of nuclear safety criteria specific to HTGRs for their future licensing in the FRG. The purpose of this assignment was to contribute to and share in the development of the safety criteria under the U.S./FRG Gas Cooled Reactor Umbrella Agreement, Direct Cycle project work statement. The resulting Federal Ministry of the Interior (BMI) draft of the safety criteria, which was issued to nuclear experts and licensing authorities in the German states, accounts for inherent safety features of the HTGR and contains general wording which is consistent with U.S. design practice and approach in all HTGR plant aspects except the BOP. Differences are found in more specific instrument radiation monitoring and control room requirements, redundant PPS circuit switchyards, and containment design for human-related external events. The impact of the proposed criteria on the HHT design is expected to be minimal and far outweighed by the future development of HTGR regulatory acceptance standards.

Major features of the BMI draft criteria are as follows. For the primary coolant boundary, a distinction is made between pressure bearing (PCPB) and non-pressure-bearing (liner) parts of the primary coolant boundary. Safety requirements for the PCPB are thermal protection and monitoring, consideration of external influences on the outside of the PCPB,

and monitoring and periodic testing of the PCPB. The liner does not have these requirements.

For the core and reactivity criteria, as for LWRs, two shutdown systems, one of which can maintain cold shutdown, are required. Inherent characteristics of the reactor can be used in the hardware design. The question of manual versus automatic activation of the reserve system was left open.

After extensive discussion on application of the single-failure criterion, it was decided to retain the concept previously defined for LWRs in the FRG interpretation of October 26, 1978. This is similar to the U.S. concept except for the way maintenance operations are considered, which sometimes leads to (N-2) instead of (N-1) redundancy. Future modifications of the concept were considered possible in light of Three Mile Island postaccident activities.

For afterheat removal, a main, non-safety system is required which must be available for the large majority of plant shutdowns. A backup safety system (CACS) is required which must consider the frequency of accidents, potential air or steam ingress, and minimum containment back-pressure (specific safety margins are not stipulated). Common parts of the two systems are not precluded if reliability is maintained and if the parts are testable. The (N-1) loop redundancy rule is sufficient for maintenance operations where the loop in repair can be restored in time, considering inherent plant characteristics. Otherwise, (N-2) loop redundancy is required.

The containment function may be met with filtered vented confinement concepts if dose exposure limits are maintained during accidents. Atmospheric cleanup or heat removal systems in the containment are not required. Periodic pressure and leak-tightness tests are required for the containment structure and penetrations. Isolation valve requirements are similar to

those in the General Design Criteria except that the positions of valves must be shown in the control room. A unique requirement was added to provide an internal barrier against liquids on the inside of buildings to protect the structure and ground water.

Instruments are divided into "event" and "consequence" categories with all output displayed in the control room and in an emergency control station (required as a backup). "Event" instruments must have redundant recording and an uninterruptible power source.

Specific redundancy requirements, whether (N-1) or (N-2), are not specified for diesel generators. As opposed to U.S. criteria, separate and redundant PPS circuit switchyards (as well as supply lines) are required.

Specific requirements were added to radiation criteria for stationary activity-measuring devices with recorded output and indication and alarms in the control room, as well as portable devices. The ALARA concept is specified for accidents as well as normal operation. Specific emphasis is placed on personnel exposure during maintenance and component replacement operations.

For external effects, the German HTGR and LWR criteria require design consideration of human-related (aircraft crash, sabotage) events as well as natural phenomena (earthquakes, storms). German requirements for seismic design are basically the same as in the U.S.

Regarding testability, a separate criterion was written specifying component testability as befits safety importance. Exceptions are allowed when additional requirements on design and quality control are satisfied. Consequences of failure of non-testable components must be limited.

In conclusion, the major German criteria do not require significant deviations from current GA design practice for the NSS/RTS portion of the HTGR-SC and HTGR-GT. Differences are found in more specific (1) instrument and control room requirements, (2) electrical switchyard requirements, (3) radiation-measuring devices, and (4) containment design for human-related external effects.

In the near-term period, technical experts and licensing authorities in the FRG will review and comment on the BMI draft of the HTGR criteria. A translation of the FRG criteria and comparison with the U.S. General Design Criteria of 10CFR50, Appendix A, should be formalized in a report to facilitate review in the U.S. and a better understanding of U.S. criteria in the FRG. This comparison should also summarize respective regulatory acceptance standards (regulatory guides, standard review plans, etc.) in the two countries. Development of acceptance standards specific to HTGRs needs to be pursued in both countries, and these standards can significantly impact the HTGR design. In the FRG, this involves mainly development of Kerntechnischer Ausschuss (KTA) regulations and Reaktor Sicherheits Kommission (RSK) guidelines. Cooperative interface should be maintained with the Germans on the detailed implications of the new criteria and developing acceptance standards on the HHT (high-temperature reactor with a helium turbine), PNP (Process Nuclear Project), and HTGR-GT projects.

9.3.4.2. Safety Assessment. In addition to the safety criteria work, an independent calculation of an HHT turbine deblading event was performed using the HTGR-GT version of the RATSAM program for the purpose of comparing analytical methods. Results for the HHT program are obtained with the PLAYGAS program (Ref. 9-1). Although some difficulties were encountered in interpreting the HHT data for input to RATSAM, reasonably good agreement between programs was obtained. Some disagreement would be expected since the HHT turbomachine performance characteristics were not available and since there is a fundamental difference in the modeling of the turbine deblading per se. In PLAYGAS, turbine deblading is simulated by a variable

area nozzle located between turbine inlet and exit regions. The area is assumed to enlarge linearly over the deblading time of 0.020 s. In RATSAM, the deblading is simulated by varying the flow resistance in the flow path containing the turbine. The change in flow resistance is performed in such a way that the same general behavior with time as the GHT simulation is approximated.

#### 9.4. REFERENCE

- 9-1. Dupont, J. F., G. Cina, and M. Dang, "PLAYGAS, A Computer Code for the Transient Analysis of Nuclear Gas Turbine Power Plants," EJR-Bericht NR. 284, paper presented at the 1st European Nuclear Conference, April 1975, Paris.

## 10. AVAILABILITY

### 10.1. SCOPE

The purpose of this task during FY-79 was to conduct availability studies as required to aid in the selection of plant features and to assist the system/component designers so that the plant availability goals can be achieved.

### 10.2. SUMMARY

During the second half of FY-79, two plant availability studies were completed. The objective of the first study was to establish a preliminary estimate of the availability of a three-loop 1200-MW(e) HTGR-GT plant and thereby establish whether high availability, in the range of 90%, could be expected from a HTGR-GT plant. The results indicate that such high availability appears to be achievable.

The objective of the second study was to quantify, to the extent possible, the relative availability that might be expected from inter-cooled and non-intercooled variants of two-loop HTGR-GT plants. The results indicate that the additional complexity of the intercooled plant could result in 1% less availability than for the non-intercooled plant.

### 10.3. DISCUSSION

#### 10.3.1. HTGR-GT Preliminary Availability Evaluation

In June 1979, a study to assess the availability potential of the HTGR-GT was completed. A preliminary program goal of attaining 90% availability in a mature plant was established. Because the scope of the study

did not permit re-evaluation of all plant systems, it was decided to use, to the extent practicable, previous analyses completed for the HTGR-SC. The unscheduled outages of the 900-MW(e) HTGR-SC which are basically the same for HTGR-3C and HTGR-GT plants are shown in Table 10-1.

The next step was to make estimates of the unscheduled outage to be expected of the systems and components exclusive to the HTGR-GT, i.e., the turbomachines, precoolers, recuperators, and PCL control valves. The unscheduled outage times for HTGR-GT exclusive systems were evaluated for a three-loop plant, and the results are shown in Table 10-2.

Table 10-2 shows that if the allocation for the HTGR-GT/HTGR-SC common systems and the HTGR-GT exclusive scheduled outage allocation can be met, an availability of about 88% can be achieved. The effect of turbomachinery ISI and planned maintenance, in which the turbomachinery is removed for inspection and a spare is installed in its place, is indicated in Table 10-2 by an increase of scheduled outage to 547 h to accomplish the task. If one turbomachine were removed every year, this would reduce the availability to about 87%. However, if turbomachine replacement is required only 3 yr out of six for a three-loop plant as presently anticipated, then the plant availability estimate falls between 87% and 88% since refueling dictates the outage time. These results indicate that the HTGR-GT concept is compatible with a goal of high availability. For an HTGR-GT plant to achieve availability in the range of 90%, there must be a continued effort in reliability and maintainability engineering throughout the program.

#### 10.3.2. Intercooled/Non-Intercooled Plant Availability Comparison

In September 1979, a study to compare the availability of non-intercooled and intercooled two-loop HTGR-GT plants was completed (Table 10-3). The study discussed above was used as a basis, with the unscheduled outage time for the components exclusive to the non-intercooled HTGR-GT;

TABLE 10-1  
 UNSCHEDULED OUTAGE HOURS ALLOCATED TO THE  
 900-MW(e) HTGR-SC REFERENCE PLANT  
 COMMON TO THE HTGR-GT

System Description	Allocated Outage (h)
Reactor, neutron and flow control and helium purification systems	22.1
Rotating machinery service	12.9
Core auxiliary cooling system	8.4
Plant control and protection systems	37.0
Cooling water systems	34.1
Generators and electrical systems	22.5
Unallocated reserve	<u>58.4</u>
Total	195.4



TABLE 10-2  
 PRELIMINARY AVAILABILITY SUMMARY FOR THREE-LOOP  
 NON-INTERCOOLED HTGR-GT

<u>Unscheduled Downtime (h/yr)</u>	
HTGR-GT/HTGR-SC common systems (see Table 10-1)	195.4
HTGR-GT Exclusive Systems	
Turbomachinery	328.0
Precoolers	10.1
Recuperators	0.6
PCL valves	73.0
	411.7
HTGR-GT Total	607.1
 <u>Scheduled Downtime (h/yr)</u>	
(1) Allocated for 90% availability	438
(2) Estimated for yearly turbomachinery replacement	547.2 <sup>(a)</sup>
 Total Downtime for HTGR-GT	
Using (1)	1045.1
Using (2)	1154.3
 Availability	
Using (1)	88.1%
Using (2)	86.8%

---

(a) If a turbomachine is replaced biennially, the availability would be between 87% and 88% owing to refueling.

TABLE 10-3  
TWO-LOOP HTGR-GT AVAILABILITY SUMMARY

	Non-Intercooled Plant	Intercooled Plant
<u>Unscheduled Outage (h/yr)</u>		
Systems common to HTGR-GT/HTGR-SC	191.8	191.8
Turbomachines <sup>(a)</sup>	218.7	240.6
Precoolers	6.8	5.0
Intercoolers	—	4.0
Recuperators	0.4	0.4
Valves (PCL)	48.7	48.7
Circulating water system	<u>114.1</u>	<u>180.1</u>
Total unscheduled downtime <sup>(b)</sup>	581	671
<u>Scheduled Outage (h/yr)</u>		
Allocated for 90% plant availability	438	438
<u>Total Outage (h/yr)</u>		
Using scheduled outage	1019	1109
<u>Plant Availability (%)</u>		
Using scheduled outage	88.4	87.3

(a) Intercooled turbomachine penalized 10% in outage time for perceived complexity.

(b) Assumes that the unscheduled outage allocated to systems common to intercooled and non-intercooled variants (top of table) is realized.

i.e., the results of the HTGR-GT exclusive components were scaled to reflect the two-loop configuration instead of the three-loop configuration. One other basic change, which involved the circulating water system (CWS), was incorporated into the second study. In the initial study, it was assumed in the cursory review of plant systems that the CWS performed similar functions for an HTGR-GT and an HTGR-SC plant and thus would cause similar unscheduled outages. In the second study, however, the changes to the CWS caused by adding the intercoolers necessitated a more detailed modeling and consideration of the CWS operating requirements. This resulted in the recognition that the CWS is significantly more complex for the HTGR-GT than for the HTGR-SC and that a greater unscheduled outage time must be expected. This will result in a readjustment of downtime allocations for the HTGR-GT system.

Several factors considered to contribute to the complexity and unscheduled outage of the CWS for the HTGR-GT are listed below:

1. Many valves are required to provide sufficient interconnections, isolation capability for repair, and heat exchanger dumping.
  - a. Each of the two pre-cooler sections (and the two inter-cooler sections) interfaces with the primary coolant, and each section therefore must have isolation and dump valves.
  - b. The higher water pressure expected for the CWS is expected to require double isolation valves for some components to enable repair with the system pressurized.
2. The effective failure rates for valves may not be reducible owing to anticipated strict leak limitations (a) because of tritium in the water and (b) because the water is treated to maintain high quality.
3. Effective repair times are longer because of the time required to shut down and start up the plant for repair of some components.

System optimization and refinement in failure criteria and effective failure rates decrease the predicted unscheduled outage for the CWS, but because of the above factors, it is expected to remain higher for a HTGR-GT than for a steam cycle plant.

The scheduled outage hour value (438 h or 18.2 days) presented in Table 10-3 for both the non-intercooled and intercooled plants is the value allocated to scheduled outage in order to meet a 90% plant availability goal. Current requirements do not include ISI of precooler, intercooler, or recuperator heat exchange tubing. If ISI of this tubing were mandated in the future, a significant increase in scheduled outage time would be likely. The increase would be greater for the intercooled plant because of the intercoolers.

#### 10.3.3. Conclusions

It is concluded that a mature HTGR-GT plant has the potential for achieving high plant availability. The intercooled variant, however, is expected to show a somewhat lower availability than a non-intercooled version.



## 11. REACTOR TURBINE SYSTEM/BALANCE OF PLANT INTEGRATION (631001)

### 11.1. SCOPE

The purpose of this task in FY-79 was to develop the reference plant layout and conceptual design for major BOP systems; issue a design information package for cost purposes; provide BOP impact assessment to the alternate, intercooled, plant study; and perform a maintenance/contamination study for selected RTS components.

### 11.2. SUMMARY

Only a nominal effort was scheduled on this task during the first half of FY-79, the bulk of the work being performed during this reporting period.

Structural sizing and layout drawings were prepared for the RCB, control auxiliaries and diesel (CAD) building, reactor service building (RSB), and fuel storage building (FSB). A plot plan illustrating the plant arrangement was also developed. The degree of detail was just sufficient to permit the preparation of cost estimates for the major BOP structures.

Design information was generated to support the cost estimate for the following BOP systems:

- Circulating Water System (CWS).
- Service Water System (SWS).
- Nuclear Service Water System (NSWS).
- Generator Plant Cooling Water System (GPCWS).

Reactor Plant Cooling Water System (RPCWS).  
Fuel Storage Pool Cooling Water System.  
Core Auxiliary Cooling Water System (CACWS).  
Helium Storage System (HSS).

A brief study was conducted to assess the differences between the containment sizes and configurations for an intercooled and a non-intercooled plant. The results indicated a significant cost increase for the containment in the intercooled concept.

A fairly extensive study was conducted to evaluate the maintenance requirements of selected major primary loop components based upon estimated contamination levels. Servicing requirements, including in-service inspection (ISI), were developed together with the sequence of events. Associated man-hour and personnel estimates for performing the various tasks were generated together with maintenance crew exposures.

Fission product plateout data were developed for MEU fuel, and dose rates were estimated for selected component locations within the primary loop. Based upon these levels and whole body dose rate limits established for contact maintenance, most of the tasks were conducted remotely.

Labor cost approximations were generated for the planned and unplanned maintenance tasks.

### 11.3. DISCUSSION

#### 11.3.1. BOP Plant Layouts

The design approach for the building arrangements is quite similar to that previously employed on other HTGR concepts, with the principal exception of the RCB.

The program decision to employ water-cooled generators permitted the generators to be housed within the RCB. This location circumvents earlier problems related to locating the generator external to the containment and the shaft penetration/seal issue. In order to minimize containment size and cost and assure adequate equilibrium backpressure for CACS operation, the generators were partially housed within "doghouse" vessel extensions from the containment at grade elevation.

A special fuel handling equipment positioner system replaces the polar crane at the spring-line elevation.

Locating the generators within the RCB introduces a problem with respect to the electrical penetrations. Currently obtainable RCB electrical penetrations are limited to ratings of 15,000 V and 520 A. The requirements for the reference plant are 24,000 V and 12,000 A. A potential solution has been determined following conceptual design work and discussions with suppliers. A development program would be required to qualify the penetrations.

The RSB houses all the equipment and facilities associated with the rapid refueling system, including the control room located above the refueling floor. Additionally, the equipment service facility, gas waste storage and process equipment, and liquid and solid radioactive waste process equipment are located within the building.

The FSB employs the pool type containerized storage system. It is sized to accommodate 10-yr spent fuel storage. It became apparent during the development of this structure that there is an economic incentive to provide an alternative, more compact, method of storage. However, time limitations and budget restraints did not permit any assessments of alternative schemes during this reporting period.



The C/D building contains the following:

1. Main control room.
2. Upper and lower cable spreading rooms.
3. Diesel generators.
4. 4160-V bus and controllers.
5. 480-V MCC and battery rooms.
6. HVAC.

The building layout with regard to services, function, and separation is similar to that recently employed on other HTGR concepts.

A plot plan was developed (see Fig. 11-1) which illustrates the overall plant arrangement and includes the other principal structures required for the BOP.

An information package was prepared, including building volumes for the Category 1 and non-category structures, for use during the preparation of the conceptual cost estimate.

#### 11.3.2. BOP Systems

The CWS is a pressurized, non-nuclear safety, closed-loop system which transfers heat from the three precoolers and rejects it to the environment through dry cooling towers. The CWS consists of two 50% capacity dry cooling towers, four 33-1/2% capacity circulating pumps (normally three operating), three dump tanks (one for each loop), and a pressurizing tank. It is designed to remove a heat load of 57.0 MW(t) ( $1.975 \times 10^6$  Btu/h) per loop.

The plant SWS is a non-nuclear safety cooling water system that provides cooling for the RPCWS, the fuel storage pool cooling water system, and the GPCWS. The SWS consists of a mechanical draft, wet cooling tower and three 50% capacity circulating pumps. It is capable of removing a total heat load of 53.0 MW(t) ( $181 \times 10^6$  Btu/h).

# DOCUMENT/ PAGE PULLED

ANO. 8008130540

NO. OF PAGES 1

REASON:

PAGE ILLEGIBLE:

HARD COPY FILED AT: PDR CF

OTHER \_\_\_\_\_

BETTER COPY REQUESTED ON \_\_\_\_\_

PAGE TOO LARGE TO FILM.

HARD COPY FILED AT: PDR CF

OTHER \_\_\_\_\_

FILMED ON APERTURE CARD NO. 8008130540

COOLING TOWER

PUMP HOUSE

PRE-COOLER DRING TUNNEL

SERVICE WATER  
METER & PUMP  
BUILDING

UHS (C)  
CACS ONLY

ISO-PURE  
BUS FROM  
GENERATOR C

CACS DRING TUNNEL

270°

THERM COOLING  
AND FUEL  
STORAGE BLDG

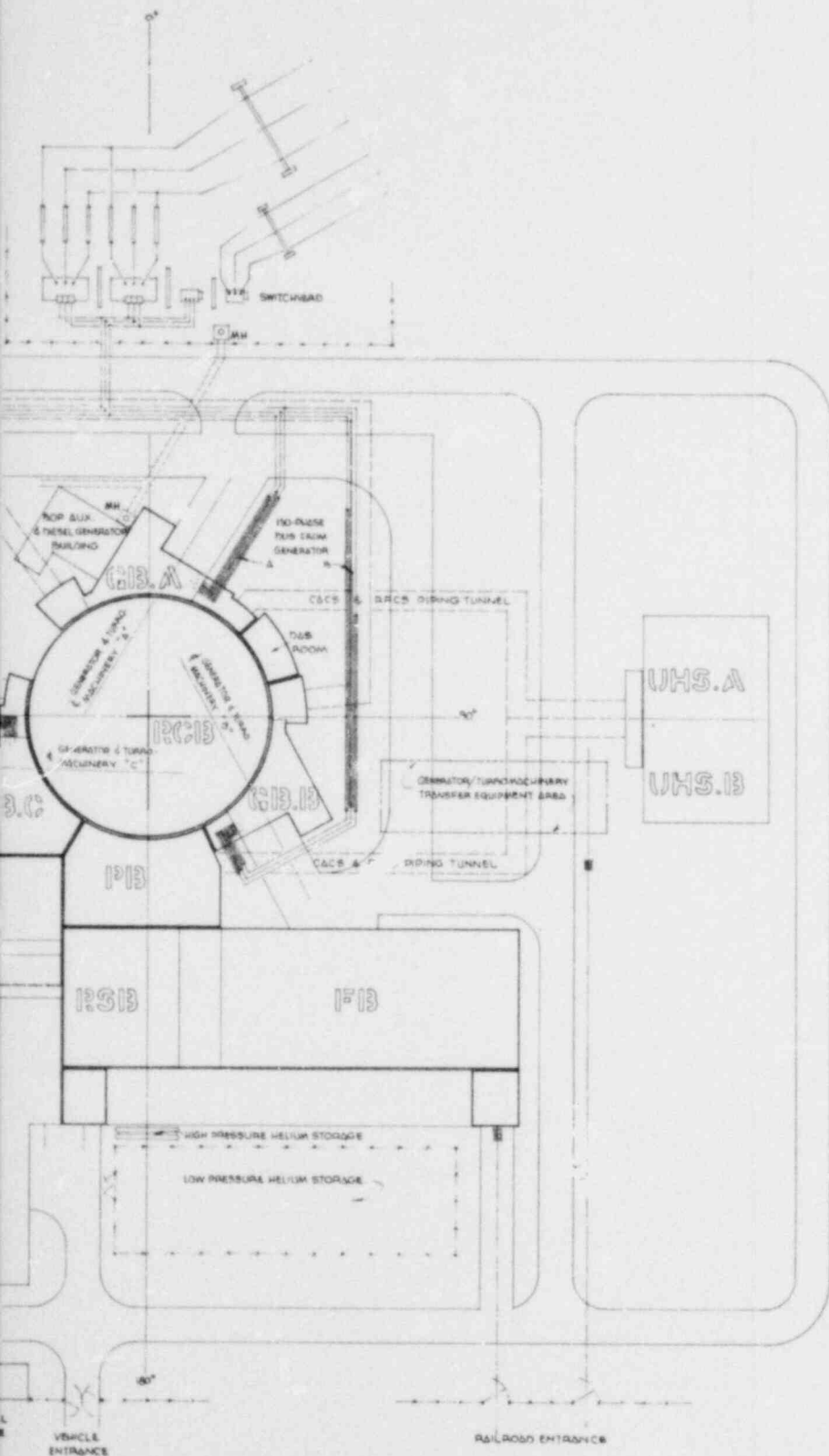
CAN

WAREHOUSE

AC

SECURITY

PERSONNEL  
ENTRANCE



LEGEND

- RCB - REACTOR CONTAINMENT BUILDING
- PB - PENETRATION BUILDING
- RSB - REACTOR SERVICE BUILDING
- FB - FUEL STORAGE BUILDING
- C&D - CONTROL AND DIESEL BUILDING
- ΔC - ACCESS CONTROL & ADMINISTRATION BUILDING
- GB - GENERATOR SERVICES BUILDING
- UHS - ULTIMATE HEAT SINK

Fig. 11-1. Plot plan showing overall HTGR-GT plant arrangement

The NSWs provides cooling for the PCRV liner, the fuel storage pool, and the auxiliary circulator motor cooling water system when the SWS is inoperative. The NSWs consists of 100% capacity wet evaporative cooling towers, two 100% capacity circulating pumps, one 100% heat exchanger, two 100% cooling water pumps, and a surge tank. The NSWs is sized to reject a heat load of 29.2 MW(t) ( $99.8 \times 10^6$  Btu/h) encountered in shutting down the plant and maintaining it in a safe shutdown condition.

The GPCWS provides cooling to the three generators and auxiliaries and to the turbocompressor service modules in the RCB. It is a non-safety, closed water system of controlled water quality rejecting heat to the SWS. The GPCWS consists of a 100% capacity heat exchanger, two 100% capacity pumps, a pressurized surge tank, and a chemical control package. It is sized to remove a heat load of 20 MW(t) ( $68.3 \times 10^6$  Btu/h).

The RPCWS provides cooling to RTS components and systems under normal and emergency plant conditions. The system normally rejects heat to the plant SWS. Under emergency conditions, the NSWs serves as the ultimate heat sink for the safety related components, i.e., PCRV liner and auxiliary circulator motors.

The fuel storage pool cooling water system consists of two 100% capacity pumps which circulate water through the SWS heat exchangers under normal conditions and to the NSWs under emergency conditions. The system has a heat rejection capacity of 6.45 MW(t) ( $22 \times 10^6$  Btu/h).

The CACWS is a nuclear safety class system supplying cooling water to the CAHEs in the CACS loops. Each loop is independent and sized to remove approximately 60.1 MW(t) ( $205 \times 10^6$  Btu/h) during the loss of pressurized main loop core cooling. Each of the three CACWS loops consists of two 100% capacity auxiliary pumps, one 100% capacity main pump, one 100% capacity air blast heat exchanger, a surge tank, and a chemical control module.

The HSS is a non-safety related system containing non-radioactive helium. It consists of two 100% capacity transfer compressors, two oil absorbers, helium storage tanks, and high-pressure supply tanks. It provides for storage and transfer of the total plant helium inventory and provides makeup, purging, and pressurizing functions for various systems and components.

A design information package for the BOP systems, including sizing data, was issued for the conceptual cost estimate.

### 11.3.3. Intercooled Versus Non-intercooled Plant Impact on BOP

This brief study evaluated the principal differences in the BOP area for an intercooled plant and a non-intercooled plant. Previous studies had been exclusively directed to the non-intercooled plant configuration. Therefore, this task concentrated solely on the differences introduced by the intercooler. The major impact may be summarized as follows:

1. The RCB is increased in size, and therefore cost, owing to the increased-diameter PCRV.
2. Increased containment net free volume results in corresponding increase to HVAC system requirements.
3. The location of the RCB access penetrations for turbogenerator removal and the removal space requirements increase the distance between the RCB and RSB within the penetration building. The penetration building increases in size accordingly.
4. The maintenance times for servicing the intercooler and removal of the turbomachine are increased over those for the non-intercooled plant.

#### 11.3.4. Maintenance/Contamination Study

An extensive study focused on the planned and unplanned maintenance requirements associated with the following primary loop components:

1. Turbocompressors.
2. Precoolers.
3. Recuperators.
4. Hot ducts.
5. Helium control valves.

These components had previously been identified, by a utility advisory committee, as being of particular concern from the maintenance and servicing aspect.

Equipment servicing requirements, including ISI, were developed together with the respective sequencing of events. Associated man-hour and personnel estimates for performing the maintenance tasks were generated.

For the initial plant, the maintenance program calls for the removal, inspection, and servicing of each turbocompressor unit on a 6-yr schedule. In-service inspection requirements and prudent judgment dictated the frequency of inspection for the other components.

Fission product plateout data were developed for MEU fuel. The main fission product nuclides contributing to unshielded gamma dose rates in this study are Ag-110m and Cs-134. At high-temperature operation [ $>800^{\circ}\text{C}$  ( $1472^{\circ}\text{F}$ )], fission product nuclides tend to diffuse into the surface of the metal, precluding standard decontamination procedures. One of the highest component dose rates (15.2 rads/h) occurs within the turbine assembly. A limit of 10 mr/h has been established for whole body dose rate for contact maintenance. It is not considered practical to achieve the required decontamination to perform hands-on maintenance for this component, and therefore

remote handling is being considered. Studies are currently under way to identify, conceptually, the remote handling tools and onsite facility requirements.

The study provides estimates of the man-hours and costs for performing the various planned and unplanned maintenance tasks, together with the annual collective dose to the maintenance crew. A great deal of uncertainty exists with respect to these values owing to the lack of adequate design definition for some components and the assumptions which, of necessity, had to be made. The results are summarized in the Maintenance/Contamination Study Design Report, which is in the process of being released for issue.



## 12. SYSTEMS DESIGN (631002)

### 12.1. SCOPE

The purpose of this task in FY-79 was to perform a review of technical issues and to conduct studies of the systems aspects of the intercooled versus the non-intercooled cycles, helium inventory control cost impact, system pressure drop and bypass, ambient air efficiency impact, and CACS cooling.

### 12.2. SUMMARY

As part of GA's assessment of the benefits associated with the HTGR-GT plant, a review of current technical issues that are related to primary system parameters was performed and documented in a design report. In addition, cost sensitivity studies were performed using CODER6 by perturbing key primary system parameters and thereby determining how reduced HTGR-GT power costs might be achieved. The results of these studies were also documented in a design report.

The reference plant design for the above investigations was the three-loop, 3000-MW(t) non-intercooled concept with a conventional liner and a "delta" PCRV configuration at 850°C turbine inlet temperature. The areas included in the design issues review were materials, limiting transients (including CACS cooldown transients and the turbine deblading event), core design and fission product release, thermal barrier, reactor internals, turbomachinery, PCRV, liners, and safety and availability. The review is intended to provide a constructive assessment of the design issues related to primary system parameters (as of August 1979) as well as an aid to component designers in their efforts to develop a technically sound and cost effective plant.

The primary system parameter review study was undertaken because the HTGR-GT must be developed and designed with constant attention toward maximizing value and safety to the utility owner. One key factor to be considered is plant capital cost. Another is availability/maintainability. In the early stages of design, a cost assessment of variations in major primary system parameters is valuable. This effort will indicate how much incentive exists for changing system parameters, which ultimately must be balanced against feasibility questions and impact on availability/maintainability. The objective of the present study is to provide an initial evaluation of the sensitivity of cost to variations of key primary system parameters about their reference design values for the 1200-MW(e) non-intercooled HTGR-GT with a conventional liner.

The primary system parameters investigated in the study are listed in Table 12-1 along with the reference values and range of survey. Two other parameters are included, capacity factor and fuel cycle length. The capacity factor for the plant is listed as 80% in the Plant Technical Description Document (TED), but all cases are also run at 70% since utilities are interested in the 70% to 80% capacity factor range. The reference fuel cycle length is 4 yr. For discussion purposes, however, the power density variation cases were also calculated with a 3-yr fuel cycle length to determine effects on fuel and overall plant costs.

Owing to the impact of fission product release on the availability/maintainability of primary system equipment, fissile particle failure fractions and several isotopic releases were evaluated as a function of variations in turbine inlet temperature. It should be noted, however, that remote maintenance appears mandatory regardless of the fuel cycle chosen if a 10-mr limit for contact maintenance is adhered to.

For the non-intercooled versus intercooled plant study, power cost optimization analyses using CODER7 and CODER8 were performed. Key system parameters were allowed to "float" within a specified range of variation while CODER searched for the minimum total power cost. Tables 12-2 and 12-3 give the performance parameters for the optimized non-intercooled

TABLE 12-1  
PARAMETERS EVALUATED IN PRIMARY SYSTEM PARAMETER STUDY

Parameter	Reference Value	Minimum Value	Maximum Value
Primary System Related			
Turbine inlet temperature, °C (°F)	850 (1562)	800 (1472)	900 (1652)
Pressure, MPa (psi)	7.932 (1150)	7.518 (1090)	8.345 (1210)
Compressor pressure ratio	2.5	2.3	2.7
Recuperator effectiveness, %	89.8	85.8	93.8
Power density, W/cm <sup>3</sup>	7.0	6.4	7.8
Others			
Capacity factor, %	80	70	80
Fuel cycle length, yr	4	3	4

TABLE 12-2  
 PERFORMANCE PARAMETERS FOR TWO-LOOP, 2000-MW(t) HTGR-GT  
 NON-INTERCOOLED REFERENCE PLANT (OPTIMIZED)

Conditions: No intercooling; no blade cooling for turbomachine; standard  
 day ambient air temperature; CODER8 run H03B/H05.

Reactor rating	2000 MW(t)
Number of loops	2
Liner option	Conventional
Compressor pressure ratio	2.6
Compressor flow (M)	563.33 kg/s (4,471,000 lb/hr)
HP compressor pressure	8.412 MPa (1220 psia)
Reactor inlet temperature	494.4°C (922°F)
Reactor outlet temperature	850.0°C (1562°F)
Turbine inlet temperature	848.9°C (1560°F)
Compressor inlet temperature	26.8°C (80.2°F)
Minimum cycle helium temperature	26.1°C (79.0°F)
Primary system pressure loss	419.9 kPa (6019 psi)
Recuperator high-pressure $\Delta P$	64.1 kPa (9.3 psi)
Core $\Delta P$	100.0 kPa (14.5 psi)
Turbine $\Delta P$	4757 kPa (690 psi)
Recuperator low-pressure $\Delta P$	72.4 kPa (10.5 psi)
Precooler $\Delta P$	11.0 kPa (1.6 psi)
Compressor pressure rise	5177 kPa (751 psi)
Recuperator effectiveness	0.905
Turbine isentropic efficiency	91.8%
Compressor isentropic efficiency	89.8%
Generator efficiency	98.8%
Turbine blade cooling flow (M)	0%
Turbine disk cooling flow (M)	2.96%
Ambient air temperature	15.0°C (59°F)
Cooling water temperature	20.6°C (69°F)
Precooler outlet water temperature	132.2°C (270°F)
Heat losses	12.33 MW(t)
Auxiliary power	8.0 MW(t)
Plant efficiency	40.0%
Net electrical output	800.0 MW(e)

TABLE 12-3  
 PERFORMANCE PARAMETERS FOR TWO-LOOP, 2000-MW(t) HTGR-GT  
 INTERCOOLED PLANT (OPTIMIZED)

Conditions: Intercooling; no blade cooling for turbomachine; standard day ambient air temperature; CODER7 run G03B/G04.

Reactor rating	2000 MW(t)
Number of loops	2
Liner option	Conventional
Compressor pressure ratio, LP/HP	1.75/1.80
Compressor pressure ratio, overall	3.15
Compressor flow (M)	494.79 kg/s (3,927,000 lb/hr)
HP compressor outlet pressure	8.618 MPa (1250 psia)
Reactor inlet temperature	445.0°C (833°F)
Reactor outlet temperature	850.0°C (1562°F)
Turbine inlet temperature	848.9°C (1560°F)
LP compressor inlet temperature	26.4°C (79.6°F)
HP compressor inlet temperature	26.7°C (80.0°F)
Minimum cycle helium temperature	26.1°C (79.0°F)
Primary system pressure loss	4.3 kPa (64.3 psi)
Recuperator high-pressure $\Delta P$	48.9 kPa (7.1 psi)
Core $\Delta P$	76.5 kPa (11.1 psi)
Turbine $\Delta P$	5.460 MPa (792 psi)
Recuperator low-pressure $\Delta P$	90.3 kPa (13.1 psi)
Precooler $\Delta P$	13.1 kPa (1.9 psi)
LP compressor pressure rise	2.075 MPa (301 psi)
HP compressor pressure rise	3.833 MPa (556 psi)
Recuperator effectiveness	0.898
Turbine isentropic efficiency	92.2%
HP compressor isentropic efficiency	90.2%
LP compressor isentropic efficiency	90.8%
Generator efficiency	98.8%
Turbine blade cooling flow (M)	0%
Turbine disk cooling flow (M)	2.96%
Ambient air temperature	15.0°C (59°F)
Cooling water temperature	20.6°C (69°F)
Precooler outlet water temperature	20.6°C (69°F)
Precooler outlet water temperature	86.9°C (188.5°F)
Intercooler outlet water temperature	65.6°C (150.0°F)
Heat losses	9.79 MW(t)
Auxiliary power	8.0 MW(t)
Plant efficiency	43.5%
Net electrical output	869 MW(e)

and intercooled plants, respectively. As indicated in the tables, the plant efficiency for the two-loop non-intercooled design is 40.0% compared with 43.5% for the intercooled design.

Plant power generation cost was evaluated on two bases: constant plant thermal rating [2000 MW(t)] and constant plant net electrical rating [800 MW(e)]. When thermal rating is maintained, the intercooled plant is approximately 5% lower in cost than the non-intercooled plant, and this difference shrinks to approximately 2% when net electric power is equal for both cases. Thus, despite the large efficiency improvement of the intercooled cycle, the additional cost of the configuration hardware tends to offset the economic impact of the efficiency gain.

Operating costs for an HTGR-GT plant can be significantly reduced with a helium inventory control system (HICS), since much higher part-load efficiencies can be achieved than with conventional control methods (bypass flow and temperature controls). A study was performed to explore implementation of this load-control technique and carry out preliminary design efforts to conceptually define the system. Follow-on efforts can be carried out to evaluate the economic viability (cost/benefit ratio) of incorporating this approach in the two-loop 800-MW(e) HTGR-GT plant.

Ground rules have been developed for an HICS, and a conceptual system design has been recommended for use with the HTGR-GT plant. It is expected that a significantly larger helium purification system will be needed along with expanded, out-of-containment storage facilities. Figure 12-1 schematically illustrates the intended plant operations with the HICS incorporated. Part-load control of the plant would be achieved using the HICS in conjunction with conventional reactor power control methods, i.e., bypass flow and temperature adjustments. For normal load decreases, up to 0.42%/min as currently defined for representative plant conditions, the HICS would operate exclusively, decreasing the helium inventory by using a helium purification system for radioactive cleanup of the helium prior to its release to out-of-containment storage. For less frequent, more

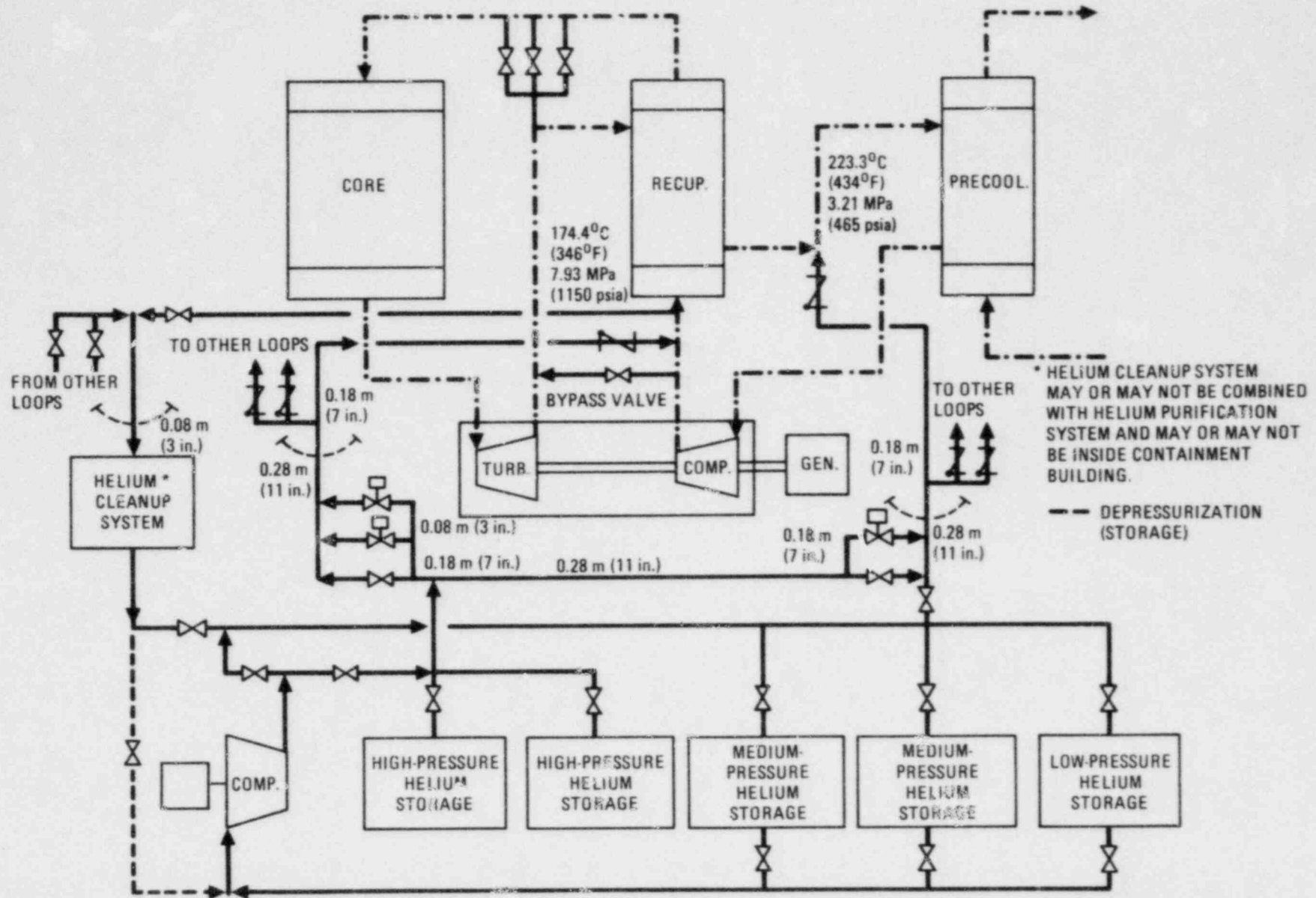


Fig. 12-1. Conceptual piping and storage system for a helium inventory control system

rapid load reductions, e.g., up to 5%/min or ramps of 10% in 10 to 20 s, the bypass flow control valve would be initially opened (for instant power decrease) and then the HJCS would be used to "catch up" with the change, i.e., through simultaneous adjustment (reclosing) of the bypass valve while helium is removed from the system at the 0.42%/min rate. All increased load requirements would be satisfied with helium supplied from external storage facilities to adjust the inventory appropriately.

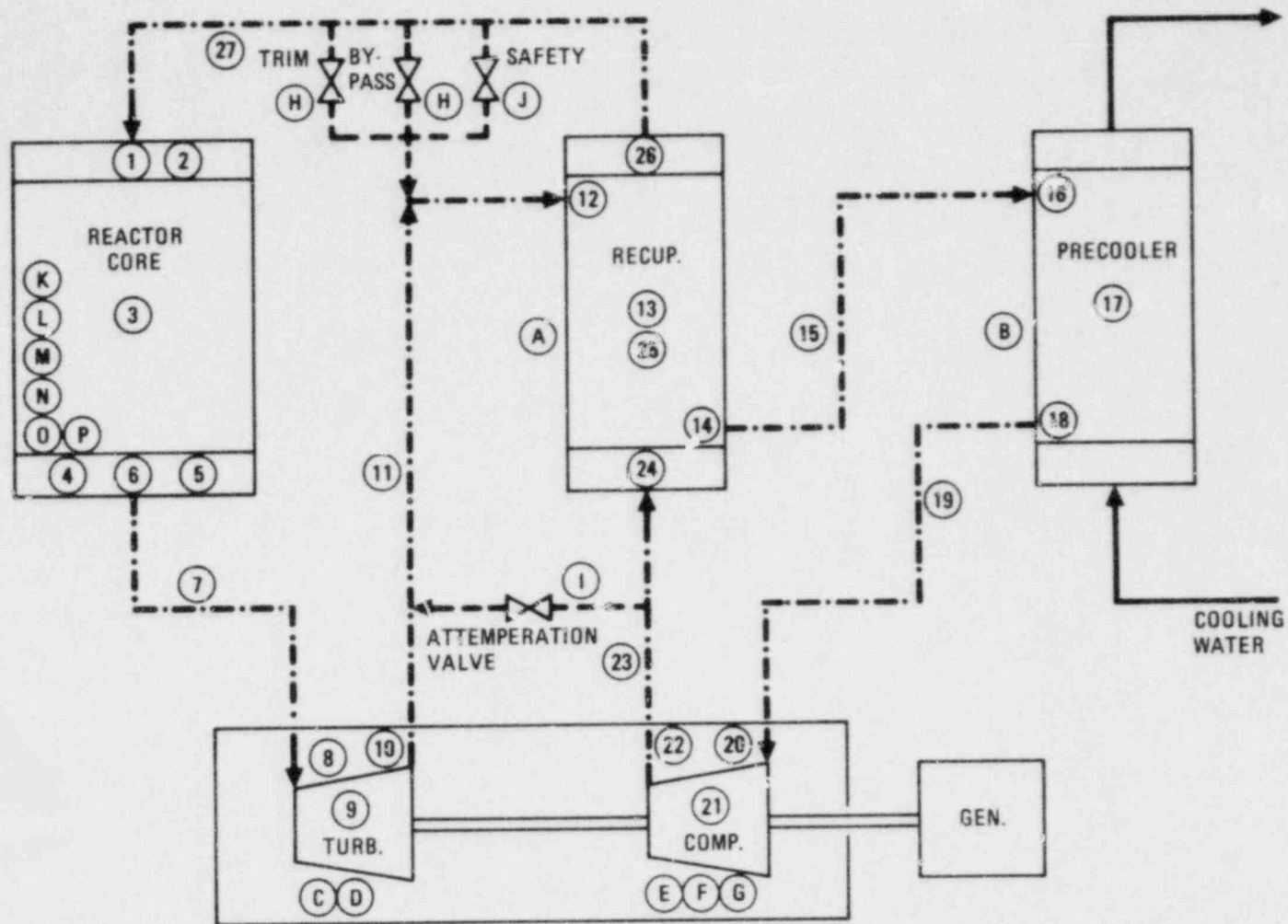
System pressure drop and bypass flows directly affect the efficiency of a power plant. The objective of recent studies in this area was to update these data to permit optimization efforts (i.e., CODER runs) on HTGR-GT designs currently being evaluated. The results of these studies can be used to guide follow-on design approaches.

Pressure drops and bypass flows were updated for the three-loop 3000-MW(t) HTGR-GT plant (see Fig. 12-2 and Table 12-4). The total primary coolant system pressure drop was found to be 520.5 kPa (75.5 psi), appreciably larger than prior values. The pressure drop increase was mainly due to increased differential pressure in the heat exchangers and in the core, determined from better design information for these components. Areas for pressure drop improvement were recommended along with guidelines for the magnitude of the differential pressure reduction.

Sizing and cost evaluations have been performed to (1) determine the influence of the major tower sizing parameters on design point plant performance and on plant cost of power, (2) compare design point performance and cost of power for an intercooled plant and a non-intercooled plant, and (3) compare plant design point performance and cost of power for different cooling tower arrangements.

Results of the parameter evaluation are generally as expected: design point plant performance decreases and cost of power increases as design point ambient temperature increases. Also, lower tower approach temperatures result in increased design point plant performance and lower cost of power. This influence is not affected by design point ambient temperature.





- NUMBERED CIRCLES: SEE TABLE 12-4 FOR PRESSURE DROPS
- LETTERED CIRCLES: SEE TABLE 12-13 FOR BYPASS/LEAKAGE FLOWS

Fig. 12-2. Pressure loss/leakage diagram for three-loop 3000-MW(t) HTGR-GT

TABLE 12-4  
PRIMARY COOLANT SYSTEM PRESSURE LOSSES

Item (see Fig. 12-2)	Loss Description	P <sup>(a)</sup>		ΔP		ΔP/P (%)
		MPa	psia	kPa	psi	
1	Core upper plenum inlet expansion	7.753	1124.38	13.58	1.97	0.175
2	Core upper plenum flow	7.751	1124.21	1.17	0.17	0.015
3	Core flow	7.660	1111.05	90.74	13.16	1.171
4	Core support blocks + lower plenum expansion	7.648	1109.30	12.07	1.75	0.158
5	Core lower plenum flow	7.645	1108.79	3.52	0.51	0.046
6	Core outlet duct contraction	7.637	1107.63	8.00	1.16	0.105
7	Core-to-turbine duct friction	7.623	1105.69	13.38	1.94	0.175
8	Turbine inlet expansion	7.592	1101.15	31.30	4.54	0.411
9	Turbine flow	3.355	486.61	—	—	—
10	Turbine exit duct contraction	3.339	484.31	15.86	2.30	0.475
11	Turbine-to recuperator (LP) duct friction	3.339	484.27	0.28	0.04	0.008
12	Recuperator (LP) inlet expansion	3.335	483.72	3.79	0.55	0.114
13	Recuperator (LP) flow	3.230	468.50	104.94	15.22	3.146
14	Recuperator (LP) exit duct contraction	3.228	468.13	2.55	0.37	0.079
15	Recuperator (LP) to precooler duct friction	3.225	467.73	2.76	0.40	0.086
16	Precooler inlet expansion	3.221	467.16	4.07	0.59	0.126
17	Precooler flow	3.187	461.56	38.61	5.60	1.199
18	Precooler exit duct contraction	3.179	461.14	2.90	0.42	0.091
19	Precooler-to-compressor duct friction	3.179	461.01	0.90	0.13	0.028
20	Compressor inlet expansion	3.172	460.00	6.96	1.01	0.219

TABLE 12-4 (Continued)

Item (see Fig. 12-2)	Loss Description	P <sup>(a)</sup>		ΔP		ΔP/P (%)
		MPa	psia	kPa	psi	
21	Compressor flow	7.929	1150.00	—	—	—
22	Compressor exit duct contraction	7.873	1141.89	55.92	8.11	0.705
23	Compressor-to- recuperator (HP) duct friction	7.870	1141.46	2.96	0.43	0.038
24	Recuperator (HP) inlet expansion	7.867	1140.96	3.45	0.50	0.044
25	Recuperator (HP) flow	7.790	1129.78	77.08	11.18	0.980
26	Recuperator (HP) exit duct contraction	7.783	1128.77	6.96	1.01	0.089
27	Recuperator (HP) to core upper plenum duct friction	7.766	1126.35	16.69	2.42	0.214
	Total	—	—	520.42	75.48	9.90 <sup>(b)</sup>

(a) Pressure on downstream end of item.

(b) These losses are not strictly additive, but for comparison purposes they are usually indicative of plant layout merit.

The impact of ambient temperature on the size and cost of the cooling tower as well as cycle performance was evaluated by developing all-dry and wet/dry cooling tower models compatible with CODER. The impact of ambient temperature on plant parameters was then evaluated to ascertain the impact of plant optimization at the various ambient temperatures.

A design report has been prepared defining the tentative CACS design bases for the two-loop 800-MW(e) HTGR-GT plant. The report, covering requirements for both the CACS and the CACWS, is currently in the review and sign-off stage.

The CACS is an engineered safety feature intended to ensure safe cool-down of the core and continued shutdown cooling in the event that the main cooling loops become unavailable. While considerable efforts have been directed at the CACS for HTGR-SC plants, little engineering has been carried out for the CACS applicable to an HTGR-GT plant. With the HTGR-GT program being the lead program at GA, such studies have been initiated, with initial emphasis directed at a design report and component sizing information to conceptually define the CACS and the CACWS.

Preliminary system parameters have been developed for the CACS (System 28) and the CACWS (System 47) for the two-loop 800-MW(e) HTGR-GT plant. Also, estimates have been made of the sizing of conceptual components for these systems (see Tables 12-5 through 12-8) and of engineering costs for such equipment (see Table 12-9). These results are based on sizing calculations carried out with the ECSEL8 code. The size of the CAHE is relatively large compared with that for HTGR-SC plants, primarily owing to the high bypass values calculated for the HTGR-GT plant. Design basis transients which the CACS must accommodate have been analyzed.

TABLE 12-5  
PRIMARY COOLANT SYSTEM PERFORMANCE

	Depressurized PCRV		Pressurized PCRV
	Pure Helium	Air Ingress	
CACS loops operating	2	2	2
Primary coolant molecular weight	4.0	14.7	4.0
Primary coolant pressure, MPa (psia)	3.84 (23.6)	3.84 (23.6)	136.68 (840)
Heat duty per CACS loop, MW (Btu/hr)	12.80(4.366 x 10 <sup>7</sup> )	17.12(5.840 x 10 <sup>7</sup> )	63.04(2.151 x 10 <sup>8</sup> )
Primary coolant circuit			
Flow per CACS loop, kg/s(lb/h)	4.22(33,493)	25.69(203,881)	40.35(320,247)
Core outlet temperature, °C(°F)	1158.3(2117)	1164.4(2128)	970.6(1779)
CAHE inlet temperature, °C(°F)	642.8(1189)	775(1427)	543.9(1011)
Core inlet temperature, °C(°F)	60(140)	333.9(633)	243.3(470)
Pressure drop, kPa(psi)			7.79(1.13)
CAHE	—	—	6.27(0.91)
Core	—	—	0.07(0.01)
Ducts and plena	—	—	1.52(0.22)
Secondary (CACWS) circuit			
Mass flow per CACS loop, kg/s (lb/h)	87.28(692,700)	87.09(691,200)	83.81(665,200)
Pump volumetric flow, m <sup>3</sup> /s (gpm)	0.088(1400)	0.088(1400)	0.088(1400)
Volumetric flow at CAHE out- let, m <sup>3</sup> /s (gpm)	0.090(1428)	0.091(1442)	0.112(1776)
CAHE inlet temperature, °C(°F)	57.2(135)	61.7(143)	118.9(246)
Air blast heat exchanger inlet temperature, °C(°F)	92.2(198)	108.9(228)	284.4(544)
Pressure drop, MPa(psi)			1.40(203)
CAHE	—	—	0.04(6)
Piping and air blast heat exchanger	—	—	1.36(197)

TABLE 12-6  
CORE AUXILIARY CIRCULATOR (SYSTEM 28-1) CONCEPTUAL STUDY RESULTS

Design power	671.1 kW (900 hp)
Maximum required power (depressurized, air ingress)	624.9 kW (838 hp)

TABLE 12-7  
CORE AUXILIARY HEAT EXCHANGER (SYSTEM 28-2) CONCEPTUAL STUDY RESULTS

Heat transfer (UA), kW/°C (Btu/h/°F)	
Depressurized, pure helium	123.6 (234,264)
Depressurized, air ingress	39.0 (73,968)
Pressurized	343.6 (651,349)
Resulting size	
Area	894.9 m <sup>2</sup> (9,633 ft <sup>2</sup> )
Length	9.81 m (32.2 ft)

TABLE 12-8  
 CORE AUXILIARY COOLING WATER SYSTEM (SYSTEM 47)  
 CONCEPTUAL STUDY RESULTS

---

Water pressure in pressurized core	10.342 MPa (1500 psia)
Air blast heat exchanger area, per loop	761.9 m <sup>2</sup> (8201 ft <sup>2</sup> )
Air blast fan power requirement, per loop	484.7 kW (650 hp)
CACWS pumping requirement, per loop	152.8 kW (205 hp)
Air blast heat exchanger configuration	
Air flow	388.3 kg/s (3.082 x 10 <sup>6</sup> lb/h)
Approach air velocity	5.92 m/s (1166 ft/min)
Number of vane-axial fans	4
Diffuser length	3.05 m (10 ft)
Fan efficiency	77%
Number of tube rows	9
Tube diameter	25.4 mm (1 in.)
Tube pitch	60.33 mm (2.375 in.)
Fin density (number per length)	0.43/mm (11/in.)
Fin height	15.88 mm (0.625 in.)
Fin thickness	0.51 mm (0.02 in.)

---

TABLE 12-9  
ENGINEERING COST ESTIMATE FOR CACS AND CACWS COMPONENTS<sup>(a)</sup>  
(1979 DOLLARS)

<u>RTS</u>	
System 28-1, auxiliary circulator	\$ 1,193,226
System 28-2, CAHE	2,283,441
System 28-3, controls (including motor speed control)	300,425
Liner, penetrations, and closures	1,111,333
Total RTS	\$ 4,888,426

<u>BOP</u>	
System 47, CACWS	
Air blast heat exchanger (ABHX) and fans	\$ 439,557
ABHX structure	1,123,755
Piping	788,778
Valves	45,228
Pumps	117,272
Misc. tanks, pumps, and services	248,669
Total	\$ 2,763,259
Tunnel, containment to ABHX structure	348,182
Standby power systems	1,347,941
Structures required by standby power	1,102,194
Total BOP	\$ 5,561,575
Total	\$10,450,001

(a) Major cost items excluded: CACS cavity and crossduct thermal barrier, portion of PCRV, circulator services, and labor on RTS components; no allowance for indeterminates.



## 12.3. DISCUSSION

### 12.3.1. Primary System Parameter-Related Design Issues

The HTGR-GT design issues related to primary system parameters are briefly reviewed below.

12.3.1.1. Materials. For the high-temperature application being considered, material lifetimes have to be verified since insufficient data exists in most cases to qualify acceptable materials for a 40-yr lifetime. Material selection is complicated by the number of limited materials with sufficient strength at design temperature to resist various imposed loadings. In addition, acoustic levels for the HTGR-GT are higher than for the HTGR-SC and induce high cycle fatigue loadings that impact material strength.

Other material issues, such as thermal aging, high-helium-velocity effects, carburization, internal oxidation, fission product effects, and wear, tend to aggravate the already difficult material selection problems. A substantial design verification and support (DV&S) program is under way to resolve the issues.

12.3.1.2. Limiting Transients. Since transient conditions can lead to limits on design parameters, nominal 100% load conditions and six limiting plant transients were simulated by the REALY2 HTGR-GT transient analysis program for the 1200-MW(e) HTGR-GT reference plant design. The transients simulated were:

1. Single loop loss of load with overspeed.
2. Single loop turbomachine shaft break.
3. Single loop total loss of precooling water flow.
4. Plant loss of load with overspeed.
5. Plant loss of cooling water flow.
6. Slow rod runout at design point operation.

The "single loop total loss of precooling water flow" transient resulted in the maximum core transient pressure in the PCRV side cavities as well as the highest precooler inlet and outlet gas temperatures. Metal temperatures at the inlet of the high-pressure side of the recuperator reached the highest observed value during this transient. The "plant loss of cooling water flow" transient resulted in the maximum inlet and outlet gas temperatures as well as maximum low-pressure recuperator/inlet and recuperator hot end metal temperatures. The "single loop loss of load with overspeed" transient showed the highest rate of pressure increase and the maximum flow rate at the low-pressure side of the recuperator. The highest rate of pressure decrease was noted during the "plant loss of load with overspeed" transient, while the highest power-to-flow ratio and turbomachine speed were predicted for the "single loop turbomachine shaft break" transient.

CACS cooldown transients are not available since specific design details of the CACS, such as heat exchanger sizes and circulator horsepower, will not be set until after the primary coolant system materials have been selected to suit their operating conditions in normal plant operation.

An event involving complete deblading of one of the turbines is expected to result in the largest depressurization rate for the primary system. Preliminary estimates of the pressure transients in the core outlet plenum have been calculated using the RATSAM8 code and indicate that a maximum depressurization rate in the core outlet plenum of  $1.503 \times 10^7 \text{ N/m}^2/\text{s}$  (2180 psi) is possible.

12.3.1.3. Core Design. Fuel element stresses for the HTGR-GT plant are slightly more favorable than in the reference HTGR-SC plant owing to a more uniform temperature distribution in the HTGR-GT plant. Nevertheless, considerable DV&S is required to resolve uncertainties in the fuel element stress areas, including verification of present analysis methods and material properties.

Fission product releases at the higher HTGR-GT fuel temperatures may be larger than for the HTGR-SC owing to greater palladium-induced corrosion of the fissile particle SiC coating of the MEU fuel. The use of MEU fuel results in significant breeding and fissioning of plutonium, resulting in a greater production of palladium isotopes than do uranium fissions. A considerable DV&S effort will be required to resolve the fission product release issue and more adequately characterize the mechanisms involved.

12.3.1.4. Thermal Barrier. The major parameter-related issues that affect reliable thermal barrier design are acoustic vibration, core outlet temperature, and rapid depressurization rates. Major design and DV&S efforts are needed to demonstrate feasibility in the areas of the lower core plenum and hot ducts.

The overall sound pressure level generated by the turbomachine is considerably larger than that generated by the circulator in the HTGR-SC plant and leads to a sonic fatigue resistance issue for thermal barrier coverplates, attachments, and insulation constructed of the various material candidates. Metallic structures are given the best chance of survival, primarily owing to their relatively high design allowable fatigue strength. However, the potential for damage to the fibrous insulation materials from acoustic vibration is very great if a "conventional" HTGR thermal barrier system is to be used.

The 850°C (1562°F) turbine inlet temperature narrows the choice of practical Class B2 material candidates to cast superalloys, carbonaceous fiber-reinforced composites (carbon-carbon), and hard ceramics. The data base for these materials is very limited, and considerable effort will be needed to qualify the candidate materials.

As mentioned earlier, the thermal barrier design is sensitive to maximum core outlet depressurization rate. This is caused by the requirement to vent the thermal barrier system in order to accommodate the large

potential pressure gradients while still retaining structural integrity. An opposing requirement is for controlled convection within the thermal barrier in order to minimize heat transfer. It is believed, however, that it is possible to design a coverplate/seal sheet arrangement that can meet both criteria.

12.3.1.5. Reactor Internals. The key issues related to the reactor internals are (1) large thermal stresses in the core support blocks resulting from core power and flow transients, (2) large thermal stresses in the permanent side reflector blocks caused by local primary coolant temperature and flow conditions, as well as radiation effects, and (3) lack of materials currently qualified to be used for the core lateral restraint and the peripheral seal assembly at the required temperature and environment for the entire plant life. DV&S programs are being developed to resolve the core restraint and seal assembly problem.

12.3.1.6. Turbomachinery. Large stresses generated by temperature gradients at the turbine inlet volute have resulted in a design change of the inlet volute to a "sandwich" construction. Since this design concept is atypical of most industrial gas turbines designed in the United States, it should be analyzed in detail. In addition, the high acoustic environment of the HTGR-GT can affect the "sandwich" integrity and should be reviewed to determine the impact on the inlet volute design. The selection of suitable materials for this application is also challenging, since service conditions in this region are similar to those of the Class B2 thermal barrier.

Another potential issue involves sealing of the different pressure regions of the turbomachine cavity. The seals must be of high quality to minimize leakages that affect cycle efficiency.

It should also be recognized that the design life of the turbomachine is significantly longer than that of industrial 850°C (1562°F) machines. Accordingly, extrapolation of materials properties significantly beyond current practice is required for the HTGR-GT case.

12.3.1.7. Liners, Penetrations, and Closures. The refueling penetration thermal design was marginal for the HTGR-SC plant and will have to be improved for the HTGR-GT plant in order to accommodate the higher-temperature environment. Another issue is that the upper CACS cavity closure would have to be designed to the ASME elevated-temperature code cases unless an actively cooled and passively insulated low-temperature design is developed.

12.3.1.8. PCRV. Potential parameter-related PCRV issues are as follows:

1. Tendon quantities may have to be increased in order to improve bottom head prestressing effectiveness.
2. High stress concentrations at the core cavity haunch and cross duct may result in a larger PCRV diameter.

12.3.1.9. Heat Exchangers. The only heat exchanger issue which appears to be parameter-related concerns the adequacy of the present design of the recuperator modules to withstand the thermal expansion imposed by the difference in temperature between the two gas streams. A design change is under consideration whereby bellows in the module could eliminate or reduce the thermal expansion issue.

12.3.1.10. Safety. A systematic and comprehensive review of the safety issues related to the HTGR-GT plant has not yet been performed. The effect of primary system parameters and plant configurations that differ significantly from the HTGR-SC is discussed in Section 9 of this report.

12.3.1.11. Availability. A plant availability engineering program has been initiated to help support the design evaluation of the HTGR-GT availability. This program is discussed in Section 10.

### 12.3.2. Primary System Parameter Review

Results from the primary system parameter review are as follows:

1. Total power cost is reduced by increasing the turbine inlet temperature beyond 850°C (1562°F). Substantial increases in plant efficiency are obtained, with a corresponding reduction in plant and fuel costs. Material integrity and lifetime considerations need to be assessed to determine a net cost of power for higher turbine inlet temperatures (see Fig. 12-3).
2. Variations in system pressure do not significantly affect total power cost. The reference pressure value, nevertheless, does appear to be at the optimum value.
3. Compressor pressure ratio variations do not significantly affect total power cost and follow the pressure variation case closely. The optimum compressor pressure ratio is 2.55, but the resulting estimated slight reduction in cost does not appear to warrant a change in compressor design.
4. Variations in recuperator effectiveness have a significant impact on total power cost, and the recuperator effectiveness based upon the current recuperator model is the optimum value for the reference design.
5. The nominal power density value of 7.0 W/cm<sup>3</sup> appears to be at or near optimum for a 3- or 4-yr fuel cycle assumption. Fairly strong cost penalties are incurred at lower power densities, while little cost incentive exists to raise the power density above the 7.0 W/cm<sup>3</sup> value.

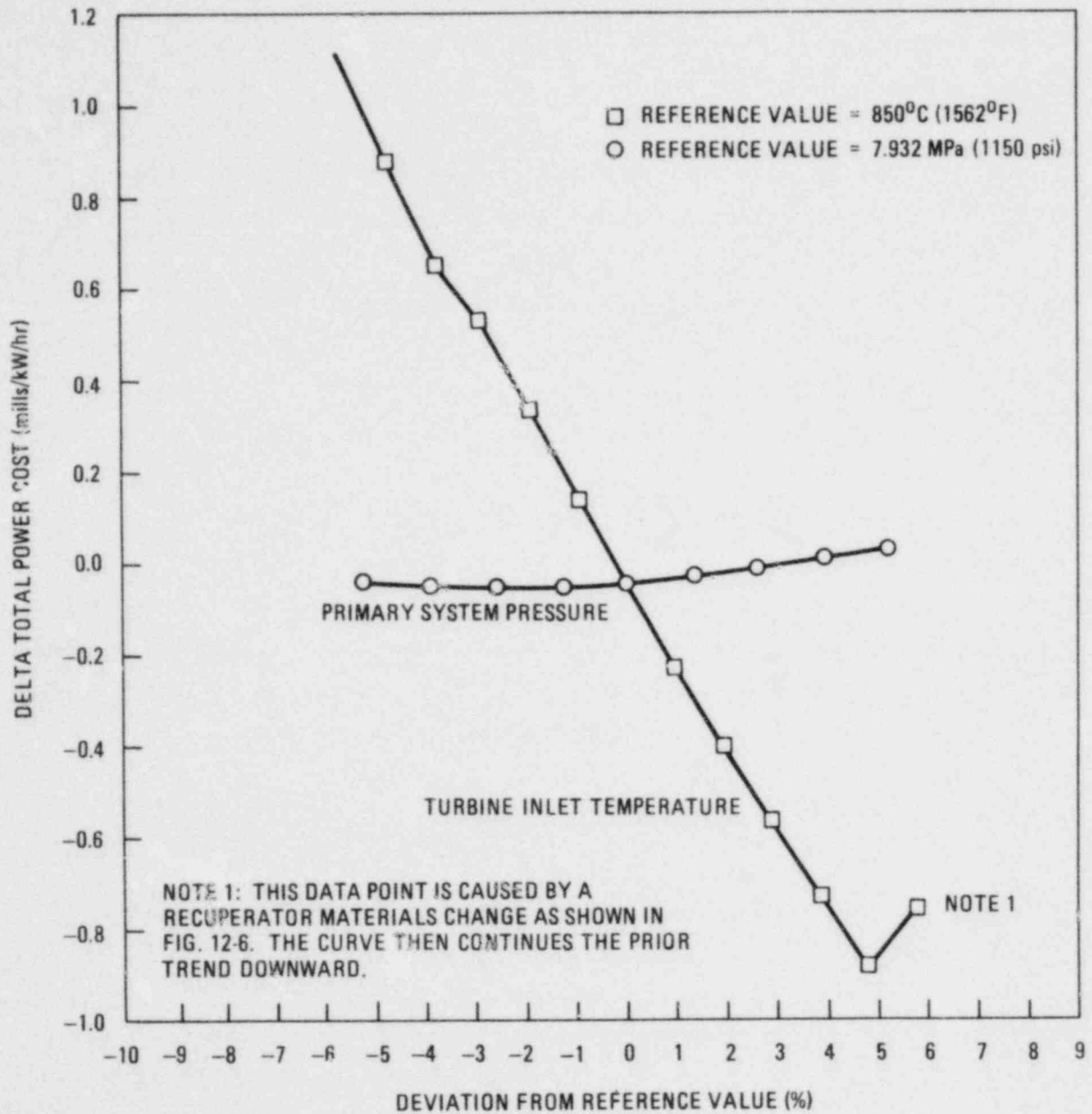


Fig. 12-3. Turbine inlet temperature and system pressure variations versus change in power cost at 80% capacity factor

6. For the 4-yr fuel cycle case, predicted fission product release is a strong function of turbine inlet temperature (i.e., fuel temperature) and has a pronounced impact on plant availability/maintainability. Since higher turbine inlet temperatures cause increased predicted fission product releases for a 4-yr fuel cycle assumption, some penalty should be associated with higher turbine inlet temperatures (e.g., increased operating and maintenance costs). No economic assessment of this penalty has yet been made.

Predicted fission product releases for the 3-yr fuel cycle are substantially lower than those of the 4-yr cycle and are a weaker function of turbine inlet temperature. However, the 3-yr fuel cycle results in higher fuel and total power costs.

The above results are preliminary estimates of cost trends and do not comprise a comprehensive cost analysis, since other significant cost impacts, such as material integrity, effects on availability, and effects on operation and maintenance costs, have not been incorporated. The analysis results are also highly dependent on the ability of the components to fit in the assigned envelopes and retain the desired performance characteristics.

#### 12.3.3. Non-Intercooled Versus Intercooled Plant Optimization Study

In the non-intercooled versus intercooled plant optimization study, CODER7 and CODER8 were used to optimize plant total power cost. CODER7 and CODER8 are equipped with an automated multiparameter plant optimization capability whereby a maximizing search is performed in the independent variable space by using direct evaluations of the objective function (total plant cost). Finite step exploration is used to guide an acceleration method based on the Fibonacci sequence for efficient use of computer time.



Figures 12-4 and 12-5 are the process flow diagrams for the non-intercooled and intercooled cycles, respectively. Generally speaking, for both cases the recuperator effectiveness increased until additional surface area cost overrode the cycle efficiency benefit, and heat exchanger cavity diameters increased to reduce shell side pressure losses. Also, precooler pitch/diameter ratio increased in order to minimize shell side pressure losses and minimize the number of helically wrapped tubes, since the precooler cost algorithm shows that the number of precooler tubes is the cost function that largely governs precooler cost. System pressure increased in both cases to reduce compressor work. Above 8.41 MPa (1220 psia) for the non-intercooled case, the additional PCRV cost associated with higher system pressure offsets the cycle benefits. In the intercooled case, the system pressure was constrained to 8.62 MPa (1250 psia) since the CODER PCRV sizing algorithm may not be accurate above that level. Note that an improvement of intercooled cycle efficiency from 43.5% might be gained by allowing system pressure to move to the 8.83 to 8.98 MPa (1280 to 1300 psia) range.

#### 12.3.4. Helium Inventory Control System for 3000-MW(t) HTGR-GT Plant

A preliminary definition of a reference HICS was developed based on the load change requirements tentatively identified for the 3000-MW(t) HTGR-GT plant (see Table 12-10 and Fig. 12-6). The HICS accommodates changes in PCRV helium inventory which, in turn, produce direct, proportionate variations in the plant power output. This control method permits much higher part-load efficiencies than are achievable by alternative, conventional power control modes (see Fig. 12-7).

For increased load changes of any anticipated requirement, the system merely supplies helium from external storage facilities to adjust the inventory appropriately. For normal, day-to-day load reductions, i.e., up to 0.42%/min, the HICS removes helium from the PCRV through a helium purification system to external storage. When less-frequent, faster load

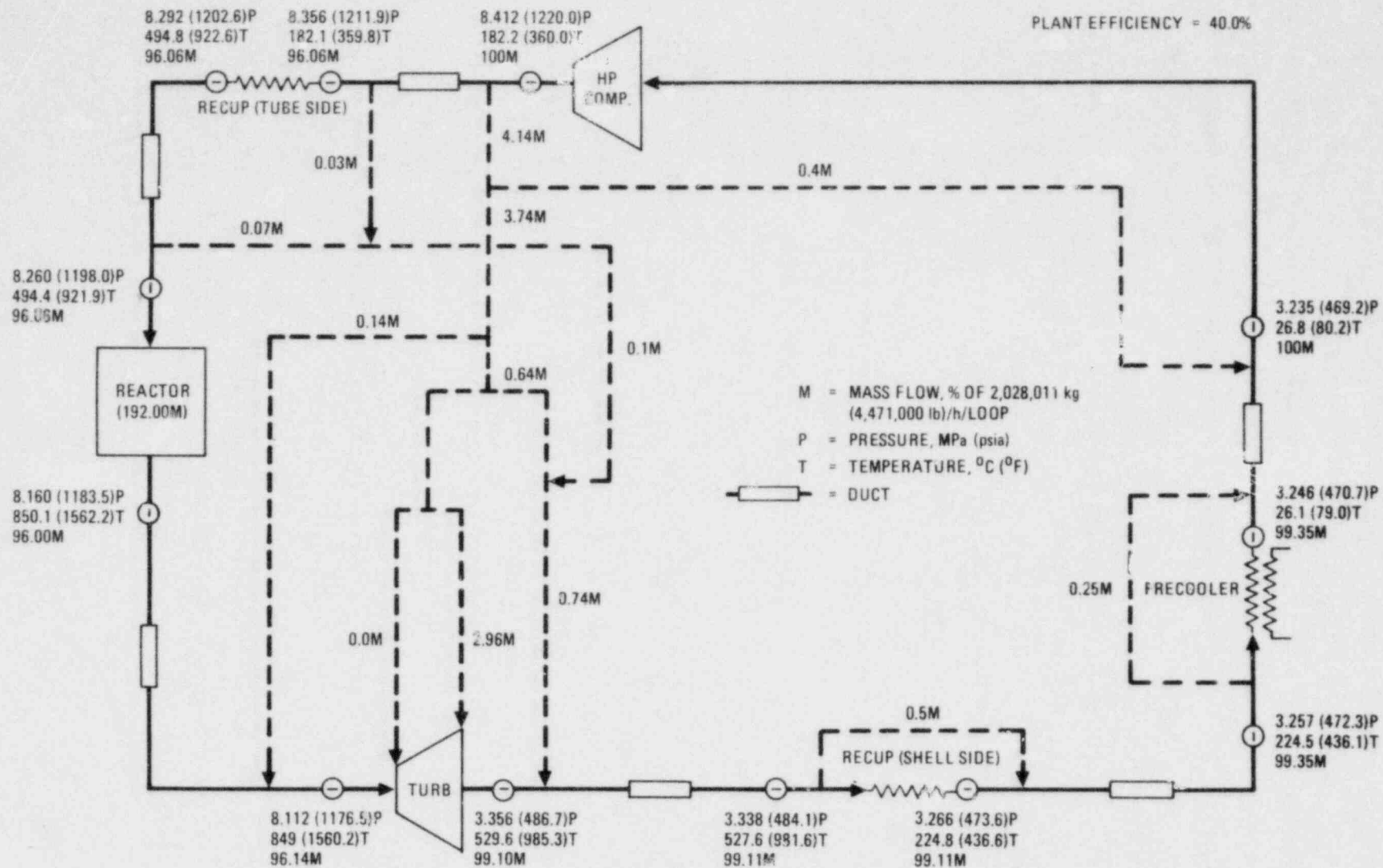


Fig. 12-4. Process flow diagram for two-loop, 800-MW(e) HTGR-GT non-intercooled plant using CODER8 (Run No. H03B/H05 optimized)

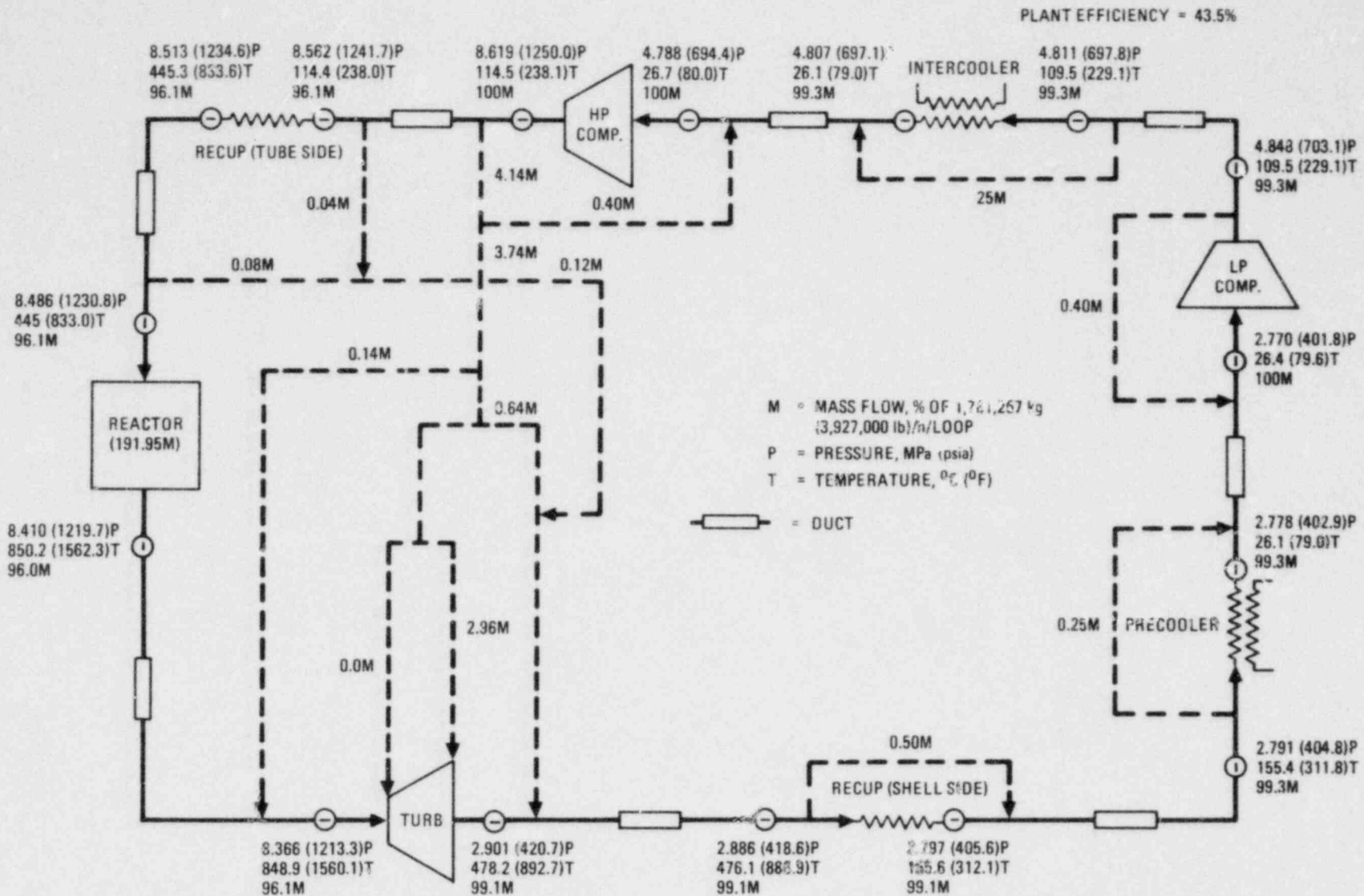


Fig. 12-5. Process flow diagram for two-loop, 800-MW(e) HTGR-GT intercooled plant using CODER7 (Run No. G03B/G04 optimized)

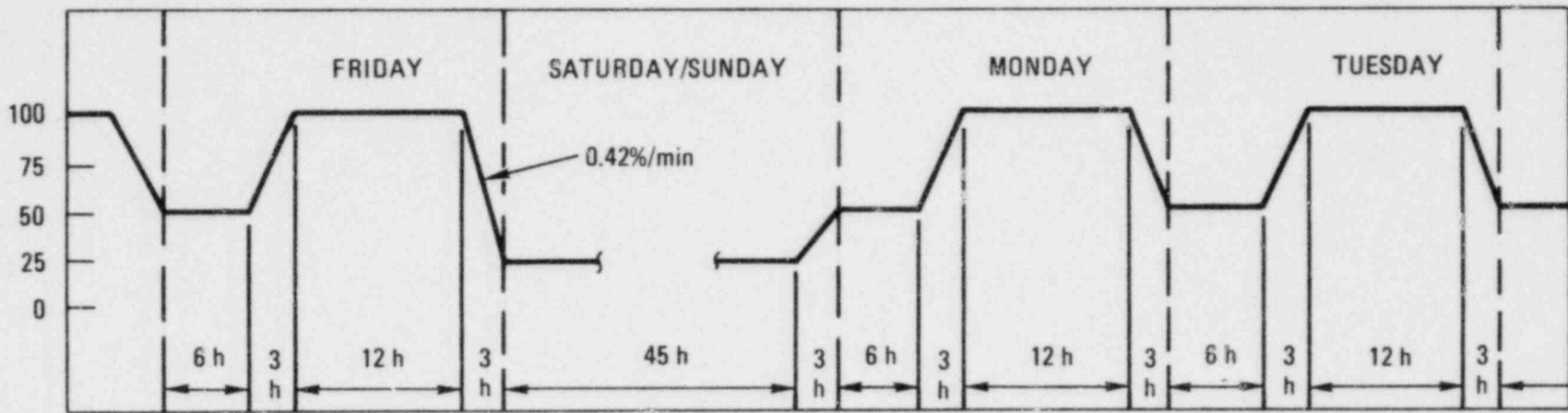
TABLE 12-10  
ANTICIPATED TRANSIENTS FOR 3000-MW(t) HTGR-GT COMMERCIAL PLANT

	Design Number of Occurrences for Plant
Normal transients	
Startup from refueling status	130
Shutdown to refueling status	80
Shutdown with full helium inventory	40
Rapid load increase (5%/min)(25%-100%)	500
Normal load increase (0.42%/min)(25%-100%)	2,600
Normal load increase (0.42%/min)(50%-100%)	10,400
Rapid load decrease (5%/min)(100%-25%)	500
Normal load decrease (0.42%/min)(100%-25%)	2,600
Normal load decrease (0.42%/min)(100%-50%)	10,400
Step load increase (+10%) <sup>(a)</sup>	2,000
Step load decrease (-10%) <sup>(a)</sup>	2,000
Upset transients	TBD <sup>(b)</sup>
Emergency transients	TBD
Faulted transients	TBD

(a) Rate of step ramp to be resolved; formerly assumed to be in 10 to 20 s with at least 2 h elapsed time between power ramps.

(b) To be determined.

12-29



NOTE: TOTAL LIFETIME SHUTDOWN CYCLES = 400

Fig. 12-6. Representation of load-following cycle

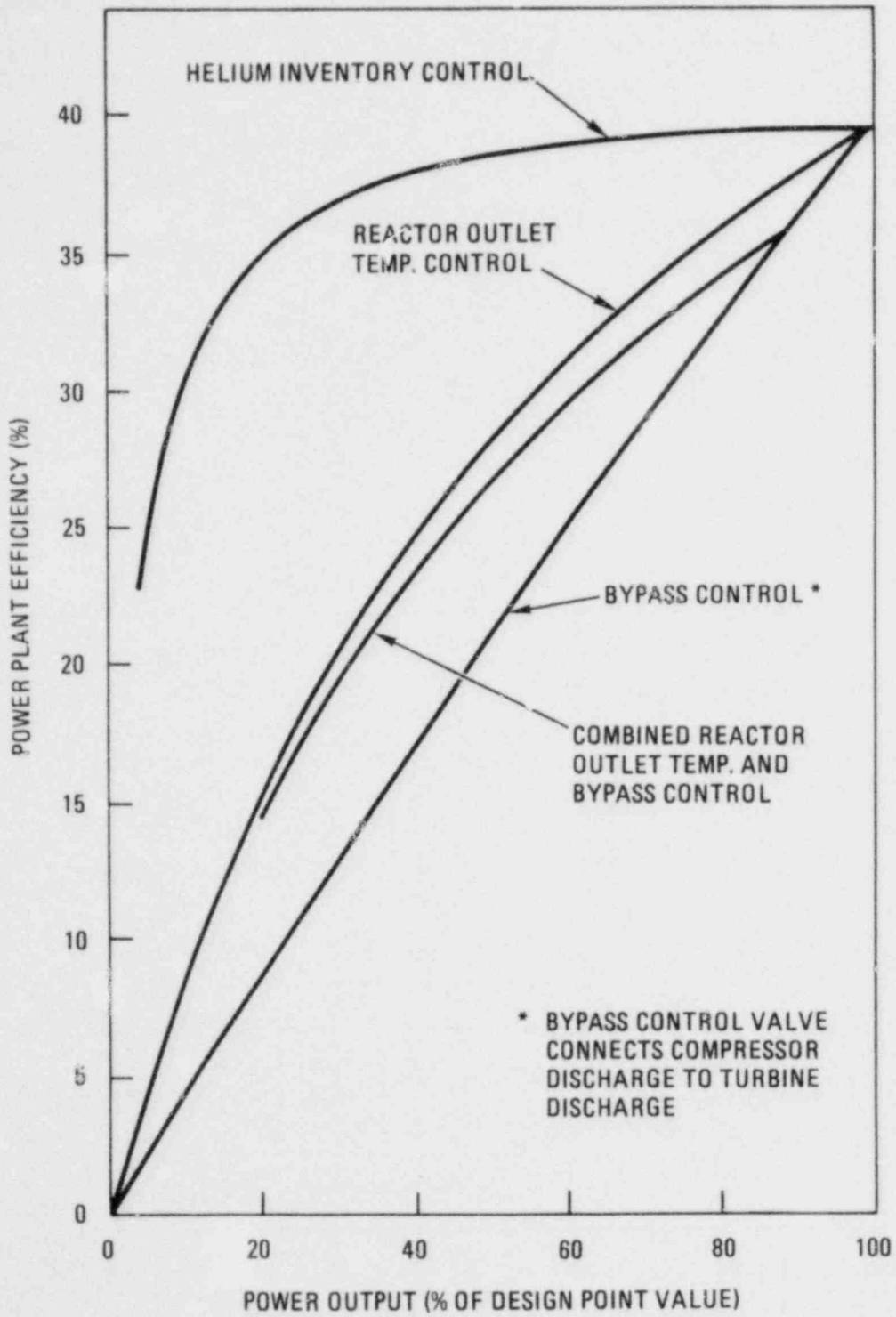


Fig. 12-7. Part-load efficiency for various control modes

reductions must be made,\* the bypass valve can first be opened (instantly), as required, and then the HICS can be used to "catch up" with the change, i.e., through simultaneous adjustment (reclosing) of the bypass valve while helium is removed from the PCRV (at the 0.42%/min rate).

A larger helium purification system will be needed to accommodate helium removal (and cleanup) for the normal load reductions of up to 0.42%/min. This requirement can be satisfied by either an added, separate system (up to 2.4 times the size of the reference unit) or by a single, combined system (up to 3.4 times the size of the reference system).

Further design studies and cost estimates will be required to evaluate the benefits which may be realized by adding the HICS to an HTGR-GT plant. The potential cost savings which can result from the improved part-load efficiencies, estimated at a capitalized cost advantage of about  $\$70 \times 10^6$  (see Table 12-11), must be balanced against the costs of additional equipment and facilities needed to incorporate the HICS into the plant design, e.g., added or increased-capacity helium purification equipment, external helium storage facilities, piping and valves, a sophisticated plant control system, etc.

A conceptual piping and storage system for an HICS, which could serve a 3000-MW(t) HTGR-GT commercial plant, is illustrated in Fig. 12-1. As indicated, inventory reductions occur from a single high-pressure point (recuperator inlet) in the PCRV; radioactive fission products are removed from the relatively cool helium [ $74.4^\circ\text{C}$  ( $346^\circ\text{F}$ )] before it is transferred to medium- or low-pressure storage tanks, which would be consolidated with the BOP-provided helium supply system. Inventory increases, for added power demands, are made by injecting helium at two locations, i.e., a high-pressure (recuperator inlet) and a low-pressure (precooler inlet) point in the system. The largest flow requirement for these inventory increases,

---

\*Up to 5%/min, or the step ramp of 10% power in 10 to 20 s.

TABLE 12-11  
 PLANT EFFICIENCY/COST SAVINGS ASSOCIATED WITH HICS

	Plant Eff. at (%) Power Level			Additional Fuel Burnup, Weekly Cycle	Overall Plant Eff., Weekly Cycle (%)	Equivalent Savings/Week	
	25%	50%	100%			MW(e)-h	\$(a)
HICS	36.5	38.7	39.5	Basis	39.0	25,350	302,680
Bypass plus temperature control	18.7	27.5	39.5	19.5	32.6	Basis	Basis

(a) 1979 dollars, based on fuel cycle cost of 11.94 mills/kW-h. Fuel cycle cost savings = (52 wk/yr) (0.8 plant factor) (\$302,680) = \$12.6 x 10<sup>6</sup>/yr. Equivalent capital investment cost = \$12.6 x 10<sup>6</sup>/(0.18 fixed charge) = \$70 x 10<sup>6</sup>.



dictated by the 10% step load demand, can be met by two containment penetrations of about 0.28-m (11-in.) diameter. This pipe size satisfies the maximum area of 645 cm<sup>2</sup> (100 in.<sup>2</sup>) imposed to limit helium leakage in the event of a DBDA.

#### 12.3.5. ΔP/P and Bypass Flows for 3000-MW(t) HTGR-GT Plant

Definition and updating of the primary system pressure drops and system leakage/bypass flows were performed for the 3000-MW(t) HTGR-GT reference commercial plant. The pressure drop data include all duct, heat exchanger, plenum, and turbomachinery (inlet and exit) losses as well as those for the core. A schematic diagram of the HTGR-GT plant is shown in Fig. 12-2 with numerical and alphabetical identification of the specific ΔP and leakage/bypass items, respectively, which were included. Data on pressure drop and leakage/bypass flows were developed only for the 100% full-power, steady-state condition.

Table 12-4 is a detailed listing of the primary coolant system pressure losses. The ΔP values found are higher than prior data; the heat exchanger components and the core contributed most of the increased pressure drop. Because of the limited effort previously placed on heat exchanger component design studies for the three-loop 3000-MW(t) plant, many dimensions necessary for pressure loss calculations were unavailable and had to be assumed or estimated. Also, a higher pressure drop was calculated for the reactor core owing to the higher helium flow rate required for the gas turbine cycle. The total pressure drop of the primary coolant system was calculated to be 520.5 kPa (75.5 psi), or a ΔP/P of about 9.9%.

Table 12-12 is a categorized summary of the pressure losses by major components and indicates potential pressure drop reductions that could be achieved through improvements in system and component design arrangements. It appears that improvements should be possible by increasing the radius of bends in all ducts, installing a diffuser section at the duct-to-component and reactor plenum inlets, and providing a rounded edge section

TABLE 12-12  
PRIMARY SYSTEM PRESSURE LOSS SUMMARY

System Component	Pressure Loss			Potential Pressure Loss Improvement		
	$\Delta P$		$\Delta P/P$ (%)	$\Delta P$		$\Delta P/P$ (%)
	kPa	psi		kPa	psi	
Helium flow ducts <sup>(a)</sup>	36.96	5.36	0.549	-6.89	-1.00	-0.102
Heat exchanger components <sup>(b)</sup>	244.35	35.44	5.868	-65.50	-9.50	-1.573
Reactor core <sup>(c)</sup>	129.0	18.72	1.670	-13.79	-2.00	-0.178
Turbomachinery <sup>(b)</sup>	110.04	15.96	1.810	-10.34	-1.50	-0.177
	520.42	75.48	9.897 <sup>(d)</sup>	-96.53	-14.00	-2.030 <sup>(d)</sup>

(a) Includes friction plus elbow turn losses.

(b) Includes inlet expansion and outlet contraction losses of the ducts.

(c) Includes upper and lower plenum flows and inlet expansion and outlet contraction losses of the plenum ducts.

(d) These losses are not strictly additive, but for comparison purposes they are usually indicative of plant layout merit.

at the component and plenum-to-duct exits. It also may be feasible to reduce the core pressure loss through design improvements in the core inlet and outlet coolant flow paths and by optimizing the graphite block coolant hole sizes and the number of graphite block columns. Improvements in pressure loss for the turbomachinery may be possible by utilizing diffusers and flow guides to minimize turning losses in the entrance and exit areas. Detailed design layout of heat exchanger components should provide sufficient information to perform an adequate pressure loss analysis and identify critical areas for improvement, such as redesign of the tube support plate to improve the associated drag coefficients. By using diffusers and rounded edge entrances into ducts, additional pressure loss improvements may be possible for the heat exchanger components.

The primary coolant system bypass/leakage flows, given as percentages of compressor discharge flow, are itemized in Table 12-13. Most of this information, except for the flows through the core region, is based on estimates that have been developed in previous studies on similar plants.

#### 12.3.6. Evaluation of Cooling Towers and Ambient Design Temperatures

Sizing and cost evaluations have been performed to (1) determine the influence of the major tower sizing parameters on design point plant performance and on plant cost of power, (2) compare design point performance and cost of power for an intercooled plant and a non-intercooled plant, and (3) compare plant design point performance and cost of power for different cooling tower arrangements.

Results of the parameter evaluation are generally as expected: design point plant performance decreases and cost of power increases as design point ambient temperature increases. Also, lower tower approach temperatures result in increased design point plant performance and lower cost of power. This influence is not affected by design point ambient temperature.

TABLE 12-13  
PRIMARY COOLANT SYSTEM BYPASS/LEAKAGE FLOWS

Bypass/Leakage Flow Description	Item (see Fig. 12-2)	Mass Flow <sup>(a,b)</sup> (%)
Recuperator shroud seal leakage <sup>(c)</sup>	A	0.5
Precooler shroud seal leakage <sup>(c)</sup>	B	0.25
Turbine blade cooling flow <sup>(c)</sup>	C	0
Turbine disk cooling flow <sup>(c)</sup>	D	2.96
Compressor (HP) cavity seal leakage to compressor inlet <sup>(c)</sup>	E	0.4
Compressor (HP) cavity seal leakage to turbine outlet <sup>(c)</sup>	F	0.64
Compressor (HP) cavity seal leakage to turbine inlet <sup>(c)</sup>	G	0.14
Control valve seat leakage <sup>(d)</sup>	H	0.1
Attemperation valve seat leakage	I	0.1
Safety valve seat leakage	J	0.1
Core peripheral seal leakage <sup>(e)</sup>	K	0.48-1.43
Core leakage		
Core gaps	L	2.95
Reflector gaps <sup>(e)</sup>	M	1.71
Core flows		
Through variable orifice regions	N	81.65
Through fixed orifice regions	O	5.52
Through control rod channels	P	3.33

(a) Percentage of compressor discharge flow.

(b) CACS leakage not included in these data. Values shown are normalized for exclusion of CACS data.

(c) These former values were not updated but were recently reviewed by UTC and are considered appropriate for the current design status.

(d) Includes both primary bypass and trim valves.

(e) Core peripheral seal leakage flow is included in (is part of) reflector gap flow.

The comparison between intercooled and non-intercooled optimized plants indicates that the design point performance (plant efficiency) of the intercooled plant is approximately three percentage points higher than that of the non-intercooled plant. Correspondingly, the cost of power for the intercooled plant is approximately 1.5 mills/kW-h less than that for the non-intercooled plant. This difference in performance and cost of power is essentially the same for different design point ambient temperatures.

The comparison of an optimized plant with a wet/dry cooling tower arrangement and an optimized plant with an all-dry natural draft cooling tower arrangement indicates that the plant with the wet/dry arrangement has higher design point plant performance and lower plant cost of power than the plant with the all-dry tower arrangement. The differences increase as the plant design point ambient temperature increases. At a design point ambient temperature of 15°C (59°F), the plant efficiency for the all-dry tower plant is approximately 0.5 percentage point lower than that for a wet/dry tower plant and the cost of power is approximately 0.5 mill/kW-h higher. At a design point ambient temperature of 38°C (100°F), the plant efficiency for the dry cooling plant is approximately 1.5 percentage points lower than that for the wet/dry tower plant and the cost of power is approximately 1.5 mills/kW-h higher.

#### 12.3.7. CACS Design Criteria

A design report (currently in the review and sign-off phase) has been prepared defining the tentative design criteria for the CACS for the two-loop 800-MW(e) HTGR-GT plant.

Design bases are established which assure a high reliability for the CACS to provide residual heat removal from the core and reactor internals in the event that the power conversion loops are not available.

In addition to firm (overall) design criteria for the CACS, the report also covers safety and non-safety performance criteria for the CACS, safety criteria for supporting systems, specific design basis transients, surveillance and monitoring requirements, design margins, and uncertainties in design parameters to be included in performance and safety analyses. These items, which are not yet developed, will be added when the design for this plant becomes better defined.

#### 12.3.8. CACS Component Sizing

Preliminary system parameters and "ballpark" sizing of components have been developed for the RTS portion of the CACS (System 28) and the CACWS (System 47). These data are presented in Tables 12-5 through 12-8. Table 12-5 gives overall system performance at three steady-state design points, i.e., peak duties in the depressurized pure helium, the depressurized air ingress, and the pressurized PCRV transients. Tables 12-6 and 12-7 specify performance parameters for the auxiliary circulator and CAHE, respectively, for the three cases. Design and configuration information on the CACWS is shown in Table 12-8. Engineering cost estimates, based on these data, are summarized in Table 12-9.

These values are the result of sizing calculations performed with the ECSEL8 code, based on data from preliminary RECA calculations which provided functions used by ECSEL. This computer program selects a minimum cost configuration for the entire CACS based upon various input factors, such as component cost functions, maximum primary coolant temperatures, pressure drop functions, certain component sizing ground rules, and performance requirements based on the system safety criteria in the various design basis transients.

The design basis events are based on the criteria proposed for the HTGR-GT in the Core Auxiliary Cooling System Design Basis Document presently in review. The document gives preliminary design basis transients

for the CACS for the HTGR-GT. These transients are the DBDA [645 cm<sup>2</sup> (100 in.<sup>2</sup>) PCRV breach], core outlet (hot duct) failure, and slow depressurization through a CACS penetration. As in the past, the DBDA is really two accidents with regard to CACS design, i.e., the depressurized pure helium and depressurized air ingress cases. In all cases except the slow depressurization, two CACS loops cool the core, the third CACS having suffered the postulated single failure. In the depressurized cases, the cooldown is at the pressure conservatively calculated for PCRV containment equilibrium at 5 h. In the duct failure event, the primary coolant is pressurized. In all events except the slow depressurization, an SSE occurs simultaneously, a rule imposed for initiating events of the most remote probability (Plant Condition 5, PC-5).

The criteria in the design report are based on an assumption that the precooler is not wholly seismic Category I, and thus the water inventory of all precoolers is considered to have been mixed with the primary coolant in the DBDA and duct failure design basis events. It now appears that the precooler might be made Category I to assure against a greater than 645 cm<sup>2</sup> (100 in.<sup>2</sup>) flow area for the DBDA. Therefore, for the present sizing calculation, no moisture is considered in the primary coolant from the precooler.

The slow depressurization event involves cooldown on one CACS loop but no SSE and takes advantage of power conversion loop inertial rundown. As a result, it is not part of the CACS sizing basis.

Bypasses calculated for the CACS sizing bases are as follows:

	<u>Bypass</u> (% of Core Flow)	<u>Bypass</u> (% of Total Flow)
Depressurized	88	47
Duct failure (pressurized)	142	59

One sizing ground rule, specified by the current general arrangement drawing, is that the CAHE is a 571 mm (22.4 in.) by 50.8 mm (2 in.) o.d. tube bayonet configuration within a 1.524 m (5 ft) diameter shroud. Based on this assumption, ECSEL can provide the CAHE surface area and length, although these two values are not system performance parameters imposed upon the design.



## 13. SYSTEM DYNAMICS (631003)

### 13.1. SCOPE

The purpose of this task in FY-79 was to analyze plant transient performance, develop control and PPS requirements, assess and develop system operational requirements, and provide transient requirements for component and subsystem design. The scope of this task also included analysis of acoustical aspects of the primary circuit, natural convection, and local flow mixing and heat transfer in the primary circuit.

### 13.2. SUMMARY

Efforts within the task were in four major areas:

1. Extension of transients with the three-loop, 1200-MW(e) plant, preliminary analyses of major transients with the two-loop, 800-MW(e) plant, and comparison of results obtained for the two plants.
2. Plant control and protection systems functional design.
3. Intercooled versus non-intercooled and warm linear versus cold liner studies.
4. Preliminary evaluations of primary circuit sound pressures, natural convection with no forced flow, and mixing of the turbine exhaust and bypass valve flow.

Additional three-loop, 1200-MW(e) plant transients were analyzed, and preliminary transient analyses of the two-loop plant were performed using

an "approximate" plant model (see Section 3). Somewhat more severe conditions are encountered for some events with the two-loop plant than for the three-loop plant. However, the preliminary analyses indicate that reasonable modification of the control and protection system functions leads to acceptable operation of the two-loop plant.

Plant shutdown control procedures and control functions were developed to provide a well-behaved transient for the severe event of reactor trip at design power. The shutdown transient was extended to long-term main loop afterheat removal out to approximately 2 days, indicating an indefinite period of main loop afterheat cooling capability. Operation of the plant control system with nominal-inventory insertion and removal was analyzed, providing scoping input to the helium handling studies to be performed in FY-80.

Studies of the control, transient behavior, and operability aspects of the intercooled versus non-intercooled and the warm liner versus cold liner plant variants were performed. Significant problem areas were identified for the warm liner variant, while no major differences were identified between the intercooled and non-intercooled designs.

An estimate of loop natural convection flow with no forced circulation (loss of offsite power) was made. The flow resistance of the turbine and compressor (assumed stationary) was so high that loop natural convection flow was essentially suppressed [ $\sim 0.005$  kg/s ( $\sim 0.01$  lbm/s) per loop with a typical velocity of less than 0.03 m/s (0.1 ft/s)].

Mixing of the turbine exhaust and bypass valve gas streams during loop shutdown was analyzed in a preliminary manner. The analysis indicates that mixing is incomplete at the entrance of the recuperator. This problem can be eliminated by the utilization of a longer duct downstream of the mixing point.

### 13.3. DISCUSSION

#### 13.3.1. Three-Loop, 1200-MW(e) and Two-Loop, 800-MW(e) Plant Analyses and Comparison

13.3.1.1. 1200-MW(e) Reference Commercial Plant Transient Analysis. The transient analysis program REALY2 was used to simulate 12 plant transients which demonstrate plant automatic load-following characteristics and plant operability in the 100% to 25% nominal power range with primary bypass, turbine inlet temperature, and helium inventory control. (Inventory control is an optional PCS control scheme whereby primary system pressure is adjusted through increase or decrease of primary coolant inventory. It provides the most efficient means for obtaining and controlling part-load plant operation (see Section 12.3.4). These transients also include two accident events at 25% nominal power.

The load-following capabilities of the HTGR-GT plant consist of (1) ramp load changes within the range of 100% to 25% of rated load at rates up to a maximum of 5% of rated load per minute, and (2) step load increase/decrease of up to a maximum of 10% of rated load with a response time of approximately 20 s. The load-following transients analyzed (see Table 13-1) considered only the 5%/min and the 10% step load changes because they establish limiting load-following conditions for the PCS; i.e., the deviations of plant variables from their normal steady-state values tend to be proportionately smaller as the rate and/or magnitude of the load change is decreased.

The two transients at 25% nominal, plant loss of precooling water and rod runout, resulted in significantly different (but not necessarily worse) plant response (Table 13-1) than the same transients of 100% nominal reported in Ref. 13-1, Table 13-1. The plant loss of precooling water transient combined with a single failure of the non-safety CWS protection function of the PCS resulted in a sequence whereby normal PCS functions essentially shut down (but did not trip) the reactor and main loops. After about 2 min, the PPS would detect low plant helium flow and subsequently it

TABLE 13-1  
1200-MW(e) HTGR-GT Reference Commercial Plant Transient Performance Comparison<sup>(a)</sup>

Transient Description	Max. Core Inlet/Outlet Temp.		Max. Power-to-Flow Ratio	Max. Press. and Temp. at LPR <sup>(b)</sup> Inlet		Max. Press. at Compressor Inlet [kPa (psia)]	Max. Flow Rate at LPR Inlet [10 <sup>6</sup> kg/h (10 <sup>6</sup> lbm/h)]	Max. Turbine Speed (rpm)	Max. Precooler Inlet and Outlet Temp.		Max. Recup. Hot End Metal Temp. [°C (°F)]	Max. Recup. Cold End Metal Temp. [°C (°F)]
	°C (°F)	°C (°F)		kPa (psia)	°C (°F)				°C (°F)	°C (°F)		
Full load 100% nominal	500 (932)	850 (1562)	1.00	3248 (471)	537 (999)	3185 (462)	2.05 (4.53)	3600	224 (436)	27 (80)	513 (955)	207 (405)
10% load reduced from 100% nom. (5%/min) w/o HIC <sup>(c)</sup>	500 (932)	850 (1562)	1.00	3296 (478)	537 (999)	3227 (468)	2.12 (4.67)	3600	224 (436)	27 (81)	516 (961)	207 (405)
25% load reduced from 100% nom. (5%/min) w/o HIC	500 (932)	850 (1562)	1.00	3296 (478)	539 (1002)	3234 (469)	2.14 (4.73)	3600	224 (436)	28 (82)	514 (958)	207 (405)
Step load change 100%-90%-100% nom. w/o HIC	501 (934)	851 (1564)	1.09	3310 (480)	538 (1000)	3234 (469)	2.14 (4.72)	3600	224 (436)	28 (83)	516 (960)	207 (405)
Step load change 100%-90%-100% nom. with HIC	<u>504 (939)</u>	<u>852 (1565)</u>	1.07	3248 (471)	537 (999)	3185 (462)	2.05 (4.53)	3600	228 (442)	27 (80)	514 (957)	208 (406)
100%-25% nom. load reduction (5%/min) w/o HIC	500 (932)	850 (1562)	1.00	3344 (485)	537 (999)	3268 (474)	2.26 (4.99)	3600	224 (436)	28 (83)	513 (955)	207 (405)
100%-25% nom. load reduction (5%/min) with HIC	500 (932)	850 (1562)	1.00	3248 (471)	538 (1000)	3185 (462)	2.06 (4.54)	3600	224 (436)	27 (80)	513 (955)	208 (406)
Primary bypass valve reclosure from 75% nom. with full helium inventory	455 (851)	777 (1430)	1.00	3254 (472)	486 (907)	3192 (463)	2.12 (4.67)	3600	215 (420)	27 (81)	468 (875)	199 (391)
Reactor trip from 100% nominal with HIC	500 (932)	850 (1562)	1.00	3951 (573)	559 (1038)	3923 (569)	2.42 (5.33)	3600	224 (436)	28 (83)	513 (955)	207 (405)
Quarter load 25% nominal	334 (634)	562 (1043)	0.62	3172 (460)	352 (665)	3103 (450)	2.16 (4.76)	3600	181 (358)	26 (79)	342 (647)	168 (335)
Plant total loss of precooling water at 25% nom. with full helium inventory	413 (776)	585 (1086)	1.06	<u>5350 (776)</u>	469 (877)	<u>5350 (776)</u>	2.44 (5.37)	<u>3614</u>	228 (443)	130 (267)	429 (805)	210 (410)
Rod runout at 25% nominal with full helium inventory	367 (693)	624 (1156)	<u>1.40</u>	3296 (478)	387 (729)	3229 (467)	2.24 (4.94)	3600	187 (368)	27 (81)	377 (710)	174 (345)

(a) Underlined numbers are the highest values predicted for given parameter.

(b) Low-pressure recuperator.

(c) Helium inventory control.

would initiate CACS startup, main loop trip, and reactor trip. Peak temperatures for this transient were lower than those reported for the case occurring from design conditions (Ref. 13-1).

The rod runout transient may or may not lead to a PPS core power to flow (P/F) trip, depending upon the initial rod position. Whereas a fully inserted rod bank has sufficient worth to induce a P/F trip, a nominally positioned (60% inserted) rod bank does not. This is attributed to the fact that a large power increase must be made before the 1.4 P/F trip setting is reached (initial P/F is approximately 0.62 for 25% load steady-state operation). Only modest temperature rises were observed in this transient.

13.3.1.2. Two-Loop 800-MW(e) Plant Transient Analysis. Six accident events were analyzed for this plant configuration (Table 13-2). Two of these transients, single loop loss of load with overspeed and reactor trip from 100% nominal with helium inventory control, were selected for their effect on the two most significant plant capabilities affected by the change from a three-loop to a two-loop plant design: (1) the ability to sustain single loop loss of load/loop shutdown events without invoking a plant shutdown and (2) the ability to provide extended main loop afterheat cooling.

Simulation results show that a single loop loss of load transient will result in a severe increase of the ratio of reactor core power to reactor core helium flow. This very short-term mismatch ( $P/F = 3.36$ ) will cause the PPS to initiate a reactor trip unless a filter network is designed into the measurement and/or evaluation of the appropriate signals. Preliminary evaluation indicates that the reactor core will not suffer any damage from this short (7.5 s above 1.4 P/F ratio) undercooling period.

Results also indicate that a reactor trip with appropriate non-safety PCS actions permits post-scrum, self-sustaining single main loop cooling without motoring of the generator. In addition, these PCS actions provide

TABLE 13-2  
TWO-LOOP 800-MW(e) HTGR-GT PLANT TRANSIENT PERFORMANCE COMPARISON<sup>(a)</sup>

Transient Description	Max. Core Inlet and Outlet Temp.		Max. P/F Ratio	Max. Press and Temp. at LPR <sup>(b)</sup> Inlet		Max. Press. at Compressor Inlet [kPA (psia)]	Max. Rate of Pressure Increase [kPA/s (psi/sec)]	Max. Flow Rate At LPR Inlet [10 <sup>6</sup> kR/h (10 <sup>6</sup> lbm/h)]	Max. Turbine Speed (rpm)	Max. Rate Of Pressure Decrease [kPA/s (psi/sec)]	Max. Precooler Inlet And Outlet Temp.		Max. Recup. Hot End Metal Temp. [°C (°F)]	Max. Recup. Cold End Metal Temp. [°C (°F)]
	°C (°F)	°C (°F)		°C (°F)	°C (°F)									
Full load 100% nominal	498 (929)	850 (1562)	1.00	3234 (469)	534 (994)	3172 (460)	-	1.96 (4.32)	3600	-	224 (436)	27 (80)	514 (957)	208 (406)
Single loop loss of load with overspeed	503 (937)	863 (1586)	<u>1.34</u>	5964 (865)	548 (1018)	5964 (865)	1296 (188)	5.58 (12.3)	<u>4150</u>	572 (83)	239 (463)	32 (89)	529 (985)	218 (425)
Single loop loss of load	502 (936)	854 (1570)	1.13	4792 (695)	545 (1013)	4620 (670)	1489 (216)	5.40 (11.9)	3858	531 (77)	238 (460)	42 (107)	519 (967)	218 (424)
Single loop total loss of precooling water flow	508 (946)	862 (1583)	<u>1.19</u>	<u>6805 (987)</u>	705 (1301)	<u>6805 (987)</u>	951 (138)	4.17 (9.2)	3615	414 (60)	309 (589)	158 (316)	588 (1090)	293 (560)
Plant total loss of precooling water flow	554 (1029)	872 (1601)	<u>1.02</u>	6130 (889)	760 (1400)	6130 (889)	903 (131)	4.17 (9.2)	3605	<u>758 (110)</u>	310 (590)	166 (330)	604 (1120)	288 (550)
Reactor trip from 100% nominal with helium inventory control	513 (955)	850 (1562)	1.00	4137 (600)	538 (1000)	4633 (672)	-	2.72 (6.0)	3600	-	226 (438)	33 (91)	518 (965)	208 (406)
25% - 100% nominal load increase (1%/min) with helium inventory control	501 (933)	851 (1564)	1.06	3275 (475)	538 (1000)	3200 (464)	-	2.09 (4.62)	3600	-	224 (436)	27 (81)	516 (960)	207 (405)

<sup>(a)</sup> Underlined numbers are the highest values predicted for given parameters.

<sup>(b)</sup> Low-pressure recuperator.

for prudent generator load runback, reactor outlet temperature control, and attemperation control to minimize thermal stresses to the reactor and PCL components. Helium inventory transfer rates of 1%/min and 5%/min with reduction to 10% inventory and a reactor outlet temperature controlled to 393°C (1100°F) were used to achieve self-sustaining main loop cooling. Owing to the lengthy nature of the reactor trip transient, an assessment of the minimum rates of helium inventory control required to provide adequate operating margins during shutdown was not performed.

Other component-limiting plant transients (Table 13-2) indicated that (1) the plant total loss of precooling water flow is the most severe transient in terms of maximum core gas temperatures and maximum heat exchanger hot end metal temperatures, (2) the single loop loss of load transient shows the most severe pressure/flow rate increase, and (3) the single loop loss of cooling water flow transient results in the maximum pressure to the low-pressure regions of the PCL and maximum recuperator cold end metal temperatures.

Although the maximum heat exchanger temperatures were higher, the two-loop plant transients were generally similar to the three-loop plant transients (Ref. 13-1).

In addition, a 1%/min upward load change transient from 25% load with reduced helium inventory conditions to 100% full load operating conditions was analyzed in order to determine the characteristics of integrated plant control combined with high- and low-pressure helium inventory insertion.

Results indicate favorable plant response using existing temperature and bypass controls (Table 13-2), although some rebiasing of the turbine inlet temperature demand versus load function would reduce or eliminate the temperature droop encountered whenever there is a mismatch between the load and helium inventory rates.

13.3.1.3. High/Low Power Difference. Two 1200-MW(e) HTGR-GT reference plant transients, plant loss of cooling water flow and rod runout, were

postulated to occur from 25% of rated plant load and resulted in significantly different (but not necessarily worse) plant response than when they were assumed to occur from 100% load.

The plant loss of cooling water transient combined with a failure of the non-safety CWS protection function of the PCS resulted in a sequence where shutdown or setback of the reactor and main loops is required. The initiating failures assumed for this transient are the multiple shear rupture of the header at the discharge of the cooling water pumps and the postulated failure of the component protection action of the PCS (main loop shutdown due to low precooler water flow). The transient was simulated by ramping water flow of all precoolers down to zero in about 4 s. The lack of water flow causes the precooler gas outlet (compressor inlet) temperature to rise, thereby slightly decreasing the mass flow through the compressors. The gas heats up as it passes through the compressors and into the high-pressure recuperator.

It was found that when this transient starts from 100% power at approximately 40 s, the water at the precooler hot end reaches saturation temperature and boiling commences. Turbine power then drops below 10% and the PCS automatically trips all generators. Upon generation trip, the primary bypass valves are opened to prevent turbine overspeed and a reactor power setback signal is issued to the neutron flux controller. As turbine speed drops below setpoint, the primary bypass valves close while the attemperation valves continue to open in order to control the recuperator temperatures. In approximately 1 min, the high-pressure recuperator outlet temperature reaches the PPS setpoint for main loop shutdown. All the main loops are tripped and the reactor is scrammed.

The above transient is different if started from the 25% load condition, because generator trip occurs about 1/2 min sooner and the PPS main loop trip on high recuperator outlet temperature does not occur at all. Instead, opening of the attemperation valves combined with non-safety reactor power setback following generator trip continuously reduces the



amount of energy available to the turbomachines. The result is a PCS shutdown of the reactor and main loops as opposed to a forced shutdown by the PPS. Eventually, however, the PPS initiates CACS startup owing to low plant helium flow, which in turn causes the main loops and reactor to be tripped.

The initiating failure for the rod runout transient is the total loss of the flux measurement signal which commands the withdrawal of the control rods at the maximum speed allowed by the rod drive mechanism. Previous incorrect operator action or failure on demand is assumed to inhibit set-back rods which should automatically compensate for large increases in core reactivity.

The increase in reactor power is small when the transient starts at 100% because of the existence of a large negative reactivity.\* A  $\Delta k$  power level of 107% was reached in approximately 140 s. The highest power-to-flow ratio attained was approximately 1.09. Power-to-flow trip of the reactor did not occur.

The rod runout transient from 25% load with full helium inventory differs in that the PPS trips the reactor on high core power-to-flow ratio in approximately 133 s. The fact that the negative reactivity coefficients are less at the lower temperatures accounts for the difference. However, the use of primary bypass control to achieve part load is the reason that the temperatures at the 25% power level are lower. If helium inventory control is used to achieve part load, it is anticipated that the transient will behave more closely with the rod runout at full load since conditions such as temperatures, core power-to-flow ratio and bypass valve settings are nearly the same as at full load.

---

\*Medium-enriched uranium, end of cycle, and initial core temperature coefficients are assumed.

### 13.3.2. Plant Control and Protection Systems Functional Design

Conceptual design of the plant control and protection systems continued during the second half of FY-79. The REALY2 code was used to scope the functional requirements for these systems. Preliminary plant transient data and conceptual design requirements data were transmitted to the component design groups. In addition, special control requirements including plant shutdown control, helium inventory control, and control rod shimming functions were defined and incorporated into the REALY2 code.

13.3.2.1. Plant Shutdown Control System. The design goal for the non-safety plant shutdown control system is the controlled removal of decay heat from the reactor core and the use of this heat to drive a single turbomachine unit, creating self-sustaining operation. The attainment of self-sustaining operation requires helium inventory reduction, control of reactor outlet temperature, shutdown of one of the two PCLs, and the capability of the remaining loop to operate at reduced speed. Furthermore, the controlled removal of decay heat via reactor outlet temperature control permits the regulation of reactor cooldown rate to alleviate thermal stresses to the reactor and PCL components. The post-scrum shutdown control actions are summarized below:

1. Generator load reduction at 2%/s followed by a generator trip at the 10% minimum load point.
2. No-load speed control of turbomachines (following generator trip) to achieve a desirable reactor outlet temperature (ROT) cooldown rate (ROT demand is run back at a rate of 17.5°C/s (0.5°F/s).
3. Trip of one of the two main loops after speed demand has dropped below 2400 rpm.
4. Continuous helium inventory removal, 10% removal in 2 min and 1%/min subsequent removal rate, until inventory is reduced to 10%.

5. Maintenance of attemperation temperature demand at design value followed by resetting of the attemperation controller to control only the high-pressure recuperator outlet temperature.

Results from the REALY2 simulation of a reactor scram from 100% nominal power indicate that a single PCL can provide controlled reactor cooldown and self-sustaining decay heat removal for more than 2 days with adequate margin. Table 13-3 gives the three-loop plant conditions at the end of 2 days from scram with 15% helium inventory. Core inlet and outlet temperatures are 475°C (887°F) and 590°C (1094°F), respectively. Turbo-machine speed is approximately 55% of nominal, and the primary bypass valve is about 14% open. The core cooling coefficient (ratio of decay heat rate to heat removal rate) is nearly 1.15. Similar self-sustaining plant conditions with 10% helium inventory and proportionally lower system pressures were obtained for the two-loop plant model.

13.3.2.2. Helium Inventory Control System. Three primary means are available for obtaining and controlling part load operation of the HTGR-GT. Bypass valve operation (bypass control), which effectively provides a shunt flow path across the core and turbine, provides rapid (fraction of a second) load change. Adjustment of turbine inlet temperature (temperature control) allows load adjustment at a slower rate (minutes). Adjustment of system pressure by increase or decrease of primary system inventory (inventory control) provides the third and most efficient means of load adjustment. Standard helium cleanup and transfer systems result in hours being required for large changes in inventory. Supplemental helium transfer systems are currently being evaluated to establish the rate and amount of inventory control which will be provided as a part of the standard HTGR-GT. This evaluation will also determine what degree of increased inventory control may be provided as an option. The helium transfer assumed in the control studies was chosen as typical and utilized to establish viable operation of the other controls in combination with inventory changes.

TABLE 13-3  
PLANT CONDITIONS TWO DAYS AFTER SCRAM

Component	Inlet Flow [kg/h (lbm/h)]	Inlet Pressure [kPa (psia)]	Inlet/Outlet Temperature [°C(°F)]
HP plenum	122,884(270,912)	760.10(110.24)	475.2/475.3 (887.3/887.5)
Core	122,804(270,737)	759.90(110.21)	475.3/589.9 (887.5/1093.8)
Turbine	128,129(282,477)	757.48(109.86)	589.9/534.7 (1093.8/944.5)
LP recuperator	187,130(412,550)	618.69(89.73)	497.11/111.8 (926.7/233.2)
LP plenum	187,130(412,550)	617.72(89.59)	111.8/111.7 (233.2/233.1)
Precooler	186,546(411,264)	617.17(89.51)	111.7/20.8 (233.0/69.4)
Compressor	187,296(412,916)	616.34(89.39)	21.4/58 (70.5/136.4)
HP recuperator	178,793(394,170)	765.14(110.97)	59.3/475.1 (138.7/887.2)

Core Parameters

Decay heat generation = 23.9 MW

Cooling coefficient = 1.147

Turbomachine Parameters

Speed = 1978 rpm

Turbine efficiency = 82.07%

Turbine pressure ratio = 1.22

Compressor efficiency = 74.61%

Compressor pressure ratio = 1.25

Bypass flow = 5488 kg/h (12,099 lbm/h)

The design objective for the helium inventory control system is the controlled removal or insertion of helium into preselected high-pressure and/or low-pressure regions of the PCL as required during plant startup/shutdown or load-following maneuvers. Figure 13-1 presents the plant efficiency versus load for the three methods of control. The very high part load efficiency obtained with inventory control is apparent. Temperature control provides reasonable efficiency in the upper range of load. Bypass control provides poor efficiency, with approximately 80% of the load reduction via bypass going to waste heat. The reference load control concept currently being evaluated is set up to take 10% load change on bypass control, with further reduction by temperature control. In addition, manually initiated inventory change is accepted by the control system and results in adjustment of the programmed setpoints of valves and temperature versus load. (For added details related to helium inventory control, see Section 12.3.4.)

Preliminary functional analysis of integrated bypass, temperature, and inventory control of various load-following and plant shutdown events has shown well-controlled stable operation with simple control functions.

13.3.2.3. Control Rod Shimming Function. During load changes between minimum and maximum load, plant operator shimming of the control rods may be required to produce sufficient rod-induced reactivity change concurrent with maintaining the position of the automatic power-regulating rod bank within specified limits. Compared with the previous, highly enriched uranium (HEU) core, the change to MEU fuel and the low-worth "power" rods necessitate larger rod movements to effect similar power changes.

Preliminary analysis of various load-following transients has shown that the required power changes can be produced smoothly through rod shimming.

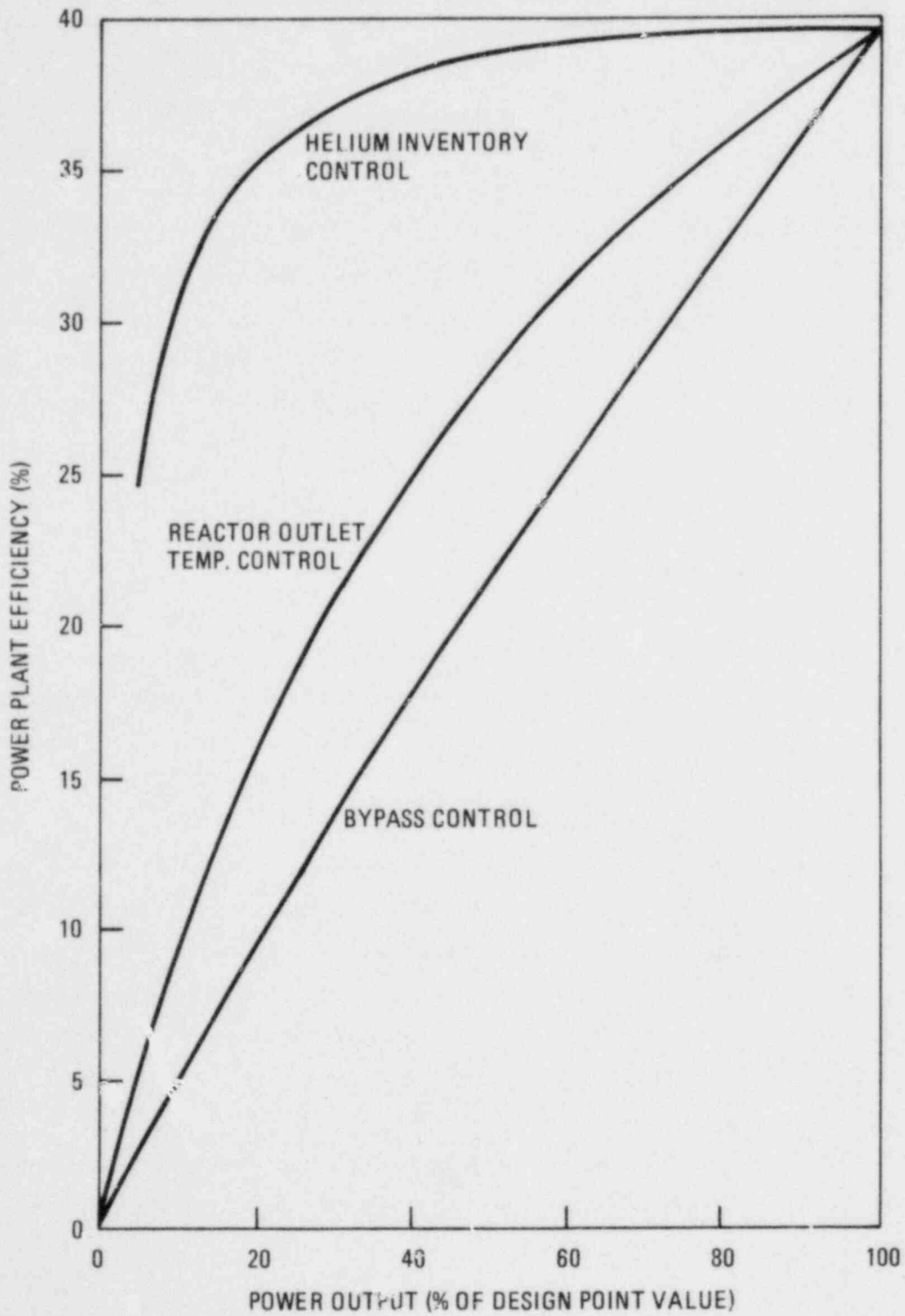


Fig. 13-1. Part-load efficiency for various plant control modes

### 13.3.3. Intercooled Versus Non-Intercooled and Warm Liner Versus Cold Liner Studies

The relative merits of alternative HTGR-GT design concepts were evaluated in two separate transient studies that were completed in FY-79: the intercooled versus non-intercooled study and the warm liner versus cold liner study.

13.3.3.1. Intercooled Versus Non-Intercooled Study. Owing to schedule and funding considerations, the comparison of the two-loop intercooled plant and the two-loop non-intercooled plant was completed using models with different design point power levels. The available models were the alternate commercial 3000-MW(t) intercooled plant model and the 2000-MW(t) non-intercooled plant model. Some of the comparisons were done on a percentage basis in order to minimize the power level mismatch. Twelve transients were studied to evaluate the control and PPS requirements for these plants. REALY2 was used in support of this work.

The greater complexity of the intercooled plant detracts from its operability. The fact that more parameters must be monitored to assure satisfactory plant operation reduces the overall response of plant operations personnel and increases the possibility that operating difficulties may be overlooked. For example, the recognition of compressor surge would apply to four compressor stages instead of two in a two-loop intercooled plant. Similar concerns would apply to the precoolers and intercoolers, where water flow conditions would have to be monitored on four units rather than two. Therefore, the simpler non-intercooled plant concept is expected to have an overall advantage in comparative operability and availability as noted in Section 10.

The PPS requirements were compared in terms of the number of control units and setpoints and are expected to be the same for the two plants.

The PCS requirements for the intercooled concept are slightly more severe in that high-pressure compressor surge margin control must be

incorporated with the primary bypass valve. That type of requirement affects only the attemperation valve in the non-intercooled concept.

13.3.3.2. Warm Liner Study. The evaluation at GA showed that it would be difficult to use the warm liner feature in multi-loop plants.

It appears for several reasons that adopting the warm liner concept makes the single loop shutdown-recovery capability either unachievable or considerably more difficult to achieve. This in turn leads to either abandoning single loop shutdown-recovery (shut down all loops, not one) or making several major modifications to the design. The addition of two main loop flow isolation valves per loop. PPS monitoring/valve actuation, and special side cavity cooling is probably required to make single loop shutdown-recovery viable. Even with the valving and other provisions, the compressor-to-compressor coupling through the core liner cavity presents possible difficulties that have not previously been assessed in the HTGR-GT concept. Also, the more complex arrangement of the primary coolant path would make the plant more difficult to operate.

Additionally, studies of the warm liner demonstration plant have shown that liner temperature could exceed 204°C (400°F) if a loss of circulating water event were allowed to proceed as in a conventional HTGR-GT plant. Since liner temperatures that high, even though occurring for only a few minutes, would seriously jeopardize an immediate plant restart, it is likely that the liner would need some cooling as a means of protection against this event.

13.3.4. Sound Pressure Level, Natural Convection, and Flow Mixing Studies

13.3.4.1. HTGR-GT Primary Circuit Sound Pressures. Sound pressures in the primary circuit due to the turbomachinery and the bypass valve were calculated.

The data base for HTGR-GT turbomachinery noise emission has been greatly strengthened by measurements from the Oberhausen gas turbine plant



and by semi-empirical predictions from United Technologies Corporation (UTC). The acoustic power spectra generated by UTC are dominated by tones emitted at the blade passage frequency and the first harmonic. Broadband noise is rather low at both low and high frequencies. Subsequently, UTC revised downward its initial estimates of turbomachinery noise to reflect proposed modifications to the outermost two stages of each end of the turbine and compressor. Using these revised sound power estimates, primary circuit sound pressures were calculated. The results are given in Table 13-4.

Calculations were also made of the sound powers emitted by the bypass valve. The resulting sound pressures for the primary circuit are too high, and at least 15 dB of attenuation will be required for the primary bypass valve. This attenuation should be straightforward because:

1. The bulk of the acoustic energy is at frequencies which are readily attenuated.
2. Little noise radiates upstream of the valve, so treatment need only be applied downstream.
3. The fluid temperatures are expected to be less than 550°C (1022°F), so a variety of materials and construction techniques are available for absorbers.

The results of these sound pressure analyses were documented in a design report.

#### 13.3.5. HTGR-GT Loop Natural Convection With No Forced Flow

An analysis was done to provide an initial estimate of natural convection loop flow in the two-loop, 800-MW(e) HTGR-GT non-intercooled plant with no forced circulation (loss of offsite power). A small computer program was written to calculate the loop flow rate provided the temperatures at various points along the loop were independently specified. Many cases

TABLE 13-4  
 PRIMARY CIRCUIT MEAN SQUARE PRESSURES IN ONE-OCTAVE BANDS (VANE-  
 BLADE MODIFICATIONS, BUT NO ATTENUATION TREATMENT)

	Octave-Band Mean Square Pressures (Pa <sup>2</sup> )						Overall Pressure <sup>(a)</sup>	
	500 Hz	1000 Hz	2000 Hz	4000 Hz	8000 Hz	16,000 Hz	Pa <sup>2</sup>	dB SPL
	Turbine exit duct	2E6 <sup>(b)</sup>	4E6	8E6	3E7	2E7	4E6	2E7
Recuperator-precooler duct	3E4	4E4	4E4	1E5	2E4	3E3	6E4	142
Compressor inlet duct	1E5	3E5	8E5	4E6	4E6	3E6	3E6	159
Compressor outlet duct	8E4	2E5	4E5	8E5	1E6	4E6	2E6	156
Recuperator-core duct	4E5	2E6	4E6	8E6	1E7	4E6	8E6	163
Core inlet plenum	2E6	3E6	8E6	2E7	3E7	1E7	3E7	167
Core outlet plenum	2E6	3E6	8E6	2E7	3E7	2E7	2E7	167
Turbine inlet duct	3E6	4E6	1E7	4E7	5E7	3E7	4E7	170

(a) Does not include a factor to account for spatial peaking near solid surfaces.

(b) 2E6 =  $2 \times 10^6$ .

were run with different combinations of core outlet and precooler outlet temperatures that are representative for natural circulation conditions. The other temperatures around the loop were then derived assuming no heat losses in the ducts, equal temperature drops through the shell and tube sides of the recuperator, and a recuperator effectiveness of 0.9. (Past experience has shown that the net driving density head is not too sensitive to the fluid temperature distribution.)

For all cases, the calculated loop natural convection flow rate was in reverse flow (upflow through the core). However, the flow resistances of the turbine and compressor were so high (both assumed stationary) that the loop natural convection was essentially suppressed [ $\sim 0.005$  kg/s ( $\sim 0.01$  lbm/s) with typical velocities of 0.03 m/s ( $\sim 1$  ft/s)]. Under these conditions, local natural convection currents with velocities of 0.03 m/s ( $\sim 1$  ft/s) may be established.

#### 13.3.6. Mixing of Turbine and Bypass Valve Gas Streams in HTGR-GT

A computer model of the mixing between the hot turbine exhaust gas and the cooler bypass valve gas stream was constructed. Because of difficulties in obtaining a converged solution, only suggested flow patterns were achieved from the computer model. A hand calculation model was then used to estimate the degree of mixing.

Figure 13-2 shows the cold bypass valve fluid impinging on the far wall and then spreading around the duct as it is blown downstream by the hot turbine exhaust flow. The calculations indicate that the flows could mix thoroughly eight duct diameters downstream. Thus, the two flows would not be thoroughly mixed at the much closer recuperator inlet (two to three duct diameters downstream) based on the present PCL layout. Alternates to this layout are being initiated.

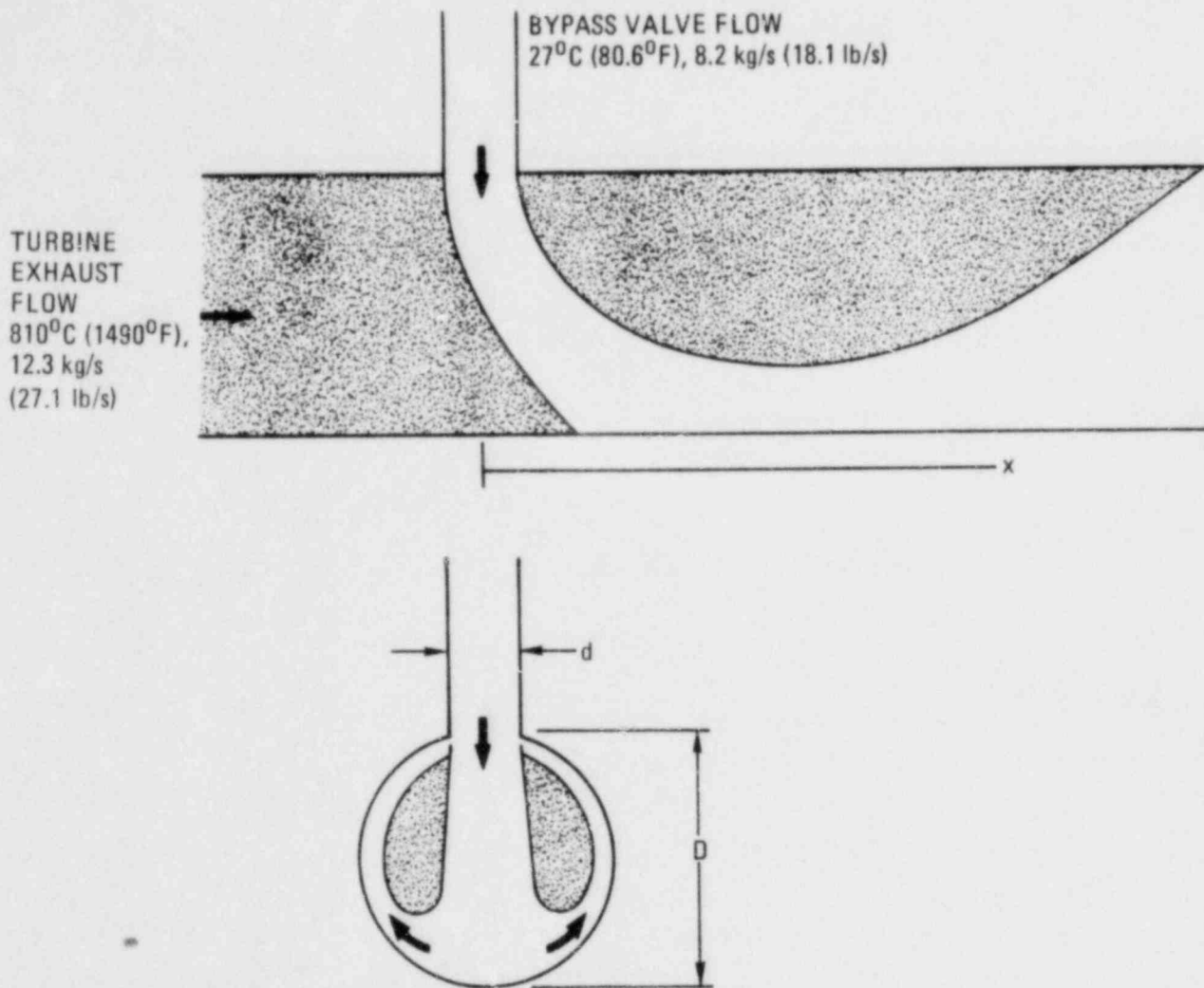


Fig. 13-2. Bypass valve/turbine exhaust flow mixing (hot fluid is gray, cold fluid is clear)

13.4. REFERENCE

- 13-1. "HTGR Gas Turbine Semiannual Progress Report for the Period Ending March 31, 1979," DOE Report GA-A15436, General Atomic Company, June 1979.

## 14. PCRV LINERS, PENETRATIONS, AND CLOSURES (631104)

### 14.1. SCOPE

The purpose of this task in FY-79 was to complete the evaluation of the warm liner concept, to study liner leak detection/collection systems as an alternative to the warm liner concept, to document the results in a design report, and to initiate design and analytical studies of large closures.

### 14.2. SUMMARY

The evaluation of the warm liner versus cold liner concept was completed and documented in a design report. The significant results of this study are summarized in Table 14-1. The disadvantages of the warm liner concept were found to outweigh its advantages, primarily owing to the design complexities that result from the presence of the warm liner flow annulus in the core cavity. Retention of the conventional, cold liner was recommended and approved for the HTGR-GT reference plant. A liner leak detection/collection system was recommended as an option for consideration by the utilities.

Analytical studies were initiated to establish sizing techniques for concrete plug and ring type closures, and design studies were initiated to pursue alternative closure configurations. These studies are scheduled to continue into FY-80.

TABLE 14-1  
SUMMARY COMPARISON OF WARM AND COLD LINER CONCEPTS

Consideration	Issue	Liner Concept with Advantage
Structures		
PCRV	Qualification of the warm liner insulating concrete is required for ASME/ACI Code revision.	Cold
Liner	The cold liner operating environment and stress/strain cycles are less severe.	Cold
Reactor internals	The warm liner requires a core barrel that is exposed to high temperatures, neutron irradiation, and large pressure differences during accidents. The many joints in the core barrel itself and the many penetrations for spring packs and concentric ducts require leak-tight seals for cycle efficiency. The core barrel must accommodate large relative movements between interfacing components while maintaining leak-tight structural integrity.	Cold
	The warm liner spring packs are exposed to much less severe thermal environment.	Warm
Thermal barrier	A great reduction in thermal barrier quantity is realized with the warm liner concept.	Warm
	With the warm liner concept, it is more difficult to design the thermal barrier to accommodate movements of core barrel plates and effects of leaks at joints.	Cold

TABLE 14-1 (Continued)

Consideration	Issue	Liner Concept with Advantage
Maintainability ISI	The warm liner can be visually inspected, but it is likely that a small crack that will cause unacceptable leakage cannot be detected.	Warm
	With the warm liner concept, the addition of the core barrel, core barrel seals, core barrel floor and top supports, and coolant flow guides and restrictions increases ISI requirements.	Cold
	The warm liner flow annulus may make remote inspection of spring packs possible.	Warm
Repair	Repair of the warm liner, although very difficult for the core cavity, is easier without a thermal barrier. Access to spring packs is better.	Warm
	With the warm liner concept, addition of the core barrel adds many components that may require repair or replacement and makes access to reactor internal components within the core barrel more difficult.	Cold
Operability	Coupling of the primary loops by the warm liner annulus results in an availability penalty for multi-loop plants or addition of isolation valves in loops. The more complicated flow path makes plant control and operator decisions more complex.	Cold



TABLE 14-1 (Continued)

Consideration	Issue	Liner Concept with Advantage
Safety/ licensing	<p>With the warm liner concept, failure of a core outlet or CACS inlet ducts or of the core barrel in the lower plenum results in the CACS flow bypassing the core. Any of these failures also leads to primary loop flow bypassing the core.</p>	Cold
Economics	<p>With the warm liner concept, the CAHE outlet gas temperature required for liner cooling [149°C (300°F)] is not suitable for core cooling because unacceptable temperatures and thermal gradients in the core structures would result. The flow stability and uniformity in the core cavity warm liner annulus is questionable under CACS operation.</p>	Cold
Capital cost	<p>Capital costs are higher for the warm liner HTGR-GT plant owing to the added core barrel and larger PCRV, even though there is much less thermal barrier.</p>	Cold
Cycle efficiency	<p>The increased efficiency of the inter-cooled cycle is negated by pressure loss owing to the complex flow path of the warm liner concept. The warm liner also has increased risk of efficiency degradation due to bypass flows and leakages.</p>	Cold

### 14.3. DISCUSSION

A stress analysis of the intersection between a refueling penetration liner and the core cavity liner was completed as a part of the warm liner evaluation. The analysis was performed for postulated dead-flow conditions to assess the effect of this high-temperature condition, which may exist with a warm core cavity liner. The results of this analysis indicated that there was insufficient margin for cyclic operation at the penetration/liner junction and that dead flow conditions would not be acceptable with a warm core cavity liner. It was concluded that some means, such as flow distribution devices, must be incorporated into a warm liner design to preclude the development of dead-flow conditions.

Another problem identified for a warm liner design is that the uncooled liners are exposed to the primary coolant and thus will react quickly to anticipated primary coolant temperature transients. The loss of cooling water transients would cause the ASME Section III, Division 2 limit on tensile stress to be exceeded in the precooler, recuperator, and turbo-machine cavity liners.

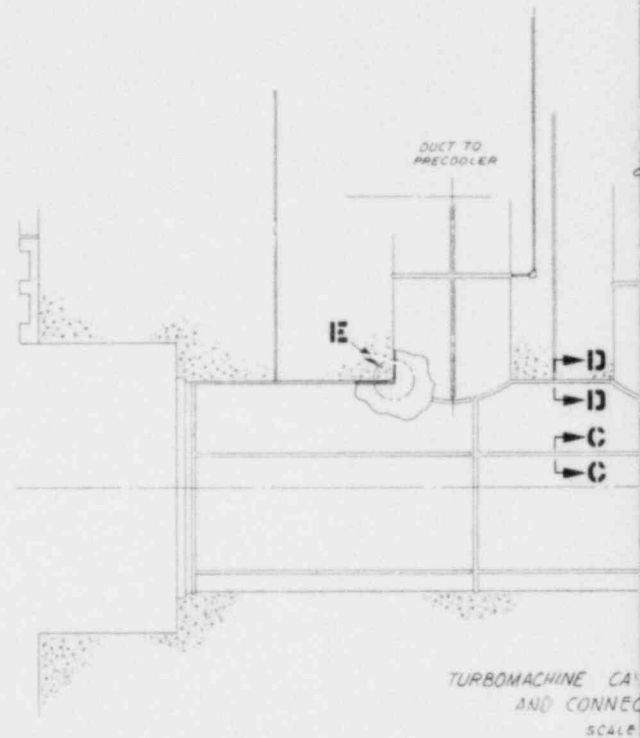
Since the warm liner experiences more severe thermal cycles and may operate in a general state of tension, it has a higher probability of service failure. For this reason, the cold liner concept was preferred from the standpoint of the liner itself.

A liner leak detection and collection system was studied as an alternative approach to mitigate the consequences of a postulated liner leak. It was decided that the primary objective of a leak collection system should be to permit continued plant operation as quickly as possible following a liner leak. This requires that (1) the escaping coolant gas can be contained or collected and processed and (2) leakage will not result in degradation of the PCRV structural integrity. The former requirement necessitates that a leakage path(s) can be detected, while the latter

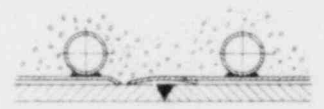
requirement indicates that the leak should be collected at or near the outer liner surface. It is also required that under normal conditions, i.e., no liner cracks, the leak collection system will not affect the leak tightness of the liner, impair the function of the PCRV cooling system, or adversely affect the strength and serviceability of the PCRV. Other desirable goals of a leak collection system design are that it be entirely passive, not contain any moving parts, and not affect or be affected by normal plant operations.

The various leak collection system designs fall into two general categories: leak chase channels and vent tubes. The first category follows the widely accepted approach used in containment liner construction, wherein channels are located at all liner welds and intersections. Penetration and closure welds would not have leak chase channels because they are subject to volumetric ISI. Representative use of a steel-formed channel system is shown in Fig. 14-1. Although the probability of a liner crack occurring is very low, if one should ever occur, it would most likely be at or near a weld joint or intersection. With a steel-formed channel and collector surrounding the leakage path, it should be possible to quickly contain the leak within the PCRV. The plant would be shut down for a very short time, containment of the leak would be readily accomplished at the collection tube termination on the periphery of the PCRV, and no pumps, process piping, or additions to the normal plant helium purification train would be required. The disadvantages of a leak chase system are that it is relatively expensive and does not protect against a crack which occurs away from a weld joint.

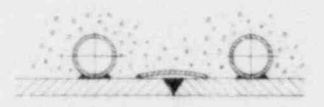
The category of vent tube designs follows the approach developed and tested by Menon in Sweden (Ref. 14-1). The leaking coolant is allowed to flow into a gridwork of tubes which surround the liner and then is vented to the periphery of the PCRV. The contaminated coolant is collected and then pumped into the reactor via a processing system. The tube gridwork may be made of perforated pipe, voids formed in the concrete, or solid pipe. When pipe is used to form the gridwork, pipe stubs may extend from the gridwork to the liner surface, where porous bushings can be used to



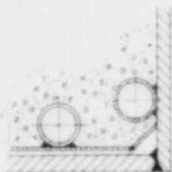
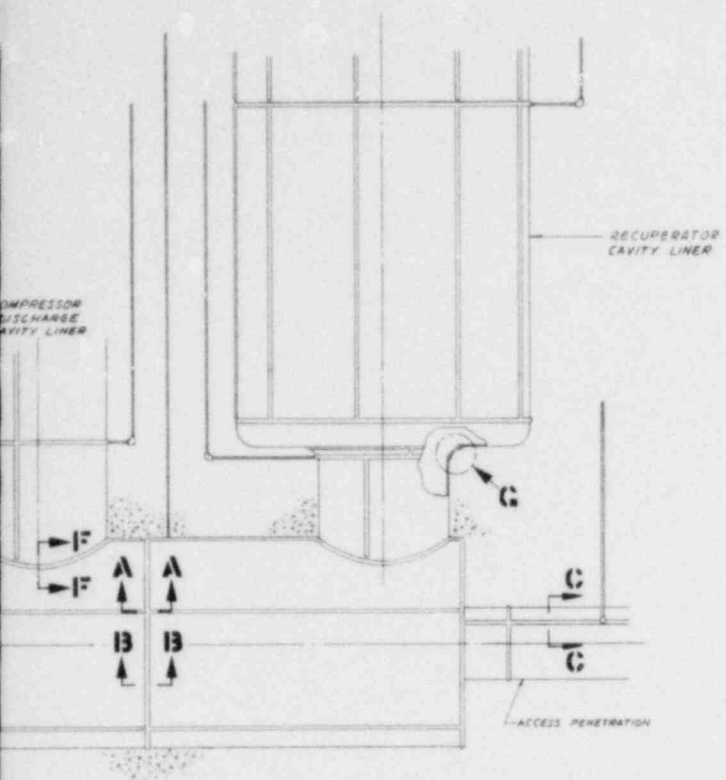
TURBOMACHINE CASING  
AND CONNECTION  
SCALE



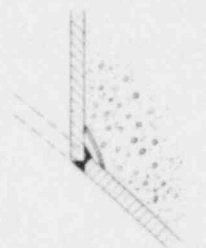
SECTION **A-A**  
SCALE - 1/2



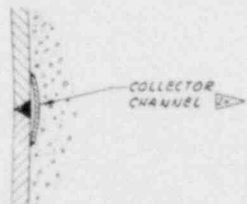
SECTION **B-B**  
SCALE - 1/2



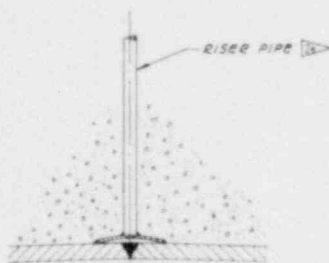
VIEW E  
SCALE - 1/2



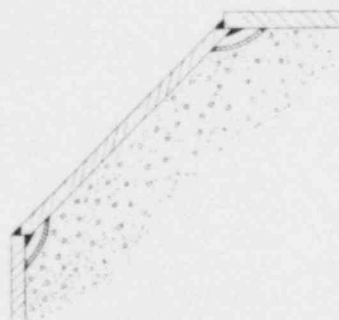
SECTION F-F  
SCALE - 1/2



SECTION C-C  
SCALE - 1/2

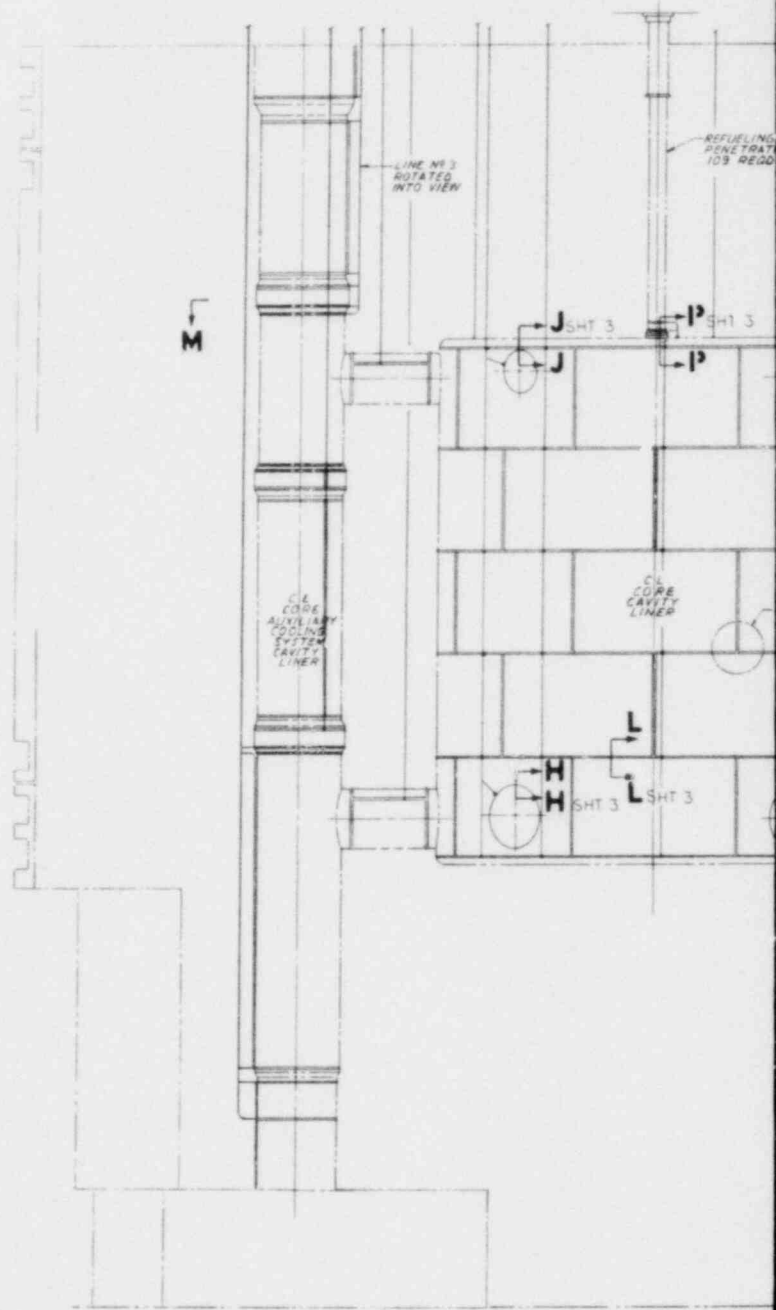


SECTION D-D  
SCALE - 1/2  
TYPICAL RISER CONNECTION



VIEW G  
SCALE - 1/2

Fig. 14-1. Liner leak chase collection system (sheet 2 of 3)



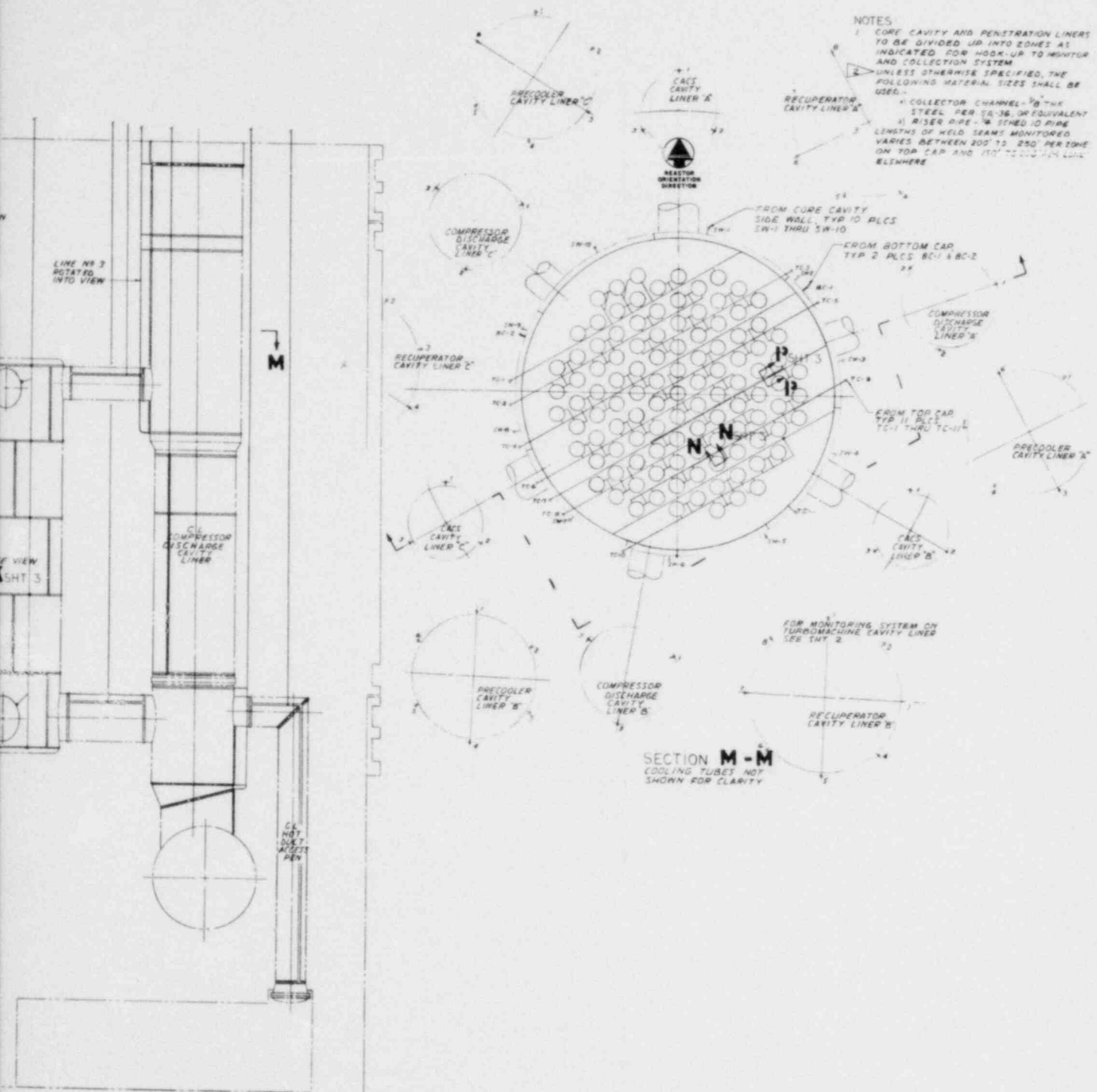
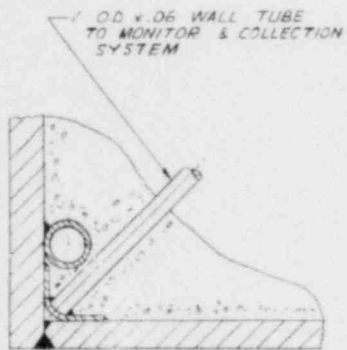
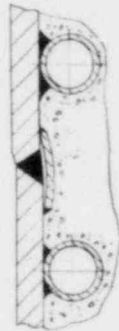


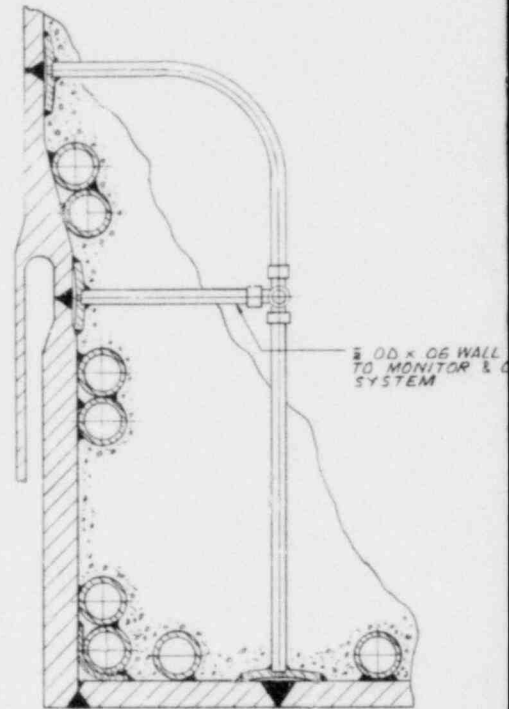
Fig. 14-1. Liner leak chase collection system (sheet 1 of 3)



SECTION **N-N** SHT 1  
 SCALE  $\frac{1}{2}$   
 ROTATED 30° CW



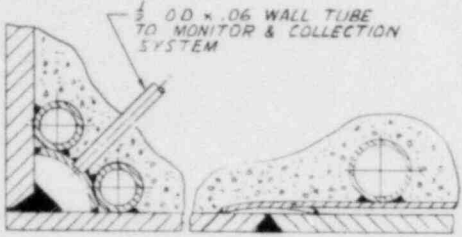
TYPICAL JOINT SHOWING  
 MAXIMUM MISMATCH



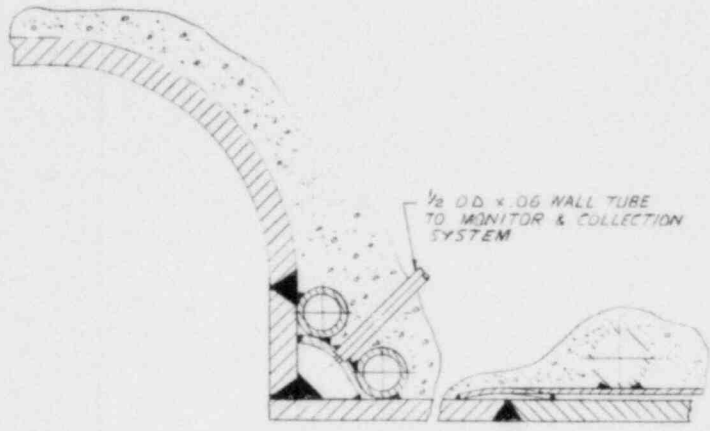
SECTION **P-P** SHT 1  
 SCALE  $\frac{1}{2}$   
 ROTATED 60° CCW



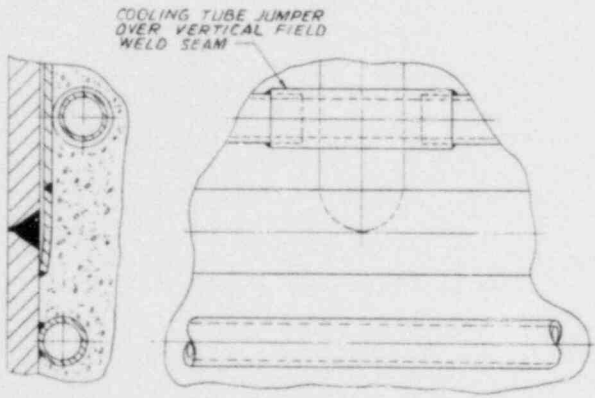
TUBE  
COLLECTION



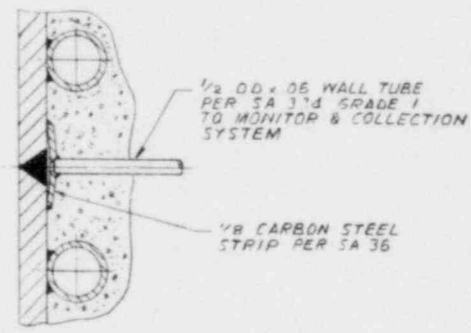
SECTION **H-H** SHT. 1  
SCALE 1/2  
TYPICAL ROUND DUCT TO  
CORE CAVITY INTERFACE



SECTION **J-J** SHT. 1  
SCALE 1/2



VIEW **K** SHT. 1  
SCALE 1/2



SECTION **L-L** SHT. 1  
SCALE 1/2  
TYPICAL CIRCUMFERENTIAL  
WELD JOINT

Fig. 14-1. Liner leak chase collection system (sheet 3 of 3)

collect the leaking helium. This should shorten the leakage path and minimize the number of vent tubes through which the contaminated coolant passes, which in turn should simplify the collection and processing of the leaking helium. A conceptual arrangement of this system for a core cavity liner is shown in Fig. 14-2. The advantages of a vent tube system are that it should be relatively inexpensive and is capable of collecting leaks wherever they occur. The disadvantages are that it will require more development testing than a leak chase system and the leakage cannot be isolated and contained, but rather must be collected and pumped into the processing system for return to the reactor.

Analytical studies of concrete closures were oriented toward establishing the direction of the load path between the plug and the ring. This directly affects the plug and ring height and movements of the omega seal between the plug and vessel. Finite element models were used in the analysis. It was concluded that it is necessary to design the components based on a nearly vertical load path, regardless of the contact angle. The impact on plug and ring size remains to be established.

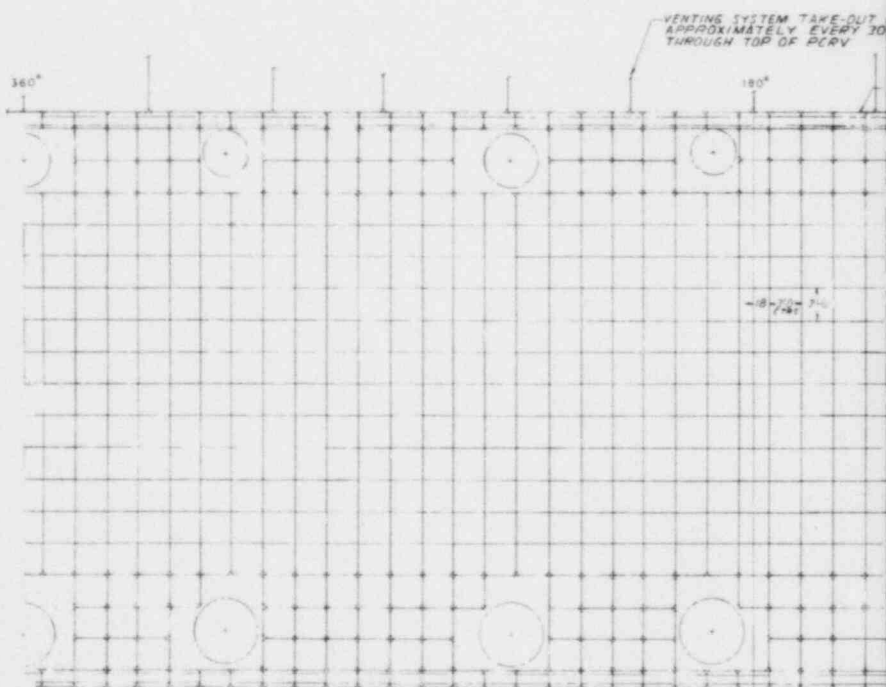
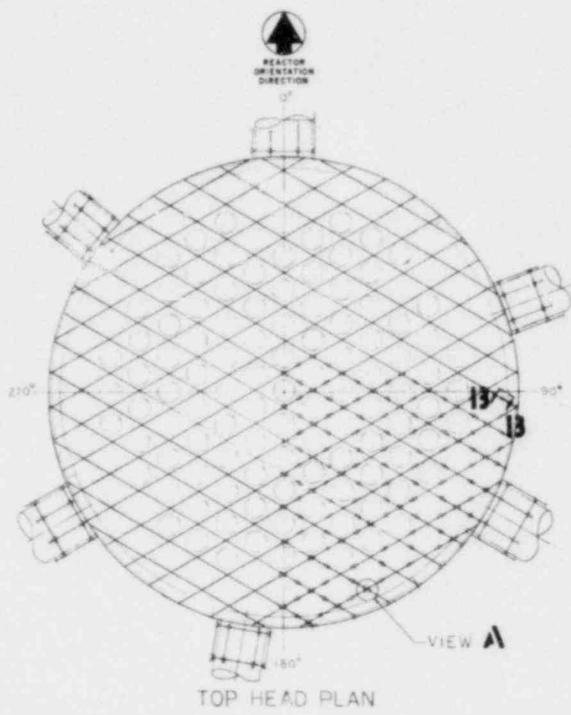
Design studies consisted of evaluating alternative closure concepts. A toggle hold-down system was rejected because it increased the height of the PCRV. A steel hold-down ring as an alternate to the prestressed concrete ring was sized and found to offer significant weight and height reduction potential. The combination of a steel ring and concrete plug is shown in Fig. 14-3. A major advantage of the steel ring is that it can be held down with anchor bolts. Therefore, it is not necessary to de-tension the PCRV tendons to remove the closure. One disadvantage of the ring is its high initial cost, since considerable steel and welding are required.

Another approach investigated was a dome closure. This followed from the position that failure of such a closure need not be postulated. Both ellipsoidal and hemispherical domes were evaluated. An ellipsoidal dome with a radius to height ratio of approximately 1.5 appeared to produce

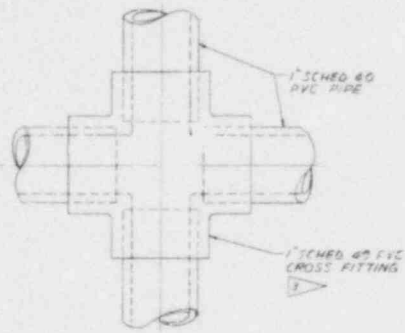
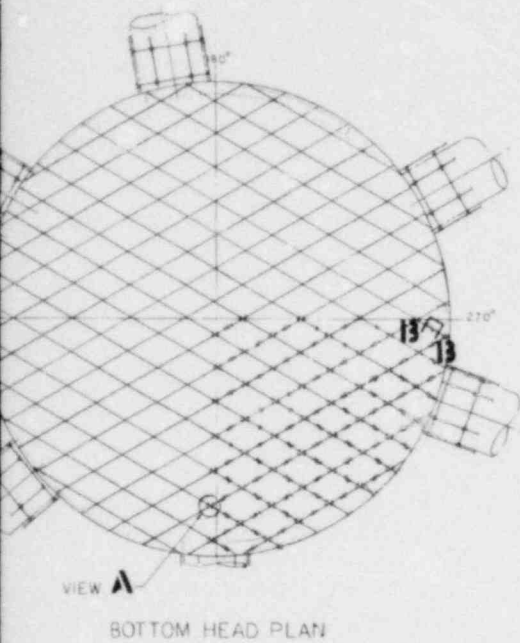
the best results. The overall height of the dome and bolting flanges was 3.05 m (10 ft), which is substantially less than any plug and ring combination. The dome is also independent of the PCRV prestressing tendons. Its major disadvantage is that the penetration thickness and annular space around the penetration required for ISI add 0.61 m (2.0 ft) to the net inside diameter of the concrete blockout at the top of the PCRV. This would probably increase the PCRV diameter, but the amount of the increase has not been determined.

#### 14.4. REFERENCE

- 14-1. Menon, S., "Verification Program of Test and Studies on Scandinavian BWR-PCRIV," in Fourth International Conference on Structural Mechanics in Reactor Technology, San Francisco, 1977.



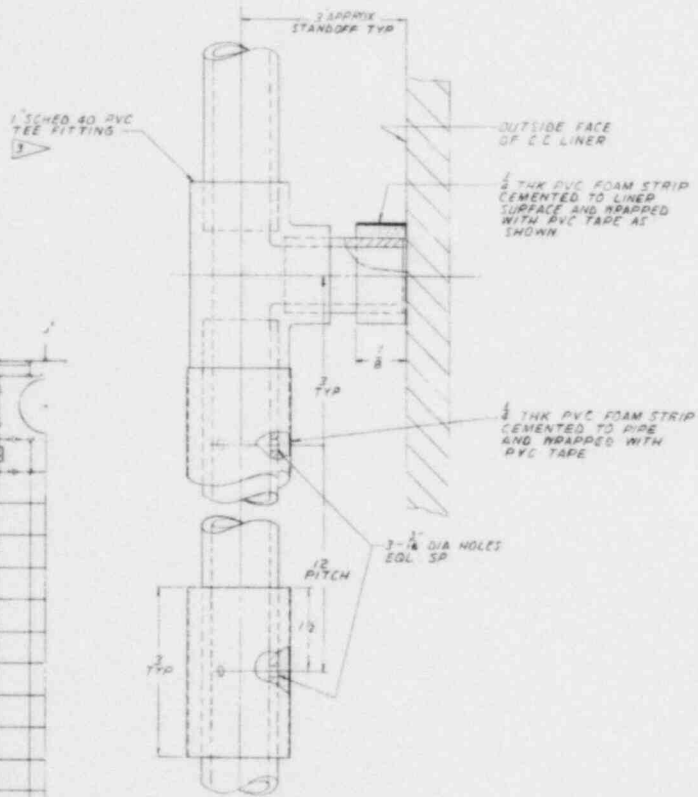
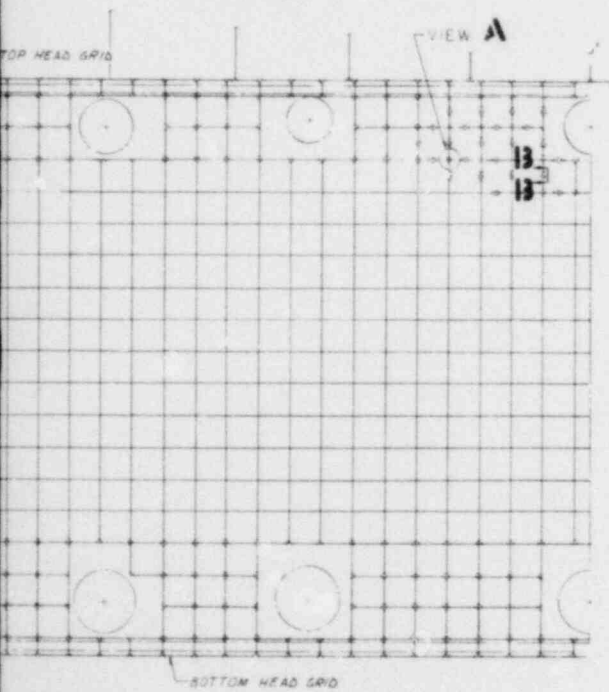
OUTER CIRCUMFERENTIAL V



VIEW A TYP  
SCALE 1/1

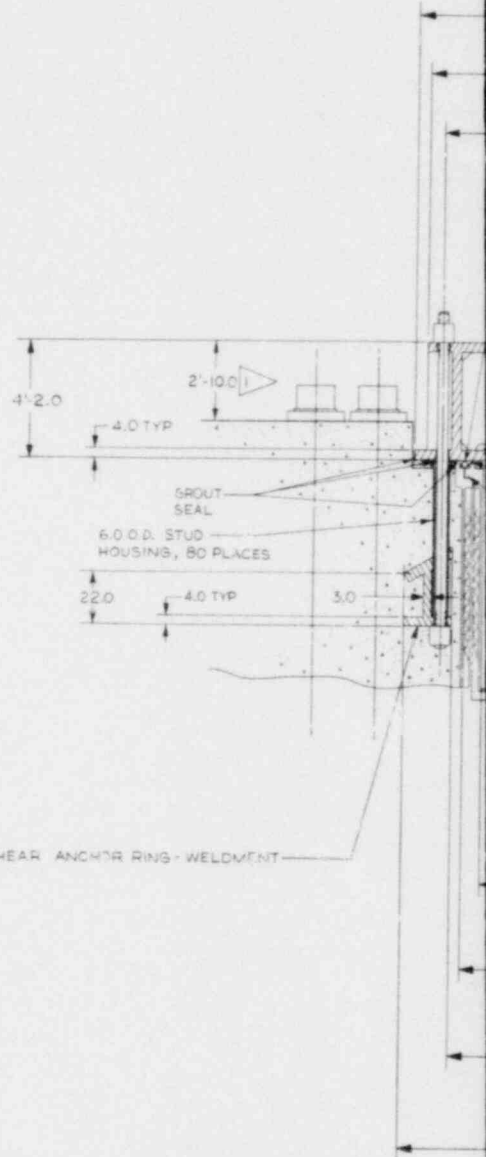
NOTES

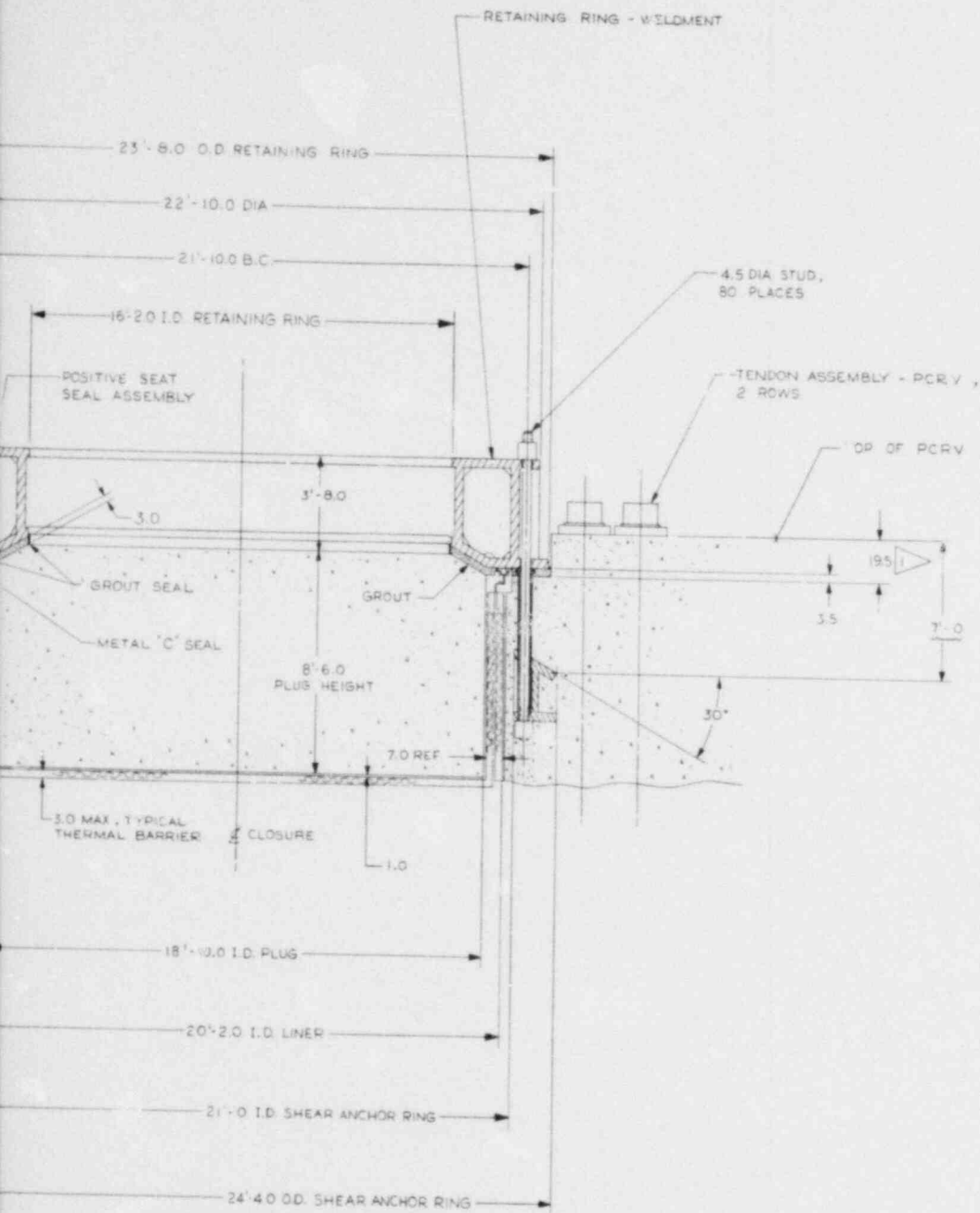
1. THIS DRAWING REPRESENTS A CORE VENTING SYSTEM CONFIGURATION FOR A CORE CAVITY LINER. SIMILAR CONFIGURATION WOULD BE UTILIZED AT OTHER CAVITY LINERS.
2. VENTING SYSTEM GRID MADE UP OF 1" SCHED 40 PVC PIPE AND STANDARD SOCKET TYPE FITTINGS ON 12" O-C-B PATTERN APPROXIMATELY 2" FROM THE OUTSIDE FACE OF THE LINER AND EMBEDDED IN THE RCRY CONCRETE. ALL SOCKET JOINT CONNECTIONS TO BE MADE USING PVC SOLVENT CEMENT.



SECTION 13-13 TYP  
SCALE 1/1  
COOLING WATER TUBES NOT SHOWN

Fig. 14-2. Core cavity liner venting system





SCALE: 1/2" = 1 FOOT

Fig. 14-3. Steel ring and concrete plug closure concept

## 15. PCRV STRUCTURES (631105)

### 15.1. SCOPE

The purpose of this task in FY-79 was to evaluate the structural characteristics of the PCRV for the three-loop plant and to develop and evaluate PCRV layouts based upon the intercooled and non-intercooled plants.

### 15.2. SUMMARY

PCRV stress analyses for the three-loop HGR-GT reference plant were performed to evaluate structural effects characteristic of the PCRV with horizontal turbomachine cavities. Preliminary evaluation of three-dimensional finite element stress results obtained for initial prestress and cavity pressure loadings indicates that the required prestressing for the turbomachine cavity region should be provided primarily by horizontal tendons.

Two conceptual PCRV layouts for the two-loop intercooled and non-intercooled plants were completed to provide PCRV sizing data for the CODER computer program. A comparative study favors the non-intercooled plant from the standpoint of PCRV design in that PCRV diameter is smaller by 2.4 m (8 ft) and the PCRV layout allows more flexibility.

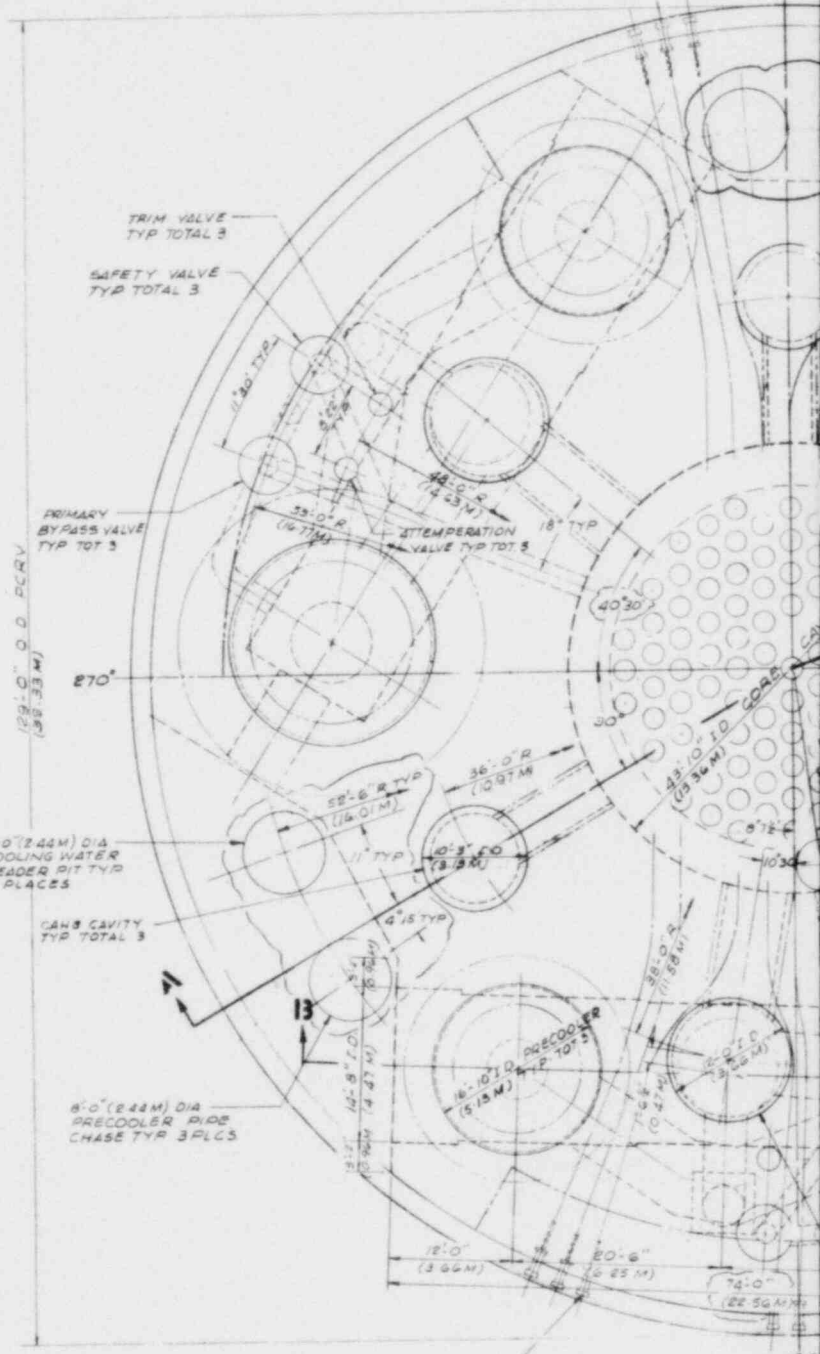


### 15.3. DISCUSSION

#### 15.3.1. Effectiveness of PCRV Prestressing at Turbomachine Cavity Region

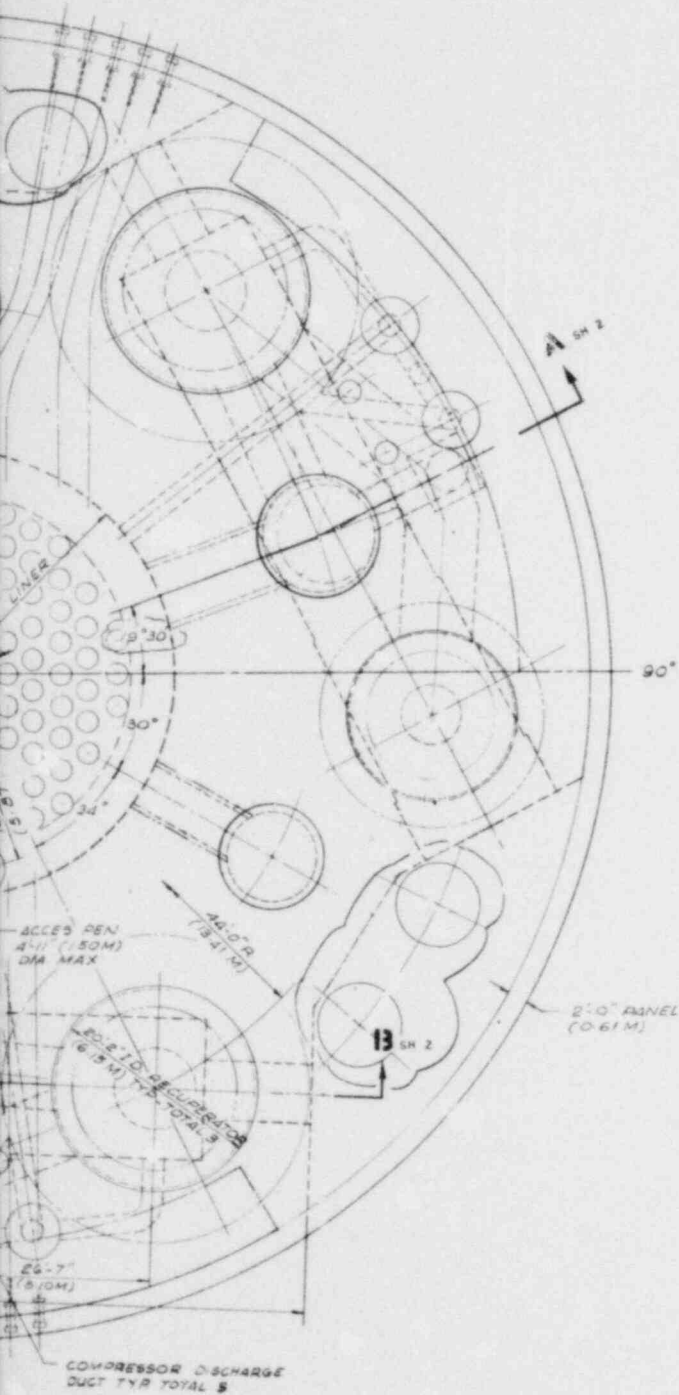
A major PCRV design consideration for the HTGR-GT plant is the inclusion of horizontal cavities for the turbomachines in the PCRV. The location of large horizontal cavities in the PCRV bottom head precludes the use of circumferential wire winding on the lower portion of the PCRV. The required prestressing in this region is provided by linear tendons. The cut-outs in the bottom head for the turbomachinery and the resulting horizontal tendon layout will have a significant impact on the PCRV sizing. To evaluate the effectiveness of PCRV prestressing at the turbomachine cavity region, a three-dimensional finite element stress analysis of the PCRV was performed. The PCRV configuration used for this investigation is based on the reference three-loop HTGR-GT plant (Fig. 15-1). Figure 15-2 shows the proposed tendon arrangement for the PCRV bottom head. It is believed that stress results obtained for the three-loop PCRV design would be indicative of the structural characteristics of the turbomachine cavity region and provide the necessary guidelines for future PCRV sizing and for establishing prestressing requirements for PCRVs with similar loop and component arrangements.

The three-dimensional finite element model of the PCRV is depicted in Fig. 15-3. The mesh consists of 222 isoparametric brick and 140 membrane elements with 1549 nodal points. The mathematical model represents a 70° sector of the lower half of the PCRV bounded by vertical planes through the centers of the compressor discharge and CAHE cavities. Also included in the model are the 3.8-m (12.5-ft) high support structure and a 6.1-m (20-ft) thick containment mat. Stress results for prestress loadings due to vertical tendons and circumferential wire windings and cavity pressure loads have been obtained. Preliminary evaluation indicates that discontinuities introduced by cut-outs have significantly reduced the effectiveness of the circumferential prestress contribution in the PCRV bottom head from wire windings. The required prestressing in the turbomachine cavity region should be provided primarily by horizontal tendons.



CO. REGION OUTLET  
TEMP PEN TYP-TOTAL 16

PLAN - PCRV TO



**GENERAL NOTES:**

1. MINIMUM LINEAR PRESTRESSING TENDON FORCE IMMEDIATELY AFTER ANCHORING SHALL BE 1735 KIPS.
2. PRECAST CONCRETE PANELS SHALL BE USED AS FORMS FOR PLACEMENT OF PCRV CONCRETE.
3. ALL TENDON BEARING PLATES SHALL BE GROUTED IN PLACE AFTER CONCRETING OF THE PCRV.
4. ALL SPECIFICATIONS FOR THE 3300 MAFI LEAD PLANT ARE APPLICABLE TO THIS DRAWING.
5. DIMENSIONS SHOWN ON THIS DRAWING ARE VERY PRELIMINARY.

6. DIMENSIONS AND OPENINGS SHOWN IN THE PCRV SUPPORT STRUCTURE ARE SUGGESTED ARRANGEMENTS ONLY. FINAL CONFIGURATION AND LOCATION ARE PART OF THE 30P DESIGN.

7. THE DUCTING BETWEEN CAVITIES SHOWN ON THE DRAWING IS SCHEMATIC AND REQUIRES VERIFICATION BY THE INTERFACING ORGANIZATIONS.

8. PCRV SIZING IS BASED ON THE INFORMATION AS FOLLOWS:
 

A. CORE CAVITY (DIA ONLY)-----	54.024490
J. RECUPERATOR CAVITY (DIA ONLY)-CE 023472640-	
C. PRECOOLER CAVITY (DIA ONLY)-CE 023472657-	
D. COMP. DISCHARGE DUCT (DIA ONLY)-54.024473	
E. CAVE CAVITY (DIA ONLY)-----	54.023457
K. TURBOMACHINE CAVITY (DIA ONLY)-54.023454	
G. MAXIMUM CAVITY PRESSURE (PSIG) USED IN THE DESIGN	

	INDIVIDUAL	EQUILIBRIUM
CORE, CAVE, COMP.		
DISCHARGE DUCT #	118	900
RECUPERATOR (HP)		
PRECOOLER, RECUP.		
HEAD (L & S TURB) 335		900
MACHINE CAVITY		

9. ADDITIONAL PRECOOLER PIPE CHASER (3) WERE INCORPORATED AS PER MEMO NO. 552 PB. 19. 79.

**QUANTITIES**

1. CONCRETE (6500 PSI):
 

PCRV	38,850 CY
PRECAST PANELS	1,590 CY
RECUPERATOR	340 CY
PRECOOLER	122 CY
2. REINFORCEMENT (ASTM A 616/A 617):
 

PCRV	2,202 TONS
PRECAST PANELS	223 TONS
RECUPERATOR	33 TONS
PRECOOLER	12 TONS
NO. OF MECHANICAL SPLICES IN PCRV	3,600
3. PRESTRESSING - LPS:
 

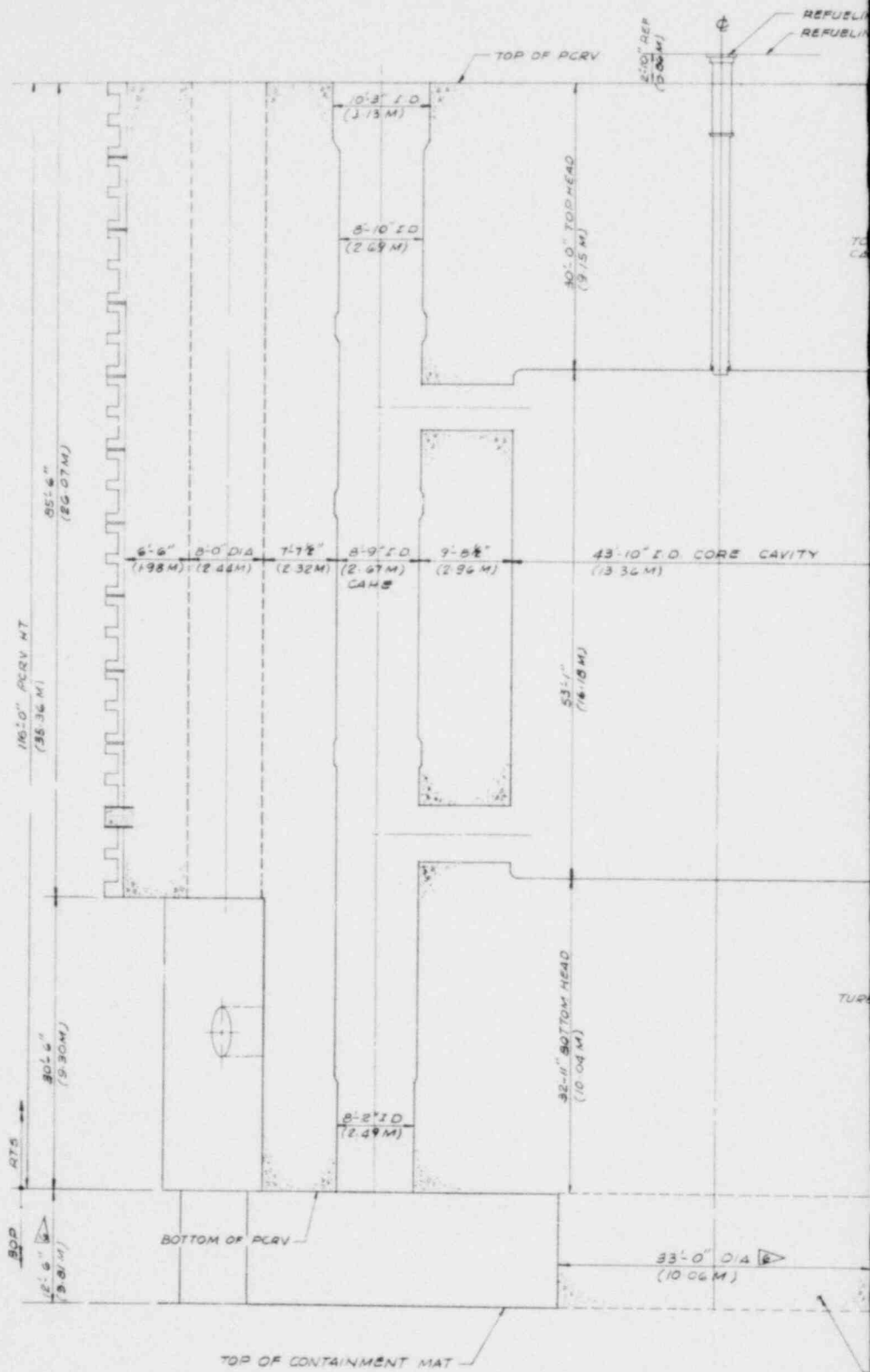
NO. OF 60- $\frac{1}{2}$ " $\phi$ STRAND TENDONS	814
LENGTH OF TENDONS (BETWEEN CONCRETE SURFACES)*	
VERTICAL TENDONS:	
1. CORE, CAVE & COMP. DISCH.	367 118 LF
2. RECUPERATOR	150 132 LF
3. PRECOOLER	33 125 LF
4. PERIPHERAL	60 154 LF
HORIZONTAL TENDONS:	
1. TURBOMACHINE	60 45 LF
2. BOTTOM HEAD	194 114 LF (178)

\* ALLOW 5 LF PER TENDON FOR TENSIONING
4. PRESTRESSING - CPS:
 

A. PCRV	
12" $\phi$ STRAND - TOTAL LENGTH	8,310 <sup>2</sup> LF
NO. OF STRAND LAYERS	37
NO. OF 10" PRECAST PANELS	212
NO. OF LOAD MONITOR PANELS	6
B. CLOSURE RINGS	
36" $\phi$ STRAND - TOTAL LENGTH	15,110 <sup>3</sup> LF
(INCLUDES STRAND FOR RECUPERATOR AND PRECOOLER)	
5. INSTRUMENTATION:
 

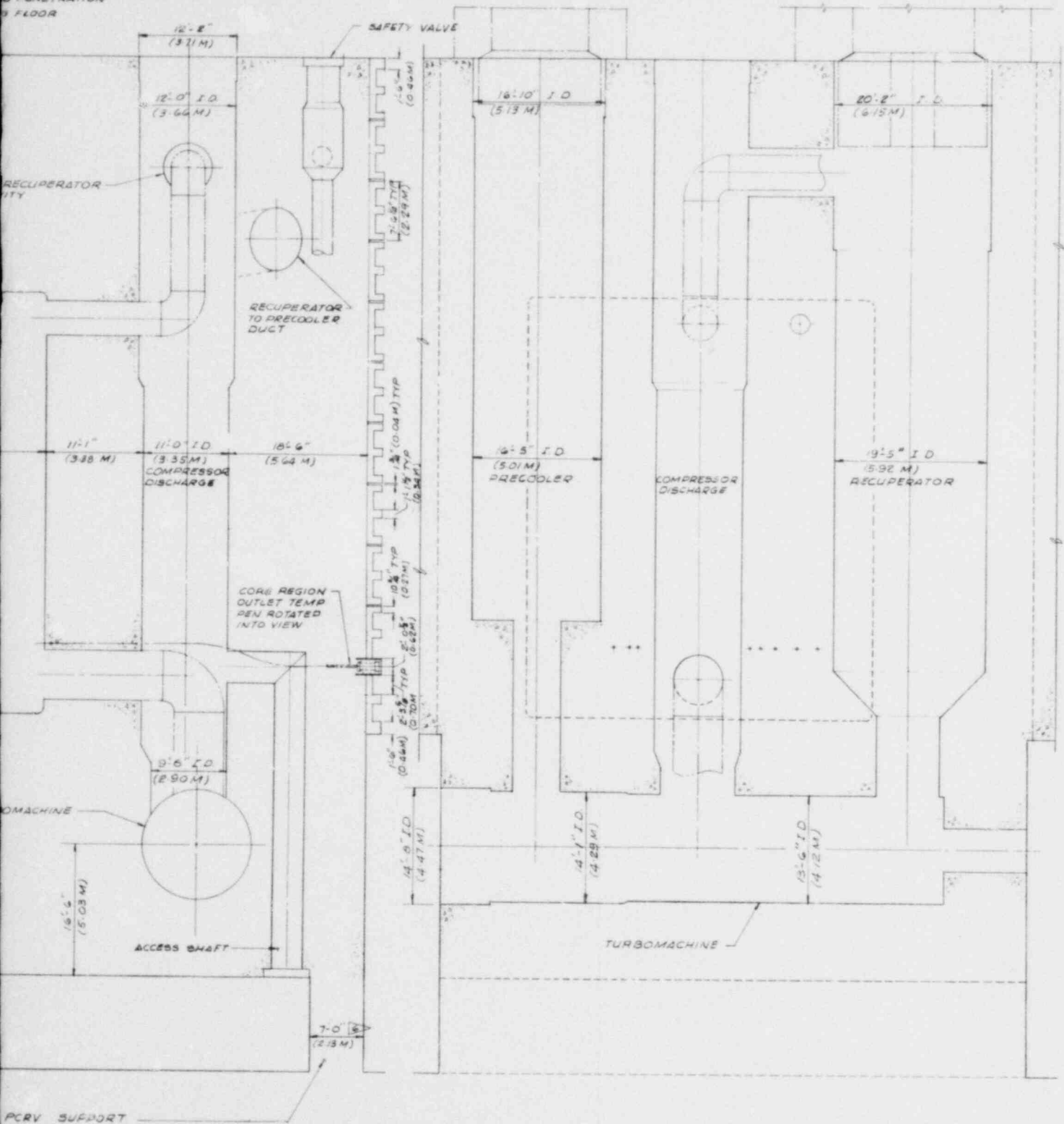
NO. OF LPS LOAD CELLS:	
1. VERTICALS	30
2. HORIZONTALS	10
NO. OF CPS LOAD CELLS	
1. PCRV	450
2. LINER	250
-ADD STRAP SENSORS TO ABOVE: PCRV - 20%	
LINER - 15%	

Fig. 15-1. PCRV for reference three-loop HTGR-GT plant (sheet 1 of 2)



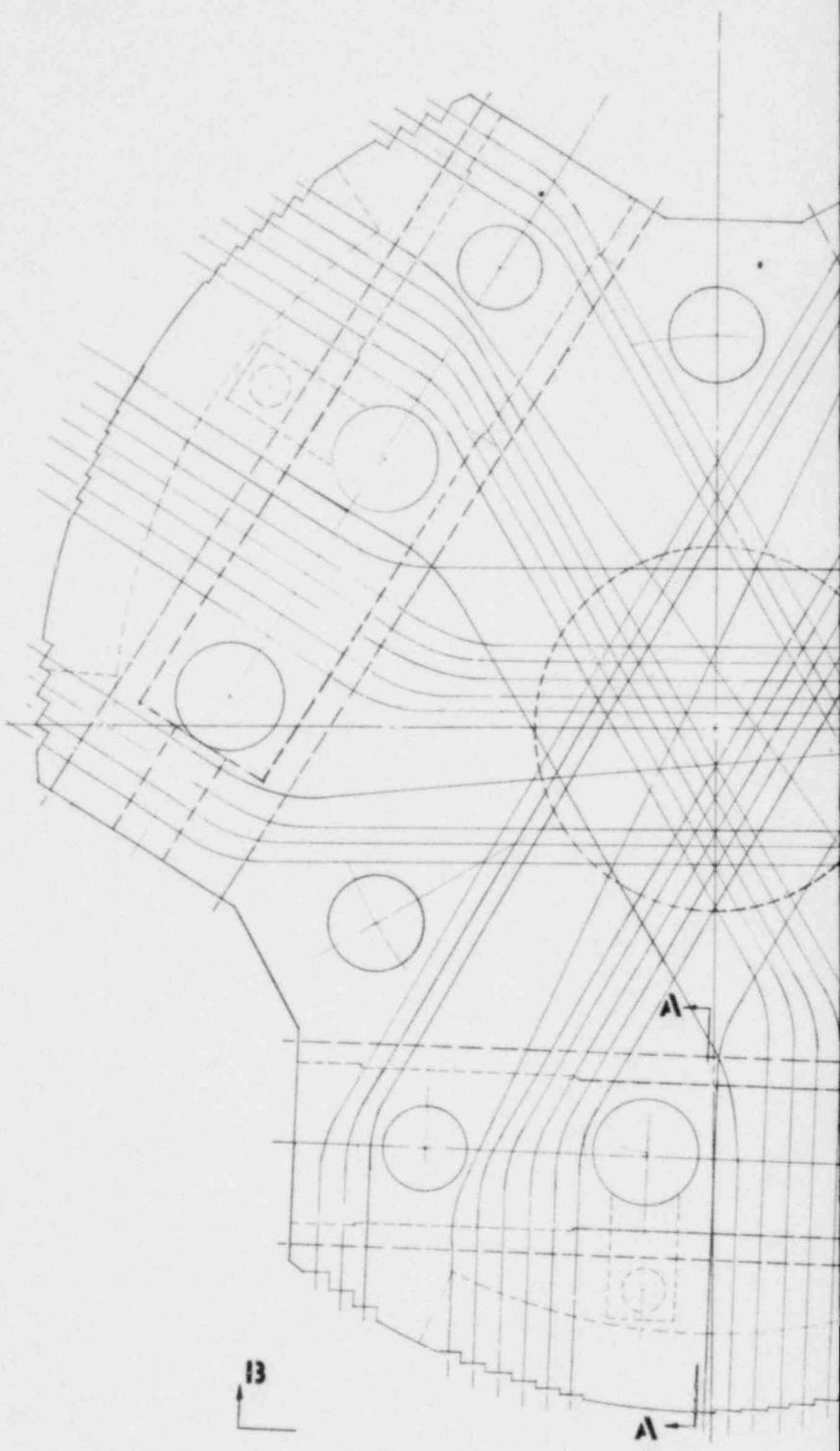
SECTION A-A SH 1

ING PENETRATION  
FLOOR



SECTION 13-13 SH 1

Fig. 15-1. PCRV for reference three-loop HTGR-GT plant (sheet 2 of 2)



SECTION THRU BOTTOM HEAD SHOWING HORIZON

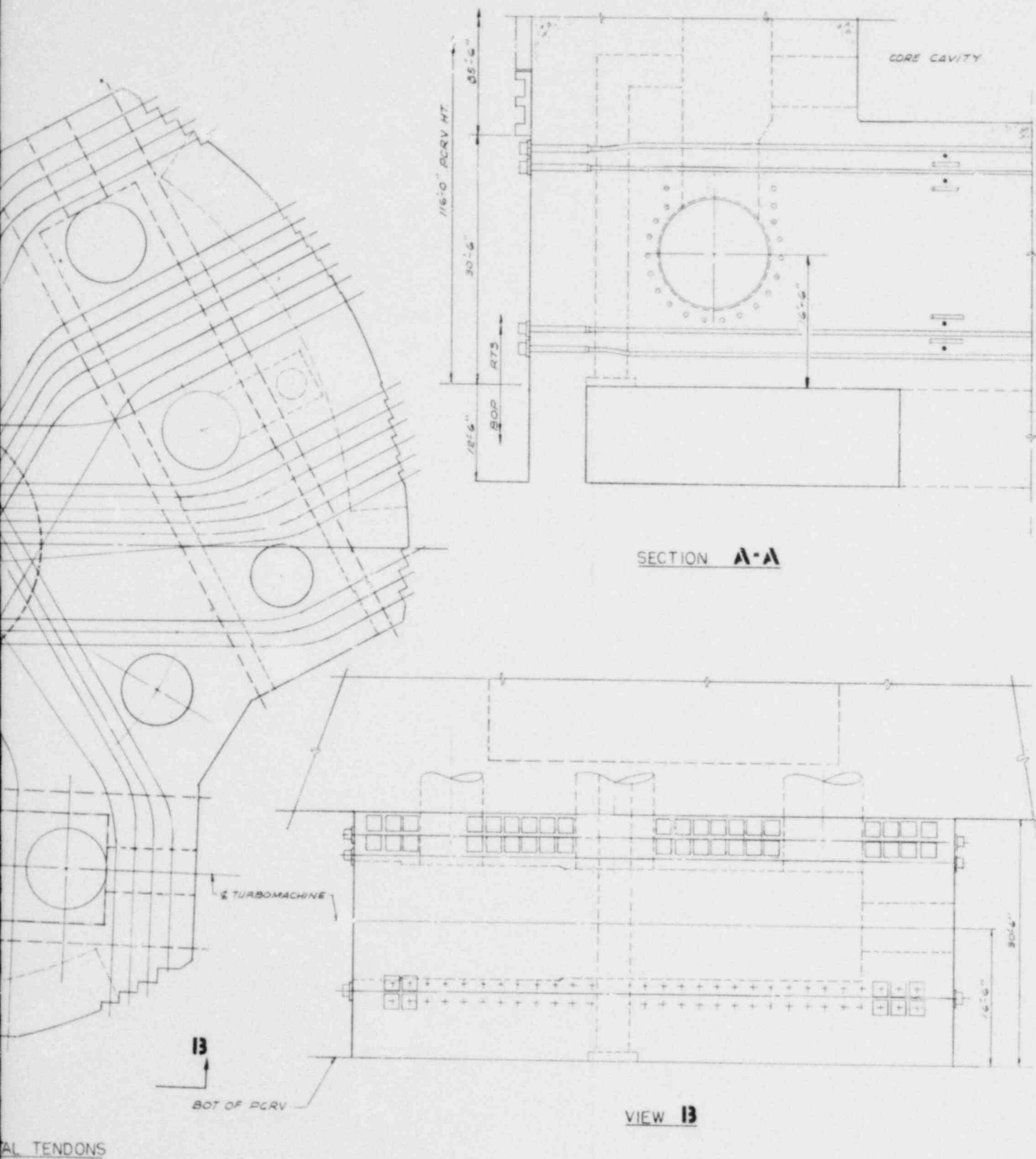


Fig. 15-2. Horizontal tendon layout for PCRV bottom head

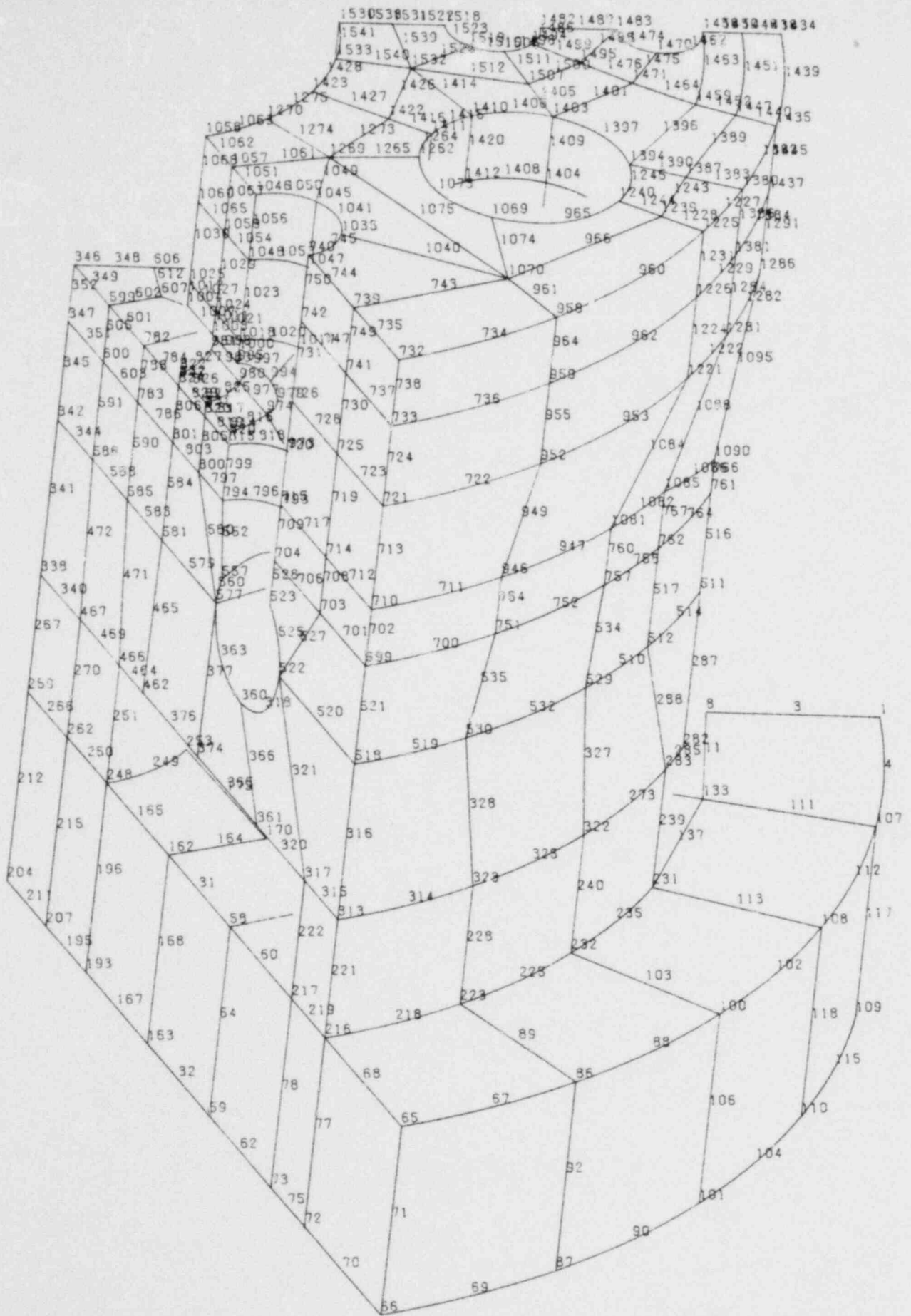


Fig. 15-3. Three-dimensional finite element model of PCRV



### 15.3.2. Two-Loop Intercooled and Non-Intercooled Plant Study

The selected basic configuration for comparing the intercooled and non-intercooled variants is the 800-MW(e) plant with two 400-MW(e) power conversion loops. The two "base case" configurations are shown in Figs. 15-4 and 15-5. The following major component PCRV cavity envelopes (liner inside diameter dimensions) and system parameters were considered for the designs:

<u>Cavity Envelopes</u>	<u>Intercooled</u>	<u>Non-intercooled</u>
Core cavity (diameter/height), m (ft-in.)	11.33/16.18 (37-2/53-1)	
Recuperator (top/middle height/diameter), m (ft-in.)	6.15/5.92 (20-2/19-5)	
Precooler (top/middle height/diameter), m (ft-in.)	4.57/4.42 (15-0/14-6)	5.13/5.50 (16-10/16-5)
Intercooler, m (ft-in.)	4.42 (14-6)	--
Turbine cavity (end/middle section/diameter), m (ft-in.)	4.75/4.57 (15-7/15-0)	
Compressor discharge duct, m (ft-in.)	3.56/3.35 (12-0/11-0)	
CACS (top/middle height/diameter), m (ft-in.)	3.12/2.67 (10-3/8-9)	
<u>System Parameters (Max. Cavity Pressure)</u>	<u>Intercooled</u>	<u>Non-intercooled</u>
High pressure, MPa (psi)		8.17 (1185)
Low pressure, MPa (psi)	2.72 (395)	3.27 (474)
Equilibrium pressure, MPa (psi)		6.21 (900)

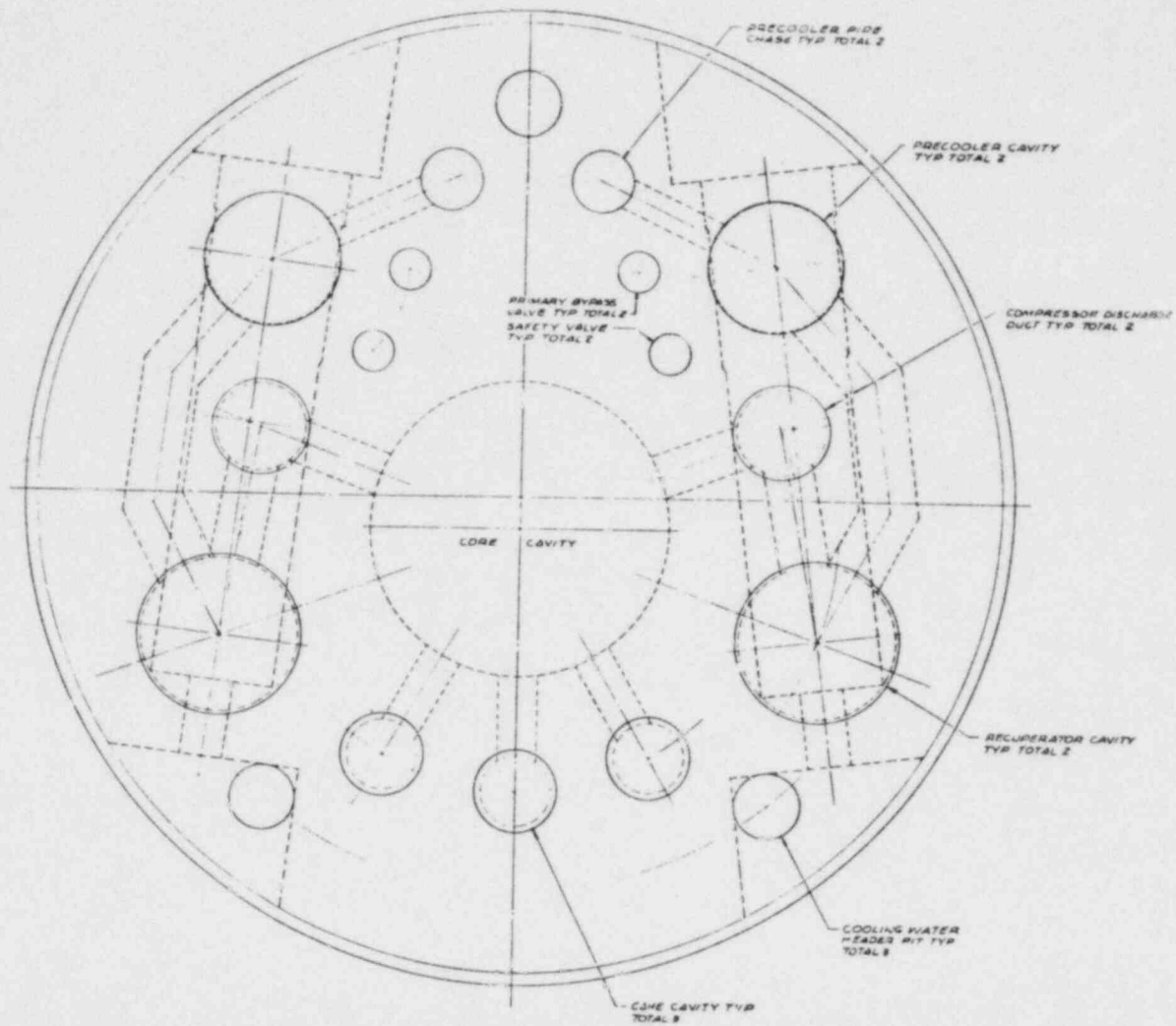


Fig. 15-4. Plan view of PCRV for two-loop, 800-MW(e) non-intercooled HTGR-GT plant

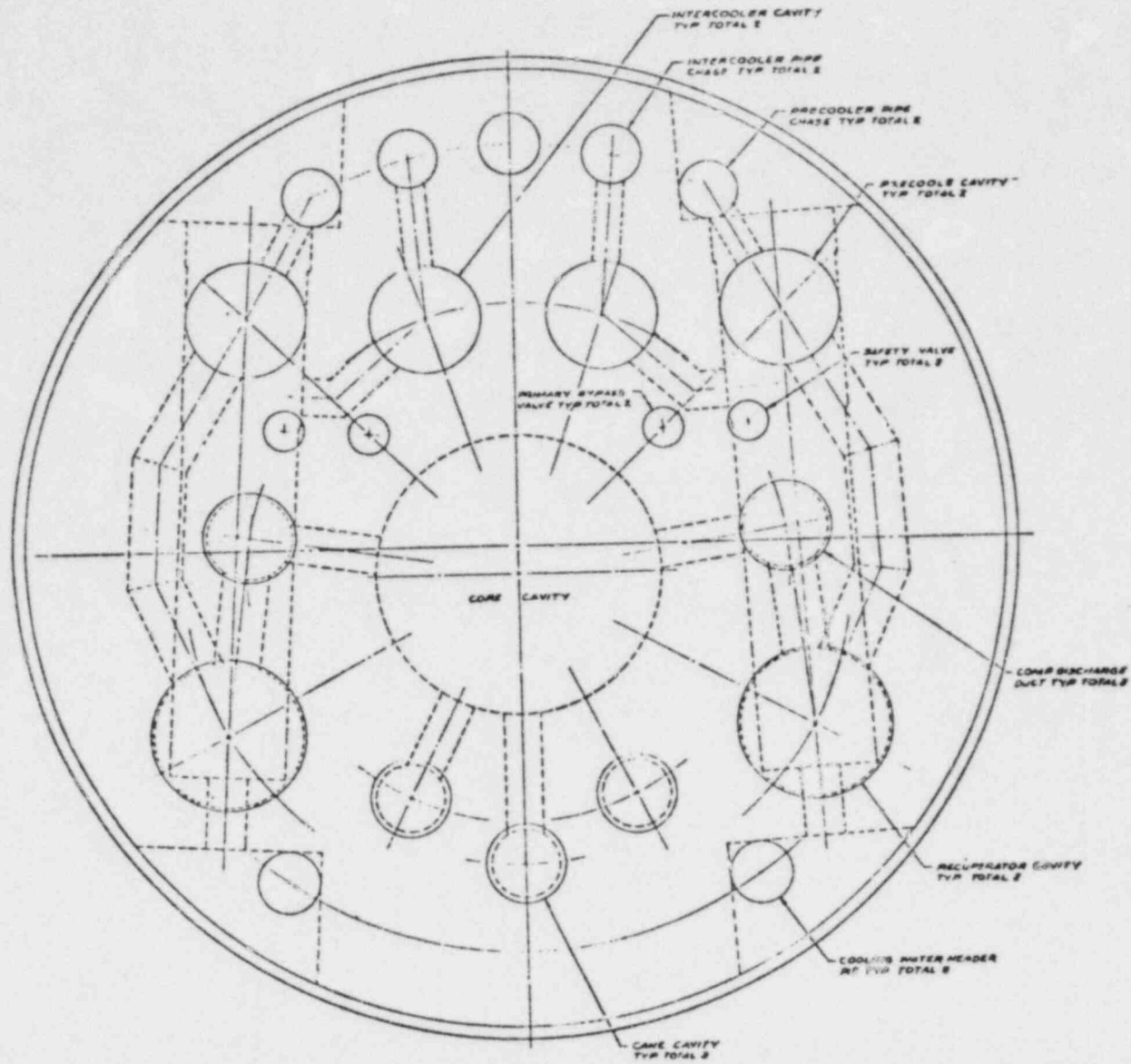


Fig. 15-5. Plan view of PCRV top head for two-loop, 800-MW(e) intercooled HTGR-GT plant

The principal dimensions of the PCRV for the two configurations are as follows:

	<u>Intercooled</u>	<u>Non-intercooled</u>
PCRV diameter, m (ft)	39.62 (130)	37.19 (122)
PCRV height, m (ft)		35.36 (116)

The two-loop plant arrangement offers a design option that was not available in the three-loop "delta" HTGR-GT configuration: the turbo-machines can be installed and removed from the turbine end of the horizontal turbomachinery cavity, thus avoiding the need to disconnect and move the generator and its bus connections.

Figures 15-6 and 15-7 depict the PCRV designs for the non-intercooled and intercooled plants, respectively. The PCRV sizing for these plants was governed mostly by the cavity closure ring space required and tendon layout except for the few ligaments which were stress governing. For the non-intercooled plant, the inner radial ligament between the core and compressor discharge duct in the barrel section and the circumferential ligament between the recuperator cavity and the compressor discharge duct in the top head were stress governing. For the intercooled plant, the circumferential ligament between the CACS and precooler cavities and between the recuperator and intercooler cavities are stress governing in the top head during initial prestressing. All other ligaments are layout controlled.

The PCRV diameter of the intercooled plant is 2.44 m (8 ft) larger than for the non-intercooled configuration. This increase is mainly due to the longer turbine cavity for the intercooled plant [2.59 m (8.5 ft)], the addition of two intercooler cavities with their closure rings, and associated pipe chases for the cooling water plumbing. The PCRV height for both concepts is governed by the combination of several component

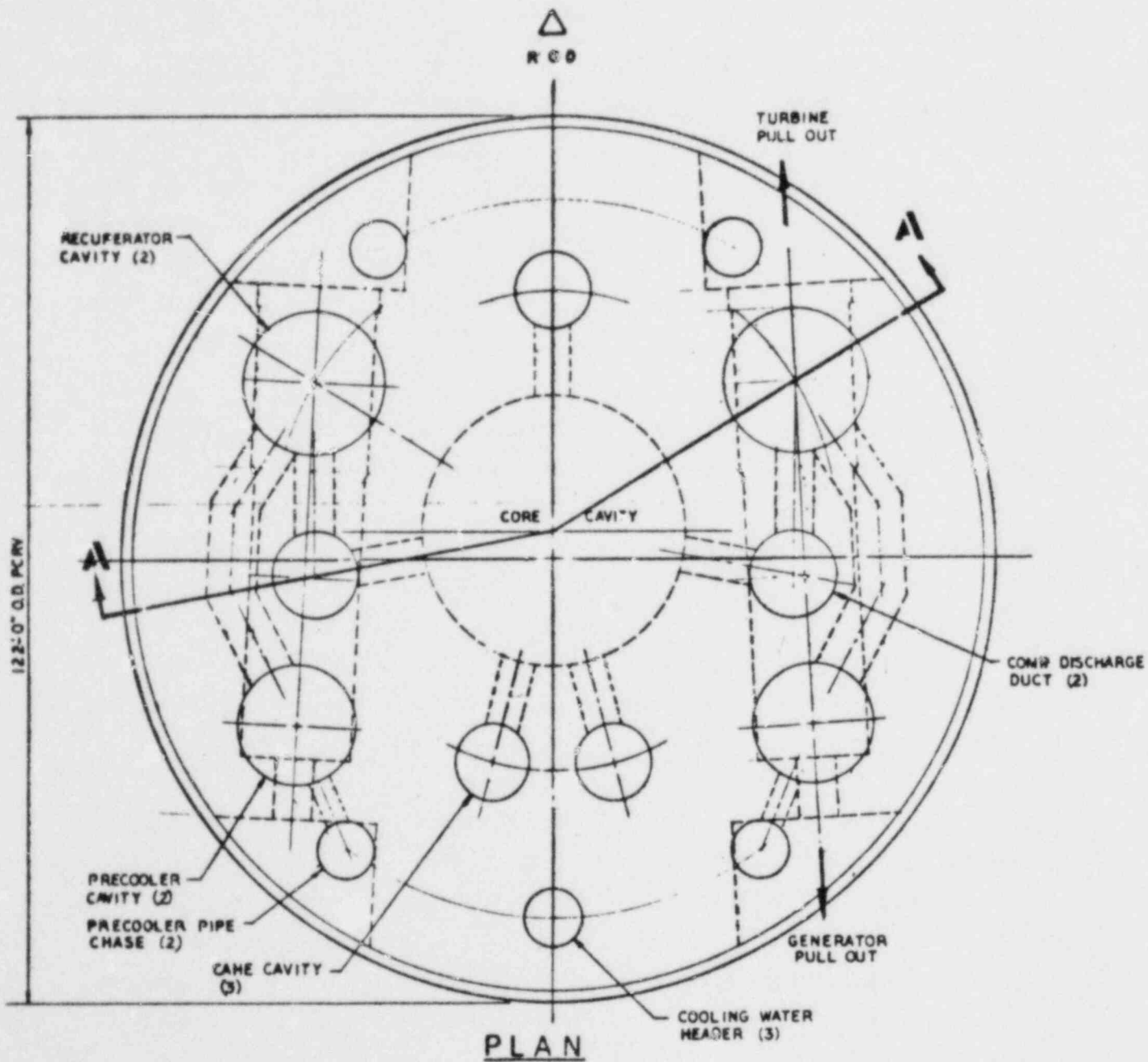


Fig. 15-6. PCR for non-intercooled HTGR-GT (sheet 1 of 2)

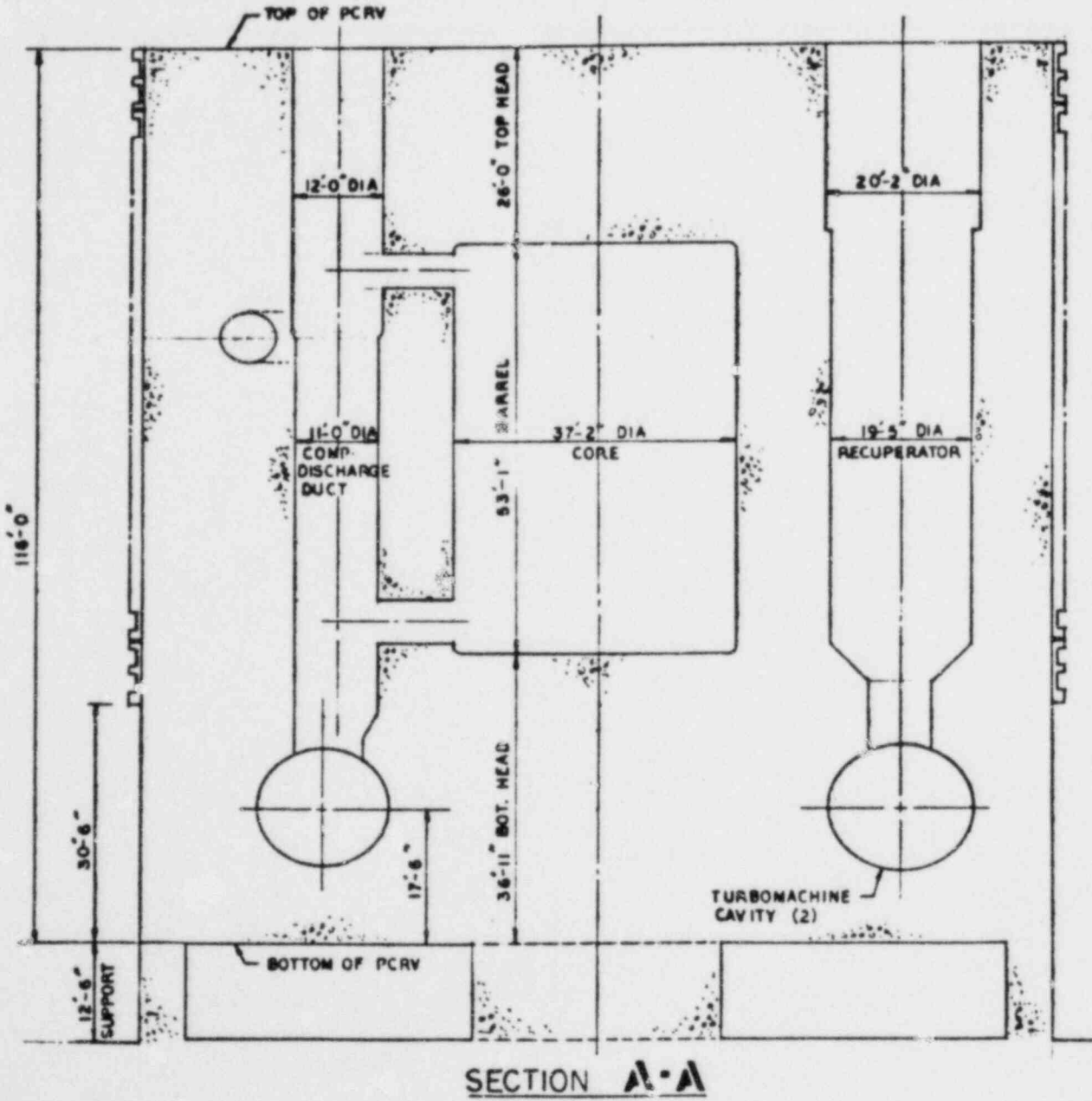


Fig. 15-6. PCRV for non-intercooled HTCR-GT (sheet 2 of 2)

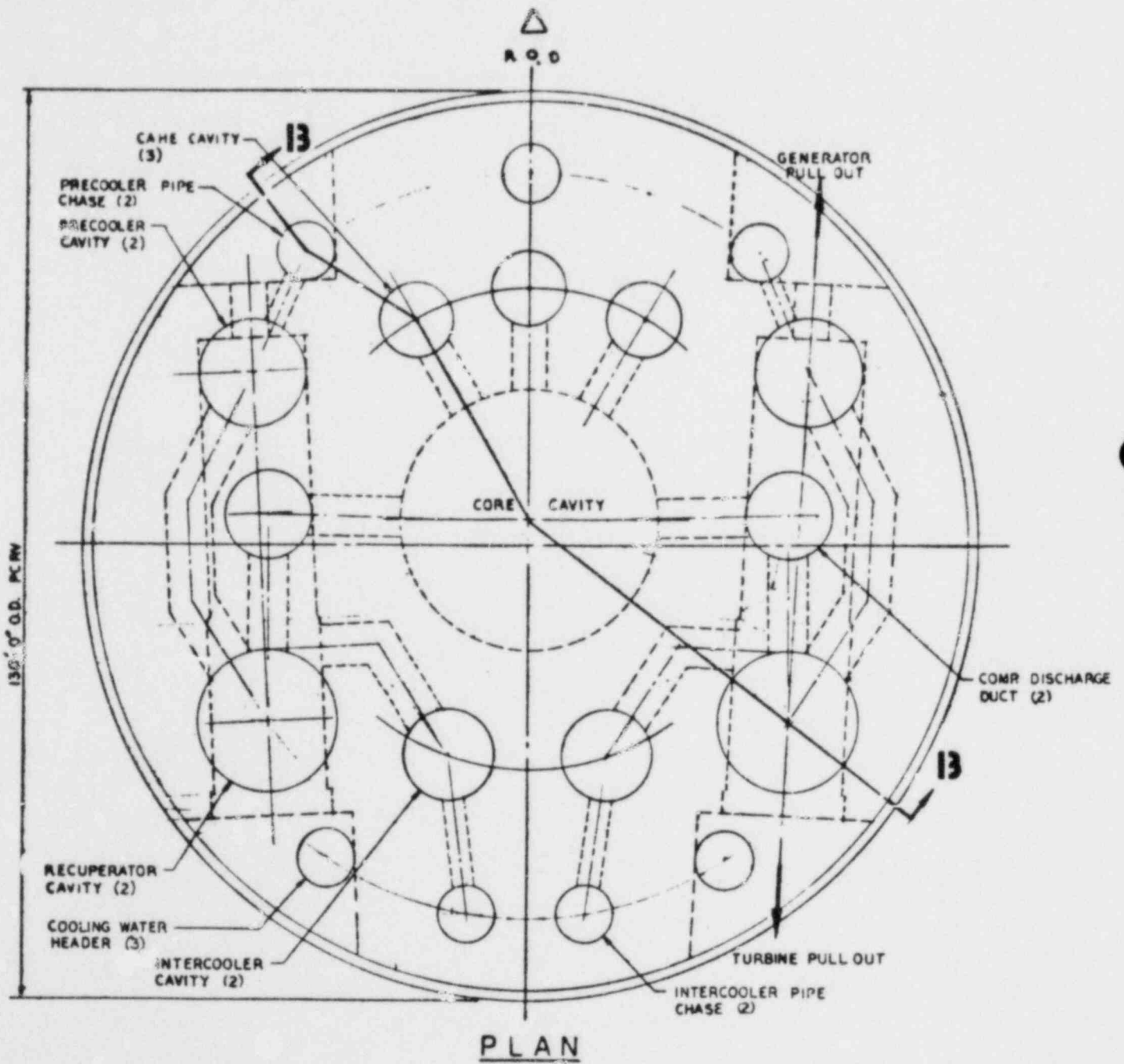
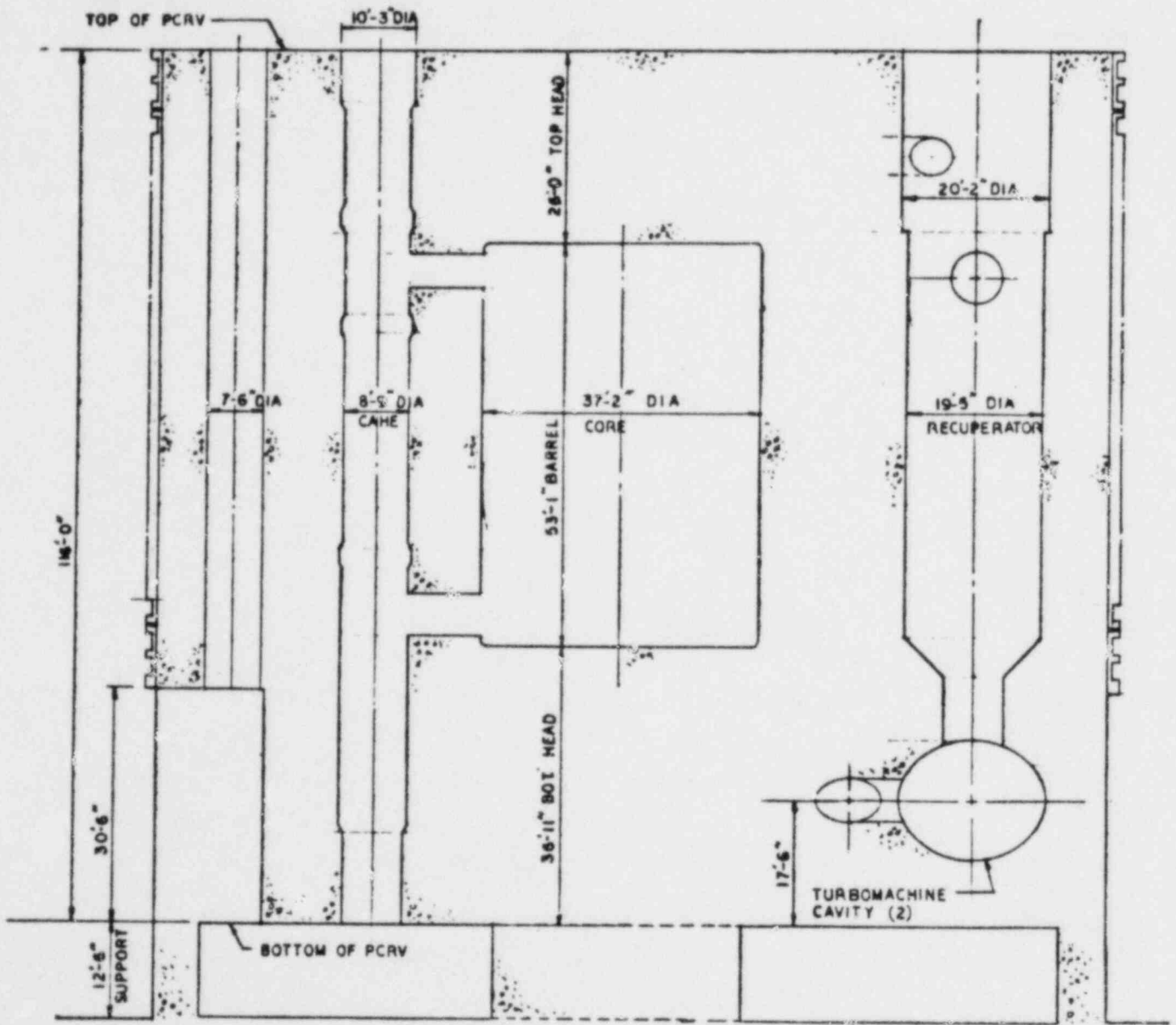


Fig. 15-7. PCRV for intercooled HTGR-GT (sheet 1 of 2)



**SECTION 13-13**

Fig. 15-17. PCRV for intercooled HTGR-GT (sheet 2 of 2)



requirements: the turbine cavity elevation in the bottom head, which is based on the requirements of the horizontal tendon layout, the space required for the recuperator, and the cavity closure plug thickness.

There are several potential cost saving improvements applicable to both concepts. These can be classified under the following major categories:

1. PCRV design changes.

- a. Increase the PCRV concrete strength from 44.8 MPa (6500 psi) to 55.2 MPa (8000 psi).
- b. Increase the linear prestressing system tendon capacity to 13.3 MN (3000 kips).
- c. Perform a crack analysis to optimize the stress-governing ligaments.

2. Major component design changes.

- a. The majority of the PCRV ligaments are controlled by layout in both plants. The concrete closure rings on top of the PCRV occupy a significant amount of space and in most cases control the location of the cavities and the size of the PCRV. Alternate closures such as inverted arch plugs or a similar concept would eliminate the huge closure rings on the PCRV top head, and the layout could be much simpler and also improve the BOP layout and refueling of the core.
- b. The compressor discharge duct in the current design is used for ISI and replacement of the hot and cold ducts and also allows helium flow from the turbine compressor to the top of the recuperator cavity. There may be a significant saving in

the PCRV diameter if this vertical duct is either eliminated or moved away from the core, i.e., not directly above the turbine cavity, and its cavity size is reduced by 50%. Hot duct removal would then be accomplished through the turbo-machinery cavity.

- c. As stated earlier, the recuperator cavity height governs the PCRV height. If this cavity is reduced in height, the PCRV height could be reduced by 1.83 m (6 ft) maximum.

While the above optimization possibilities would result in PCRV size reduction, further investigation is necessary to establish their feasibility. It should be noted, however, that the size reduction so achieved is not cumulative.

From a PCRV standpoint, the two-loop, 400-MW(e) non-intercooled plant is favored over its intercooled counterpart for the following reasons:

1. The PCRV diameter is 2.44 m (8 ft) smaller than in the intercooled plant.
2. It provides more flexibility in canting of the turbine (especially in the divergent position) without affecting the PCRV diameter.
3. It permits easy incorporation of the enhanced core cooling system, again without affecting the PCRV diameter.
4. More top head layout space is available because of the absence of intercooler cavities and their associated pipe chases and simpler tendon layout.

## 16. THERMAL BARRIER (631106)

### 16.1. SCOPE

The purpose of this task in FY-79 was to develop design features for high-temperature thermal barrier designs and to complete the evaluation of the HHT conceptual hot duct thermal barrier for applicability to the GA HTGR-GT reference plant.

### 16.2. SUMMARY

An evaluation of the HHT hot duct design was completed. The design was found to be complex with potential heat transmission and maintenance problems. The three major issues of concern in developing a reliable thermal barrier design, i.e., acoustic vibration, high core outlet temperatures, and rapid depressurization rates, were evaluated.

### 16.3. DISCUSSION

#### 16.3.1. Evaluation of HHT Thermal Barrier Designs

A thorough review and analysis of the HHT hot duct designs proved difficult, since the information made available to GA was inadequate for reviewing all aspects of the designs.

In general, it was found that the HHT ducts were structurally too complex and would require extensive efforts to achieve an acceptable degree of simplicity. Except for some local movements and possible leakage through "sealing" devices, the warm ducts (such as the core inlet and turbine outlet ducts) were considered to be minor problem areas. The main problems are centered around the core outlet duct.

16.3.1.1. Assumed Design Conditions. The function of the core outlet duct is to transfer the hot gas from the lower core plenum to the turbine as efficiently and safely as possible. The general design parameters of interest are:

Temperature:	860°C (1581°F) [mixed mean].
Pressure:	7.01 MPa (1017 psi).
Differential pressure:	+26.0 MPa/s (+3771 psi/s) for 20 ms once in 40 yr. -60.0 MPa/s (-8702 psi/s) for 20 ms once in 40 yr.
Velocity:	102 m/s (335 ft/s).
Acoustic noise level:	500 Pa (148 dB).*
Seismic load:	Unknown.

16.3.1.2. Critique of HRB HHT Conceptual Designs. Written descriptions of these designs have not been made available to GA. Also, the drawings are without significant callouts. Therefore, much of the following is based on assumption and interpretation.

It appears that the thermal barrier coverplate material is carbon-carbon (C-C). It also appears that fibrous blanket material is used as an insulator. This is consistent with GA's current thinking, although cast superalloys are strongly considered for coverplates as long as the normal condition core outlet temperature remains in the range of 850° to 900°C (1562° to 1652°F). The HRB design concept appears to have provided an adequate means of accommodating pressure changes by incorporating a groove on the back side of the coverplate. However, the functional performance of the secondary plate between the insulation and the primary coverplate is questionable. It would appear that the system permits pressure changes but does nothing to reduce permeation within the insulation.

---

\*General Atomic currently uses 10,000 Pa (174 dB) for turbine-generated noise.

The effect would be excessive heat transfer (or at least local hot spots) at the "cold" face.

The method of retaining and restraining the coverplates as shown in HRB drawings is unique and complex. Apparently, the internal coaxial duct is designed to be completely fabricated outside of the plant (because of the sequence and location of the welds and back side attachments). Therefore, it must be assumed that the duct must be removed in its entirety for repair or replacement. In situ inspection of anything other than the coverplates is impossible. Remote removal of such a large duct section through complex angles seems to be difficult. Since local distortion of the supports and guides is to be expected, the new replacement duct will be difficult to mate.

In summary, the HRB HHT duct concepts as presented are very complex, which is undesirable in high-temperature structural design. The complexity is particularly evident in the attachments, ring seals, gimbaled sections, expansion joints, and supports. If in situ inspection, repair, and replacement are criteria, then the duct designs should be simplified.

16.3.1.3. Applicability of HRB HHT Designs to GA HTGR-GT. The designs as presented are more schematical than detailed and have limited applicability to the GA thermal barrier designs. General Atomic considers the major thermal-barrier-related problems to be resistance to acoustic vibration and accommodation of rapid pressure transients, as discussed in Section 16.3.2. Also important, but of lesser consequence, are factors associated with long-term thermal stability and the necessity of ISI.

The degree of ISI and repair/replaceability must be clearly defined. This definition is the basis of the thermal barrier and structural portions of the ducts, whether it is the HRB approach of complete, intact duct replacement or the approach of remotely replacing individual components of the thermal barrier.

### 16.3.2. High-Temperature Thermal Barrier Design Development

There are three major issues of concern in developing reliable thermal barrier designs: acoustic vibration, high core outlet temperatures, and rapid depressurization rates.

The first issue to be considered is vibration. The overall sound pressure levels generated by the turbomachinery are projected to range up to 166 dB. At these levels, the fatigue resistance of coverplates, attachments, and insulation is extremely low. Changes in primary system parameters, such as system pressure, temperature, or flow rate, can indirectly impact the acoustic vibration issue by affecting the thermal barrier material properties and potentially reducing fatigue resistance.

Among the material choices, metallic structures are given the best chance of survival, primarily owing to a relatively high design allowable fatigue strength. However, the potential for damage to the fibrous insulation materials from acoustic vibration is very great if a "conventional" HTGR thermal barrier system is to be used. A possible solution to this problem is to encapsulate and quilt the insulation package, thereby enhancing the sonic tolerance level of the fiber blankets. This subject is discussed in more detail in Section 16.3.2.4.

Second, the proposed core outlet temperature of 850°C (1562°F) limits the choice of materials for the hot regions to cast superalloys, C-C, and hard ceramics. General Atomic has developed designs using all of these materials. The least practical at this time appears to be the hard ceramic configuration in combination with structural graphite. This is primarily because of attachment complexities and changing the duct cross section from round to rectangular to ease construction and installation. Recent discussions with suppliers of both castings and C-C indicate practical utilization opportunities of these materials for the proposed application. It must be noted, however, that the data base for these materials is very limited, especially in regard to fatigue and long-term creep. DV&S programs will be progressing to fill this void.

Finally, there are opposing requirements for controlled convection within the thermal barrier in order to minimize heat transfer and the necessity for rapid venting of the system during a depressurization accident. The effects of rapid depressurization on the thermal barrier are discussed in more detail in Section 16.3.2.3.

16.3.2.1. Candidate Alloy Evaluation. Based upon representative parameters for thermal and mechanical stress resistance and the ability to sustain imposed acoustic loads, an evaluation of candidate thermal barrier structural metallics was performed. The major candidates are given in Table 16-1.

The only coverplate materials currently being considered for Class A thermal barrier are low carbon steels such as ASTM A36 or AISI 1020, because no other grade of material has been shown to be economically competitive. For the Class B1 application, the choice is less clear. All of the alloys mentioned for this class have individual advantages. The eventual choice will probably be made on the basis of an economical tradeoff with the more expensive Class B2 choice. All the Class B2 metals are cast nickel-base superalloys. An evaluation by GA's Structural Materials Department regarding castability and material properties is in progress. At this time, the favored candidate is IN 713LC.

16.3.2.2. Class B2 Coverplate Evaluation. The coverplate and attachment configurations must perform satisfactorily under the following conditions:

1. Long-term loading of the insulation pressure.
2. Short-term loading due to rapid depressurization (see Section 16.3.2.3).
3. Fatigue loading due to acoustic vibration (see Section 16.3.2.4).

TABLE 16-1  
MAJOR CANDIDATE THERMAL BARRIER METALLICS AND DESIGN TEMPERATURE LIMITS

Material	Thermal Barrier Class	Thermal Barrier Temperature Limit [ $^{\circ}\text{C}$ ( $^{\circ}\text{F}$ )]		
		Normal Design Condition at 300,000 h	Emergency Design Condition at 10 h	Faulted Design Condition at 1 h
Carbon steel	A	371 (700)	482 (900)	593 (1100)
2-1/4 Cr-1 Mo	B1	538 (1000)	649 (1200)	Not yet defined, depends on material selection.
304 SS	B1	593 (1100)	816 (1500)	
316 SS	B1	621 (1150)	816 (1500)	
Alloy 800H	B1	677 (1250)	>816 (>1500)	
Hastelloy X	B1	704 (1300)	>899 (>1650)	
IN 100 or Rene 100	B2	910 (1670)	982 (1800)	1093 (2000)
IN 162	B2	910 (1670)	982 (1800)	1093 (2000)
IN 713LC	B2	910 (1670)	982 (1800)	1093 (2000)
IN 738	B2	910 (1670)	982 (1800)	1093 (2000)



4. Thermal loading of the primary coolant due to steady-state and transient operation.
5. Long-term effects of the primary coolant on the material properties of the casting materials.

To date, preliminary analyses have been completed for stresses induced by mechanical loading, thermal loading, and loads due to acoustic vibration. The favored configuration (Fig. 16-1) was found to be structurally adequate when using the properties of IN 713LC.

The analyses have shown that the maximum stress due to the mechanical loading occurs at the coverplate-attachment intersection, where the largest bending moment from the insulation pressure is induced. The maximum stress due to thermal loading resulting from the temperature gradient through the structure was found to occur at the base of the attachment during steady-state operation and at the top of the attachment during normal operation thermal cycling.

Before the evaluation of these proposed cast coverplates is complete, it will be necessary to include the short-term loading due to rapid depressurization and the thermal loading of the primary coolant due to accident transients. The effect of the reactor environment on the basic material properties must also be determined.

16.3.2.3. Effects of Rapid Depressurization. An investigation of the effect of rapid depressurization on the thermal barrier in the HTGR-GT was completed. The turbine deblading accident is considered to have the most severe pressure transients and was therefore the accident used in this study. An evaluation of the required coverplate vent area to accommodate rapid depressurization indicates that the vent area [1.6% of the coverplate area yields a 103-kPa (15-psi) pressure drop] is feasible.

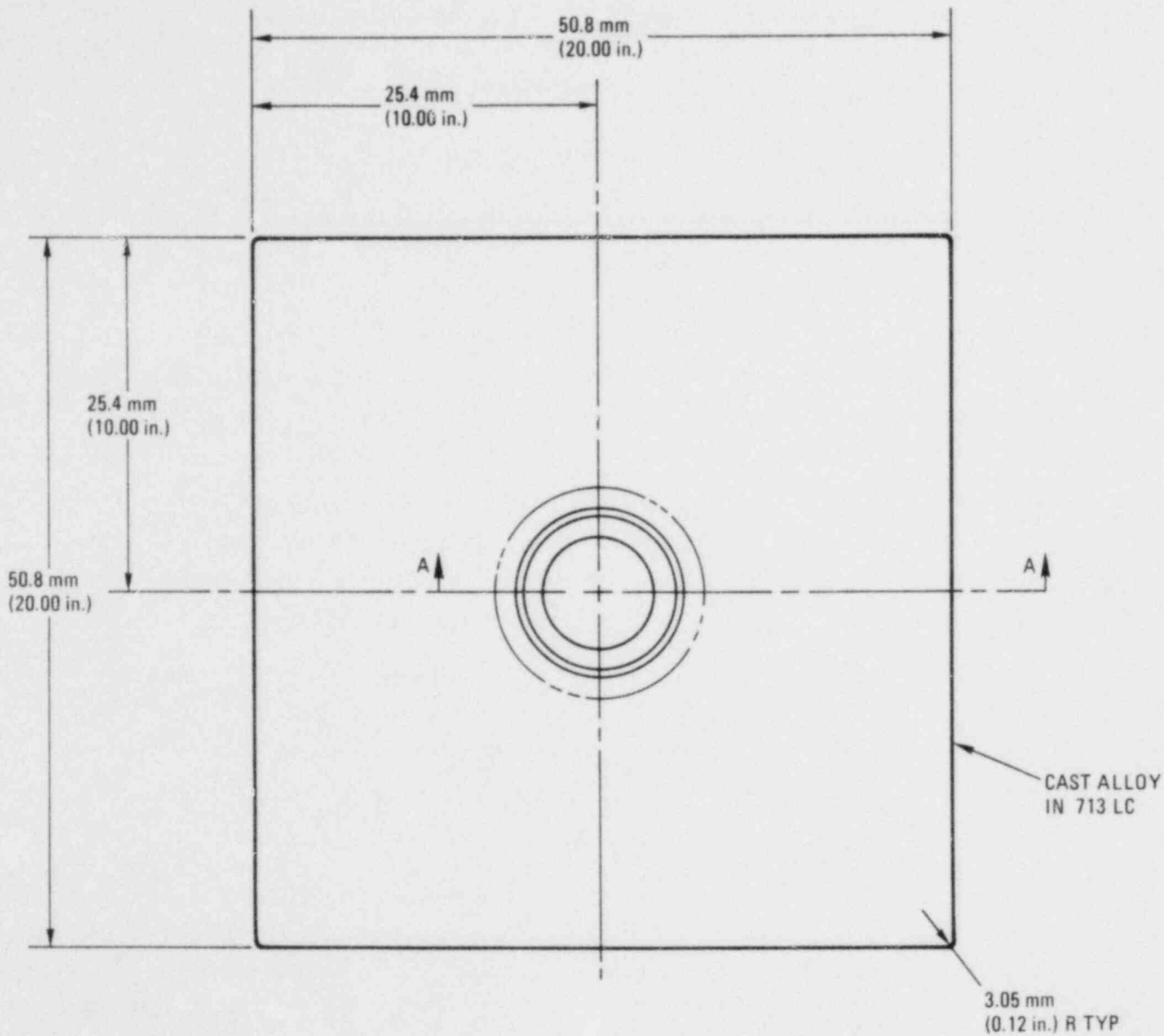


Fig. 16-1. Thermal barrier coverplate with integrated attachment fixture  
 (sheet 1 of 2)

16-9

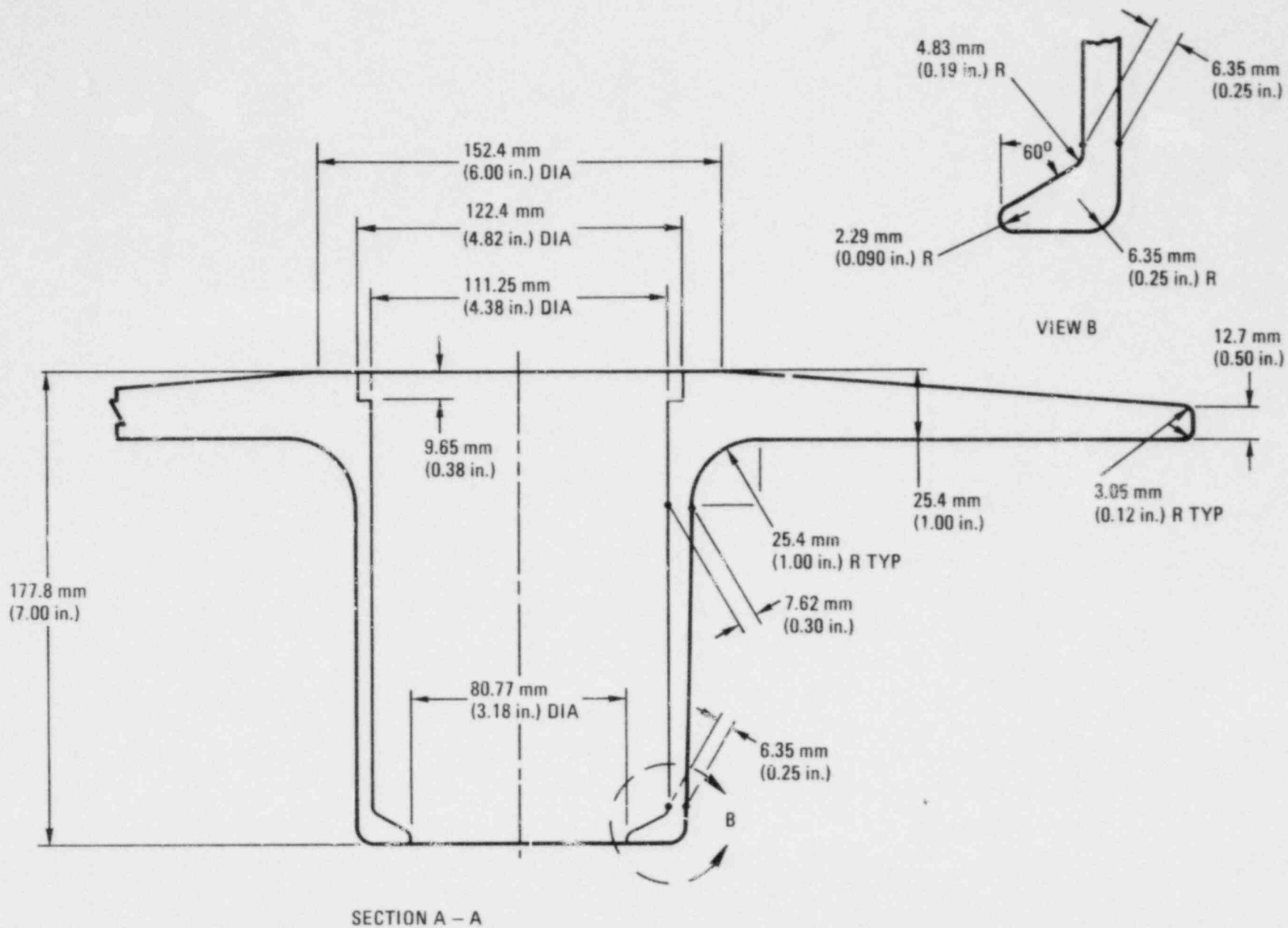


Fig. 16-1. Thermal barrier coverplate with integrated central attachment fixture (sheet 2 of 2)

Further study of rapid depressurization during the turbine deblading accident indicated that there may be a venting problem due to depressurization of the fibrous insulation because of the flow resistance of the fibers. Limited test results indicate a potentially serious problem associated with the rapid depressurization of the fibers. This is especially true for the lower main cross duct (hot duct) where a maximum depressurization rate of 56.9 MPa/s (8255 psi/s) may yield a pressure load of 0.35 MPa (50 psi) on the coverplates. It is recommended that permeation and depressurization tests for the HTGR-GT conditions be conducted in coordination with analyses.

At the present time, the evaluation of the effects of pressure upon the thermal barrier requires more information in a number of areas, most of which involve rapid depressurization caused by the turbine deblading accident. These areas are as follows:

1. A study should be performed to determine whether the helium flow through the thermal barrier during the turbine deblading accident can be considered Darcian flow or is actually a non-Darcian flow, which is not easily characterized.
2. Because of the rapid temperature decrease caused by the adiabatic expansion of the helium, the effects of the turbine deblading accident should be evaluated with respect to the potential thermal shock on the thermal barrier components.
3. The rapid temperature and pressure decreases induced by the turbine deblading accident need to be evaluated in terms of two-dimensional effects of the transient in the duct.

16.3.2.4. Acoustic Analysis. During this study, the acoustic response of two candidate Class B thermal barrier configurations currently being proposed for the HTGR-GT was analyzed. It was concluded that a 51 x 51 cm (20 by 20 in.) plate with a central attachment fixture appeared feasible.

Based on acoustic load considerations only, either IN 713LC or a C-C composite can be satisfactory. It is felt that the present concept (see Fig. 16-1) is structurally satisfactory for the currently predicted acoustic loads. However, before a given coverplate attachment fixture can be designed with confidence, it will be necessary to:

1. Determine the narrow band root mean square acoustic load as a function of frequency.
2. Determine the high-cycle fatigue strength of the candidate materials (IN 713LC and C-C) in reactor helium. Currently, there are only limited data on IN 713LC in air and almost no data on C-C.
3. Experimentally determine the coverplate damping characteristics in reactor helium. Currently, the coverplate damping in reactor helium is based on a theory which needs verification.
4. Investigate the effect of coverplate curvature on the coverplate response and the attachment fixture loads. Thus far, all analysis and testing have been done assuming flat coverplates. However, it is recognized that in the current HTGR-GT configuration all coverplates will have some curvature.
5. Investigate the effect of varying the coverplate thickness with a tapered plate (as shown in Fig. 16-1) on the coverplate response and the attachment fixture loads. As indicated in item 4 above, all the analysis and testing have been done on flat plates of uniform cross section. However, it appears that this is not an optimum or realistic configuration.
6. Determine the loading on attachment fixtures, since the results of GA's acoustic analysis do not include this information.

7. Verify the coverplate boundary conditions.
8. Experimentally determine the effect of coverplate motion on fiber damage.

While a comprehensive vibration test program has been outlined to obtain the necessary information, GA would benefit from relevant existing test data. Therefore, efforts are being made to obtain information previously generated in the United Kingdom under the Advanced Gas-Cooled Reactor program.

## 17. REACTOR INTERNALS (6317)

### 17.1. REACTOR INTERNALS DESIGN

#### 17.1.1. Scope

The purpose of this task in FY-79 was to improve the level of confidence in developing the structural/mechanical design of the HTGR-GT reactor internals.

#### 17.1.2. Summary

Work performed under this task was as follows:

1. A structural and mechanical evaluation of the HHT reactor internals under seismic excitation was conducted.
2. Preliminary cost information on the reactor internals of the three-loop HTGR-GT commercial plant was estimated for input to the CODER program.

A structural and mechanical evaluation of the HHT coaxial, high-temperature gas ducts was performed. This study was limited to the structural and mechanical aspects of HRB's design of the HHT high-temperature gas ducts. The thermal insulation of the ducts was reviewed separately. The amount of available information did not permit a definite conclusion as to the feasibility of the present design. However, potential problem areas were identified and recommendations for needed analytical and experimental programs were made.

A preliminary seismic evaluation of the reactor internals structures was completed. This study was primarily qualitative owing to the lack of data on the internals of the HHT and the absence of a supporting seismic analysis.

Cost information on reactor internals was estimated for input to CODER. The cost information on the reactor internals of the three-loop HTGR-GT commercial plant was incomplete and will have to be revised when materials for the high-temperature metallic internals are chosen.

#### 17.1.3. Discussion

The primary results of the structural and mechanical evaluation of HHT's coaxial, high-temperature gas ducts are summarized below:

1. The choice of material for the shells of the CAHE inlet ducts should be reviewed to ensure that a steel with the required high-temperature properties is chosen. (A)\*
2. The turbine outlet duct appears to have inadequate buckling strength and may need stiffening. Also, all the bends are subjected to a complex combination of loads, and it is recommended that their buckling strength be carefully confirmed through detailed analysis. (A)
3. A comprehensive analysis should be performed to determine the ability of the ducts to withstand acoustic and seismic loads. This analysis would also provide a necessary input to the vibration tests planned by HRB. (A, in part)

---

\* (A) indicates applicability to the GA three-loop HTGR-GT reference design.



4. The present HHT ducts are very complex, and an effort should be made to simplify the design and to reduce the number of components. It is believed that a simpler design will enhance safety and reliability, reduce installation and removal problems, and lower costs. The flange coupling system is incomplete. (A)
5. The design of the various types of sliding joints should be developed in more detail so that leakage estimates can be made over the range of possible seal conditions. (A)

Wherever feasible, the use of bellows, which is preferred by GA, should be considered as an alternative and a backup to ring seals. (A)

6. The various types of supports, particularly the snubbers, should also be defined in more detail so that the effect of relative movements and duct vibrations can be determined. (A)
7. Lastly, it should be pointed out that two major considerations outside the scope of this study need particular attention: (1) the effectiveness and integrity of the thermal barrier on the inside (A), and (2) the uniformity and continuity of the cooling flow on the outside of the ducts. (A)

The conclusions from the preliminary seismic evaluation of the HHT reactor internals structures are as follows:

1. The overturning and rotational stability of the core barrel side wall is doubtful. Radial keys between side wall and PCRV liner should be added to ensure it.
2. The buckling stability of the side reflector must be investigated.

3. The presence of radial gaps between the inner blocks of the side reflector, and also between the outer blocks of the bottom reflector and core support floor, is needed to permit the spring packs to keep the outer side reflector and the bottom reflector and core support floor tight. However, these gaps may prove detrimental to the internals by amplifying their seismic response and their collisions.
4. The pendulum-like arrangement of the top reflector may cause excessive impact against the side reflector.
5. Relative horizontal movements of the core support floor and the core barrel floor may not be acceptable for the core support posts as designed.
6. Both a more precise definition of the properties and geometry (including gaps) of the internals and a seismic analysis of the dynamic PCRV-internals core system are necessary to quantify the above-mentioned problems and to verify the seismic adequacy of the design proposed for the HHT, especially that of the lateral restraint.

## 17.2. HOT DUCT DESIGN - FREE-STANDING SECTION

### 17.2.1. Scope

The purpose of this task is to improve the level of confidence in developing the structural/mechanical design of the HTGR-GT free-standing ducts.

### 17.2.2. Summary

The conceptual design layouts of the core inlet and core outlet ducts for the two-loop HTGR-GT plant were released (see Fig. 17-1). The conceptual design of these ducts included the remote handling and coupling system, provisions for flexibility, and supports and seals.

### 17.2.3. Discussion

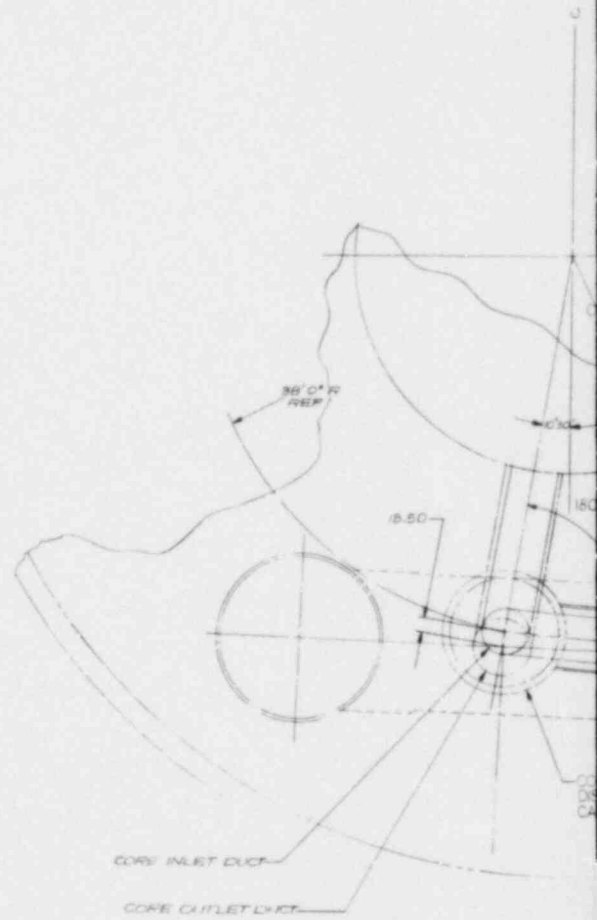
17.2.3.1. Core Outlet Duct. The core outlet duct design incorporates a coupling mechanism which is accessible via remote handling equipment through a 1.2-m (4-ft) diameter access shaft in the PCRV from the bottom head. The coupling mechanism required modification in order to be operated from a horizontal position. However, it is basically identical to the previous design, which required operation vertically from the top head of the PCRV through the compressor discharge cavity. The earlier plant configuration did not route the core inlet coolant through a free-standing duct in the upper end of the compressor discharge cavity; therefore, the core outlet duct was accessible without obstruction from the top of the PCRV. The current design requires removal of the core inlet duct prior to removal of the core outlet duct should that become necessary for inspection and/or replacement.

The duct design includes the use of bellows to accommodate movements imposed by the turbomachine. Stresses in the duct shell, without the benefit of bellows, exceed the allowable limits. Protective guards were added for the bellows to prevent damage during handling. A secondary seal was also incorporated into the design. This provides a backup to the bellows in the event of failure. The assembly has been designed for the most recent estimates of pressure differences across the duct as a result of a turbine deliading accident.

A guide-rail structure was designed such that both the core inlet and core outlet ducts have a means of horizontal restraint and also have provisions for remote installation and removal. Handling features are provided on the ducts for the remote handling equipment.

The core outlet duct/turbine inlet seal design is intended to be similar in concept to the refueling penetration/control rod drive seal ring assembly used in the Fort St. Vrain plant.

17.2.3.2. Core Inlet Duct. The free-standing core inlet duct is a recent addition to the plant design configuration. The vertical section of the duct, including the coupling mechanism and bellows, was designed similarly to the core outlet duct. The horizontal section of the duct was segmented to permit installation and removal around the 90° bend at the compressor discharge cavity/recuperator outlet cavity interface. Handling lugs were provided as well as spring-loaded roller supports for the horizontal section. As described above for the core outlet duct, a guide-rail structure is provided for the vertical section of the duct in the compressor discharge cavity. A seal ring assembly is planned for the recuperator/core inlet duct similar to that described for the core outlet duct/turbomachine interface. Additional conceptual design work is required in this area.



ORIENTATION  
SECTION  
SCALE: 1/2"

NOTES:

- 1. REF DRG: 0247/B, G-T HYBR 3 LOOP
- 2. ESTIMATED WEIGHTS (INCLUDING THERMAL BARRIER):  
 CORE INLET DUCT: 25,000 LBS  
 CORE OUTLET DUCT: 25,000 LBS  
 VERTICAL SECTION: 25,000 LBS  
 HORIZONTAL SECTION: 10,000 LBS

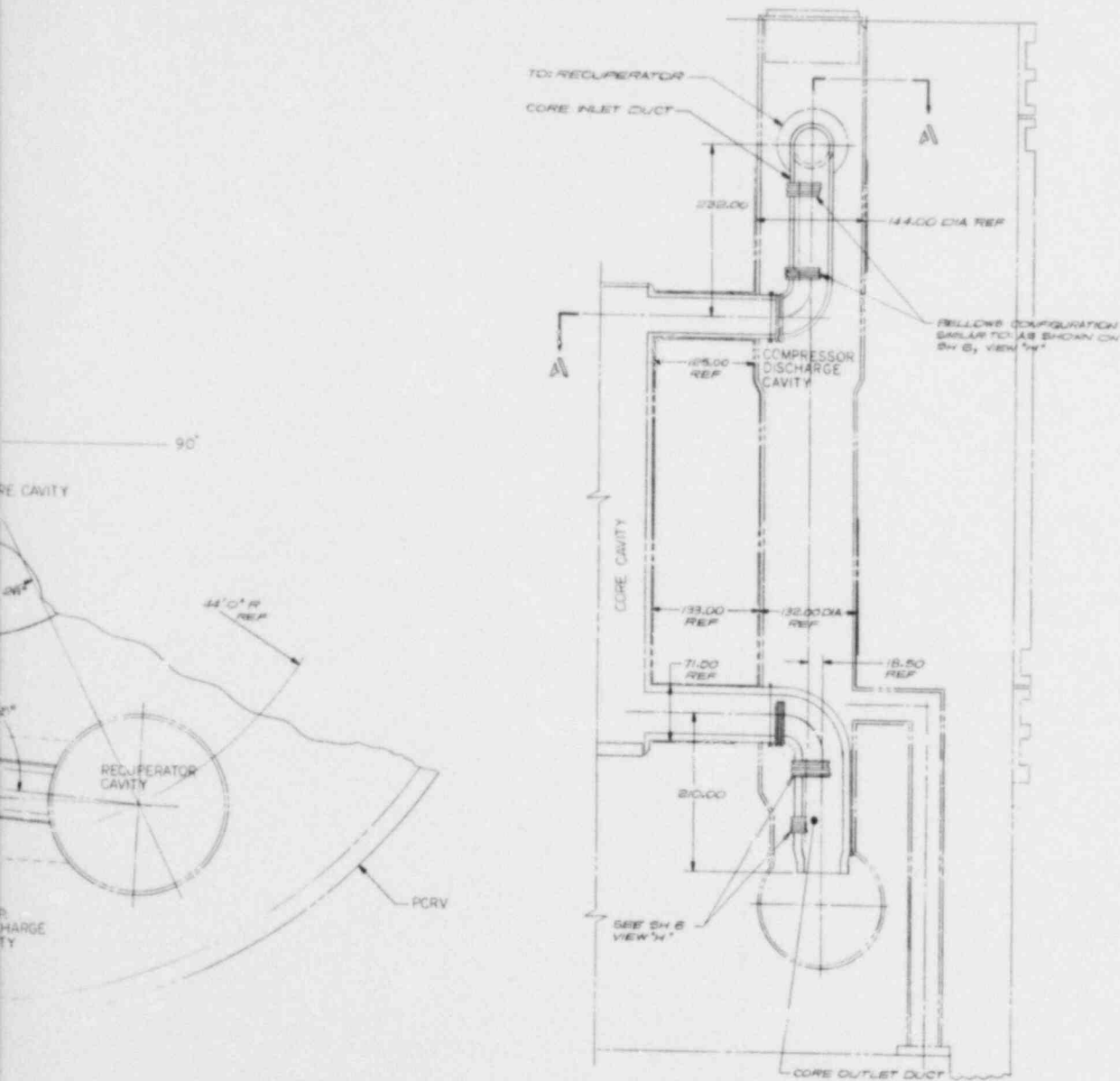
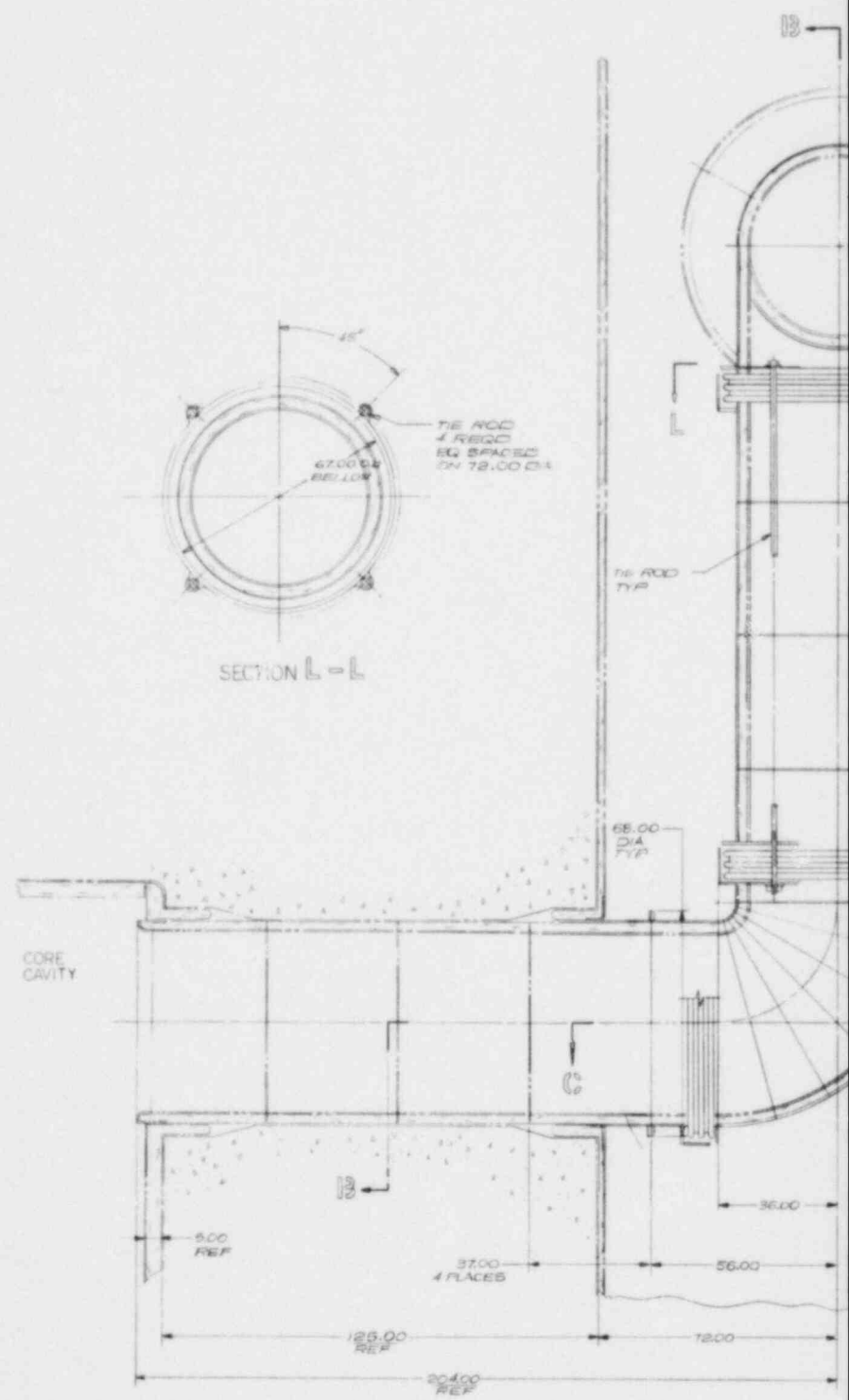
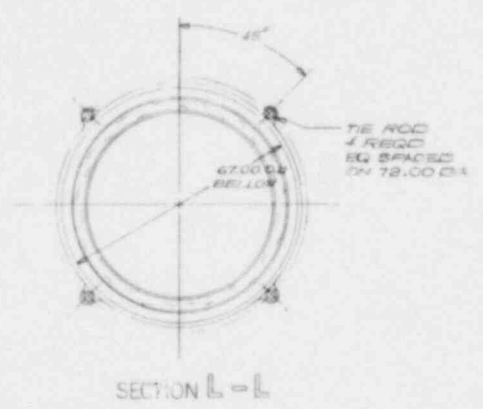


Fig. 17-1. Conceptual core inlet and core outlet ducts (sheet 1 of 6)



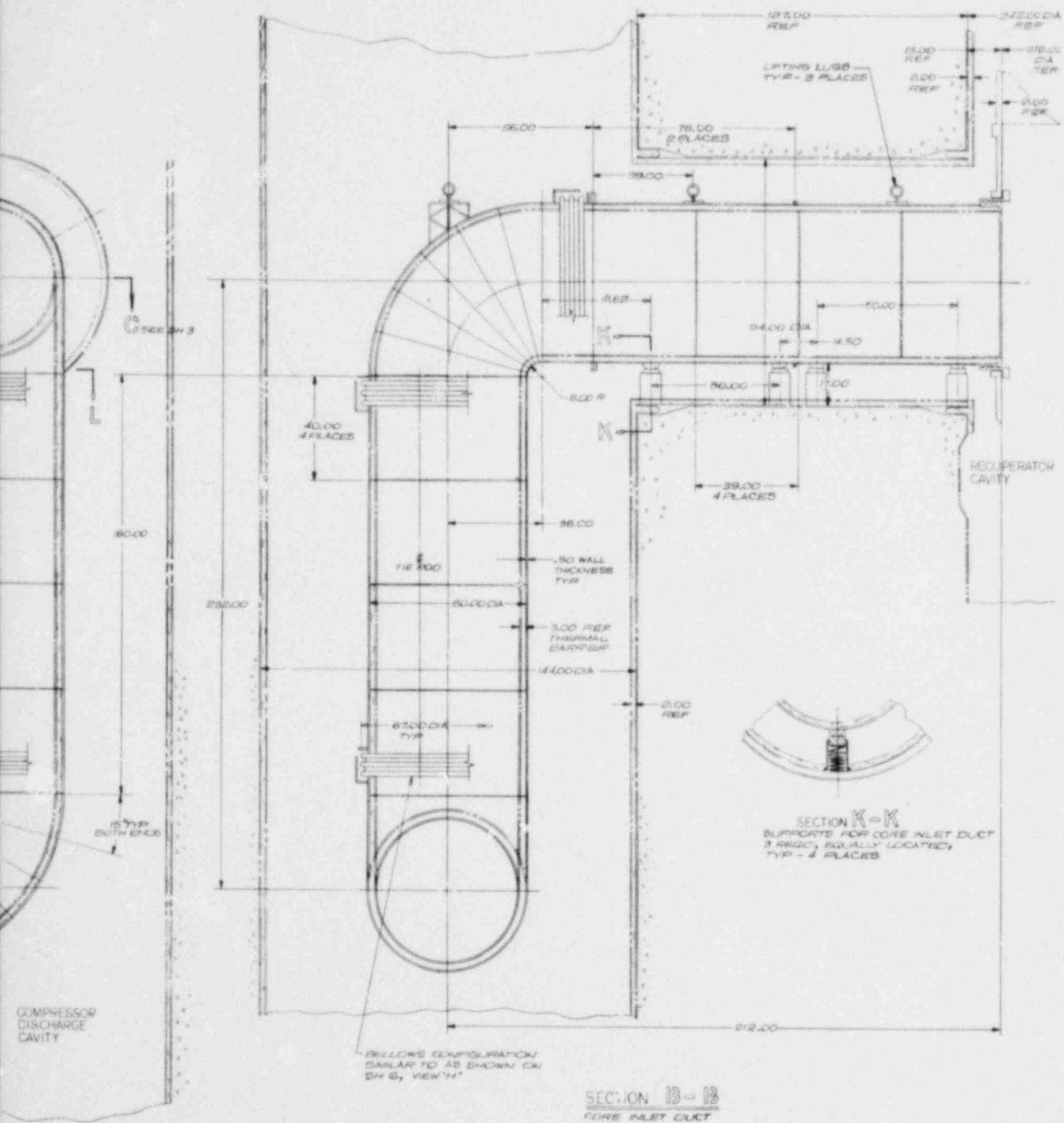
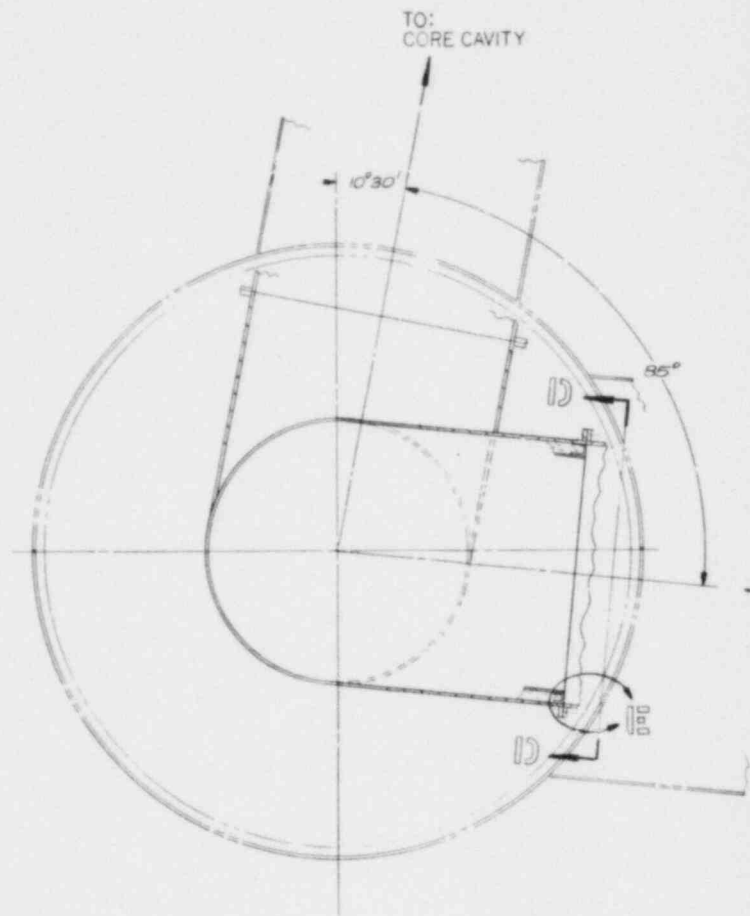
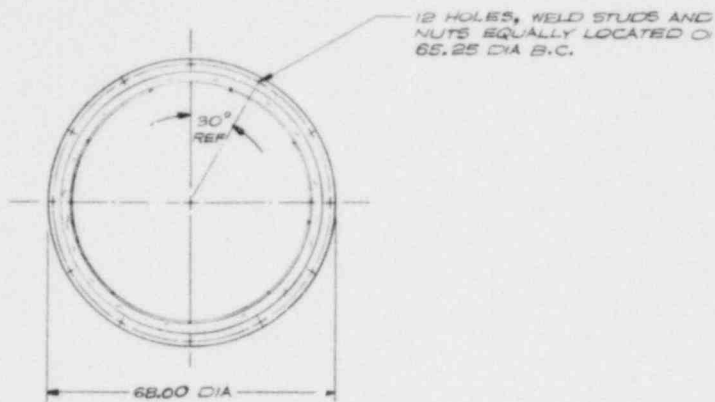


Fig. 17-1. Conceptual core inlet and core outlet ducts (sheet 2 of 6)



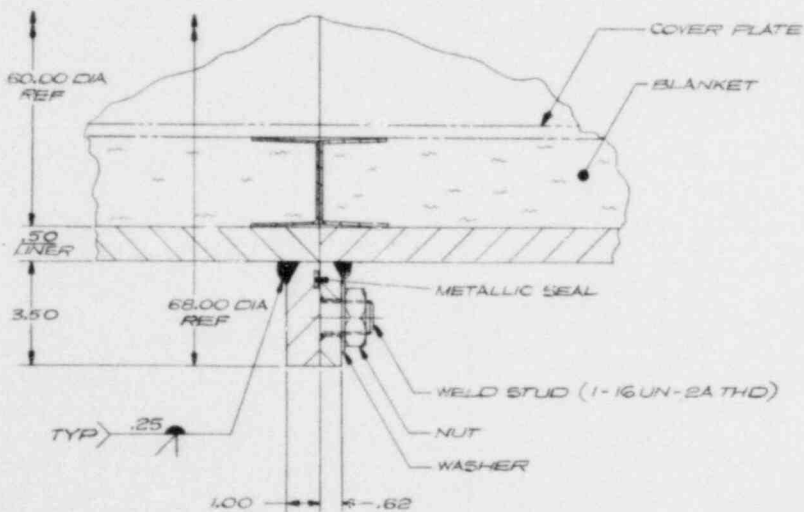


SECTION C-C  
TYP. ELBOW & JUCT  
ANGULAR ORIENTATION



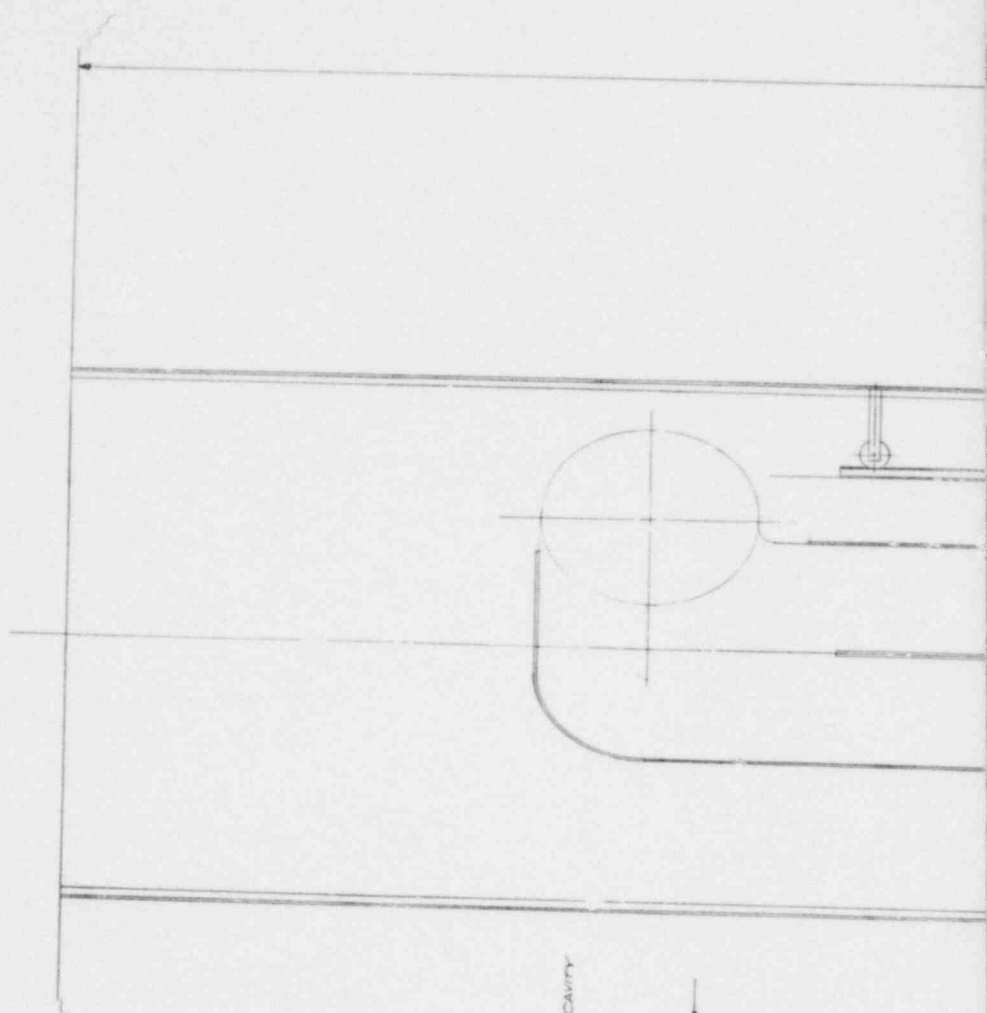
VIEW D-D  
TYP AT EACH CONNECTION OF DUCT

FROM:  
RECUPERATOR  
CAVITY



VIEW E-E  
SCALE:  $\frac{1}{2}$   
OPTIONAL

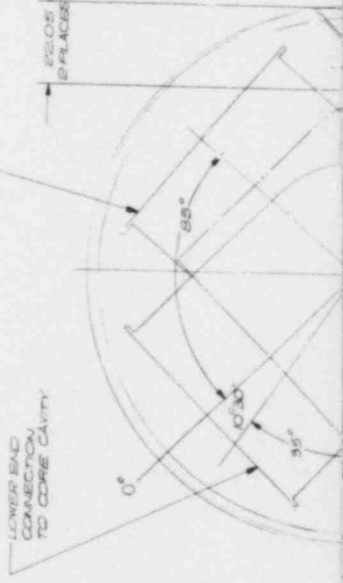
Fig. 17-1. Conceptual core inlet and core outlet ducts (sheet 3 of 6)



UPPER END CONNECTION FROM RECUP CAVITY

22.05  
2 PLACES

LOWER END CONNECTION TO CORE CAVITY



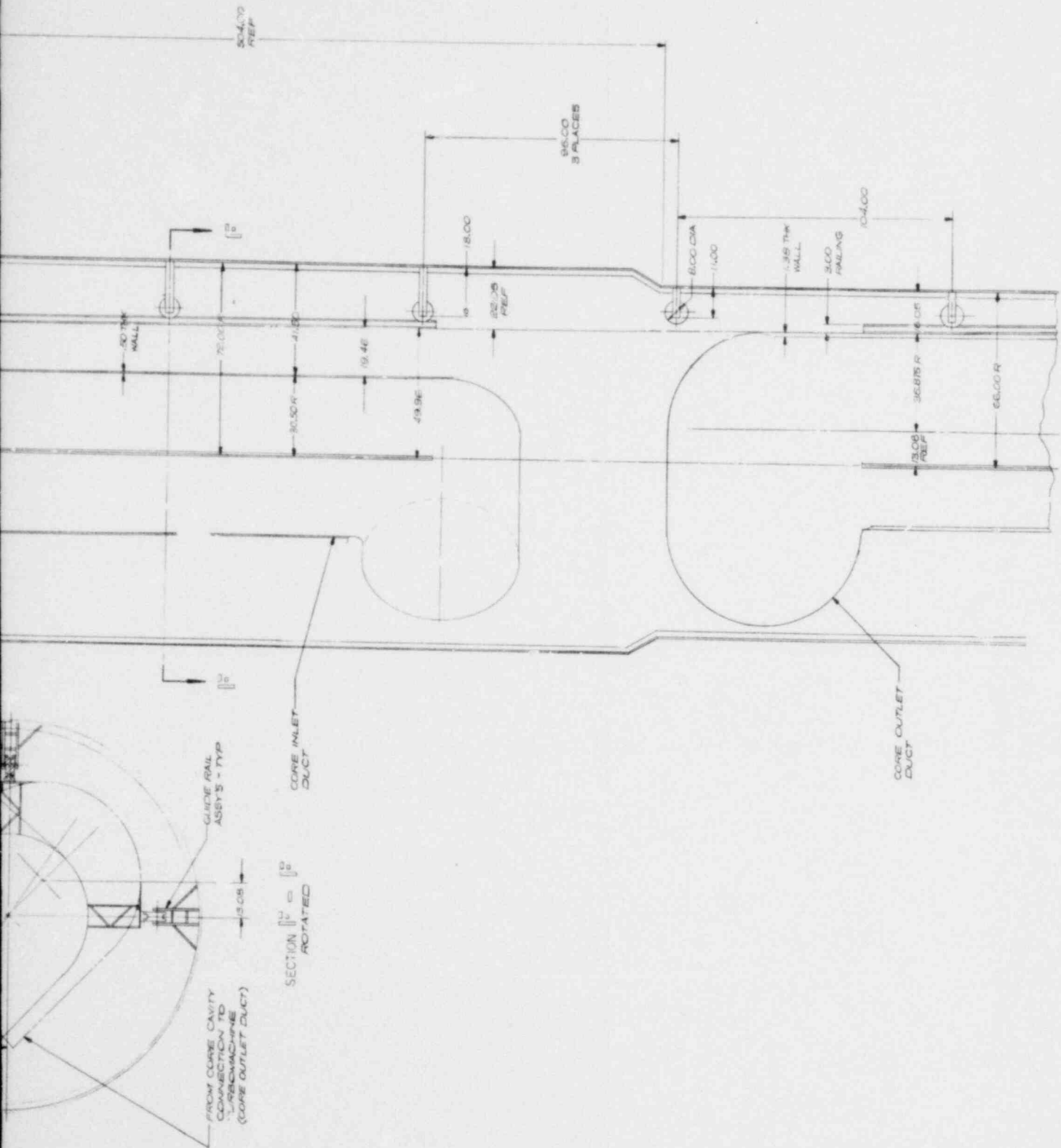
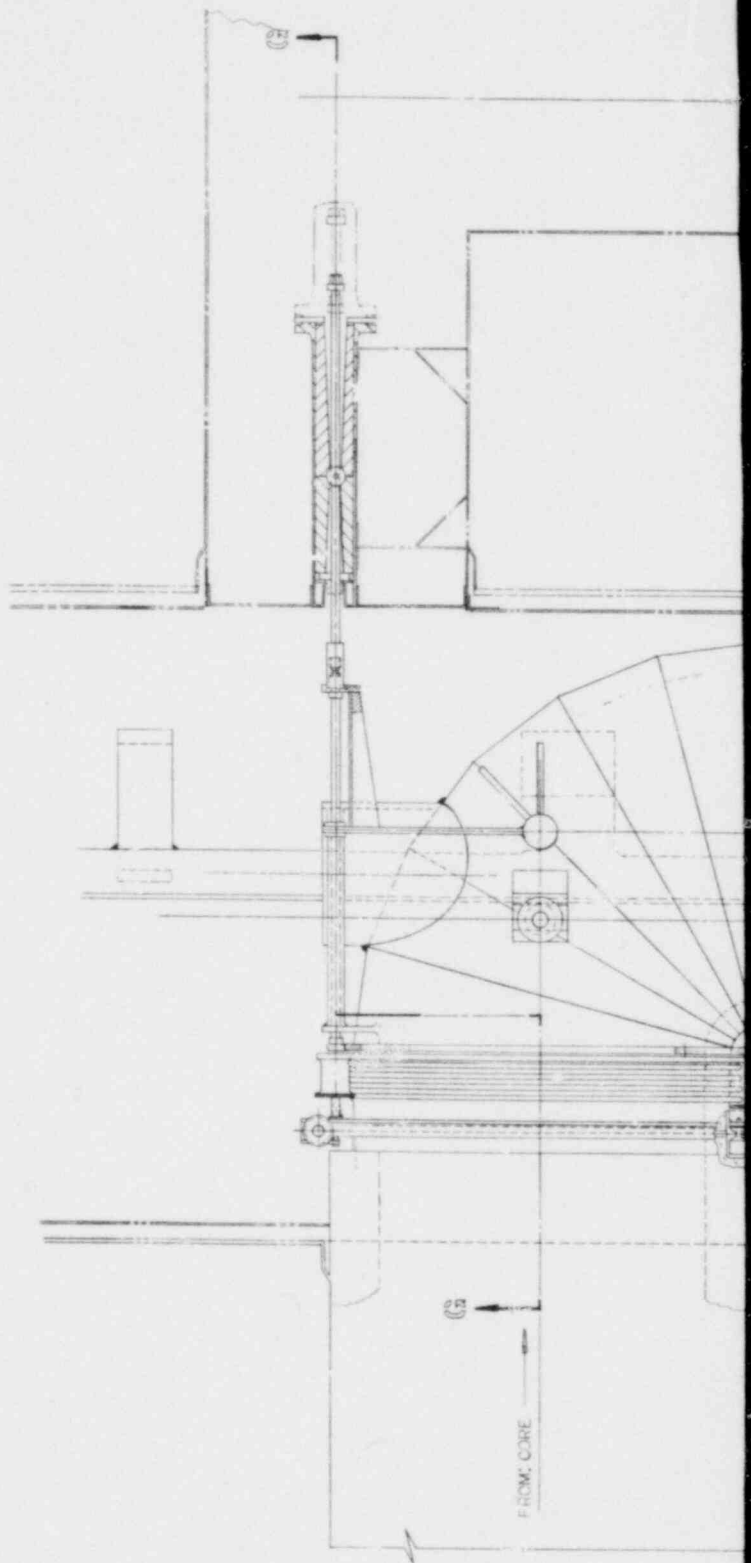
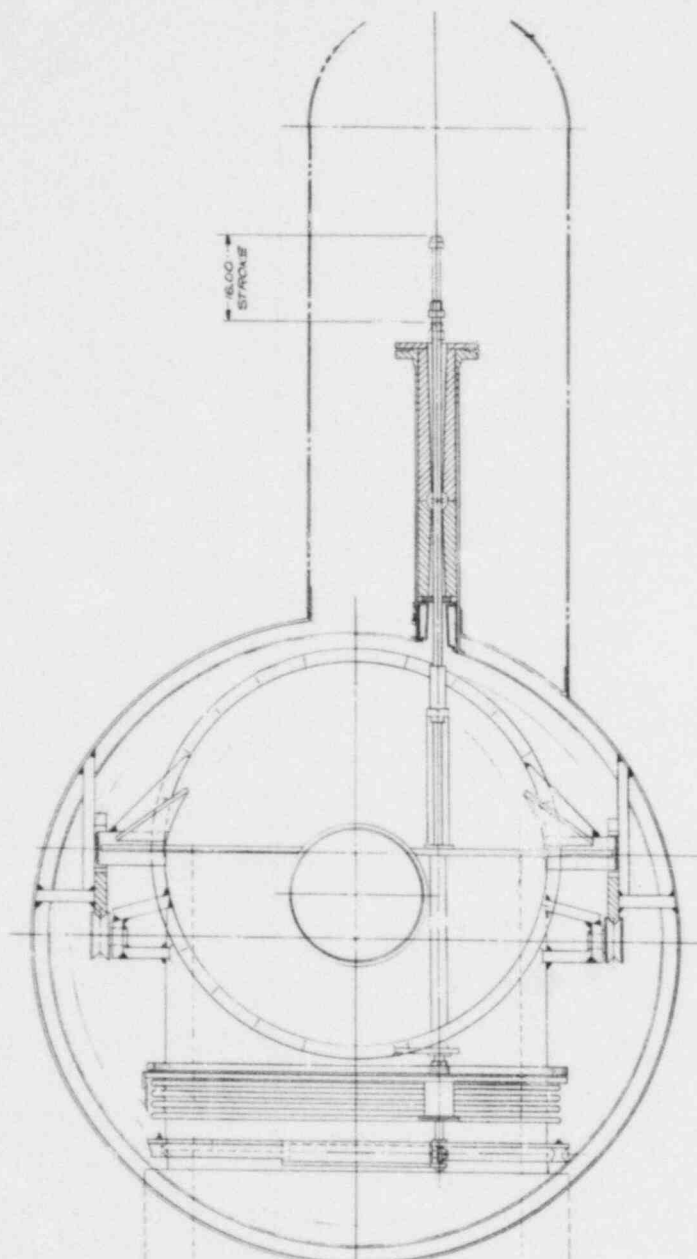
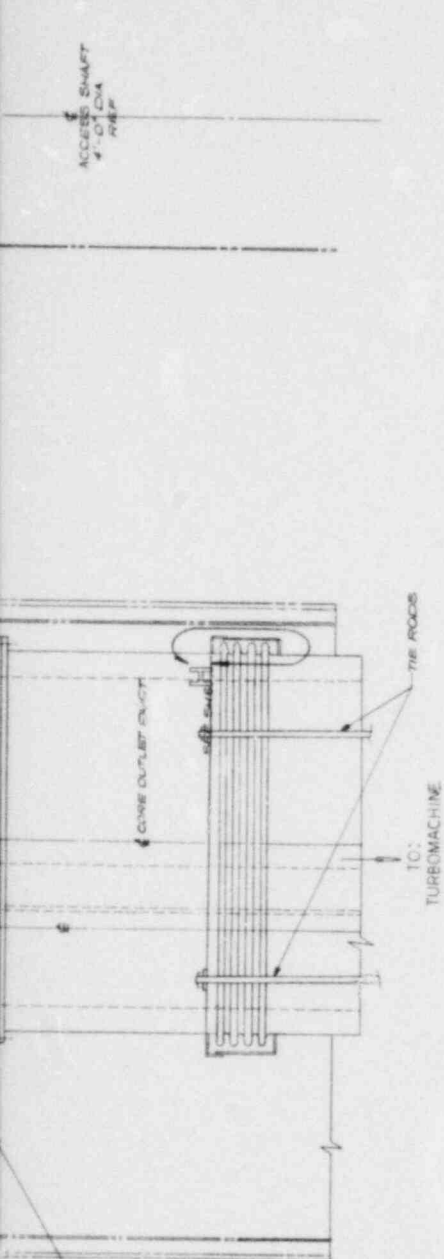


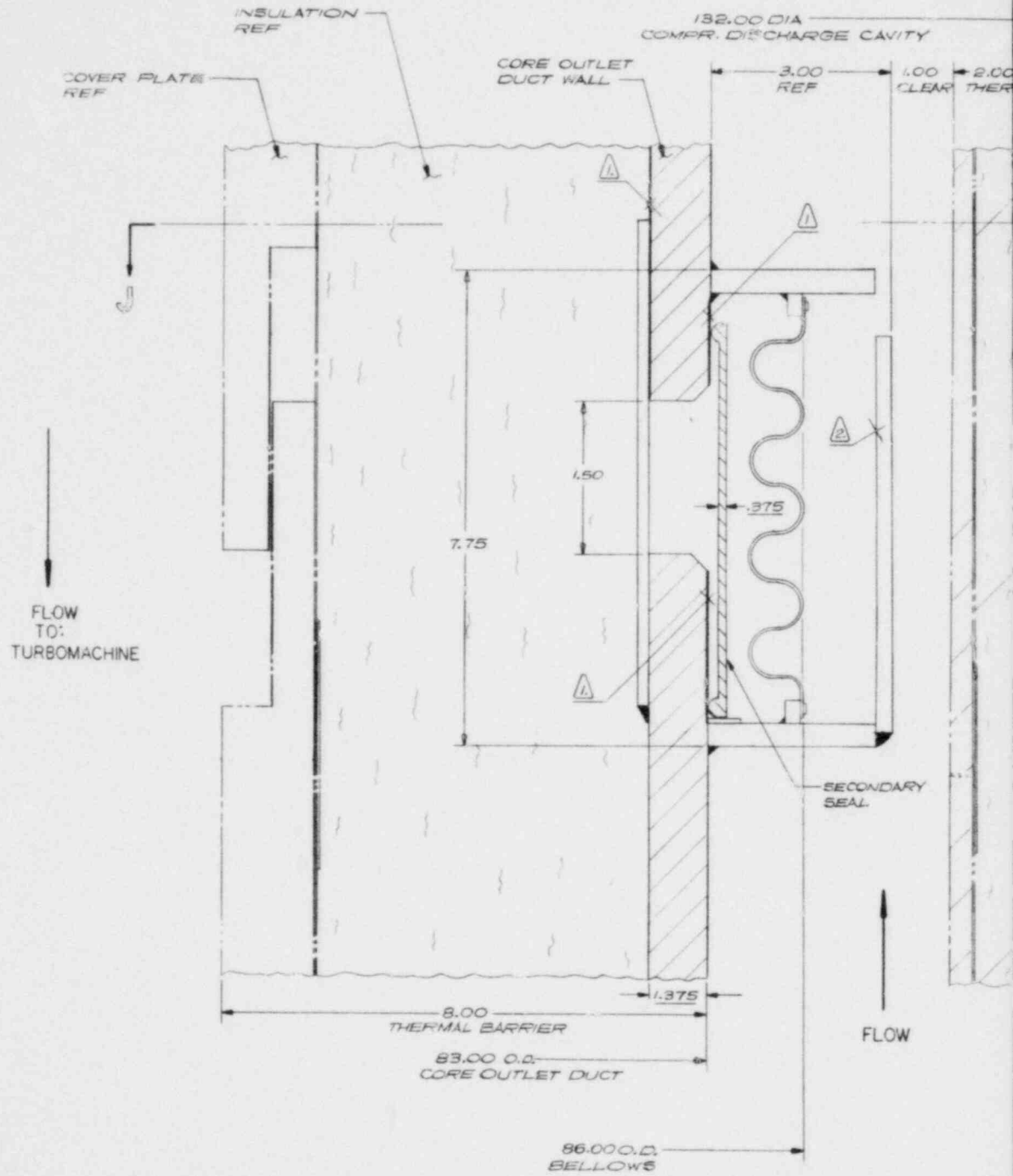
Fig. 17-1. Conceptual core inlet and core outlet ducts (sheet 4 of 6)



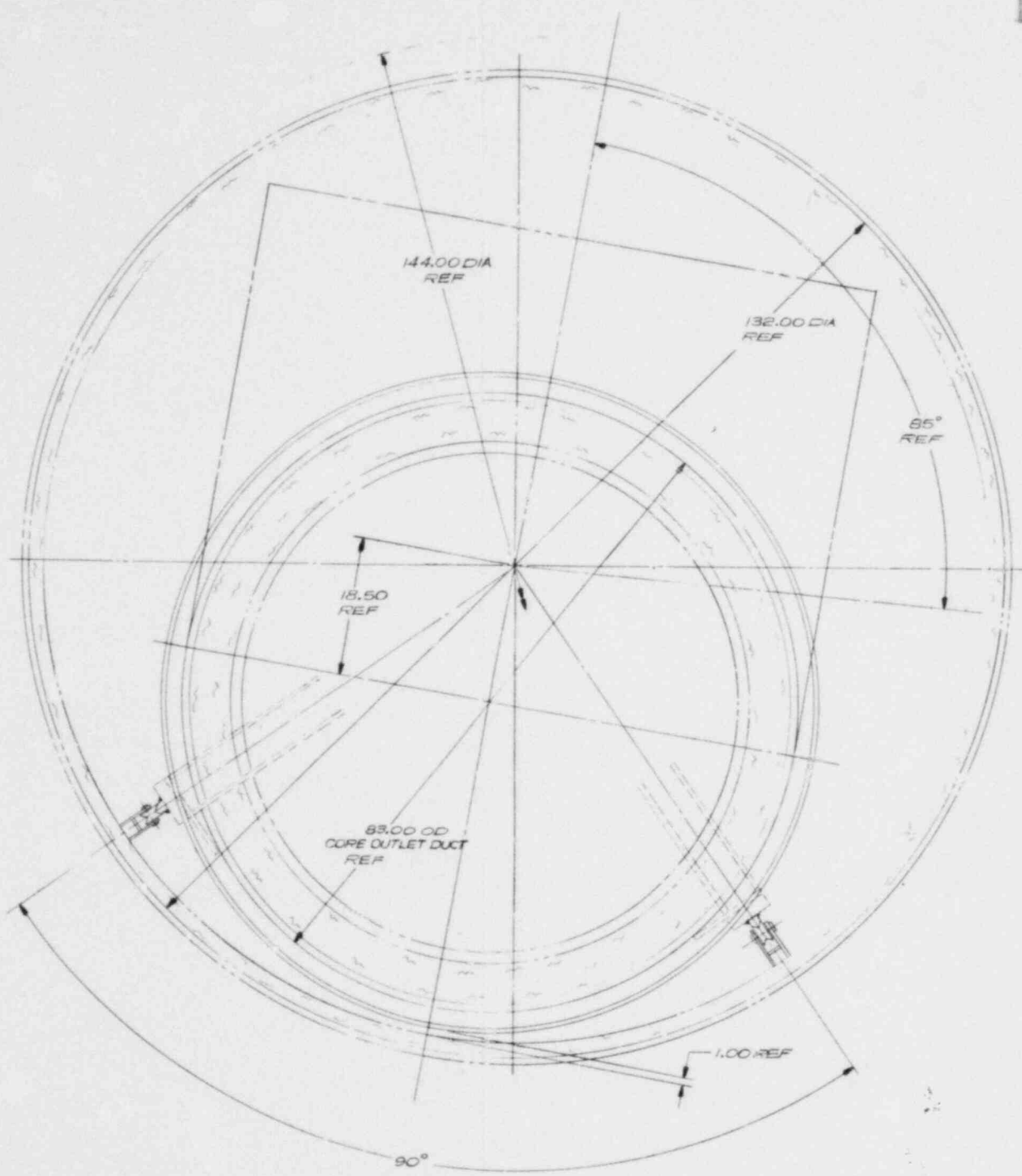


SECTION (A-A)  
SCALE: 1/2"  
(CORE OUTLET DUCT)

Fig. 17-1. Conceptual core inlet and core outlet ducts (sheet 5 of 6)



VIEW H  
 PART 54 5  
 SCALE: 1/1



SECTION J = J  
SCALE: 1/8

Fig. 17-1. Conceptual core inlet and core outlet ducts (sheet 6 of 6)



### 17.3. HOT DUCT DESIGN - THERMAL BARRIER

#### 17.3.1. Scope

The purpose of this task is to improve the level of confidence in the feasibility of employing one or more candidate materials for the thermal barrier of the hot duct.

#### 17.3.2. Summary

Concepts emphasizing repair and replaceability were examined using C-C and nickel-base alloy castings. Configurations were shown to be within the state-of-the-art of fabrication and met all the present criteria of application. An evaluation was made comparing a coaxial and an embedded horizontal duct, with the latter being preferred on the basis of system reliability.

#### 17.3.3. Discussion

From the viewpoint of assembly, removal, and replacement, a thermal barrier constructed of C-C cylinders with high-temperature insulation "washers" is the most advantageous (Fig. 17-2). However, it is very costly (~\$1.5M per duct for C-C versus \$0.55M for a cast superalloy version). Also, at this time, there is less confidence in the structural integrity of C-C compared with castings. Therefore, emphasis has more recently been placed on metallic configurations.

A variety of alloys have been identified as candidates for the HTGR-GT environment (Ref. 17-1). These include IN 100, IN 162, IN 519, IN 617, IN 625, IN 713LC, and IN 738. Of these, the most attractive appears to be IN 713LC. A concept using coverplates instead of cylindrical sections is shown in Fig. 17-3, and a representative cast coverplate is shown in Fig. 17-4.

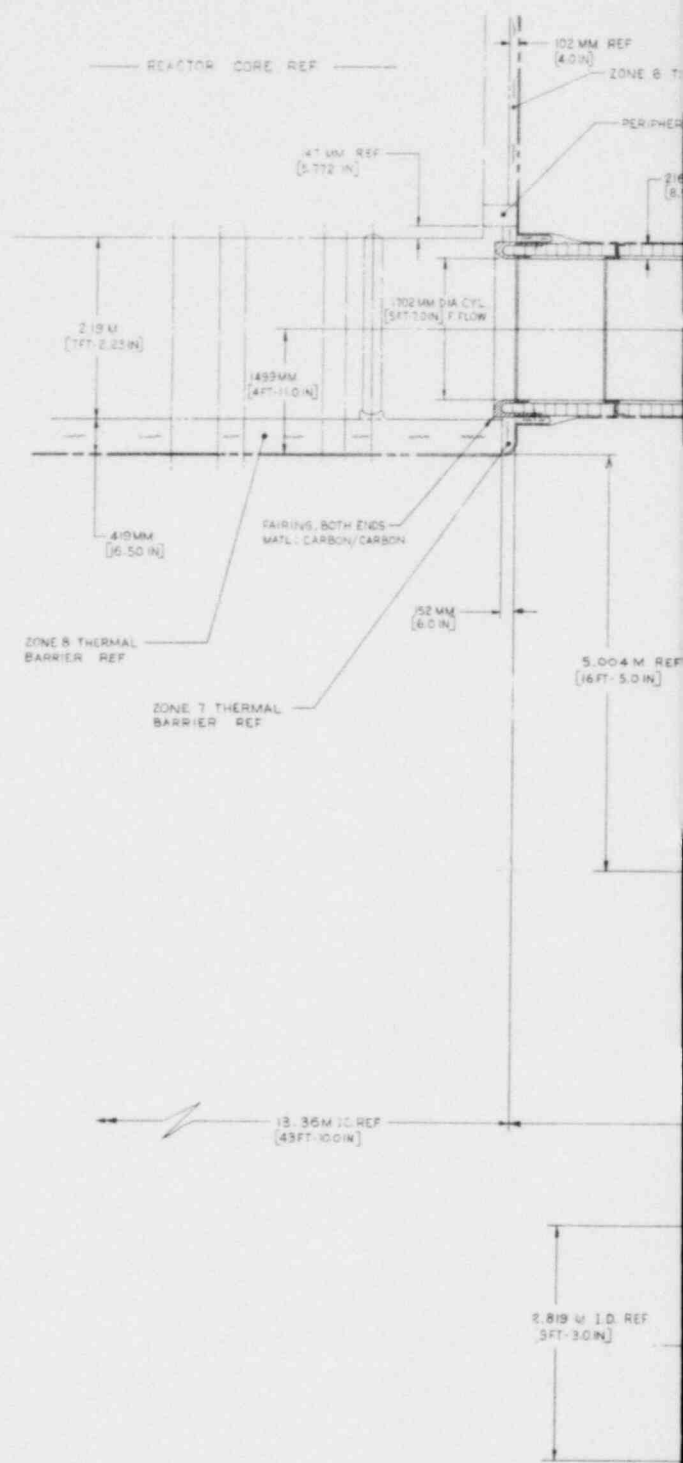
One of the potential design problems associated with superalloy castings is size limitation. If thermal and inlet fairings are required as anticipated, the problem will be accentuated by the need to provide a relatively smooth surface in order to minimize gas flow disruption.

Casting vendors have indicated that cast cylindrical sections (such as would be required for the thermal shield) might be limited to 610-mm (2-ft) lengths. A 1524-mm (5-ft) diameter was considered possible by the vendors. With these limitations, a configuration such as that shown in Fig. 17-5 can be considered. While this concept accommodates the gas flow conditions and is castable, there is some question concerning its ability to withstand rapid depressurization conditions. It also presents some difficulties with regard to removability. Hence, a modular thermal shield concept was investigated.

If repair and/or replaceability of the hot ducts is considered to be mandatory, then the C-C cylinder concept (Fig. 17-2) becomes increasingly attractive. The components are relatively few in number and simple in construction. It is believed that remote replacement of the thermal barrier in the horizontal region of the hot duct is both possible and practical. This was intended from the beginning because of the severe vibration and pressure transient environment to which the system is expected to be subjected and the uncertainty (at least at this design/development stage) of being able to sustain this environment during the 40-yr design life.

Nevertheless, because of the concern for replaceability, alternative concepts have been examined. One such concept consists of a horizontal coaxial duct that would enable both the primary structure and the thermal barrier to be removed as a unit. This concept is shown in Fig. 17-3.

Owing to the restriction on the size of the compressor discharge duct diameter, it is not possible to remove the horizontal portion of the duct in one piece. It is believed that two sections are possible, but three



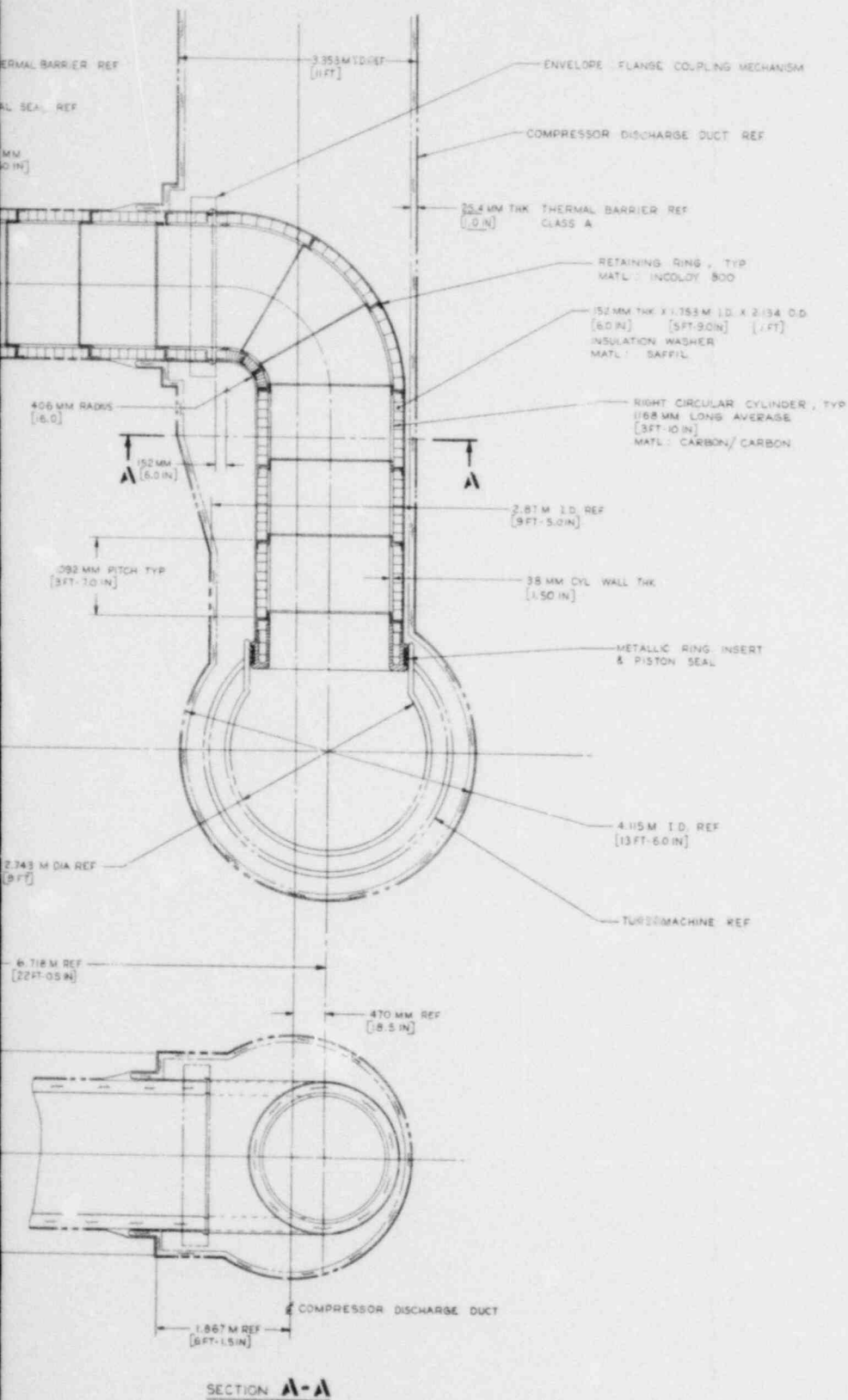
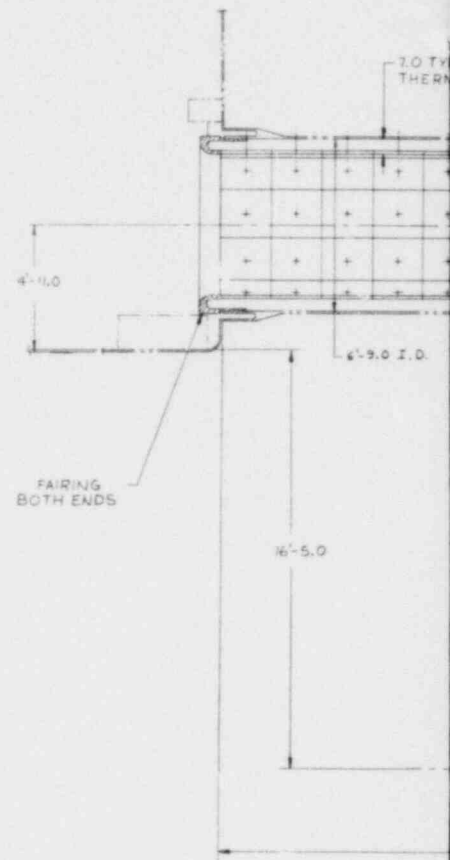
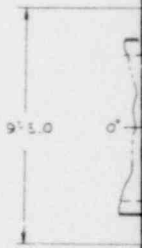
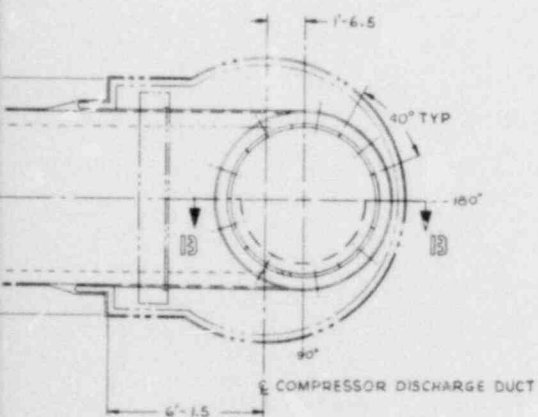
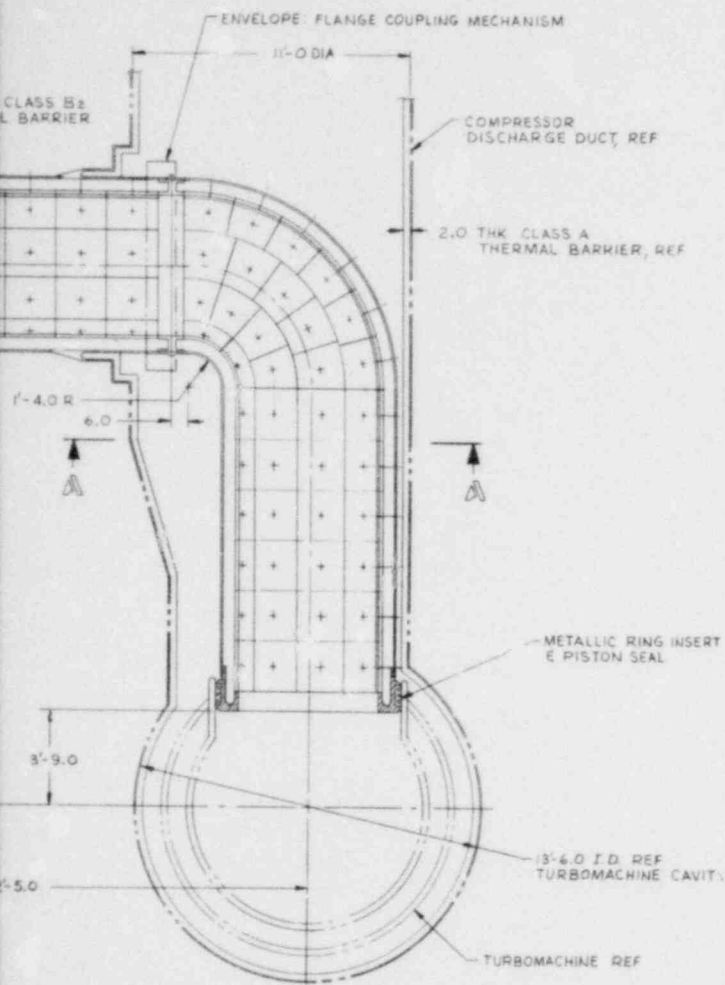


Fig. 17-2. Carbon-carbon/insulation washer hot duct thermal barrier concept



ORIENTATION VIEW  
SCALE: 1/24

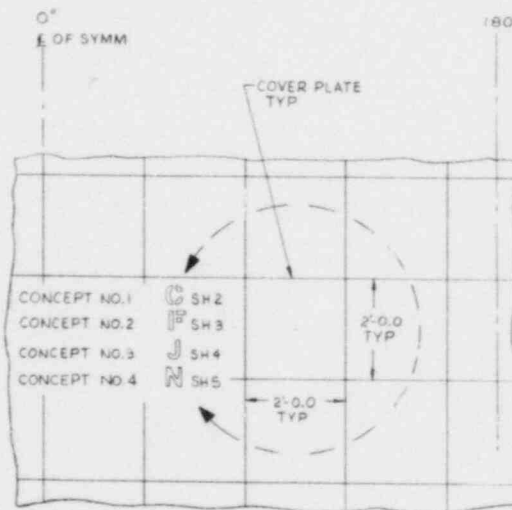




SECTION A-A  
SCALE: 1/24

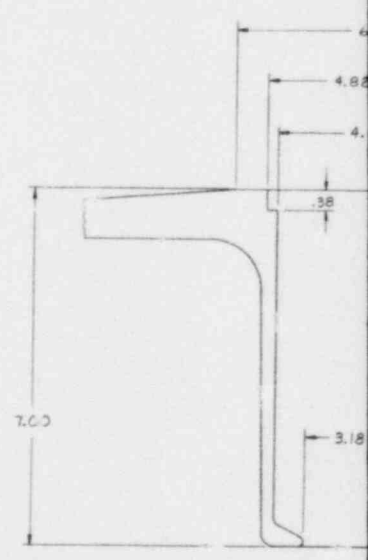
NOTES:

- 1 BLANKET ASSY MAY CONSIST OF LAYERS OF SAFFIL FIBER BLANKETS, CUT .25 OVER SIZE SHOWN, FOR LINER TOLERANCE ACCUMULATION.
- 2 BLANKET ASSY TO BE ENCLOSED IN A HIGH TEMPERATURE CLOTH FABRIC.

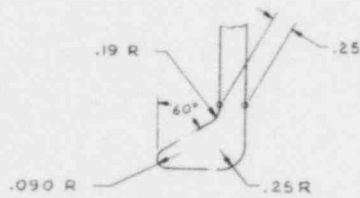
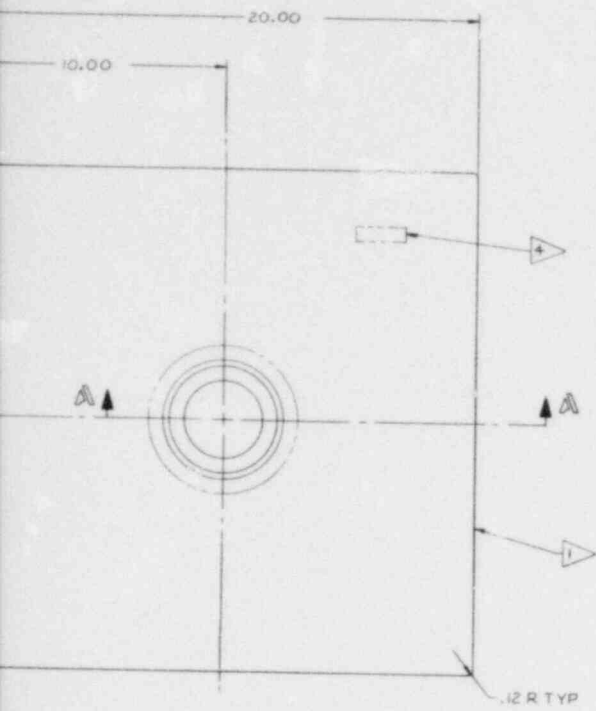


SECTION B-B  
PARTIAL CIRCUMFERENTIAL ELEVATION VIEW  
SCALE: 1/12

Fig. 17-3. Cast coverplate hot duct thermal barrier concept



SECTION  
SCALE: 1/1



VIEW B  
SCALE: 2/1

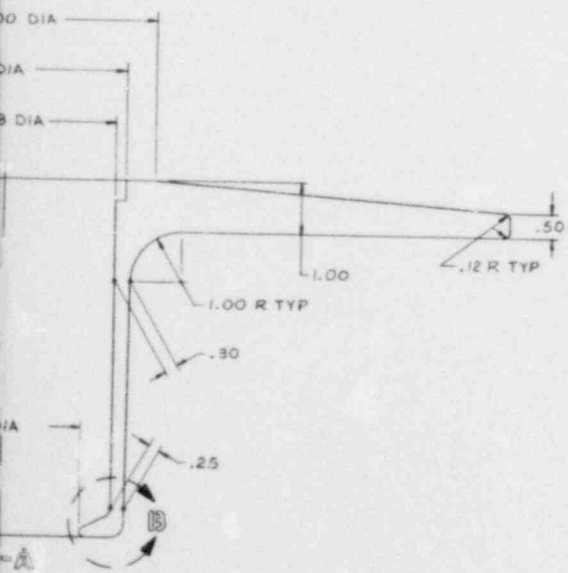
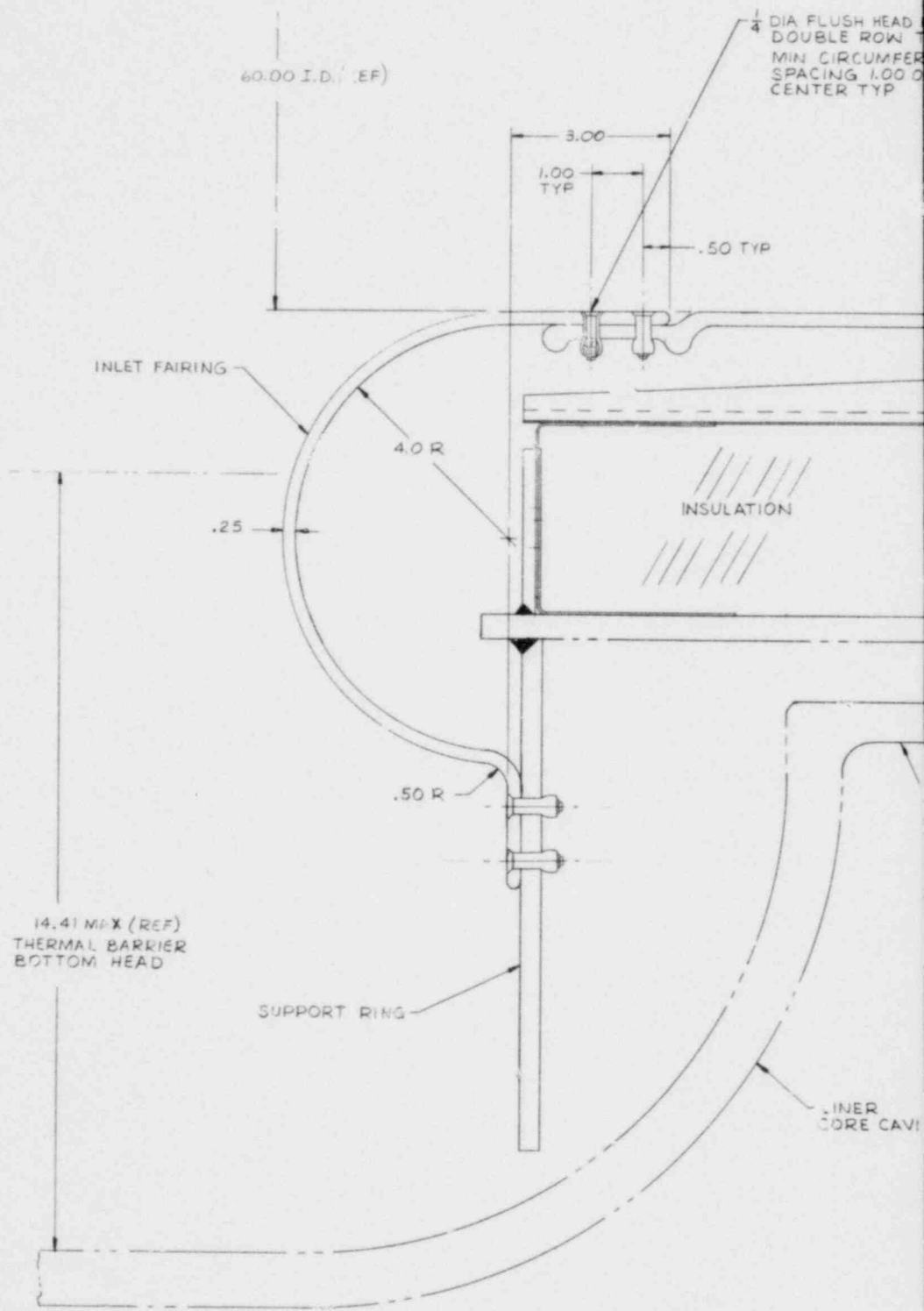
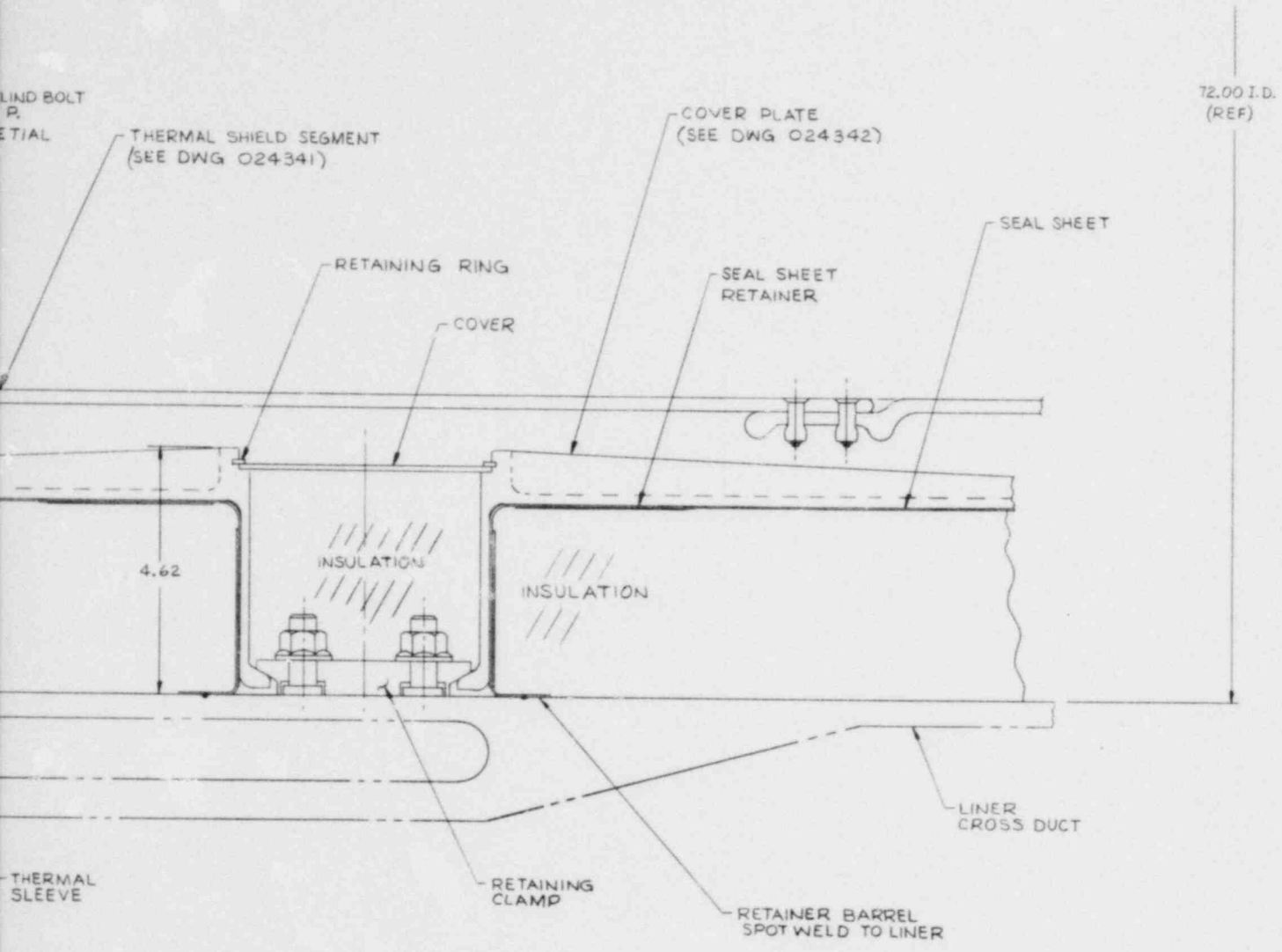


Fig. 17-4. Castable thermal barrier coverplate

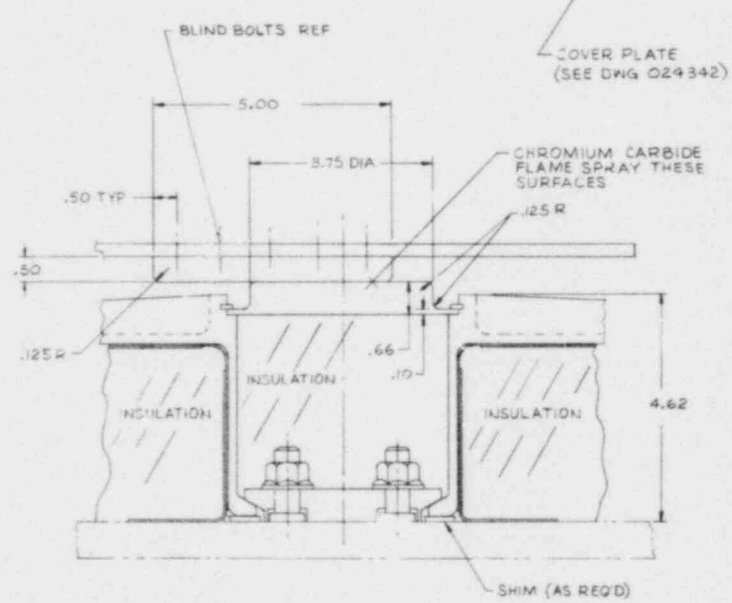
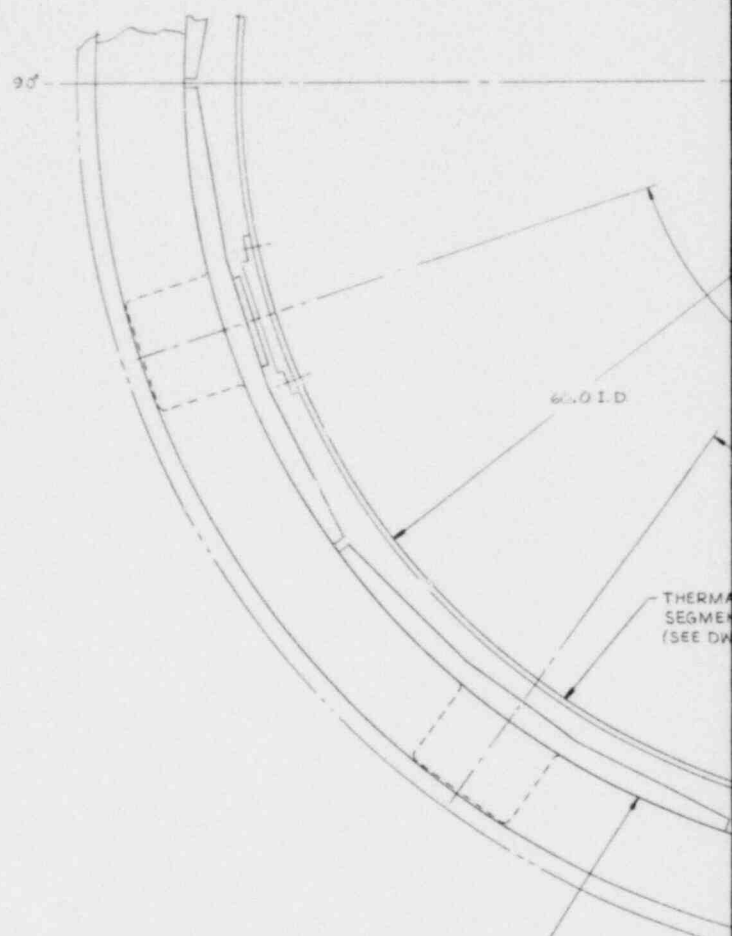






VIEW  $\frac{3}{8}$  SH1  
 SCALE: 1/1

Fig. 17-5. Castable hot duct thermal shield concept (sheet 1 of 2)



SECTION H-H SH1 & SH3  
 SCALE: 1/1  
 TYP. PLACES

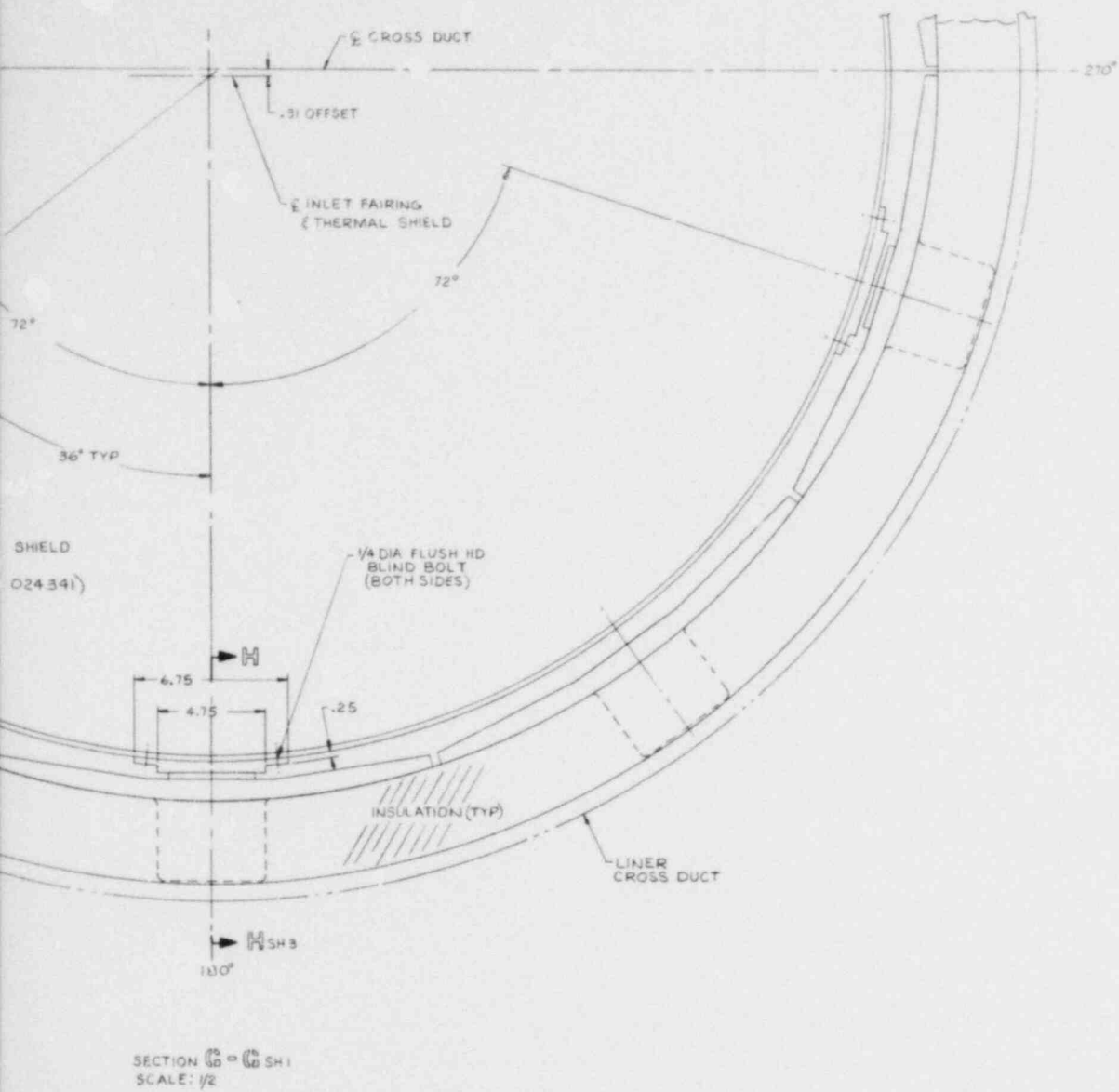


Fig. 17-5. Castable hot duct thermal shield concept (sheet 2 of 2)

are more practical. This leads to at least one joint, such as that indicated in Fig. 17-3. However, it is desirable to minimize the number of joints because of inherent sealing difficulties. Gas bypass could cause deterioration of both the primary structure and the thermal barrier (not to mention system-related effects).

The above problem is accentuated by the necessity for a sliding seal at the lower core plenum sidewall-to-duct interface. In this case, a piston seal might be possible as has been suggested by HRB designers, but the initial fit-up and in-service distortions due to thermal gradients raise the potential for gas bypass. It is also necessary to protect this seal from direct gas impingement. Hence, a thermal shield is indicated at the duct inlet in conjunction with a secondary seal attached to the lower plenum sidewall thermal barrier. Protection of this region is very critical, and considerable attention must be given to ensuring it.

In order to ease assembly, removal, and replacement, it is felt that guide rails and rollers are desirable. (This approach has also been taken by HRB in their HHT duct design.) The presence of the rails contributes to the potential for additional heat transfer to the liner and the associated cooling water system. In order to permit thermal expansion, the rollers must not be rigid. A spring-loaded mechanism is envisioned. This lends itself to compounded vibration problems in an already critical area.

In summary, it is believed that it is not desirable to baseline design a coaxial horizontal duct. Instead, a rigid primary structure with an in situ replaceable thermal barrier is more practical. It is believed that the current cylindrical, segmented C-C duct with modular insulation washers is a practical state-of-the-art approach.

17.4. REFERENCE

- 17-1. Wattier, J.B. (compiler), "Preliminary Assessment of Structural Materials for Use at Temperatures in the Range 1200°F to 2000°F," General Atomic Company, unpublished data, July 1979.

## 18. TURBOMACHINERY

### 18.1. SCOPE

The purpose of this task in FY-79 was for United Technologies Corporation (UTC), under subcontract to GA, to conduct turbomachinery design studies in support of the HTGR-GT plant design effort.

### 18.2. SUMMARY

The studies conducted by UTC supported mechanical, systems, metallurgical, and safety studies being conducted by GA related to the HTGR-GT plant.

The conceptual layout for the 400-MW(e) turbomachine was updated. Techniques for attenuating the sound power level were identified. These techniques included increased blade/vane spacing, adjusted relative number of blades and vanes, and introduction of acoustic liners in selected locations. The changes necessary to accommodate the requirements for remote handling were also addressed. The turbomachine component weights were summarized, and the turbine cooling flow distribution was estimated. The predicted compressor operating maps were extended into the low-pressure-ratio regions. A preliminary study of the mechanism by which a welded rotor fails was initiated. Evaluation of industrial experience showed that welded rotor failures are unlikely. Turbine disk rim stresses were evaluated for various system transient conditions. Results indicate satisfactory turbomachine operation for decay heat removal after a reactor scram. The rate of pressure change during a rotor deblading event was predicted. Available high-speed recording data were reviewed, and their applicability was established. Results from these high-speed records show the major portion of the pressure change occurred in less than 0.1 s. The materials

selected for the turbomachine were reviewed. Alternate candidates were provided for critical areas. A technique for maintaining the rotor bearings in situ was provided. A conceptual layout for an intercooled 400-MW(e) configuration was prepared. A turbomachine/generator development program and its associated schedule and cost were defined. The impact of codes and licensing criteria on the turbomachine design was evaluated.

### 18.3. DISCUSSION

#### 18.3.1. 400-MW(e) Turbomachine Conceptual Design

Design effort concentrated on the 400-MW(e) turbomachine configuration. The primary emphasis was to update the conceptual layout. This was accomplished in two sequences.

The first included a design of the turbine inlet duct which placed the piston ring seals on the inner surface of the PCRV duct. This design has the advantage of reducing the overall diameter of the engine. In addition, the contour of the compressor inlet case was changed to increase the plenum entrance area. Axial retention for the compressor containment ring was also provided.

The second revision included recommendations for disk containment and noise attenuation. The inlet and discharge vane/blade spacing of both the compressor and turbine were increased to decrease the sound power levels. As a result, the span between bearings was increased. The length of the disk containment rings was increased to accommodate the increase in rotor length plus an additional overhang at each end to further ensure the safety of surrounding parts. A seal was provided for the bore of the front hub to prevent cycle flow leakage into the outer cavity during maintenance actions.

The original hot duct configuration was reintroduced based on system interface considerations. This final updated configuration is shown in Fig. 18-1.



### 18.3.2. Sound Power Level Study

Several means were examined for reducing upstream and downstream noise emissions from the compressor and turbine of the HTCR-GT.

These methods fall into four categories:

1. Modifying the number of blades and vanes.
2. Increasing the spacing between the rotor and stator stages.
3. Providing sound-absorbing linings for turbomachinery cases and/or ducting (inlet and discharge).
4. Modifying inlet and discharge duct configurations to provide noise reductions by use of a sonic throat (for inlet) and further acoustic treatment.

Not all of these methods need be applied to all components. For example, if the recommended blade and vane numbers can be employed, the current rotor-stator spacing can be retained. Similarly, if satisfactory inlet ducts that incorporate a sonic throat can be designed, it will be unnecessary to modify the blade and vane numbers and the spacing in the inlet stages.

Estimates of the overall power level (OAPWL) reductions were obtained using some of these methods. Either blade vane modifications or increased spacing is worth about 4 dB in OAPWL. Treating the diffuser sections of the compressor and the turbine discharge with perforated facing - honeycomb backing space acoustic liners should provide about 9-dB discharge noise OAPWL reduction. Similar treatment upstream of the compressor and turbine would reduce the sound power levels in these regions by approximately 12 to 14 dB. Use of sonic inlets should result

in at least 20-dB reduction in inlet noise. Further noise reductions could be obtained by sound-absorbing liner applications outside of the main turbomachine components. For design of such structures, an estimate of the spectral distribution of target noise reduction is required to provide better criteria than the OAPWL reductions employed here.

#### 18.3.3. Turbomachine Weight Summary

Weights of the 400-MW(e) turbomachine components were estimated as shown in Table 18-1. The basis for the estimates is the layout shown in Fig. 18-1.

#### 18.3.4. Turbine Cooling Flow Distribution

The turbine cooling flow distribution was defined for the 400-MW(e), welded rotor turbomachine. The estimated distribution is shown in Fig. 18-2. The prediction is based on the optimized turbine configuration using tangential fir tree attachments. Total cooling flow, including case cooling, is 3.6% of compressor discharge flow.

#### 18.3.5. 400-MW(e) Intercooled Turbomachine Conceptual Design

A conceptual layout for a 400-MW(e) intercooled turbomachine was prepared. The primary requirement was for estimated dimensions for use in interfacing structural layout development. An improved performance compressor was assumed with fewer stages, similar to that in the 500-MW(e) non-intercooled concept. This allowed achieving the 2.5 pressure ratio with 16 stages which were split into two 8-stage compressors upstream and downstream of the intercooler. Sound attenuation spacing between blades and vanes was approximated for both the compressor and turbine inlets and exits. The resulting overall turbomachine length was 15.4 m (50.5 ft) with a bearing span of approximately 11.5 m (38 ft). The diameter was retained at 4 m (13 ft) to accommodate GA's hot duct configuration. Figure 18-3 is a reduced version of the layout (Fig. 18-1).

TABLE 18-1  
 400-MW(e) TURBOMACHINE WEIGHT SUMMARY  
 (BASED ON FIG. 18-1)

Component	Units per Engine	Weight [tonnes (tons)]
Compressor discharge case	2	20.63(20.30) each
Turbine inlet duct	2	2.90(2.85) each
Turbine containment ring and case	1	39.52(38.9)
Turbine stator case and vanes	2	8.12(7.99) each
Turbine exhaust case	1	22.24(21.89)
Turbine bearing and seals	1	4.78(4.70)
Turbine rotor assembly (bladed)	1	22.91(22.55)
Compressor discharge duct	2	0.23(0.23) each
Compressor containment rig and case	1	63.41(62.41)
Compressor stator case and vanes	2	4.60(4.53) each
Compressor inlet case	1	20.52(20.20)
Compressor bearing and seals	1	4.78(4.70)
Compressor rotor assembly (bladed)	1	21.07(20.74)
	Total	272.20(267.9)

TOTAL FLOW = 3.6% OF COMPRESSOR INLET FLOW RATE  
CASE FLOW = 0.64%  
TURBINE ROTOR FLOW = 2.96%

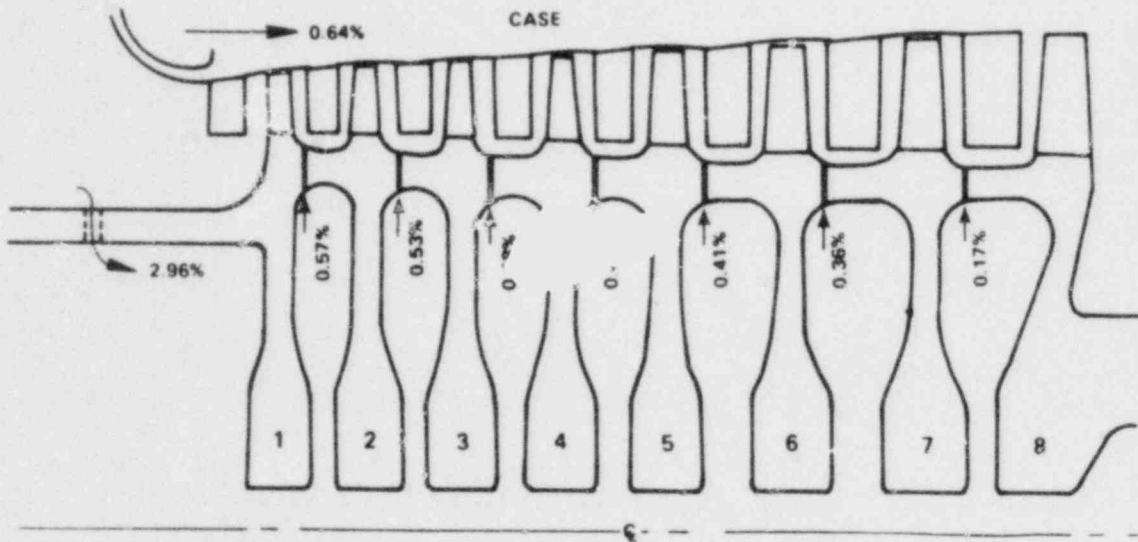


Fig. 18-2. Estimated secondary cooling flow distribution

# DOCUMENT/ PAGE PULLED

ANO. 8008130540-1

NO. OF PAGES 1

REASON:

PAGE ILLEGIBLE:

HARD COPY FILED AT PDR CF

OTHER \_\_\_\_\_

BETTER COPY REQUESTED ON \_\_\_\_\_

PAGE TOO LARGE TO FILM.

HARD COPY FILED AT: PDR CF

OTHER \_\_\_\_\_

FILMED ON APERTURE CARD NO. 8008130540-1

#### 18.3.6. Compressor Map

The turbomachine compressor map was revised to include additional definition in the range of low pressure ratios. The low pressure ratio operating range was required for systems analysis studies of off-design and transient conditions. The revised map is shown in Figs. 18-4 and 18-5. For consistency, the base map used for extrapolation was that prepared in 1976 for the HTGR-GT program.

#### 18.3.7. In Situ Bearing Maintenance

Figures 18-6 through 18-12 depict the concept of in situ bearing maintenance for the HTGR-GT. Basically, the procedure has been changed from a manual operation to primarily a mechanical powered one. The key to the process is a unique piece of access equipment (Fig. 18-6) that permits a mechanic to be transported into the work area, carrying the required power tools and fixturing.

The maintenance truck (Fig. 18-6) is a self-propelled vehicle supporting a horizontal work truss. The outer end of the work truss carries a platform and control panel. The operator will lie mine-car fashion to operate the truck. An access path will be provided through the length of the truss, permitting a second man to crawl in to aid the operator. The truss also carries mounting provisions for carrying the required pneumatic tools and attachment fixtures, as well as lifting provisions for removing engine services. This piece of equipment could be adapted readily for remote control if necessary.

In situ maintenance of the journal bearings is accomplished by the following steps:

##### Turbine Bearings

- a. The operator attaches lifting provisions to the engine service pipes for support, then breaks the mechanical joints. The pipes can then be lifted slightly and removed as shown in Fig. 18-7.

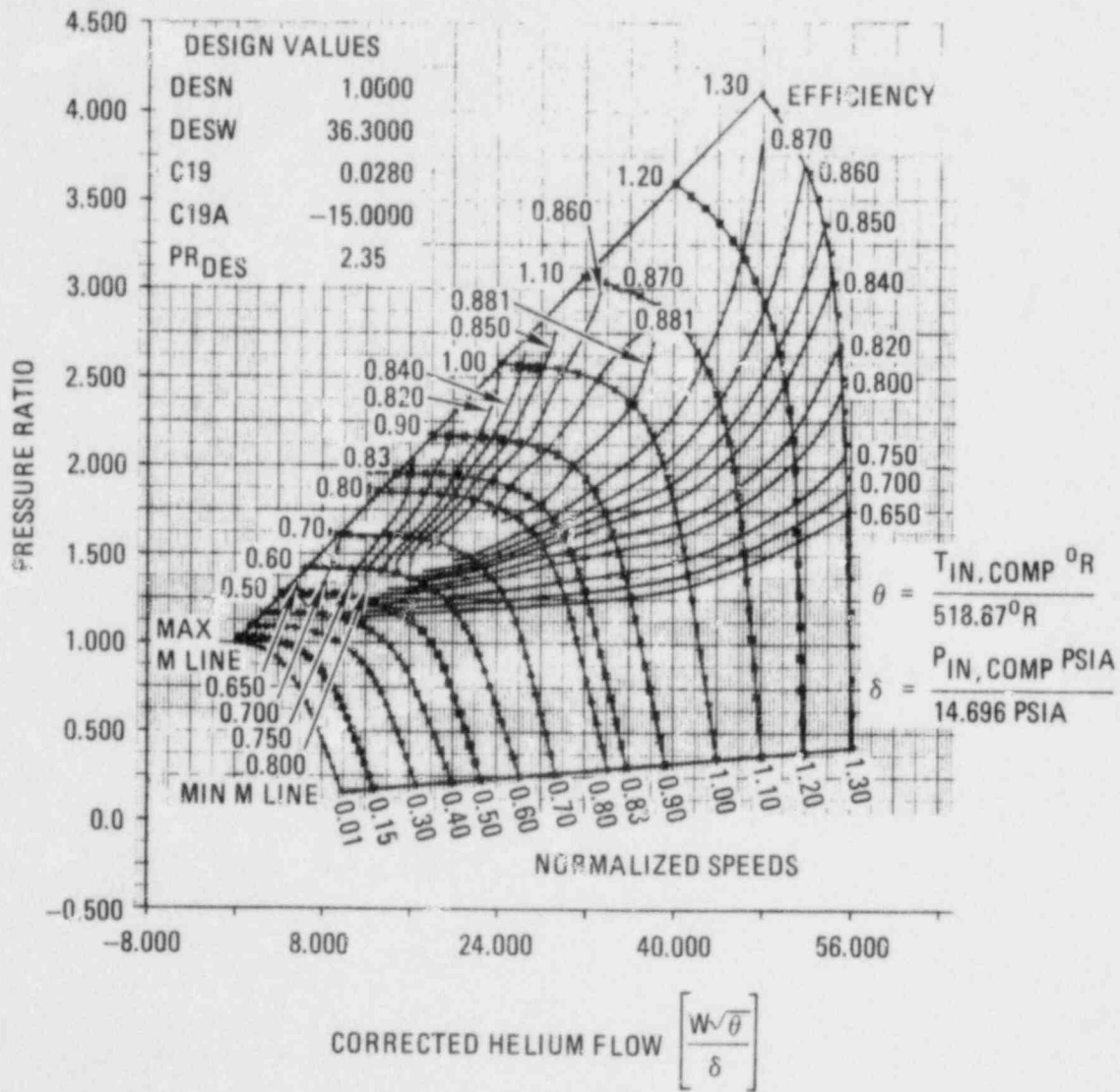


Fig. 18-4. Turbomachine compressor map high efficiencies

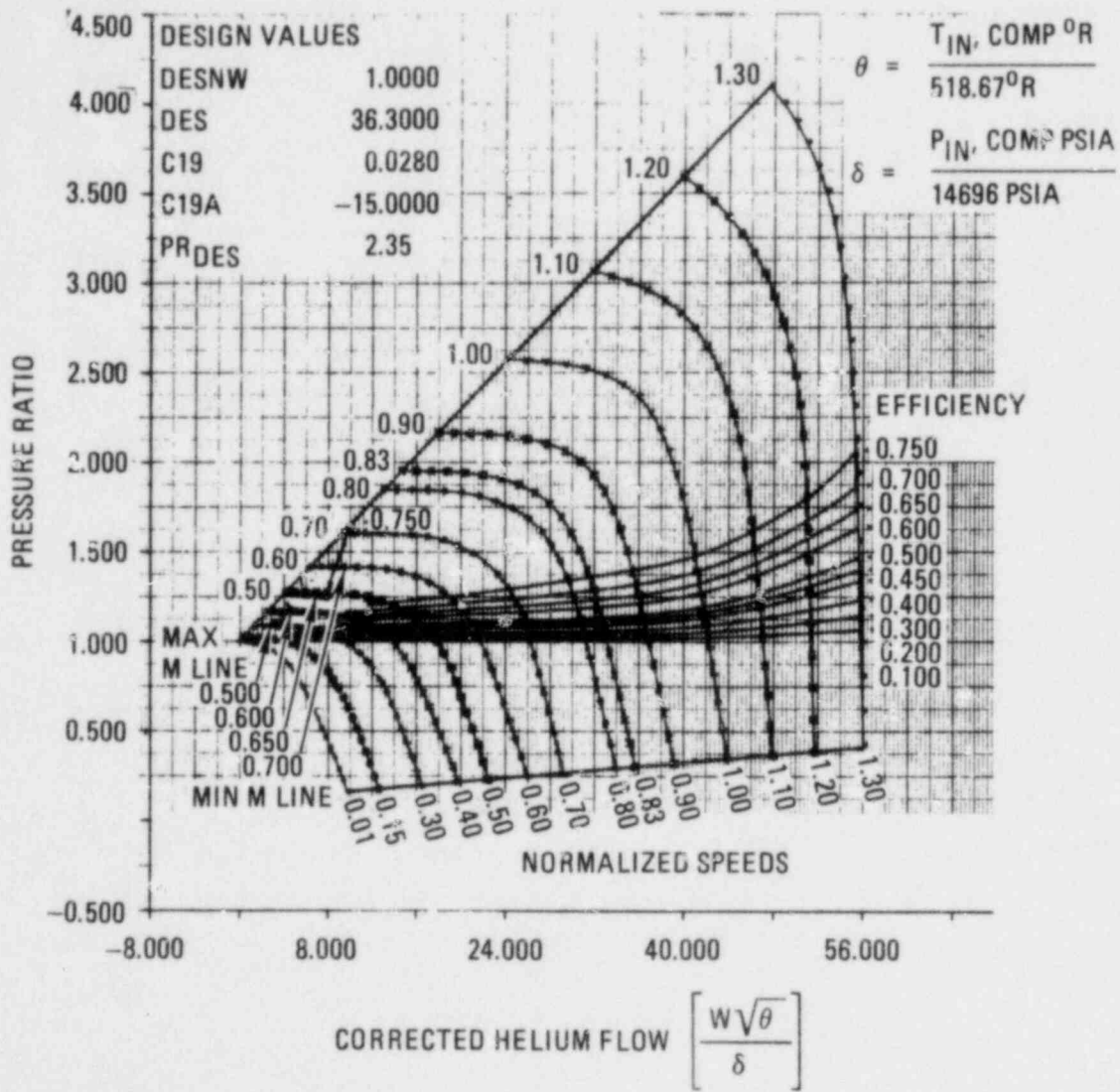


Fig. 18-5. Turbomachine compressor map low efficiencies



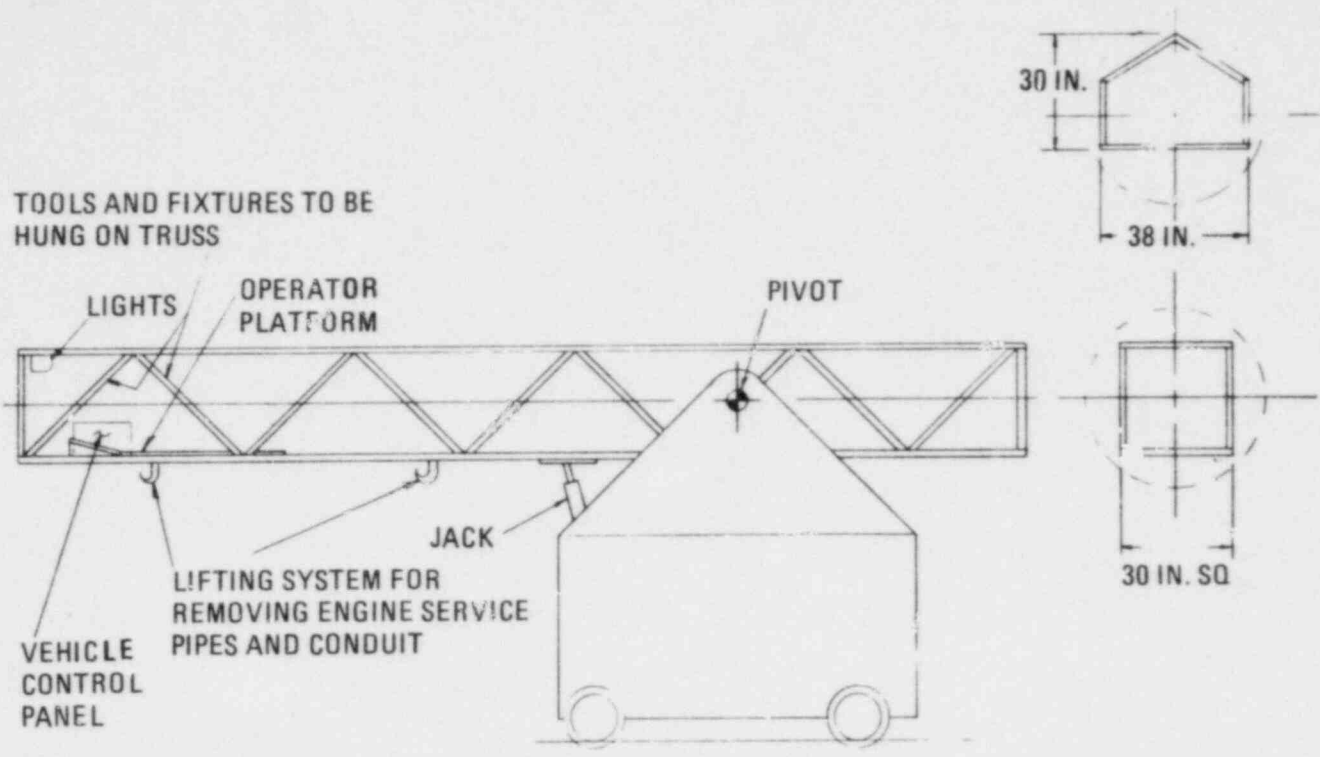


Fig. 18-6. Self-propelled maintenance truck

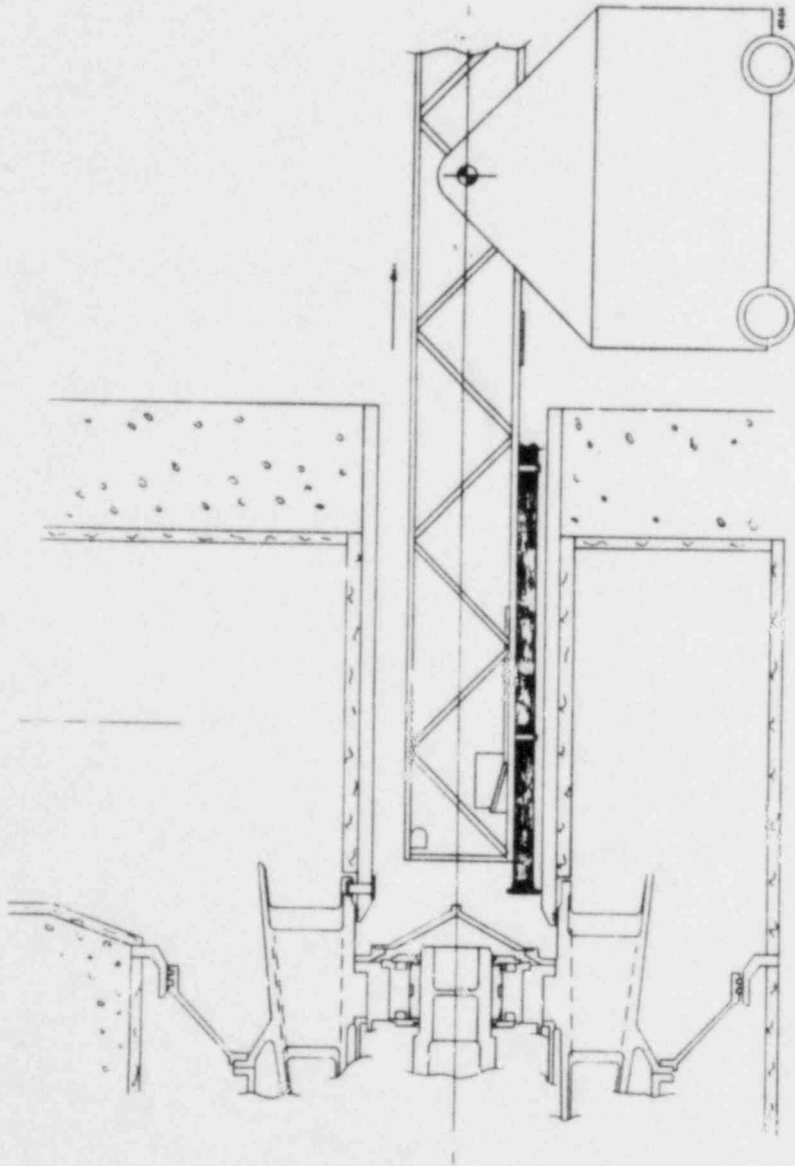


Fig. 18-7. Removal of engine services

- b. After depositing the service pipes, the truck returns and the operator attaches fixtures from the frame to the bearing compartment cover. The bolt circle is broken with a pneumatic wrench, and the cover is backed out of the tunnel (Fig. 18-8). This process is repeated for removal of the bearing sideplate.
- c. The operator brings in the required support fixtures, jacks, and rotor attachment tool (Fig. 18-9). The rotor is lifted off the journal bearing to permit inspection and/or removal of pads.
- d. The bearing removal fixtures are screwed into the tapped holes provided at both ends of the individual pads. The pad is removed by backing the truck out through the tunnel (Fig. 18-10).

#### Compressor Bearings

- e. Prior to compressor bearing maintenance, the generator, thrust bearing, and output shaft must be removed (Fig. 18-11).
- f. The maintenance truck enters through the center of the PCRV plug and the attachment fixtures are mated to the shaft coupling (Fig. 18-12). The operator uses the pneumatic wrench to break the bolt flanges, and the coupling is backed away.

The remaining steps are very similar to steps b, c, and d.

It should be noted that the maintenance procedures for the compressor end bearings would require movement of the generator if the generator is close coupled. Based upon guidance from the utilities, this is not acceptable, and as a result the maintenance of the compressor end bearing is being re-evaluated.

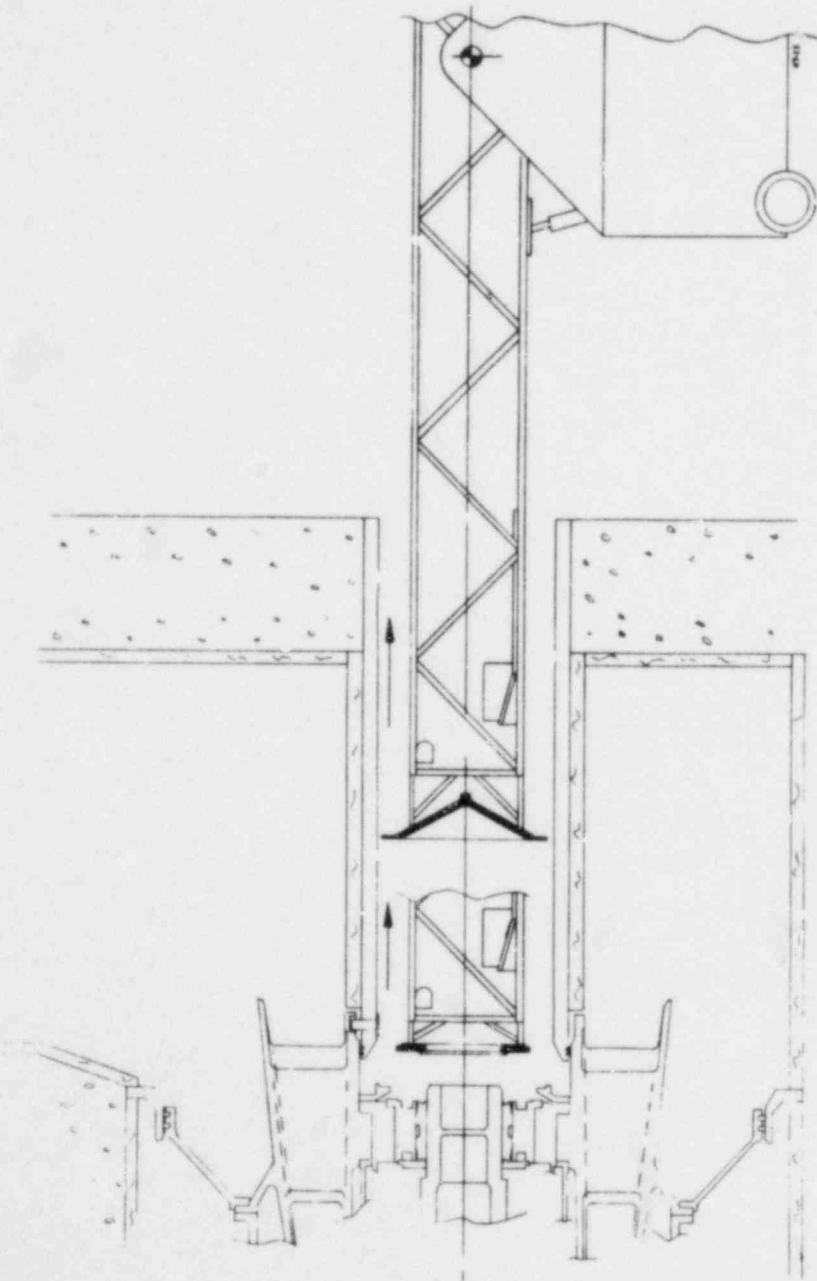


Fig. 18-8. Removal of compartment cover/bearing sideplate

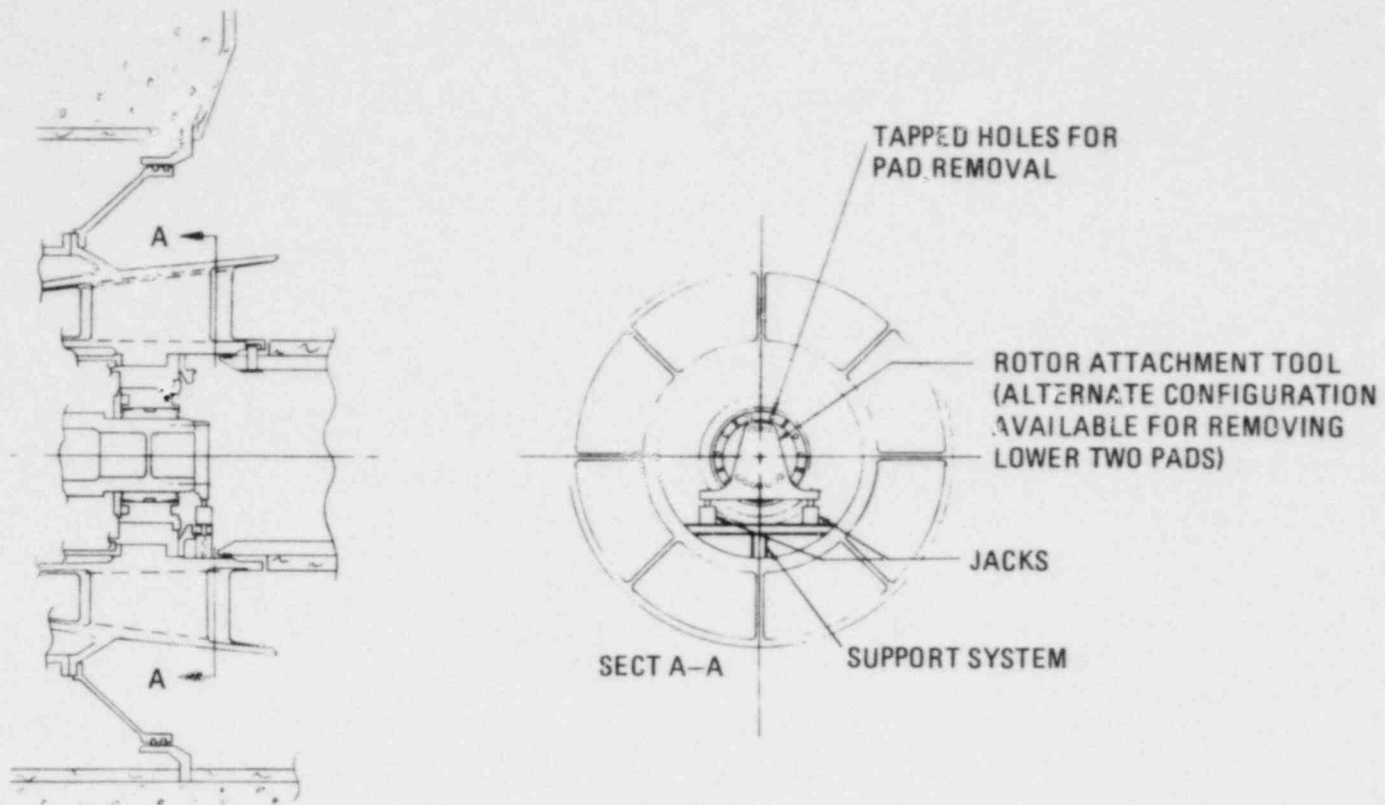


Fig. 18-9. Jacking system

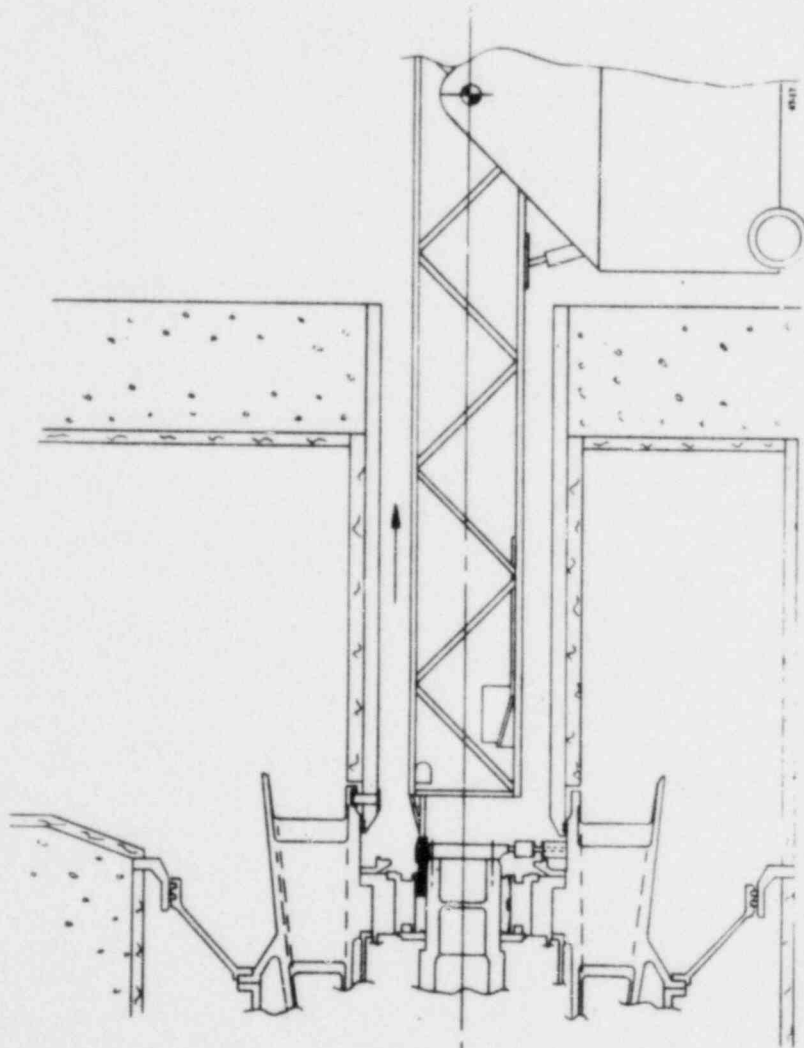


Fig. 18-10. Bearing pad removal

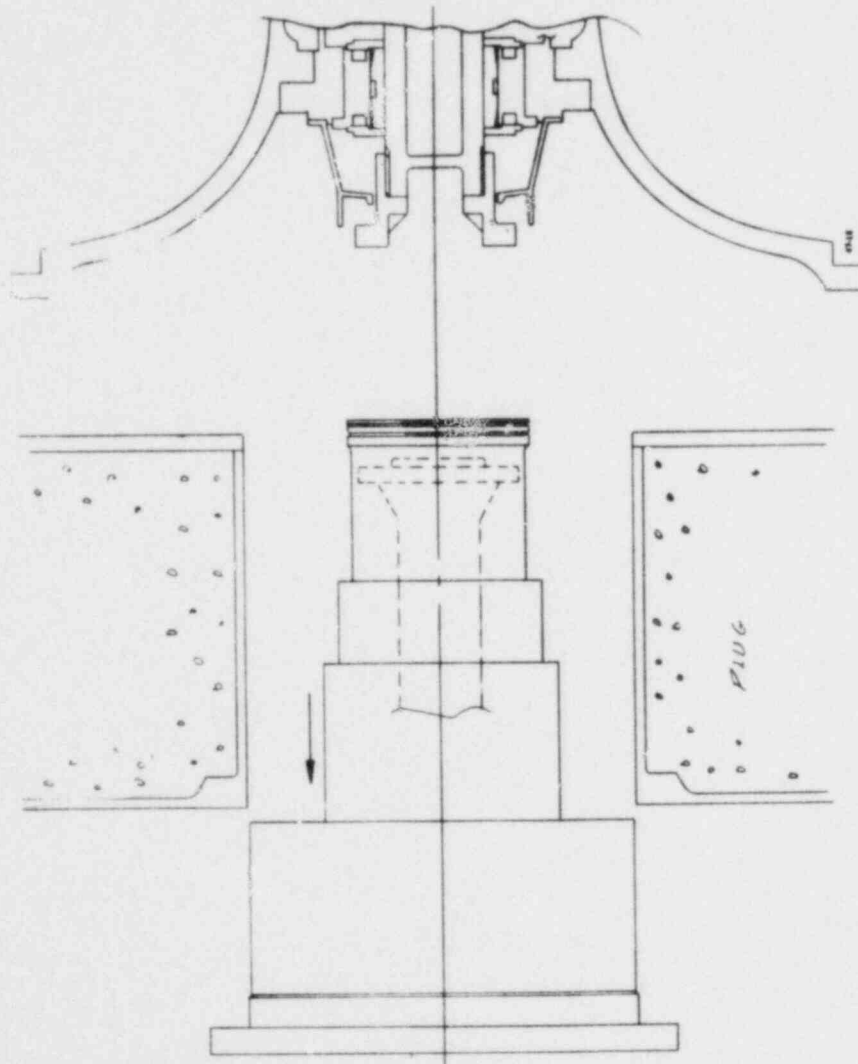


Fig. 18-11. Removal of shaft and thrust bearings

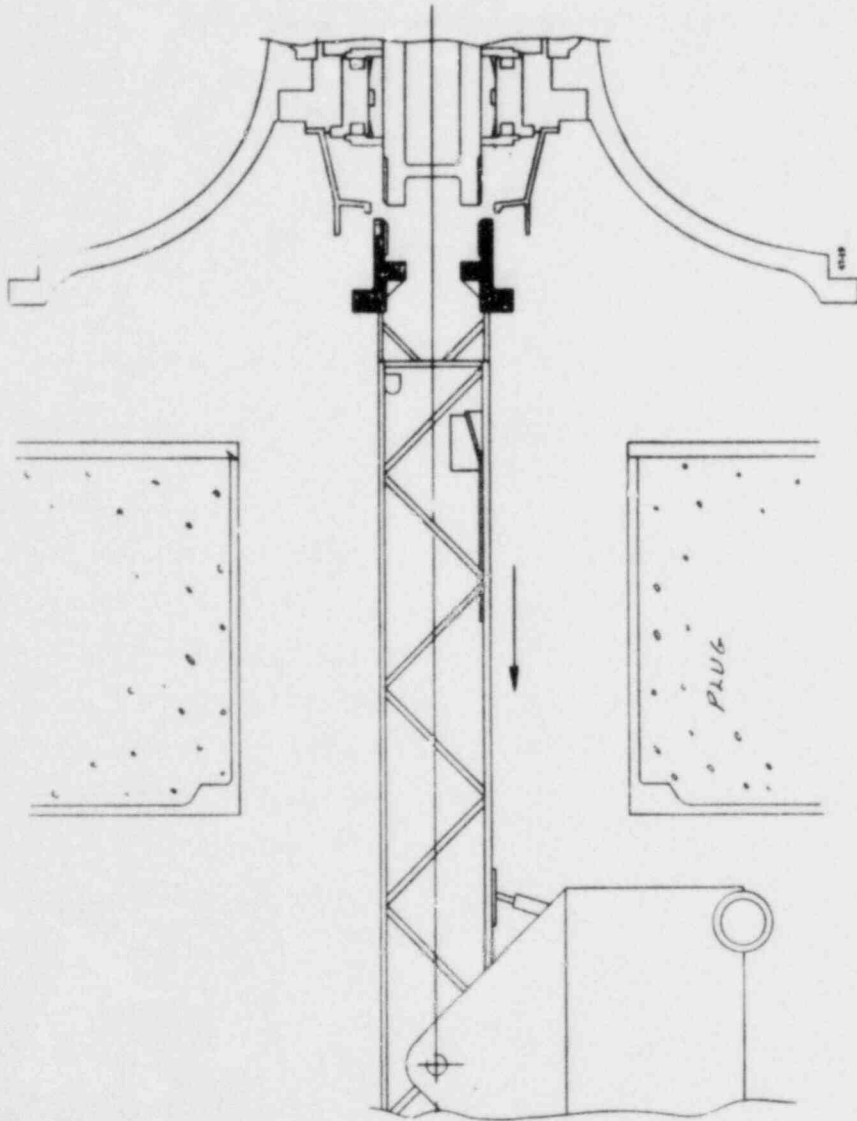


Fig. 18-12. Removal of shaft coupling



### 18.3.8. Turbomachine Noise Reduction

Several means were examined for reducing upstream and downstream noise emissions from the compressor and turbine of the HTGR-GT. These include modifying the blade and vane numbers, increasing the rotor-stator spacing, providing acoustic liners for the component cases, and using special inlet and exhaust ducting. Not all these methods need be applied to all components. For example, if the recommended blade and vane numbers can be employed, the current rotor-stator spacing can be retained. Similarly, if satisfactory inlet ducts that incorporate a sonic throat can be designed, it will be unnecessary to modify the blade and vane numbers and the spacing in the inlet stages.

Estimates of the overall power level (OAPWL) reductions were obtained for some of these measures. Either blade-vane modifications or increased spacing is worth about 4 dB of OAPWL. Treating the diffuser sections of the compressor and the turbine discharge with perforated facing - honeycomb backing space acoustic liners should provide about 9 dB discharge noise OAPWL reduction. Similar treatment upstream of the compressor and turbine would reduce the sound power levels in these regions by approximately 12 to 14 dB. Use of sonic inlets results in at least 20-dB reduction in inlet noise. Further noise reductions could be obtained by sound-absorbing liner applications outside of the main turbomachine components. For design of such structures, an estimate of the spectral distribution of target noise reduction is required to provide better criteria than the overall power reductions employed here.

### 18.3.9. Depressurization During Deblading

A study was conducted to address the question of an assumed deblading of the HTGR-GT turbine. The primary information sought was the rate at which the turbine flow path resistance to flow changed with time, i.e., how fast the failed turbine parts clear the annular gas path area. With these data, the system depressurization rate could then be calculated.

The approach taken was to search for available hardware data resulting from this type of failure and to simulate the HTGR-GT system in a computer program, so that the data obtained from open cycle hardware could be rationalized to a closed cycle configuration. The UTC Volume Dynamics Simulation Program (VDS) was used to simulate the power plant system. VDS is a digital system used for pressure-volume dynamics simulations in the milliseconds to minute time regime. It is used to model the process control logic of a power plant during normal operation, power transients, failure modes, startup, and shutdown. Power plant interface conditions are defined by the user, and pressure, flow compositions (where applicable), mass storage, and flow direction are calculated at each system location. Temperature at each location is user input either as set values or as dynamic calculations. Temperatures of fluid mixes are calculated based on the temperatures and properties of the mixing streams.

The VDS input was the three-loop version of the HTGR-GT with system volumes as provided by GA. The compressor map was included so that the compressors in the two operating loops (one loop failed) would maintain their characteristics during the transients. The operating turbines were modeled as orifices. The failed turbine and its compressor were modeled as variable area orifices with the rate of change of area being a variable input. The results of a simulated turbine failure are shown in Figs. 18-13 through 18-17. It was assumed in this case that the turbine area changed linearly over a 150-ms period. The other assumptions associated with this simulation are shown in Fig. 18-18 and Table 18-2.

At the time these data were generated, it was understood that this simulation was deficient from the standpoint of completeness because it did not take into account the transient momentum terms associated with the acceleration of the mass in the various parts of the system. A more complete analysis was conducted by GA based on inputs from UTC.

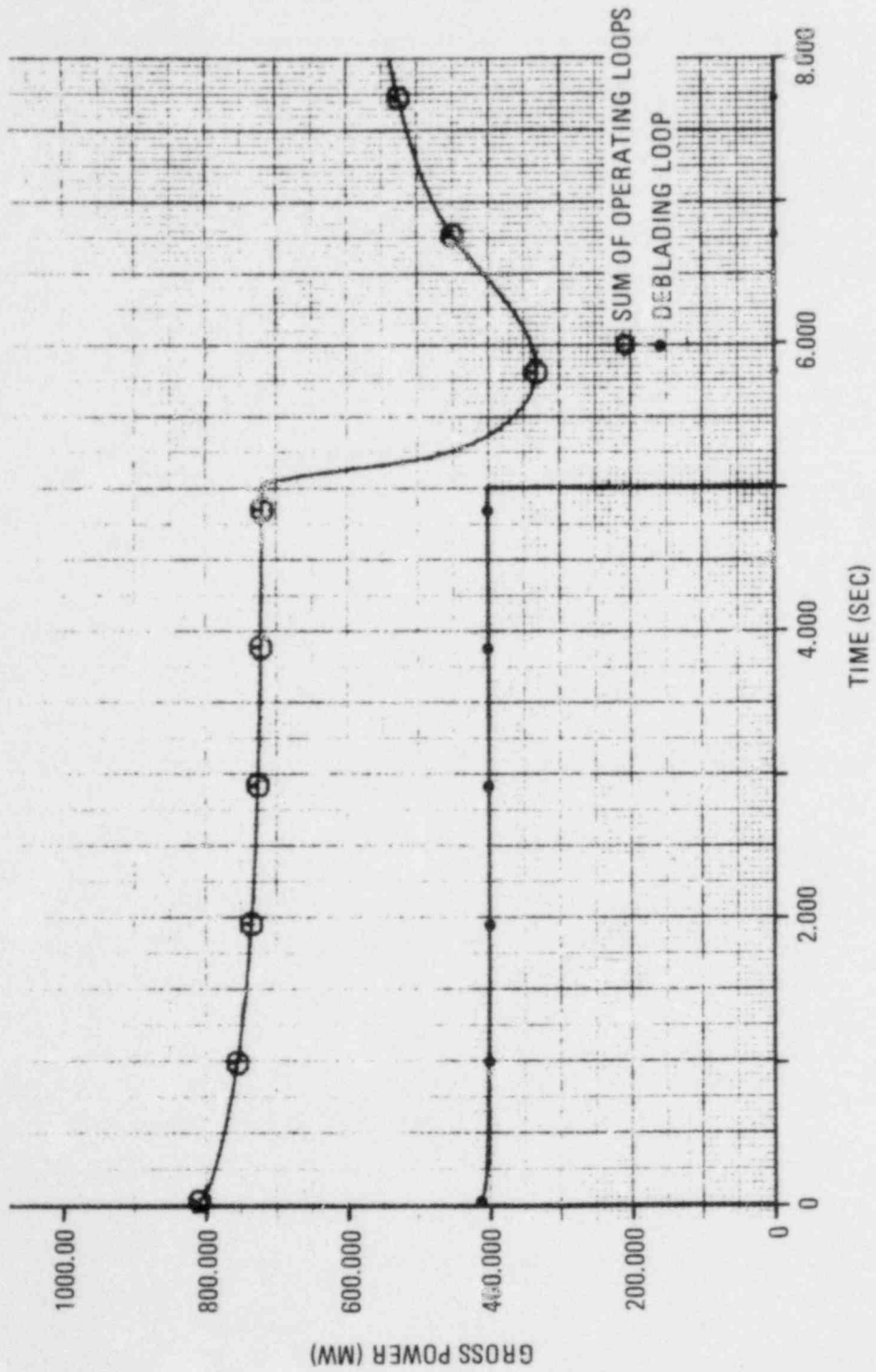


Fig. 18-13. Turbine deblading computer simulation - gross power versus time

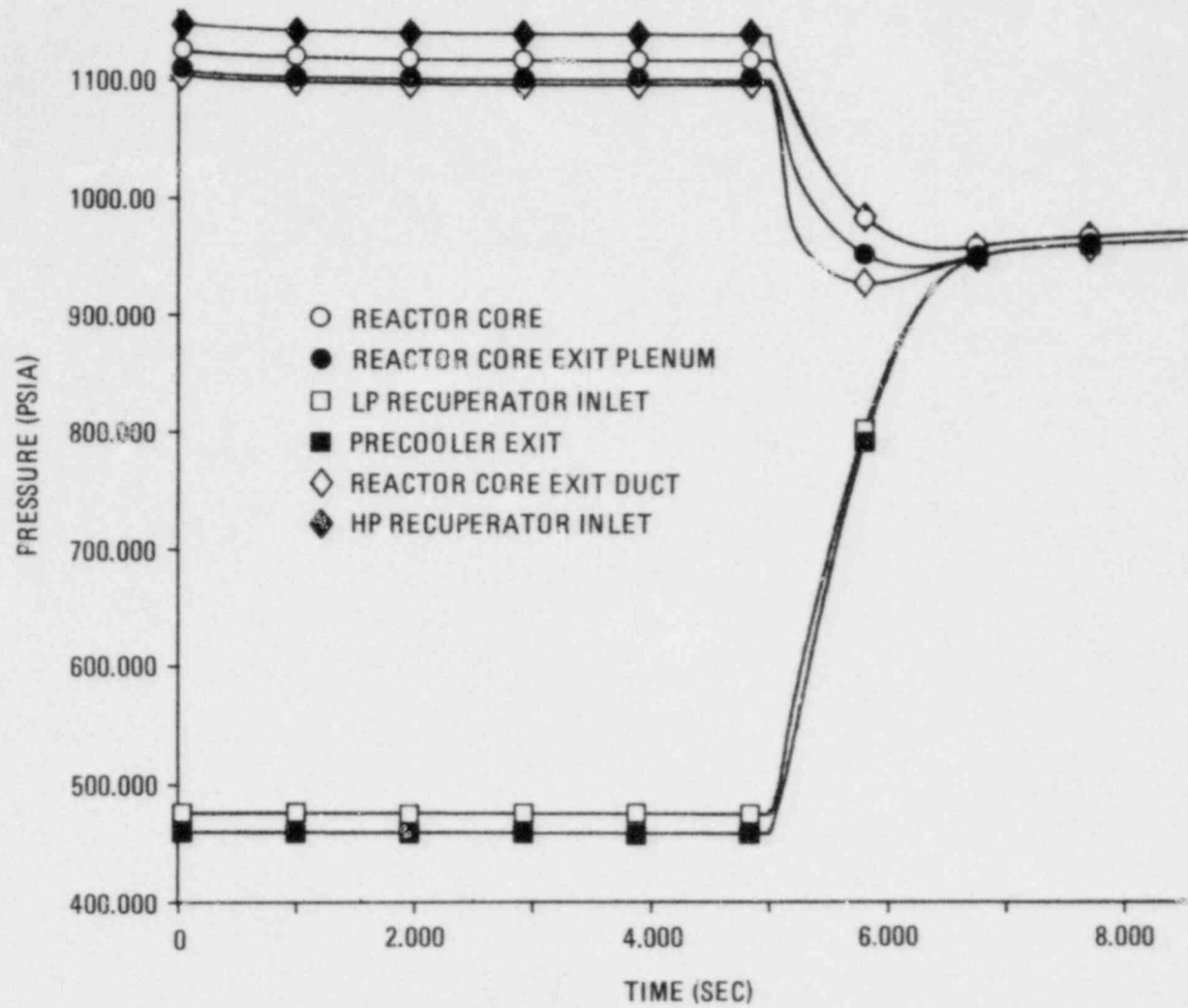


Fig. 18-14. Turbine deblading computer simulation - pressure versus time

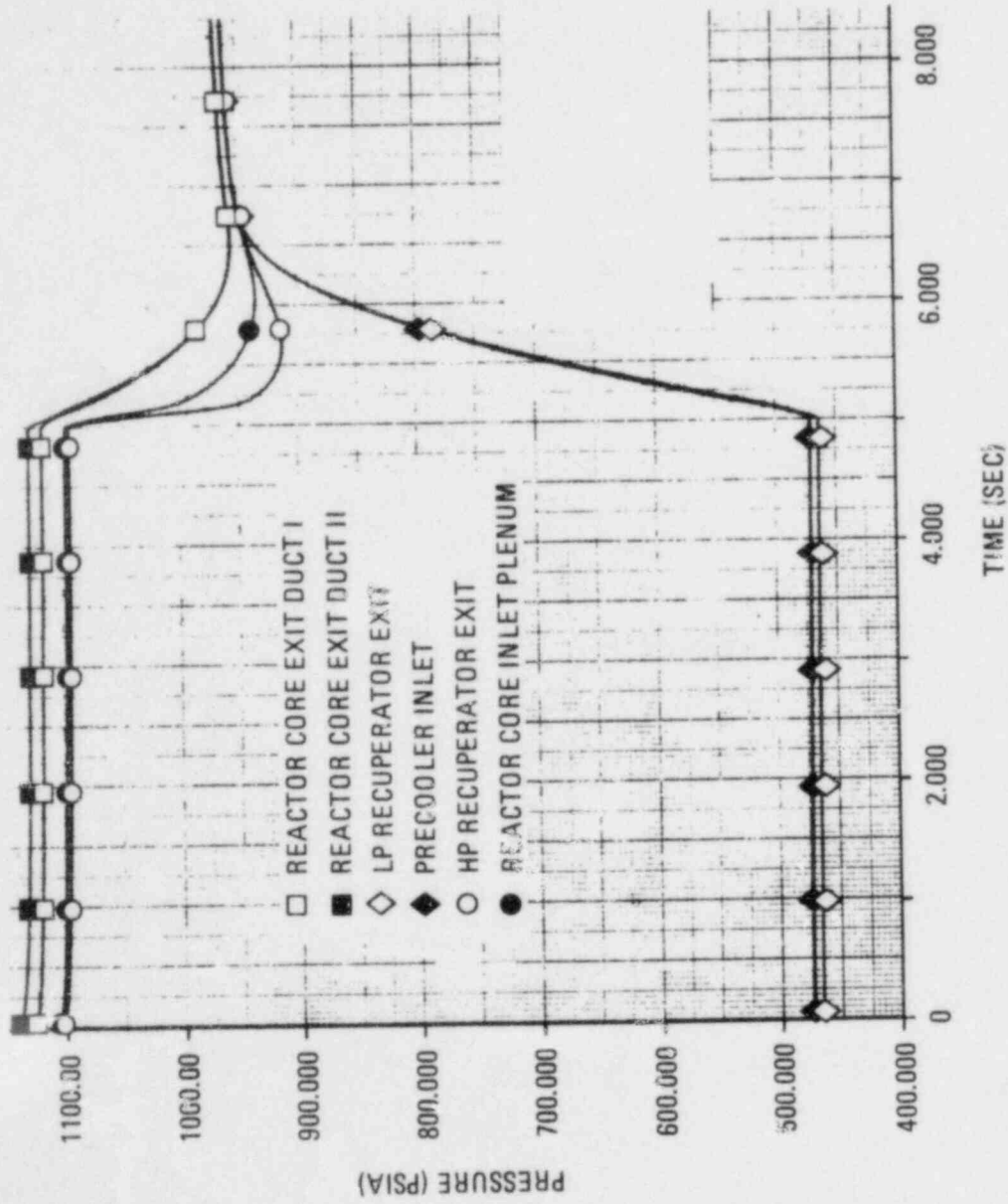


Fig. 18-15. Turbine deblading computer simulation - pressure versus time

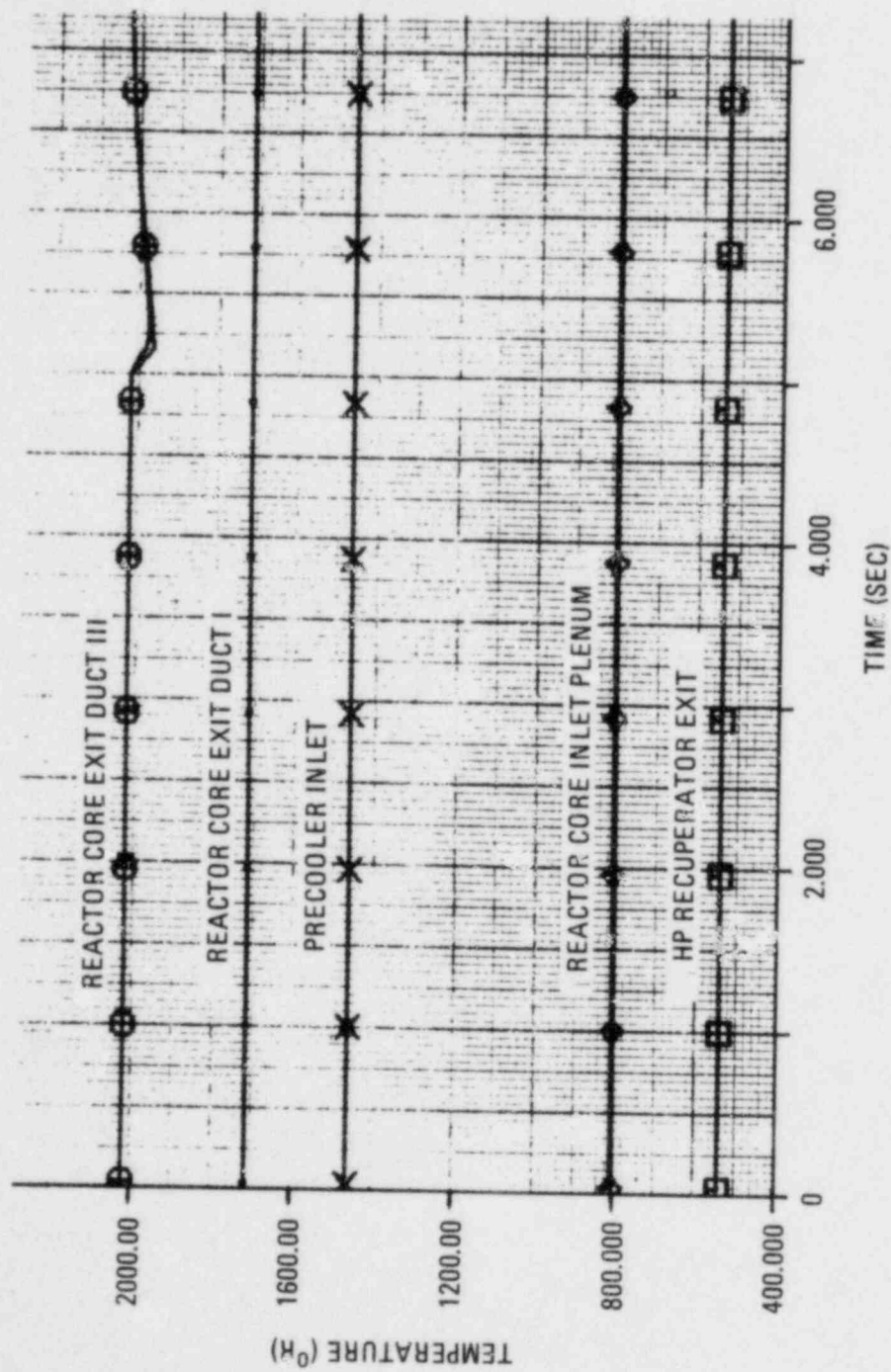


Fig. 18-16. Turbine deblading computer simulation - temperature versus time

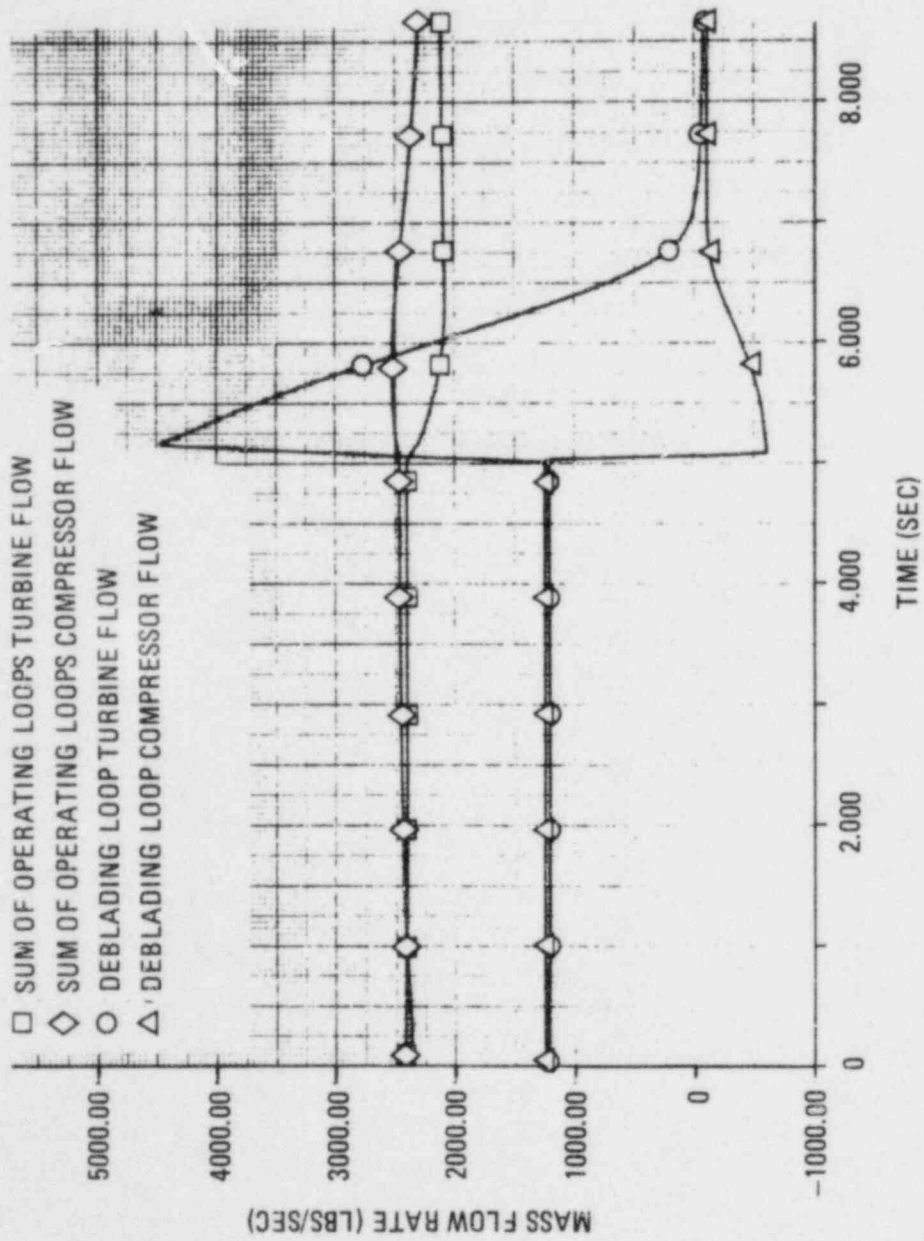


Fig. 18-17. Turbine deblading computer simulation - mass flow rate versus time

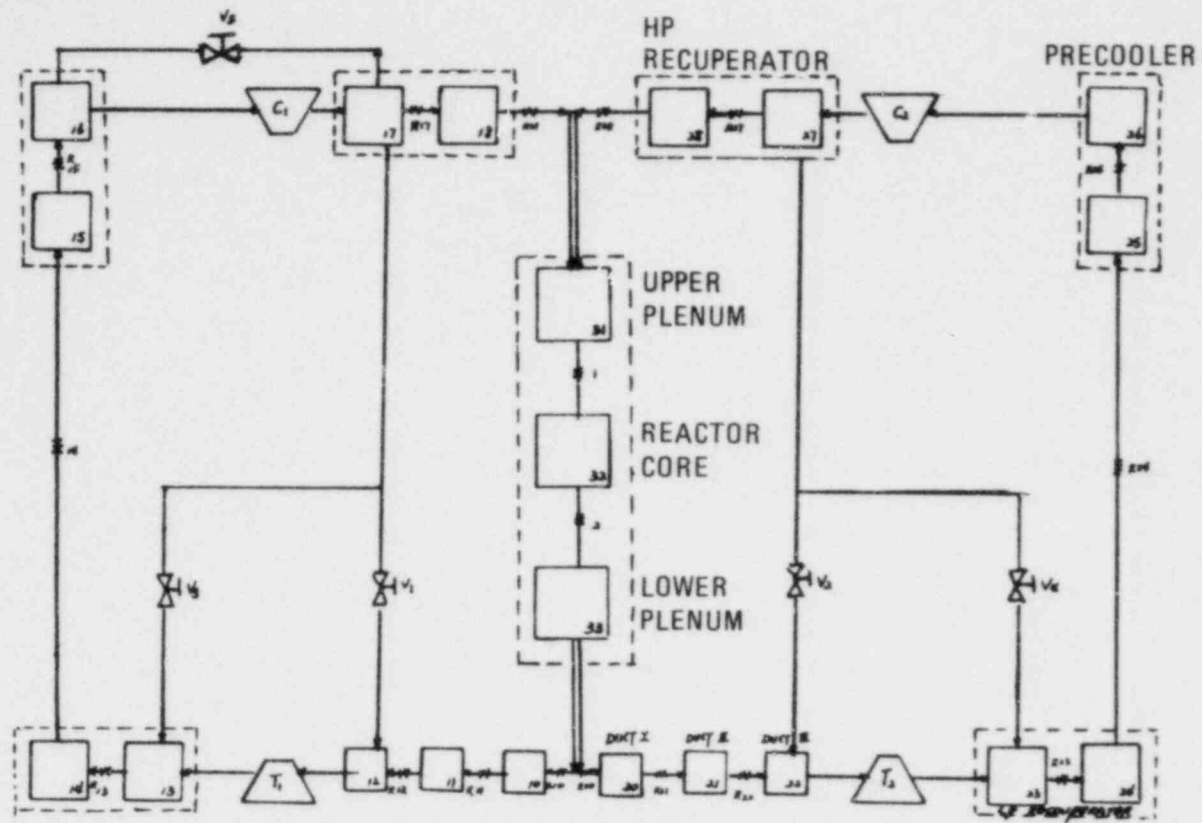


Fig. 18-18. HTGR-GT Volume Dynamics Simulation system schematic



TABLE 18-2  
HTGR-GT VOLUME DYNAMICS SIMULATION  
(INITIAL STEADY-STATE CONDITIONS)

Volume Number	Volume [m <sup>2</sup> (ft <sup>2</sup> )]	Temperature (°R)	Pressure [MPa (psia)]	Resistance Number	Pressure Drop [kPa (psi)]	Flow [kg/s (lb/s)]
10	55.40 (596)	2022	7.65 (1109)	10	13.8 (2)	551 (1215)
11	55.40 (596)	2022	7.63 (1107)	11	13.8 (2)	551 (1215)
12	55.40 (596)	2022	7.62 (1105)	12	13.8 (2)	551 (1215)
13	754.53 (8117.5)	1463	3.28 (476)	13	20.9 (3)	555 (1224)
14	754.53 (8117.5)	897.3	3.26 (473)	14	48.3 (7)	555 (1224)
15	390.86 (4205)	897.3	3.21 (466)	15	41.4 (6)	555 (1224)
16	390.86 (4205)	540	3.17 (460)	17	69.0 (10)	551 (1215)
17	0.093(1)	806.4	7.93 (1150)	18	75.8 (11)	551 (1215)
18	1831.4 (19,703)	1110.5	7.86 (1140)	20	27.6 (4)	1102 (2430)
20	110.80 (1192)	2022	7.65 (1109)	21	27.6 (4)	1102 (2430)
21	110.80 (1192)	2022	7.63 (1107)	22	27.6 (4)	1102 (2430)
22	110.80 (1192)	2022	7.62 (1105)	23	41.4 (6)	1110 (2448)
23	1509.24 (16,237)	1463	3.28 (476)	24	96.5 (14)	1110 (2448)
24	1509.24 (16,237)	897.3	3.26 (473)	25	82.7 (12)	1110 (2448)
25	781.71 (8410)	897.3	3.21 (466)	27	137.9 (20)	1102 (2430)
26	781.71 (8410)	540	3.17 (460)	28	151.7 (22)	1102 (2430)
27	0.186(2)	806.4	7.93 (1150)	31	6.90 (1)	1652 (3644)
28	3362.81 (39,406)	1110.5	7.86 (1140)	32	117.2 (17)	1652 (3644)
31	1505.80 (16,200)	1414.6	7.78 (1129)			
32	451.93 (4862)	1717.3	7.77 (1128)			
33	845.29 (9094)	2022	7.66 (1111)			

Information available from hardware experience is shown in Fig. 18-19, where the static pressure measured upstream of an open cycle turbine during an overstress test turbine failure is presented. The period between 0 and 1.0 s is expanded in Fig. 18-20. The pressure transducer was close coupled to the static tap with a response rate between 1/16 and 1/8 s. Other measured parameters indicated the heat supply continued throughout the failure. Since the upstream choked hardware remained intact during the test, it would tend to hold the measured pressure up. Also, a significant portion of the turbine blading remained intact after the rotor was stopped. Rotor speed at the time of failure was approximately 9000 rpm.

#### 18.3.10. Welded Rotor Failure Mechanism

A study was performed to investigate the mechanism by which a welded rotor might fail. Welded rotor failure modes were reviewed, and it was concluded that a failure of an entire rotor was an unlikely event.

The probability of failure can be further minimized by:

1. Including in the design progressive margins which would cause the component with the least damage impact to fail first.
2. Setting high disk burst margins.
3. Limiting critical stresses based on fracture mechanics criteria compatible with the minimum detectable flaw size.
4. Establishing rigid quality assurance procedures.

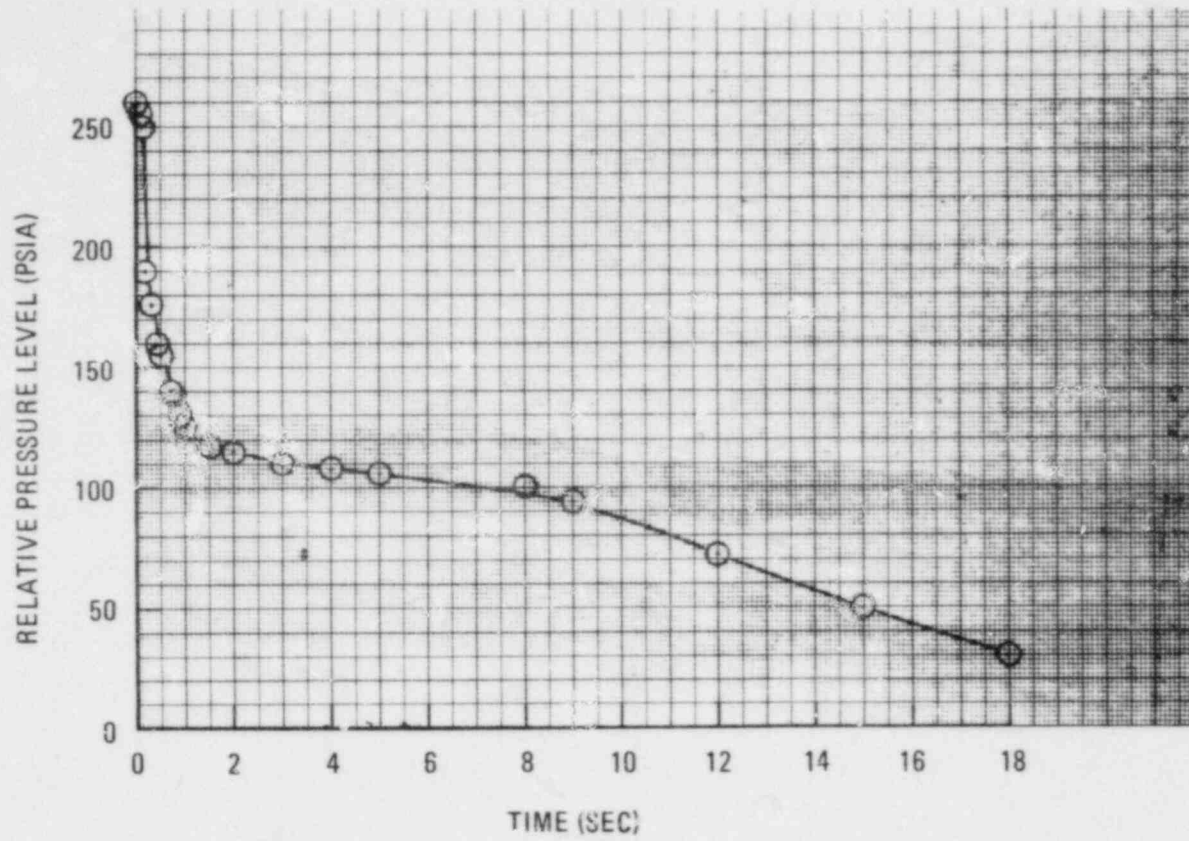


Fig. 18-19. Depressurization during turbine failure with 0 to 1.0 s period expanded (based on test data)

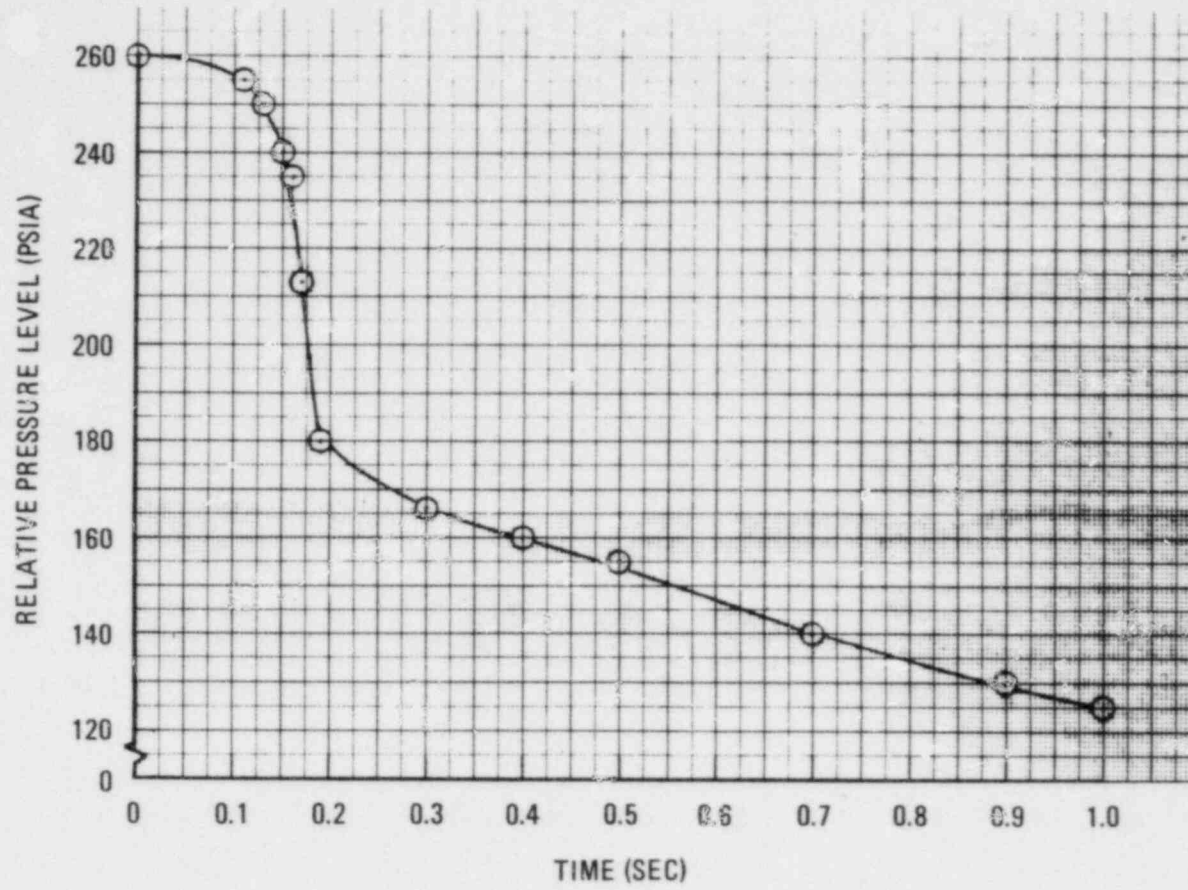


Fig. 18-20. Depressurization during turbine failure (based on test data)

Disk failure, the least likely rotor failure, may result from:

1. Exceeding the design stress level owing to speed and/or temperature exceeding maximum design levels.
2. Weakness of material due to a metallurgical defect, an unexpected crack, or changes due to the environment (corrosion, embrittlement, etc.).

Disk failure will originate in regions of high stress. The highest stress occurs at the bore of the disks and the second highest at the web of the disk. Failures originating at the bore will lead to bursting when the crack size exceeds the critical flaw size.

Based on fracture mechanics and limited information on Ladish D6AC material, Fig. 18-21 shows that 0.049 mm (0.192 in.) is the critical crack length for a 0.69-MPa (100,000-psi) stress level that is reached at 20% overspeed. Assuming a 0.016-mm (0.062-in.) minimum detectable flaw, its size will grow 0.229 mm (0.009 in.) in 1000 cycles. However, the likelihood of 1000 cycles coupled with overspeed is very small, and the crack could either be detected by inspection during overhaul or remain safe during the 280,000-h life of the engine. Larger cracks will grow much more rapidly but are more likely to be detected before leading to rupture.

At the rated speed of 3600 rpm, the bore stress is reduced to  $100,000/1.2^2 = 478$  MPa (69,400 psi) with a corresponding reduction of crack sensitivity and crack growth. With the maximum bore stress set at 689.5 MPa (100,000 psi) at 20% overspeed, the disks have a burst margin of 1.44 at maximum engine speed of 4320 rpm compared with the 1.25 margin used in other gas turbine designs.

If the disk develops a flaw that reaches critical flaw size, a crack may propagate to the rim in 1 ms. In this case, the three or four fragments of the disk are still attached to the spacers and become instantaneous

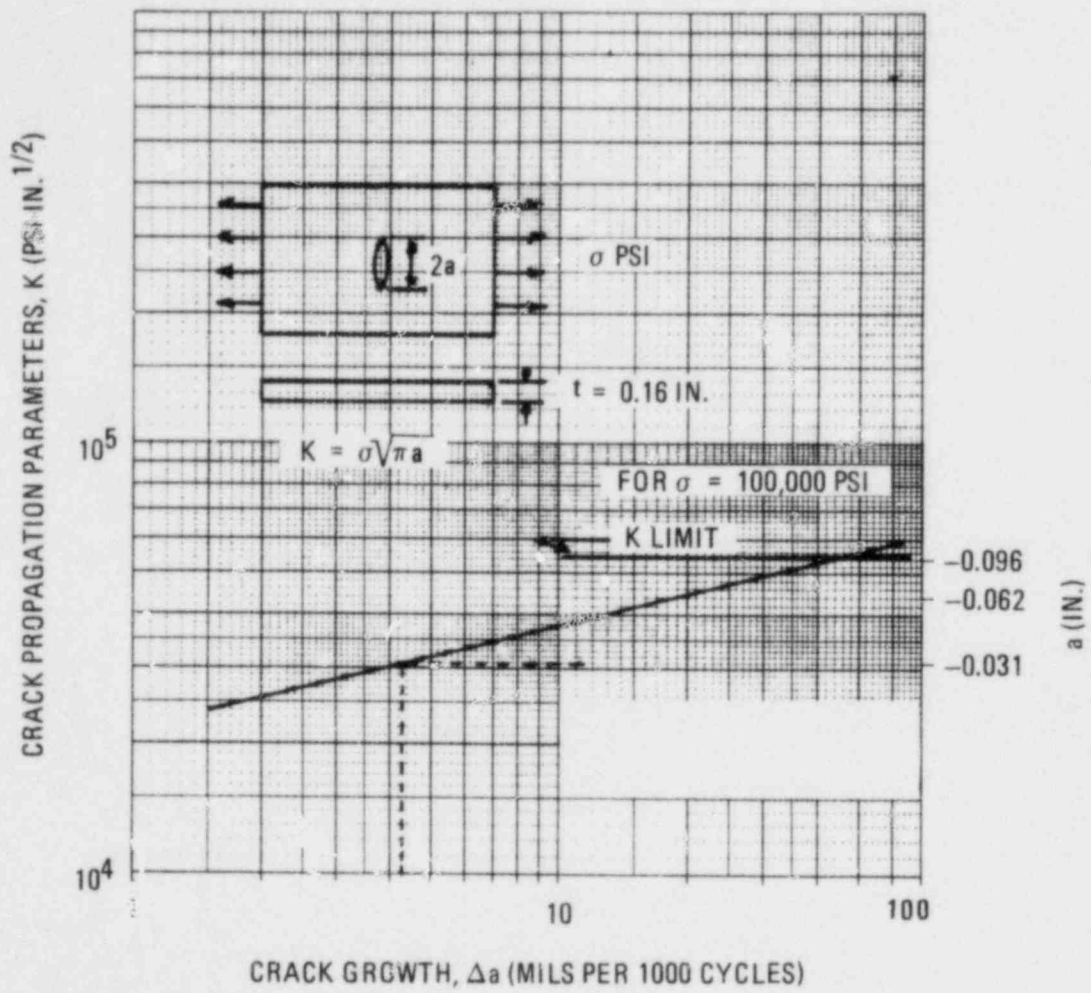


Fig. 18-21. Rotor disk crack growth diagram

additional loads on both the spacers and the adjoining disks. It is therefore possible that the overload will result in bursting of these disks, since there is no time for deceleration of the rotor and reduction of centrifugal forces.

Another possible disk failure could originate at the web with high radial stress, the second highest stress level in the disk. Results from prior work covering the first and eighth turbine disks show this stress to be 76% to 92% of the bore stress. Failure of this type will tear out a fragment of the disk without causing a complete burst; it will cause excessive unbalance and rotor deflections. It can again be assumed that the engine will be shut down before any catastrophic failure occurs.

Further work is needed to determine if in the case of a disk or shaft failure, deterioration of driving torque and mechanical interferences are sufficient to prevent or limit propagation of the failure. The design system should include progressive design margins which would cause the component with the least damage impact to fail first. The probable sequence would be:

1. Blades.
2. Blade roots.
3. Blade attachments.
4. Disk lugs.
5. Disk segment or disk.

Thus, most rotor failures would result in blade loss only and would not involve the disks and main rotor structure.

The HTGR-GT design has as a criterion that the loss of up to 10% of the blades in a single stage will not produce major damage. In the event of such a failure, other blades and blade rows can and frequently will be involved, but the engine can be shut down before any catastrophic failure occurs. Disk damage in these cases is limited to the blade attachment region.

Experience with welded rotors shows no catastrophic failures. Use of welded rotors is justified because:

1. The design system permits thorough analysis of stresses.
2. Welding of the rotor permits the use of smaller, higher-quality disk forgings.
3. Welding techniques have progressed and guarantee very high-quality, reliable joints.
4. Inspection procedures reveal even very small imperfections and permit monitoring of possible crack growth during the life of the engine.
5. Welded rotors avoid the stress concentrations associated with bolt holes.

#### 18.3.11. Turbine Disk Rim Stress Studies

A study was performed to evaluate the tolerance of the turbomachine to various static and transient off-design operating conditions. For purposes of the study, turbine rim stress was used as the parameter for acceptability. The following off-design conditions were evaluated:

1. Reactor scram coastdown transient.
2. Plant loss of load.
3. Single loop loss of load with overspeed.
4. Plant loss of coolant water flow.



These conditions involve both short-time transients, <1 h, and long-time operating conditions, >1 h. The study was conducted in two parts, consisting of a structural evaluation defining the maximum allowable short-time and long-time rim temperatures and a thermal evaluation of the rim temperature during the selected off-design conditions.

The conclusions from the study are as follows:

1. The coastdown and plant loss of load transients do not impose unacceptable levels of turbine rim stress.
2. Further review of the system characteristics during the single loop loss of load and loss of coolant water conditions is required. If the identified reverse flow occurs under these conditions within a reasonable period of time after the loop shutdown, turbo-machine operation will be acceptable. However, if reverse flow does not occur, the turbine will be exposed to a reactor outlet temperature of 816°C (1500°F) with no cooling flow available. The adverse impact on turbine materials under these conditions will be a function of the exposure time at temperature.

18.3.11.1. Structural Analysis. One of the features of the UTC design is the use of Ladish D6AC as a turbine and compressor disk material. This material has excellent low-temperature strength (Fig. 18-22) but weakens rapidly above 482°C (900°F) and has little structural strength above 649°C (1200°F). A key feature of the design is a cooling scheme which employs compressor exit flow at 177°C (350°F) to wash over and cool the turbine rim. The base line design maintains the maximum turbine disk temperature at 288°C (550°F) by using 3.6% of the compressor flow for cooling.

Any changes in operation that affect speed, turbine inlet temperature, or available cooling flow will alter the turbine rim temperature. The objective of the structural analysis is to set the maximum allowable turbine

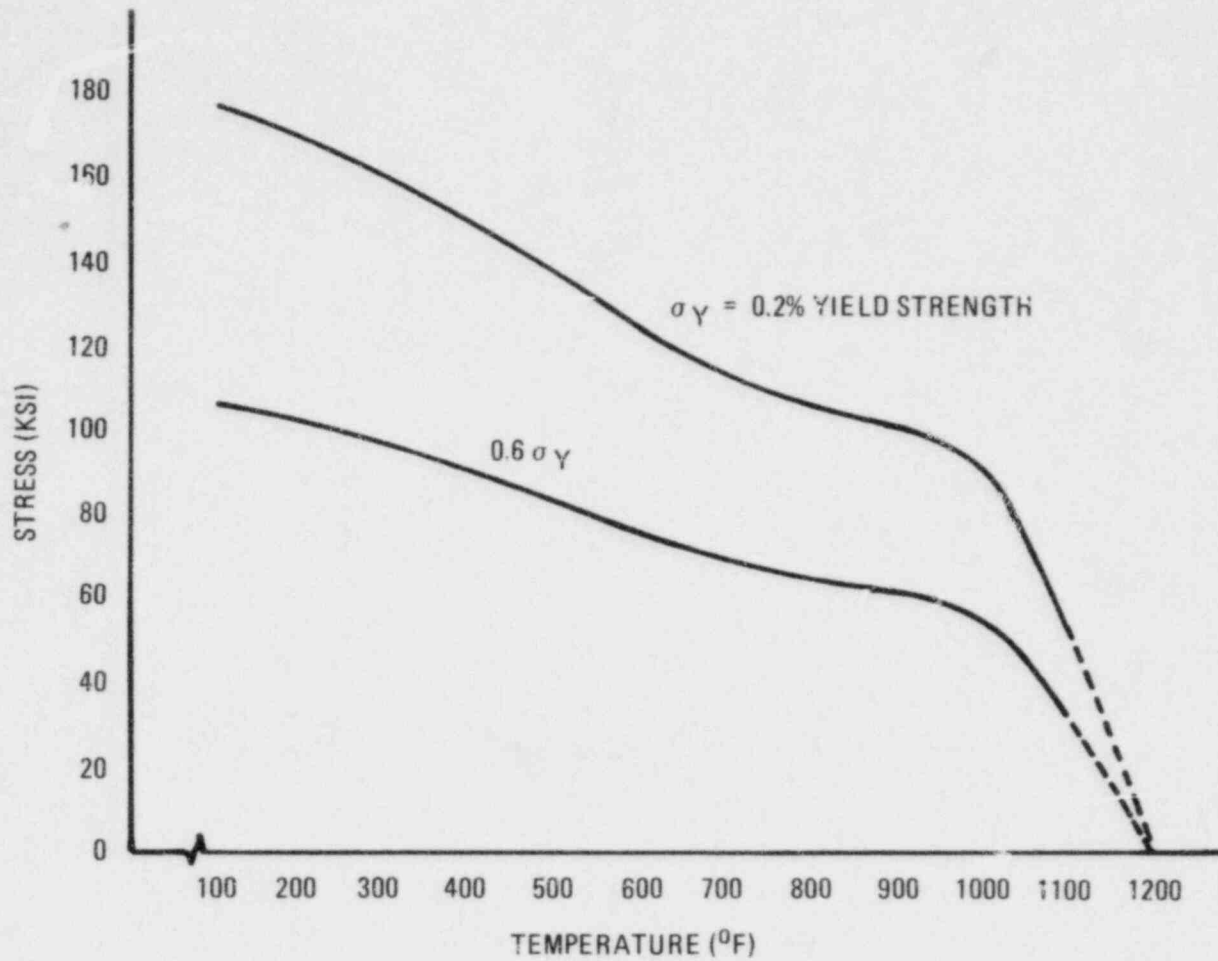


Fig. 18-22. Ladish D6AC minimum yield strength versus temperature

rim temperatures. Disk stress level in the turbine blade fir tree attachment sets the maximum allowable turbine rim temperature. The UTC design system analyzes these stresses by means of a computer program and compares the results with either 60% of the 0.2% offset yield strength at 20% overspeed or 60% of the 280,000-h stress rupture strength at normal operating speed. The latest fir tree attachment analysis for the HTGR-GT turbo-machine indicates that the design is governed by the stresses in the eighth-stage turbine,  $\sigma_{max} = 353 \text{ MPa}$  (51,200 psi) at  $288^\circ\text{C}$  ( $550^\circ\text{F}$ ) and  $0.6\sigma_y = 538 \text{ MPa}$  (78,000 psi).

Figure 18-23 relates the maximum allowable turbine rim temperature to the turbine rim stress. It shows that at the overspeed condition, the turbine rim temperature could reach  $538^\circ\text{C}$  ( $1000^\circ\text{F}$ ) and still meet the design criteria. The maximum allowable short-time turbine rim temperature ranges from  $538^\circ\text{C}$  ( $1000^\circ\text{F}$ ) to  $649^\circ\text{C}$  ( $1200^\circ\text{F}$ ), depending on speed. The upper limit was arbitrarily set at  $649^\circ\text{C}$  ( $1200^\circ\text{F}$ ) based on the rapid decline in mechanical properties at this temperature.

For an off-design condition which lasts longer than 1 h, a slightly different approach is taken which uses stress rupture allowables. Figure 18-24 shows the relationship between stress, temperature, and time. The results indicate that at normal operating speed [ $\sigma = 244.8 \text{ MPa}$  (35,500 psi)], the design life would be 3000 h at  $482^\circ\text{C}$  ( $900^\circ\text{F}$ ) but only 50 h at  $538^\circ\text{C}$  ( $1000^\circ\text{F}$ ). Therefore, based on the sensitivity of temperature to the stress rupture properties and extrapolation of the data, the maximum allowable long-time turbine rim temperature has been set at  $510^\circ\text{C}$  ( $950^\circ\text{F}$ ).

18.3.11.2. Thermal Analysis. Two transient events were analyzed in detail, the scram coastdown transient and the plant loss of load. Transients associated with single loop loss of load with overspeed and plant loss of cooling water flow were evaluated in somewhat less detail. The detailed analyses of the first two events provided familiarity with the major contributing factors which affect rim temperatures. Accordingly, these factors were considered in evaluating the last two events.

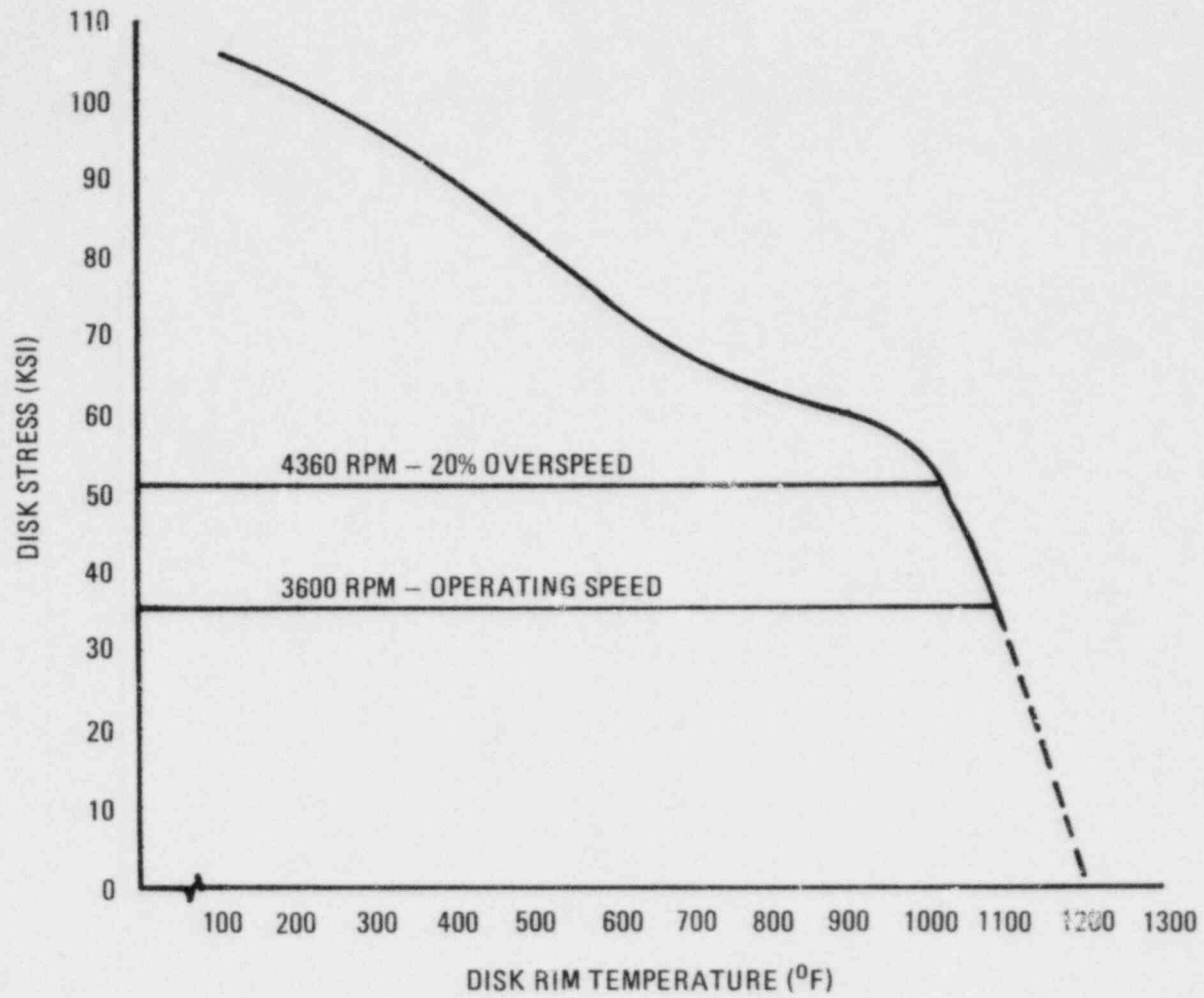


Fig. 18-23. Disk stress versus maximum allowable short-time rim temperature

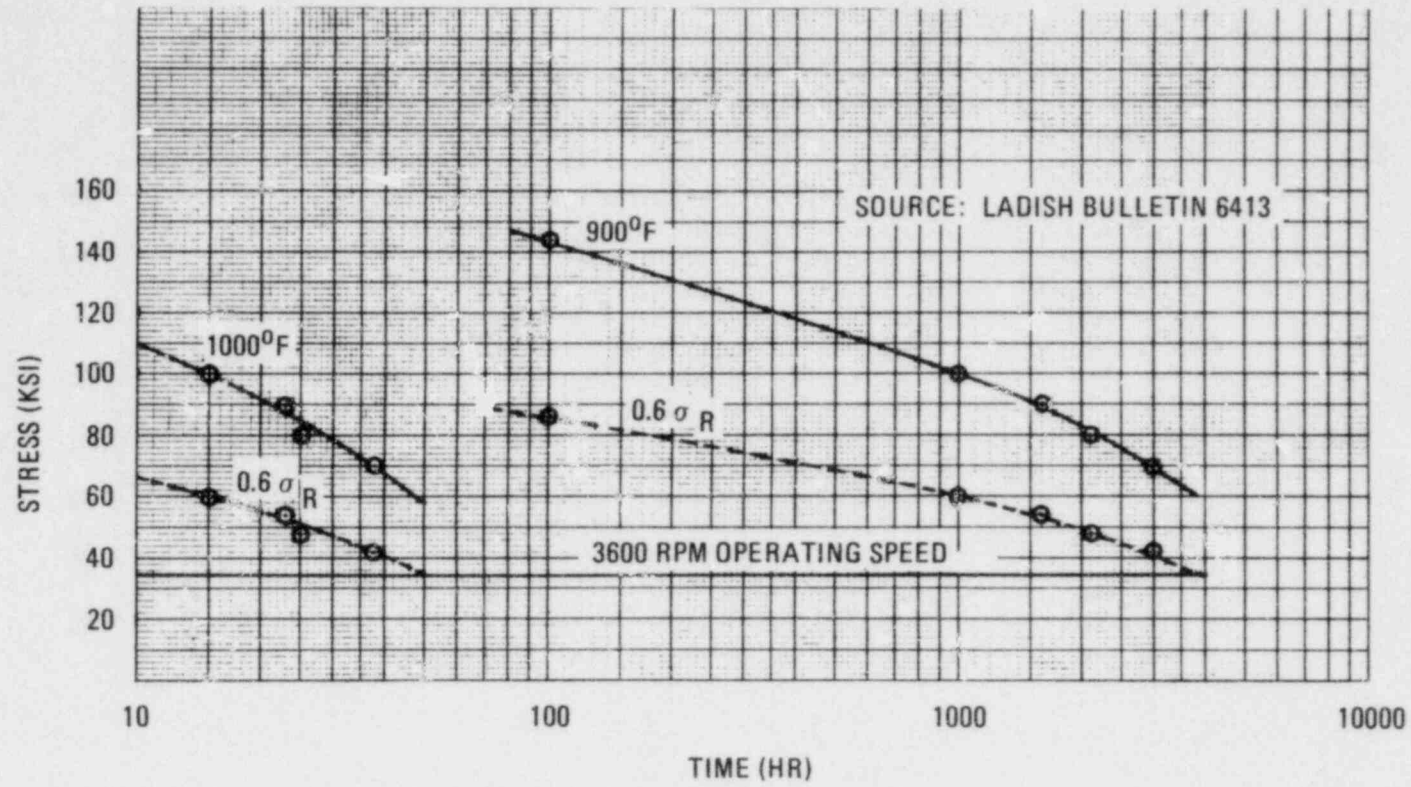


Fig. 18-24. Ladish D6AC stress rupture strength

The fundamental analytical techniques were established consistent with those used previously by UTC. The FT-50 engine was used as a reference. Some internal temperatures for the HTGR-GT were determined via appropriate ratioing techniques. The gas temperatures adjacent to the turbine disk outside diameter reflect the turbine rim temperatures (see  $T_{\text{gas(mix)}}$  in Fig. 18-25). Pending further studies, the rim outside diameter temperatures have been assumed to be cooled within 10°C (50°F) of the gas mixture.

The major parameters associated with the coastdown and plant loss of load transients are presented in Table 18-3.

The parameters controlling the gas mixture temperatures are as follows (Fig. 18-25):

1.  $W_{\text{in}}$  = hot gas ingested into the cavity between the vane and blade. The rate of ingestion is proportional to gas absolute velocity at the root, gas density, and gap.
2.  $W_{\text{cool}}$  = rate of coolant flow through the coolant passage. All coolant flow per stage was assumed to flow into the passage upstream of the vane. Actually, a small portion will flow through the passage going to the bottom of each "fir tree." The gas cooling rates depend on turbine/compressor pressures and temperatures.
3.  $W_{\text{BB}}$  = rate of seal blow-by. This rate depends on seal design, pressure ratio across the seal, upstream absolute pressure, and temperature. The baseline blow-by rates were determined from prior analytical results.
4. Heat generated from disk and seal windage. The heat generation rates were determined to have only a -6.7°C (20°F) or less increase in gas mixture temperatures and were therefore ignored for the present level of analysis.

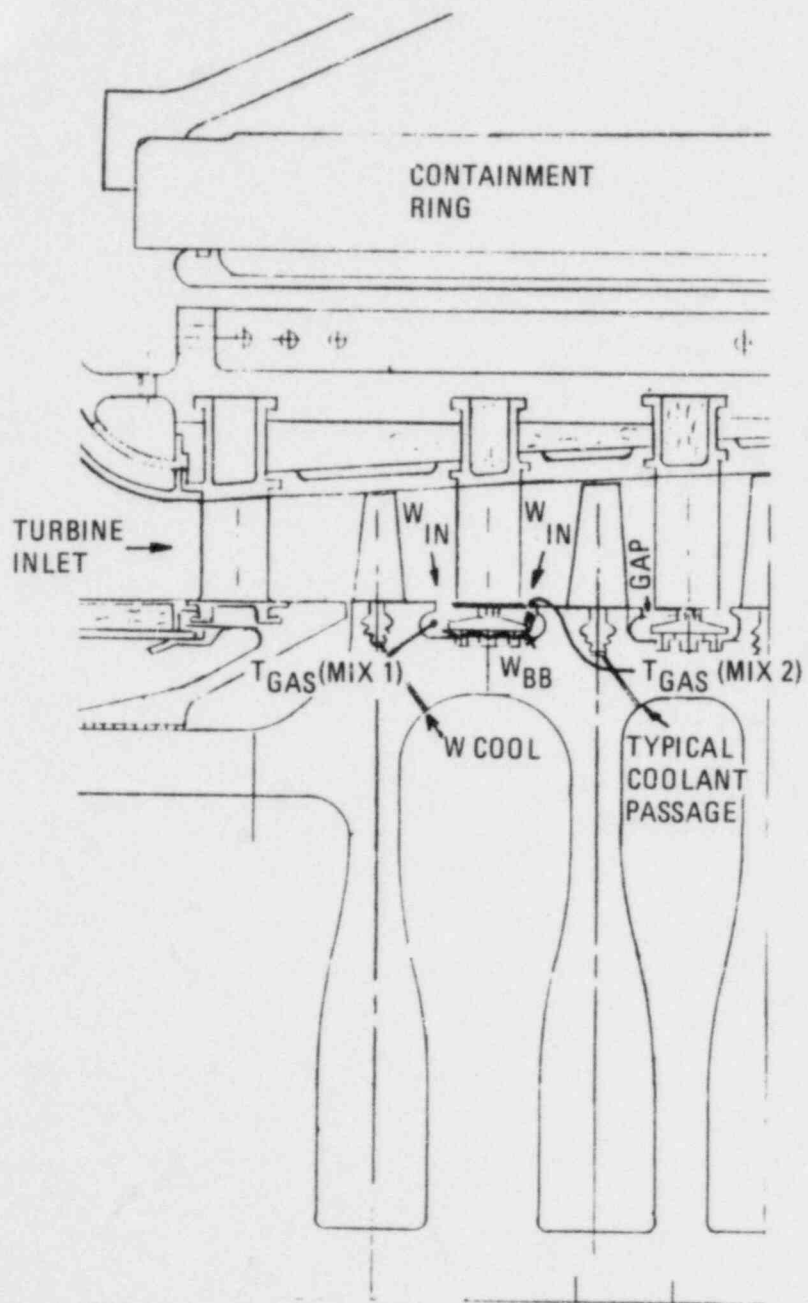


Fig. 18-25. 400-MW(e) turbine section

TABLE 18-3  
 MAJOR PARAMETERS FOR REACTOR SCRAM COASTDOWN AND  
 PLANT LOSS OF LOAD TRANSIENTS

Parameter	Time = 0 (100% power)	Reactor Scram Coastdown <sup>(a)</sup>				Plant Loss of Load <sup>(b)</sup>	
		t=10 h	t=1 day	t=1-1/2 day	t=80 s	t=180 s	t=299 s
Compressor exit temperature, °C (°F)	174 (346)	56 (133)	102 (215)	86 (187)	142 (287)	181 (359)	181 (357)
Compressor exit pressure, MPa (psia)	7.92 (1150)	2.61 (379)	1.31 (190)	0.78 (114)	6.97 (1011)	7.84 (1138)	7.88 (1144)
Turbomachine speed, rpm	3600	1970	3180	2780	3600	3600	3600
Turbine inlet temperature, °C (°F)	849 (1560)	747 (1377)	727 (1341)	588 (1091)	851 (1564)	843 (1551)	851 (1563)
Turbine inlet pressure, MPa (psia)	7.66 (1112)	2.57 (373)	1.27 (184)	0.76 (111)	6.07 (967)	7.56 (1097)	7.60 (1103)
Turbine inlet flow rate, kg/h (lb/h)	1.95x10 <sup>6</sup> (4.3x10 <sup>6</sup> )	0.38x10 <sup>6</sup> (0.84x10 <sup>6</sup> )	0.29x10 <sup>6</sup> (0.64x10 <sup>6</sup> )	0.18x10 <sup>6</sup> (0.39x10 <sup>6</sup> )	1.45x10 <sup>6</sup> (3.2x10 <sup>6</sup> )	1.95x10 <sup>6</sup> (4.3x10 <sup>6</sup> )	1.95x10 <sup>6</sup> (4.3x10 <sup>6</sup> )
Turbine exit temperature, °C (°F)	534 (998)	644 (1192)	542 (1009)	456 (852)	632 (1170)	557 (1034)	556 (1032)
Turbine exit pressure, MPa (psia)	3.27 (476)	2.14 (311)	0.81 (117)	0.52 (76)	4.13 (600)	3.55 (516)	3.50 (508)

(a) Reactor scram starts transient; inventory control is used. One turbomachine loop operating to provide reactor cooling. Turbomachine speed adjusted to maximize turbine efficiency and minimize reactor heat losses.

(b) Plant loss of load starts transient. Bypass control of turbomachine. Load restored at 160 s.



The  $W_{cool}$  rates for the coastdown and plant loss of power transients were determined. These rates were ratioed from the baseline rate per stage as shown in Fig. 18-26. The pressures for each stage (transient) conditions were obtained by dividing the overall pressure ratio into eight equal pressure ratios,

$$\left(\frac{P_u}{P_d}\right)_{\text{Stage}} = \left(\frac{P_{in}}{P_{out}}\right)^{1/8},$$

which is standard turbine preliminary design practice. Since the overall temperature change through the turbine was relatively small, it was considered sufficiently accurate to also divide the overall temperature ratio into eight equal temperature ratios.

The analysis was limited to evaluating the rim temperatures of the areas upstream and downstream of the second vane and upstream and downstream of the eighth vane.

#### 18.3.11.3. Results.

##### Coastdown Transient due to Reactor Scram

The results show that the maximum cavity gas mixture temperatures occur during the baseline condition [see Table 18-4(A)]. The maximum estimated gas cavity temperature occurs downstream of the second vane.

The transient creates no problems since the maximum metal rim temperature is 54°C (130°F) below the long-term allowable temperature.

##### Plant Loss of Load

The conditions for this transient are nearly the same as for the baseline 100% power point except at  $t = 80$  s. Analysis of the gas mixture temperatures at 80 s showed a drop in temperature. Temperatures at other

TOTAL FLOW = 3.6% OF COMPRESSOR INLET FLOW RATE  
CASE FLOW = 0.64%  
TURBINE ROTOR FLOW = 2.96%

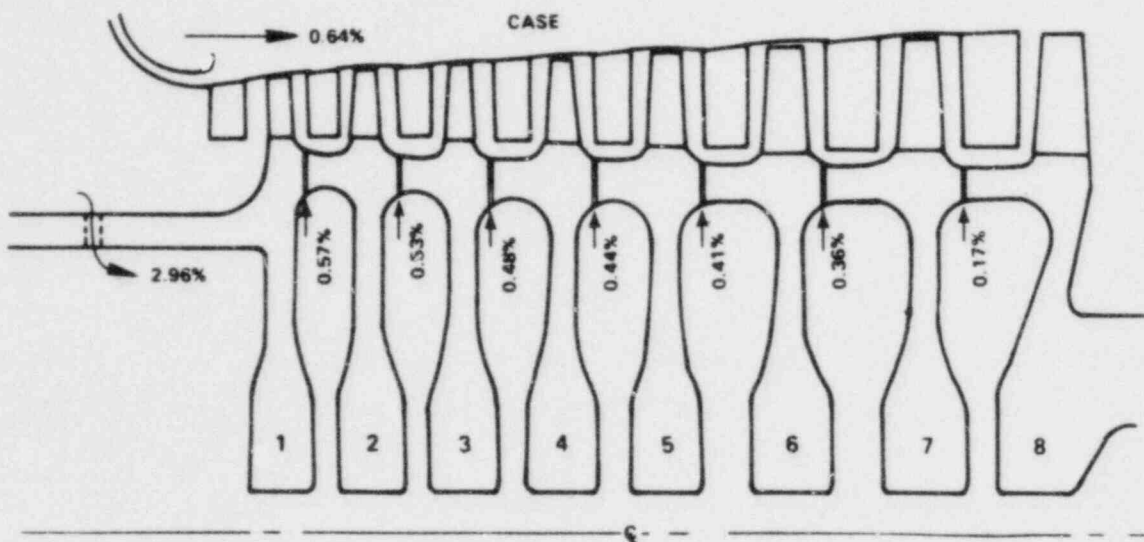


Fig. 18-26. Estimated secondary cooling flow distribution

TABLE 18-4(A)  
ESTIMATED GAS TEMPERATURES FOR COASTDOWN  
INITIATED BY REACTOR SCRAM

Time	Estimated Gas Temperature in Cavities (Rim O.D.) [°C (°F)]			
	Upstream Vane 2	Downstream Vane 2	Upstream Vane 8	Downstream Vane 8
Baseline 100% power 3600 rpm	Base	Base	Base	Base
t = 10 h 1970 rpm	- 121 - (250)	- 116 - (240)	- 93 - (200)	- 54 - (130)
t = 1 day 3180 rpm	- 71 - (160)	- 54 - (130)	- 54 - (130)	- 32 - (90)
t = 1½ day 2780 rpm	- 110 - (230)	- 143 - (290)	- 88 - (190)	- 93 - (200)

TABLE 18-4(B)  
ESTIMATED GAS TEMPERATURES FOR PLANT LOSS OF LOAD

Time	Estimated Gas Temperature in Cavities (Rim O.D.) [°C (°F)]			
	Upstream Vane 2	Downstream Vane 2	Upstream Vane 8	Downstream Vane 8
Baseline 100% power 3600 rpm	Base	Base	Base	Base
t = 80 s 3600 rpm	- 21 - (70)	- 99 - (210)	- 18 (0)	+ 16 + (60)
t = 180 s 3600 rpm	(a)	(a)	(a)	(a)
t = 299 s 3600 rpm	(a)	(a)	(a)	(a)

(a) These temperatures are approximately baseline since conditions are nearly the same.

times are expected to be very close to baseline. The maximum metal rim temperature is well below the allowable short-term level.

#### Single Loop Loss of Load with Overspeed

In the loops which continue to operate, the speed holds constant but the pressures in the turbine and compressor drop  $\sim 20\%$ . The differential pressure between the compressor outlet and turbine inlet appears to drop by about one-half that for the baseline 100% power point. This will reduce coolant gas flow in the inlet turbine stages while the hot gas ingestion temperature only drops slightly. A gas cavity temperature rise of  $49^\circ\text{C}$  ( $120^\circ\text{F}$ ) is estimated to occur near vane 2.

In the non-operating loop, the rotor initially overspeeds 16% and then drops to  $\sim 6\%$  of the design speed in 50 s. The differential pressure and flow in the turbine become very small. The compressor-turbine  $\Delta P \approx 0$  and thus precludes significant coolant flow. The initial, rapid, almost steep increase in temperature [to  $816^\circ\text{C}$  ( $1500^\circ\text{F}$ )] in the turbine exit could produce a rim temperature rise of  $\sim 10^\circ\text{C}$  ( $\sim 50^\circ\text{F}$ ). However, this effect is not as severe as the end point condition in which the turbine gas temperature appears to level out. The associated turbine rim temperature would increase since  $W_{\text{cool}} \approx 0$ .

Both operating and non-operating loops exceed the allowable rim temperature limit. (The long term is assumed after the transient end point conditions are established.) This could be reduced to tolerable rim temperature levels by controlling the end point turbine gas temperature.

#### Plant Loss of Coolant Water Flow

The initiating failure for this transient is the multiple shear rupture of the header at the pump discharge. Turbine speed begins to drop in 50 s and reaches  $\sim 5\%$  of design speed in 110 s.

The turbine and compressor differential pressures drop to 0 after 60 s, thereby reducing the compressor coolant flow to insignificant levels. The turbine inlet and exit gas temperatures reach 871°C (1600°F) in 100 s. This would bring the turbine rim temperature up to 871°C (1600°F) if allowed to "soak" at the temperature, since there is no coolant flow predicted at this point.

The 871°C (1600°F) temperature for the metal rim far exceeds the allowable level (long term assumed after the end point condition is reached). The excessive rim temperatures could be reduced to acceptable levels by maintaining sufficient coolant flow at the low-rpm point. This may require auxiliary equipment.

#### 18.3.12. Creep/Fatigue Interaction

The UTC gas turbine design system recognizes the existence of creep/fatigue interactions in the design of high-temperature components, e.g., turbine blades, vanes, and burner cans. Laboratory creep/fatigue testing of turbine blade materials (generally nickel-base alloys having low ductility) has shown that the Linear Damage Law is non-conservative. UTC has adopted a creep design system called "ductility exhaustion" which has exhibited good agreement with both laboratory tests and turbine blade field experience. Details of this method can be found in Ref. 18-1.

The method is based on the concept that there is a finite amount of ductility available (established by baseline thermal fatigue tests). A cycle by cycle evaluation of the ductility used and the ductility remaining is conducted with a digital computer program. In this analysis the total strain is composed of creep strain and fatigue strain converted to equivalent creep strain.

Strain range partitioning (SRP) was investigated for turbine blade design but was abandoned because of poor results. This may have been due to the fact that the closed, stabilized strain loop required for SRP

analysis is violated by the ever-increasing tensile creep strain caused by the rotational stresses. However, SRP is currently being employed to design burner cans.

In the current design of the HTGR-GT, no creep/fatigue analyses were conducted. This type of analysis can be performed only when finite element modeling of the turbine airfoil allows detailed thermal stress analysis. For preliminary conceptual studies, the guideline is that the total creep strain must be held to <1% over the life of the engine. Cooling schemes and material selections are chosen accordingly.

All secondary stresses are considered and used in low cycle fatigue analysis. For example, they would be used in the low cycle fatigue analysis of disk life, but would not be used in evaluating burst margins.

In general, the design of the high-temperature critical components of the HTGR-GT has been influenced more by long-time creep considerations than by either low cycle fatigue or high cycle fatigue.

### 18.3.13. Turbomachine Materials Selection Review

18.3.13.1. Summary. Materials selections for the HTGR-GT turbomachinery (Ref. 18-2) were based on a normal, i.e., oxidizing, gas turbine operating environment and were expected to be valid for the "inert" helium environment of the HTGR-GT. Subsequent testing in a simulated HTGR-GT helium coolant showed that the impurities in the helium interacted with many structural materials and resulted in appreciable degradation of their properties. In light of this information, the turbomachinery materials selections were reviewed and updated.

The susceptibility of some of the previously selected HTGR-GT turbomachinery materials to degradation, resulting from the interaction of the alloys with the impurities in the helium coolant, required a revision of

the original materials list. An updated list is shown in Table 18-5. The long design life (280,000 h) and lack of long-term compatibility data necessitate continuous re-evaluation of the selected materials as additional data become available. The materials problems would be alleviated if a shorter design life for the critical components were considered.

Some potential problems and concerns as well as suggested solutions are discussed in the remainder of this section. It is concluded that materials technology is currently available to resolve the problems associated with HTGR-GT materials requirements. However, extensive testing is necessary to provide a sufficient data base for the long design life requirements.

18.3.13.2. Areas of Concern. The original materials selected for the HTGR-GT are listed in Table 13-6. Recent HTGR-GT helium coolant compatibility data (Refs. 18-3, 18-4) and a better definition of the operating environment, e.g., sound level, presence of fission products, etc., indicate that some of the original selections would be unsuitable for this application. In addition, other potential problems and concerns have been identified which must be addressed. Specific areas of concern are as follows:

#### Existing Problems

1. Severe carburization of the Hastelloy X turbine inlet duct material, resulting from prolonged exposure to the impurities in the HTGR-GT helium at elevated temperatures (Ref. 18-3, 18-4).
2. Self-welding of materials in intimate contact at elevated temperatures.

TABLE 18-5  
 UPDATED HTGR-GT TURBOMACHINERY MATERIALS SELECTION

Components	Materials	
	Compressor	Turbine
Disks	Ladish D6AC low-alloy steel	Ladish D6AC low-alloy steel
Hubs	9Ni-4Co-0.2C steel	9Ni-4Co-0.2C steel
Blades	AMS 6414 (AISI 4340) low-alloy steel	PWA 658 (IN100) Ni-base alloy
Vanes	AMS 6414 (AISI 4340) low-alloy steel	PWA 1447 (MAR-M-247) Ni-base alloy
Cases	ASTM A-515 Gr 55 carbon steel	ASTM A-515 Gr 55 carbon steel
Mounts	ASTM A-387 Gr 12 } ASTM A-217 WC6 } low-alloy steels	ASTM A-387 Gr 12 }
Ducts		ASTM A-217 WC6 } low-alloy steels
Containment ring	AMS 5613 (AISI 410) stainless steel	AMS 5613 (AISI 410) stainless steel
Blade tip seals	AMS 5613 (AISI 410) stainless steel	AM5783 (Hastelloy S) coated <sup>(a)</sup>
High-temperature ducts	AMS 5613 (AISI 410) stainless steel	AM5783 (Hastelloy S) coated <sup>(a)</sup>
Insulation	AMS 5613 (AISI 410) stainless steel	PWA 385 (Kaowool)

<sup>(a)</sup> Coating to be determined.



### Anticipated Problems

1. Deterioration of the structural integrity of alloys of construction by fission product interactions (Refs. 18-5, 18-6).
2. Sonic fatigue of fibrous insulation and structural materials (Ref. 18-7).

### Additional Concerns

1. Long-term metallurgical stability of structural alloys exposed to elevated temperatures.
2. Extrapolation of mechanical property data to 280,000 h.
3. Manufacturing of large components.
  - a. Welded compressor and turbine rotors.
  - b. Compressor and turbine containment rings.
4. Strength margin for first and second stage turbine blade material.

Specific suggestions for resolving each of the above problems are discussed below.

#### 18.3.13.3. Suggested Solutions.

##### Carburization of Hastelloy X

Test results (Ref. 18-3, 18-4) indicate that Hastelloy X is inadequate for the turbine inlet duct material because it is susceptible to severe carburization in an HTGR-GT helium environment. In addition, it is metallurgically unstable and tends to embrittle when exposed for prolonged

periods of time to temperatures in the range of 649° to 982°C (1200° to 1800°F). The use of compatible cast alloys, e.g., IN100, for this application is impractical. Lack of experience ruled out the use of non-metallic materials. As a result, a coated high-temperature alloy is proposed for evaluation.

Hastelloy S is more stable than Hastelloy X and is recommended for evaluation as a substrate material. A simple aluminide, e.g., PWA 273, a rare earth aluminide (Ref. 18-8), and Ni-40Cr-3Al-2Ti are suggested for evaluation as carburization resistant coatings. The last composition has been evaluated at Pratt & Whitney Aircraft and found to have good oxidation and hot corrosion resistance. Its chemistry suggests that it will be carburization resistant as well. The recommended alloy is weaker than Hastelloy X, but this can be compensated for by design.

The oxide dispersion strengthened alloys MA956 and MA754 were also considered for inlet duct application. However, they have been tentatively dropped from consideration because of their tendency to form voids when exposed to temperatures above 760°C (1400°F) (Ref. 18-9). The effect of this phenomenon, the cause of which is unknown, on mechanical properties is being investigated.

#### Self-Welding

The use of suitable hard-face coatings on contacting surfaces exposed to elevated temperatures should eliminate this problem. A  $\text{Cr}_{23}\text{C}_6$ -NiCr coating has been shown to be a promising candidate (Ref. 18-4) and should be considered for gas turbine applications. Since the development of wear-resistant coatings for a helium environment is being actively pursued, it is highly probable that additional candidates will be identified.

### Fission Product Interaction

Although it has been demonstrated that the interaction of fission products with structural alloys can be quite detrimental (Refs. 18-5, 18-6), no data are available to indicate what effect fission products will have on the selected gas turbine materials in an HTGR-GT environment. The magnitude of this problem can be assessed only by a suitable test program.

### Sonic Fatigue

The predicted noise level in the HTGR-GT gas turbine (Ref. 18-10) is higher than the sound pressure level which is sufficient to fatigue aluminum and glass fiber panels (Ref. 18-7). The effect of this noise level on the selected gas turbine materials is unknown and would have to be determined by laboratory testing. Since a design study is currently under way to reduce the noise level of the gas turbine engine, action on this problem should be postponed until this study is completed.

### Long-Term Metallurgical Stability

Although metallurgical stability is taken into consideration when selecting materials for elevated-temperature applications, there is insufficient long-term experimental data to substantiate the selections for the 280,000-h design life. Testing currently under way at GA should provide the necessary substantiation.

### Extrapolation of Data to 280,000 Hours

The current UTC approach to extrapolating short-time data to predict long-term behavior is to use a modified Larson-Miller extrapolation. The modification consists of appropriately debiting the extrapolated values to give a more conservative Larson-Miller curve. This method has been proven to work well for other alloy systems for which long-term creep data are

available. However, the accuracy of any extensively extrapolated curve is questionable, and a minimum of 30,000 h of test time would be desirable to improve the probability of correctly predicting a 280,000-h creep life.

#### Manufacturing of Large Components

Welded Compressor and Turbine Rotors. The material originally selected for this application is Ladish D6AC high-strength low-alloy steel. The high carbon content (0.45%) and lack of D6AC welding experience at Pratt & Whitney Aircraft and the Power Systems Division of UTC prompted a review of the suitability of this selection.

The Chemical Systems Division of UTC has considerable experience in welding this alloy. They have developed gas tungsten arc welding (GTAW) schedules which have been used successfully in D6AC rocket motor case manufacture. They also have been successful in electron beam welding this alloy. Electron beam welding of the D6AC alloy has been well documented in the literature (Refs. 18-11, 18-12). The consensus is that this alloy can be readily electron beam welded in thick sections provided the weld joints are preheated. Weld tensile properties equivalent to the parent metal properties can be achieved after heat treatment.

In view of the above, it is concluded that the D6AC alloy is a suitable candidate for the welded rotor. Another candidate, a 9Ni-4Co steel, has been selected as an alternate should improved weldability and a higher-temperature capability, at an equivalent strength level, become desirable. However, the 9Ni-4Co alloy is more expensive than D6AC.

Compressor and Turbine Containment Rings. The size [2.4 m (8 ft) o.d. x 3.4 m (11 ft) long] of the containment rings is expected to present some manufacturing problems, but the ability to forge rings this large is considered to be within the state of the art. For example, the Ladish Company and Standard Steel have been identified as manufacturers having the

capability of fabricating parts of this size. A development effort may be required to define the manufacturing techniques and heat treatments needed to optimize the end product.

#### Turbine Blade Material

The IN100 nickel-base alloy originally selected for the turbine blades and vanes has been shown (Ref. 18-3) to be one of the materials most resistant to the impurities in the HTGR-GT helium coolant. Structural analysis, based on extrapolated data, indicates that this alloy has the required creep strength, but because of the extensive extrapolation involved, an additional safety margin would be desirable, particularly for the first and second stage turbine blades. As a result, two other state-of-the-art alloys were evaluated. Creep curves generated by Pratt & Whitney Aircraft show that both MAR-M-247 (PWA 1447) and the directionally solidified modified MAR-M-200 (PWA 1422) alloys have strength equivalent to that of the IN100 (PWA 658) alloy at 843°C (1550°F) and would be suitable airfoil candidates. Since the PWA 1447 alloy is easier to manufacture than the PWA 1422 alloy, the former has been selected as an alternate to the IN100 turbine blade and vane material. A program is currently under way at Pratt & Whitney Aircraft to develop single crystal superalloys for turbine airfoils (Ref. 18-13). This program may yield suitable airfoil materials for the HTGR-GT gas turbine and will be closely monitored.

The development of HTGR-GT gas turbine materials is by no means complete, and many questions must still be answered and problems resolved by laboratory testing. However, there are currently a number of candidate materials which have an excellent chance of meeting the HTGR-GT turbomachinery requirements. These are listed in Table 18-6, and their chemical compositions are given in Table 18-7. The very long HTGR-GT design life requires the use of extensive extrapolation to predict alloy behavior. These predictions should be continuously evaluated as more test data become available. To alleviate critical materials problems, a shorter design life should be considered.

TABLE 18-6  
INITIAL HTGR-GT TURBOMACHINERY MATERIALS SELECTION

Components	Materials	
	Compressor	Turbine
Disk } Hubs } Seals }	Ladish D6AC low-alloy steel (vacuum consumable electrode melted)	Ladish D6AC low-alloy steel (vacuum consumable electrode melted)
Blades } Vanes }	AMS 6414 (AISI 4340) low-alloy steel (consumable electrode melted)	PWA 658 (IN100) Ni-base alloy (vacuum melted)
Cases	ASTM A-515 Gr 55 carbon steel	ASTM A-515 Gr 55 carbon steel
Mounts Ducts	ASTM A-387 Gr 12 } ASTM A-217 WC6 } low-alloy steels	ASTM A-387 Gr 12 } ASTM A-217 WC6 } low-alloy steels
Containment ring	AMS 5613 (AISI 410) stainless steel	AMS 5613 (AISI 410) stainless steel
Blade tip seals High-temperature ducts	AMS 5613 (AISI 410) stainless steel AMS 5613 (AISI 410) stainless steel	PWA 1038 (Hastelloy X) Ni-base alloy PWA 1038 (Hastelloy X) Ni-base alloy
Insulation	AMS 5613 (AISI 410) stainless steel	PWA 385 (Kaowool)

TABLE 18-7  
 CHEMICAL COMPOSITIONS OF CANDIDATE MATERIALS FOR HTGR-GT TURBOMACHINERY

	C	Cr	Ni	Mo	Mn	Co	Al	Ti	Fe	Other
IN100	0.18	9.5	Bal.	3.0	--	15.0	5.5	4.8	--	0.01 B, 0.6 Zr, 1.0 V
MAR-M-247	0.16	8.2	Bal.	0.6	--	10.0	5.5	1.0	--	3 Ta, 0.02 B, 0.09 Zr, 1.5 Hf
Hastelloy X	0.10	22.0	Bal.	9.0	0.50	1.5	--	--	18.5	0.6 W, 1.0 Si
Hastelloy S	0.02	15.8	Bal.	15.2	0.70	2.0	0.30	--	3.0	0.5 Si, 0.02 B, 0.05 La, 10 W
AISI 410	0.10	12.5	0.50	0.50	1.0	--	--	--	Bal.	1.0 Si
Ladish D6AC	0.45	1.0	0.5	1.0	0.75	--	--	--	Bal.	0.1 V
HP9-4-20	0.20	0.75	9.0	--	0.30	4.5	--	--	Bal.	0.1 V
AISI 4340	0.40	0.75	1.8	0.25	0.70	--	--	--	Bal.	0.25 Si
ASTM A-515 Gr 55	0.20	--	--	--	0.70	--	--	--	Bal.	0.2 Si
ASTM A-387 Gr 12	0.17	1.0	--	0.50	0.50	--	--	--	Bal.	0.2 Si
ASTM A-217 WC6	0.20	1.25	--	0.50	0.60	--	--	--	Bal.	0.6 Si

18-60

#### 18.3.14. Turbomachine Development Program

18.3.14.1. Program Approach. The HTGR-GT turbomachine will inherit considerable design system and development technology from existing aircraft and industrial gas turbines. The design concept will be conservative without forfeiting the fundamental efficiency and reliability required for utility economics.

The sophisticated design systems developed for aircraft and industrial gas turbines will yield an engine design of assured success. There will be little or no need to extend the fundamental state of the art, so feasibility tests will not be required. There will be a need to conduct a design system verification program for components and for the system to the extent practical. This program will assure that all design requirements have been met and will provide a data base for licensing activities.

18.3.14.2. Testing Required. The HTGR-GT turbomachine is a reasonable extrapolation in size from current industrial power plants, such as the FT-50 or the Frame 7. However, the closed cycle, helium working fluid configuration and the size present a unique test facility requirement. A number of the turbomachine aspects must be tested and verified with the helium working fluid. These include:

1. Bearings and seals.
2. Compressor performance rig.
3. Turbine performance rig.
4. Materials compatibility.

Other tests may be accomplished without a helium environment. These include:

1. Disk and rotor spin and burst tests.
2. Complete rotor spin test.
3. Containment ring tests.
4. Flow distribution tests.



These tests would be run in air or in a vacuum. A vacuum would be pulled on spin test rigs to minimize drive power requirements.

18.3.14.3. Helium Testing. The turbomachinery supplier would design and build a test facility which would provide a large-volume, temperature-controlled helium stream. The facility would provide flows to 54.4 kg/s (120 lb/s) or 1/10 the rated PCL flow. This flow would be sufficient to test 1/10 scale compressors and turbines. These rigs would be run in time sequence so as to provide economy in the helium supply system. Performance mapping of these components requires relatively short-duration tests which lend themselves to sequencing.

Bearing and seal tests would include both performance and life characteristics tests. Because of the small quantities of helium required for buffering and for simulating main loop pressure variations (a few pounds per second), these tests would be run in parallel with the compressor and turbine tests.

18.3.14.4. Bearing and Seal Testing. The bearing and seal configurations in the HTGR-GT turbomachine are designs that have been successfully operated in other applications. In the HTGR-GT application, there is a very stringent oil leakage limit [ $0.028 \text{ m}^3$  ( $1 \text{ ft}^3/\text{yr}$ )]. Oil ingress has a very harmful impact on core and heat exchanger operation. In addition, the bearing diameters are large and the DN factor (surface speed) is high. The generator drive shaft seal is a safety class component because it seals a rotating penetration through the PCRV and prevents contamination of the secondary containment building.

For these reasons, extensive testing is planned to optimize bearing and seal configurations and flows and to provide verification of the integrity of the designs. The test rigs will be operated at design conditions and under extreme transients and off-design conditions to assure that adequate margins are available. After the completion of tests that verify the designs meet all performance parameters, endurance testing will be performed to identify and eliminate any random or wearout failure modes.

The two main shaft bearings are tilted pad journal bearings. These main support bearings are identical, so only one journal bearing rig is planned. This rig will also include the double-buffered, labyrinth seal arrangement and the lubricating and helium cleanup system.

The thrust bearing is a double-acting tilted pad design. It is designed to handle the rotor thrust plus loads associated with an earthquake shock up to 6.7 on the Richter scale. The thrust bearing is located at the compressor end of the turbomachine near the PCRV shaft penetration. Its lubricating system is located in the secondary containment building so as to minimize oil ingress problems.

The PCRV penetration seal is a multiple piston ring, floating oil lubricated seal. It incorporates a hydraulically operated shutdown face seal. It is a safety class component.

To achieve further economy, it is planned to use common drives for the bearing and seal rigs. Although the thrust bearing rig does not require a helium supply, it will be operated along with the other bearing and seal rigs so it can share common resources of equipment, instrumentation, techniques, and engineering coverage.

18.3.14.5. Compressor and Turbine Performance Tests. The turbomachinery computer model gas dynamic analysis for the compressor and turbine design accurately describes the required gas path configuration. Although experience with numerous power plants designed using this computer program has shown excellent correlation between calculated and actual results, compressor and turbine performance tests are included in the HTGR-GT program. Compressor and turbine efficiency and compressor surge margin are very critical to the success of the installation. Also, although design with helium as a working fluid poses serious concerns, actual experience is very limited and design assumptions should be proven.

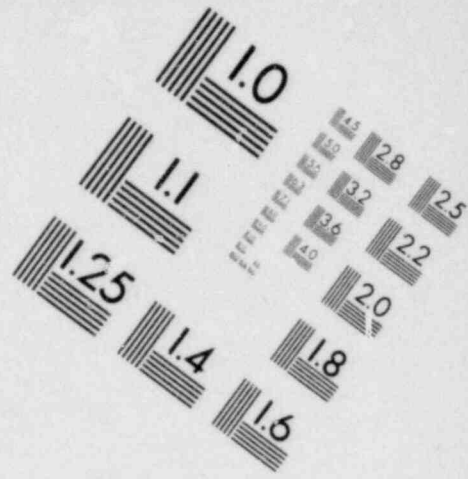
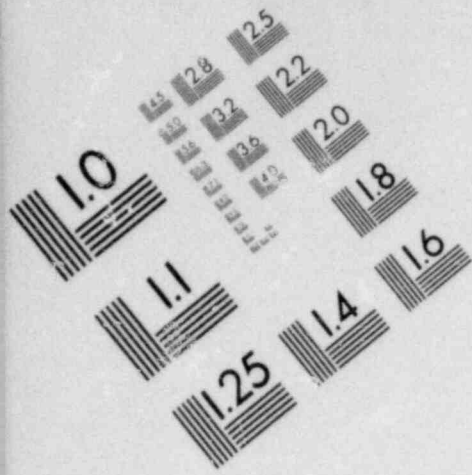
Gas dynamic design considerations readily yield to scaling effects. For economic and practical considerations, 1/10 scale helium compressor and turbine rigs would be built and run to confirm design efficiencies and compressor surge margin.

Compressor and turbine performance mapping tests will be performed so that pressure ratios versus corrected flow may be plotted for various rotor speeds. By measuring these parameters in test rigs as opposed to engine operation, performance limits off the normal operating line may be evaluated.

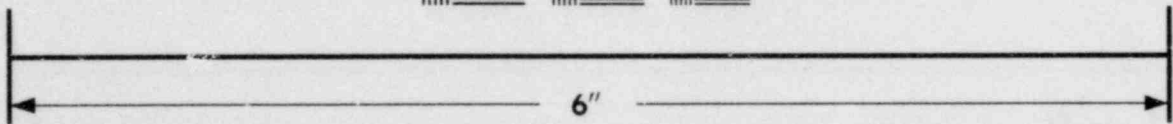
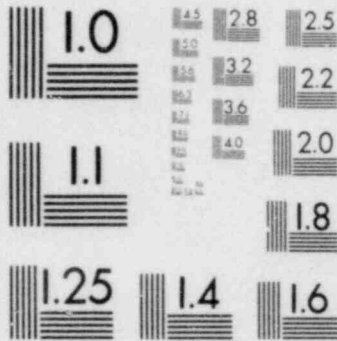
18.3.14.6. Rotor Stress Tests. Stresses in rotors do not scale well. Some information on stress concentration effects is obtainable by scaled rig tests, but the expense is not justified. Therefore, a spin test program on critical full-scale disks and rotor segments will be conducted to verify the design margins. The disks and rotor sections will be tested in a vacuum to minimize drive costs and to allow sufficient overstress conditions.

Containment of rotor failures is a plant safety consideration. Both compressor and turbine sections are shrouded by heavy wall containment rings designed to prevent blade, disk, or rotor segment failures from propagating to the cavity liner or other parts of the installation. Containment rings will be tested as part of the blade, disk, and rotor segment spin tests to failure. These tests are normally conducted in pits with the shaft in a vertical orientation. Data from these tests will be critical for licensing considerations.

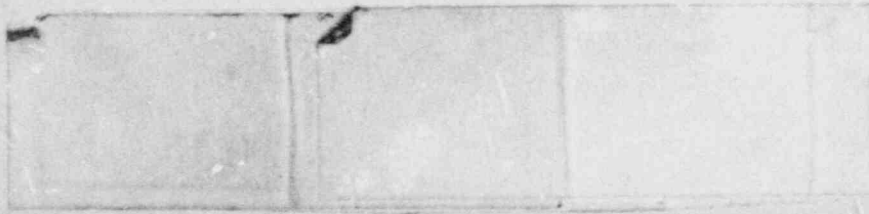
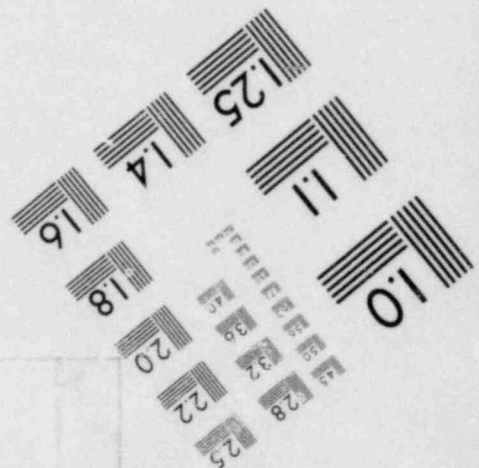
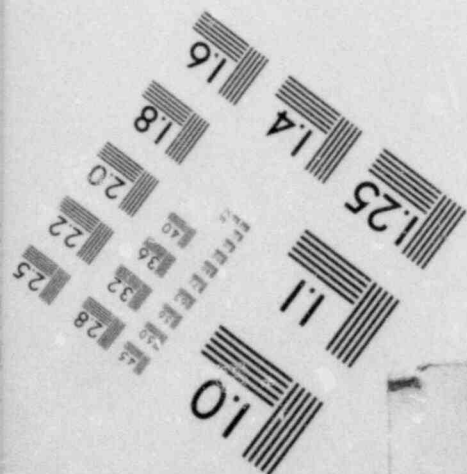
A rig is planned for balancing complete rotors. It will simulate the dynamic environment, including the three main shaft bearings and their support cases. The rotor will be shrouded so that a vacuum can be drawn to reduce drive motor capacity requirements to a practical level. Vibration tests will be performed after balancing to verify design analysis of critical speed mode and vibration energy levels.



**IMAGE EVALUATION  
TEST TARGET (MT-3)**



**MICROCOPY RESOLUTION TEST CHART**



18.3.14.7. Diagnostic Instrumentation. Both digital and analog simulations are used in design, operation, checkout, and training activities. Condition monitoring instrumentation and response systems warn of and control unwanted excursions. These include vibration, strain gauge, pressure, and temperature monitoring of all critical parameters. A preset response to out-of-limits operation is programmed.

18.3.15. Turbomachine/Generator Development Schedule

A development schedule for the gas turbine and generator and their associated ancillaries was prepared (see Fig. 18-27). This schedule was made consistent with GA requirements. The major considerations included:

1. Phase I - Program Definition in FY-80.
2. Phase II - Conceptual Design in FY-81 and FY-82.
3. Phase III - Detailed Design and Licensing in FY-83 through FY-87.
4. Phase IV - Construction and Startup in FY-88 through FY-95.

18.3.16. Turbomachine/Generator Development Cost

The costs for development of the turbomachine and generator were estimated. These costs are shown in Table 18-8 in relation to the development schedule.

Construction of facilities required for the component development program is estimated to cost approximately \$50 M. Construction would be completed by FY-84, with conceptual design of the facilities starting in FY-80. This cost is a rough estimate to be used for planning purposes only.

18.3.17. Preliminary Evaluation of Impact of Codes and Licensing Criteria on Turbomachinery Design

Many existing codes (NRC, FAA, ASME, and ANSI) have sections that are applicable to the HTGR-GT turbomachine. The chances for misinterpretation or misapplication are many because the codes were all written for other

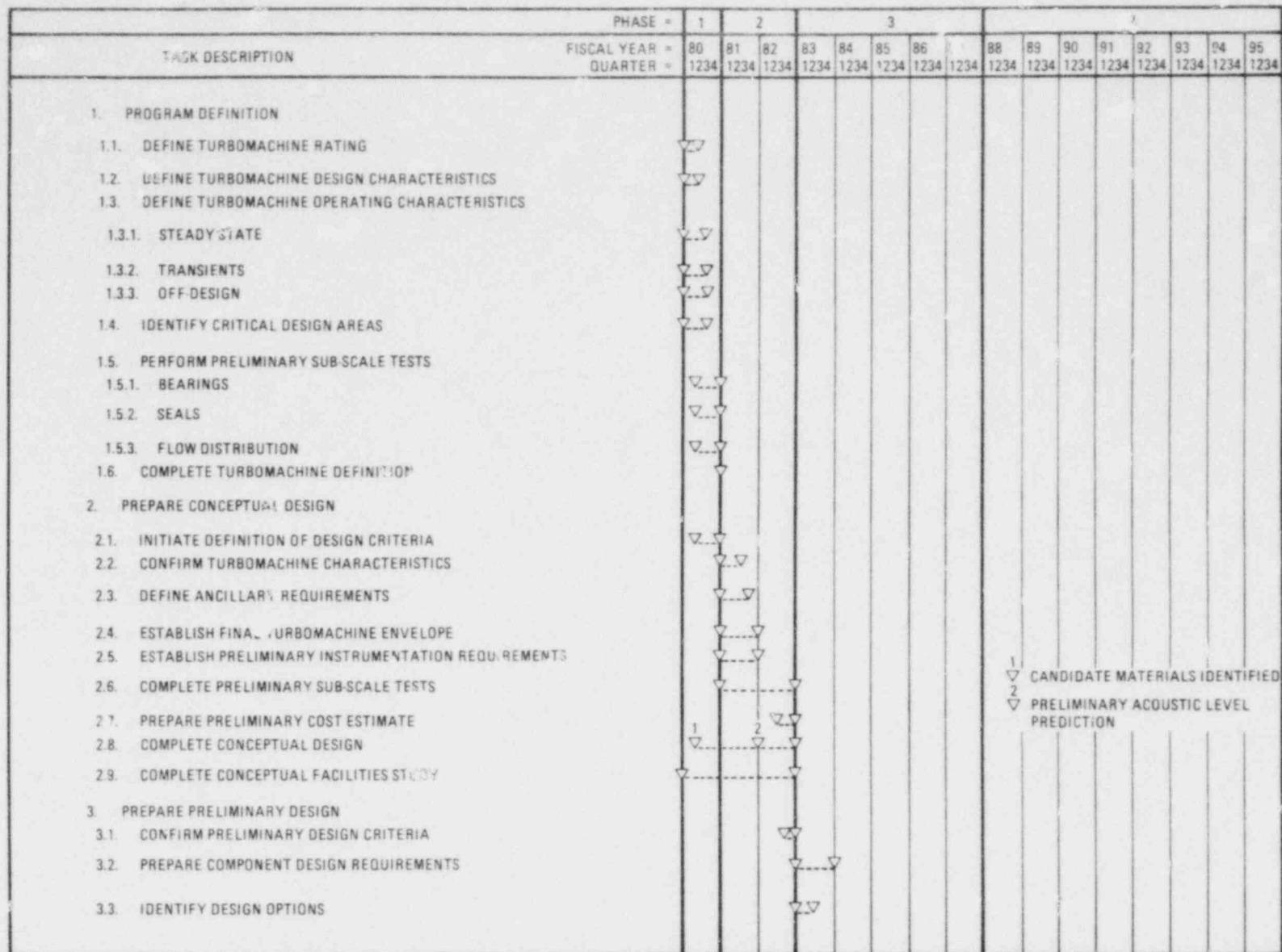


Fig. 18-27. 400-MW(e) HTGR-GT turbomachine/generator development schedule (sheet 1 of 7)

18-67

TASK DESCRIPTION	PHASE =																
	1			2			3										
	FISCAL YEAR =	80	81	82	83	84	85	86	87	88	89	90	91	92	93	94	95
QUARTER =	1234	1234	1234	1234	1234	1234	1234	1234	1234	1234	1234	1234	1234	1234	1234	1234	1234
3.4. SELECT DESIGN																	
3.4.1. PERFORM ANALYTICAL STUDIES				▽	▽												
3.4.2. PROVIDE MODELS																	
3.4.2.1. MOCKUP				▽	▽												
3.4.2.2. COMPUTER MODEL				▽	▽												
3.5. IDENTIFY AND RESOLVE CRITICAL DESIGN AREAS																	
3.5.1. JOURNAL BEARINGS				▽	▽												
3.5.2. THRUST BEARING				▽	▽												
3.5.3. DRIVE SHAFT SEAL				▽	▽												
3.5.4. BEARING COMPARTMENT SEALS AND BUFFERING SYSTEM				▽	▽	3											
3.5.5. OUTER SEALS				▽	▽												
3.5.6. REMOTE INSTALLATION AND REMOVAL				▽	▽												
3.5.7. COMPRESSOR																	
3.5.7.1. SURGE				▽	▽												
3.5.7.2. EFFICIENCY				▽	▽												
3.5.7.3. FLOW				▽	▽												
3.5.8. TURBINE																	
3.5.8.1. EFFICIENCY				▽	▽												
3.5.8.2. FLOW				▽	▽												
3.5.8.3. COOLING				▽	▽												
3.5.9. CONTAINMENT RINGS				▽	▽												
3.5.10. DUCT FLOW DISTRIBUTION																	
3.5.10.1. COMPRESSOR INLET				▽	▽												
3.5.10.2. COMPRESSOR EXIT				▽	▽												
3.5.10.3. TURBINE INLET				▽	▽												
3.5.10.4. TURBINE EXIT				▽	▽												

3  
 ▽ ROTOR AND SEAL FAILURE ANALYSIS  
 • OIL AND WATER INGRESS STUDIES

Fig. 18-27. 400-MW(e) HTGR-GT turbomachine/generator development schedule (sheet 2 of 7)





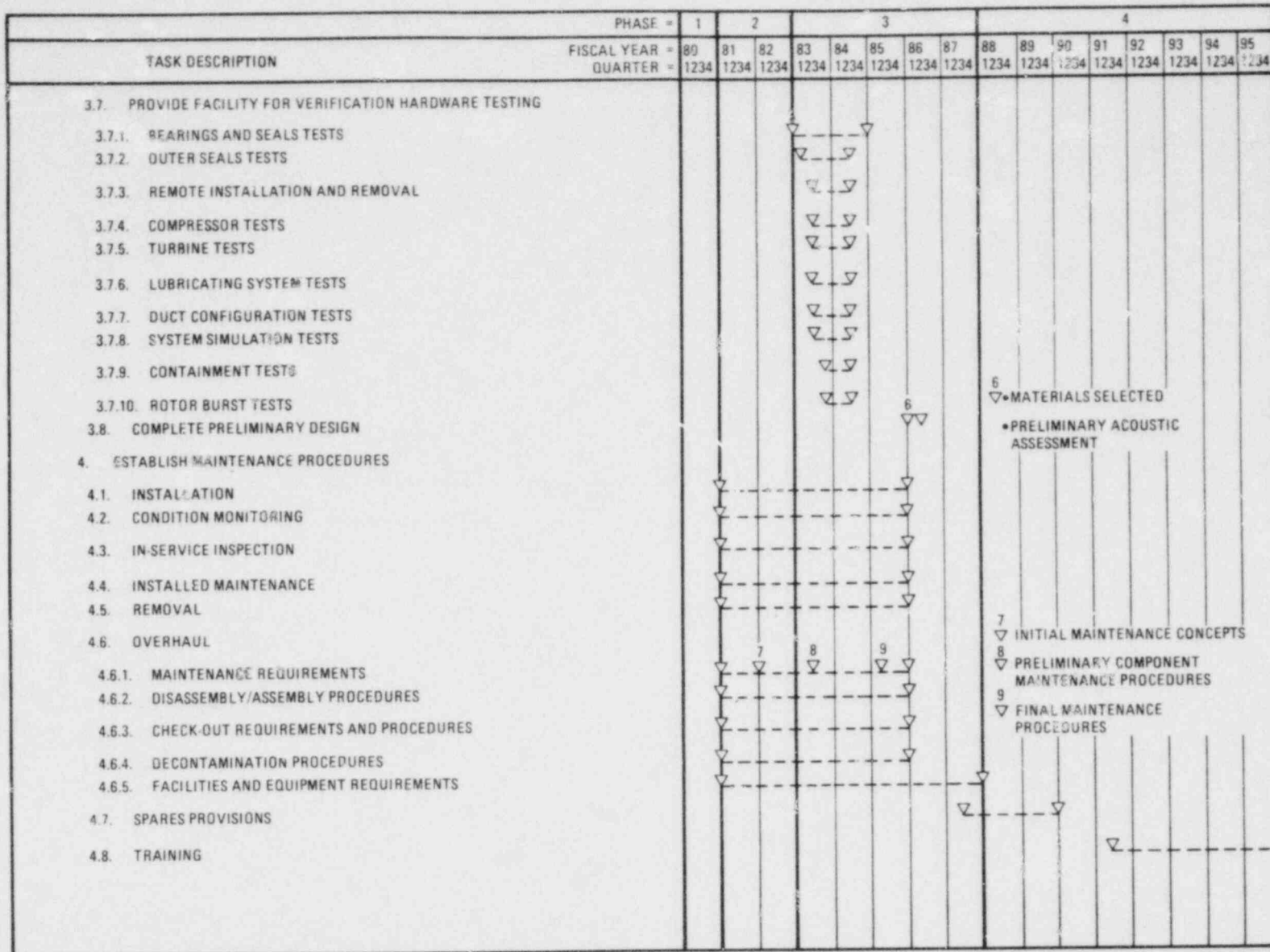


Fig. 18-27. 400-MW(e) HTGR-GT turbomachine/generator development schedule (sheet 4 of 7)

18-70

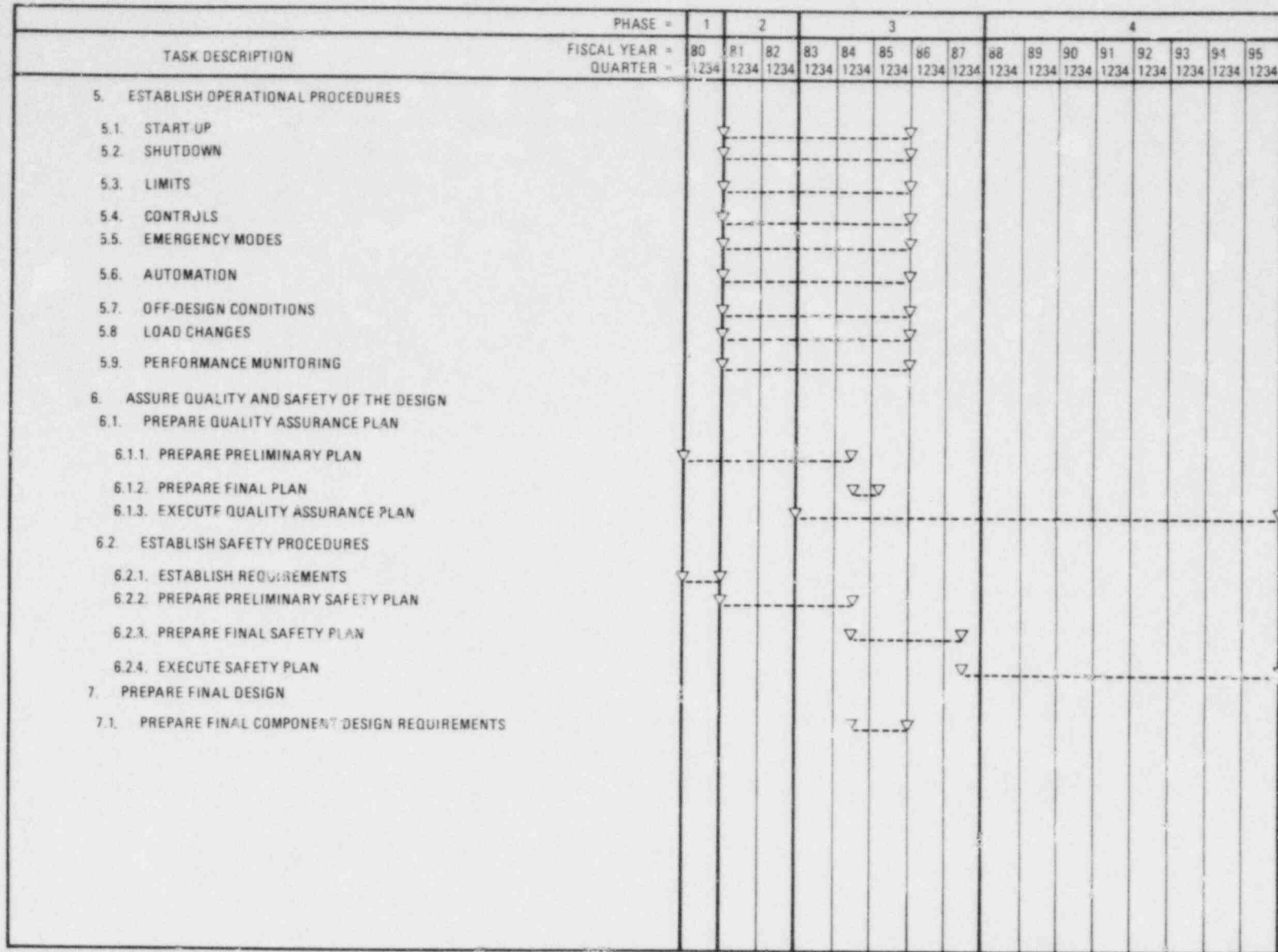


Fig. 18-27. 400-MW(e) HTGR-GT turbomachine/generator development schedule (sheet 5 of 7)

18-71

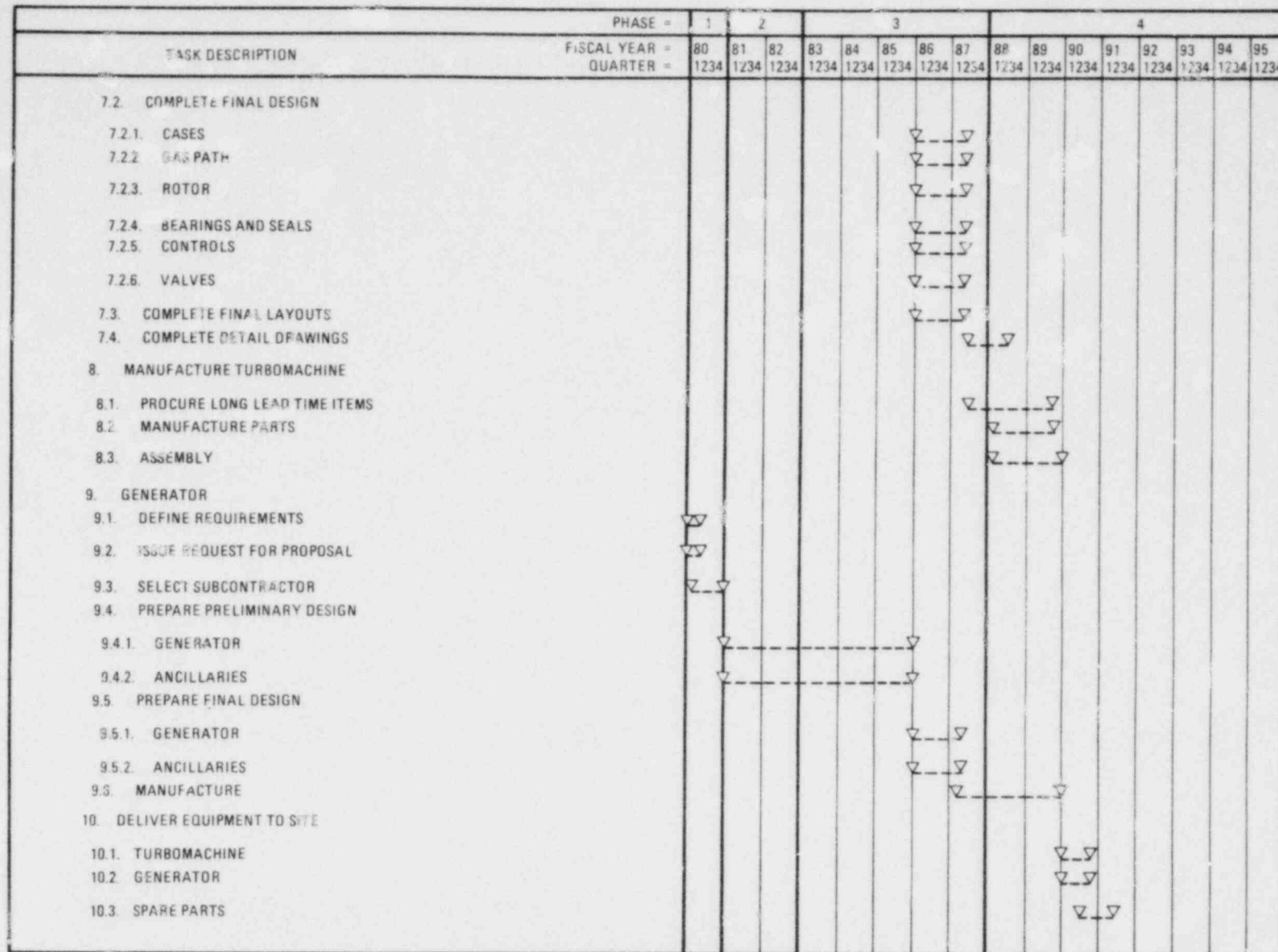


Fig. 18-27. 400-MW(e) HTGR-GT turbomachine/generator development schedule (sheet 6 of 7)

18-72

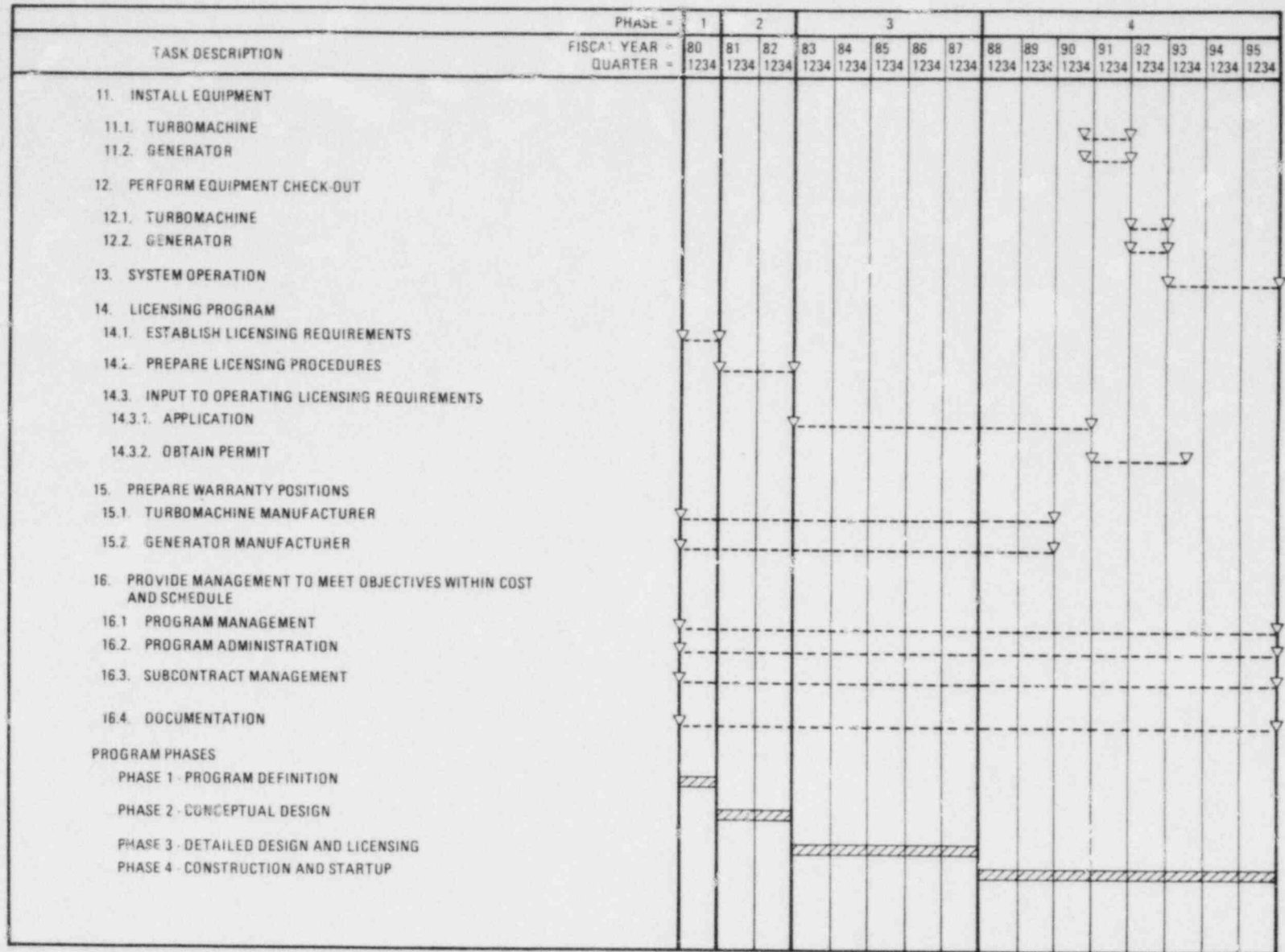


Fig. 18-27. 400-MW(e) HTGR-GT turbomachine/generator development schedule (sheet 7 of 7)

TABLE 18-8  
400-MW(e) HTGR-GT TURBOMACHINE/GENERATOR  
DEVELOPMENT COST (1979 DOLLARS)<sup>(a)</sup>

---

A. Development Program - \$ Millions (including special tooling and special test equipment)

---

	<u>Turbomachine</u>	<u>Generator</u>
1980	1	0.1
1981	1.6	0.1
1982	2.7	0.1
1983	4.7	0.1
1984	9	0.2
1985	10	0.2
1986	14	0.2
1987	22	0.3
1988	33	0.4
1989	14	0.3
1990	4	0.2
1991	1	0.2
1992	1	0.1
1993	1	0.1
1994	1	0.1
1995	1	0.1
	<hr style="width: 50%; margin: 0 auto;"/> \$121 M	<hr style="width: 50%; margin: 0 auto;"/> \$2.8 M

---

B. Cost of Equipment To Be Delivered to the Site - \$ Millions

---

Turbomachinery	11.4
Generator	10.5
Auxiliaries	<hr style="width: 50%; margin: 0 auto;"/> 1.1
Total per 400-MW(e) Set	\$23.0 M

---

<sup>(a)</sup> These costs were estimated in accordance with FY-79 work. They are based on conceptual design information. They are not a quotation and should be used for planning purposes only.

equipment or other applications. It is planned that a specific code document which excerpts, restates, and organizes all the requirements will be prepared and negotiated for rigorous application to the preliminary and final design of the turbomachine.

Design activity to date has utilized standards for FAA certification, including FAR33, "Air Worthiness Standards: Engines." Industrial turbomachines were designed to meet specific utility specifications. These have also been used as a guide for conceptual design activity of the HTGR-GT turbomachine.

The purpose of this task was to make a preliminary review of the additional codes which must be addressed. Adherence to these codes is necessary to obtain required licensing for operation. The results of this preliminary review are summarized below.

18.3.17.1. NCR General Design Criteria for Nuclear Power Plants:

Criterion 1, Quality Standards and Records. The quality assurance program used during the design, development, and manufacture of the HTGR-GT turbomachine must be consistent with CFR10 Part 50, Appendix B. Applicable ASME and ANSI 45 standards must also be complied with.

18.3.17.2. NRC General Design Criteria for Nuclear Power Plants:

Criterion 2, Design Bases for Protection Against Natural Phenomena. Consideration of seismic events must be included in the turbomachine design. Both the shaft and thrust bearing designs must include the additional seismic loads. A flexible coupling between the turbomachine and generator will accommodate some relative displacement between these two major pieces of equipment. Safe shutdown after the seismic occurrence is essential.

18.3.17.3. NRC General Design Criteria for Nuclear Power Plants:

Criterion 4, Environmental and Missile Design Bases. This criterion requires that structures, systems, and components of nuclear power plants important to safety be protected against the effects of missiles that might result from equipment failures. Failure of a turbomachine turbine

disk could result in high-energy missiles, since turbine disks have large masses and rotate at relatively high speeds. The present WIGR-GT turbomachine minimizes the probability of disk failure through conservative design margins and incorporation of a welded rotor. In addition, the system includes overspeed protection.

The following areas of turbine rotor integrity must be addressed:

1. Material selection.
2. Fracture toughness.
3. High-temperature properties.
4. Preservice inspection.
5. Turbine disk design.
6. ISI.

In considering the above, the NRC Standard Review Plan, Section 10.2.3, Turbine Disk Integrity, should be used as a standard.

In addition to the above measures to assure disk integrity, the turbomachine overspeed protection system should be completely redundant. This redundancy should extend to both instrumentation and controls.

In the unlikely event of a disk or rotor segment failure, large, high-energy missiles could be produced. The turbomachine design addresses containment of these particles. Single piece rings have been included around both the compressor and turbine rotors. The standards to be considered for these containment rings should be NCR Regulatory Guide 1.115 and Standard Review Plan 3.5.3, Turbine Missiles.

18.3.17.4. NRC General Design Criteria for Nuclear Power Plants. The following criteria should be addressed:

1. Criterion 30, Quality of Reactor Coolant Pressure Boundary.

2. Criterion 31, Fracture Prevention of Reactor Coolant Pressure Boundary.
3. Criterion 32, Inspection of Reactor Coolant Pressure Boundary.
4. Criterion 33, Reactor Coolant Pressure Boundary Penetrating Containment.

These four criteria should be imposed on the turbomachine shaft seal at the PCRV interface. This seal is a safety class item.

18.3.17.5. CFR 10 Part 20: Standards for Protection Against Radiation.

The turbomachine design must accommodate maintenance which is consistent with permissible levels of radiation as set forth in this standard. Both preliminary forms of maintenance, i.e., in situ, including in-service inspection, and on-site overhaul after turbomachine removal, are significantly impacted by the turbomachinery contamination level. The contamination level will determine if maintenance procedures can be performed "hands-on" or if remote handling is required.

18.3.17.6. CFR 10 Part 50.55a: Codes and Standards. To the extent applicable, the following codes and standards should be imposed on the turbomachine design:

1. ASME Boiler and Pressure Vessel Code, Section III -- for pressure parts.
2. Power Piping Code, ANSI B31.1 -- for pressure piping.
3. ASME Code for Pumps and Valves for Nuclear Power and Power Piping Codes, ANSI B31.1 -- for pumps and valves.
4. Criteria for Protection Systems for Nuclear Power Generating Stations, IEEE 279 -- for protection systems.



#### 18.4. REFERENCES

- 18-1. "Ductability Exhaustion for Prediction of Thermal Fatigue and Creep Interaction," in "Fatigue at Elevated Temperatures," ASTM Special Publication STP 520, p. 625.
- 18-2. Rosenwasser, S. N., and W. R. Johnson, "Gas-Turbine HTGR Materials Screening Test Program Interim Report," ERDA Report GA-A13931, General Atomic Company, June 30, 1976.
- 18-3. Rosenwasser, S. N., and W. R. Johnson, "Gas Turbine and Advanced HTGR Materials Screening Test Program, 10,000-Hour Results and Semiannual Progress Report for the Period Ending March 31, 1977," ERDA Report GA-A14407, General Atomic Company, July 1977.
- 18-4. "HTGR General Technology Program Quarterly Progress Report for the Period Ending July 31, 1978," DOE Report GA-A15006, General Atomic Company, August 1978.
- 18-5. Maiya, P. S., and D. E. Busch, "Grain-Boundary Penetration of Type 316 Stainless Steel Exposed to Cesium or Cesium and Tellurium," Met. Trans., **6A**, 409 (1975).
- 18-6. Aitken, E. A., and M. G. Adamson, "Recent Advances in Delineation of the Mechanism of Intergranular Attack in Stainless Steel by Fission Products," ANS Trans. **23**, 153 (June 1976).
- 18-7. Hayes, J. A., "Sonic Fatigue Tolerance of Glass Filament Structure: Experimental Results," North American Aviation Technical Report AFFDL-TR-6678, December 1966.
- 18-8. Long, R. H., M. C. Sze, and H. Unger, "Aluminum-Rare Earth Coating Counters Corrosion Failures," Metal Prog. **107**(2), 52-53 (1975).
- 18-9. Evans, J., and M. Gell, "Materials for Advanced Turbine Engine," Contract NAS3-20072 Quarterly Report, Pratt & Whitney Aircraft Group, Commercial Products Division, July 31, 1979.
- 18-10. Sofrin, T. G., "400 MW High Temperature Gas-Cooled Reactor Turbomachinery Noise Estimates," United Technologies Corporation, April 4, 1979.

- 18-11. McGregor, W. P., A. G. Metcalfe, and J. R. Warren, "Electron Beam Welding of Thick Sections," Air Force Materials Laboratory Report AFML-TR-69-198, August 1969.
- 18-12. Williams, A. J., and C. F. Martin, "Properties of Electron Beam Welds in Ultra High Strength Steels," Publication No. U2537, Chico Corporation, March 23, 1964.
- 18-13. Nguyen-Dinh, X., and D. N. Duhl, "Single Superalloy Turbine Airfoils for Marine Gas Turbine Engines," Pratt & Whitney Aircraft Group, Government Products Division, Report FR-12124, August 10, 1979.

## 19. TURBOMACHINE REMOTE MAINTENANCE

### 19.1. SCOPE

The purpose of this task during FY-79 was to study the remote maintenance tooling requirements for a contaminated turbomachine and to determine the impact that this remote tooling has on the turbomachinery.

### 19.2. SUMMARY

Initial results are presented from a design study to describe procedures, equipment, and facilities necessary to remotely inspect, overhaul, and repair a radioactively contaminated 400-MW(e) nuclear gas turbine after it has been removed from its operating location within the PCRV.

The primary objective of this effort has been to define the impact of remote maintenance on the current gas turbine design and to familiarize gas turbine designers with remote methods and techniques that are often utilized in the maintenance of radioactively contaminated nuclear equipment. This will allow the turbine designer to consider remote handling and remote tooling early in the design of the turbomachinery and will assist in minimizing the time necessary to complete inspection and maintenance operations. Similarly, remote handling equipment engineers were familiarized with the unique requirements of gas turbines, thus establishing their goals for support of turbomachine maintenance.

An additional objective of this study has been to develop a pictorial sequence of disassembly operations showing major fixtures and facility equipment as the basis for a remote maintenance facility design. This

study also identified major tooling and repair facility equipment necessary to perform the basic remote disassembly operations.

It should be recognized that a detailed design should not proceed until the remote equipment designer and the gas turbine designer have considered interface requirements and upgraded basic concepts accordingly. Section 19.3.5 identifies items for additional development and issues requiring resolution prior to detailed design of turbomachinery or a repair facility.

The remote operations, tooling, and estimated maintenance items described herein will be improved as the detailed machine design evolves. It is noteworthy that Brown Boveri & Cie (BBC) estimated that only 775 h would be required for a complete turbine overhaul outage with the much larger [816-tonne (900-ton)] gas turbine proposed for the HHT demonstration project, a concept very similar to the HTGR-GT concept. The GA maintenance study resulted in 2832 h required for the smaller 400-MW(e) turbomachinery.

### 19.3. DISCUSSION

#### 19.3.1. Introduction

In the development of the HTGR-GT, the need for remote maintenance of the turbomachinery was recognized since immersion of a large gas turbine directly into the primary circuit of a high-temperature radioactive system results in significant contamination of the turbomachinery. Periodic inspection and overhaul of the gas turbine, as well as unplanned repairs or modifications, will require removal of the turbomachinery from the PCRV, shielded transport to a maintenance facility, and remote disassembly of the machine. The purpose of this study was to define the impact of remote maintenance on the gas turbine design. The procedures, methods, tooling, and equipment that might be necessary to maintain the gas turbine at an onsite remote maintenance facility were considered.

The degree to which gas turbine maintenance should be performed remotely, or whether fully remote maintenance is most cost effective, has not yet been established. A fully remote procedure for complete disassembly of the gas turbine as an initial approach is described herein. As the design progresses, it may be determined that fully remote maintenance capability should be provided.

Provisions for contact maintenance and decontamination of the gas turbine will depend on detailed analysis of many factors, including equipment reliability, effects of decontamination, materials development, exposure guidelines and regulations, outage time and maintenance time goals, plant staffing requirements, capital investments, and experience at other facilities.

The approach used in this study has been as follows:

1. GA and UTC joint determination of gas turbine disassembly operations and their sequence.
2. Development of conceptual remote maintenance procedures and equipment design input.
3. Estimation of time required for fully remote maintenance operations.
4. Compilation of a list of equipment required for fully remote maintenance of a nuclear gas turbine.

#### 19.3.2. Maintenance Criteria

This task was carried out based on the assumptions described below.

19.3.2.1. Plant Configuration. The plant was assumed to be a 3000-MW(t), direct cycle three-loop configuration with a non-intercooled, single-shaft gas turbine directly driving a water-cooled generator located inside the containment.

19.3.2.2. Inspection Interval. Based on information from the HHT program and U.S. utilities, major overhaul and inspection intervals requiring removal of the gas turbine will be scheduled every 6 yrs. This may routinely include turbine reblading. To make this inspection interval practical, extensive diagnostic monitoring of the gas turbine will be employed during operation, common high reliability and component life will be emphasized in the design, and in situ access is being made possible at both ends of the machine.

19.3.2.3. Onsite Repair. Inspection, overhaul, and repair of the gas turbine will be performed onsite. This approach removes constraints on the gas turbine design, such as maximum size, the need for a qualified shielded shipping cask, and the need to reduce surface contamination levels prior to shipment.

19.3.2.4. Turbine Outage. All planned turbine inspection and servicing will be performed during annual refueling outages.

19.3.2.5. Spare Turbomachine. A spare turbomachine will be made available for installation into the PCRV whenever an installed machine must be removed for servicing.

19.3.2.6. Radiation Protection. Minimizing personnel exposure is a major concern in all aspects of the gas turbine maintenance cycle. Low personnel exposure and production of very little radioactive waste are important assets to HTGR designs, as evidenced by experience at Fort St. Vrain and with other gas-cooled reactors. Even though the current HTGR-GT can be designed to limit personnel exposure, offsite releases, and waste production to within the federal guidelines of 10CFR20, 10CFR50, and various other regulatory guides at the present time, future exposure goals may be much lower than present guidelines. With this in mind much more emphasis is being placed on remote maintenance in advanced nuclear applications.

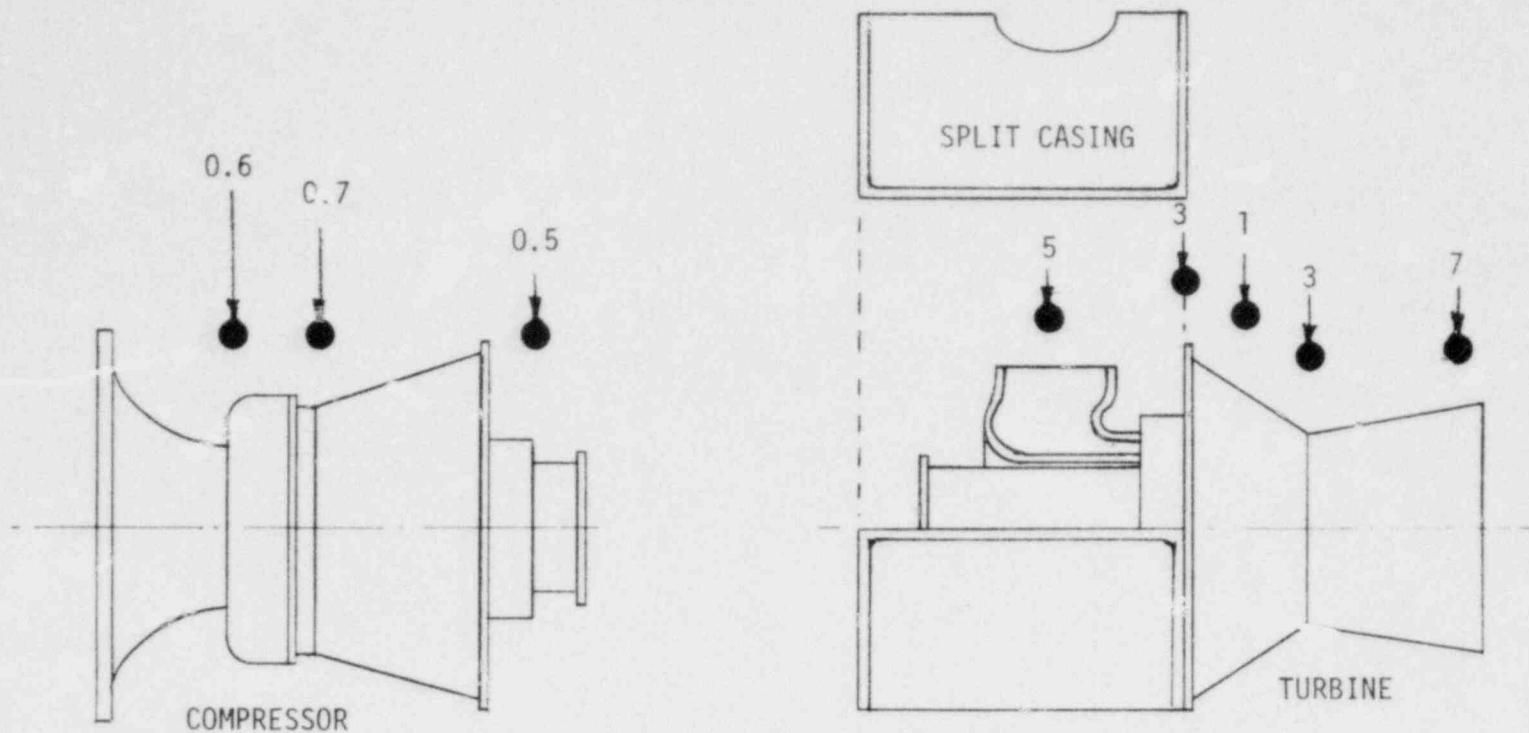
Figure 19-1 illustrates turbomachine radiation levels due to fission product plateout. Source terms were based on MEU fuel, Level A activities, 6-yr plant operation, and 100-day decay following plant shutdown. Preferential plateout factors were assigned to the various contaminating nuclides in various regions of the primary circuit and various sections of the turbomachine to account for the effects of material type, surface condition, gas velocity, and operating temperature on the deposition of various nuclides. Figure 19-2 indicates the dose rates that might be expected in the vicinity of the exposed turbine and compressor rotors for design plateout assumptions. A 10-day decay period will result in dose rates approximately 30% higher than indicated in Figs. 19-1 and 19-2.

There are several approaches to mitigating both source and effects in order to minimize personnel exposure. The source reduction measures include, for example:

1. Fuel improvement to reduce fission product releases.
2. Reliability improvement to reduce the need for maintenance of contaminated equipment or access to radiation areas.
3. Design ingenuity to minimize the need to expose individuals to high radiation levels in the performance of maintenance tasks.
4. Decontamination to remove radiation source contaminants.

The following techniques are widely accepted as the most effective means of lessening maintenance worker radiation exposure:

1. Time.
  - a. Allow time for decay of source activity.



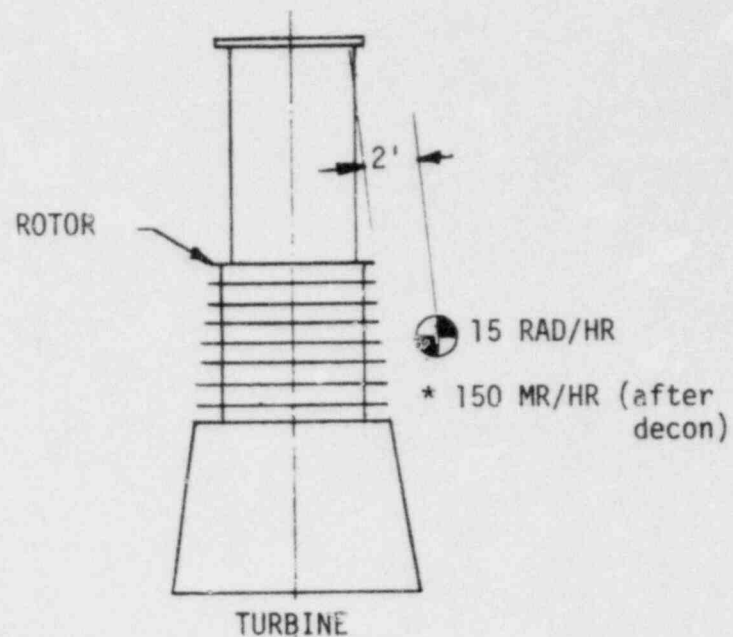
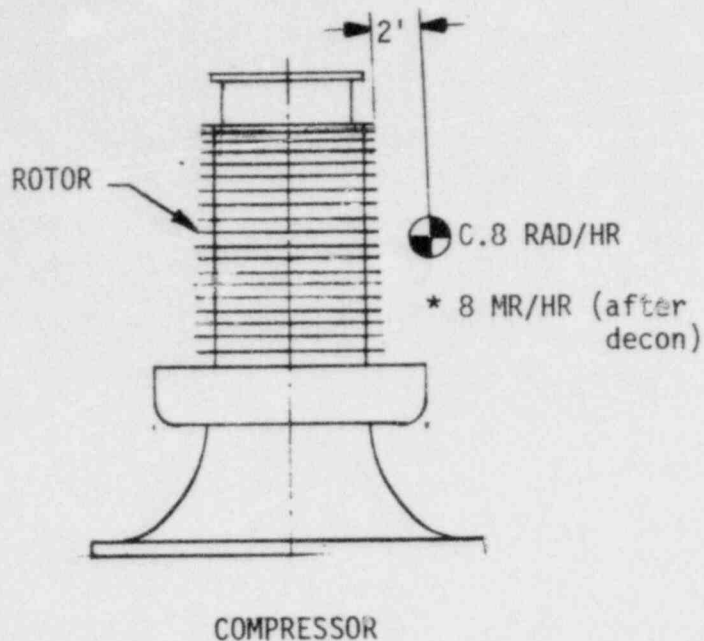
DOSE RATES SHOWN ARE IN RADS/HR AND ARE BASED ON --

- 100 DAYS DECAY
- NO DECONTAMINATION

NOTE: A 10 day decay period will result in dose rates approximately 30% higher than shown.

Fig. 19-1. Turbomachine radiation level after 100-day decay





NOTES:

1. MAXIMUM RADIATION EXPOSURE NEAR ROTORS.
2. GOAL FOR CONTACT MAINTENANCE < 10 MR/HR.
3. PLAN FOR REMOTE DISASSEMBLY OF TURBINE.
4. COMPRESSOR POSSIBLY MAY BE MAINTAINED BY CONTACT.

\* Based upon estimated decontamination factor = 100

NOTE: A 10 day decay period will result in dose rates approximately 30% higher than shown.

Fig. 19-2. Turbine and compressor dose rates

- b. Minimize the time necessary to do work in radiation areas.
  - c. Develop work procedures; plan work.
2. Distance.
- a. Maximize the distance from radiation sources in the performance of work tasks.
3. Shielding.
- a. Take advantage of self-shielding effects of components and structures.
  - b. Add shielding where its use can be justified.
4. Remote operations.
- a. Perform high-level radiation operations using remote equipment.

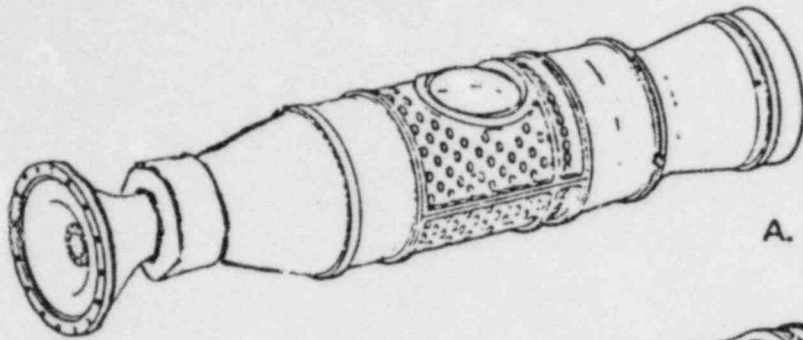
The remote maintenance facility approach to gas turbine maintenance takes maximum advantage of all four factors of time, distance, shielding, and remote operations, so minimal worker exposure is possible. This approach also permits immediate repairs to be made on the turbomachine using remote equipment, without waiting for lengthy decay to permit contact repair operations.

#### 19.3.3. Maintenance Procedure

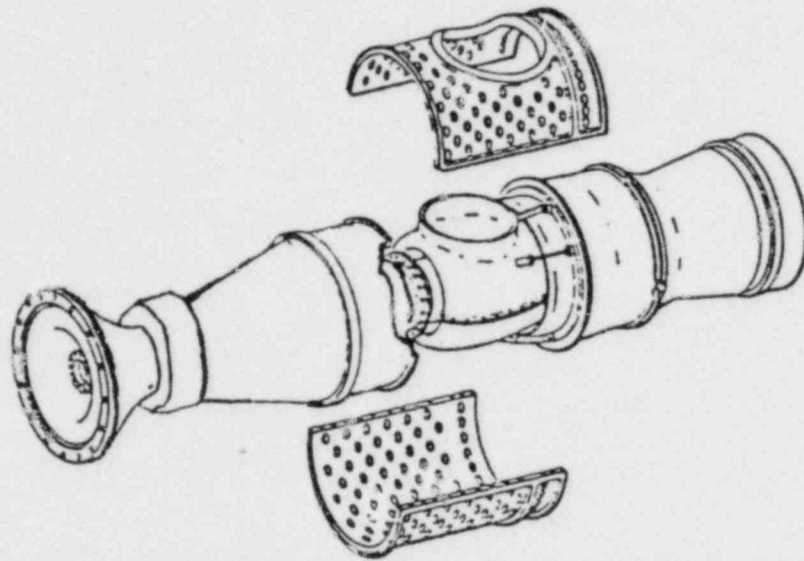
A straightforward approach has been used in developing conceptual procedures for gas turbine maintenance. Gas turbine inspection and

maintenance operations were identified by the turbomachinery designer. Figure 19-3 presents an exploded view of the 400-MW(e) turbomachine which was the basis for the study. The required operations were put into logical sequences using functional flow diagrams beginning with the overall outage sequence shown in Fig. 19-4. These overall steps were broken down into a second level of detail as shown in Fig. 19-5. Third level detail was then developed and tooling concepts and procedures were conceived. Time estimates were also made at this third level. Figure 19-6 is typical of the third-level detail developed. (More detailed information is given in Ref. 19-1). Time estimates were then summarized to the third level functional flow diagram steps and to the second and first levels. It should be recognized that the time summaries (Tables 19-1 and 19-2) provide only a gross sum of the hours to follow a complete remote disassembly and reassembly sequence as described, including the removal of every bolt and nut on the turbomachine and every compressor and turbine blade on the turbomachine without any refinement in the present machine design.

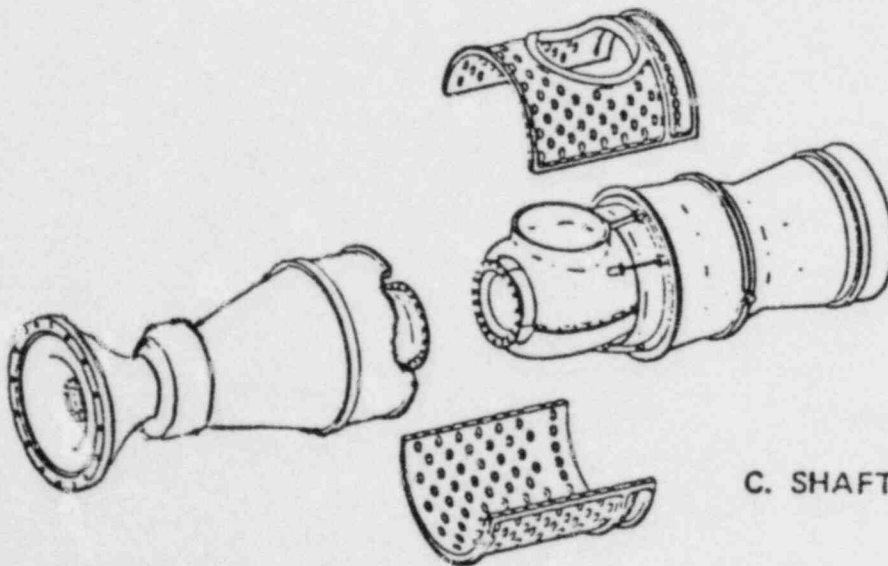
Tables 19-1 and 19-2 and their detailed breakdown as presented in Ref. 19-1 show which areas in the disassembly procedure consume the majority of disassembly and reassembly time and also allows critical path identification. It is believed that operating times can be improved significantly, equipment can be standardized and simplified, and in situ operations can be refined to minimize personnel exposure. This also applies to removal of the turbomachine from the PCRV and transportation to a maintenance facility. For the 846-tonne (900-ton) turbomachine in the HHT program, BBC estimated that a complete gas turbine overhaul, including removal and reinstallation in the PCRV, might be accomplished in 775 h. While there is little question that such a repair time could be achieved, tradeoffs must be made with facility cost, potential impact on plant downtime, value of exposure reduction, plant configuration, fuel cost, and impact on PCRV design and the design of the gas turbine.



A. FULLY ASSEMBLED



B. SPLIT CASES SEPARATED

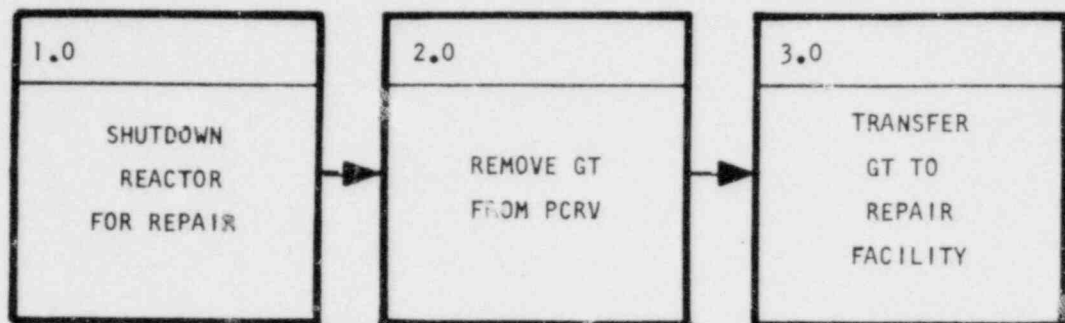


C. SHAFT SEPARATED

Fig. 19-3. Turbomachine - exploded view

GT-HTGR TURBINE

REMOVE



# REPAIR/REPLACEMENT CYCLE

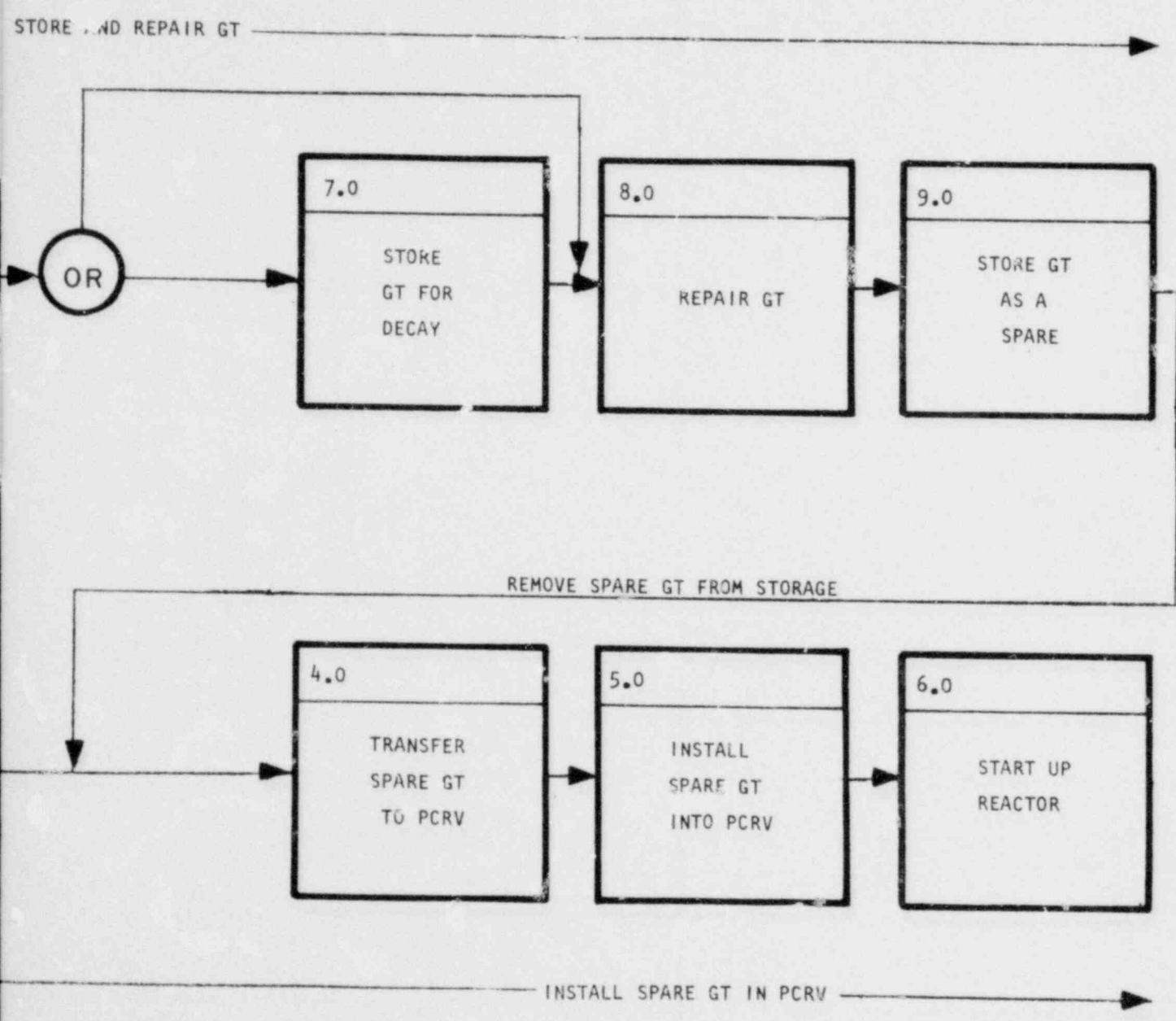


Fig. 19-4. First level functional flow diagram

19-13

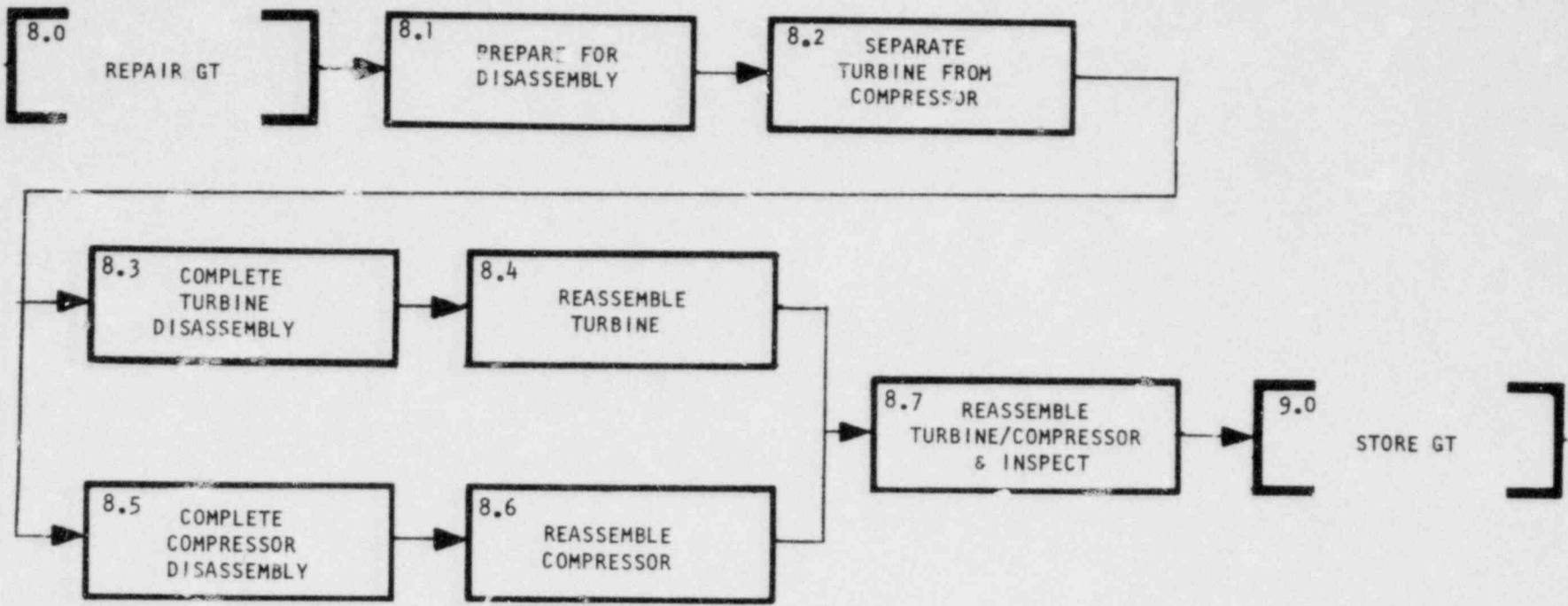


Fig. 19-5. Second level -repair gas turbine

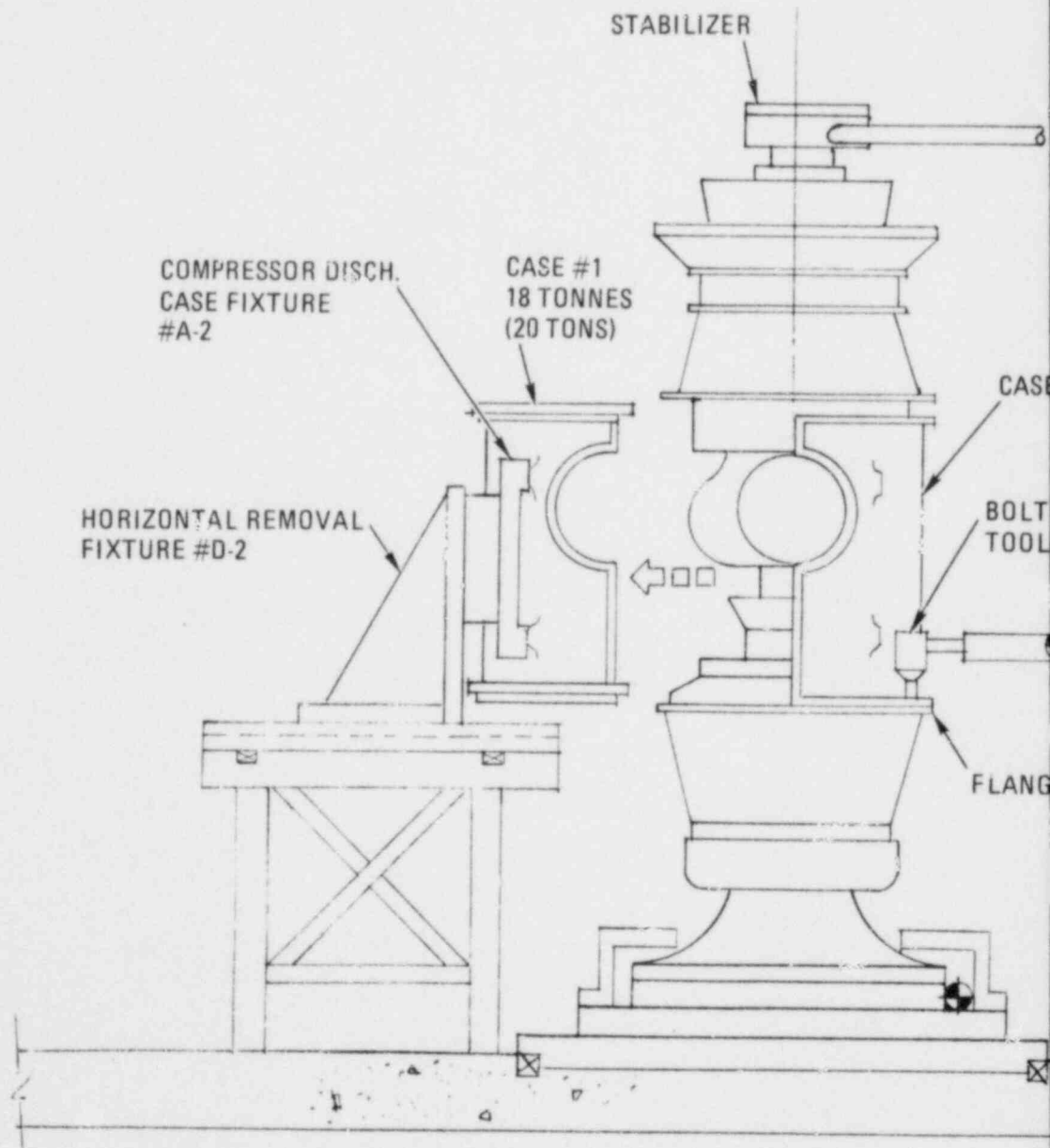
TABLE 19-1  
 FIRST LEVEL TIME SUMMARY FOR  
 GAS TURBINE REPAIR OUTAGE

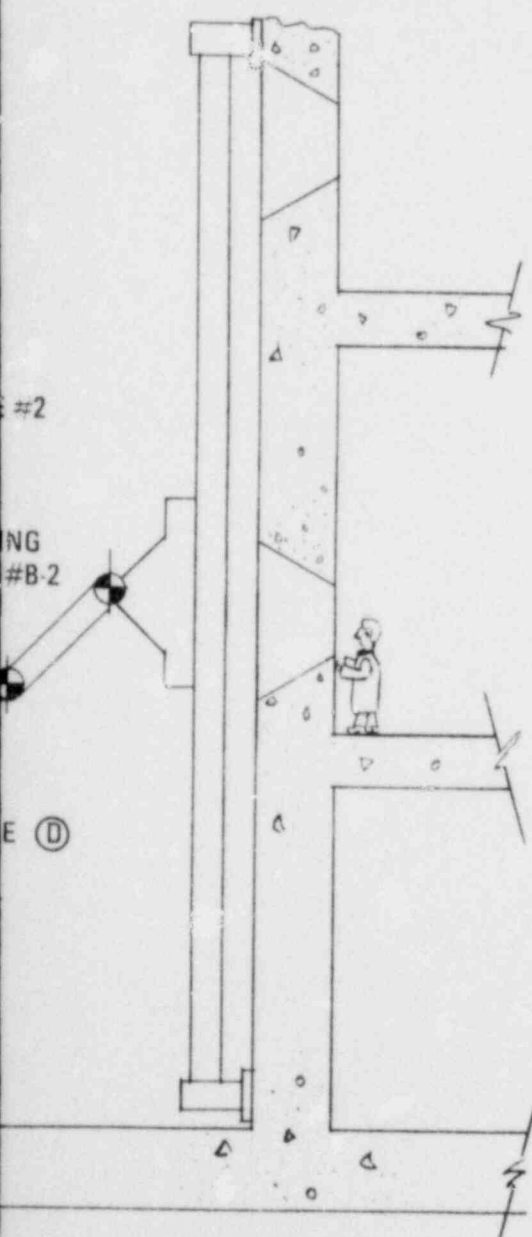
1.0 Shut Down Reactor for Repair	2 days
2.0 Remove Gas Turbine from PCRV	10.5 days <sup>(a)</sup>
3.0 Transfer Gas Turbine to Repair Facility	1 day
4.0 Transfer Spare Gas Turbine to PCRV	1 day
5.0 Install Spare Gas Turbine in PCRV	10.5 days <sup>(a)</sup>
6.0 Start up Reactor	2 days
7.0 Store Gas Turbine for Decay	10 days
8.0 Repair Gas Turbine	177 days
9.0 Store Gas Turbine as a Spare	As required

---

<sup>(a)</sup> Based on an estimate of 21 days (at two shifts per day) to remove and install the gas turbine from the PCRV (Ref. 19-2).







STEP	TOOLING	TIME
● LIFT COMPRESSOR EXHAUST CASE #1 AND REMOVE	HORIZONTAL REMOVAL FIXTURE #D-2, CASE HANDLING FIXTURE #A-2	1 HR
● DISCONNECT FIXTURE #A-2		2 HRS
● UNBOLT CASE #2 AT FLANGE (D)	BOLTING TOOL #B-2	40 HRS
● ROTATE GT 180° AND INSTALL FIXTURE #A-2 ON CASE #2	HORIZONTAL REMOVAL FIXTURE #D-2 CASE HANDLING FIXTURE #A-2	4 HRS
● LIFT AND REMOVE CASE #2		1 HR
● DISCONNECT FIXTURE #A-2		2 HRS
TOTAL TIME:		50 HRS

Fig. 19-6. Schematic for removing 180-deg split cases

TABLE 19-2

## 8.0 REPAIR GAS TURBINE - TIME SUMMARY

(Total disassembly time including removal of  
all bolts and all blades)

8.1 Prepare for Disassembly	20 h
8.2 Separate Turbine from Compressor	465 h
8.3 Disassemble Turbine	482 h <sup>(a)</sup>
8.4 Reassemble Turbine	532 h <sup>(a)</sup>
8.5 Disassemble Compressor	904 h
8.6 Reassemble Compressor	930 h
8.7 Reassemble Turbine/Compressor Unit and Inspect	513 h
	<hr/>
Total Time	2832 h <sup>(b)</sup>

(a) Steps 8.3 and 8.4 are in parallel with steps 8.5 and 8.6 and do not add to the critical path which results when all compressor blades are replaced.

(b) 177 days at two shifts per day.

19.3.3.1. Functional Flow Diagrams. The overall size of the 272-tonne (300-ton) gas turbine contemplated for the reference HTGR-GT is shown in Fig. 19-7 and is broken down into major component weights in Fig. 19-8. Periodically, a gas turbine would be removed from the PCRV and placed in storage for decay while a spare turbomachine was reinstalled in the PCRV to allow plant operation. The removed turbomachine would then be overhauled immediately at an onsite maintenance facility and placed in storage for instant future use. This concept is shown schematically in Fig. 19-9 and described in a functional flow diagram in Fig. 19-4. Figure 19-4 illustrates the movement of both a spare turbomachine and a turbomachine to be overhauled in an overall first level sequence. As shown, the decay period can be completely eliminated if total remote facilities and equipment are provided for turbine disassembly.

Step 8.0 in Fig. 19-4 could be accomplished in an onsite facility as shown schematically in Fig. 19-10 following the second level sequence illustrated in Fig. 19-5. Reference 19-2 summarizes removal of the gas turbine from the PCRV and the operations which precede this step.

19.3.3.2. Repair Times. Gross estimates of the time to accomplish each step in the first, second, and third level sequences are summarized in Tables 19-1 and 19-2. All estimates for steps 1.0 through 7.0 in Table 19-1 are roughly estimated. This places the turbomachinery repair time estimate (step 8.0) in perspective with the overall outage downtime. Steps 1.0, 2.0, 5.0, and 6.0 might be summed to provide an estimate of total downtime for an unplanned or planned turbine outage. The estimate provided in step 8.0 is the result of this investigation and represents only the gross sum from Table 19-2. As discussed earlier, a much lower estimated gas turbine repair time will be realized as the concept is refined. Design improvements will be made to reduce the time required to perform the most time-consuming operations. Also, only those operations will be performed which are necessary to ensure reliable operation of the turbomachine or are necessary to effect repairs.

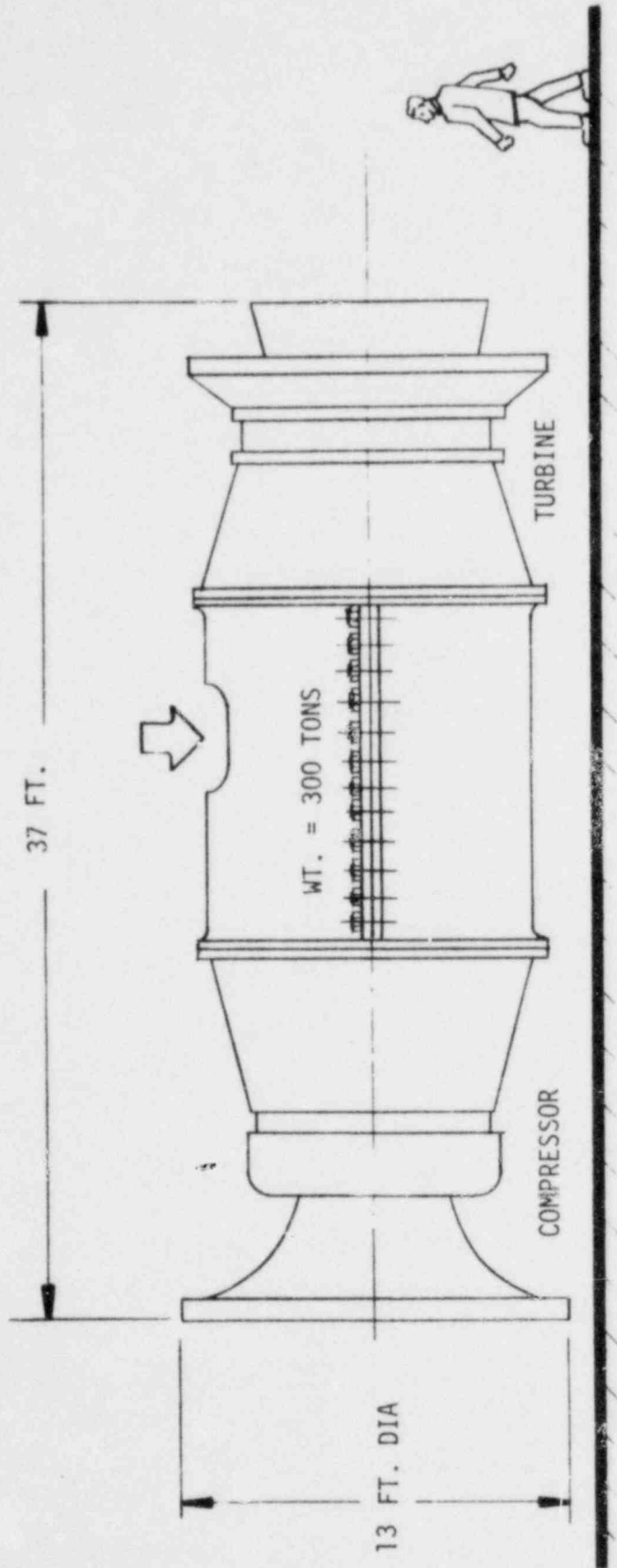


Fig. 19-7. Turbomachine envelope dimensions and weight

19.3.3.3. Disassembly of Gas Turbine. The detailed disassembly and reassembly procedures are described in Ref. 19-1.

19.3.3.4. Remote Maintenance Equipment. Table 19-3 lists tools and fixtures identified for gas turbine remote maintenance. Items such as horizontal removal fixture #D-2 could perform all side removal and access functions and replace all similar fixtures. Similar bolt heads could be used to minimize the amount of manipulator tooling required. Load pallets could be devised to allow storage and handling of similarly sized turbo-machinery parts.

Casing sections might be grappled, removed, and placed on a load pallet with no special attachment fixtures required.

Major features necessary in the remote maintenance facility will include turbine and compressor turntables serviced by manipulators and a horizontal removal fixture. An inspection stand and decontamination equipment will also be major features of the facility.

#### 19.3.4. Remote Maintenance Facility

As stated previously, one of the purposes of this study has been to describe remote maintenance equipment and features which must be considered in the development of the gas turbine. In a similar manner, the gas turbine design and HTGR-GT plant design will dictate the requirements for a remote maintenance facility.

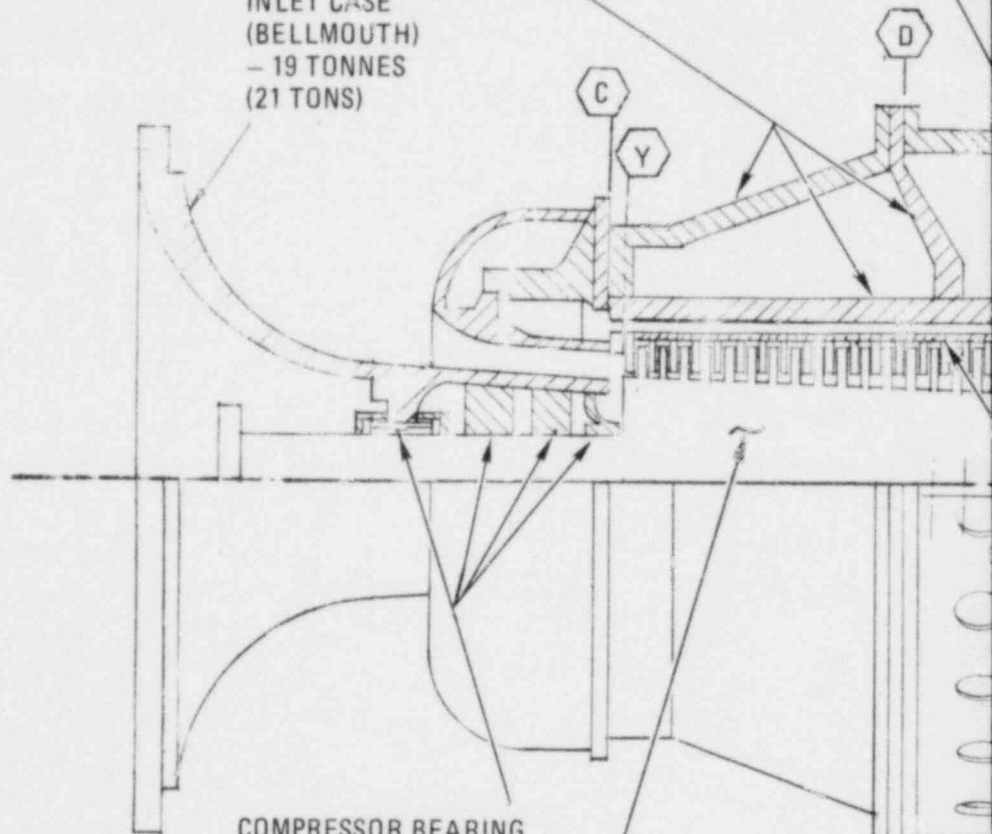
19.3.4.1. Location. For a three-loop plant, location of the repair facility with respect to the PCRV is not critical, since transportation of the gas turbine between the PCRV and the repair/storage facility should not be a critical path operation. Good rail and truck access should be provided to allow receipt of turbomachinery on two high-capacity flat cars. Proximity to the PCRV becomes a much more important concern for a two-loop design plant, since direct transfer of the turbomachine to the repair facility without a shielded cask is a potential feature of the two-loop concept.

COMPRESSOR CONTAINMENT  
RING AND CASES -  
57 TONNES (63 TONS)

COMPRESSOR EXHAUST  
DIFFUSER DUCTS (2)  
- 0.23 TONNE (0.25 TON)  
EACH

TURBINE  
DUCTS  
- 2.7 TONNES  
(3 TONS)

COMPRESSOR  
INLET CASE  
(BELLMOUTH)  
- 19 TONNES  
(21 TONS)



COMPRESSOR BEARING  
AND SEALS -  
4.5 TONNES (5 TONS)

COMPRESSOR ROTOR  
AND BLADES -  
19 TONNES (21 TONS)

COMPRESSOR  
DISCHARGE  
CASES (2)  
- 18 TONNES  
(20 TONS) EACH

INLET  
(2)  
TONNES  
(5) EACH

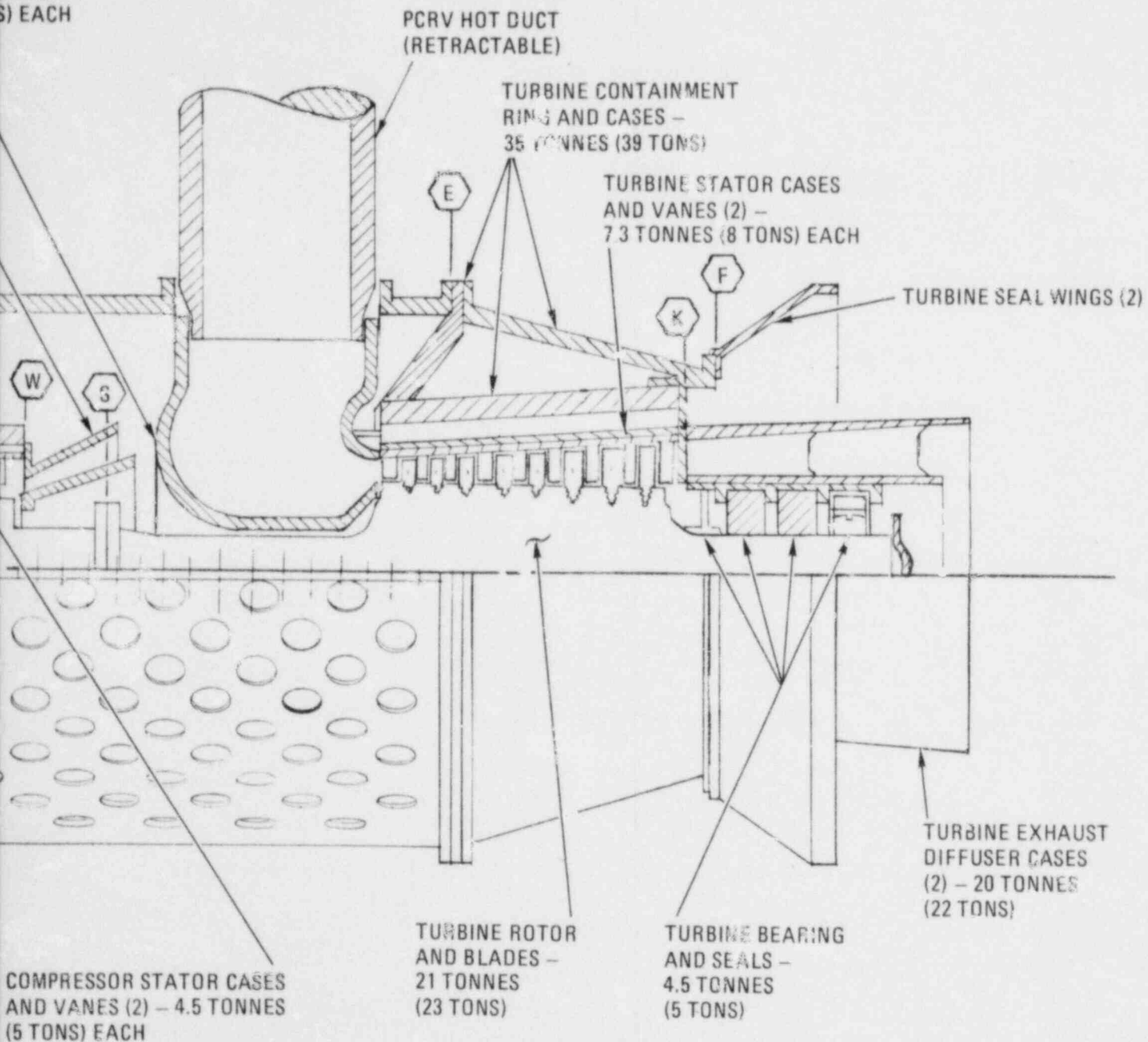
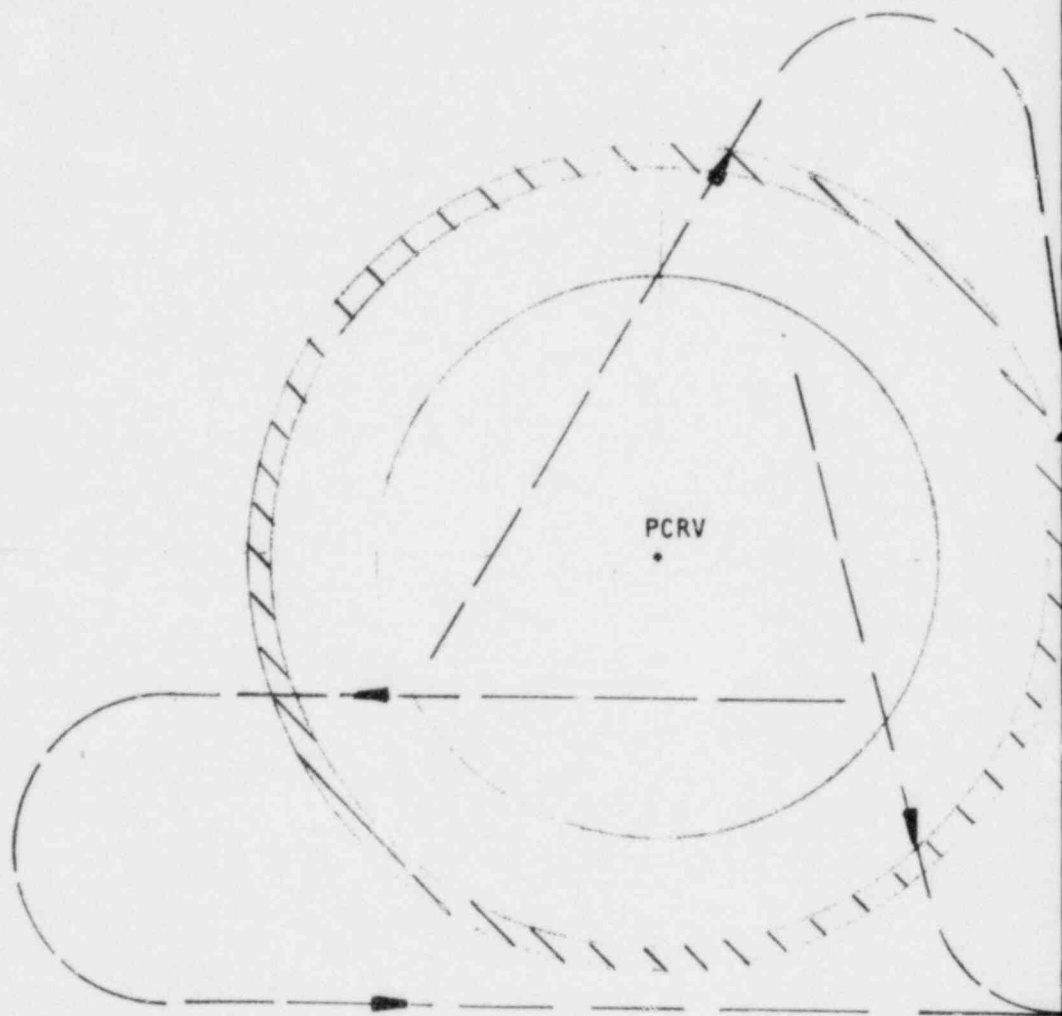


Fig. 19-8. 100-MW(e) gas turbine





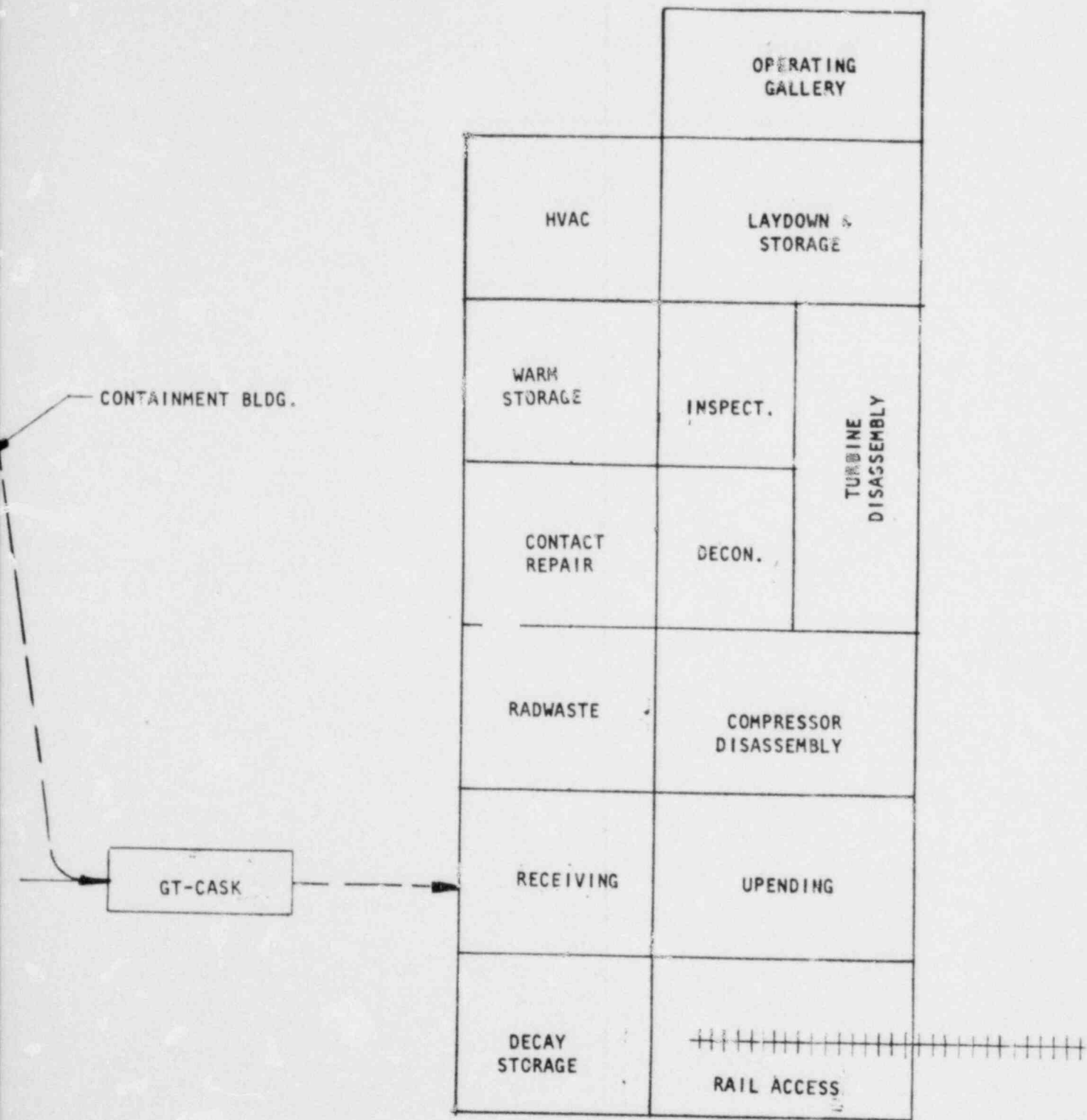
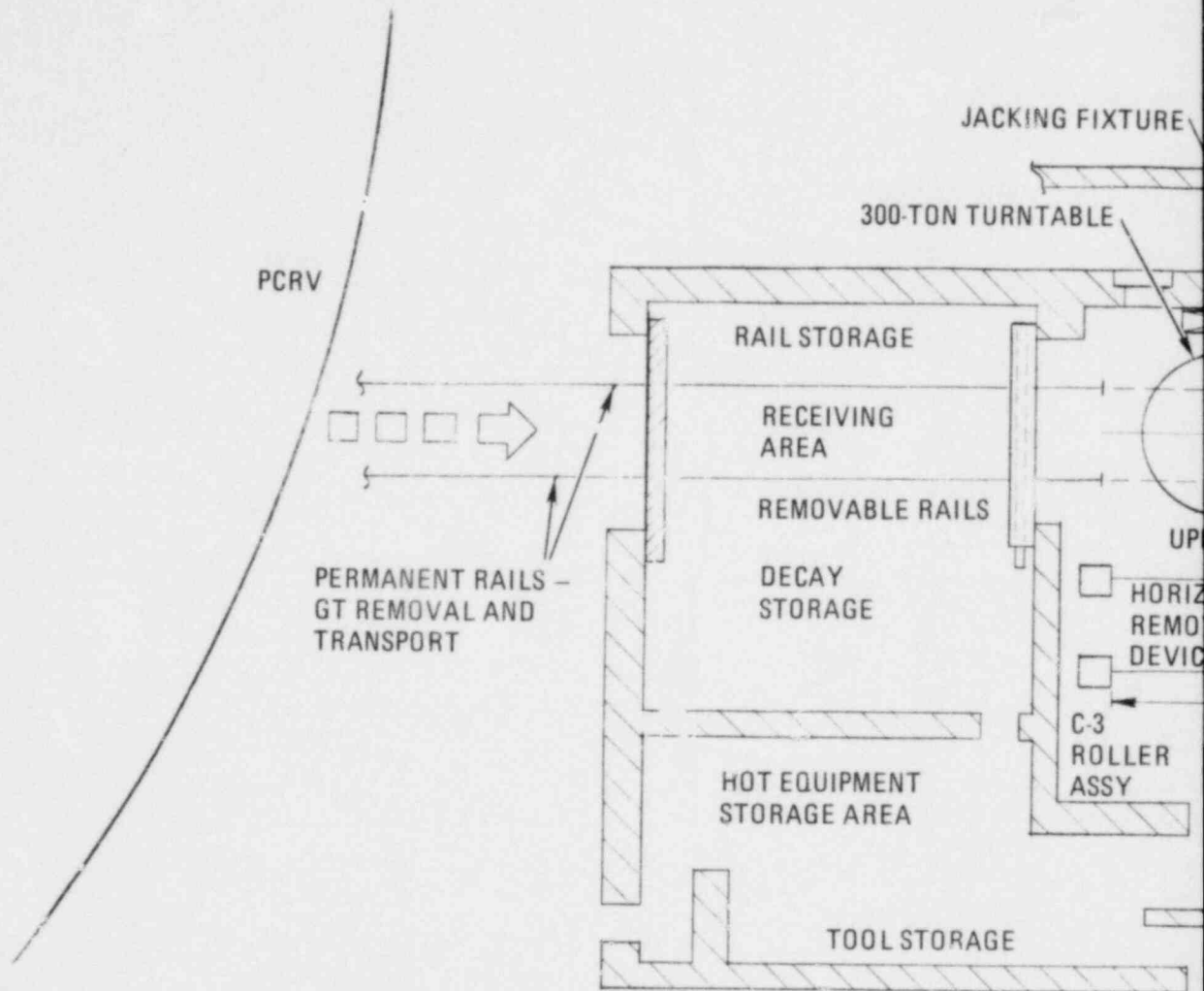


Fig. 19-9. Functional arrangement of a remote repair facility



**NOTES:**

1. DISASSEMBLY AREA CAN BE SERVICED BY A 136 TONNE (150-TON) OVERHEAD CRANE (SPAN IS MINIMIZED ALSO).
2. D-2 PERFORMS ALL HORIZONTAL ACCESS REMOVAL AND LIFTING OPERATIONS.
3. ACCESS AREA IS SERVICED BY A SMALL OVERHEAD CRANE.
4. ARRANGEMENT IS COMPATIBLE WITH A TWO OR THREE LOOP PLANT AND MINIMIZES USE OF SPACE ADJACENT TO THE PCR AND CONTAINMENT.

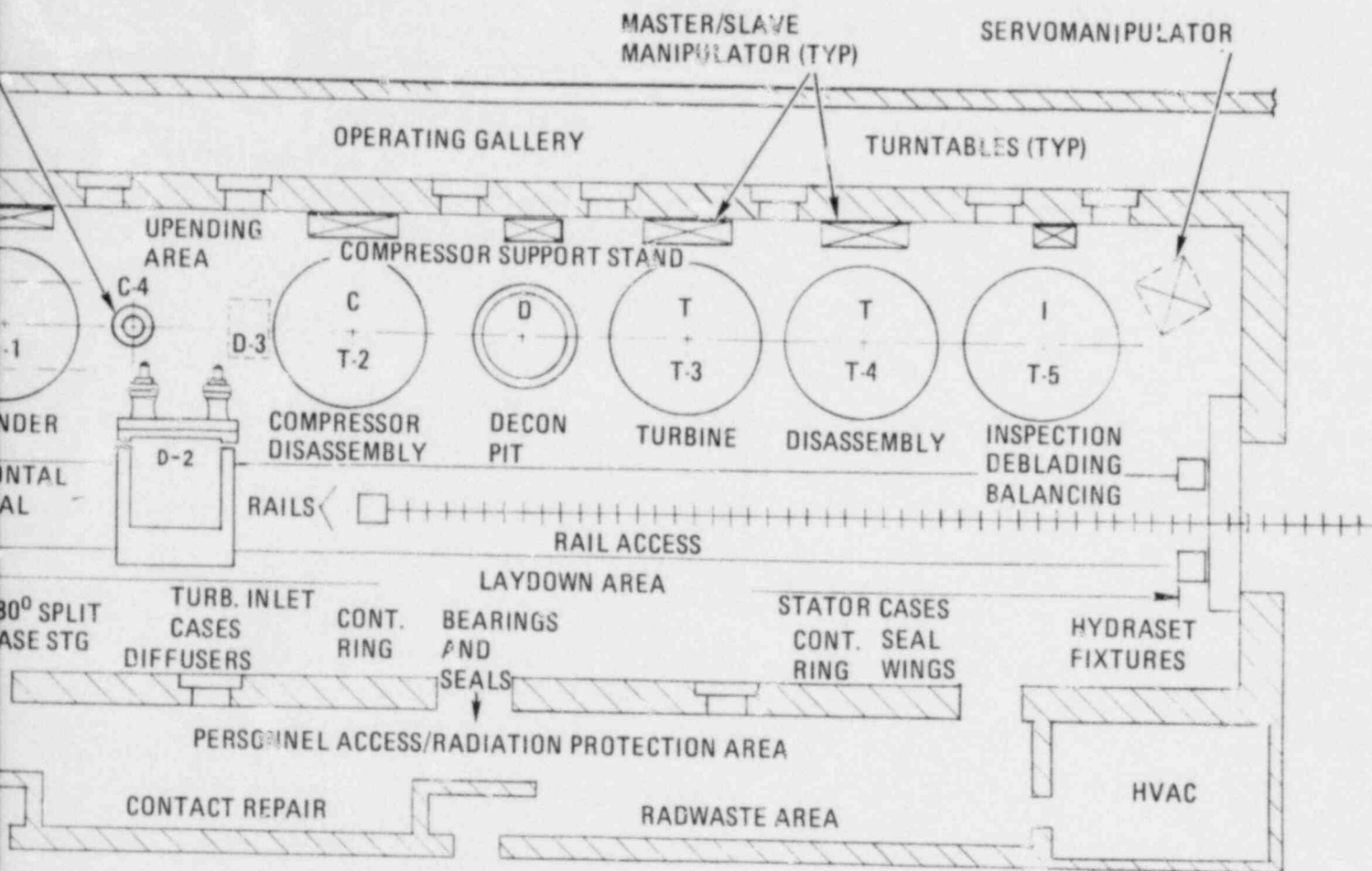


Fig. 19-10. Functional layout of a remote repair facility

TABLE 19-3  
TOOLING REQUIREMENTS SUMMARY

Handling and Lift Fixtures

A-1	Trunnion Lift Fixture
A-2	Compressor Discharge Case Handling Fixture
A-3	Split Case Lift Fixture
A-4	Diffuser Handling Fixture
A-5	Diffuser Lift Fixture
A-6	Inlet Duct Handling Fixture
A-7	Inlet Duct Lift Fixture
A-8	Compressor Containment Assembly Lift Fixture
A-9	Rotor Shaft Lift Fixture
A-10	Compressor Stator Case Removal Fixture
A-11	Bearing Fixture
A-12	Bearing Housing Fixture
A-13	Compressor Inlet Duct Lift Fixture
A-14	Compressor Rotor Lift Fixture
A-15	Seal Wing Lift Fixture
A-16	Turbine Diffuser Lift Fixture
A-17	Turbine Stator Case Removal Fixture
A-18	Turbine Rotor Lift Fixture

Bolting Tools

B-1 through B-12

Special Fixtures

C-1	Turbine End Rotor/Stator Lock
C-2	Compressor End Rotor/Stator Lock
C-3	Turbomachine Roller Assembly
C-4	Compressor End Support Jack

TABLE 19-3 (Continued)

C-5	Compressor Inboard Stabilizer Lock
C-6	Turbine Inboard Stabilizer Lock
C-7	Compressor Bearing/Seal Removal Fixture
C-8	First Labyrinth Seal Rotor Lock
C-9	Second Labyrinth Seal Rotor Lock
C-10	Turbine Bearing/Seal Removal Fixture

Disassembly Stands/Fixtures

D-1	Tilting Removal Fixture
D-2	Horizontal Removal Fixture
D-3	Compressor Support Stand
D-4	Compressor Disassembly Stands
D-5	Compressor Inlet Duct Support Stands
D-6	Inspection Stand
D-7	Turbine Containment Disassembly Stand
D-8	Turbine Containment Assembly Support Stand
D-9	Turbine Disassembly Stand
D-10	Turbine Exhaust Duct Support Stand
D-11	Turbine Rotor Stabilizer

19.3.4.2. Major Facility Features. A gas turbine maintenance facility must be designed to support the operations described in Section 19.3.3.1, including:

1. Receipt of the gas turbine transportation cask.
2. Decay storage.
3. Removal of the gas turbine from its cask.
4. Fully remote machine disassembly.
5. Decontamination of rotors, stators, and small parts.
6. Visual examination and dimensional surveys.
7. Blade examination, removal, and reinstallation.
8. Reassembly.
9. Balancing.
10. Testing.
11. Long-term storage protection.
12. Welding, grinding, and machining.

A 272-tonne (300-ton) capacity bridge crane with sufficient inching capability to support the operations described in this report is required. This will include a significant amount of head room for vertical disassembly. The crane capacity could be reduced to 137 tonnes (150 tons), as shown in Fig. 19-10, if the upending operation were performed on a turntable and the requirement to transfer the entire turbocompressor to a turntable could be eliminated.

Gamma shielding must be sufficient for unlimited 40 h/wk access to remote operating consoles and all normal working areas.

If it is determined that frequent personnel access to the repair cell is desirable, a ventilation system must be provided to remove airborne contaminants to allow access without the use of breathing equipment.

Because of the long inspection intervals contemplated for the HTGR-GT, facilities should be provided for training maintenance personnel prior to receipt of a contaminated gas turbine.

19.3.4.3. Service Requirements. Detailed facility design would include consideration of the following:

1. Tool racks, support stands, and typical maintenance support equipment.
2. Viewing equipment such as lead glass windows, telescopes, and closed circuit TV.
3. Storage space, including turbomachinery component laydown space, rigging setup space, locker storage, and radiation protection and contamination control equipment storage.
4. Decontamination facilities.
5. Ventilation and airborne contamination control equipment.
6. Treatment and processing interfaces for radioactive liquids, gases, and solids.
7. Radiation/contamination monitoring equipment.
8. Personnel access, monitoring, and health physics areas.
9. Utilities, including service air, breathing air, demineralized water, electrical outlets, welding connections, etc.
10. Provisions for maintenance of the facility, such as access ladders and platforms, lubrication aids, and provisions for cleaning.



#### 19.3.5. Conclusions and Recommendations

Plant availability, worker exposure, and HTGR-GT capital and operating costs are strongly influenced by the maintenance of the turbomachinery. Simplification and streamlining of the methods and procedures must be stressed as the detailed design evolves. Areas for future development and issues which must be resolved prior to development of a detailed maintenance plan include turbomachinery design, tooling design, in situ maintenance, turbomachinery removal and transport, and decontamination.

#### 19.4. REFERENCES

- 19-1. "Remote Maintenance of a 400 MW(e) Helium Gas Turbine," DOE Report GA-A15587, General Atomic Company, to be published.
- 19-2. "HTGR-GT Plant Maintenance Studies," DOE Report GA-A14858, General Atomic Company, March 1979.

## 20. REMOTE MAINTENANCE FACILITY (63200400)

### 20.1. SCOPE

The scope of this task in FY-79 was to develop preconceptual designs and a cost estimate of tooling associated with the remote disassembly and reassembly of the turbomachine for the 400-MW(e) HTGR-GT non-intercooled plant.

### 20.2. SUMMARY

Studies were made of the space required for laydown of turbomachine components and fixtures for disassembly and assembly of the turbomachine to facilitate this work, as well as to accommodate supporting services such as decontamination and rotor balancing. The floor area needed was found to be approximately 1060 m<sup>2</sup> (11,400 ft<sup>2</sup>). This work/storage area would be provided with crane coverage.

Studies were also performed, with the previous disassembly sequence studies as a basis, to identify fixture and tooling requirements for turbomachine maintenance. The major fixtures and tools were outlined on layout criteria requirement sketches, and the minor ones were identified and tabulated.

Finally, a preconceptual rough cost estimate was prepared for the fixtures and tools identified in the study.

### 20.3. DISCUSSION

A remote maintenance study for the 400-MW(e) HTGR-GT turbomachine was performed in which identifications were made for the remote disassembly process and inspection of the turbomachine. Concurrently, identifications and simple configuration outlines were made of the major fixtures and tools required.

Based on this study and supplemental judgment, an initial facility size with a fixed area of about  $930 \text{ m}^2$  ( $10,000 \text{ ft}^2$ ) was developed, primarily as an early aid in the plant design work. As a basic maintenance philosophy it was decided to retain the scheme whereby the turbomachine is tilted to a vertical orientation in the facility while being serviced. The reason is primarily related to retention of the structural integrity of the turbomachine during the several steps of disassembly.

This first facility concept envisioned a large elevator type device in a pit area, with a turntable being part of the elevator. This elevating platform would be double decked to accommodate insertion of the spare turbomachine immediately following removal of the unit to be serviced. Upending the machine and placing it on the turntable would also facilitate its rotation in relation to the tooling and the viewing windows.

The balance of the floor area was identified as needed for (1) a turbomachine component laydown area, (2) storage of tools and fixtures, (3) rotor balancing, and (4) an area provided with inspection facilities.

In recognition of the very broad basis on which this facility design was developed, the study continued with an identification, size determination, and general configuration study of each of the turbomachine parts removed from the assembly and temporarily stored within a designated floor area within the maintenance facility.

Evaluations were then made of the fixtures and tools configured in the earlier study of the turbomachine disassembly process. It was found that several fixtures could be combined and interchangeable tool attachments used. Emphasis was placed on initial identification of those tools and fixtures that appeared to have a significant effect upon the tool fixture storage floor area and the work space around the turbomachine.

The fixtures were identified in rough outlines on Plant Layout Requirement Sheets which also were provided with other available data such as sizes, estimated weights, etc. A total of twelve major items were thus identified. The Plant Layout Requirement Sheets were used in the preparation of a preconceptual layout drawing of the maintenance facility floor plan (Fig. 20-1). The layout identifies the significant space allocations, such as:

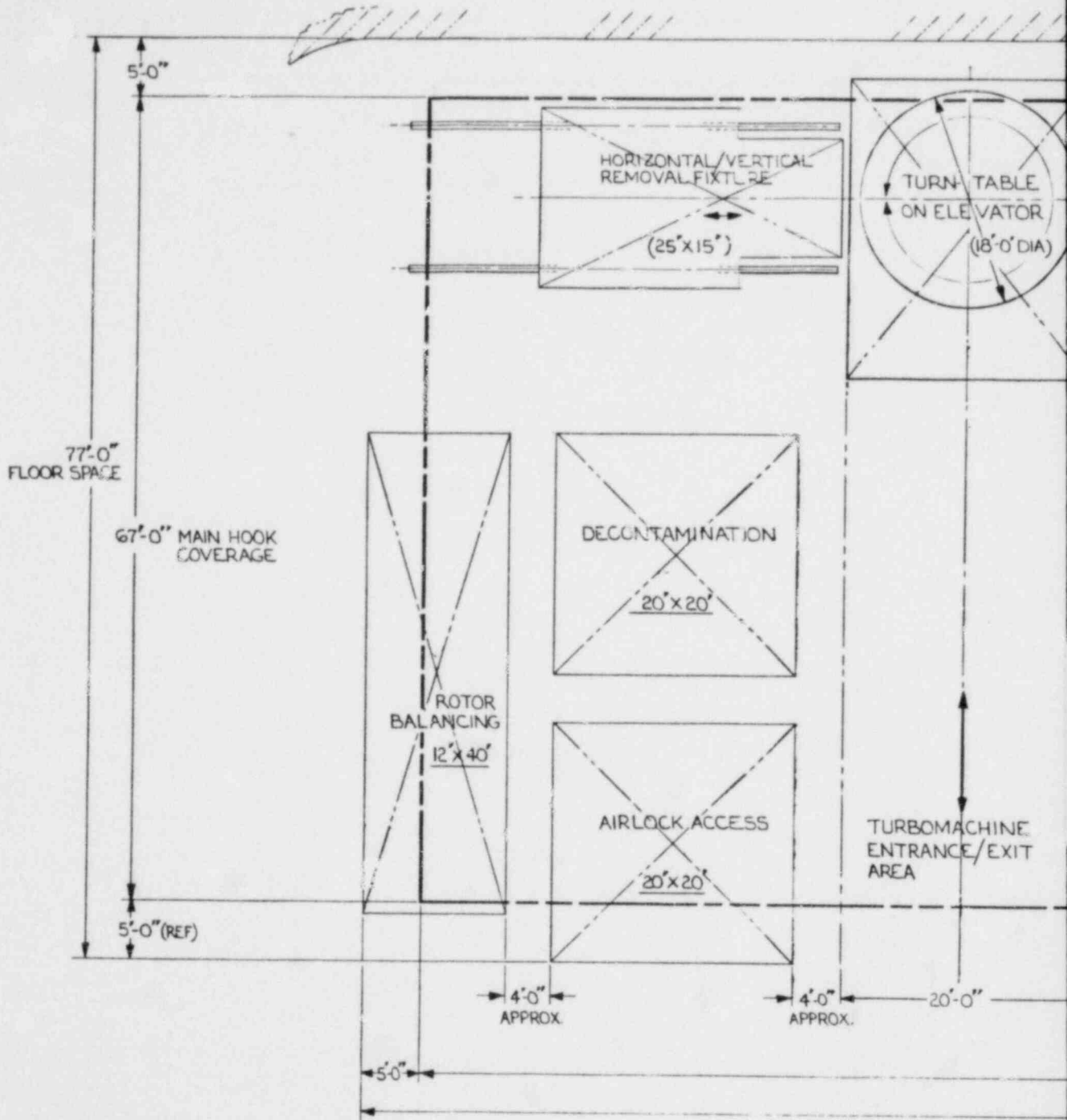
1. Turbomachine entrance/exit area.
2. Turntable and elevator.
3. Work area with track-mounted, removable fixtures and wall-mounted manipulator(s).
4. Storage for fixtures and related equipment.
5. Tool storage.
6. Auxiliary work area.
7. Decontamination area.
8. Airlock access.
9. Rotor balancing space.

In this facility layout, the total usable floor area was found to be about 1060 m<sup>2</sup> (11,400 ft<sup>2</sup>) compared with the earlier, very rough estimate of needed floor space of about 930 m<sup>2</sup> (10,000 ft<sup>2</sup>). The difference is partly due to deletion of below-the-floor storage of the spare turbo-machine, which required a very large, high-capacity elevator type device. The turntable feature was retained. It was shown as being mounted on a smaller elevator type device, but subject to further plant design studies to determine if building height could effectively be reduced by utilizing the elevator while uprighting the turbomachine for disassembly.

A preconceptual cost estimate of fixtures and tooling for turbomachine remote maintenance was then prepared. The gas turbine remote maintenance study performed by GA (Ref. 20-1) was used as a basis for the estimate, since it contained preconceptual outlines of the tooling and fixturing as envisioned at that time. As reported above, it was concluded that the quantity of major fixtures shown could be reduced to 12 basic ones, while the remaining 25 would consist of either attachments to the large fixtures and tools or smaller but independent units. The Plant Layout Requirement Sheets thus prepared facilitated the development of projected weights of the fixtures and tools. A cost per weight unit was then applied to arrive at a "first cut" estimated cost. The unit cost varied between components depending on type of structure, degree of complexity, amount of mechanistic complexity, and instrumentation.

For the second group of equipment, containing the 25 additional handling fixtures and attachments, lump sum estimates were made, since little or no design information had been generated at that time.

A third category containing such items as remote manipulators, balancing equipment, TV systems, lights, etc., was accommodated by cost allowances only, because of the lack of particulars.



SCALE = 3/4"

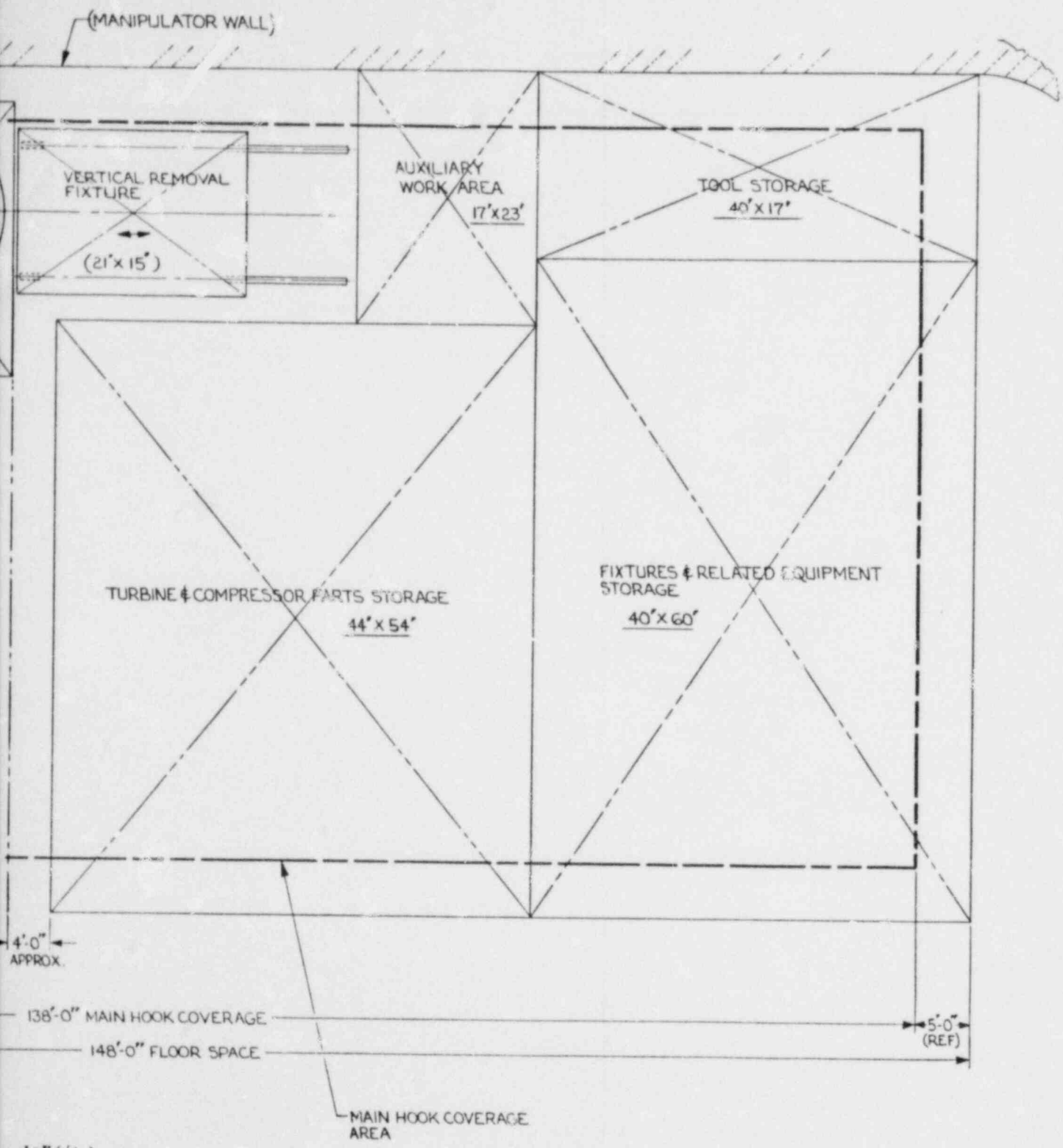


Fig. 20-1. Remote maintenance facility floor plan

For obvious reasons, an estimate of this type is marked by uncertainties since it is based on preconceptual studies. Therefore, using a cost range may be more appropriate until more detailed design studies have been performed which lead to well-defined technical definitions and thus better and firmer cost projections.

#### 20.4. REFERENCE

- 20-1. "Remote Maintenance of a 400 MW(e) Helium Gas Turbine," DOE Report GA-A15587, General Atomic Company, to be published.



## 21. CONTROL VALVE (632003)

### 21.1. SCOPE

The purpose of this task in FY-79 was to determine the trim, attemper-  
tion, primary bypass, and safety valve functional requirements and to design  
the valves to meet these requirements.

### 21.2. SUMMARY

Conceptual designs for the four valves have been completed. Design  
criteria for each valve are presented in Table 21-1. These criteria are  
preliminary and will be revised as the valve designs progress and various  
problems are resolved.

### 21.3. DISCUSSION

Several problems have been identified that affect valve design:

1. To take advantage of inherent PCRV strength and radiation shield-  
ing ability and to reduce valve space envelope requirements to a  
minimum, the valve conceptual designs show the valve bodies  
encased in concrete. This arrangement has been reviewed, and  
problems have been identified in the areas of code compliance  
stress analysis, prototype testability, and valve alignment  
during operation and initial construction.
2. Primary loop flow and pressure drop analysis indicates the need  
for very large, fast-acting valves in primary bypass and safety  
valve service. The analysis shows that valve characteristic and

TABLE 21-1  
VALVE CRITERIA FOR THREE-LOOP, 400-MW(e) HTGR-GT NON-INTERCOOLED REFERENCE PLANT

	Control Valve	Trim Valve	Safety Valve	Attemperation Valve
Design pressure [MPa (psig)]	8.17 (1185)	8.17 (1185)	8.17 (1185)	8.17 (1185)
Design temperature	Per analysis	Per analysis	Per analysis	Per analysis
Normal inlet pressure [MPa (psia)]	7.93 (1150)	7.93 (1150)	7.93 (1150)	7.93 (1150)
Normal temperature [°C (°F)]	498 (928)	498 (928)	498 (928)	174 (346)
Flow area, 100% open [mm <sup>2</sup> (in. <sup>2</sup> )]	493 x 10 <sup>3</sup> (765)	41 x 10 <sup>3</sup> (65)	493 x 10 <sup>3</sup> (765)	73 x 10 <sup>3</sup> (113)
0%-100% travel time open (s)	1	1	1	1
Control range (%)	0-100	0-100	Not required	0-100
Position resolution	0.2% of stroke	0.2% of stroke	N/A	0.2% of stroke
Loss of power position	Open: ΔP > 20 Closed: ΔP < 20	Open: ΔP > 20 Closed: ΔP < 20	Open: ΔP > 20 Closed: ΔP < 20	Open: ΔP > 20 Closed: ΔP < 20
Maximum pressure drop [MPa (psi)]	4.65 (675)	4.65 (675)	4.65 (675)	4.65 (675)
Type of control contour	Linear	Equal per- centage	Quick open	Linear
Normal ΔP [MPa (psi)]	4.65 (675)	4.65 (675)	4.65 (675)	4.65 (675)
Seat leakage normal ΔP [kg/s (lb/h)]	0.19 (1500)	0.19 (1500)	0.19 (1500)	0.19 (1500)
10% step change, time constant (s)	0.25	0.25	N/A	0.4

size are interrelated such that valve size can be reduced if a quick-opening characteristic can be achieved when the valve starts its opening stroke. A quick-opening characteristic is easily achievable with the safety valve but is more difficult with the primary bypass valve because the normal function of the valve is flow control. Flow control implies a linear or exponential characteristic as opposed to a quick-opening characteristic. Various solutions to the problem are being investigated. These involve the use of multiple valves much like conventional steam chest throttle valve arrangements and special valve disk designs, caged and uncaged, that can achieve a quick-opening characteristic at the start of the stroke and a linear characteristic thereafter.

3. Mechanical design problems resulting from high stem forces and valve speed persist. The use of valve balancing chambers to reduce stem forces is being investigated along with the effect of the chambers on valve speed.

Steps are being taken to conduct a nation-wide survey of valve designers and fabricators. At the conclusion of the survey, one or more large-valve designers will be engaged to assist GA in completing the valve mechanical designs if adequate valves or valve manifolds are not commercially available.

## 22. HEAT EXCHANGERS (6321)

The heat exchanger design effort is divided between GA and its sub-contractor Combustion Engineering (CE).

### 22.1. SCOPE

The purpose of this task in FY-79 was to perform conceptual design work on the heat exchangers for the two-loop demonstration plant in an effort to update the reference designs. To accomplish this, the following subtasks were to be performed:

1. Evaluate heat exchanger designs developed by CE in FY-78 and early FY-79. The evaluation should include identification and resolution of critical technical issues.
  - a. Study the differential expansion of the integral return tube (IRT) recuperator concept and recommend a solution to the high stress/limited tube life problem associated with the design. A module layout should be generated, and the impact on the recuperator envelope should be identified and a revised envelope drawing prepared, as appropriate.
  - b. Evaluate the seismic capability of the hexagonal module support structure and identify a potential solution to the seismic inadequacy. The solution should be incorporated in the revised envelope.
  - c. Determine the impact of the solution of issues a and b on the pressure drop and component cost.

- d. Evaluate the impact of high sound power levels on the heat exchanger designs. The most recent sound power level estimates which relate to the heat exchangers are:

Compressor inlet	152.7 dB
Compressor discharge	150.6 dB
Turbine discharge	163.8 dB

2. Evaluate Sulzer/GA heat exchanger design criteria.
  - a. Evaluate the CE designs based on their ability to meet HHT design criteria.
  - b. Provide comments pertaining to the compatibility of the HHT and U.S. design criteria.
  - c. Identify those heat exchanger areas which are major contributors to the high heat exchange costs and recommend possible methods for potential cost reduction.
3. As part of the 500-MW(e) HTGR-GT heat exchanger study, develop a preconceptual top assembly sketch of the 500-MW(e) HTGR-GT loop recuperator and precooler.
4. As part of the alternate heat exchanger design effort, develop an alternative recuperator design concept which stresses design simplicity, ease of maintenance, ease of fabrication, low pressure drop, low cost, and increased safety and reliability.

## 22.2. SUMMARY

In FY-78 and early FY-79, CE developed mechanical designs and cost estimates for the primary loop heat exchangers (recuperator, precooler, and/or intercooler) for three different plant configurations. Based on suggestions by both GA and CE for further definition of the design concepts,

the effort in the third and fourth quarters of FY-79 focused on the recuperator. Two important structural feasibility issues associated with the hexagonal module recuperator were investigated, and design solutions were identified which do not significantly impact heat exchanger envelope, pressure loss, or component cost.

As part of an overall effort to identify areas of capital cost reduction for the HTGR-GT plant, CE reviewed its cost estimates on the heat exchangers to identify potential cost reductions. The general result is a recuperator concept which departs from the hexagonal module approach in a number of ways. A trend toward large, round modules will not only lead to reduced component costs but has advantages of design simplicity and ease of maintenance. An alternate to the hexagonal module concept was developed which employs 19 round modules. The cavity diameter penalty associated with the concept tends to be offset by lower pressure losses and lower capital cost.

The review of both U.S. (GA) and HHT (HRB) design requirements revealed that the recuperator requirements are quite similar and reflect basically the same philosophy toward the design, manufacture, operation, and inspection of the heat exchangers. In addition, most of the U.S. (GA and CE) recuperator concepts could be configured to meet the HHT requirements. In particular, the trend toward larger modules and possibly round modules will produce concepts which will readily meet the implied HHT requirement to inspect individual recuperator tubes.

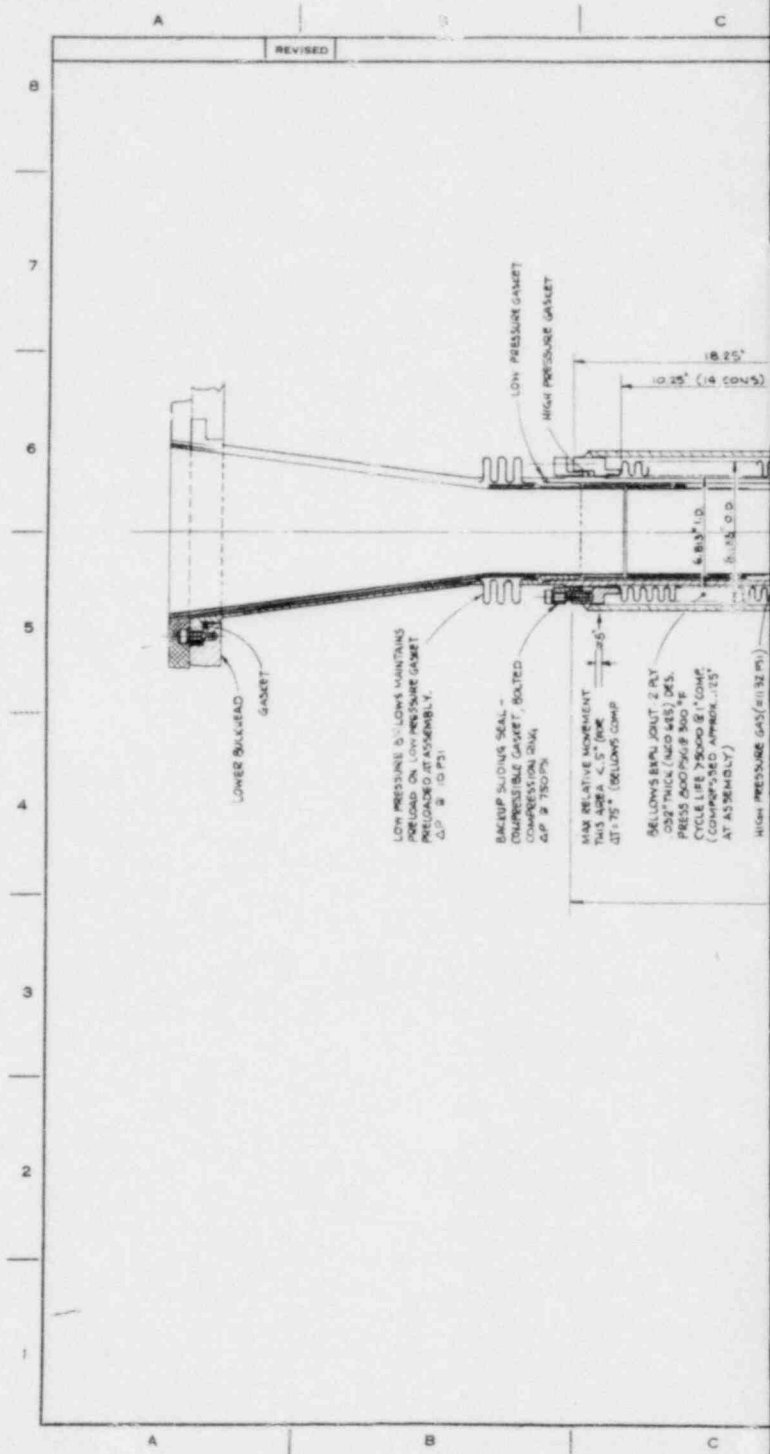
As a result of the reviews of the designs developed by CE in FY-78/79, CE cost estimates, and U.S./HHT design criteria, alternate recuperator concepts were studied by GA. These studies resulted in two alternate concepts to the 83-module reference design and the 19-module design discussed above: (1) a concept with seven round modules developing the 19-module design even further and (2) a "stayed tubesheet" concept. Both concepts show increased potential for cost reduction, design simplicity, ease of maintenance, and improved safety and reliability. All four concepts will be compared with the aim of selecting a preferred concept early in FY-80.

## 22.3. DISCUSSION

### 22.3.1. Heat Exchanger Design Issues Study

The objective of this task was the resolution of design issues that were identified by CE during a review of the CE heat exchanger effort in 1978. In 1979, CE addressed these design issues and recommended design modifications that should resolve the stress problems in the module tubes and module lateral support structure. The high stresses in the module tubes were caused by differential thermal expansion between the tubes and IRT. The proposed solution to the problem was to incorporate a bellows expansion joint between the tubes and IRT to reduce tube stresses. The arrangement of the module with an expansion joint is shown in Fig. 22-1. The problem of high stresses and large deflections in the hexagonal module support structure was caused by inadequate seismic support points tying the structure to the shell (shroud). The design modification to resolve this structural problem is shown in Fig. 22-2. Stresses and deflections were greatly reduced by providing continuous support points around the periphery of the "honeycomb" to replace the six points at which it was previously supported.

Based on a review of estimated acoustic inputs to the recuperator structure from the turbine and compressor, the tentative conclusion is that sound levels of these magnitudes will have no significant impact upon the bulk of the recuperator structure, but that further study is needed to verify the adequacy of those elements that might be more affected, such as the small heat transfer tubes and thin thermal liners. Acoustic testing programs should be included in future planning.





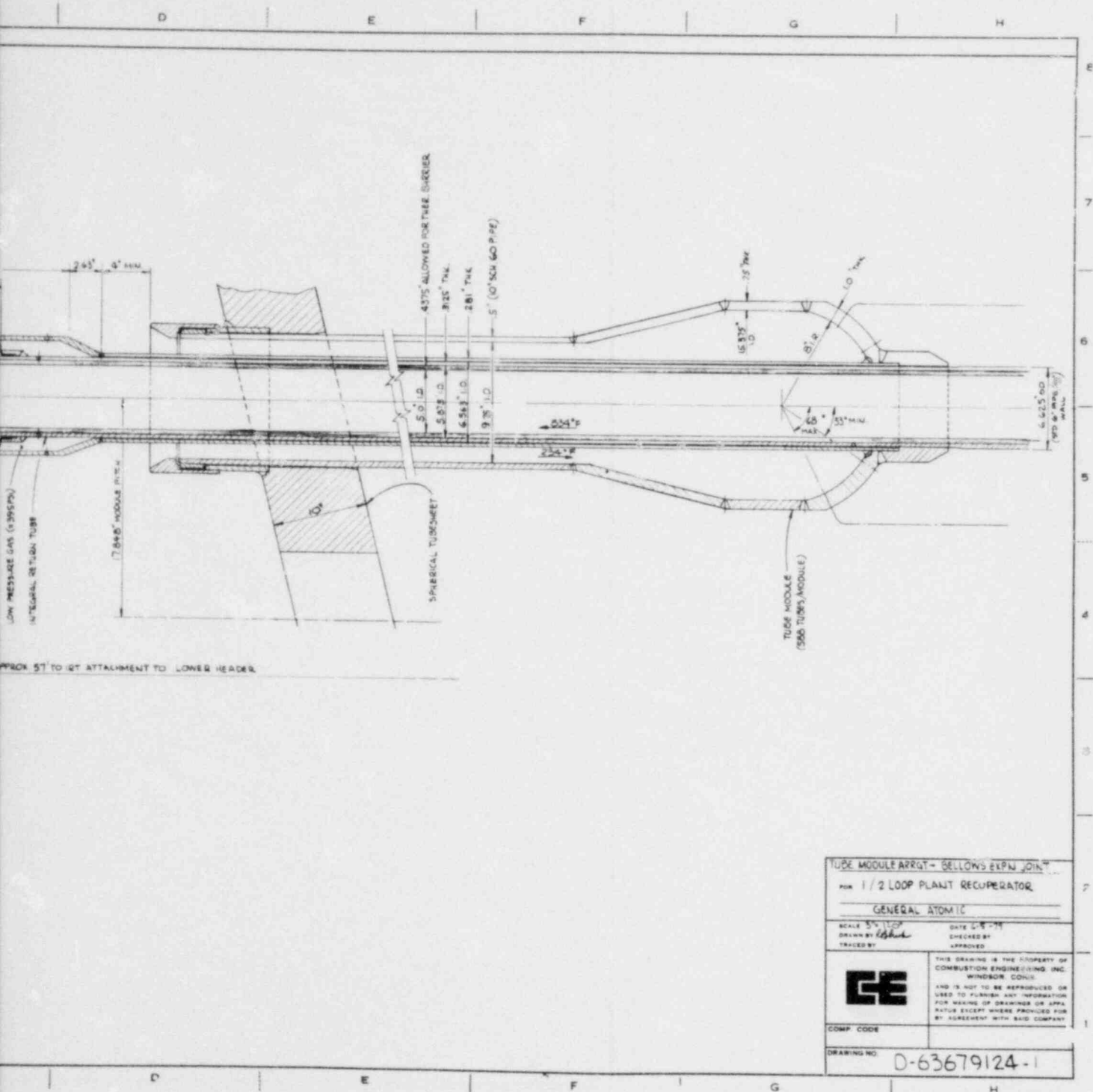
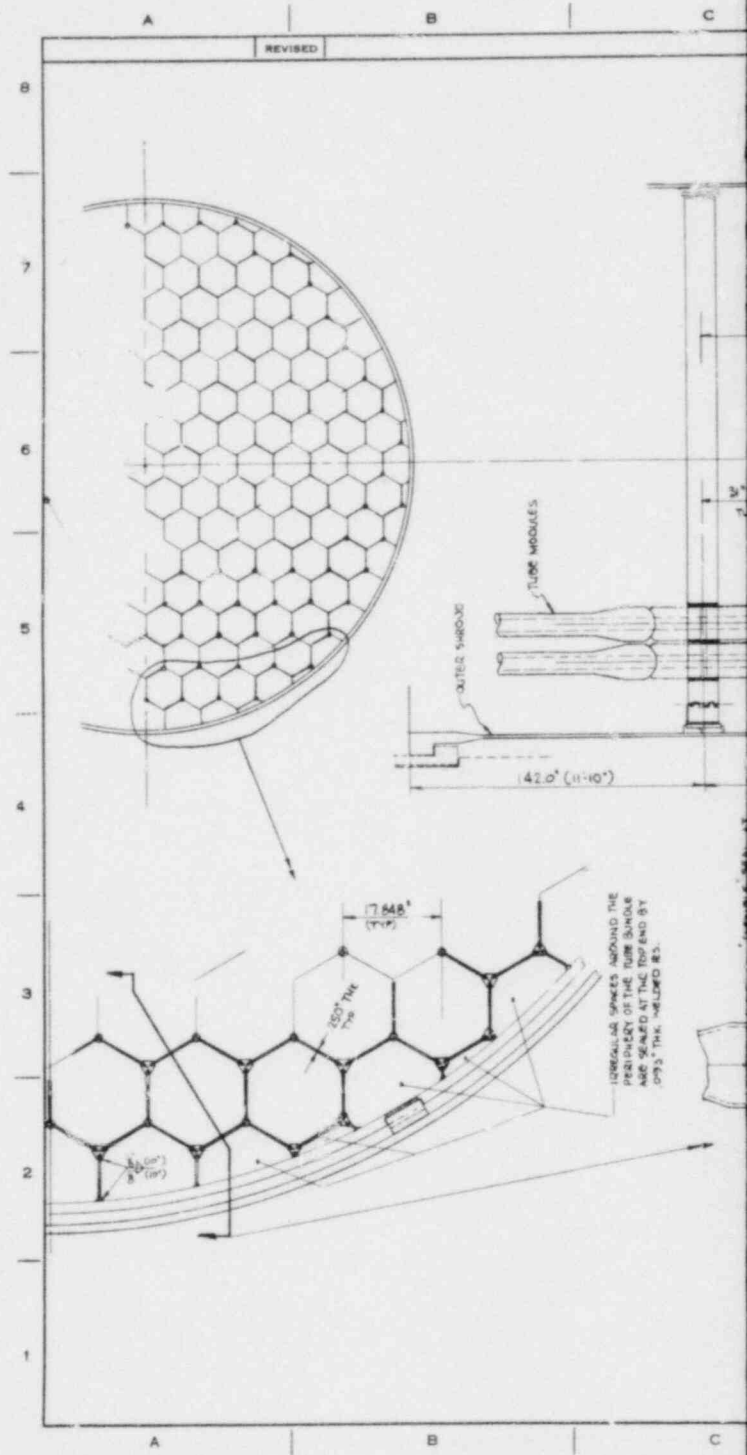
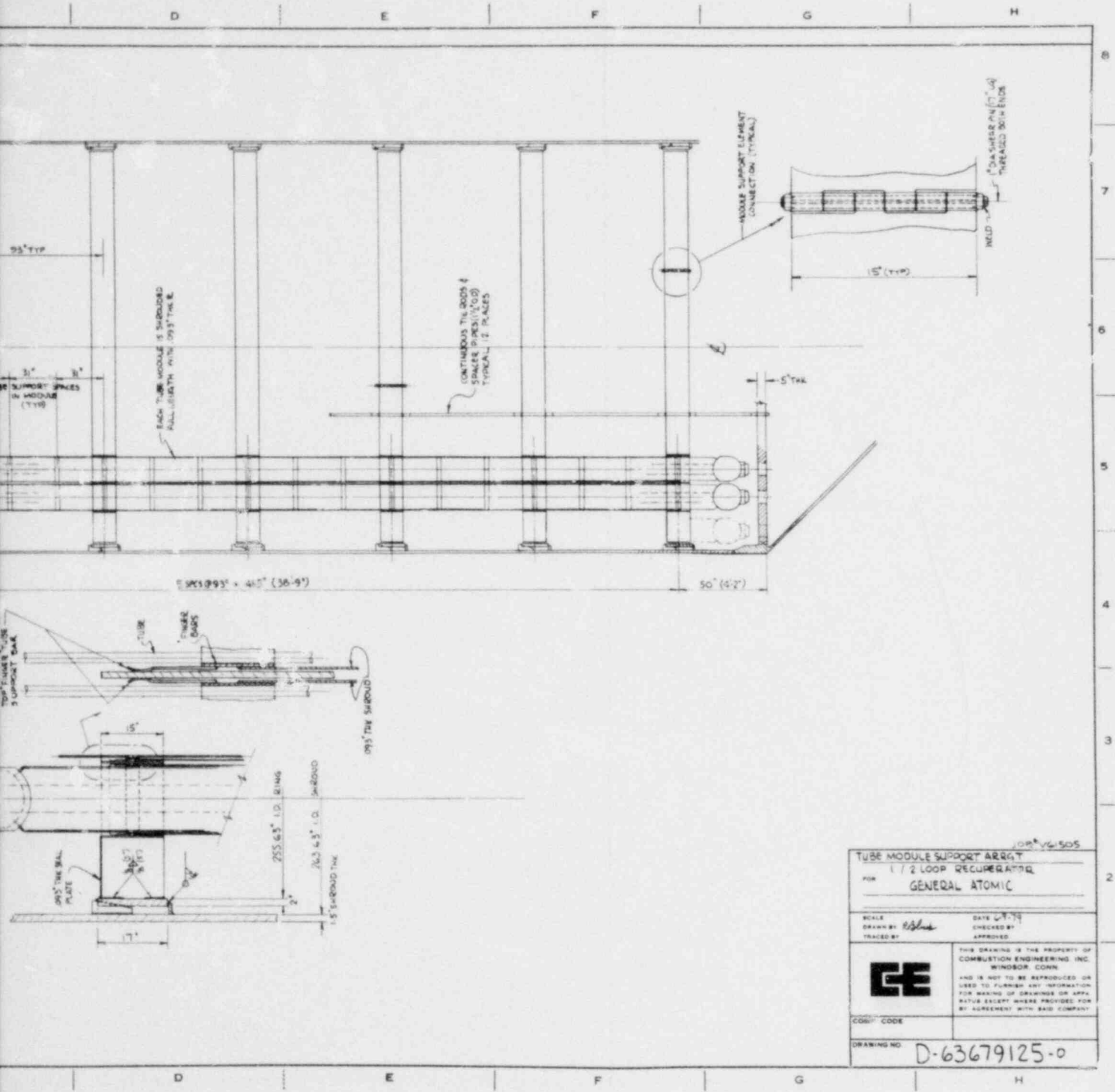


Fig. 22-1. Heat exchanger module arrangement with expansion joint





COR. V6-505

TUBE MODULE SUPPORT ARRANGEMENT FOR 1/2 LOOP RECUPERATOR GENERAL ATOMIC	
SCALE DRAWN BY: <i>elsh</i>	DATE: 6-7-79 CHECKED BY: APPROVED:
<b>GE</b>	THIS DRAWING IS THE PROPERTY OF COMBUSTION ENGINEERING INC. WINDSOR, CONN. AND IS NOT TO BE REPRODUCED OR USED TO FURNISH ANY INFORMATION FOR MAKING OF DRAWINGS OR APPURTENANCE EXCEPT WHERE PROVIDED FOR BY AGREEMENT WITH SAID COMPANY.
	COSBY CODE
DRAWING NO. D-63679125-0	

Fig. 22-2. Design modification of hexagonal heat exchanger module support structure

### 22.3.2. Evaluation of Sulzer/GA Heat Exchanger Design Criteria

In this study, HHT (HRB) design criteria were compared with comparable U.S. (GA) criteria, and U.S. recuperator design concepts were evaluated based on their ability to meet the HHT requirements. The following areas were reviewed:

1. Design criteria for the HHT recuperator.
2. HTGR-GT heat exchangers/ground rules, guidelines, and design requirements.

These criteria are still in preliminary form, and much information that should be included is not yet available. Until the criteria become more complete and self-contained, only a cursory evaluation of their technical compatibility can be made.

The major conclusions that can be drawn from this evaluation are as follows:

1. In general, the two documents are quite similar in their requirements or ground rules and reflect basically the same philosophy and approach toward the design, manufacture, operation, and inspection of the heat exchangers. While there are numerous instances in which the two documents do not agree, these differences would have no major impact upon recuperator design.
2. There is nothing particularly unique or radical about the proposed alternate recuperator designs that would preclude their use in accordance with the HHT criteria. Some minor modifications would have to be made in the designs, but none would have a significant impact on the concepts. The implied HHT requirement to inspect recuperator tubes will significantly constrain module size and accessibility and probably precludes the small hexagonal module approach developed in FY-78.

A heat exchanger cost reduction study was performed, but this study was severely limited in scope in that time did not permit cost estimating. The conclusion from the study is that further work should be devoted to quantifying cost savings associated with:

1. Flat tubesheets (rather than spherical).
2. Large modules (reduced number of modules).
3. Simpler, round tube modules rather than close packed hexagonal modules.

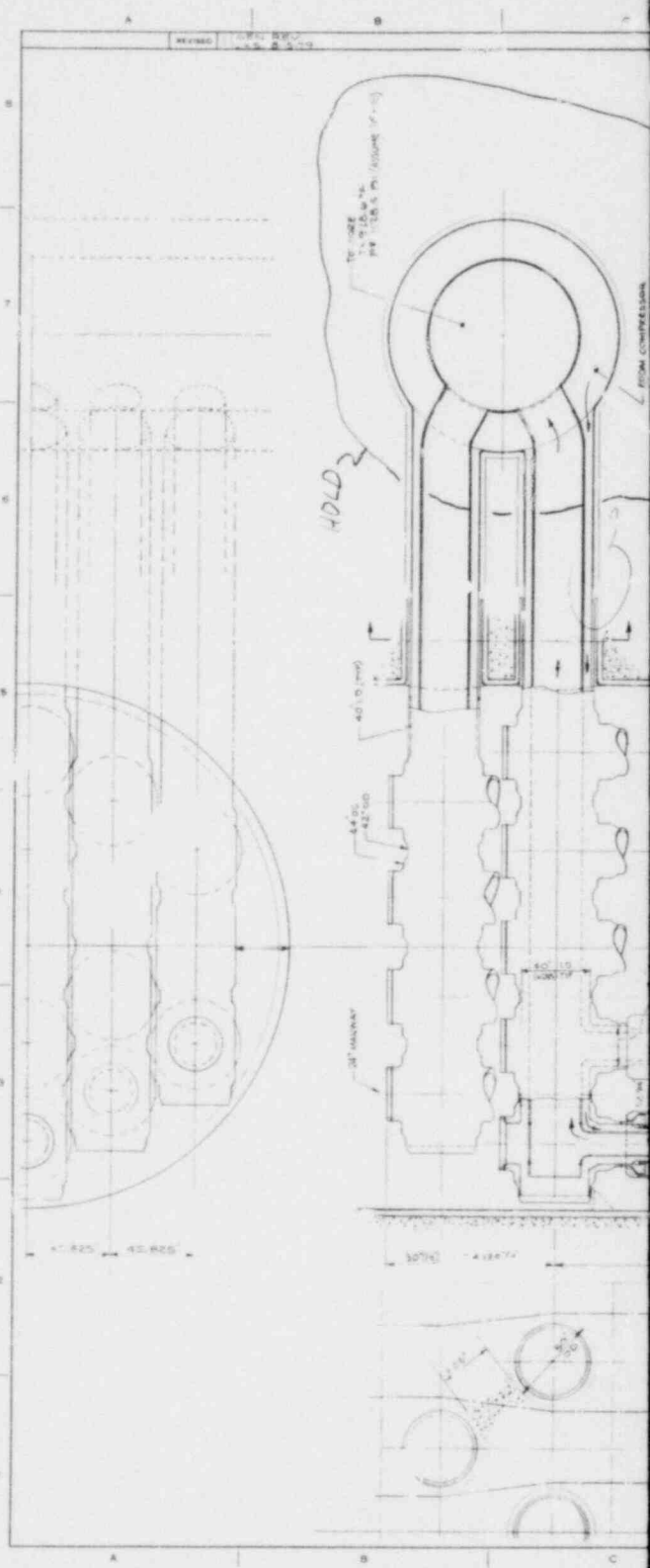
#### 22.3.3. 500-MW(e) HTGR-GT Heat Exchanger Study

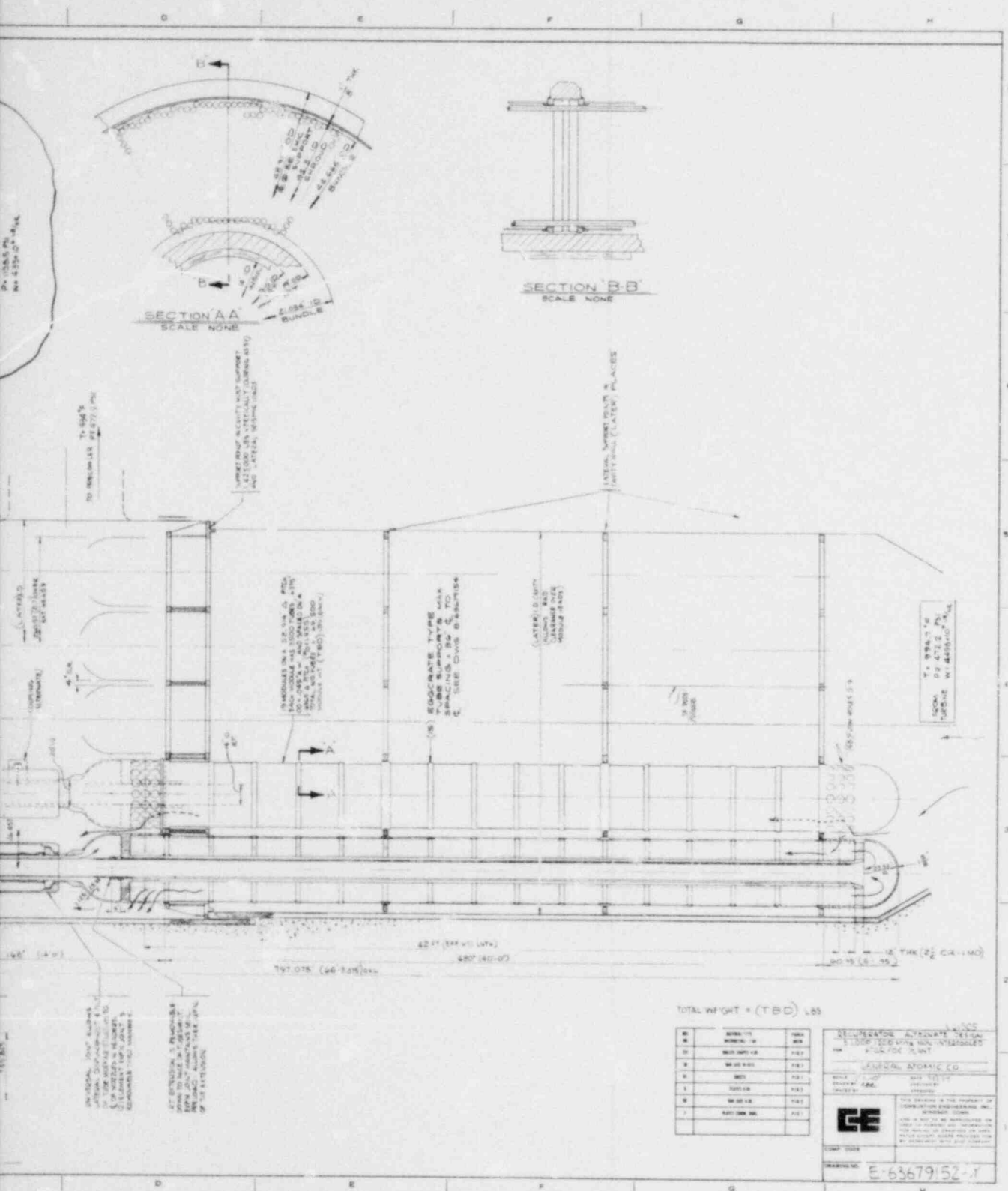
Sketches of the recuperator and precooler for the 500-MW(e) HTGR-GT were prepared by CE. The sketches were merely scaled up from the three-loop, 1200-MW(e) non-intercooled plant design.

#### 2.3.4. Alternate Heat Exchanger Design

The alternate recuperator design proposed by CE is illustrated in Fig. 22-3. Briefly, the concept utilizes a series of five parallel headers to support 19 large modules within the recuperator cavity. (These headers replace the single, large dished head found in the reference design.) A separate module support structure in the cavity provides a horizontal load path for the modules into the PCRV concrete. The support structure assumes no vertical loads from the modules or headers except for initial assembly, at which time the structure supports the modules while the five horizontal headers are being welded into place.

After the headers are in place, the modules are lifted off the structure and attached to the headers. A manway is provided in the headers at each of the 19 module positions. Removal of the manway cover and parts of the insulated return pipe provides excellent access to the top tubesheet for





TOTAL WEIGHT = (TBD) LBS

NO	DESCRIPTION	QTY	UNIT
1	...	...	...
2	...	...	...
3	...	...	...
4	...	...	...
5	...	...	...
6	...	...	...
7	...	...	...

RECUPERATOR ALTERNATE DESIGN  
 1.000 TUBES 100% INTERLOCKED  
 100% FOR 100% FLOW

GENERAL APOTHEC CO.  
 100% FOR 100% FLOW

THIS DRAWING IS THE PROPERTY OF  
 GENERAL APOTHEC CO. AND IS NOT TO BE  
 REPRODUCED OR TRANSMITTED IN ANY  
 FORM OR BY ANY MEANS, ELECTRONIC OR  
 MECHANICAL, INCLUDING PHOTOCOPYING,  
 RECORDING, OR BY ANY INFORMATION  
 STORAGE AND RETRIEVAL SYSTEM, WITHOUT  
 THE WRITTEN PERMISSION OF GENERAL  
 APOTHEC CO.

COMP CODE  
 DRAWING NO. E-63679152-1

Fig. 22-3. CE alternate recuperator design

tube inspection and/or plugging. The tubes are completely straight and are welded to flat tubesheets at either end of the module. The modules are round, and each module is individually shrouded. The five headers are staggered in the vertical direction to provide concrete ligament where they penetrate the cavity wall. The staggering also provides access for inspection of the header welds and for cutting and rewelding the headers in the event module replacement is ever required. A universal pipe joint in the pipe connecting the module to the header allows unrestrained lateral shift and tilt of the module centerline relative to the centerline of the header nozzle to which it is attached. The 19 modules are arranged in a triangular pattern with a 134.4-cm (52.914-in.) pitch. There are 3500 A.W. tubes, 1.111-cm (0.4375-in.) o.d. by 0.114 cm (0.045 in.), in each module. Tube supports are of a type commonly referred to as "eggcrates" and are illustrated in Fig. 22-4.

Preliminary structural analysis has been performed to justify the feasibility of the concept, and pressure drop calculations have been made that compare favorably with those made for the reference recuperator concept.

A comparison of recuperator concepts is shown in Table 22-1, which begins with the one-loop/two-loop intercooled plant recuperator (161 modules), followed by the modified one-loop/two-loop design (as a result of design issues), the three-loop, 83-module concept, and finally the 19-module alternate concept.

The alternate recuperator designs proposed by GA are illustrated in Figs. 22-5 (seven modules) and 22-6 (stayed tubesheet). The seven-module concept is a further development of the 19-module concept proposed by CE. The number of modules has been further reduced and increased in size. This provides the fabrication/handling/cost benefits associated with the 19-module concept while also providing module shrouds of sufficient diameter/stiffness so that the lateral support requirements are significantly simplified (one at top and one at bottom only). Additionally, a



TABLE 22-1  
RECUPERATOR CONCEPT COMPARISON

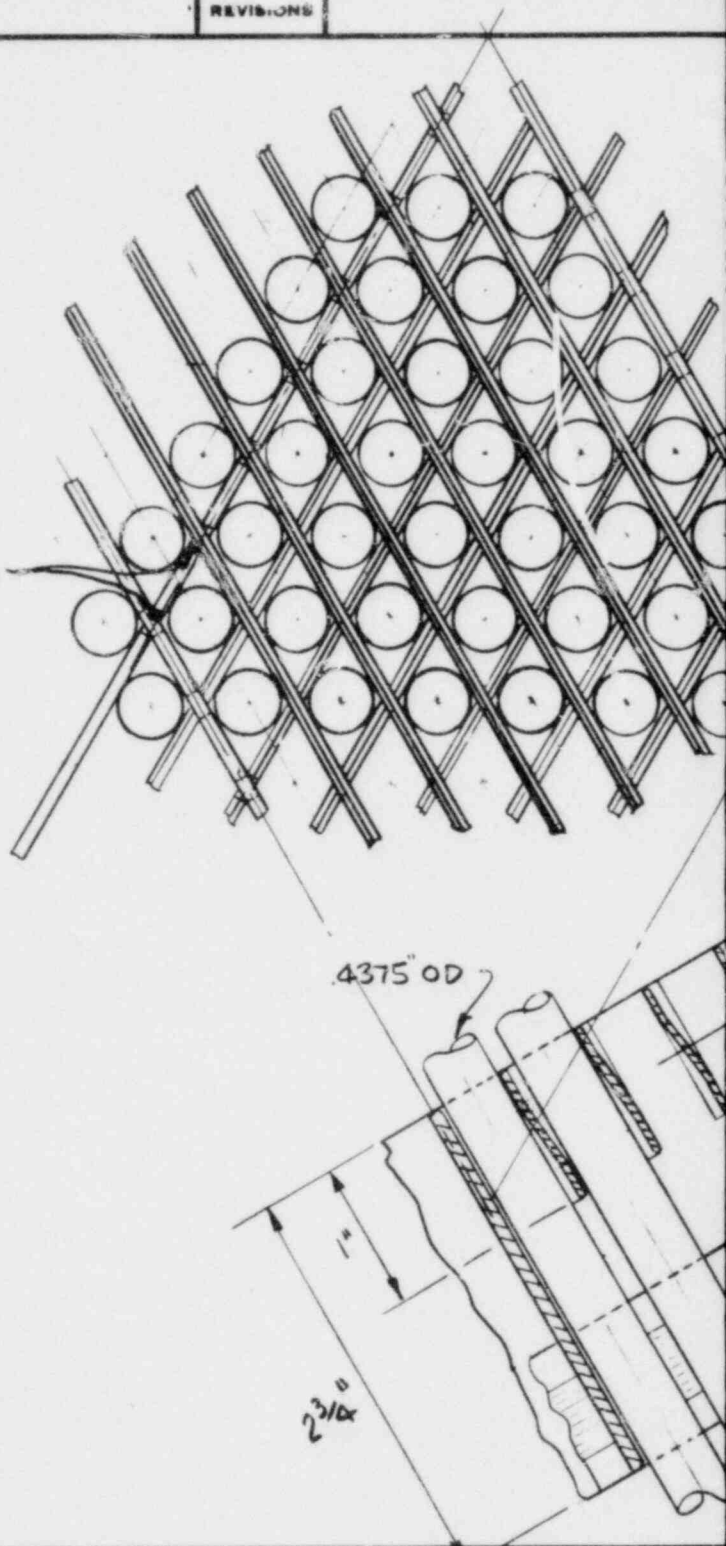
	1-Loop/2-Loop	Modified 1-Loop/2-Loop	3-Loop	Alternate Concept
Thermal rating, MW(t)/HX	1253	1253	918	918
Heat exchanger surface, m <sup>2</sup> (ft) <sup>2</sup> /HX	42,312 (455,406)	42,312 (455,406)	28,400 (305,732)	28,400 (305,732)
Number of tubes/heat exchanger	94,668	94,668	66,732	66,500
Number of modules/heat exchanger	161 (hex.)	161 (hex.)	83 (hex.)	19 (round)
Number of tubes/module	588	588	804	3500
Tube size, cm(in.)	1.1113 x 0.0813(0.4375 x 0.032)		1.1113 x 0.1114(0.4375 x 0.045)	
Pitch-to-diameter ratio	1.455	1.455	1.4	1.455
Diameter, m(ft)	6.8 (22.3)	6.9 (22.55)	5.64 (18.5)	6.7 (22)
Height, m(ft)	24.5 (80.0)	21.2 (69.4)	20.4 (67)	20.2 (66.4)
Weight, tonnes (tons)	1043 (1027)	1041 (1025)	813 (800)	813 (800)
Pressure loss, %	2.4	2.4	3.7	1.9
ISI repair	Module	Module	Module	Module/tube
HP/LP gas boundary	Large spherical head	Large spherical head	Large spherical head	Headers

REVISIONS

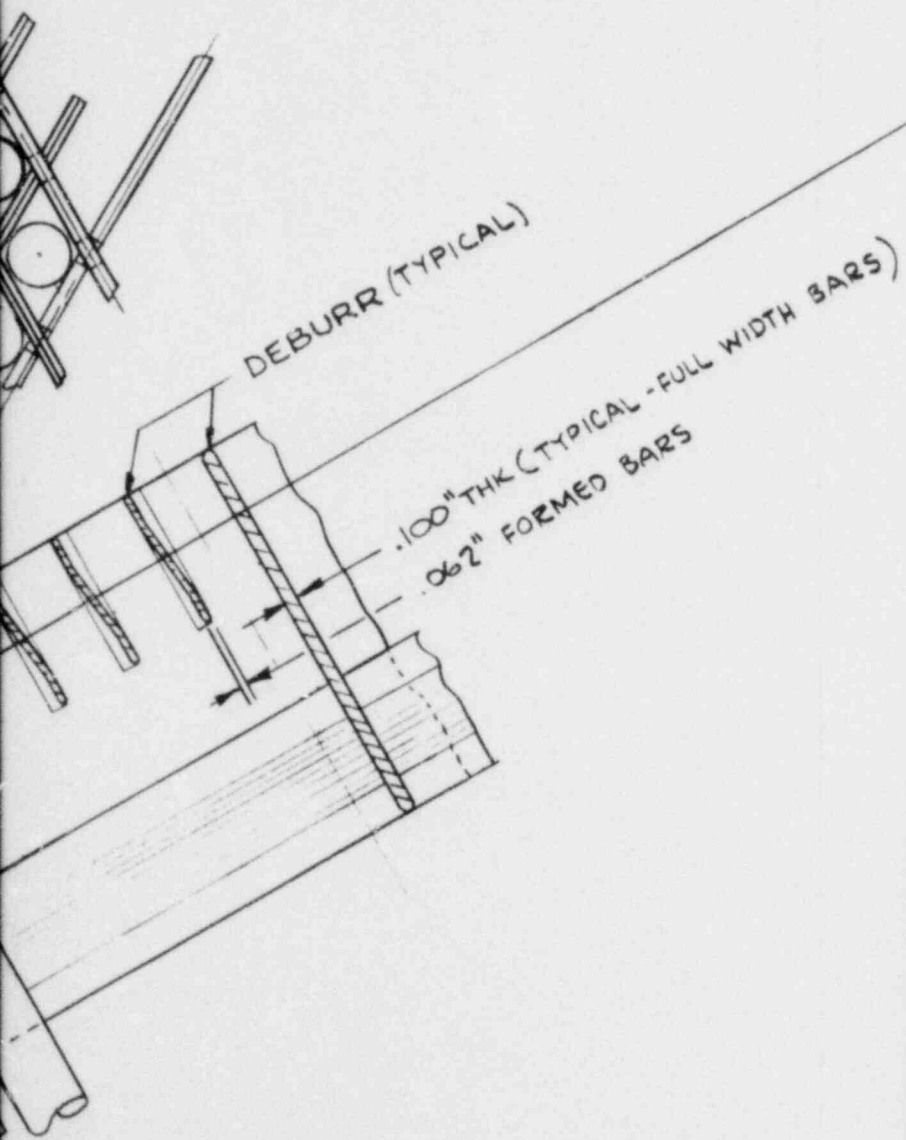
TACK WELD

4.375" OD

2 3/16"



WIDE BARS 7x7 SPCS (TYP ALL TUBES)  
 TOTAL AREA = 17.192 IN<sup>2</sup> (49 TUBE GROUP)  
 AREA TUBES = 7.366 IN<sup>2</sup> (49 "  
 FLOW AREA = 9.826 IN<sup>2</sup> (BETWEEN SUPPTS) } @ P/O = 1.455



% BLOCKAGE THRU ONE PLANE

P/O 1.4 = 31.33%  
 P/O 1.455 = 28.33%  
 P/O 1.5 = 26.3%


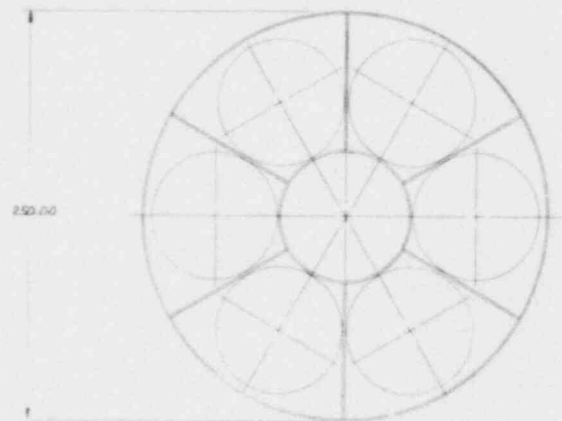
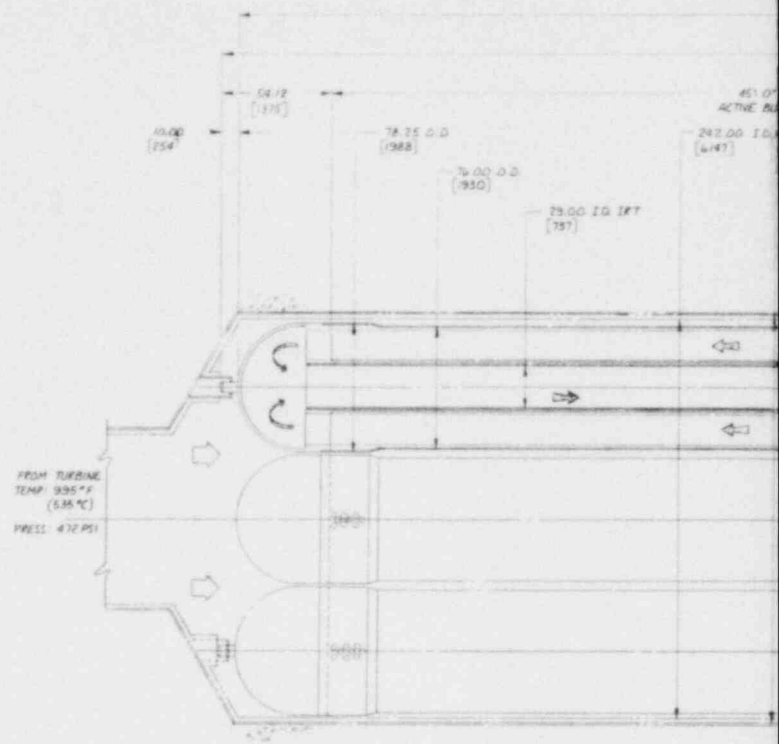
<b>TYPICAL EGGCRATE TYPE</b> <b>FOR TUBE SUPPTS FOR CELL</b>	
SCALE FULL SIZE DRAWN BY BULLEN TRACED BY	DATE 7-27-79 CHECKED BY APPROVED <i>l. Bullock 7-27</i>
	THIS DRAWING IS THE PROPERTY OF <b>COMBUSTION ENGINEERING, INC.</b> WINDSOR, CONN. AND IS NOT TO BE REPRODUCED, OR USED TO FURNISH ANY INFORMATION FOR MAKING OF DRAWINGS OR APPA- RATUS EXCEPT WHERE PROVIDED FOR BY AGREEMENT WITH SAID COMPANY.
	COMP. CODE:
DRAWING NO. <b>B-63679154-0</b>	

Fig. 22-4. "Eggcrate" tube supports for heat exchanger module

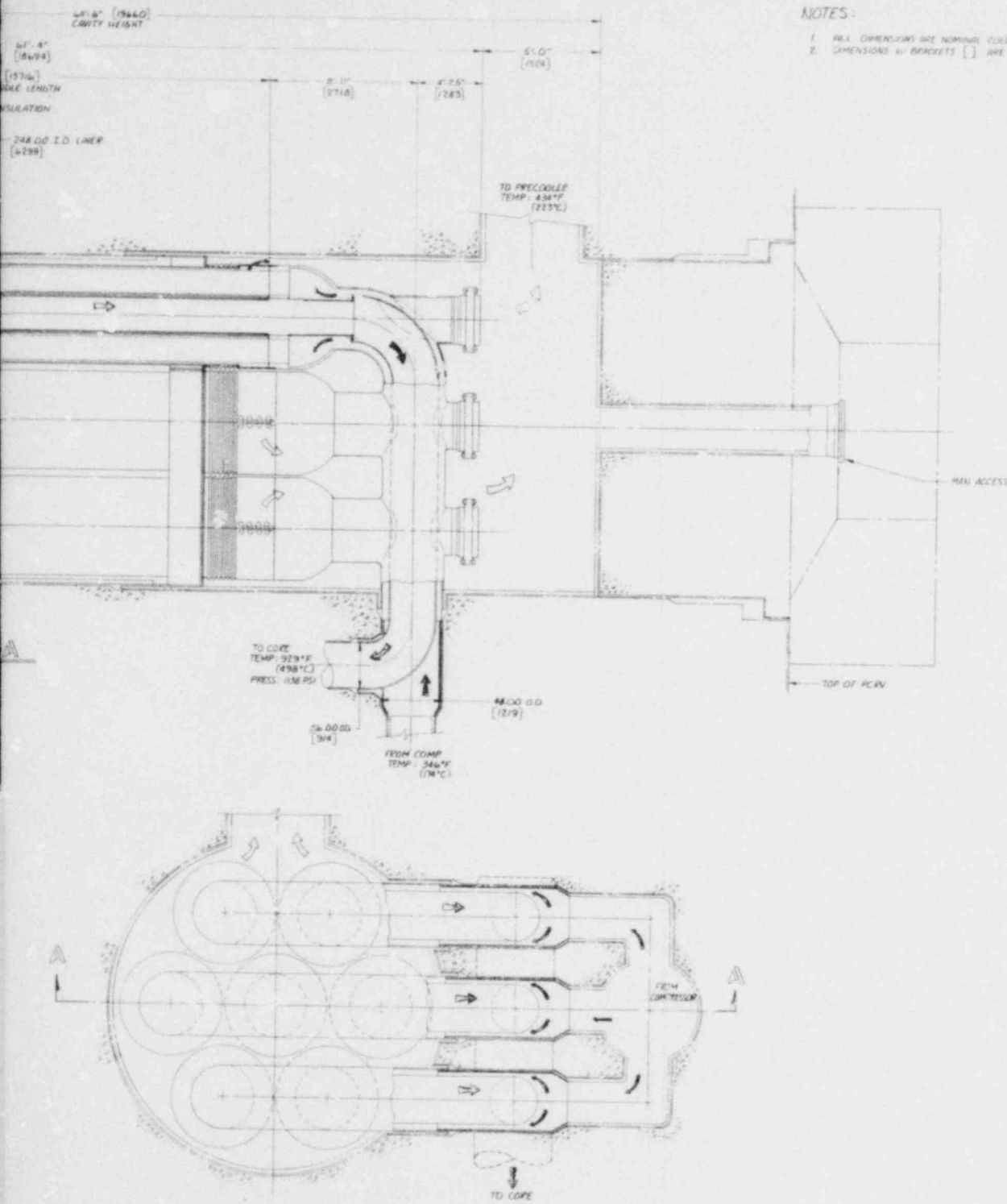
reduction in the number of modules reduces the number of headers to three, thereby reducing the overall height of the unit and providing additional access in the header area.

The stayed tubesheet design (Fig. 22-6), although not unique in concept, is unique in application. This concept comprises two flat tubesheets (one at the top and one at the bottom) which are connected by 45,000 straight [1.666-cm (0.656-in.) diameter by 0.109-cm (0.043-in.) wall] stainless steel tubes. An outer shroud extends the full length of the tubes, is attached to the lower tubesheet, and is perforated top and bottom for shell side gas flow. A pipe in the middle of the bundle is provided for inspection access, and the tubes are supported laterally by "eggcrate" supports as illustrated in Fig. 22-4. Low-pressure gas from the turbine enters the upper plenum, flows down through the tubes, and exits the lower cavity via a duct to the precooler. High-pressure gas from the compressor enters the bundle at the lower end, turns 90° and flows upward parallel to the tubes, turns 90° at the top, and exits to the core. The tubes therefore are externally pressurized and loaded in tension, thus "staying" the tubesheets. Preliminary analysis indicates that this concept reduces capital and plant operating costs while improving safety and reliability.

All four concepts will be evaluated and compared by GA and CE. The HHT seven-module concept data (if available) will also be included in the comparison. Selection of a preferred design is scheduled for early FY-80.

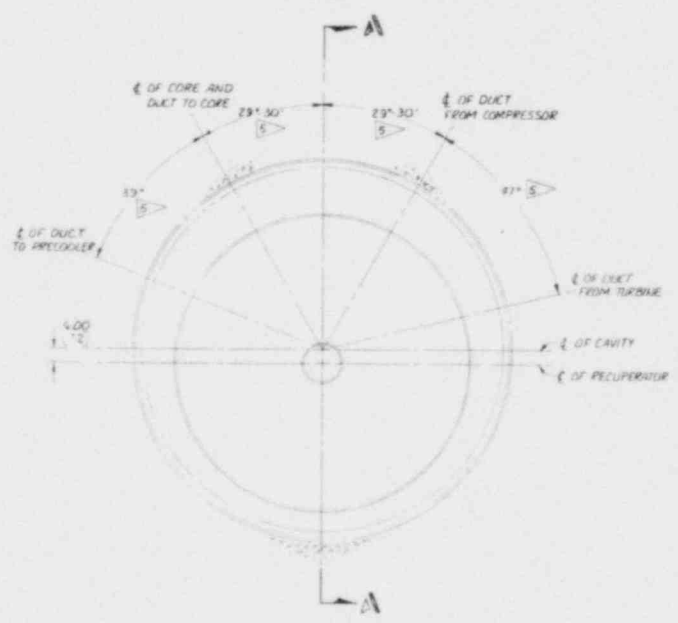
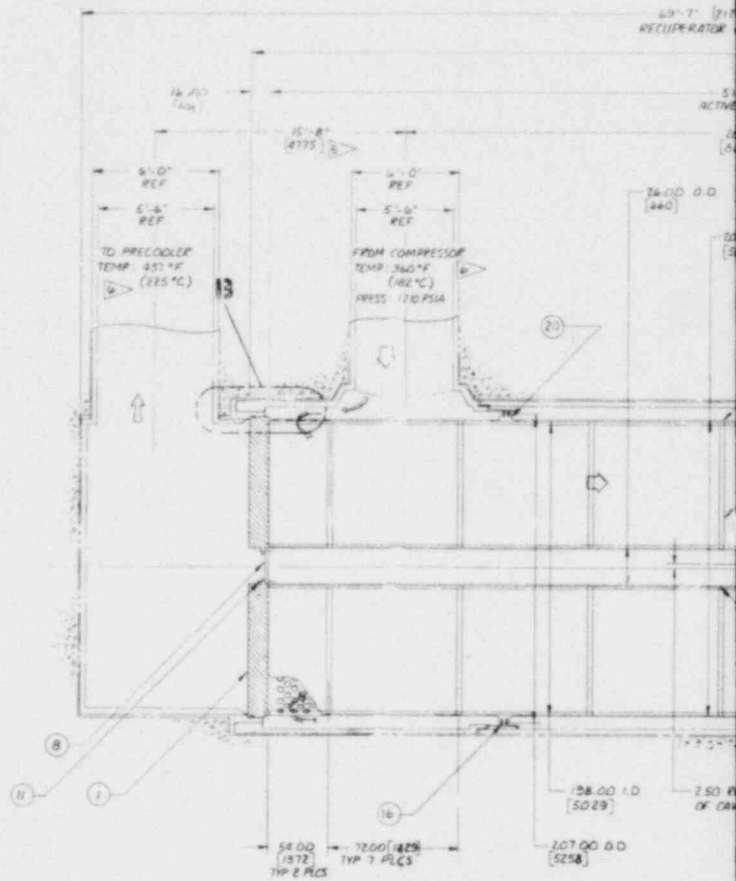


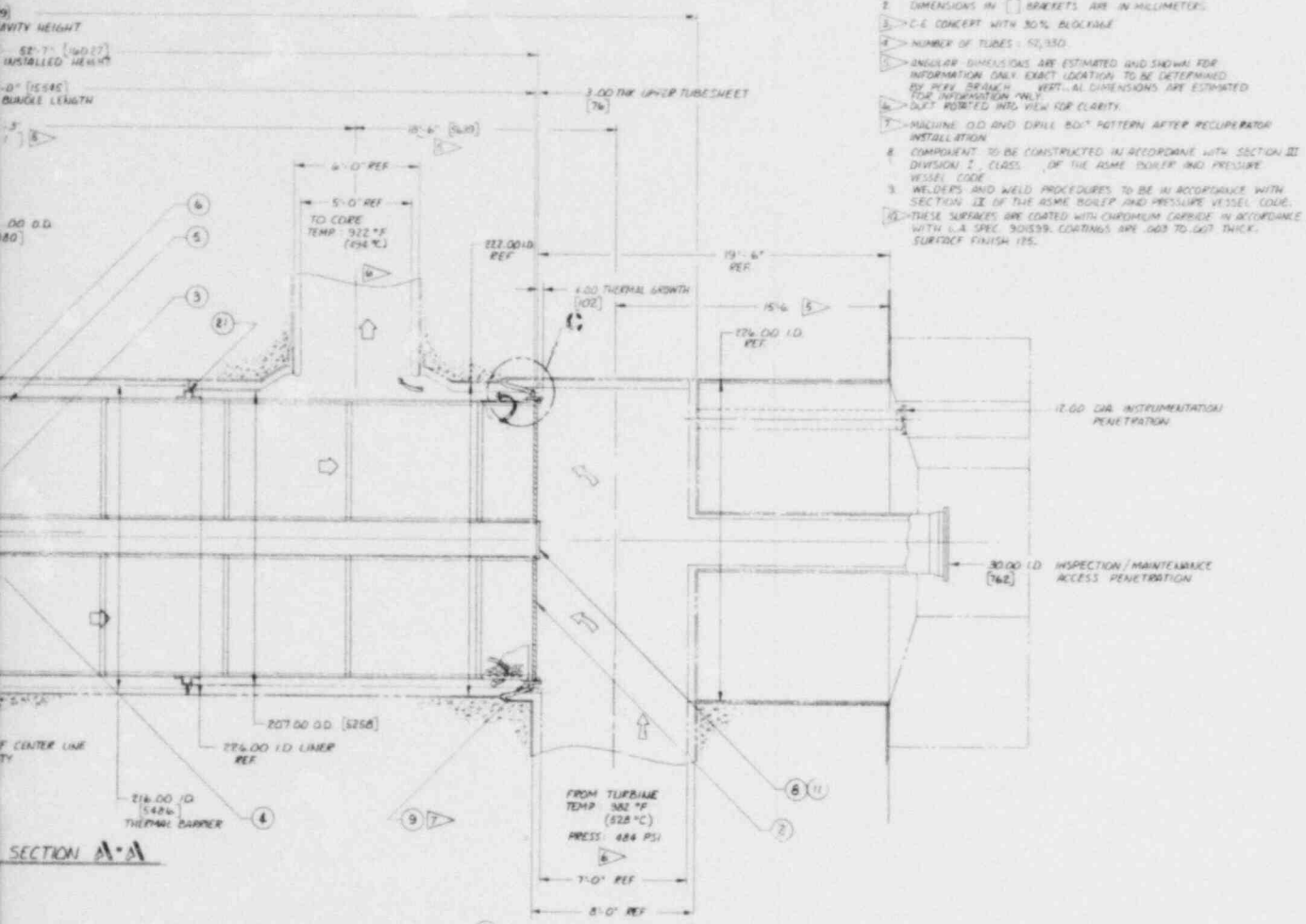
SUPPORT STRUCTURE



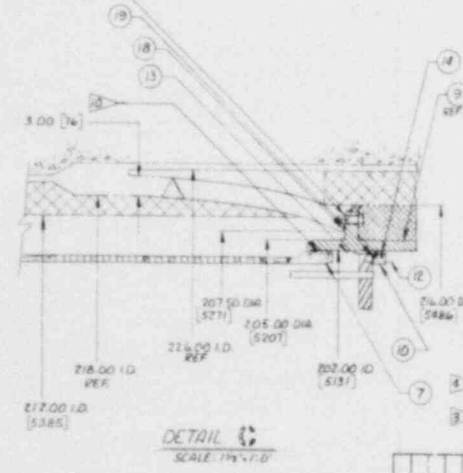
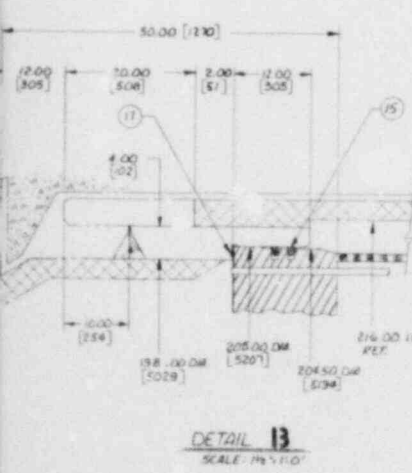
NOTES:  
 1. ALL DIMENSIONS ARE NOMINAL COLD CONDITION  
 2. DIMENSIONS IN BRACKETS [ ] ARE IN MILLIMETERS

Fig. 22-5. GA seven-module alternate recuperator design





- NOTES**
1. ALL DIMENSIONS ARE NOMINAL COLD CONDITION
  2. DIMENSIONS IN [ ] BRACKETS ARE IN MILLIMETERS
  3. C-E CONCEPT WITH 30% BLOCKAGE
  4. NUMBER OF TUBES = 52,350
  5. ANGULAR DIMENSIONS ARE ESTIMATED AND SHOWN FOR INFORMATION ONLY EXACT LOCATION TO BE DETERMINED BY PERFORMING VERTICAL DIMENSIONS ARE ESTIMATED FOR INFORMATION ONLY
  6. DUCT POINTED INTO VIEW FOR CLARITY
  7. MACHINE OLD AND DRILL BOX PATTERN AFTER RECUPERATOR INSTALLATION
  8. COMPONENT TO BE CONSTRUCTED IN ACCORDANCE WITH SECTION III DIVISION 1, CLASS OF THE ASME BOILER AND PRESSURE VESSEL CODE
  9. WELDERS AND WELD PROCEDURES TO BE IN ACCORDANCE WITH SECTION II OF THE ASME BOILER AND PRESSURE VESSEL CODE
  10. THESE SURFACES ARE COATED WITH CHROMIUM CARBIDE IN ACCORDANCE WITH U.S. SPEC. 301539. COATINGS ARE .003 TO .007 THICK. SURFACE FINISH 125.



ITEM	PART NO.	DESCRIPTION	MAT. MATL. SPEC.
1 21		FLOW RESTRICTOR 1/2" x 1/2" x 1/2" x 1/2"	SA 240 TYPE 316
1 20		SEAL RING FLANGE 1/2" x 1/2" x 1/2" x 1/2"	SA 182 TYPE 316
1 19		GASKET FLEXIBLE 1/2" x 1/2" x 1/2" x 1/2"	SA 240 TYPE 316
1 18		GASKET FLEXIBLE 1/2" x 1/2" x 1/2" x 1/2"	SA 240 TYPE 316
1 17		GASKET FLEXIBLE 1/2" x 1/2" x 1/2" x 1/2"	SA 240 TYPE 316
2 16		SEAL PISTON RING 209" O.D.	SA 240 TYPE 304
2 15		SEAL PISTON RING 206" O.D.	SA 240 TYPE 304
2 14		SEAL PISTON RING 202" O.D.	SA 240 TYPE 304
1 13		SEAL FINISHER (LATER)	
1 12		BOLT 1/2" DIA x 3" LG.	SA 437 TYPE 718
1 11		BOLTS 1/2" DIA x 4" LG.	SA 437 TYPE 718
1 10		BACK-UP SEAL HOLDER 1/2" x 1/2" x 1/2" x 1/2"	SA 240 TYPE 316
1 9		SWIM 20" O.D. x 2 1/2" O.D. x 1/2"	SA 240 TYPE 316
2 8		ACCESS COVER 24" O.D. x 2 1/2" THK	SA 240 TYPE 316
1 7		SHROUD RING RING 1/2" x 1/2" x 1/2" x 1/2"	SA 240 TYPE 316
1 6		SHROUD RING 1/2" x 1/2" THK	SA 240 TYPE 316
1 5		TUBE 1/2" O.D. x 1/2" WALL x 1/2" x 1/2"	SA 240 TYPE 316
1 4		PIPE 24" O.D. x 1/2" WALL	SA 240 TYPE 316
1 3		TUBE SUPPORT SPID 1/2" x 1/2" x 1/2" x 1/2"	SA 240 TYPE 316
1 2		HOT TUBESHEET 1/2" THK x 202" O.D.	SA 240 TYPE 316
1 1		COLD TUBESHEET 1/2" THK x 206" O.D.	SA 240 CL 1

ESTIMATED WEIGHT: 1014,000 LBS.  
459,997 KGS.

Fig. 22-6. GA stayed tubesheet alternate recuperator design



## 23. PLANT PROTECTION SYSTEM (6332)

### 23.1. SCOPE

The purpose of this task in FY-79 was to establish conceptual design requirements and interfaces for the plant protection system (PPS).

### 23.2. SUMMARY

The PPS effort consisted of (1) reviewing previously generated data, (2) identifying major technical problems, (3) preparing block diagrams for the PPS, and (4) initiating work on the PPS system description and design basis.

The review of previous work in the PPS area continued, and a technical problem list was compiled identifying 17 issues. The most significant problem is how to measure primary coolant loop and total plant helium flow.

The PPS instrument block diagrams (Fig. 22-1) were issued and work was begun on preparation of the PPS system description and design basis documentation.

### 23.3. DISCUSSION

#### 23.3.1. Review and Problem Areas

A review of the previous work in the PPS area continued, and a technical problem list was compiled. Seventeen unresolved areas have been identified. (This is in addition to the questions related to the combination of the control and protection on the previously reported safety and

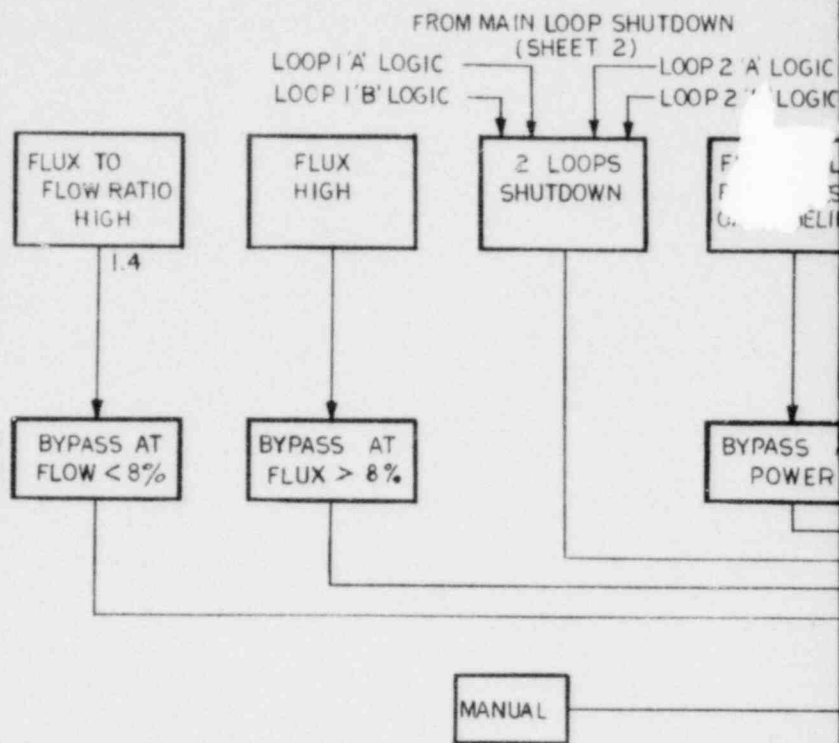
primary bypass valves.) Many of these technical problems relate to the selection of trip parameters or the need for various protective actions and interlocks. Some relate to the basic plant configuration or control (i.e., precooler safety class, isolation needs, and leak detection; whether the plant has helium inventory control and its potential impact; etc.). While these problems will generally be answered in the normal plant design evolution, their recognition assists in future work planning.

The most significant problem is how to measure primary coolant loop and total plant helium flow. These parameters are used in the reactor trip system and the CACS initiation system. This problem will need to be specifically addressed in the future and may require specific generic funding.

#### 23.3.2. Design

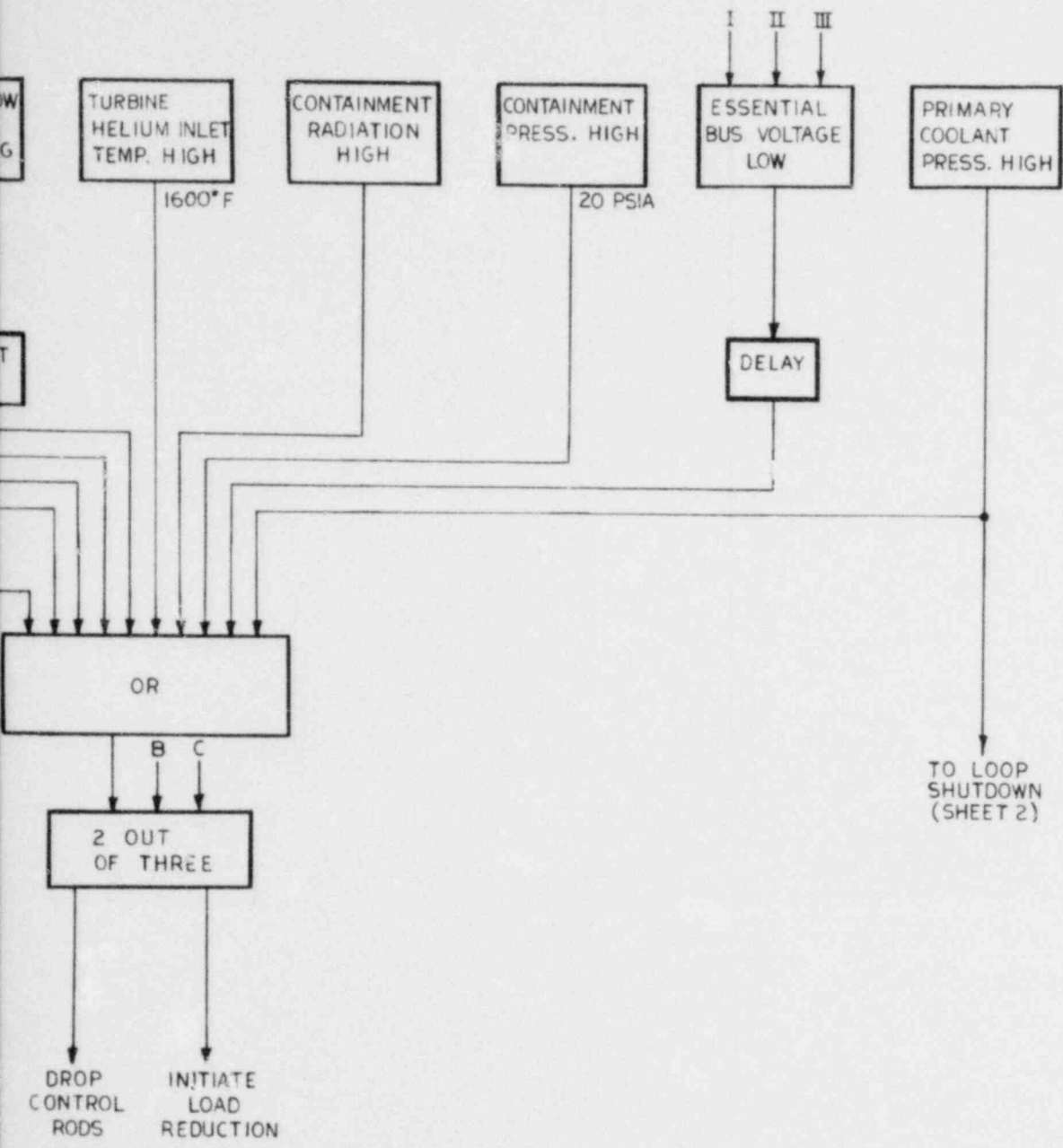
The PPS instrument block diagrams (Fig. 23-1) were issued. These block diagrams show the major PPS function, their initiating parameters, and basic logic. The major subsystems are (1) the reactor trip system, (2) the main loop shutdown system, (3) the CACS initiation system, (4) the precooler isolation and dump system, and (5) the rod withdrawal interlock. The latter may not be required in the PPS and further study may lead to its downgrading.

Work has begun on preparation of the PPS system description/criteria and the supporting PPS design basis (as required by IEEE-279 and IEEE-603). These are both on-going tasks and will be an iterative process between plant systems design, systems dynamics analysis, and the PPS instrumentation and control.



CHANNEL

R



A SHOWN: CHANNEL B,C IDENTICAL

REACTOR TRIP SYSTEM

Fig. 23-1- Plant protection system instrument block diagram (sheet 1 of 4)

POWER  
CONVERSION  
LOOP TEMP  
HIGH

975°

T/M SPEED  
HIGH

110%

MANUAL

TRI  
SAFE  
BYPA  
VALV  
&  
PRIM  
BYPASS

A LOGIC FOR ONE LOOP

MAIN LOOP

(SHOWN FOR L

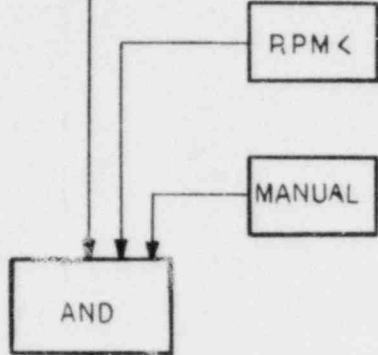
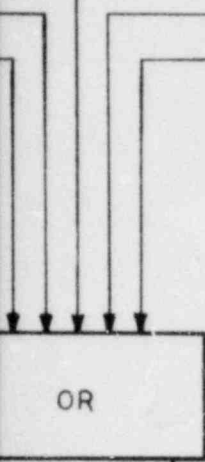
FROM REACTOR  
TRIP SYSTEM  
(SHEET-1)

FROM CACS  
INITIATION SYSTEM  
(SHEET-3)

PRI COOLANT  
PRESS HIGH

CACS  
START

T/M PRIMARY  
SEAL  
LEAKAGE HI



POWER  
SETBACK  
(PCS)

SET T/M  
SHAFT SEAL

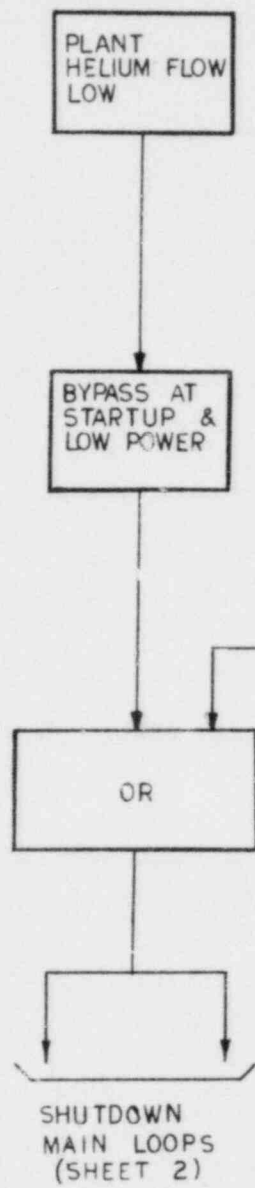
TY  
SS  
E  
RY  
VALVE

SHOWN - B LOGIC IDENTICAL

# SHUTDOWN SYSTEM

OP #1, SIMILIAR FOR LOOP 2)

Fig. 23-1. Plant protection system  
instrument block diagram  
(sheet 2 of 4)



A LOGIC FOR ONE LOOP SHOWN - B LOGIC IDENTICAL

CACS INITIATION SYSTEM

UAL

TWO OR MORE  
CONTROL RODS  
COMMANDED OUT



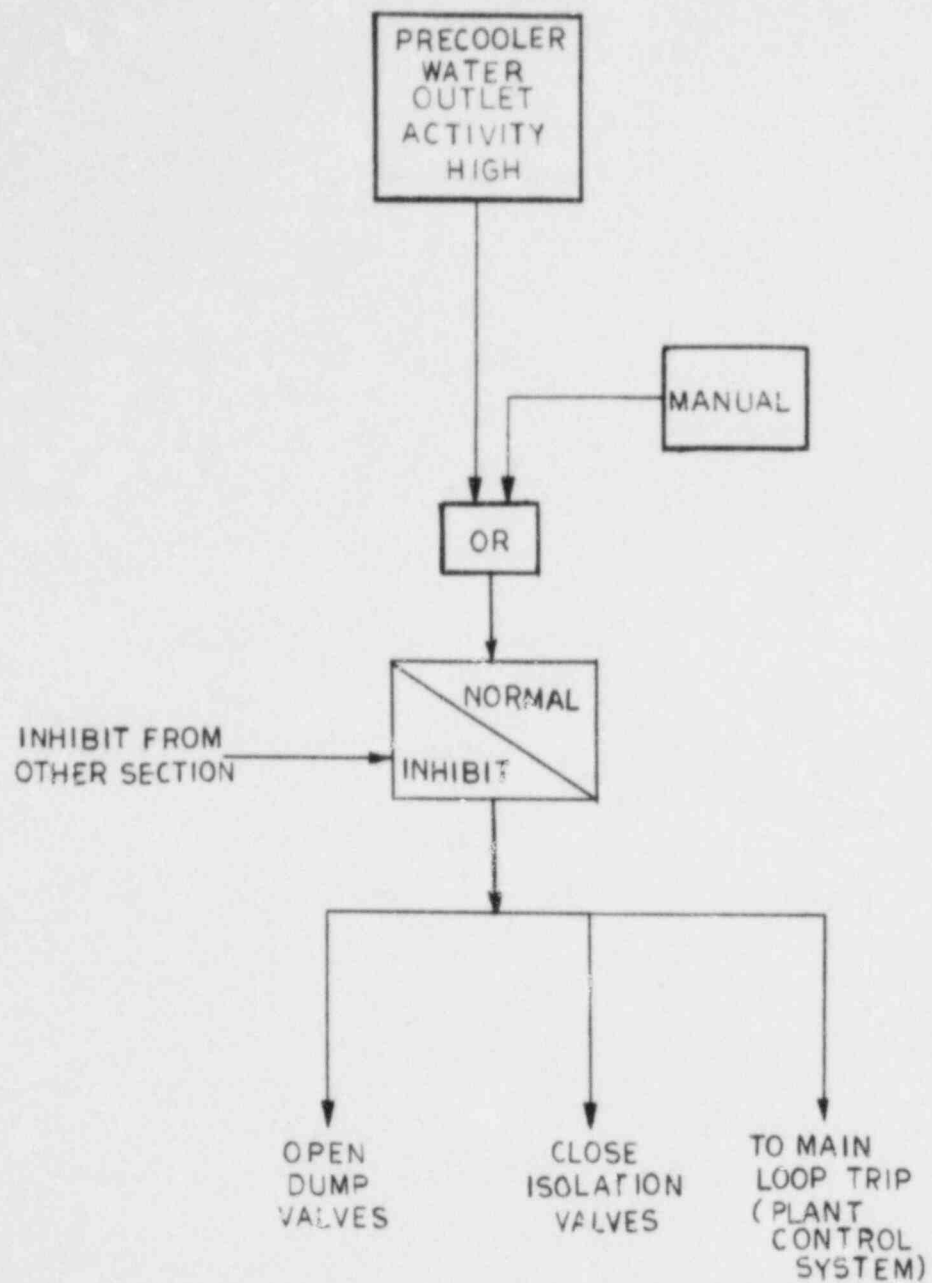
BLOCK MOTOR  
CONTROL CENTER  
OUTPUT TO RODS

ROD WITHDRAWAL  
INTERLOCK

M

Fig. 23-1. Plant protection system  
instrument block diagram  
(sheet 3 of 4)





'A' LOGIC SHOWN FOR ONE - HALF A LOOP

'B' LOGIC IDENTICAL

PRECOOLER ISOLATION  
& DUMP SYSTEM

Fig. 23-1. Plant protection system instrument block diagram (sheet 4 of 4)

## 24. PLANT CONTROL SYSTEM (6333)

### 24.1 SCOPE

The purpose of this task in FY-79 was to synthesize a PCS conceptual design.

### 24.2. SUMMARY

A candidate primary bypass valve control scheme is shown in Fig. 24-1. The initial effort to lay out the turbine inlet temperature, electrical power, turbine speed, attemperation, and surge margin controls is shown in Fig. 24-2. Technical problems encountered during early phases of conceptual design have been described. Possible turbomachinery outputs for a PCS condition monitoring system have been listed.

### 24.3. DISCUSSION

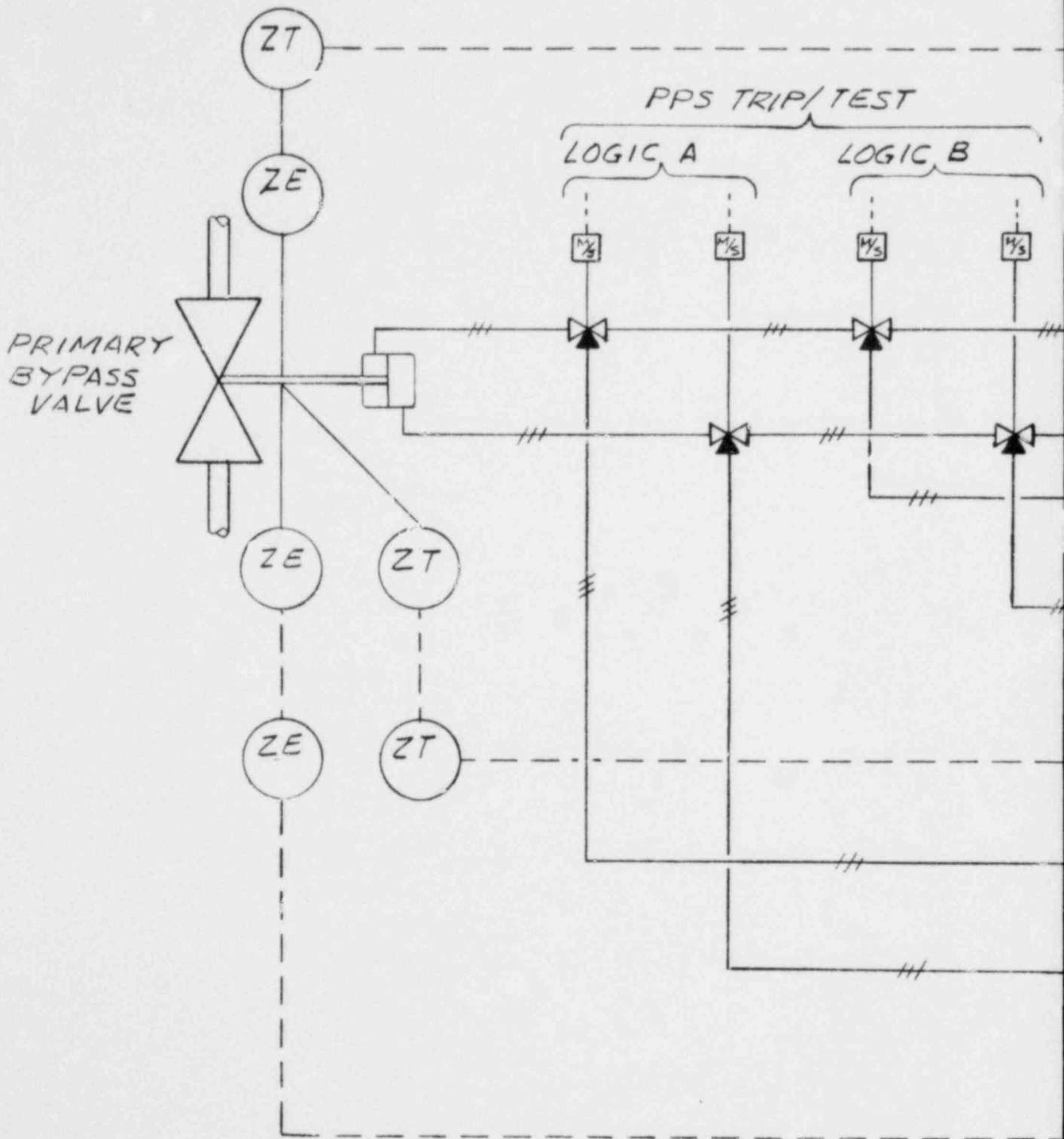
The work accomplished in the FY-79 effort is directly related to key FY-80 planned tasks. The plans for FY-80 are as follows:

1. Synthesize the conceptual design of the bypass valve control system.
2. Resolve the separation of the control and safety valve functions.
3. Summarize the major technical problems encountered during PCS conceptual design.
4. Develop a hybrid computer model for the control valve auxiliary system.
5. Prepare the conceptual design of the PCS condition monitoring system.

6. Develop the SYSL digital computer model of the control system dynamics.
7. Integrate auxiliary system control (turbomachinery primary seal system criteria, etc.) into the plant conceptual design.
8. Conceptually design the turbomachinery startup and shutdown controls.
9. Prepare the conceptual requirements for the control room.
10. Evaluate the feasibility of a control valve design using the hybrid computer model.

The primary bypass valve control circuit shown in Figs. 5-1 and 24-1 was configured in FY-79 and will be refined as tasks 1, 2, 3, 4, and 10 are accomplished during FY-80. The adequacy of the safety and control function separation (at the solenoid valves) shown in Fig. 24-1 will be evaluated. As the figure shows, an electrohydraulic servo valve has been proposed for the primary bypass valve actuator loop. Figure 24-2 shows the inner loop frequency response range for the servo valve. Closed loop servo valve/cylinder/bypass valve response will be obtained using the hybrid computer model in the future. The computer model will help determine the magnitude of problems such as required actuation times, force profiles, full-load speed control capability, discontinuous full-load valve control system response, application of split range primary/trim bypass control, integration of inventory control, and the use of more, smaller bypass control valves. It is anticipated that changes in valve geometry and control philosophy will be recommended on the basis of model response.

Figure 24-3 depicts a possible arrangement of the turbine inlet temperature, electrical power, turbine speed, attemperation, and surge margin controls. As the diagram illustrates, many "first cut" control system components were identified during FY-79. It is expected that many of the details of Fig. 24-3 will change as PCS effort continues in FY-80.



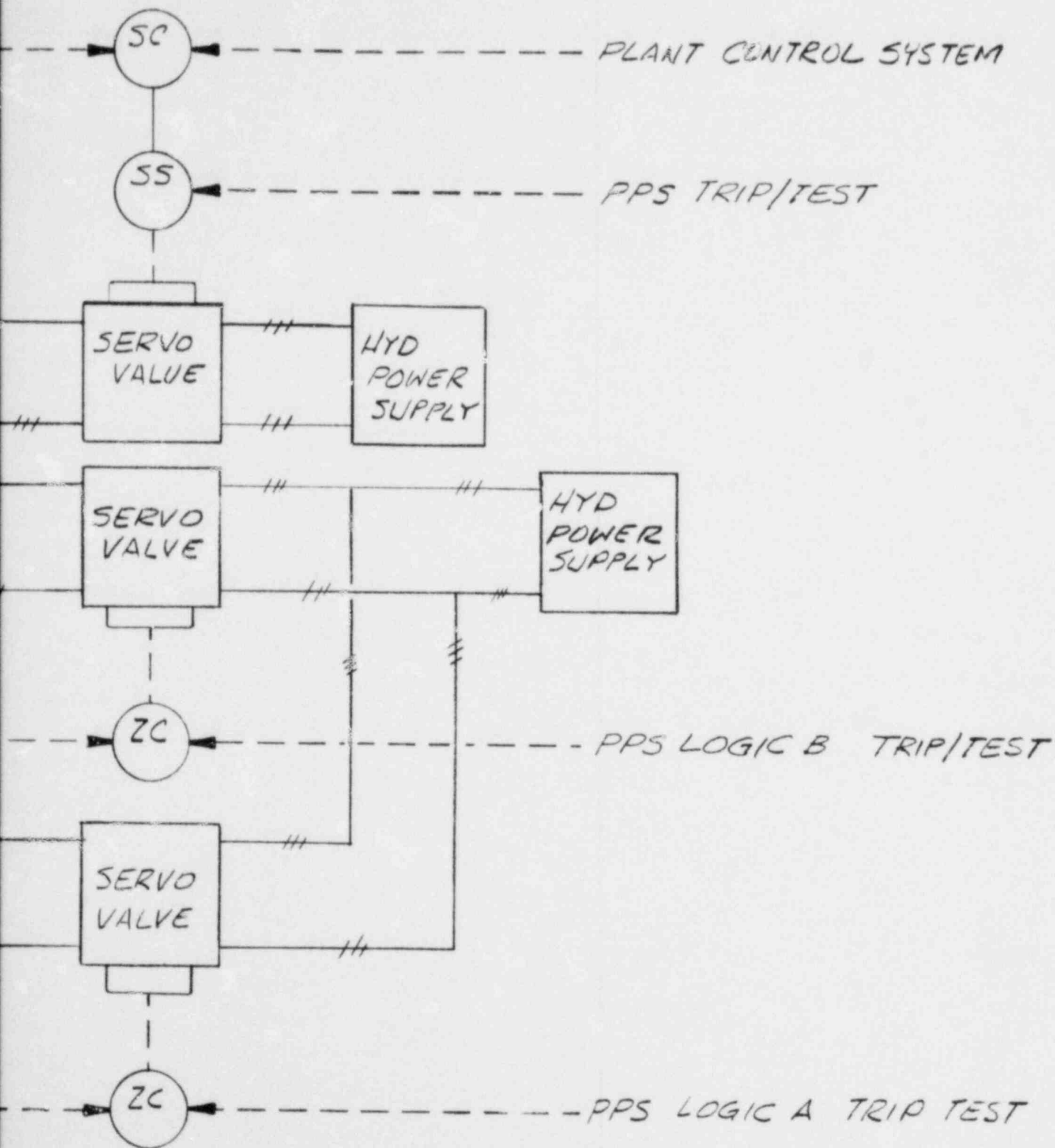
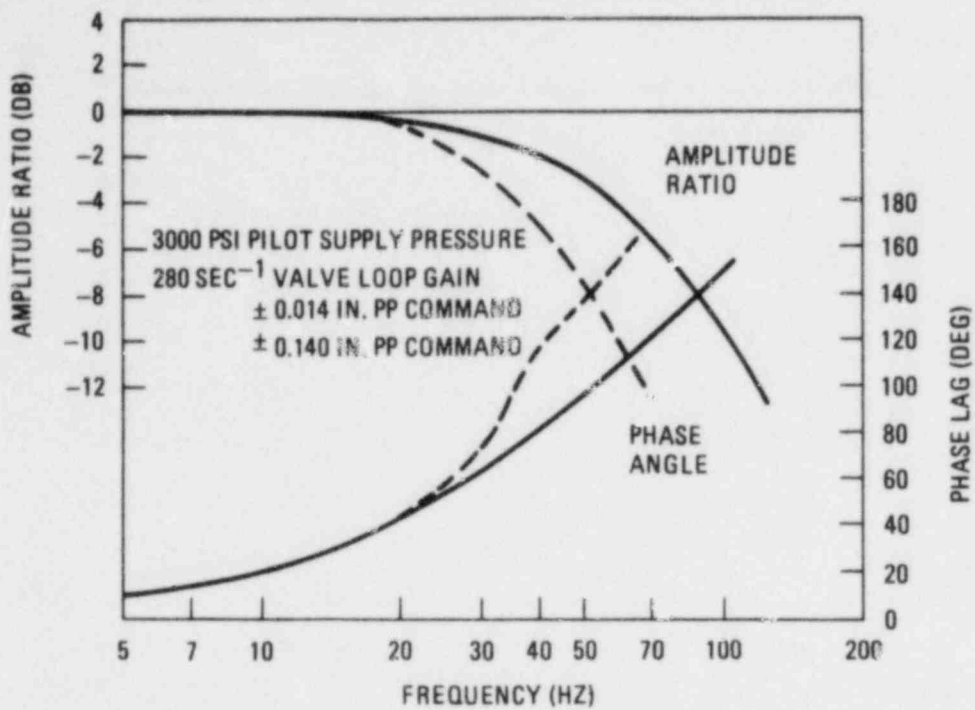
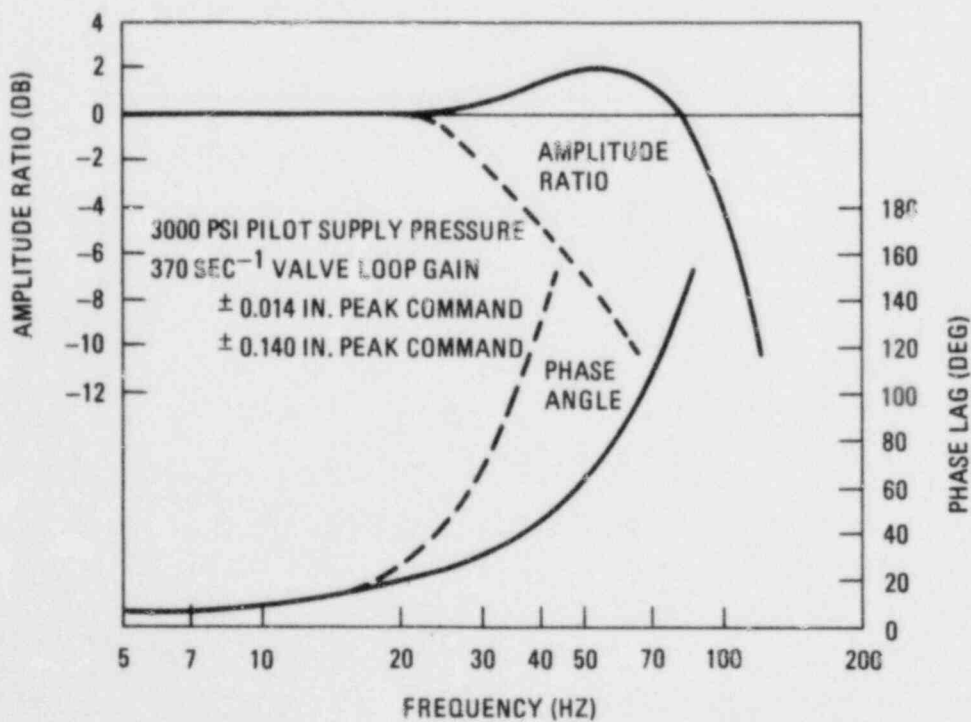


Fig. 24-1. Instrument diagram for primary bypass valve

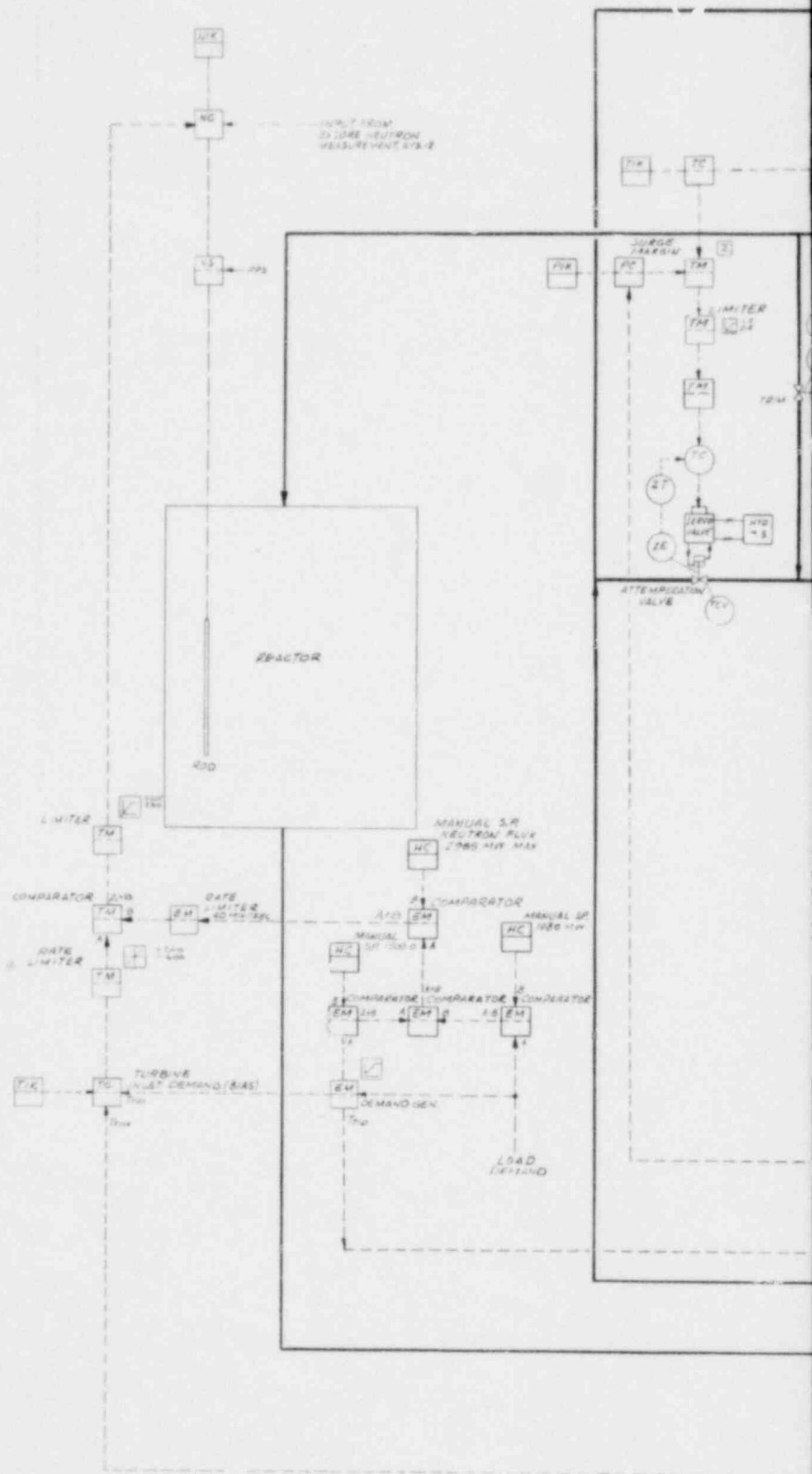


(a) FREQUENCY RESPONSE WITH  $280 \text{ SEC}^{-1}$  LOOP GAIN



(b) FREQUENCY RESPONSE WITH  $370 \text{ SEC}^{-1}$  LOOP GAIN

Fig. 24-2. Frequency response of electrohydraulic servo valve for primary bypass valve actuation system



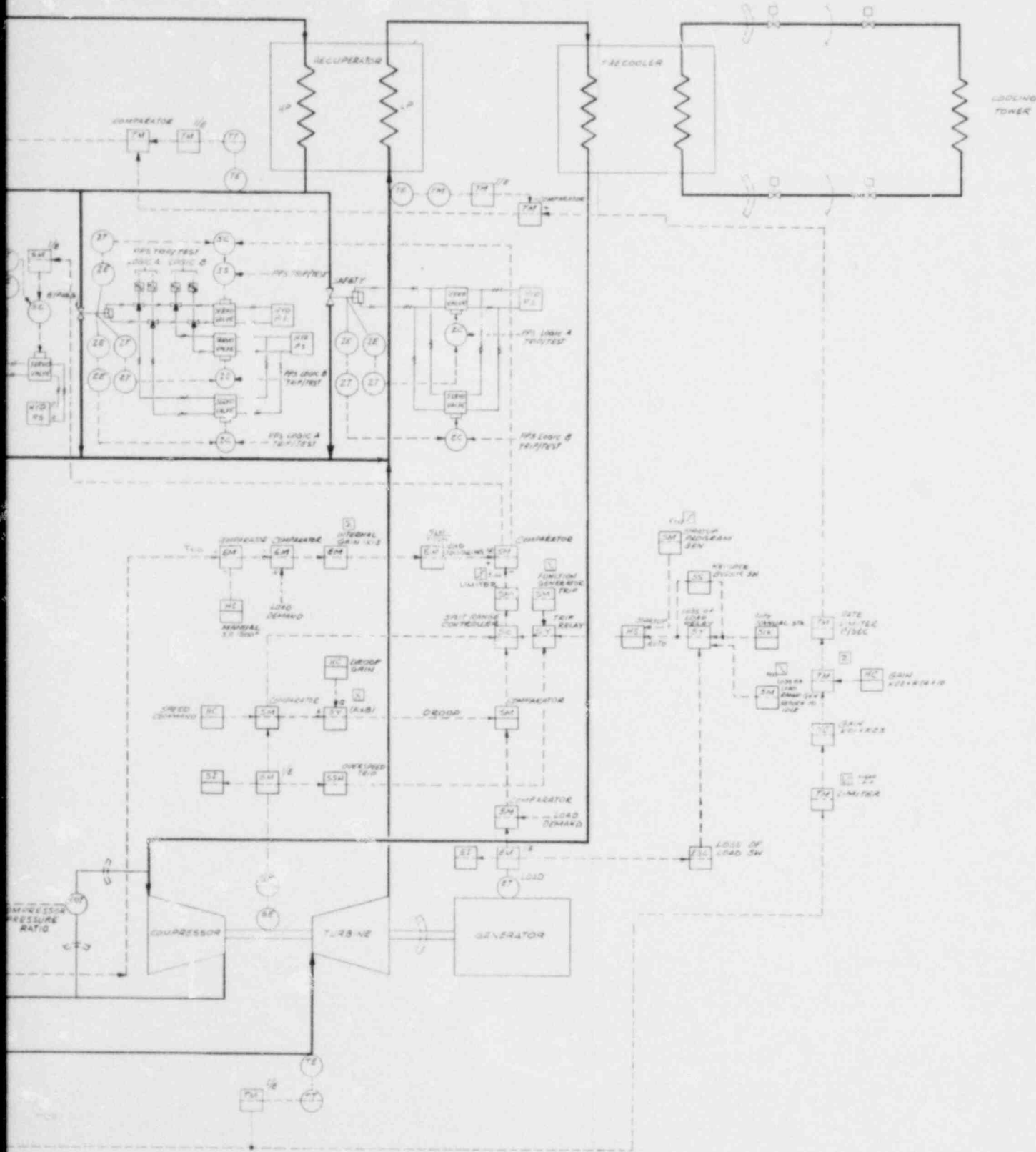


Fig. 24-3. Instrument diagram for plant control system



APPENDIX A  
TURBOMACHINE NOISE REDUCTION

Several means were examined for reducing upstream and downstream noise emissions from the compressor and turbine of the HTGR-GT.

These methods fall into four categories:

1. Modifying the number of blades and vanes.
2. Increasing the spacing between the rotor and stator stages.
3. Providing sound-absorbing linings for turbomachinery cases and/or ducting (inlet and discharge).
4. Modifying inlet and discharge duct configurations to provide noise reductions by use of a sonic throat (for inlet) and further acoustic treatment.

Not all of these methods need be applied to all components. For example, if the recommended blade and vane numbers can be employed, the current rotor-stator spacing can be retained. Similarly, if satisfactory inlet ducts that incorporate a sonic throat can be designed, it will be unnecessary to modify the blade and vane numbers and the spacing in the inlet stages.

Estimates of the overall power level (OAPWL) reductions were obtained using some of these methods. Either blade vane modifications or increased spacing is worth about 4 dB in OAPWL. Treating the diffuser sections of the compressor and the turbine discharge with perforated facing - honeycomb

backing space acoustic liners should provide about 9-dB discharge noise OAPWL reduction. Similar treatment upstream of the compressor and turbine would reduce the sound power levels in these regions by approximately 12 to 14 dB. Use of sonic inlets should result in at least 20-dB reduction in inlet noise. Further noise reductions could be obtained by sound-absorbing liner applications outside of the main turbomachine components. For design of such structures, an estimate of the spectral distribution of target noise reduction is required to provide better criteria than the OAPWL reductions employed here.

#### A.1. NUMBER OF BLADES AND VANES

In a compressor or turbine, sound at blade-passage frequency and its harmonics is generated primarily by the interactions of the aerodynamic fields between adjacent rotor and stator stages. The noise or sound pressure has a characteristic structure of spatial distribution in the duct consisting of a set of pressure patterns having a number,  $m$ , of lobe pattern spins in the duct at a speed  $B/m$  times rotor speed (where  $B$  is the number of rotor blades) for the fundamental  $2B/m$  for the first overtone. (This is required for the patterns to generate the correct frequency.) Clearly, low  $m$ -lobe patterns spin more rapidly than high  $m$ -lobe patterns.

The pattern spin speed is crucial for the tangential Mach number at which the pattern sweeps the wall. This dictates one or the other of two very different types of behavior. If the pattern circumferential wall speed is supersonic, the pattern will spiral its way to the duct outlet and radiate noise. This is called propagation. On the other hand, if the pattern wall speed is subsonic, the strength of the pattern will decay exponentially with axial distance. These axial decay rates can be made very high so that substantial noise reductions can be achieved by proper design.

The number of lobes,  $m$ , in these patterns can be expressed in terms of the number of rotor blades,  $B$ , and stator vanes,  $V$ , as follows:

$$m = nB \pm kV \quad , \quad (A-1)$$

where  $n = 1$  for blade passage frequency (BPF),  $n = 2$  for 2BPF, etc., and  $k$  is an index taking values  $k = 1, 2, 3 \dots$

To obtain decay of all patterns of some harmonic,  $n$ , requires only that the least absolute value of  $m$  be large enough so that the pattern Mach number,  $M_m = (nB/m)M_B$ , is less than 1.

Usually, it is desired to decay patterns for both BPF and 2BPF. In aircraft power plants where the blade Mach number,  $M_B$ , is moderately high subsonic,  $V$  must be selected to be greater than four times the number of blades,  $B$ . This requirement can seldom be met. However, because of the low Mach numbers in most of the HTGR-GT stages, it is possible to exploit the following property (Ref. A-1): If the blade Mach number,  $M_B$ , is less than  $1/3$ , then selection of vane numbers according to

$$B(1 + M_B) < V < 2B(1 - M_B) \quad (A-2)$$

leads to decaying patterns of sound at the fundamental and first harmonic of BPF.

This property has guided selection of blade and vane numbers in the outermost three stages of the HTGR-GT compressor and turbine, with one exception: The first stage compressor inlet Mach number is too high to meet the requirement that Eq. A-2 applies. In this case only,  $V$  is selected to decay only the fundamental BPF. The harmonic 2BPF will unavoidably propagate.

In addition to satisfying Eq. A-2, the blade and vane numbers were determined by repeated trials to provide a substantial amount of decay: 20 to 25 dB or more. Interactions between non-adjacent stages were also considered because of the known persistence of wakes through several stages.

The blade and vane numbers for the compressor and turbine inlet and discharge stages are presented below.

Compressor Inlet Stages

Stage	Blade and Vane Numbers			
	Modified		Current	
	Rotor	Stator	Rotor	Stator
1GV		114		102
R1	77		77	
S1		116		78
R2	80		80	
S2		118		81
R3	82		82	
S3		120		83

Notes

1. If the sonic throat inlet is used, the current blade and vane numbers can be retained.
2. For use with other inlets, the modified numbers should be used.
3. The modified numbers decay BPF but cannot control 2BPF.
4. A length of at least 12.7 cm (5 in.) forward of the 1GV leading edge should be provided before the inlet outer diameter increases.

Compressor Discharge Stages

Stage	Blade and Vane Numbers			
	Modified		Current	
	Rotor	Stator	Rotor	Stator
S15		154		113
R16	114		114	
S16		156		115
R17	117		117	
S17		158		118
R18	120		120	
S18		160		121

Note

1. Provide at least 15.2 cm (6 in.) aft of the S18 trailing edge before increasing the outside diameter of the discharge annulus.

Turbine Inlet Stages

Stage	Blade and Vane Numbers			
	Modified		Current	
	Rotor	Stator	Rotor	Stator
S1		120		54
R1	90		94	
S2		118		70
R2	86		86	
S3		116		58
R3	76		76	
S4		114		52

Notes

1. If the sonic throat inlet is used, the current blade and vane numbers can be used.
2. If another inlet is used, the modified numbers should be used.
3. In this case, provide at least 15.2 cm (6 in.) forward of the S1 leading edge before increasing the outside diameter of the inlet duct.

### Turbine Discharge Stages

Stage	Blade and Vane Numbers			
	Modified		Current	
	Rotor	Stator	Rotor	Stator
S6		64		38
R6	48		52	
S7		62		34
R7	46		46	
S8		62		32
R8	44		42	

#### Note

1. Provide at least 25.4 cm (10 in.) aft of the R8 trailing edge before increasing the outside diameter of the discharge duct annulus.

#### A.2. INCREASED SEPARATION BETWEEN ROTOR AND STATOR STAGES

The effect of increased spacing between rotor and stator stages is to reduce levels of propagating narrow band tone noise. In practical terms, neither "breadboard" noise nor "haystack" noise at a cutoff frequency is significantly affected (Ref. A-2).

The modified blade and vane numbers ensure that BPF and 2BPF coherent tone noise will decay and not propagate for HTGR-GT compressor discharge and turbine inlet and discharge. Consequently, it would be unproductive to increase spacing for these three regions.

For the compressor inlet, the 2BPF noise will propagate and increased spacing should be provided. An axial separation on the order of two chords of the upstream airfoil should be the goal. If a sonic inlet is used, no change in spacing (or blade and vane numbers) is needed in the compressor inlet.

If the recommended blade and vane modifications cannot be made, then two-chord spacing must be provided for at least the outermost two stages.

Generally, the coherent discrete frequency blade-vane interaction noise may be reduced at least 20 dB by modifying the vane number to eliminate a propagating mode (Ref. A-3). Unfortunately, this reduction applies only to the phase-locked, very narrow band noise level. When the frequency bandwidth is increased, haystack noise provides a floor level. This noise is associated with cutting of turbulent eddies by the rotor.

It is possible to provide a reasonable estimate of the effects of modified blade and vane numbers and spacing. The original HTGR-GT noise figures (Ref. A-4) were obtained by improving penalty estimates on noise data taken on a baseline direct two-step (Q2S) fan. The baseline had blade and vane numbers selected to cut off the BPF noise and two-chord spacing to reduce 2BPF noise. To obtain reference numbers for the HTGR-GT using certain blade and vane numbers and close spacing, penalties of 6 dB were assigned to each of the 1/3 octave bands containing the fundamental and first overtone of each of the two rotors. These modified spectra were used in the scaling procedures (Ref. A-4) to generate HTGR-GT noise estimates.

In the new HTGR-GT design incorporating correct blade and vane numbers and/or spacing, the noise levels can be obtained by simply scaling the original Q2S fan data before the penalties are applied. More simply, the differences between "penalized" and basic spectra of the Q2S fan should provide reasonable estimates of the effects of the proposed HTGR-GT improvements.

The estimated reductions in OAPWL vary slightly for the four HTGR-GT regions, but for practical purposes may be taken as 4 dB. The implication of this very nominal 4-dB reduction is that large, further noise reductions must be provided by means other than redesign of the basic turbomachine

components. These means include extensive use of sound-absorbing treatment and use of sonic throat inlets for the compressor and turbine. Provision of so-called turbulence control structures which were contemplated to augment inlet noise reduction were examined. These structures provide estimated reductions of only 1 or 2 dB OAPWL and are thus insufficiently effective to be considered.

### A.3. SOUND-ABSORBING TREATMENT FOR TURBOMACHINERY CASES

The HTGR-GT turbomachinery layout was examined to determine the feasibility of installing sound-absorbing treatment. Generally, there is insufficient axial length in the outermost stages to justify treatment in or between the stages themselves. However, the inlet and diffuser case sections of both the compressor and turbine discharge do provide an opportunity to treat an effective length of passage. These locations were examined to obtain estimates of the noise reductions possible.

For the compressor and turbine inlet and discharge ducts, treatments were examined that provide peak attenuation at the peak frequency of the discharge spectra and that would have a reasonably broad bandwidth of attenuation. These characteristics can be provided by construction of the following form. A perforated facing sheet of metal provides the duct flow surface (on both the outside and inside surfaces of the duct annulus). Separated from the perforated facing by a backing space is the solid outer casing. Finally, the annular regions between the facing sheet and backing casing is partitioned radially, usually with a metal honeycomb structure. In the HTGR-GT application, this form of treatment construction has the advantage of not employing any material that would be more adversely affected by the environment than the main turbomachinery components.

A simplified version of the method described in Ref. A-5 was used to obtain estimates of the attenuation characteristics of such liners. After a few trials, liners were selected for these regions. Figures A-1 and A-2



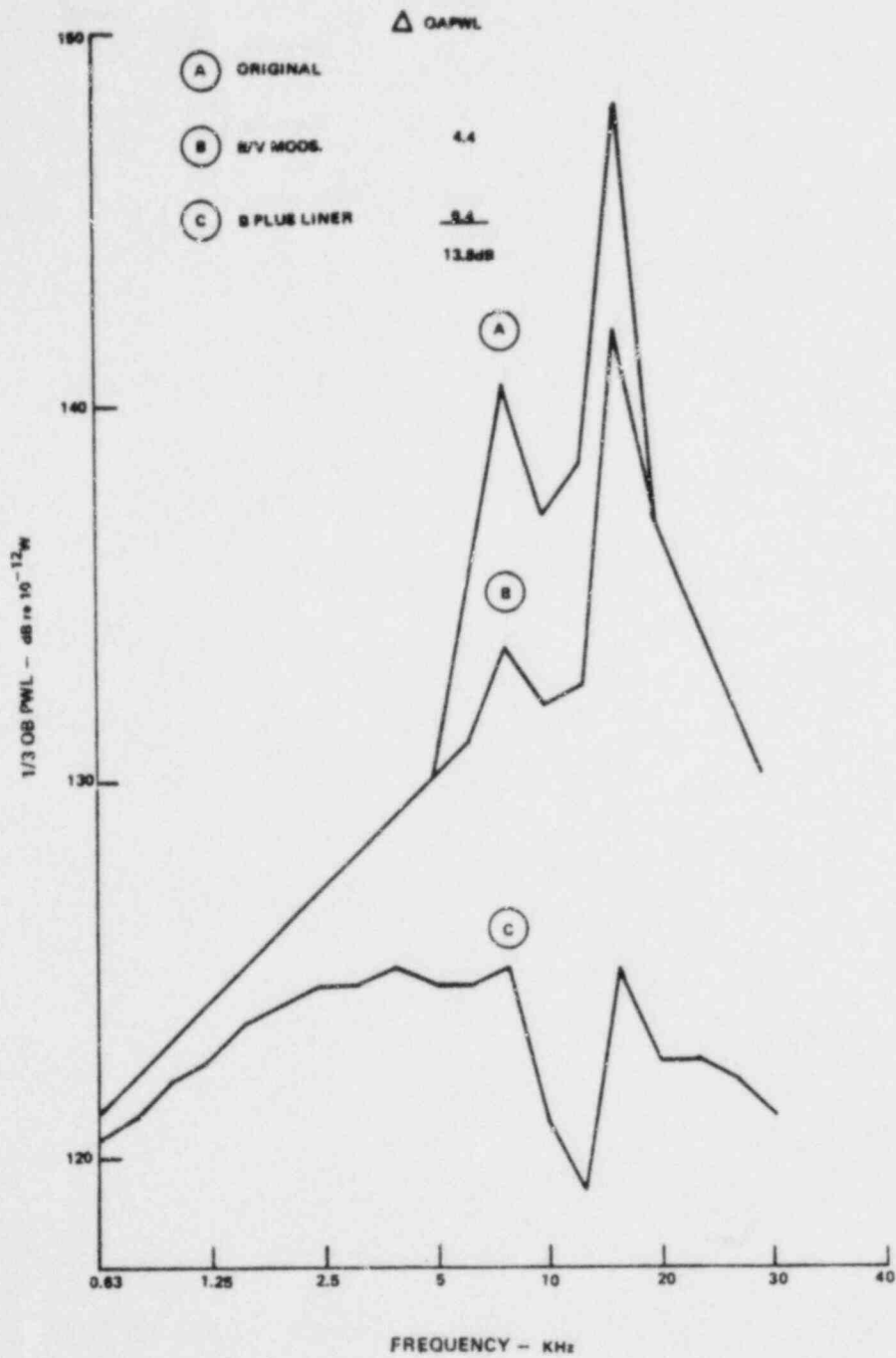


Fig. A-1. Estimated compressor discharge spectra for 400-MW(e) HTGR-GT

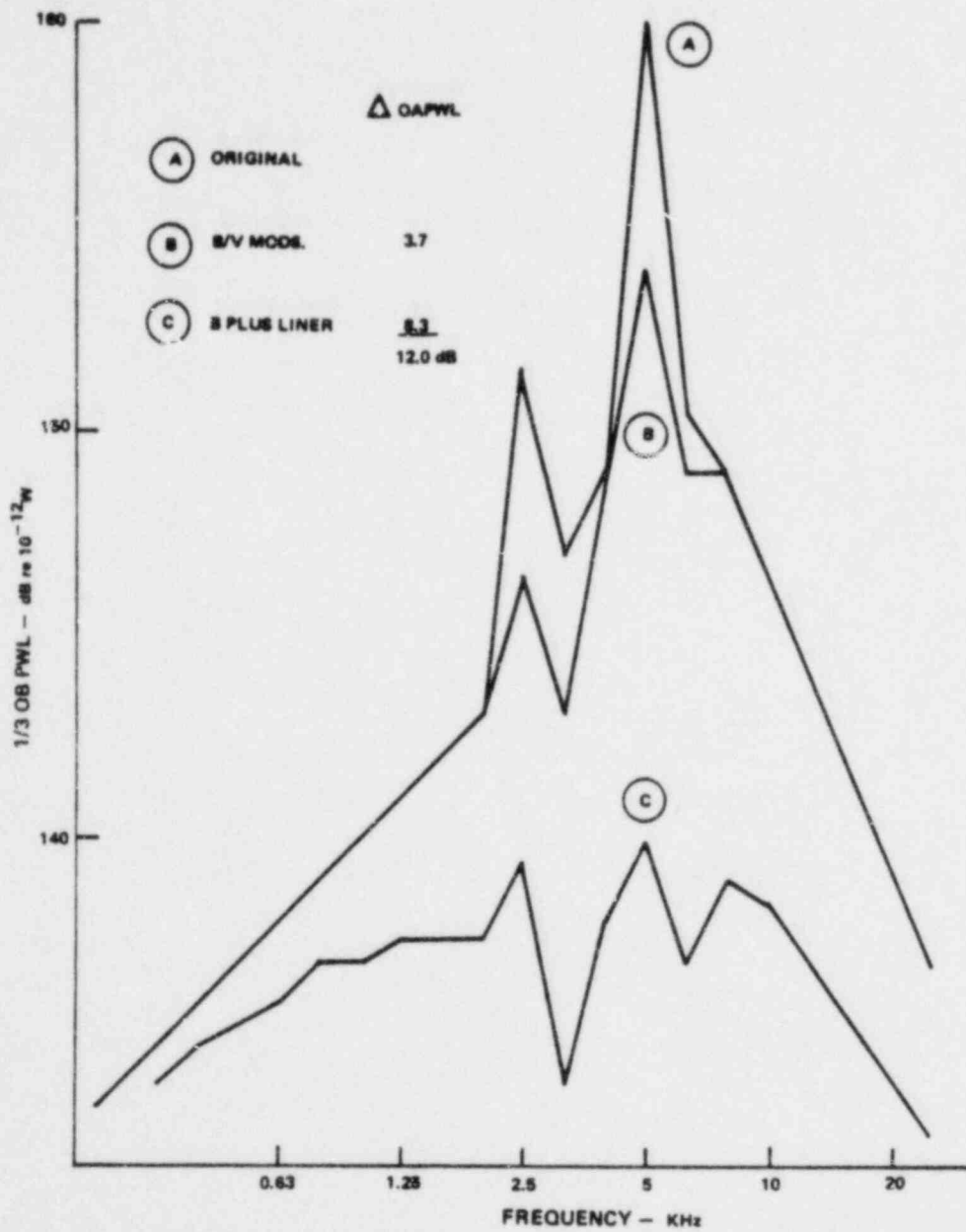


Fig. A-2. Estimated turbine discharge spectra for 400-MW(e) HTGR-GT

present the following information for compressor discharge and turbine discharge: original spectrum estimates, estimated spectra incorporating cutoff blade and vane numbers and/or spacing as previously described, and the estimated spectra resulting from added use of treatment. Figures A-3 and A-4 present similar information for the compressor and turbine areas for three different lengths of extended acoustically treated annular inlet passages.

As shown in Figs. A-1 and A-2, the peak liner attenuations are on the order of 15 dB in the 1/3 octave band to which they are tuned, but the reduction in overall power is approximately 9 dB. Coupled with an overall reduction of 4 dB through cutoff blade and vane redesign, an overall noise reduction of about 13 dB has been achieved so far.

Detailed specification of liner physical parameters, such as percent open area, facing thickness, etc., has not been needed to arrive at the attenuation estimates. Based on experience, the depth of the backing volume is usually between 1/8 and 1/4 wavelength. This gives an annular backing depth between 1.27 and 2.54 cm (1/2 and 1 in.) for the compressor discharge duct and between 3.81 and 7.62 cm (1.5 and 3 in.) for the turbine. The backing depth is 2.54 to 5.08 cm (1 to 2 in.) at the compressor inlet and 5.08 to 10.16 cm (2 to 4 in.) at the turbine inlet. These dimensions seem feasible, but the turbine duct structure incorporating bearing support struts will need extensive redesign to accommodate the treatment.

It is likely that further attenuation will be required. The most obvious structure for this purpose is a set of splitters in the main ducts. Before such added treatment is designed, or even if the treatment described above is considered satisfactory, better estimates of the required spectral distribution of attenuations are needed. It may be that, from the standpoint of structural response, more attenuation should be targeted for the higher frequency at the expense of low-frequency reduction. In other words, a more refined basis for selecting the attenuation spectrum should be found before further work is done on sound-absorbing liner design.

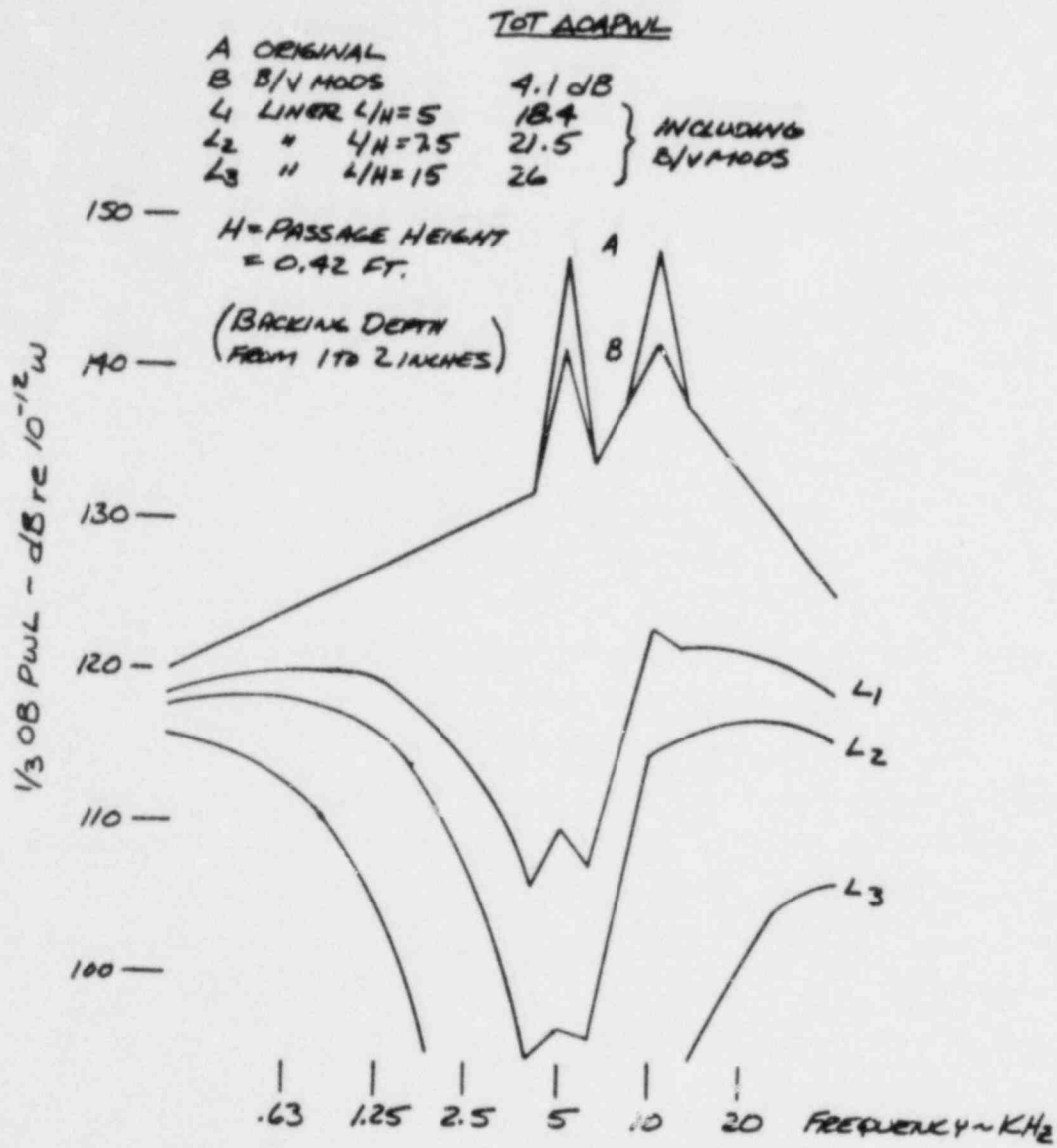


Fig. A-3. Estimated noise reduction potential at compressor inlet of 400-MW(e) HTGR-GT

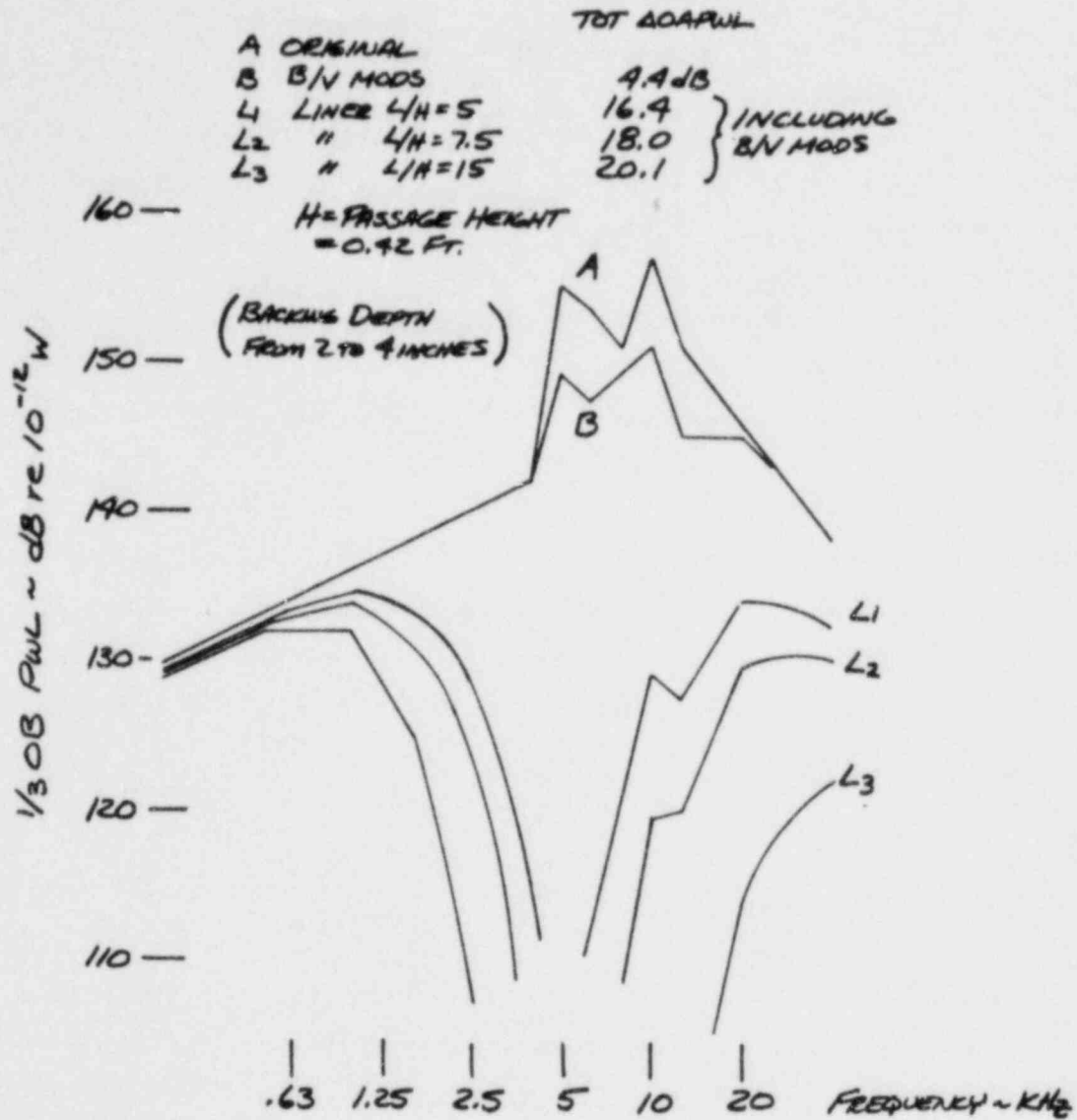


Fig. A-4. Estimated noise reduction potential at turbine inlet of 400-MW(e) HTGR-GT

#### A.4. INLET AND DISCHARGE DUCT MODIFICATIONS

##### A.4.1. Sonic Throat Inlets for Compressor and Turbine

Use of sonic inlets has been shown to be an extremely effective means of reducing noise. As shown in Ref. A-6, this reduction extends over the entire frequency range. The amount of reduction is at least 20 dB. The actual amount depends on the ability to lower noise transmitted from sonics other than the inlet. Furthermore, at part-sonic operation with a throat Mach number of 0.9, as much as 15 dB suppression has been measured. These benefits were observed in the referenced tests with no penalty of aft noise increase.

Since this noise reduction device is so effective, means for incorporating a sonic throat in redesigned compressor and turbine inlets should be examined carefully. If it turns out that turbomachinery performance would be penalized excessively, use of such a device with a throat Mach number of 0.9 or 0.8 together with cutoff blade/vane numbers and/or spacing should be considered.

##### A.4.2. Extended Inlet and Discharge Ducts with Treatment

For the discharge ducts of the compressor and turbine, and for the inlets, if sonic throat design is ruled out, added noise reductions may be achieved by extending these ducts and employing absorbing construction. To fit in the existing spaces, it may be possible to secure the added treatment length by having a folded-back or convoluted geometry. Before examining details of the treatment, two items should be examined. First, the type of duct that could provide significant added length within the structure should be explored in layout. Secondly, estimates should be made of the "allowable" power spectra that should result from all noise reduction measures. Then it will be possible to estimate the reduction from these added treated ducts and to determine if still additional treatment in the loop system is needed.

#### A.5. REFERENCES

- A-1. Tyler, J.M., and T.G. Sofrin, "Noise Abatement Method and Apparatus" U.S. Patent 3,194,487, July 13, 1965.
- A-2. Chin, C.Y., "Acoustic Data Analysis for Rotor-Stator Spacing Test," United Technologies Research Center, July 12, 1977.
- A-3. Sofrin, T.G., and D.C. Mathews, "Asymmetric Stator Interaction Noise," AIAA Paper No. 79-0638, March 1979.
- A-4. Sofrin, T.G., "400MW High Temperature Gas - Cooled Reactor Turbomachinery Noise Estimates," United Technologies Corporation, Power Systems Division, April 4, 1979.
- A-5. Minner, E.L., and E.J. Rice, "Computer Method for Design of Acoustic Liners for Turbofan Engines," NASA Lewis Research Center Report NASA TM X-3317, October 1976.
- A-6. Sofrin, T.G., and N. Rilaff, Jr., "Two-Stage Low Noise, Advanced Technology Fan, V. Acoustic Final Report," Pratt & Whitney Aircraft Report NASA CR 134831, September 1975.